

A CHEMICAL BIOLOGY APPROACH TO DISCOVER THE BIOLOGICAL
TARGETS OF THE ANTIEPILEPTIC DRUG LACOSAMIDE

Pierre Philippe Morieux

A dissertation submitted to the faculty of the University of North Carolina at Chapel Hill in partial fulfillment of the requirements for the degree of Doctor of Philosophy in Pharmaceutical Sciences at the Eshelman School of Pharmacy (Division of Medicinal Chemistry and Natural Products)

Chapel Hill
2010

Approved by:

Pr. Harold Kohn

Pr. Rihe Liu

Pr. Qisheng Zhang

Pr. Stephen Frye

Pr. Robert Rosenberg

ABSTRACT

PIERRE PHILIPPE MORIEUX: A Chemical Biology Approach to Discover the
Biological Targets of the Antiepileptic Drug Lacosamide
(Under the direction of Harold Kohn)

Lacosamide (Vimpat[®]) is a potent antiepileptic drug that received market approval for the adjunctive treatment of partial-onset seizures in adults in Europe and the United States. The pharmacological studies document that lacosamide has a unique profile of activity that differentiates it from existing antiepileptic agents. Based on these findings, we hypothesized that lacosamide binds to different proteins, with low-to-modest affinity. This research project aims to identify the lacosamide biological targets that modulate function and toxicity. We propose a novel target identification approach where an affinity bait (AB) and a chemical reporter (CR) group are strategically placed within the lacosamide framework. These compounds are termed lacosamide AB&CR agents. The AB moiety leads to permanent capture of the binding protein while the bioorthogonal CR unit is used for either detection or isolation of the complex upon reaction with a probe. The understanding of lacosamide's mechanism(s) of action will help increase our understanding of epileptic disorders, and permit the rational development of new clinical agents.

In the first part of our study, we explored the structure-activity relationship (SAR) for the 3-oxy site in lacosamide. We showed that incorporation of non-bulky,

hydrophobic groups at this site provided lacosamide derivatives with excellent activities in animal seizure models. This information was used to design and stereospecifically synthesize a series of lacosamide AB&CR agents where either the AB or the CR group was installed at the 3-oxy site. Most lacosamide AB&CR agents were evaluated for anticonvulsant activity in animal models.

In the second part of our study, the lacosamide AB&CR agents were utilized to interrogate the rat brain soluble and membrane-bound proteome for potential binding partners of lacosamide. We used several subcellular fractionation methods to deconvolute the rat brain proteome. Within each subcellular fraction, different protein purification methods were employed to partition the lysate and aid the identification process. Several potential proteins were selectively targeted by the lacosamide AB&CR agents. Further analysis did not confirm that these proteins were directly linked to lacosamide function. These studies documented the strengths and limitations of the AB&CR strategy for receptor identification and are discussed.

DEDICATION

To my high school chemistry teacher Michel Schiano, for making me love chemistry and for developing my scientific curiosity.

To my niece Chloé Confais-Morieux, and my nephew Romain Morieux. I am looking forward to catch up with my uncle duties.

ACKNOWLEDGMENTS

I am deeply indebted to the many persons, friends and colleagues, that I have been working and interacting with in the last 5 years.

My Ph.D. advisor Dr. Harold Kohn, who worked hard to start the exchange program with the Ecole Nationale Supérieure de Chimie de Paris that brought me to UNC Chapel Hill. Hal has been a great mentor and teacher. Among many things, he has taught me how to be a responsible and rigorous scientist. Most importantly, he has always respected and trusted me, and has let me think and work independently, while his door always remained open when I needed help.

My Ph.D. committee members, Dr. Rihe Liu, Dr. Qisheng Zhang, Dr. Stephen Frye, and Dr. Robert Rosenberg for their advice and insightful comments during these years. I wish to especially thank Dr. Rihe Liu, for opening the door to his lab by letting me rotate, then work in his laboratory at my own bench, for considering me as part of his team, and for guiding me through the biology learning process.

My family, Christian and Sumiko Morieux, Christine, Guillaume and Chloé Confais-Morieux, Pascal, Sandrine and Romain Morieux, as well as my very special friends Anthony Lefèvre and May Christian for their immense, never-ending support that has kept me going during all these years away from home.

My former roommate and friend Duy Tran, his wife Shauna, and their daughter Madeline. I wish the three of you all my best.

Alexander, Nana, Emilia, Liudmila, and Daniel Tropsha for all the great times spent together at their home cooking and sharing Russian culture.

Present and former members of the Kohn laboratory, Dr. Ki Duk Park, Amber King, Dr. Christophe Salomé, Dr. Jason Dinsmore, Dr. Pranjal Baruah, and Elise Salomé for being such pleasant labmates and persons, for their day-to-day assistance and help with chemistry and everything else.

Present and former members of the Liu laboratory, Steven Cotten, Dr. Alex Valencia, Dr. Biao Dong, and Dr. Dongwook Kim, for all their friendship, help, availability for discussion, and the time they took to teach an organic chemist how to conduct biology experiments.

From the Queen Mary University of London, Pr. Simon Gaskell, and from the University of Manchester, Onrapak Reamtong, and Dr. Claire Evers, who performed the mass spectrometry analysis for this project.

All the other present and former graduate students, post-docs, technicians, and faculty members in Beard Hall for all the friendship, help with reagents, technical assistance, ideas, scientific discussions, less scientific discussions, and for making life as a graduate student easier. From Dr. Scott Singleton's lab, Dr. Tim Wigle, Dr. Daniel Cline, Dr. Mallinath Hadimani, Dr. Anna Gromova, Demet Guntas, Keri Flanagan, and Morgan Chapman. From Dr. Alexander Tropsha's lab, Chris Grulke, Tong-Yi Wong, Dr. Denis Fourches, and former member Dr. Weifan Zheng. From

Dr. Mike Jarstfer's lab, Dr. Flori Sassano, Vijay Sekaran, Joana Soares, Dr. Laura Bonifacio, and Dr. Ian Moon. From Dr. Jian Liu's lab, Dr. Heather Bethea, Courtney Jones, Liz Pempe, and Sherket Peterson. From Dr. Andrew Lee's lab, Mary Carroll, Tony Law, Dr. Chad Petit, Tina Galban, Dr. Matthew Whitley, and Dr. Karl Koshlap. From Dr. K.H. Lee's lab, Dr. Qian Shi. From Dr. David Lawrence's lab, Danielle Cook. Thanks to new first-year students Jean-Marc Grandjean and Natalie Rice to who I wish all my best for their graduate career, and finally to my former teaching assistantship advisor Dr. Robert Shrewsbury for being such a nice and enjoyable person.

I would also like to have a special thank for all the persons behind the scenes who have been so helpful all these years keeping me on track administratively and taking care of business when needed. These persons are Amber Allen, Joanne Shanklin, Terri McGowan, Sherrie Settle, Phyllis Smith, Jeanie Stroud, Raj Kshatriya, Paula Press, Barbara Dearry, Pat Shields, and Carrie Goldsmith.

Last but certainly not least, I would like to thank the National Institute of Neurological Disorders and Stroke of the National Institutes of Health for funding this project with a Ruth Kirschstein National Research Service Award Fellowship (F31NS060358) and a National Institutes of Health Grant (R01NS054112), as well as the UNC Eshelman School of Pharmacy for their financial support. The content of this dissertation is solely the responsibility of the author and does not necessarily represent the official views of the National Institute of Neurological Disorders and Stroke or the National Institutes of Health.

PREFACE

“You do what you are”

I look at the work in my dissertation and see a reflection of myself. Who am I? A scientist passionate about what he does. A person who does not settle for mediocre and goes the extra step. An apprentice eager to learn, understand, and share new information. A human being who wants to help people not as lucky as he is. What am I? A hybrid, a reaction mixture, an alloy, a blend of different cultures, backgrounds, and trainings. What do I like to do? Synthesize compounds with a purpose. Design, craft and tailor molecular tools. As a reference to metalworkers, I like to look at myself like a carbonsmith.

I was born in December 1982 in Washington, D.C., from a French father, Christian Morieux, and a Japanese mother, Sumiko Morieux (née Ouchi), making me French/Japanese by blood, and French/American by citizenship. I speak French, English, fairly decent German, I can write, read, and speak Japanese at a more basic level, and these days I am trying to learn some Spanish. I am the youngest of three, with one sister, Christine, and one brother, Pascal. I always like to point out a unique feature of my family, which is that the five of us were each born in a different country, France and Japan for my parents, Beirut, Lebanon for my sister, and Algiers, Algeria for my brother. The origin of this diversity lies with my father's former

jobs as a French diplomat. Thanks to him, I have had the chance to be exposed to many different cultures and to grow in an open-minded familial environment. I am also the only scientist in my family. My father was a French teacher before being a diplomat, my mother was a journalist in Japan, and my brother and sister both went through a business/economy curriculum.

After my birth in the U.S., my family came back to live in France in 1985 for several years, and then moved to Rabat, Morocco, in 1989, where I spent 3 years going at a French elementary school. I learnt to read, speak and write Arabic as a child, but I unfortunately lost everything within years as we came back to France. After a couple more years in Paris, my father was nominated in 1995 as a cultural counselor at the French Embassy in Tokyo, Japan. We stayed there for 5 years, my high school years, where I attended the Lycée Franco-Japonais de Tokyo (LFJT), the French school in Tokyo. There, I met a person who played a very important role in my life, Michel Schiano, my physics and chemistry teacher. Michel had a passionate way to teach his classes and always tried to get his students exposed to more than the chemistry program requirements. He's the person who got me hooked on chemistry. He worked hard to have students from the French school in Tokyo participate in the French Chemistry National Olympiads. His efforts paid out and he made the LFJT the first French school in a foreign country to take part in the French National Chemistry Olympiads. Training under his supervision, I participated in the 16th Olympiads in 2000 where I ranked 10th, well beyond our expectations. Michel also taught us to look outside of science and got me interested in theater. He directed small theater plays with students, in which I was enrolled two consecutive

years. I then obtained my Baccalauréat in science in 2000, and me and my parents moved back to Paris.

The year following my return was not as bright. The next logical thing for me to do was to start my higher education in the classes préparatoires, the French traditional way to enter famous graduate schools Ecoles d'Ingénieurs. With chemistry on my mind, I set myself the goal to enter the Ecole Nationale Supérieure de Chimie de Paris (ENSCP), one of the most prestigious Ecole d'Ingénieurs in chemistry in France. However, the classe préparatoire work schedule proved to be as tough as advertised. With over 12 h of abstract mathematics, 10 h of physics, and only 2 h of chemistry per week, it did not take me long to start failing classes. Well before the end of the 1st year I knew I would not pass and looked for a reorientation. I joined the Institut Universitaire de Technologie of Orsay (IUT d'Orsay) in 2001, and followed a two-year training program as a chemistry technician. All the classes had a more practical aspect which was cruelly missing in the classes préparatoires. In this much more favorable, hands-on environment, I performed much better and learnt a lot, theoretically and practically, and I also continued playing theater. As part of my training, I completed my first internship as a chemistry technician in 2003 at BASF in Ludwigshafen am Rhein, Germany, for over a month. Ranking first of my class, I was able to apply for a parallel admission in the ENSCP where I was accepted in the fall of 2003 (class of 2006).

In the beginning of my second year, in the fall of 2004, a seminar was given by an English teacher at the Ecole Nationale Supérieure de Chimie de Rennes, Pierre Briend, a friend of Harold Kohn, who advertised for a Ph.D. exchange

program with the University of North Carolina at Chapel Hill. At this point in my studies, I was orienting myself towards research and organic synthesis, and decided to take advantage of this offer. I applied to the Division of Medicinal Chemistry and Natural Products and was accepted in 2005. I finished my second year at the ENSCP with a summer internship at Glaxosmithkline Stevenage's Medecines Research Center in Stevenage, U.K. There I worked, indirectly, for one of my future Ph.D. committee members, Dr. Stephen Frye. Within the four days following the end of my internship in Stevenage, in August 2005, I hopped back to Paris, grabbed my luggage and took off for Chapel Hill.

Exposed almost exclusively to chemistry in my training in France, I decided to learn something different and conducted my first laboratory rotation with Dr. Rihe Liu, learning basic biology techniques. I then moved on to work with Dr. Alexander Tropsha where I learnt more about computational chemistry and QSAR. In the summer of 2006, I joined Dr. Harold Kohn's laboratory and started working on my Ph.D. research project to identify the biological targets of lacosamide. Within the first year, Hal encouraged me to apply for a competitive NIH NRSA F31 fellowship, which he helped me obtain. I started working on the organic synthesis of molecular derivatives of lacosamide and later decided to learn how to use them myself in a biological environment. Several years down the road, and despite the fact that we did not find what we were looking for, I am more than happy with the overall result. With all this acquired knowledge I now have the ability to understand and speak both the language of chemistry and the language of biology. In the future I intend to perfect and take full advantage of this set of skills.

All these years as a graduate student, I have sadly witnessed some of my peers and even faculty members openly disregard, or look down on scientific fields other than their own. Biologists and pharmacologists looking at organic or computational chemistry with disdain. Organic chemists sneering at biology. I wish that my work serves as an invitation to other scientists, to reach out of their own field and learn about new areas of research. I believe it is a great approach to tackle the tough challenges we face as health scientists. It may, of course, feel scary to go to new, unknown places, but in my own experience it sure is a lot of fun!

TABLE OF CONTENTS

LIST OF TABLES.....	xxi
LIST OF FIGURES.....	xxii
LIST OF SCHEMES.....	xxv
Chapter	
1. NEUROBIOLOGY OF EPILEPTIC DISORDERS	1
1.1. Basic neurobiology	1
1.1.1. Anatomy of neurons	1
1.1.2. Glial cells are crucial constituents of the brain.....	3
1.1.3. Neurons are polarized by differences in intracellular and extracellular ionic concentrations	4
1.1.4. Mechanism of generation and propagation of action potentials.....	5
1.2. Epilepsy(ies): a multifaceted neurological disorder.....	8
1.2.1. A burden for people and economy	8
1.2.2. Brief classification of epileptic seizures	9
1.2.3. Small molecules to treat epilepsy: the need for antiepileptic drugs with new mechanisms of action.....	10
1.2.4. Animal models used in the pharmacological evaluation of AEDs	11
1.2.4.1. Maximal electroshock seizure test.....	12
1.2.4.2. 6 Hertz test.....	12
1.2.4.3. Pentylentetrazole administration	12

1.2.4.4.	Pilocarpine administration	13
1.2.4.5.	Audiogenic seizure animal models	14
1.2.4.6.	Electrical kindling models	15
1.2.4.7.	Neurological toxicity evaluation	15
1.3.	Pharmacology of traditional and recent AEDs	16
1.3.1.	Ion channels are primary pharmacological targets to prevent seizures	16
1.3.1.1.	Voltage-gated sodium channels	16
1.3.1.2.	Voltage-gated calcium channels.....	19
1.3.2.	Targeting synaptic transmission helps control neuronal excitability.....	20
1.3.2.1.	GABA _A receptors.....	20
1.3.2.2.	Glutamate receptors.....	23
1.3.3.	Pharmacology of traditional AEDs.....	25
1.3.3.1.	Phenytoin	26
1.3.3.2.	Carbamazepine	27
1.3.3.3.	Ethosuximide.....	28
1.3.3.4.	Valproic acid.....	29
1.3.3.5.	Benzodiazepines	30
1.3.3.6.	Summary	31
1.3.4.	Pharmacology of recent AEDs	32
1.3.4.1.	Lamotrigine.....	32
1.3.4.2.	Topiramate	33
1.3.4.3.	Felbamate	34
1.3.4.4.	Tiagabine.....	35
1.3.4.5.	Summary.....	36

1.4.	The emergence of new anticonvulsant entities and biological targets	37
1.4.1.	What is new in antiepileptic drug development.....	37
1.4.1.1.	Levetiracetam.....	37
1.4.1.2.	Retigabine	38
1.4.1.3.	2-Deoxy-D-glucose	39
1.4.2.	Challenges for treating epilepsy	40
1.4.3.	Future hopes	41
1.4.4.	Functionalized Amino Acids (FAAs) are potent anticonvulsants with a broad spectrum of activity and a unique mechanism of action	42
1.4.4.1.	Lacosamide	42
1.4.4.2.	Rationale and hypothesis to search and identify the biological targets of (<i>R</i>)-LCM.....	43
2.	ORGANIC SYNTHESIS OF LACOSAMIDE DERIVATIVES.....	45
2.1.	Selecting the chemical parts to build molecular tools	45
2.1.1.	Current methods for drug target identification	45
2.1.2.	The use of small chemical groups for selective protein modification	46
2.1.2.1.	Electrophilic groups	47
2.1.2.1.1.	Isothiocyanate	48
2.1.2.1.2.	Aldehyde	49
2.1.2.1.3.	Epoxides	50
2.1.2.2.	Photoreactive groups	51
2.1.2.2.1.	Aromatic azide	52
2.1.2.2.2.	Diazirines	53
2.1.2.2.3.	Benzophenone.....	54
2.1.3.	Bioorthogonal groups and click chemistry	55

2.2.	Structure-activity relationship of FAAs.....	58
2.2.1.	FAAs.....	58
2.2.2.	Synthetic approaches to side chain modification.....	60
2.2.2.1.	Functionalization using O-alkylation.....	60
2.2.2.2.	Functionalization using aziridine ring-opening, a general approach to LCM O-substituted derivatives	62
2.2.2.2.1.	Synthesis via <i>N</i> -Trt aziridine carboxylate esters.....	62
2.2.2.2.2.	Synthesis using dialkoxyphosphoranes derivatives	64
2.2.3.	Structure activity relationship of the LCM 3-oxy-substituent.....	67
2.2.3.1.	Choice of compounds.....	67
2.2.3.2.	Pharmacological results	72
2.2.3.3.	Discussion.....	77
2.2.4.	Experimental Section.....	81
2.2.4.1.	Synthetic procedures.....	82
2.2.4.1.1.	General procedure for the aziridine ring-opening with alcohols. Method A	82
2.2.4.1.2.	General procedure for the ester hydrolysis of <i>N</i> -acetylserine esters with LiOH. Method B	82
2.2.4.1.3.	General procedure for the MAC reaction. Method C	83
2.2.4.1.4.	General procedure for the DMTMM coupling reaction. Method D	83
2.2.4.1.5.	General procedure for the Swern oxidation reaction. Method E	84
2.2.4.1.6.	General procedure for the Corey-Chaykovsky epoxidation. Method F.....	84
2.2.4.1.7.	General procedure for the Williamson ether synthesis. Method G	85
2.2.4.1.8.	General procedure for the Pd-catalyzed hydrogenation reaction. Method H	85

2.2.4.1.9.	General procedure for the aromatic aldehyde deprotection. Method I	86
2.2.4.1.10.	General Procedure for the <i>m</i> -CPBA epoxidation. Method J	86
2.2.4.2.	Synthesis of <i>N</i> -acetylaziridine carboxylate esters and carboxamides	86
2.2.4.3.	Synthesis of <i>O</i> -substituted <i>N</i> -acetylserine esters	95
2.2.4.4.	Synthesis of <i>O</i> -substituted <i>N</i> -acetylserine derivatives.....	113
2.2.4.5.	Synthesis of <i>O</i> -substituted derivatives of lacosamide	124
2.3.	Synthesis of a molecular toolkit for use in chemical biology studies	154
2.3.1.	Synthetic strategies to different AB, CR and AB&CR derivatives	154
2.3.1.1.	Introduction of aldehyde AB groups	156
2.3.1.2.	Introduction of isothiocyanate AB groups	158
2.3.1.3.	Introduction of epoxide AB groups	159
2.3.1.4.	Introduction of azide CR groups	160
2.3.1.5.	Introduction of alkyne CR groups	161
2.3.1.6.	Introduction of diazirine and benzophenone photoAB groups (<i>work of Dr. Christophe Salomé</i>).....	161
2.3.1.7.	Summary	162
2.3.2.	Biotin and fluorescent alkyne and azide Probes	163
2.3.3.	Experimental Section.....	166
2.3.3.1.	Synthesis of <i>para</i> -substituted benzylamines	166
2.3.3.2.	Synthesis of lacosamide AB derivatives	170
2.3.3.3.	Synthesis of lacosamide AB&CR derivatives	181
2.3.3.3.1.	Derivatives bearing the CR group on the C(2) side chain	181
2.3.3.3.2.	Derivatives bearing the CR group on the aromatic ring.....	194
2.3.3.4.	Synthesis of biotin and fluorescent Probes	205

3.	PROTEIN CHEMISTRY IN THE EYE OF THE CHEMIST	213
3.1.	General procedures for rat brain fractionation	213
3.1.1.	The nuclear fraction (N1)	216
3.1.2.	The mitochondrial fraction (P2)	218
3.1.3.	The membrane fraction (P3).....	218
3.1.4.	The cytoplasmic fraction (S3)	219
3.2.	Ammonium sulfate fractionation	219
3.3.	Ion exchange chromatography	221
3.4.	Click chemistry	226
4.	SCREENING THE RAT BRAIN CYTOPLASMIC FRACTION.....	230
4.1.	The use of epoxide-based AB&CR molecules as selective labeling agents.....	230
4.1.1.	Rationale	230
4.1.2.	Labeling and fractionation experiments of cytoplasmic proteins.....	231
4.1.3.	Identification of a protein of interest in the soluble fraction.....	233
4.2.	Brain-type creatine kinase B (CKB)	235
4.2.1.	CKB is selectively labeled by epoxide-based AB&CR agents	235
4.2.2.	Competition experiments with (<i>R</i>)-LCM and a known CKB inhibitor	238
4.2.3.	Possible significance of CKB as a target for epilepsy.....	240
4.2.4.	Creatine Kinase B activity assay	241
4.2.5.	Identification of modification sites of CKB.....	244
4.2.6.	Interaction of lacosamide with CKB	249
4.3.	Photoaffinity labeling of the cytoplasmic lysate.....	251
4.3.1.	A potential protein target for (<i>S</i>)-LCM.....	254
4.3.2.	Enrichment procedure for the ~25 kDa protein.....	258

4.4.	Discussion	262
4.5.	Conclusions	267
4.6.	Experimental Section	268
4.6.1.	Preparation of the rat brain cytoplasmic lysate	268
4.6.2.	Cytoplasmic protein labeling with AB&CR agents	268
4.6.3.	General procedure for lysate fractionation	269
4.6.4.	Click chemistry	270
4.6.5.	ITC experiments	270
4.6.6.	Creatine Kinase B enzymatic assay	271
4.6.7.	Cloning of CK-B	273
4.6.8.	Overexpression and purification of CK-B	275
5.	MEMBRANE-BOUND FRACTION SCREENING	277
5.1.	Using non-denaturing detergents to solubilize membrane-bound proteins	277
5.1.1.	Preparation of detergent-solubilized membrane extract from rat brain	279
5.1.2.	Solubilized membrane fraction screening	280
5.1.3.	Interactions between fluorescent Probes and detergent molecules	285
5.2.	Screening whole membrane extracts for potential targets	286
5.2.1.	Rationale for the synaptosomal fraction screening	287
5.2.2.	Screening the synaptosomal and microsomal fractions	290
5.3.	Discussion	299
5.4.	Conclusions	304
5.5.	Experimental Section	305
5.5.1.	Preparation of the solubilized membrane lysate	305

5.5.2.	Protocol for the enrichment of synaptosomes by phase partitioning.....	306
5.5.3.	Photolabeling of the membrane fraction	308
5.5.4.	Click chemistry on intact labeled membrane proteins (Methods A and B)	309
5.5.5.	Protocol for the cryopreservation step	310
6.	CONCLUSIONS AND FUTURE DIRECTIONS.....	311
6.1.	The importance of the lysate source.....	312
6.2.	Other subcellular fractions and proteins for screening.....	313
6.3.	Drug target identification methods	315
	REFERENCES.....	318

LIST OF TABLES

Table 1. The Structure activity relationship of <i>O</i> -substituted (<i>R</i>)-lacosamide derivatives.....	69
Table 2. Representative list of the CKB tryptic digests identified from the fractionated cytoplasmic lysate	235
Table 3. List of peptides identified after trypsin digestion of streptavidin beads for the cytoplasmic sample treated with 10 μ M (<i>R</i>)- 179	237
Table 4. Components used for the PCR amplification of the CKB gene from a human cDNA library.....	274
Table 5. Components used for the ligation reaction between CKB and pET28a vector digested products	274
Table 6. Representative list of tryptic fragments identified in the Coomassie stained band corresponding to ~60 kDa	296

LIST OF FIGURES

Figure 1. General morphology of a neuron (art by Mariana Ruiz Villareal)	2
Figure 2. Typical intracellular and extracellular ionic concentrations for a mammalian neuron.....	5
Figure 3. Schematic representation of the different phases occurring during the generation of an AP.....	6
Figure 4. Chemical structures of various chemoconvulsants used in animal testing.....	14
Figure 5. Schematic representation of a voltage-gated Na ⁺ channel α -subunit	17
Figure 6. Simplified representation of a GABA _A R structure	21
Figure 7. Chemical structures of cognate ligands of ionotropic glutamate receptors.....	23
Figure 8. General topology of an ionotropic glutamate receptor subunit.....	24
Figure 9. Structures of the different AB&CR agents synthesized for chemical biology studies.....	163
Figure 10. Structures of epoxide-based AB&CR agents used in the rat brain cytoplasmic fraction screening	231
Figure 11. Structures of the different Probes used to react with the CR groups after protein labeling.....	232
Figure 12. 6% SDS-PAGE gel of rat brain cytoplasmic AMS cuts containing a protein of interest labeled by (R)- 179 but not (R)- 175	233
Figure 13. 8% SDS-PAGE gel of rat brain cytoplasmic preferentially labeled by (R)- 179 over (S)- 179	234
Figure 14. In-gel fluorescence scan of the brain cytoplasmic lysate (6% SDS-PAGE gel).....	236
Figure 15. 8% SDS-PAGE gel of the cytoplasmic lysate M4555 cut.....	238
Figure 16. 12.5% SDS-PAGE gel Coomassie stain of overexpressed purified human CKB enzyme after His-tag, AMS, and Q-Sepharose [®] fractionation.....	241

Figure 17. Comparison of enzymatic activities of human commercial CKB and overexpressed CKB.....	243
Figure 18. Crystal structure of human CKB (PDB ID: 3B6R)	244
Figure 19. CKB enzymatic inhibition assay with (<i>R</i>)- 180 (abbreviated EXRKY). ...	246
Figure 20. MS analysis of intact CKB (~50 μ g) modified with (<i>R</i>)- 180 at different concentrations	247
Figure 21. Fluorescence scan (very low sensitivity, PMT 300) of CKB samples treated with various concentrations of (<i>R</i>)- 180	248
Figure 22. Left picture: ITC trace of the interaction between CKB and (<i>R</i>)-LCM.....	250
Figure 23. Structures of electrophilic AB&CR agents 172 , and photoAB&CR agents 181 , 169 , 168 , and 170 used in the screening of the rat brain cytoplasmic lysate.	251
Figure 24. Left: in-gel fluorescence of different AMS cut from the cytoplasmic lysate after labeling with various AB&CR agents.	253
Figure 25. Left: in-gel fluorescence of different AMS cut from the cytoplasmic lysate after labeling with various AB&CR agents	254
Figure 26. Left: in-gel fluorescence of different AMS cuts (M0030, M3045, M4555) from the cytoplasmic lysate after labeling with various AB&CR agents.	255
Figure 27. Left: in-gel fluorescence of different AMS cuts (M5565, M6590) from the cytoplasmic lysate after labeling with various AB&CR agents	256
Figure 28. 12.5% SDS-PAGE gel of the rat cytoplasmic M3555 cut.....	257
Figure 29. Fluorescence scan of the cytoplasmic AMS cut M3555 after labeling with (<i>R</i>)- 169 or (<i>S</i>)- 169 at various concentrations (10% SDS-PAGE gel) and click chemistry with 196	258
Figure 30. 10% SDS-PAGE gel of the rat brain cytoplasmic lysate M3555 labeled with 1 μ M (<i>R</i>)- 169 or (<i>S</i>)- 169	260
Figure 31. Structure of non-ionic and zwitterionic detergents used in our study of the membrane proteome.....	278

Figure 32. 12.5% SDS PAGE gel of the detergent-solubilized (β -DDM, or CHAPS) membrane fraction (P2+P3) labeled with photoAB&CR agents 181 , 169 , 168 , and 170	281
Figure 33. 10% SDS-PAGE gel (minigel) of the membrane fraction (P2+P3) solubilized with a panel of detergents, flow-through of the S and Q Sepharose [®] (pH 7.4) fractionation steps	282
Figure 34. 10% SDS-PAGE gel (large size) of the membrane fraction (P2+P3) solubilized with a single detergent or sequentially-solubilized with two different surfactants	284
Figure 35. General approach to the purification of synaptosomes by phase partitioning.....	288
Figure 36. Western blot of the crude brain homogenate and synaptosomes.....	290
Figure 37. Fluorescence scan of the synaptosomal fraction screened with photoAB&CR agents 181 , 169 , 168 , and 180 (6%SDS PAGE gel).	291
Figure 38. 10% SDS-PAGE gel of the synaptosomal fraction labeled with (<i>R</i>)- 169 and (<i>S</i>)- 169	294
Figure 39. 8% SDS-PAGE gels of the intact membrane-bound fraction after photolabeling, click chemistry with 196 using Method B and 1% SDS 25 mM HEPES (pH 7.4)	295
Figure 40. Coomassie stain of the enriched protein of interest (8% SDS-PAGE gel).....	296
Figure 41. In-gel fluorescence scan of freshly prepared (non cryopreserved) microsomal fraction from the rat brain.	297
Figure 42. In-gel fluorescence scan of purified BSA and HSA labeled with photoAB&CR agent 169	298
Figure 43. In-gel fluorescence scan of purified BSA and HSA labeled with photoAB&CR agent 181 , 168 , and 170	299

LIST OF SCHEMES

Scheme 1. Simplified representation of the propagation of an action potential along the axon.....	7
Scheme 2. Schematic representation of the fast inactivation hinged lid mechanism of VGSCs.	18
Scheme 3. Proposed strategy to identify the target proteins of (<i>R</i>)-LCM with AB&CR agents.	47
Scheme 4. The NCS group reacts with a lysine residue to form a covalent thiourea linkage.	49
Scheme 5. The aldehyde groups 10 and 13 react with an amine to give imine intermediates 11 and 14	49
Scheme 6. Epoxides undergo ring-opening with a variety of nucleophilic amino acids.....	50
Scheme 7. Irradiation of 22 leads to the singlet nitrene 23	52
Scheme 8. Irradiation of the diazirine moiety (27 , 30) generates the corresponding carbene (28 , 31) which undergoes nucleophilic attack or C-H bond insertion (31 , 32).	53
Scheme 9. Excitation of the C=O bond in 33 reversibly leads to an excited diradical 34 that undergoes C-H bond insertion reaction (35 , 36).	55
Scheme 10. Terminal alkynes and azides lead to different triazole regioisomers under different conditions	56
Scheme 11. Staudinger ligation reaction	56
Scheme 12. Two examples of strain-promoted cyclooctyne addition reactions.	57
Scheme 13. Structure of FAAs.....	58
Scheme 14. Synthetic pathway to enantiomerically pure <i>O</i> -alkoxysubstituted derivatives of lacosamide: route 1	60
Scheme 15. Synthetic pathway to enantiomerically pure <i>O</i> -alkoxysubstituted derivatives of lacosamide: route 2	61
Scheme 16. Synthetic pathway to enantiomerically pure <i>O</i> -alkoxysubstituted derivatives of lacosamide: route 3	62

Scheme 17. Different synthetic pathways used to access enantiomerically pure aziridine ester carboxylates	63
Scheme 18. Synthetic route to dialkoxytriphenylphosphoranes DTPP and DTPP-F ₆	65
Scheme 19. Synthetic pathway to enantiomerically pure O-alkoxysubstituted derivatives of (<i>R</i>)-LCM: route 4	66
Scheme 20. Synthesis of acid 123 to prepare the side chain aldehyde AB group	113
Scheme 21. Different reactions used to obtain 55 derivatives after the amide coupling step (route 3).	125
Scheme 22. Synthesis of the deuterated analog of (<i>R</i>)-lacosamide (<i>R</i>)- 1-d₃ (route 1).....	126
Scheme 23. Synthetic routes to <i>para</i> -substituted benzylamines used in the synthesis of AB, CR and AB&CR agents	154
Scheme 24. Synthesis of the lacosamide AB derivative 151 (route 1).....	157
Scheme 25. First attempt to synthesize the side chain aldehyde AB group (route 3).	157
Scheme 26. Synthesis of the side chain aldehyde AB group (route 3)	158
Scheme 27. Synthesis of aromatic isothiocyanate AB&CR derivatives (route 3)	158
Scheme 28. Synthesis of the side chain isothiocyanate AB&CR (route 3).....	159
Scheme 29. Synthesis of aromatic epoxide AB&CR agents (route 3).....	159
Scheme 30. Synthesis of the side chain epoxide AB&CR agents (route 3)	160
Scheme 31. Synthesis of 2-azidoethanol (top) and AB&CR agents bearing an aromatic azide (bottom) (route 3).....	160
Scheme 32. Synthesis of the alkyne-containing AB&CR agents (route 3)	161
Scheme 33. Synthesis of 2-(3-methyl-3 <i>H</i> -diazirin-3-yl)ethanol and the corresponding AB&CR agent (top), and photoAB&CR agents bearing an aromatic diazirine or benzophenone (bottom) (route 3).....	162
Scheme 34. Synthetic pathway to azide and alkyne-containing PEG linkers.....	164

Scheme 35. Synthesis of PEG-containing D-biotin Probes	165
Scheme 36. Synthesis of PEG-containing TAMRA fluorescent Probes.....	165
Scheme 37. Synthesis of the AB derivative 197 bearing the epoxide at the benzylamide <i>para</i> position.	170
Scheme 38. Structure of the different intermediates and chemical reactions used in the synthesis of AB&CR agents 171 , 173 , 174 , 175 and 176	181
Scheme 39. Structure of the different intermediates and chemical reactions used in the synthesis of AB&CR agents 178 , 179 , and 180	194
Scheme 40. Subcellular fractionation using differential centrifugation	215
Scheme 41. Chemical reactions used in the CKB activity assay.	242

LIST OF ABBREVIATIONS

(COCl) ₂	Oxalyl chloride
(R)	Rectus
(S)	Sinister
(v/v)	Volume per volume
(w/v)	Weight per volume
(w/w)	Weight per weight
[α] ²⁵ _D	Optical rotation at 25 degrees Celsius using the D line of sodium
+ESI	Positive electrospray ionization
°C	Degree Celsius
β-DDM	β-Dodecylmaltoside
Δ	Heating
δ	Chemical shift
μA	Microampere
μM	Micromole per liter
2DG	2-Deoxy-D-glucose
AB	Affinity bait
AB&CR	Affinity bait and chemical reporter
ABPP	Activity-based protein profiling
Ac	Acetyl

Ac ₂ O	Acetic anhydride
ADP	Adenosine diphosphate
AED	Antiepileptic drug
Ag ₂ O	Silver (I) oxide
AMP	Adenosine monophosphate
AMPA	α-Amino-3-hydroxy-5-methyl-4-isoxazolepropionic acid
AMPAR	α-Amino-3-hydroxy-5-methyl-4-isoxazolepropionic acid receptor
AMS	Ammonium sulfate
AP	Action potential
app	Apparent
Ar	Aryl; Argon
ASP	Anticonvulsant Screening Program
Asp, D	Aspartic acid
ATP	Adenosine triphosphate
BASP1	Brain acid soluble protein 1
BF ₃ •Et ₂ O	Boron trifluoride diethyl etherate
BME	β-Mercaptoethanol
Bn	Benzyl
Boc	<i>Tert</i> -butoxycarbonyl
Boc ₂ O	di- <i>tert</i> -butyl-dicarbonate
br	Broad

Br ₂	Bromine
BSA	Bovine serum albumin
BuLi	<i>n</i> -Butyllithium
BVT	Brivaracetam
BZD	Benzodiazepine
<i>c</i>	Concentration in mg per 0.1 mL
C=O	Carbon-oxygen double bond
CA2	Carbonic anhydrase 2
Ca ²⁺	Calcium (II)
CaCl ₂	Calcium (II) chloride
Calcd	Calculated
CaM	Calmodulin
CBZ	Carbamazepine
Cbz	Carboxybenzyloxy
CD ₃ OD	Perdeuterated methanol
CDCl ₃	Deuterated chloroform
cDNA	Cloned deoxyribonucleic acid
C-H	Carbon-hydrogen bond
CH ₂	Methylene
CH ₂ Cl ₂	Methylene chloride
CH ₃ CN	Acetonitrile

CHAPS	3-[(3-Cholamidopropyl)dimethylammonio]-1-propanesulfonate hydrate
CHCl ₃	Chloroform
CKB	Brain-type creatine kinase
CKB ^{-/-}	Brain-type creatine kinase double knockout
Cl ⁻	Chloride (-I)
CMC	Critical micellar concentration
CNS	Central nervous system
C-O	Carbon-oxygen single bond
COX IV	Cytochrome c oxidase subunit IV
Cr	Creatine
CR	Chemical Reporter
CRMP2	Collapsin response mediator protein 2
Cu(I)	Copper (+I)
Cu ²⁺	Copper (+II) ion
CuAAC	Cu(I)-catalyzed azide-alkyne cycloaddition
CuSO ₄ •5H ₂ O	Copper (+II) sulfate pentahydrate
CV	Column volume
Cys, C	Cysteine
d	Day; doublet
D	Dextrorotatory
Da	Dalton

dB	Decibel
DBA/2	Dilute brown non-agouti
dd	Doublet of doublet
ddH ₂ O	Double distilled water
DEPC	Diethylpyrocarbonate
DIEA	Diisopropylethylamine
DITC	Di-(imidazolyl)thionocarbonate
DMAP	Dimethylaminopyridine
DMF	<i>N,N</i> -Dimethylformamide
DMSO	Dimethylsulfoxide
DMSO- <i>d</i> ₆	Perdeuterated dimethylsulfoxide
DMTMM	4-(4,6-Dimethoxy-1,3,5-triazin-2-yl)-4-methylmorpholinium chloride
DNA	Deoxyribonucleic acid
DNFB	2,4-Dinitrofluorobenzene
DPT	Di-(2-pyridyl)thionocarbonate
dt	Doublet of triplet
DTPP	Diethoxytriphenylphosphorane
DTPP-F ₆	Di-(2,2,2-trifluoroethoxy)triphenylphosphorane
DTT	Dithiothreitol
<i>E. coli</i>	<i>Escherichia coli</i>
<i>E</i> _{Ca}	Equilibrium potential for calcium ions

E_{Cl}	Equilibrium potential for chloride ions
ED ₅₀	Effective dose (50%)
EDTA	Ethylenediamine tetraacetate
EEG	Electroencephalogram
E_{K}	Equilibrium potential for potassium ions
E_{Na}	Equilibrium potential for sodium ions
equiv	Equivalent
ESM	Ethosuximide
Et, CH ₂ CH ₃	Ethyl
Et ₂ O	Diethyl ether
Et ₃ N	Triethylamine
EtOAc	Ethyl acetate
EtOH	Ethanol
F	Phenylalanine
FAA	Functionalized amino acid
FBM	Felbamate
FDA	Food and Drug Administration
FITC	Fluorescein isothiocyanate
g	Unit of gravity
G6PDH	Glucose-6-phosphate dehydrogenase
GABA	γ -Aminobutyric acid

GABAR	γ -Aminobutyric acid receptor
GABA-T	γ -Aminobutyric acid transaminase
GAD	Glutamic acid decarboxylase
GAPDH	Glyceraldehyde-3-phosphate dehydrogenase
GAT	γ -Aminobutyric acid transporter
GBP	Gabapentin
Glu, E	Glutamic acid
GPCR	G-protein coupled receptor
h	Hour
H ₂	Hydrogen gas
H ₂ O	Water
HAT	Histone acetyltransferase
HCl	Hydrogen chloride
HDAC	Histone deacetylase
HEPES	(4-(2-Hydroxyethyl)-1-piperazineethanesulfonic acid
His	Histidine
His-tag	6-Histidine tag
HK	Hexokinase
HRMS	High resolution mass spectrometry
HSA	Human serum albumin
Hz	Hertz

I	Isoleucine
IBCF	Isobutylchloroformate
IC ₅₀	Inhibitory concentration (50%)
iGluR	Ionotropic glutamate receptor
ip	Intraperitoneally
<i>i</i> -Pr	Isopropyl
<i>i</i> -PrOH	Isopropanol
IPTG	Isopropyl β-D-1-thiogalactopyranoside
IR	Infrared
ITC	Isothermal titration calorimetry
IUPHAR	International union for basic and clinical pharmacology
iv	Intravenous
<i>J</i>	Coupling constant
K ⁺	Potassium (+I) ion
KA	Kainic acid
KAR	Kainic acid receptor
KCC2	Potassium and chloride cotransporter 2
KCl	Potassium chloride
K _d	Dissociation constant
kDa	Kilodalton
kg	Kilogram

L	Levorotatory
L	Liter
LB	Luria broth
LCM	Lacosamide
LGIC	Ligand-gated ion channel
LiAlH ₄ , LAH	Lithium aluminum hydride
LiCl	Lithium chloride
LiOH	Lithium hydroxide
LSAMP	Limbic system-associated protein
LTG	Lamotrigine
LVT	Levetiracetam
Lys, K	Lysine
m	Multiplet
M	Mole per liter
mA	milliampere
MASS1	Monogenic audiogenic seizure susceptibility 1
<i>m</i> -CPBA	<i>Meta</i> -chloroperbenzoic acid
Me, CH ₃	Methyl
Mel	Methyl iodide
MeOH	Methanol
MES	Maximal electroshock seizure (epilepsy), Morpholineethanesulfonic acid (buffer)

Met, M	Methionine
mg	Milligram
Mg(OAc) ₂	Magnesium (+II) acetate
mg.kg ⁻¹	milligram per kilogram
Mg ²⁺	Magnesium (+II) ion
MgCl ₂	Magnesium (+II) chloride
mGluR	Metabotropic glutamate receptor
min	Minute
mM	Millimole per liter
mmol	millimole
mp	Melting point
<i>M_r</i> , MW	Molecular weight
ms	Millisecond
Ms	Methanesulfonyl, mesyl
MsCl	Methanesulfonyl chloride
mV	millivolt
MWCO	Molecular weight cut-off
N ₂	Nitrogen gas
N ₃	Azide
Na Asc	Sodium ascorbate
Na ⁺	Sodium (+I) ion

Na ₂ SO ₄	Anhydrous sodium sulfate
NaBH ₃ CN	Sodium cyanoborohydride
NaBH ₄	Sodium borohydride
NaBr	Sodium bromide
NADP	β-Nicotinamide adenine dinucleotide phosphate, oxidated form
NADPH	β-Nicotinamide adenine dinucleotide phosphate, reduced form
NaH	Sodium hydride
NaHCO ₃	Sodium hydrogenocarbonate
NaN ₃	Sodium azide
NaOEt	Sodium ethoxide
<i>n</i> Bu ₄ NF	Tetra- <i>n</i> -butylammonium fluoride
NCS	Isothiocyanate
NH ₃	Ammonia
NINDS	National Institute of Neurological Disorders and Stroke
nM	Nanomole per liter
nm	Nanometer
NMDA	<i>N</i> -methyl-D-aspartate
NMDAR	<i>N</i> -methyl-D-aspartate receptor
NMM	<i>N</i> -methylmorpholine
NMR	Nuclear magnetic resonance
Nu	Nucleophile

OD	Optical density
PAGE	Polyacrylamide gel electrophoresis
PCr	Phosphocreatine
PCR	Polymerase chain reaction
Pd	Palladium
Pd/C	Palladium on charcoal
PDB	Protein Data Bank
PEG	Polyethylene glycol
Ph	Phenyl
pH	Potentiometric hydrogen ion concentration
photoAB	Photoaffinity bait
photoAB&CR	Photoaffinity bait and chemical reporter
PHT	Phenytoin
PI	Protective index
PILO	Pilocarpine
PKA	Protein Kinase A
PKC	Protein kinase C
PMSF	<i>Para</i> -methylsulfonylfluoride
PMT	Photomultiplier tube
PNS	Peripheral nervous system
po	Perorally

PPh ₃	Triphenylphosphine
PPh ₃ (O)	Triphenylphosphine oxide
ppm	Part per million
Pr	Propyl
<i>p</i> TSA	<i>Para</i> -toluenesulfonic acid
<i>p</i> TsCl	<i>Para</i> -toluenesulfonyl chloride
PTZ	Pentylentetrazole
<i>R_f</i>	Retention factor
RGB	Retigabine
RNA	Ribonucleic acid
rpm	Revolution per minute
Ru(II)	Ruthenium (+II)
s	Second (time); singlet (NMR)
SA	Serum albumin
SAR	Structure activity relationship
SBP	Sulfobathophenanthroline
sc	Subcutaneous
SDS	Sodium dodecyl sulfate
SE	Status epilepticus
SiO ₂	Silica
SNAP-25	Synaptosomal-associated protein 25

SRF	Sustained repetitive firing of neurons
STX	Saxitoxin
SV2A	Synaptic vesicle protein 2A
t	Triplet
T	Threonine
TAMRA	Tetramethylrhodamine
TBDMS	<i>Tert</i> -butyldimethylsilyl
TBST	Tris-buffered saline tween-20
TBTA	Tris[(1-benzyl-1 <i>H</i> -1,2,3-triazol-4-yl)methyl]amine
<i>t</i> -Bu	<i>Tert</i> -butyl
<i>t</i> -BuOH	<i>Tert</i> -butanol
<i>t</i> -BuONO	<i>Tert</i> -butyl nitrite
TCEP HCl	Tris(2-carboxyethyl)phosphine hydrochloride
TD ₅₀	Median toxic dose (50%)
TFA	Trifluoroacetic acid
TGB	Tiagabine
THF	Tetrahydrofuran
TLC	Thin layer chromatography
TLE	Temporal lobe epilepsy
TMS	Trimethylsilyl
TMSN ₃	Trimethylsilyl azide

TPEN	<i>N,N,N',N'</i> -Tetrakis(2-pyridylmethyl)ethylenediamine
TPM	Topiramate
Tris HCl	Tris(hydroxymethyl)aminomethane hydrochloride
Trt	Triphenylmethyl
TTX	Tetrodotoxin
TX100	Triton X-100
U.mL ⁻¹	Unit per milliliter
UV	Ultraviolet
VGCC	Voltage-gated calcium channel
VGIC	Voltage-gated ion channel
VGKC	Voltage-gated potassium channel
VGSC	Voltage-gated sodium channel
VLGR1	Very large G-protein coupled receptor 1
VPA	Valproic acid
vs	Versus
Zn ²⁺	Zinc (+II) ion
Zw3-14	Zwittergent 3-14, 3-(<i>N,N</i> -dimethylmyristylammonio)propanesulfonate

CHAPTER 1

NEUROBIOLOGY OF EPILEPTIC DISORDERS

1.1. Basic neurobiology

1.1.1. Anatomy of neurons

Neurons are nerve cells found in the central nervous system (CNS) and the peripheral nervous system (PNS).¹ They are responsible for processing and transmitting sensory information.² Their discovery in the late part of the 19th century was made possible by the pioneering work of two scientists, Camillo Golgi³ and Santiago Ramón y Cajal,^{4,5} who shared the 1906 Nobel Prize for Physiology or Medicine.⁶ A normal human brain contains approximately 100 billion neurons,⁷ and the numerous types of stimuli we perceive come, in part, from the diversity of receptors and proteins localized within the brain.^{1,2}

Like other cells, neurons are polarized by an electrochemical gradient generated by the differences between intracellular and extracellular ionic concentrations.^{1,2} However, only a select set of cells (e.g., neurons) have the ability to electrically respond to a change in membrane potential. When the cell depolarizes and the potential reaches a certain threshold, it fires an electrical signal termed action potential (AP). In most cases, APs lead to neurotransmitter release from the presynaptic neuron, and the reception of the chemical signal is converted into

another electrical signal (excitatory or inhibitory) by the postsynaptic cell.^{1,2} Neurons' morphologies and functions are intimately linked,⁸ and they typically contain the following elements (Figure 1).

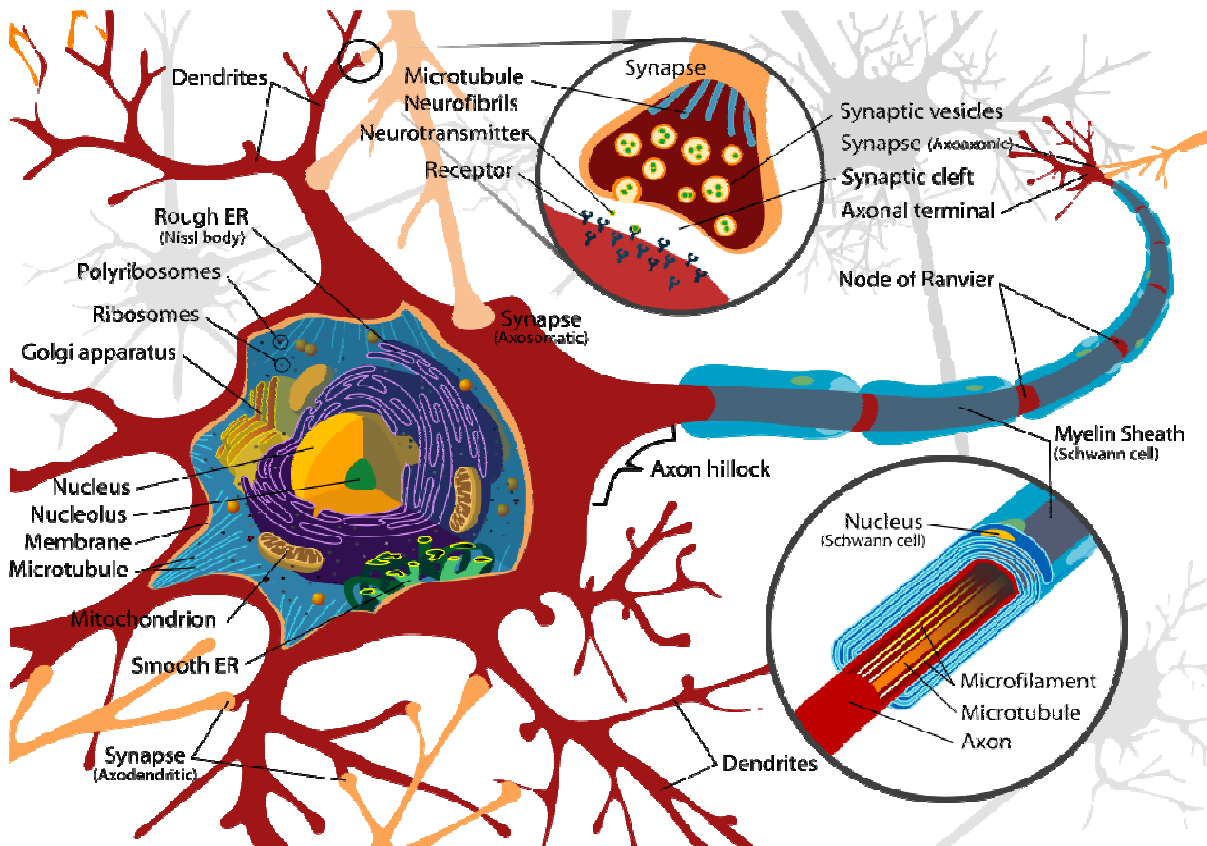


Figure 1. General morphology of a neuron (art by Mariana Ruiz Villareal)

- Dendrites, which are branched processes extending from the neuron, are designed to receive stimuli.
- The perikaryon or soma, core of the neuron, which contains the nuclear structure and organelles.
- The axon, a cellular wire-like projection towards other cells, acts as a transmitter of electrical information.

- Synapses, located at the end of the axon, are neuronal structures divided in three compartments: the presynaptic button, the synaptic cleft, and a post-synaptic density.

Upon reception of the AP, the depolarization of the presynaptic terminal releases vesicles filled with neurotransmitters into the synaptic cleft.⁹ These neurochemicals, small molecules or peptides, interact with their cognate receptor to propagate or modulate signal transduction.⁹

1.1.2. Glial cells are crucial constituents of the brain

In a human brain, neurons represent approximately 10% of the brain tissue.¹⁰ The remaining 90% are accounted for by non-neuronal cells called glia (greek for “glue”).¹⁰ Glial cells are present in both the CNS (astrocytes, oligodendrocytes, microglia) and the PNS (Schwann cells) where they play various roles.^{1,2,11-14} Unlike neurons, glial cells are capable of undergoing mitosis and unable to generate action potentials.¹⁰ They are also characterized by a lack of axon. One of their most basic roles is to provide a physical and energetic support to neurons and other brain cells.^{1,2,10} Once thought of only fulfilling these “passive” tasks, glial cells in general have recently been shown to play crucial roles in neuronal signaling pathways.^{11,13,14} In addition, overactivation of some types of glial cells is implicated in some neurological conditions.

Astrocytes are a type of cell indispensable to a neuron.^{12,14} Briefly presented, their role ranges from tuning blood flow to different regions of the brain, clearing the synaptic cleft of excess neurotransmitter for recycling, to supplying neuronal cells

with nutrients and oxygen.^{12,14} Microglia is the immune cell of the brain that is responsible for removing dead cells through phagocytosis.¹⁰ Finally, oligodendrocytes and Schwann cells are a type of glia that forms a sheath of myelin, a lipid-rich membrane, which wraps around certain axons.^{1,10,13} This electrical insulation increases the conduction speed of APs. Axonal regions exposed to the external milieu between two segments of myelin are called nodes of Ranvier. In these areas, the axonal membrane generally expresses high levels of ion channels that are essential for APs propagation.^{1,2}

1.1.3. Neurons are polarized by differences in intracellular and extracellular ionic concentrations

Elaborate protein machinery allows neurons to maintain a membrane potential. In mammalian neuronal cells, the typical resting state membrane potential is approximately -70 mV and the intracellular part of the neuron is, therefore, more negatively charged. The concentration of K^+ ions is greater inside the cell while concentrations of Na^+ , Ca^{2+} , and Cl^- are higher outside the cell (Figure 2). Highly selective membrane-spanning receptors called ion channels allow one specific type of ion to cross the membrane. For example, when a K^+ -specific channel opens, K^+ ions tend to flow down the outwardly directed concentration gradient. As more and more positively charged ions leave the cell, the intracellular negative charge increases and creates an inwardly directed voltage gradient. This electrical force tends to attract K^+ ions inside the cell or slow the exiting ones. When the thermodynamic and electric forces cancel each other, the membrane is at its

equilibrium potential (E_K for potassium ions is equal to -102 mV), a value unique to each ionic species.

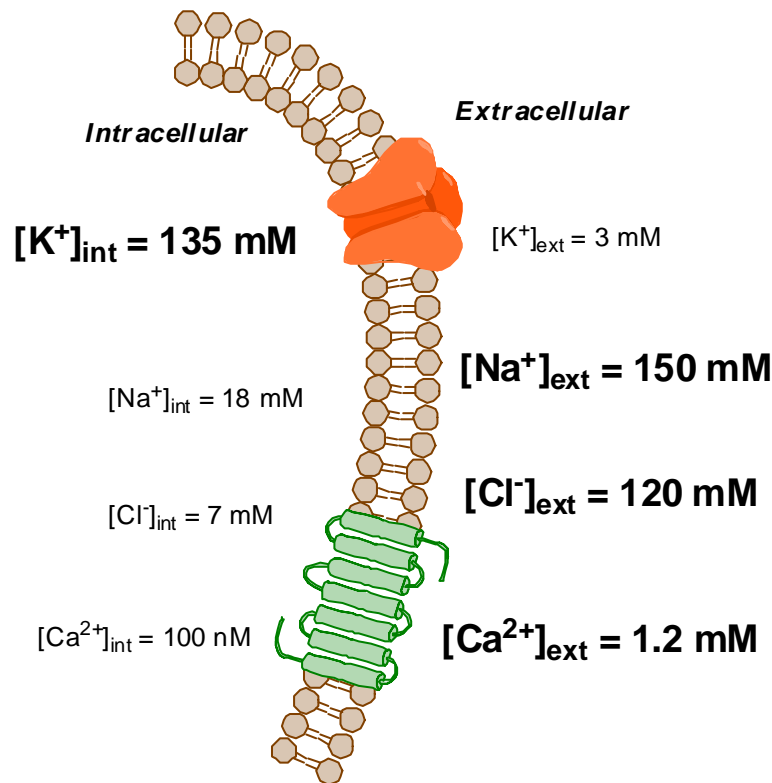


Figure 2. Typical intracellular and extracellular ionic concentrations for a mammalian neuron.

In addition to ion channels, a variety of ion pumps allow to maintain the unequal ionic distribution across the lipid bilayer. One of these, the Na^+/K^+ -ATPase, maintains the Na^+ and K^+ gradients across the cell membrane by extruding three sodium ions and transporting two potassium ions inside the cell.

1.1.4. Mechanism of generation and propagation of action potentials

Different events are involved in the generation of an AP (Figure 3). First the membrane is at its resting potential (approx. -70 mV) (1) until a stimulus triggers the

opening of a small fraction of closed Na^+ channels on the membrane. Due to the concentration gradient, Na^+ ions start entering the cell leading to a membrane depolarization (2). If the initial depolarization reaches a threshold of approximately -55 mV, an AP is generated. If the threshold value is not met, no AP is produced. Upon reaching the threshold, a greater fraction of Na^+ channels open, leading to a rapid influx of Na^+ ions, which locally depolarizes the cell.

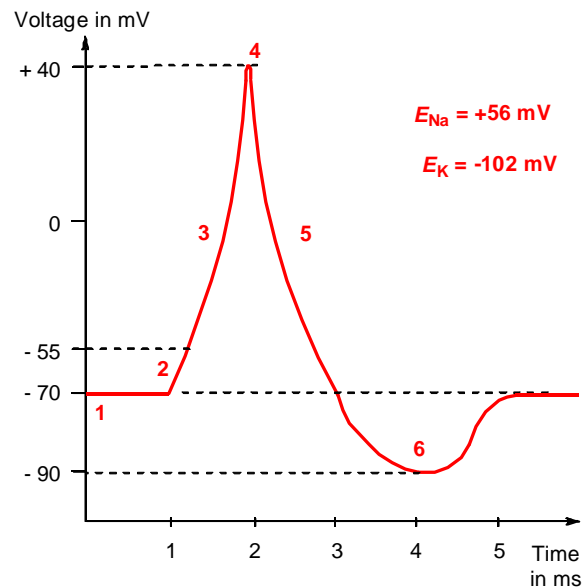
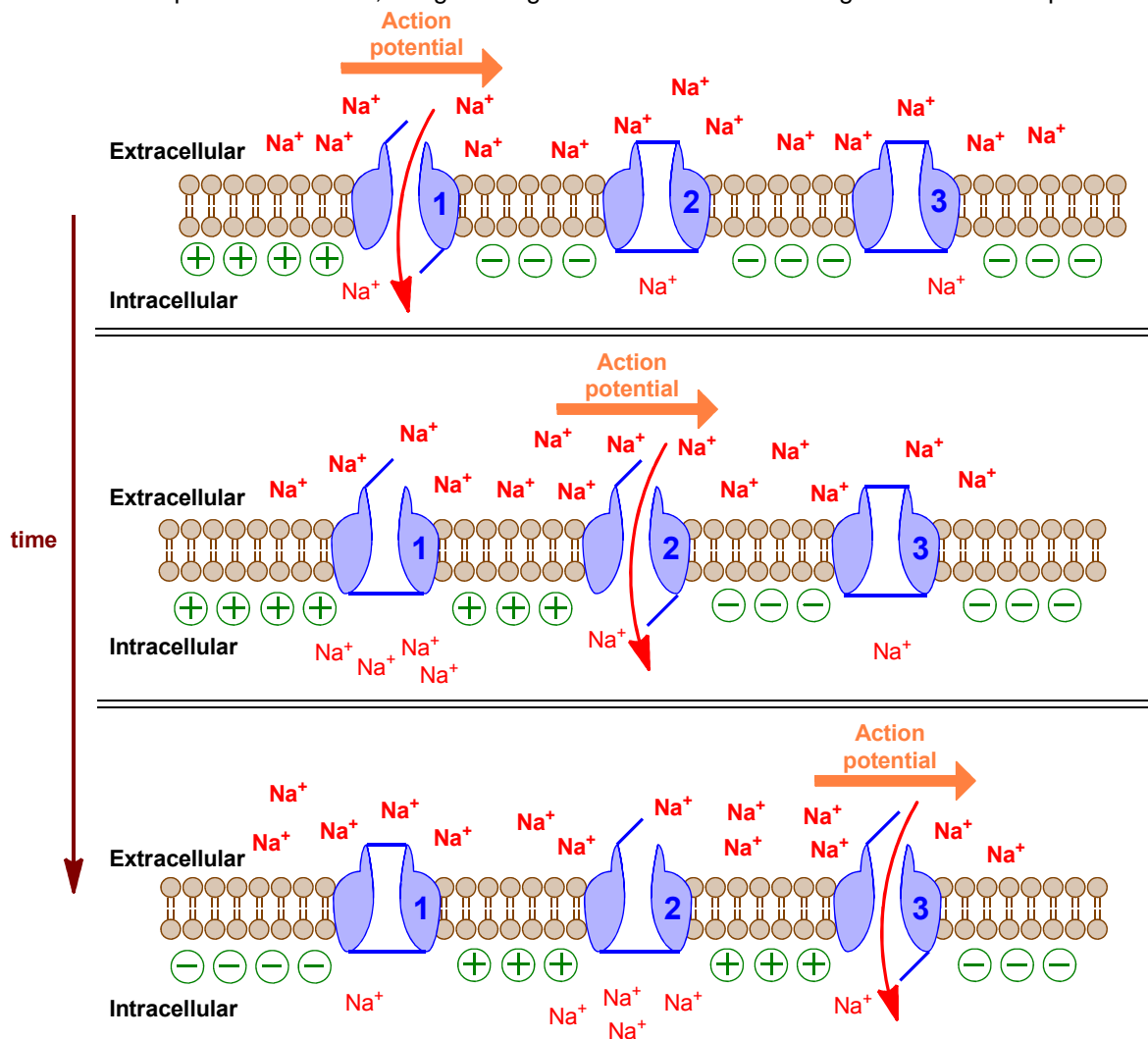


Figure 3. Schematic representation of the different phases occurring during the generation of an AP.

The membrane potential rapidly moves towards the equilibrium potential of Na^+ ions ($E_{\text{Na}} = +56 \text{ mV}$) (3). Before E_{Na} can be reached, the membrane depolarization causes Na^+ channels to go into their inactive state (4), while nearby K^+ channels open and lead to an efflux of K^+ ions. As K^+ ions flow out, the membrane potential moves towards E_{K} (5). Before -102 mV can be reached, most K^+ channels go into their inactive state. During this refractory period (6), no AP can

occur. The initial membrane potential is then restored by action of specific K^+ channels.¹⁵ After the resting concentrations are reached, another action potential may be fired. The AP generated travels unidirectionally down the axon by successive openings and closings of adjacent Na^+ channels expressed along the axonal membrane in a process termed “saltatory conduction” (Scheme 1).

Scheme 1. Simplified representation of the propagation of an action potential along the axon. Na^+ channels are represented in blue, the green signs indicate localized changes in membrane potential.



As its intracellular environment becomes more depolarized, Na⁺ channel **1** opens and leads to a local influx of sodium ions (top drawing). This localized increase in Na⁺ causes a membrane depolarization in the surroundings of Na⁺ channel **2**, causing it to open, while **1** goes into its inactivated state (Scheme 1, middle drawing). Open **2** leads to Na⁺ influx and membrane depolarization near to **3**, and its subsequent opening. As the AP travels down the axon towards the synapse, **1** goes from its inactivated to its closed state to allow transmission of another AP (Scheme 1, bottom drawing). This mechanism illustrates the physiological relevance of the refractory period, as it allows an AP to propagate in only one direction.

1.2. Epilepsy(ies): a multifaceted neurological disorder

1.2.1. A burden for people and economy

Epilepsy, also known as seizure disorder, is a chronic neurological condition that affects all populations¹⁶ and is characterized by recurrent unprovoked epileptic seizures.¹⁷⁻¹⁹ Such seizures are defined as discrete events resulting from simultaneous neuronal firing leading to an abnormal cellular behavior.^{17,20} This disorder adversely affects the quality of life of approximately 50 million people worldwide,²¹ that include 2 million people in the U.S. of which there are 340,000 children.²²⁻²⁴ The U.S. annual cost of epilepsy is estimated at \$15.5 billion in both medical costs and lost or reduced earnings and productivity.²⁵ Epilepsy is an extremely broad term that encompasses a large number of different seizure types.^{20,26} While genetic mutations have been associated with some forms of epilepsy,²⁷ the etiology of epileptic seizures often remains unknown.^{21,25}

1.2.2. Brief classification of epileptic seizures

Epileptic seizures can be classified according to the nature of the patient's electroencephalogram (EEG), brain scans, both of which are related to the seizure phenotype, and the level of consciousness of the patient.^{20,26} So far over 40 different types of epilepsy have been reported.²⁸ Seizures confined to one region of one brain hemisphere are termed partial or focal, as opposed to generalized seizures that affect both hemispheres. The adjectives "complex" and "simple" respectively designate seizures that occur with and without loss of consciousness and "ictal" is the adjective that refers to a seizure.²⁰ Seizures can also evolve, for example from simple partial to complex generalized seizures and may or may not be convulsive.

Tonic-clonic, or grand mal seizures are the most common generalized seizures and they are typically (and misconceptually) associated with the word "epilepsy" itself.^{26,29} They are characterized by a tonic phase, where the person violently arches in a strained position, followed by a clonic phase, during which the person experiences repetitive and uncontrolled jerks that may lead to injuries.^{26,30}

Absence, or petit mal seizures are a type of generalized seizures characterized by a person's sudden interruption of activity, accompanied by a blank stare. This attack may or may not be accompanied with mild clonic, tonic or atonic components.^{26,31} Atonic seizures are characterized by a sudden loss of muscle tone that may lead the person to abruptly fall on the ground, sometimes resulting in severe injury.²⁶

Finally, status epilepticus (SE) is a potentially life-threatening condition where a generalized seizure, convulsive or non-convulsive, lasts for an extended period of time.³²⁻³⁴ The precise duration after which a seizing person is considered to have SE is not clearly defined and ranges from 10 to 30 min during which the individual is unconscious.^{33,35} Studies have shown that prolonged SE may lead to severe neuronal damage in epileptic patients.^{36,37}

1.2.3. Small molecules to treat epilepsy: the need for antiepileptic drugs with new mechanisms of action

Epileptic seizures are typically treated with one or more antiepileptic drugs (AEDs). There are ~40 available AEDs on the market and they are classified into three categories: traditional, recent, and emerging.³⁸⁻⁴¹ Most traditional and recent anticonvulsants have been associated with well-defined pharmacological profiles. In many cases, they interact with either voltage-gated sodium channels,⁴² calcium channels,⁴³ or with the benzodiazepine-binding site of the GABA_A receptor.⁴⁴⁻⁴⁶ Despite the availability of drugs, approximately *one third* of the patients diagnosed with epilepsy are refractory to treatment⁴⁷⁻⁵⁰ and almost 40% of treated patients experience adverse side effects with current medications.⁵¹ Current research on antiepileptic agents is hindered by the relatively few biological targets identified for epileptic seizures and by the need to conduct labor intensive animal behavioral tests for compound screening.

To respond to this health problem, the National Institute of Neurological Disorders and Stroke (NINDS) in 1975 created the Epilepsy Branch and the Epilepsy

Advisory Committee to expedite the development of more efficacious antiepileptic agents.⁵² The Anticonvulsant Screening Program (ASP) is a division of the NINDS that allows research institutions to test small molecules in a variety of animal or *in vitro* pharmacological tests at no cost.²⁸ The requirement is the preparation of the compound on a 500–1000 mg scale which will be tested in mice and rats against a variety of seizure models.

1.2.4. Animal models used in the pharmacological evaluation of AEDs

Many animal models have been advanced to study epileptic syndromes.⁵³ Here, we briefly review the main pharmacological tests used at the ASP to identify new anticonvulsant molecules. The qualitative and quantitative assessments of a molecule are conducted at different time points ranging from 15 min to 4 h after administration. The anticonvulsant and toxicological profiles of compounds are mainly determined by intraperitoneal (ip) or peroral (po) administration to rodents. The dosage may range from 1 to 300 mg of compounds per kg of body weight, with several animals tested at each dosage. The dose at which half of the animals are protected is termed effective dose (50%) or ED₅₀. Similarly, the median toxic dose (50%) or TD₅₀ is the dosage at which half of the animals display neurological impairment. The ratio of the TD₅₀ over the ED₅₀ is called the protective index (PI).

1.2.4.1. Maximal electroshock seizure test

The maximal electroshock seizure (MES) test consists in applying an electrical current to the animal via corneal electrodes and represents a model for generalized tonic-clonic seizures.⁵⁴ The electrical signal (60 Hz current, delivered for 0.2 sec) has a high frequency/short duration nature which elicits maximal seizures generally lasting no more than 30 sec.⁵⁵ A brief initial tonic flexion, and prolonged tonic extension period, followed by terminal clonus are characteristic of MES seizures.⁵⁵ Protection is defined as a failure of the animal to extend hindlimbs to an angle with the trunk greater than 90°. ⁵⁶

1.2.4.2. 6 Hertz test

The 6 Hz test is analogous to the MES test except for the nature of the electrical signal applied. A low frequency/long duration signal (6 Hz current, delivered for 3 sec, 32 or 44 mA intensity) triggers a different type of seizures in the animal that are representative of complex partial seizures.^{57,58} Characteristics of 6 Hz-induced seizures are the immobility of the animal, accompanied by forelimb clonus, vibrissae (whiskers) twitching, and Straub-tail (elevated tail).⁵⁹ The absence of these signs upon electrical stimulation is defined as seizure protection.

1.2.4.3. Pentylenetetrazole administration

The subcutaneous pentylenetetrazole (scPTZ) test measures the ability of a compound to raise the seizure threshold produced by a chemoconvulsant (PTZ,

Scheme 5).⁶⁰ At a dose specific to the rodent model, PTZ induces clonic seizures and the test is considered a model for absence seizures.⁵² A compound is considered protective if it abolishes the spasms triggered by the PTZ administration.⁵² It is pharmacologically different from either the intravenous (iv)PTZ or the ipPTZ tests. In the iv route, the animal will start experiencing a series of myoclonic jerks (rapid contraction and relaxation of muscles) in a time-dependent manner.⁶¹ These jerks will worsen and ultimately lead to loss of righting and clonic seizure. In the ip route, defined, subconvulsive doses of PTZ are administered at given time intervals. A gradual, reproducible response can then be observed, with initial jerks and full-blown seizure each starting after a specific number of injections.⁶² In these tests, a molecule is considered protective if it can elevate the threshold PTZ dose necessary for convulsions and delay (iv) or increase the number of injections (ip) necessary for the onset of seizure.^{61,62} Molecules with efficacy in the scPTZ test may have no effect in the ipPTZ or ivPTZ tests and vice-versa.⁶³

1.2.4.4. Pilocarpine administration

In the lithium pilocarpine-induced status epilepticus (SE) model, animals are treated ip with a solution of LiCl 20 h prior to ip injection of pilocarpine (PILO), which results in the development of SE within 30 min after administration of PILO.⁶⁴ When administered alone, PILO induces secondarily generalized seizures that evolve into SE.⁶⁵ A variety of chemoconvulsants such as kainic acid,⁶⁶ picrotoxin,⁶⁷ and bicuculline⁶⁷ can be used to induce SE (Figure 4). After the SE period (8–24 h), animals will develop spontaneous recurrent seizures over a long-term period (up to 2

months).⁶⁵ These seizures are representative of complex partial seizures observed in humans.²⁰ Protection is defined by the suppression of recurring seizures.

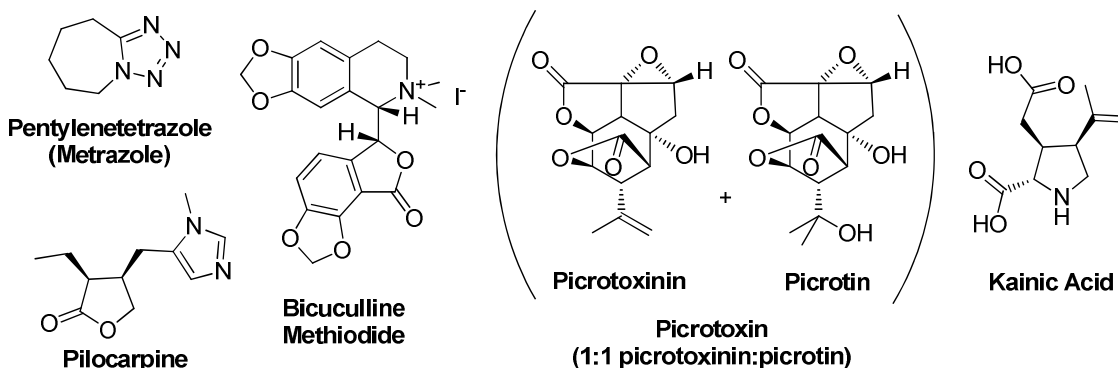


Figure 4. Chemical structures of various chemoconvulsants used in animal testing. Pentylene-tetrazole, bicuculline and picrotoxin are GABA receptor antagonists. Kainic acid is a glutamate receptor agonist.

1.2.4.5. Audiogenic seizure animal models

The Frings mouse model is a model of generalized reflex epilepsy in which the seizure is triggered by a loud noise.⁶⁸ The epileptic phenotype is caused by a mutation in the *mass1* gene (monogenic audiogenic seizure susceptibility 1) which causes a premature termination of the membrane protein “very large G-protein coupled receptor 1” (VLGR1 or MASS1, 6300 amino acid residues).^{69,70} The characteristic response of Frings mice to an intense stimulus (100 dB, 20 s) is wild running, followed by a loss of righting reflex that occurs with forelimb and hindlimb tonic extension.⁵² Seizure protection is defined as the ability of a molecule to prevent tonic hindlimb extension.⁵² The DBA/2 (dilute brown non-agouti) mouse is another genetic model used for audiogenic seizures.⁷¹

1.2.4.6. Electrical kindling models

The rapid hippocampal kindling test is a model representative of focal seizures.^{52,72} The term kindling refers to repetitive, infrequent stimulations that sensitize a specific region of the brain, progressively leading to a fully kindled state.⁷² Once this stage is reached, stimulations that initially did not elicit a reaction will consistently trigger an enhanced response.⁷² In the rat hippocampal kindling model, electrodes are surgically implanted in the hippocampus and kindled seizures are produced by a 10 s train of 1 ms biphasic 200 μ A pulses (50 Hz) delivered every 30 min for 6 h on alternating days for a total of 60 stimulations (5 stimulus days).⁵² Behavioral seizures are scored according to the Racine scale,⁷³ that ranges from 1 (whiskers twitching) to 5 (forelimb clonus, rearing and falling). Another brain region commonly used for the kindling procedure is the amygdala.⁷⁴ Compounds evaluated in this model are dosed based on their activity in other seizure tests. A molecule can be tested for its ability to stop kindled seizures (anticonvulsant activity), or its ability to delay the acquisition of the kindled state (antiepileptogenic effect).⁵²

1.2.4.7. Neurological toxicity evaluation

The rotarod test is a measure of neurological toxicity, where a mouse is placed on a rotating rod (6 rpm).⁷⁵ Control mice have the ability to maintain themselves on the rod for an extended period of time.⁷⁵ Neurological impairment is defined as the inability of the mouse to remain on the rod for 1 min in three successive trials.⁵² In rats, the behavioral toxicity of the compound is assessed. The positional stance test consists in lowering one hind leg over the edge of a table. A

neurologically impaired rat will fail to lift its leg back to a normal position.⁵² The gait and stance tests consists in observing symptoms of impairment in the animal, such as zigzag gait, abnormal posture, and lack of exploratory behavior or catalepsy.⁵²

1.3. Pharmacology of traditional and recent AEDs

1.3.1. Ion channels are primary pharmacological targets to prevent seizures

Ion channels belong to a superfamily of transmembrane proteins that regulate intracellular and extracellular concentrations of cations and anions essential for triggering action potentials that propagate information or elicit biological responses.^{1,2} This superfamily of receptors can further be divided into two main classes, the Voltage-Gated Ion Channels (VGIC) and the Ligand-Gated Ion Channels (LGIC).^{1,2} VGICs respond to changes in the membrane potential, while LGICs respond to binding of an endogenous neurotransmitter or an exogenous molecule. Ion channels play a crucial role in electrophysiological events pertaining to epilepsy and it is therefore not surprising that they are targeted by numerous AEDs.⁷⁶⁻⁷⁸

1.3.1.1. Voltage-gated sodium channels

Voltage-gated sodium channels (VGSCs) are large Na⁺-specific ion channels that respond to changes in membrane potential. They are composed of one α subunit (~260 kDa) consisting of 4 domains (I–IV) that form a central pore, each containing 6 membrane-spanning α helical segments (S1–S6) (Figure 5), with intracellular N- and C-termini.⁷⁶ The S4 segment of each domain contains one

positively charged amino acid every three residues.⁷⁹ These residues control the channel gating and respond to depolarization by moving across the membrane and initiating the activation of the receptor.⁸⁰ The ionic selectivity of the channel is determined by repetitive amino acid motifs in the membrane-reentrant loop between S5 and S6 of each domain, and a mutation of three residues in the S5S6 loop of each domain is enough to turn the Na⁺ channel into a Ca²⁺ channel.⁸¹

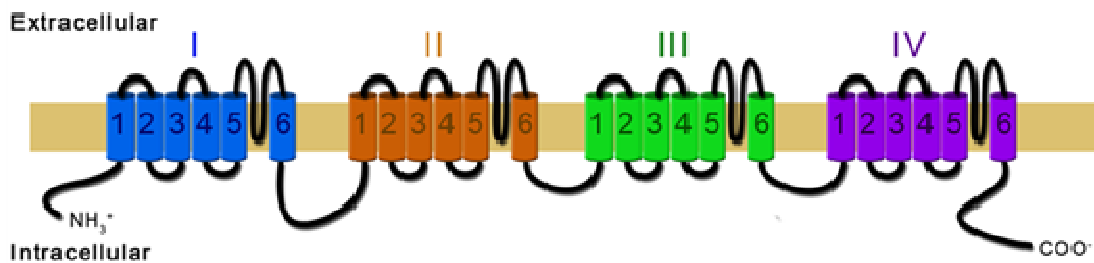


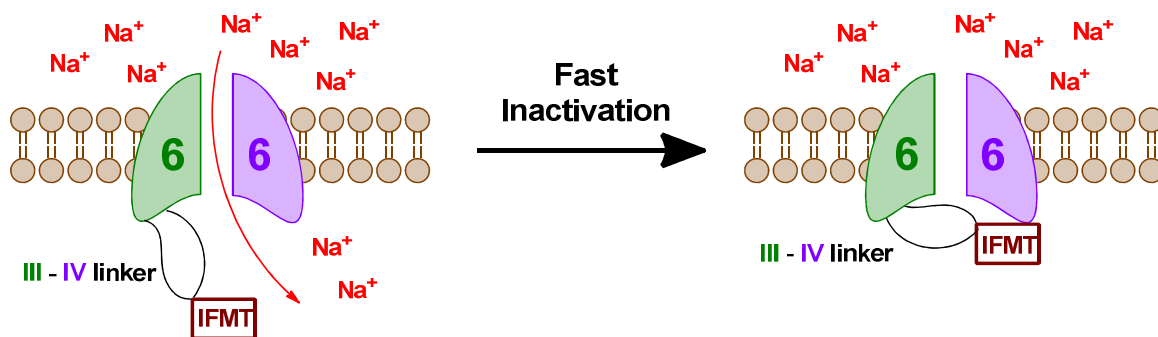
Figure 5. Schematic representation of a voltage-gated Na⁺ channel α -subunit

Native VGSCs are associated with one or more β 1, β 2, or β 3 subunits (~30 kDa) that can influence the gating properties of the channel, the kinetics of channel activation, as well as protein interactions with cell adhesion molecules.⁸²⁻⁸⁴ In humans, 9 different types of voltage-gated Na⁺ channels exist and they are designated Na_v1.1–Na_v1.9.⁸⁰ Among these, Na_v1.1–Na_v1.3 and Na_v1.6 are the main VGSCs found in the CNS.⁸⁰ Mutations in Scn1A, Scn2A and Scn1B, the genes that respectively code for the α subunits of Na_v1.1 and Na_v1.2, and the β 1 subunit, are associated with severe forms of infant epilepsy.^{85-87,27}

As described earlier, VGSCs can adopt different conformations depending on their state. When firing an AP, the channel goes from the closed (resting) state to the

open (activated) state to the inactivated state. Two distinct inactivation pathways exist, fast and slow, from which the Na^+ channel can recover. The fast inactivation pathway happens within a few milliseconds of channel opening, and involves a “hinged lid” mechanism.⁷⁶ The short intracellular region between domains III and IV physically obstructs the pore by docking a conserved hydrophobic peptide sequence isoleucine, phenylalanine, methionine, threonine (**IFMT**) into domain IV S6 segment (Scheme 2).⁸⁸ Recovery from the fast inactivated state depends on the membrane potential and time. This mechanism is responsible for the refractory period allowing APs to propagate in only one direction (Scheme 1).

Scheme 2. Schematic representation of the fast inactivation hinged lid mechanism of VGSCs.



The VGSC slow inactivation pathway is a biological process independent of the fast inactivation.⁸⁹ Although its precise mechanism is subject to controversy, it is likely to involve a rearrangement of the pore, as well as specific domains of the channel.⁸⁹⁻⁹² The “slow” terminology refers to the prolonged time required for the channel to recover from its inactivated state, ranging from hundreds of milliseconds to a second.⁷⁶ This pathway is a cellular mechanism that only takes place under

conditions that may be relevant to an epileptic seizure such as high frequency depolarizations, or under sustained membrane depolarization (membrane potential at -60 or -55 mV). This type of inactivation acts as a protective way to lessen excessive neuronal excitability.⁷⁶

1.3.1.2. Voltage-gated calcium channels

Voltage-gated Ca^{2+} channels (VGCCs), also termed voltage-dependent calcium channels (VDCCs) are transmembrane receptors that mediate calcium influx into the cell. Ten different types of VGCCs exist, $\text{Ca}_v1.1$ – 1.4 , $\text{Ca}_v2.1$ – 2.3 , and $\text{Ca}_v3.1$ – 3.3 , that are comprised of four to five subunits, the largest and most important of which is the α_1 subunit (190–250 kDa).⁹³ Analogous to the VGSCs α subunit, the VGCC α_1 subunit is made of four domains (I–IV) each containing 6 α -helical membrane-spanning segments (S1–S6) where the S4 segment senses changes in membrane potential. Ion selectivity is controlled by the loop between S5 and S6 segments of domains I, III and IV.⁹³ VGCCs additionally possess an intracellular β subunit, as well as a disulfide-linked transmembrane δ subunit, and an extracellular α_2 subunit that forms a $\alpha_2\delta$ complex, and less frequently an intracellular γ subunit.⁹⁴ The pharmacological and electrophysiological properties of the Ca^{2+} channel are primarily determined by the different types of α_1 subunits whereas β , $\alpha_2\delta$ and γ subunits serve as modulators.⁹⁴ The alphabetical designation of VGCCs comes from the distinct types of currents they elicit and their sensitivity to established channel blockers: L-type for “long-lasting” ($\text{Ca}_v1.1$ – $\text{Ca}_v1.4$), N-type for

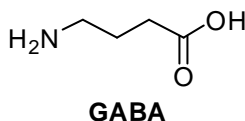
“neural” ($\text{Ca}_v2.2$), P/Q-type for “Purkinje neuron”⁹⁵ ($\text{Ca}_v2.1$), R-type for “resistant to the other blockers” ($\text{Ca}_v2.3$), and T-type for “transient” ($\text{Ca}_v3.1$ – $\text{Ca}_v3.3$).⁹³

The VGCC-mediated influx of Ca^{2+} ions has several consequences. Electrophysiologically, the increase of intracellular calcium leads to a depolarization of the neuron ($E_{\text{Ca}} = +120 \text{ mV}$).¹ Pharmacologically, Ca^{2+} is an important second messenger signaling molecule that can start a cascade of cellular downstream events ranging from activation of protein kinase C (PKC), calmodulin (CaM) and Ca^{2+} -dependent proteases to triggering the transcription of pro-apoptotic factors.⁹⁶⁻

101

1.3.2. Targeting synaptic transmission helps control neuronal excitability

1.3.2.1. GABA_A receptors



γ -Aminobutyric acid (GABA) is the major inhibitory neurotransmitter in the CNS. GABA receptors are a family of homo- or heteromeric transmembrane receptors that elicit their biological responses upon binding of GABA.¹⁰² GABA_A receptors (GABA_ARs) are ligand-gated ion channels, or ionotropic receptors, while GABA_B receptors (GABA_BRs) are G-protein coupled receptors (GPCRs), or metabotropic receptors. GABA_C receptors (GABA_CRs) have recently been reclassified by the *International Union for basic and clinical Pharmacology* (IUPHAR)

as the ρ subfamily of GABA_AR based of their closely related sequence, structure and function.¹⁰³ That reclassification is, however, subject to controversy.¹⁰⁴

There are 19 types of subunits, α 1–6, β 1–3, γ 1–3, δ , ε , θ , π , and ρ 1–3, that can assemble into a pentameric GABA_ARs forming a central pore (Figure 6).¹⁰⁵ Each subunit possesses 4 transmembrane segments, with extracellular N- and C-termini. The extracellular N-terminal peptide chain contains a disulfide bridge that is characteristic of the so-called Cys-loop superfamily of receptors, to which other pentameric LGICs belong.¹⁰⁶

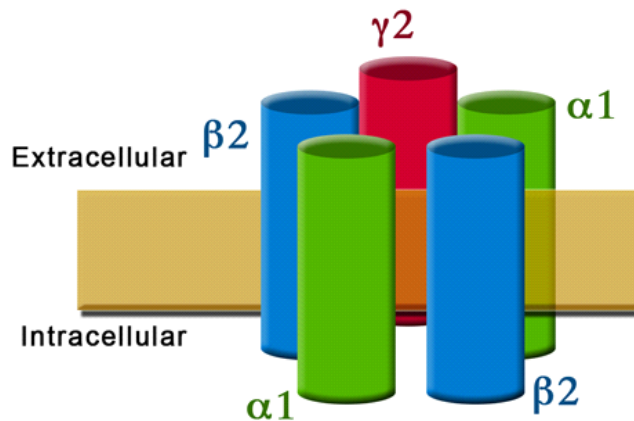


Figure 6. Simplified representation of a GABA_AR structure

GABA_ARs containing ρ subunits (or GABA_CRs) are primarily located in the retina.¹⁰³ The differences in subunit composition translate into different GABA_ARs pharmacological and electrophysiological properties and reports indicate that receptors comprised of subunits $\alpha 1\beta 2\gamma 2$ (Figure 6) are the most abundant in the brain.¹⁰² The binding site for GABA is located between an α and a β subunit, and up to two GABA molecules can, therefore, bind to the receptor.¹⁰⁷ Genetic forms of

juvenile epilepsies have been linked to mutations in the GABA_ARs $\alpha 1$ and $\gamma 2$ subunits.^{108,109}

GABAergic neurons are equipped with a machinery of enzymes and transporters that play an essential role in GABA-mediated signaling. GABA itself is biosynthetically derived from the excitatory amino acid L-glutamate through action of the glutamic acid decarboxylase enzyme (GAD).¹¹⁰ GABA transporters (GAT) are present on the presynaptic membrane as well as on the membrane of astrocytes located near the synaptic cleft.^{11,111-113} These transporters are responsible for excess GABA uptake into the glial cell or the presynaptic density, where GABA transaminase (GABA-T) further processes GABA into succinic semialdehyde.¹¹⁴

The biological effects of GABA are primarily mediated by GABA_ARs, which are GABA-activated chloride channels that are primarily localized on the post-synaptic membrane.⁷⁷ The higher extracellular concentration of Cl⁻ ions leads to an inward flux upon channel opening. The electrophysiological basis of GABA-mediated inhibition can be explained by the equilibrium potential for chloride ions ($E_{Cl} = -75$ mV) which is slightly more negative than the average resting membrane potential (-70 mV). An influx of negatively charged chloride ions leads to a hyperpolarization of the post-synaptic neuron, thus reducing its probability of firing an AP.¹ It is important to note that the inhibitory effect of GABA is due to the average E_{Cl} in mature neurons. Changes in the intra- and extracellular concentrations of chloride ions can lead to an E_{Cl} value less negative than the resting membrane potential, thus rendering GABA excitatory.¹¹⁵ Such conditions have been reported to occur in

developing cultured neurons,^{116,117} as well as in the brain of patients suffering from temporal lobe epilepsy (TLE).^{118,119}

1.3.2.2. Glutamate receptors

L-Glutamate is the main CNS excitatory neurotransmitter and acts at a variety of biological receptors. Mirroring the GABA_ARs and GABA_BRs, two different classes of glutamate receptors exist: the ionotropic glutamate receptors (iGluRs) that are LGICs permeable to several ionic species, and the metabotropic glutamate receptors (mGluRs) that are GPCRs.^{120,121} While a recent investigation pointed out the potential anticonvulsant effects of mGluRs subtype-specific agonists and antagonists,¹²¹ we will principally review the pharmacology of the ionotropic class.

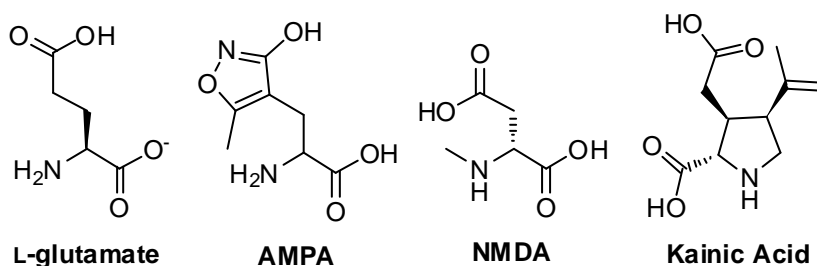


Figure 7. Chemical structures of cognate ligands of ionotropic glutamate receptors

iGluRs are divided into three major families, the α -amino-3-hydroxy-5-methyl-4-isoxazolepropionic acid (AMPA) receptors (AMPA_Rs), the kainate (KA) receptors (KARs) and the *N*-methyl-D-aspartate (NMDA) receptors (NMDA_Rs) named after their selective small-molecule agonists (Figure 7).¹²² Another less studied class called δ receptors are classified as orphan iGluRs.¹²³

All classes of receptors have a similar heteromeric protein structure, comprised of four subunits forming the central pore.¹²⁰ Four different types of subunits exist for AMPARs (GluA1–GluA4), five types for KARs (GluK1–GluK5), seven for NMDARs (GluN1, GluN2A–D, GluN3A, GluN3B) and two for δ receptors (GluD1, GluD2).¹⁰⁶ The subunit nomenclature used above has recently been introduced (as of January 2009) by the nomenclature committee of IUPHAR (NC-IUPHAR) in order to bring a consistent nomenclature of LGICs.¹⁰⁶ iGluRs generally assemble into dimers of dimers: NMDARs comprise two sets of one mandatory GluN1 (former NR1) and one GluN2 or GluN3 (former NR2 and NR3) subunits,¹²⁴ and AMPARs contain a dimer of two GluA subunits that most often contains a GluA2.¹²⁵ The composition of the receptors varies with different brain regions and determines their electrophysiological and pharmacological properties.^{124,125}

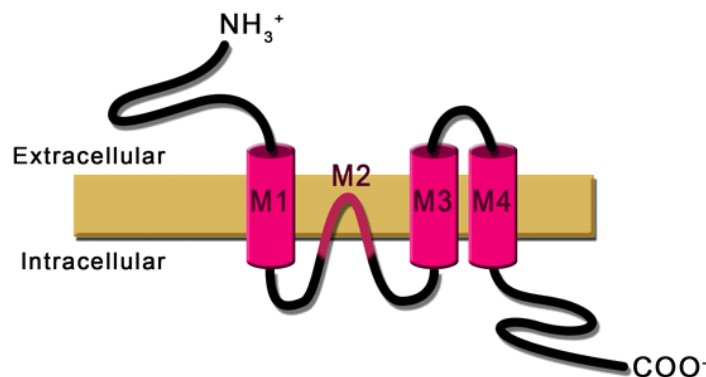


Figure 8. General topology of an ionotropic glutamate receptor subunit.

The subunits possess the same topology among AMPA, KA, and NMDA receptors: they are made of three transmembrane domains (M1, M3, M4) and one re-entrant membrane loop facing the intracellular side (M2), with extracellular N-

terminus and intracellular C-terminus (Figure 8).¹²² The amino acid composition of the M2 loop determines the ion selectivity of the channel.^{126,127}

While AMPA and kainate receptors are only permeable to Na^+ , NMDA receptors are primarily permeable to Ca^{2+} .¹²⁵ In addition, the activation of NMDA receptors is unique in that it can occur through a ligand-gated mechanism involving glutamate and either glycine or D-serine, as well as through a voltage-dependent mechanism that can be modulated by Mg^{2+} ions.¹²⁴ The glutamate binding site is located on a GluN2 subunit, while either glycine or D-serine bind to a GluN1 subunit.

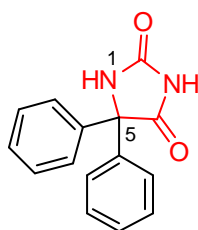
L-Glutamate and glutamate receptors mediate an important pathological process called excitotoxicity.¹²⁸ Excess glutamate may give rise to overactivation of iGluRs, such as NMDARs, leading to an increase of intracellular Ca^{2+} . In large excess, calcium cannot be adequately buffered and activates Ca^{2+} -dependent proteases.¹²⁹ In addition, excess Ca^{2+} may trigger swelling of mitochondria and release of proapoptotic molecules, leading to programmed death of the post-synaptic neuron.¹³⁰ Prolonged NMDARs overactivation and bioenergetic failure may ultimately drive the dying neuron to release excess glutamate towards other neurons, starting a neurodegenerative chain reaction.¹³¹

1.3.3. Pharmacology of traditional AEDs

In this section we briefly discuss leading marketed drugs with antiepileptic activity. AEDs that were identified as potential therapeutic agents in the early 1930s to the early 1970s are termed traditional. Despite their early year of discovery, traditional AEDs are still used for the treatment of epileptic seizures. As is the case

for many of these therapeutic agents, the complete mechanism of action of traditional AEDs still remains unknown.

1.3.3.1. Phenytoin



Phenytoin (PHT)

5,5-Diphenylhydantoin (phenytoin, PHT, Dilantin[®]) is an AED that was introduced in 1938 after its anticonvulsant effects were observed on electrically shocked laboratory animals.¹³² It remains clinically used for the treatment of partial and tonic-clonic seizures but is ineffective in the treatment of absence seizures.⁵⁵ This pharmacological profile correlates with the high potency of the compound in the MES test, and its lack of activity in the scPTZ test.⁵⁵ Investigation of the structure activity relationship (SAR) of PHT analogs showed that the presence of the unmodified hydantoin ring (in red) was necessary for activity.¹³³ Replacing the 5-phenyl groups by alkyl groups leads to compounds with sedative effects, of which PHT is devoid.¹³⁴

The primary mechanism of action of phenytoin has been established as the stabilization of the fast inactivated state of VGSCs, by binding to the intracellular part of the Na⁺ channel (Scheme 7).^{76,135} Indeed, *in vitro* studies showed PHT cannot prevent an initial action potential but blocks firing of a second one.⁷⁶ This blockade only affects epileptiform APs termed sustained high-frequency repetitive firing of

neurons (SRF),¹³⁶ without impairing spontaneous low frequency APs.^{137,78} Importantly, the PHT block of VGSCs is highly voltage-dependent, with a 12-fold greater inhibitory effect at depolarized membrane potentials ($IC_{50} = 10 \mu M$ at -60 mV) than at hyperpolarized potentials ($IC_{50} = 120 \mu M$ at -85 mV).¹³⁸

1.3.3.2. Carbamazepine



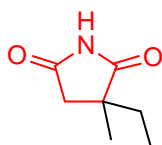
**Carbamazepine
(CBZ)**

5*H*-Dibenzo[*b,f*]azepine-5-carboxamide (carbamazepine, CBZ, Tegretol[®]) is an iminostilbene derivative (iminostilbene in red) with mood-stabilizing and anticonvulsant properties that was introduced as an AED in the 1970's.¹³⁹ Despite a lack of structural similarity, CBZ has an animal pharmacological profile closely related to that of PHT, being very potent in the MES test while having very limited efficacy in the scPTZ test.⁵⁵ Like phenytoin, this profile correlates with the use of CBZ for the treatment of tonic-clonic and partial seizures but not absence seizures.¹³⁶

Based on their similar pharmacological profiles, it is not surprising that CBZ exerts its action through the fast inactivation of VGSCs.¹³⁵ Like phenytoin, carbamazepine is able to block SRF *in vitro* in a voltage-dependent fashion.^{140,141} The main difference between PHT and CBZ resides in their binding kinetics with the VGSCs, with CBZ binding 5 times faster than PHT, but with 3-fold less affinity.¹⁴²

This difference may account for the different therapeutic responses observed among subgroups of patients.^{76,142} CBZ was also shown to have a weak inhibitory effect *in vitro* on NMDARs-mediated Ca^{2+} influx.¹⁴³ This effect was, however, highly potentiated in the presence of high extracellular K^{+} concentration (50 mM KCl), a physiological concentration pertinent to epileptic seizures.¹⁴³

1.3.3.3. Ethosuximide



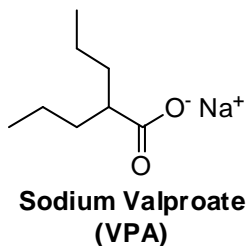
**Ethosuximide
(ESM)**

(*R,S*)-3-Ethyl-3-methyl-pyrrolidine-2,5-dione (ethosuximide, ESM, Zarontin[®]) is a member of the succinimide (succinimide core in red) family of anticonvulsants.¹³⁶ It was introduced in 1960 as an antiepileptic drug for the treatment of absence seizures in humans, and is ineffective against generalized tonic-clonic seizures. This profile correlates with the drug's animal pharmacology, ESM being able to prevent scPTZ- but not MES-induced seizures.⁵⁵

The accepted mechanism of action responsible for suppressing absence seizures is the blockade of T-type calcium currents,^{144,145} although different biological mechanisms are potentially implicated in the generation of absence seizures.¹⁴⁶ Unambiguous data concerning ESM reduction of Ca^{2+} currents was only recently published using cloned human T-type calcium channels, showing that T-type VGCCs block by ethosuximide is both voltage- and state-dependent.¹⁴⁷ ESM has a greater inhibitory effect on VGCCs at a depolarized membrane potential (IC_{50}

~2.5 mM at -75 mV, $\text{Ca}_v3.1$) than at a hyperpolarized potential (IC_{50} ~18 mM at -100 mV, $\text{Ca}_v3.1$),¹⁴⁷ a phenomenon reminiscent of the actions of PHT and CBZ on VGSCs.

1.3.3.4. Valproic acid

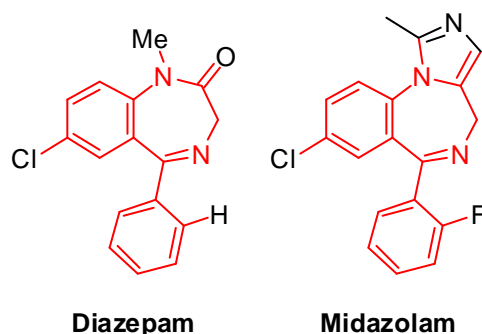


2-Propylvaleric acid (valproic acid, VPA, Depakene®) sodium salt is a branched fatty acid whose antiepileptic properties were fortuitously discovered in 1962, at which time it was used as a vehicle to evaluate new AEDs in animal models.¹⁴⁸ As positive results were obtained with any drug candidate at any dosage, the testing of valproate itself led to confirmation of its protective effects against seizures.¹⁴⁹ First marketed in 1967, it is still commonly used nowadays and has protective effects similar to ESM against absence seizures, and to CBZ and PHT against both tonic-clonic and partial seizures. Moreover, it is active in a variety of refractory epileptic disorders.¹⁵⁰ To date, VPA has one of the widest spectra of antiepileptic activity.¹⁵⁰

The exact mechanism(s) of action of VPA is still subject to debate. VPA prevents MES-induced seizures with an efficacy comparable to PHT and CBZ, correlating with its use against generalized tonic-clonic and partial seizures.⁵⁵ Some studies indicate that valproate is able to reduce SRF in rat hippocampal cultured neurons,¹⁵¹ probably through action on VGSCs. However, these results vary greatly

with preparation from different brain regions.^{152,153} VPA does not seem to interact with the PHT binding site of VGSCs.¹⁵⁴ Similar to ESM, VPA's interaction with T-type VGCCs has been studied to explain its absence seizure protective effect.¹⁵⁵ T-Currents blockade by VPA proved to be specific to the type of neuron used for the *in vitro* culture.¹⁵⁶ In addition to its suggested interactions with VGICs, VPA has been shown to interact with GABA synthetic and degradative enzymes,¹⁵⁰ without directly interacting with GABA_ARs.¹⁵⁷ Paralleling its effects on VGSCs and VGCCs, VPA displayed a brain regional specificity in its activating properties of glutamic acid decarboxylase (GAD).¹⁵⁷ In *ex vivo* and *in vitro* experiments, the valproate-induced increase in GAD activity matched the increase in GABA levels and its anticonvulsant effect.^{158,159,157}

1.3.3.5. Benzodiazepines



Diazepam (Valium[®]) belongs to the family of benzodiazepines (BZDs, benzodiazepine core in red), a class of drugs useful for treating a variety of neurological conditions, ranging from anxiety, agitation, insomnia, muscle spasms to seizures.¹⁶⁰ In 1963, diazepam, the second marketed BZD, was prescribed for its antidepressant properties. The anticonvulsant properties of BZDs were discovered

early in animal models. They are very potent in both the MES and scPTZ tests, but exhibit a pronounced neurotoxicity and short duration of action.⁵⁵ Benzodiazepines are unfortunately rendered useless for a chronic treatment of epilepsy due to the rapid onset of tolerance.¹⁶¹ However, as an acute treatment, rectal administration of diazepam remains today the first-line emergency treatment against status epilepticus,¹⁶² along with the more recent buccal formulation of midazolam¹⁶³ (Versed®).

The pharmacology of BZDs has been extensively studied, and have been shown to interact as positive allosteric modulators of GABA_ARs.^{102,103,105,164,165} BZDs bind with at the interface of α and γ subunits and enhance hyperpolarizing chloride currents by increasing the frequency of channel opening.¹⁶⁶ This sole mechanism of action, however, can not explain all the pharmacological properties of benzodiazepines.¹⁶⁷ BZDs have been demonstrated to have an inhibitory effect on Ca²⁺ uptake through action on VGCCs,¹⁶⁸ and were shown *in vitro* to act on VGSCs by reducing SRF, which may correlate with the protective effects of the drug in animal seizure tests.¹⁶⁹

1.3.3.6. Summary

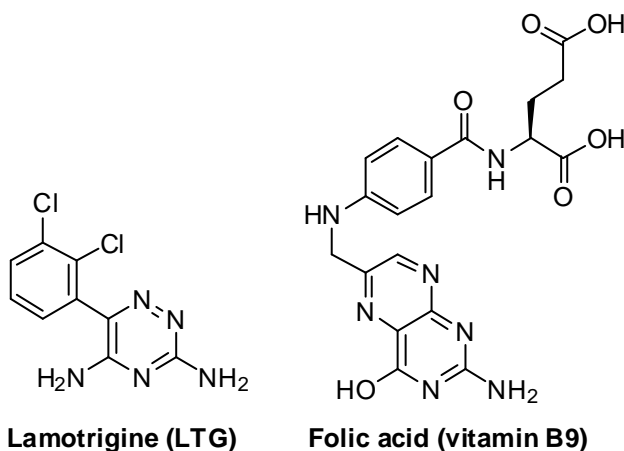
Except for the family of benzodiazepines, most traditional AEDs mainly target VGICs. The prototypical drugs PHT, CBZ, VPA, ESM have proven to be invaluable tools for our understanding of biochemical mechanisms underlying epilepsy. Early research has led to the paradigm that blockades of Na⁺ currents and transient Ca²⁺ currents, respectively, translate into protection against tonic-clonic and absence

seizures. The two respective animal models corresponding to these seizures are the MES and the scPTZ tests. In view of more recent studies, it has also become clearer that the neurotransmitter modulation through LGICs may account for part of the anticonvulsant properties of these AEDs.

1.3.4. Pharmacology of recent AEDs

One of the driving forces that led to the development of new AEDs was their undesirable side effects associated with long-term treatments.¹⁷⁰⁻¹⁷² The class of recent AEDs (mid-1970's to mid-1990's) has provided new chemical entities with diverse pharmacological profiles and mechanisms of actions. The compounds discussed in the following section are not exhaustive, but rather serve as an illustration of the variety of new mechanisms of action relevant to the treatment of epilepsy.

1.3.4.1. Lamotrigine

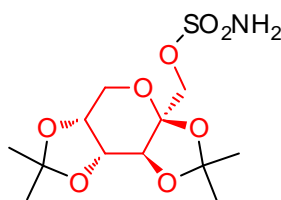


6-(2,3-Dichlorophenyl)-1,2,4-triazine-3,5-diamine (lamotrigine, LTG, Lamictal[®]) is an AED introduced in 1995 for the treatment of partial and generalized

tonic-clonic seizures. LTG was rationally designed based on the observation that folate derivatives possess proconvulsant activity in animals.^{173,174} LTG, however, is only a weak folate antagonist, a property that has not been linked to its antiepileptic effects.¹⁷⁵ In animal models, the pharmacological profile of LTG was similar to that of PHT and CBZ.¹⁷⁶

LTG blocked voltage-gated Na⁺ channels by stabilizing the fast inactivated state of the channel.¹⁷⁷ In early studies, LTG was suggested to act at the slow inactivation pathway of VGSCs.¹⁷⁸ However, this pathway could not be distinguished from an alternative mechanism where the binding kinetics of LTG to the channel were slow.^{76,179} In animal cultured neurons, lamotrigine demonstrated the ability to reduce SRF in a state- and voltage-dependent manner similar to that of PHT and CBZ.^{180,181,177} Interestingly, evidence supports that LTG, although very different in structure from PHT and CBZ, binds, if not at the same fast-inactivation site, to a closely related receptor site.¹⁸²

1.3.4.2. Topiramate



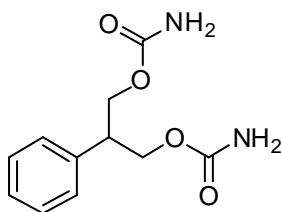
Topiramate (TPM)

2,3:4,5-Bis-O-(1-methylethylidene)-β-D-fructopyranose sulfamate (topiramate, TPM, Topamax[®]) is a recent AED with unusual structural features. The sulfamate derivative of D-fructose (in red) is used to treat simple and complex partial

seizures.¹⁸³ Originally synthesized in 1979 as a potential antidiabetic inhibitor of fructose 1,6-bisphosphatase, TPM was also tested the same year for anticonvulsant activity in mice where it displayed excellent anticonvulsant activity.^{184,185} Following the same trend as its predecessors PHT, CBZ, and LTG, TPM displayed a marked protection in the MES test, and little effect in the scPTZ test.¹⁸⁶ A distinct feature of TPM was its extended duration of action (up to 16 h).¹⁸⁶

In vitro experiments on neuronal cultures have identified three different potential mechanisms to explain the anticonvulsant activity of TPM. Similar to PHT, TPM reduced VGSC-dependent SRF ($IC_{50} < 100 \mu M$) in rat hippocampal neurons.¹⁸⁷ In addition, TPM showed selective blockade of KARs ($IC_{50} < 5 \mu M$) but not NMDARs,¹⁸⁸ and potentiated GABA_AR-mediated chloride currents (~150% increase in GABA-evoked Cl⁻ currents at 10 μM) by binding to a site distinct from the BZD site.¹⁸⁹

1.3.4.3. Felbamate



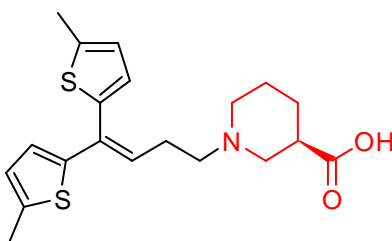
Felbamate (FBM)

2-Phenylpropane-1,3-diol dicarbamate (felbamate, FBM, Felbatol[®]) is a broad spectrum AED that was approved in 1993 for the treatment of partial and generalized seizures in adults and Lennox-Gastaut Syndrome (LGS) in children. At

non-toxic doses, FBM proved effective against both MES- and scPTZ- induced seizures in mice and rats.¹⁹⁰

Like TPM, FBM possesses several distinct mechanisms of action that may account for its broad range of activities. In mice and rat cultured neurons it reduced VGSC-dependent SRF ($IC_{50} = 28 \mu M$, rat striatal neurons),^{191,192} and inhibited cloned human and rat VGSCs by stabilizing the fast-inactivated state of the channel.¹⁹³ At physiological concentrations (10–100 μM), it was shown to potentiate GABA-elicited currents through action on GABA_ARs, in ways that differed with the neuronal *in vitro* preparations (e.g., mouse cortical neurons, rat hippocampal neurons).^{194,195} In addition, FBM was shown to function as an antagonist on NMDA-evoked excitatory currents, albeit at high concentrations ($IC_{50} \sim 2 \text{ mM}$).¹⁹⁵ Knowing that administered anticonvulsant doses of FBM led to whole brain peak levels of 0.6 to 0.8 mM in rats,¹⁹⁶ it is likely that a modest inhibition of NMDARs may have occurred.

1.3.4.4. Tiagabine



Tiagabine (TGB)

(*R*)-1-[4,4-Bis(3-methylthiophen-2-yl)but-3-enyl] piperidine-3-carboxylic acid (tiagabine, TGB, Gabitril[®]), is an antiepileptic drug advanced in the mid-1990's for the treatment of partial seizures.¹⁹⁷ TGB is another example of rationally designed molecule, based on the observation that nipecotic acid (in red) has inhibitory

properties on the GABA reuptake system.¹⁹⁸ Tiagabine is a more lipophilic analog of nipecotic acid with protective effects against scPTZ-induced, audiogenic, and amygdala kindled seizures, and moderate efficacy in the MES test.¹⁹⁷

Unlike other traditional or recent AEDs, the mechanism of action of TGB is well-defined. Tiagabine has a potent inhibitory activity on GABA reuptake in glial ($IC_{50} = 182$ nM) and neuronal ($IC_{50} = 446$ nM) cultured cells, thereby prolonging the effects of GABA on its post synaptic cognate receptors.¹⁹⁹ The difference between the two IC_{50} values may be explained by different cellular levels of GAT-1, the GABA transporter selectively targeted by TGB.²⁰⁰ Tiagabine was found to have little to no effect on a variety of neurotransmitter transporters, GPCRs, GABARs, Na^+ or Ca^{2+} VGICs.^{201,197}

1.3.4.5. Summary

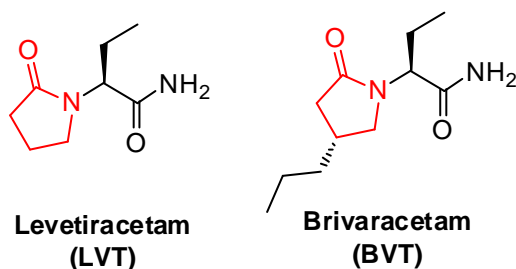
Recent AEDs are characterized by diversified, sometimes unusual, scaffolds compared with to traditional antiepileptics. An interesting feature of this class of drugs is the growing importance of rational design in the conception of the molecule. The rationally targeted pathway, however, turned out in some cases to be completely unrelated to the anticonvulsant properties of the molecule. AEDs such as TPM and FBM are unique in that they target both inhibitory and excitatory neurotransmitter receptors. TGB, in addition to modulating VGSCs, is the first antiepileptic rationally designed to effectively target one protein.

1.4. The emergence of new anticonvulsant entities and biological targets

1.4.1. What is new in antiepileptic drug development

The field of AEDs development is constantly evolving. The first decade of this millennium has seen the emergence of new therapeutic molecules acting on novel biological pathways. Following is a select list of such anticonvulsant molecules either marketed for the treatment of epilepsy or that are currently undergoing clinical trials.

1.4.1.1. Levetiracetam

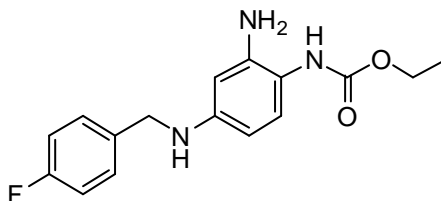


(S)-2-(2-Oxopyrrolidin-1-yl)butanamide (Levetiracetam, LVT, Keppra[®]) is a recently approved AED (1999) for the treatment of partial onset seizures in humans and is structurally related to racetams, a class of pyrrolidine (in red) CNS-targeting agents.²⁰² LVT is unique in that it was not identified as active in the traditional MES and scPTZ animal models.^{202,203} Instead, LVT proved very potent in the 6 Hz test and is one of the reasons why this pharmacological test was reintroduced as an important anticonvulsant screening method.⁵⁷ Levetiracetam has been proposed to have antiepileptogenic properties, in addition to its antiepileptic effects.²⁰⁴ Such a profile may be linked to LVT's ability to prevent the acquisition of kindled seizures in

animals.²⁰⁵ There are, however, some conflicting results about these properties of levetiracetam.²⁰⁶

LVT is also unique with respect to its mechanism of action. LVT has been shown to interact with the Synaptic Vesicle 2A (SV2A) protein, a macromolecule involved in the synaptic vesicle fusion process.²⁰⁷⁻²⁰⁹ A correlation between interaction of SV2A and efficacy against partial and generalized seizures has been established.²¹⁰ Indeed, a tighter interaction with SV2A has been advanced as the primary mechanism of action of brivaracetam (BVT),²¹¹ the second-generation analog of LVT currently undergoing Phase III clinical trials. Unlike its predecessor, BVT also appears to act on VGSCs, which may account for some of its anticonvulsant activity.²¹²

1.4.1.2. Retigabine



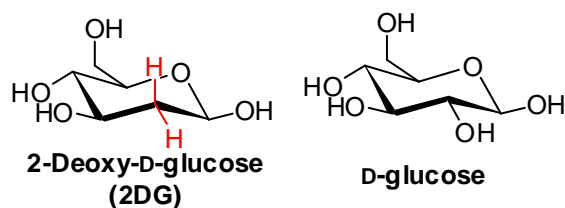
Retigabine (RGB)

Ethyl *N*-[2-amino-4-[(4-fluorophenyl)methylamino]phenyl]carbamate (Retigabine, RGB, D-23129) is a new anticonvulsant currently undergoing phase III clinical trials for the treatment of refractory partial-onset seizures.²¹² RGB has demonstrated efficacy in many animal seizure tests like the MES and 6 Hz tests, in addition to several chemoconvulsant-induced seizure tests such as scPTZ and

picrotoxin.²¹³ Furthermore, it prevents sound-induced seizures in the Frings and DBA/2 mice models.²¹⁴

The novel mechanism of action of RGB is the activation of $K_v7.2$ – $K_v7.5$, a primarily neuronal subfamily of voltage-gated potassium channels (VGKCs).^{215,216,207} Like VGCCs, these K^+ channels are characterized, in part, by the type of current they elicit.²¹⁷ Retigabine activates (1–10 μ M) VGKC-mediated M-currents that are hyperpolarizing, with slow activation and deactivation kinetics.^{218,219} RGB's effect is prevented by known, subtype-specific, VGKC blockers.²¹⁹

1.4.1.3. 2-Deoxy-D-glucose



2-Deoxy-D-glucose (2DG) is a rather simple molecule with very promising anticonvulsant properties and is expected to undergo phase I clinical trial evaluation for the treatment of epilepsy in 2010.²¹² Closely related to glucose, 2DG is taken up into cells by glucose transporters, but lacking the 2-hydroxyl group, the molecule cannot be metabolized and therefore act as an inhibitor of glycolysis.²²⁰

The ketogenic diet is a nutritional approach to the treatment of refractory epilepsy that consists in switching to a high-fat, low-carbohydrate food intake.²²¹ As a state of high energy demand, seizures rely on energetic pathways to “exist”.²²² By switching from glucose to fat as the primary source of fuel, this diet is efficient at preventing epileptic seizures in patients.²²² These beneficial results can, however,

rapidly be lost by a small ingestion of excess carbohydrate.²²³ Based on this observation, it was hypothesized that a glycolysis inhibitor may have protective effects against seizures and indeed, 2DG was found to have antiepileptic and antiepileptogenic effects in a variety of animal seizure models.²²⁴

1.4.2. Challenges for treating epilepsy

Most of the AEDs highlighted in this introductory chapter, from traditional drugs to recently discovered entities, have been presented in a favorable light, with their therapeutic mechanism of action as the focus. However, not mentioned are the sometimes life-threatening side-effects of some AEDs. As with most CNS-targeting agents, treatment with antiepileptics is often accompanied with a diverse set of side-effects, that can range from mild (drowsiness, nausea, sedation),²²⁵ to severe (liver failure, aplastic anemia, teratogenicity).²²⁶ Mostly for traditional and some recent AEDs, drug-drug interactions are numerous and multi-drug therapy, a standard practice in the treatment of epilepsy, requires caution by the practitioner.²²⁷ In addition, antiepileptics are either classified by the Food and Drug Administration (FDA) as Schedule V substances because of an associated increased risk of suicidal thoughts, or as Schedule IV for AEDs with strong sedative effects (barbiturates and some benzodiazepines).

To tackle the problem of toxic side-effects often arising from a metabolite of the drug, one of the endeavors of AED research has been the development of prodrugs or metabolically stable analogs of already marketed molecules. This effort is exemplified by the modification of the traditional AED carbamazepine to the

second and third generation derivatives, oxcarbazepine and eslicarbazepine, respectively.^{228,229} While these AEDs provide patients with safer treatment alternatives, they do not constitute a major breakthrough for the elucidation of new biological mechanisms underlying epilepsy.

1.4.3. Future hopes

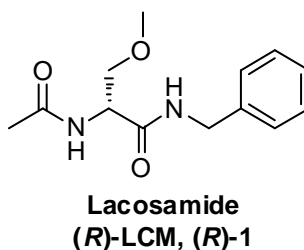
Fortunately, change in AED development is likely to occur as scientists examine epilepsy in a new light. Although far from complete, our knowledge and understanding of epileptic disorders have greatly expanded since the early days of AED development. Importantly, researchers now realize the necessity to tackle the problem of epilepsy differently. Most marketed antiepileptics work as a prophylactic treatment, meaning preventing the symptoms rather than curing them. Research focus has begun to slowly shift towards the development of “disease-modifying” molecules and their related biology.

One interesting observation that began in the late 1980's, was the emergence of the word “antiepileptogenic” in epilepsy-related literature abstracts, a term that has gained greater prominence in the literature with each increasing year (Pubmed search). Antiepileptogenesis is a concept that designates the prevention or slowing of biological processes that eventually lead to an epileptic state. Recurring seizures have been shown to induce neuronal growth through a mechanism called mossy fiber sprouting.^{230,231} The abnormal neural connections resulting from this process are thought to be essential for the initial development of seizures.²³² A better understanding of key macromolecules involved in neurogenesis will provide us with

new opportunities to help people with epilepsy. In addition, we can expect advances in seizure control using “disease”-representative models such as the kindled animal models, rather than tests that use healthy animals (e.g., MES, scPTZ, 6 Hz tests).

1.4.4. Functionalized Amino Acids (FAAs) are potent anticonvulsants with a broad spectrum of activity and a unique mechanism of action

1.4.4.1. Lacosamide



(*R*)-*N*-Benzyl 2-acetamido-3-methoxypropionamide (lacosamide, (*R*)-LCM, Vimpat[®], (*R*)-1) is a functionalized amino acid (FAA) derived from D-serine that gained marketing approval for the treatment of partial-onset seizures in Europe (2008) and in the United States (2009).^{203,233} FAAs were originally identified as potent anticonvulsant entities in the mid-1980s. Interestingly, the derivatives with the natural amino acid configuration displayed 10–20 fold less anticonvulsant activity.²³⁴⁻²⁴¹ (*R*)-LCM was extensively evaluated at the NINDS ASP and displayed excellent protection in the MES test, the Frings mouse model, the hippocampal kindled rat model and the 6 Hz test.²⁴² Compared with other standard AEDs, such as CBZ, PHT and LTG, the pharmacological profile of (*R*)-LCM was unique, leading to the speculation that (*R*)-LCM's mechanism of action was different from existing anti-epileptic agents.^{233,243,244}

(*R*)-LCM function has been extensively studied using electrophysiology. Early studies showed that lacosamide had no effect on VGSCs (fast inactivation), VGCCs and VGKCs.^{245,246} Radioligand displacement binding assays with (*R*)-LCM were conducted against a panel of GPCRs and LGICs, including GABA, adrenergic, dopamine, serotonin and muscarinic acetylcholine receptors.²³³ (*R*)-LCM did not show any specific binding to these receptors at concentrations up to 10 μ M. Because of its structural similarity to the unnatural amino acid D-serine, it was suggested that (*R*)-LCM might exert its action via the glycine binding site of NMDARs. However, binding studies showed no effect of (*R*)-LCM on this receptor at therapeutically relevant concentrations.²³³

1.4.4.2. Rationale and hypothesis to search and identify the biological targets of (*R*)-LCM

With little known about the mechanism of action of (*R*)-LCM, we initiated a chemical biology study to identify binding partners of (*R*)-LCM, by screening the rat brain proteome. Our rationale for this approach was based on the several observations. First, (*R*)-LCM and its FAA derivatives displayed very potent anticonvulsant activity in the rat. Second, AEDs, like many CNS agents, tend to have multiple targets for which they have a modest binding affinity. This phenomenon may be accounted for, in part, by their lower molecular weight and, in most cases, their relatively simple structures. The diminished structural size and complexity of most AEDs likely lessens the extent of protein-drug interactions (e.g., hydrogen bonds, hydrophobic, dipole-dipole, van der Waals) that foster binding. The average

molecular weight of the structurally diverse AEDs presented in this introductory chapter is $\sim 220 \text{ g.mol}^{-1}$ and (*R*)-LCM itself is 250 g.mol^{-1} . Third, the established or likely targets for anticonvulsant molecules are either soluble or membrane-bound proteins.

Shortly after the start of our investigation, (*R*)-LCM was reported to exert its function by enhancing the slow inactivation of VGSCs,^{135,243} and by modulating the Collapsin Response Mediator Protein 2 (CRMP-2).²⁴⁷ These target sites/pathways were novel for anticonvulsants and supported earlier assertions that (*R*)-LCM functioned via mechanisms *different* from existing antiepileptic agents. In light of the complex nature of AED function, we asked if there were additional (*R*)-LCM targets.

CHAPTER 2

ORGANIC SYNTHESIS OF LACOSAMIDE DERIVATIVES

2.1. Selecting the chemical parts to build molecular tools

2.1.1. Current methods for drug target identification

Many approaches exist for elucidating drug function.²⁴⁸⁻²⁵⁹ Microarrays, RNA interference (RNA_i) and forward chemical genetics are three recent strategies. The first of these allows identification of genes or proteins whose expression profile is modified in the presence of the drug.²⁶⁰ The second approach uses small RNAs to partially or completely silence or knock-down specific genes, and, therefore, proteins.²⁶¹ Though useful in rational drug discovery strategies, these methods do not identify the target's binding region for drug function. Forward chemical genetics is an attractive chemical biology approach that employs small molecules to elucidate biological pathways and protein targets by eliciting a certain phenotype.²⁵⁰⁻²⁵⁵ Again, this method doesn't allow the identification of the target itself.

The most common approach for drug target identification is an affinity-based strategy where modified small molecules are immobilized on a matrix, and then incubated with purified proteins. Although protein targets have been successfully identified by this approach^{262,263} the method does have limitations. The most

significant of these is that the structure of the ligand has been optimized. Subsequent introduction of a chemical bulky group (*i.e.*, biotin) often results in the disruption of key binding interactions, and with it, a loss of the drug's affinity for its target.

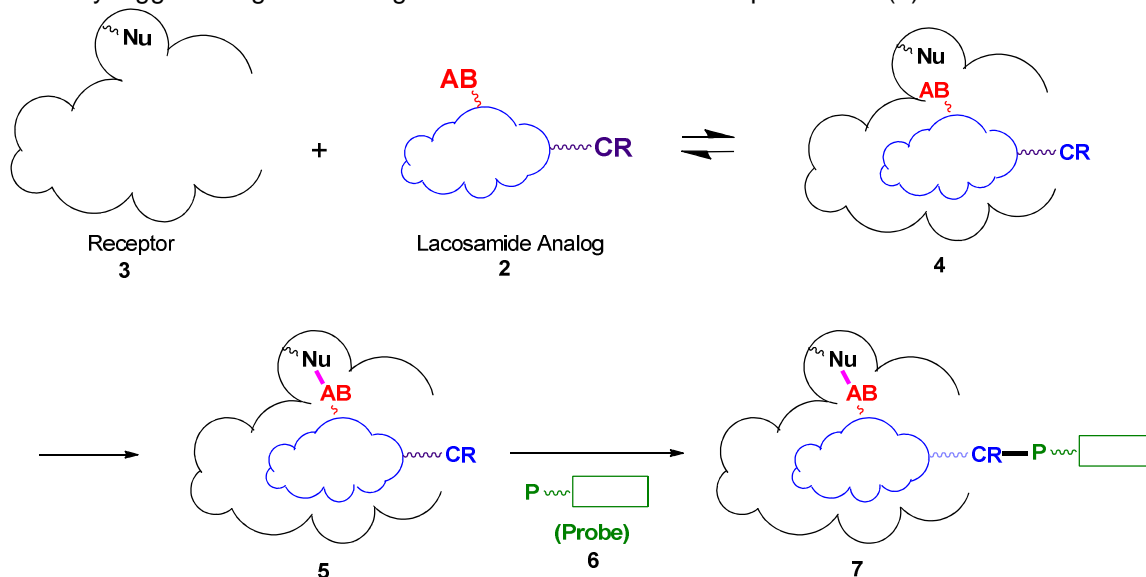
2.1.2. The use of small chemical groups for selective protein modification

Medicinal chemists and biochemists have traditionally appended reactive chemical groups on organic molecules to covalently label or inactivate macromolecules.²⁶⁴⁻²⁷⁴ We term these small reactive moieties **Affinity Bait (AB)** groups. More recently the concept of bioorthogonal chemistry was advanced as a powerful approach to study or identify protein targets.²⁷⁵⁻²⁸² Alkynes and azides are two small, bioorthogonal groups: they are inert under biological conditions, yet quickly react with each other under Cu^I-catalyzed conditions ("Click Chemistry").^{283,284} The alkyne and azide groups have been termed **Chemical Reporter (CR)** groups.

Our approach to target protein identification is based on the incorporation of both **AB** and **CR** groups on a low molecular weight compound. In this study, we focus on the mode of action of the novel AED lacosamide ((*R*)-**1**, LCM). Thus, we term these bi-functional derivatives as LCM **AB&CR** agents **2** (Scheme 3). Upon binding with the receptor (**3**), the **AB** group first creates a covalent linkage between the target protein and lacosamide (**4**, **5**). The **CR** group then reacts with a bioorthogonal **Probe (P, 6)** containing a fluorophore or a biotin moiety to permit

complex **7**'s detection or purification, respectively. The following section provides a rationale for the choice of **AB** and **CR** groups used in our chemical biology study.

Scheme 3. Proposed strategy to identify the target proteins of (*R*)-LCM with AB&CR agents. The AB&CR analog **2** covalently modified receptor **3**. The covalent receptor/AB&CR complex **5** is then selectively tagged using a bioorthogonal Probe **6** for detection or purification (**7**).



2.1.2.1. Electrophilic groups

One common application of the **AB** methodology is the development of selective enzyme inhibitors.²⁸⁵⁻²⁸⁷ Typically, an electrophilic moiety is appended on the small molecule, peptide or peptidomimetic. The covalent bond formed between the active residue and the ligand leads to irreversible inhibition of the enzyme. Cravatt and coworkers have used an **AB&CR** methodology, Activity-Based Protein Profiling (ABPP), to characterize the reactivity profile of various **AB** groups within different classes of enzymes.^{275,283,288} Interestingly, the nature of the electrophilic groups can be modulated to target a specific class of protease. For example

epoxide-containing peptides derivatives are commonly used to inactivate cysteine proteases,^{269,274} while chloromethylketone groups are more prone to react with serine proteases.²⁸⁹

Almost any electrophile can, in principle, be used for protein modification. However, successful implementation of this approach requires the **AB** to display the adequate balance between chemical selectivity and reactivity. Employing very potent electrophilic moieties will inevitably lead to high levels of non-specific labeling.²⁹⁰

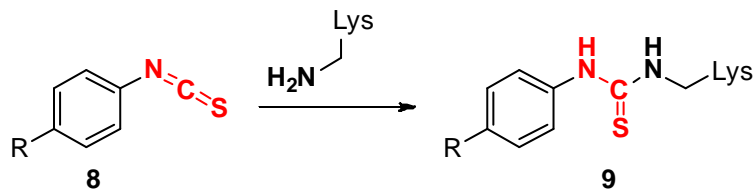
Covalent protein modification through small reactive groups is widely used in protein biology. Among the commonly utilized groups are the aromatic isothiocyanate,²⁹¹ the maleimide,²⁹² and the succinimidyl ester.²⁹³ These electrophiles can react in a non-specific fashion since their adduction only requires an accessible lysine (isothiocyanate and succinimidyl ester) or cysteine (maleimide) residue. Fluorescein isothiocyanate (FITC),^{291,294} and biotin succinimidyl esters,²⁹³ are two examples of widely used low-molecular weight, non-specific protein modifiers.²⁹⁵ Nonetheless, researchers have demonstrated that electrophilic groups can selectively target non-catalytic amino acid residues.^{290,296,297}

2.1.2.1.1. Isothiocyanate

The aromatic isothiocyanate (NCS) may be considered a general amine-reactive chemical moiety with respect to proteins.²⁹⁴ However, many studies document its utility as a selective, irreversible protein modifier. Indeed, brain G-protein coupled receptors (GPCRs) such as the δ -opioid,²⁶⁴ cannabinoid,²⁶⁵ *N*-methyl-D-aspartate (NMDA),²⁹⁸ and α 2-adrenergic receptors,²⁶⁶ have been labeled *in*

vitro, and under certain conditions *in vivo*, by synthetic NCS-derivatives of their cognate ligand. Thus, this moiety can potentially be used as an **AB** group (**8**) for selective protein modification through a lysine residue within a binding pocket (Scheme 4).

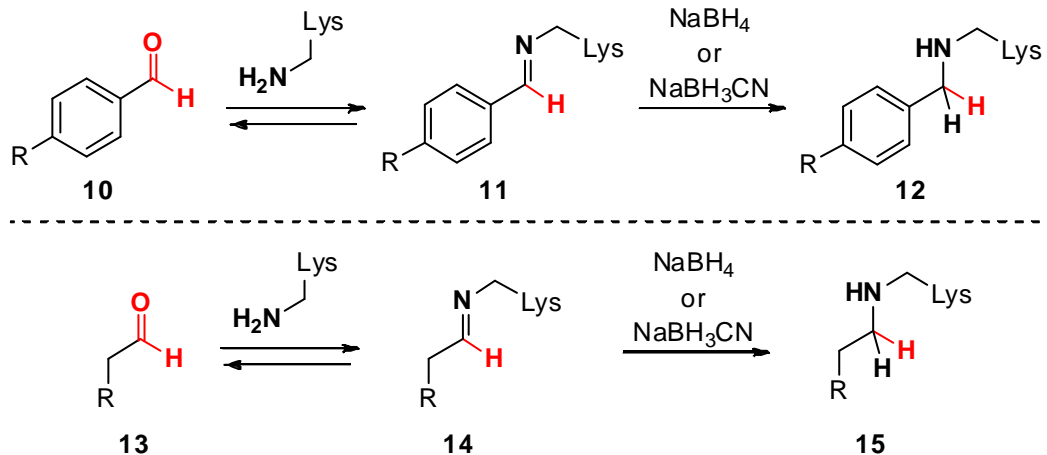
Scheme 4. The NCS group reacts with a lysine residue to form a covalent thiourea linkage.



2.1.2.1.2. Aldehyde

Carbonyl compounds without an adjacent halomethyl group can also selectively label proteins.²⁹⁹ Researchers have used aldehyde-containing small molecules to react with protein lysine residues (Scheme 5).³⁰⁰

Scheme 5. The aldehyde groups **10** and **13** react with an amine to give imine intermediates **11** and **14**. The transient species is then reduced to form a covalent amine bond using a hydride source.

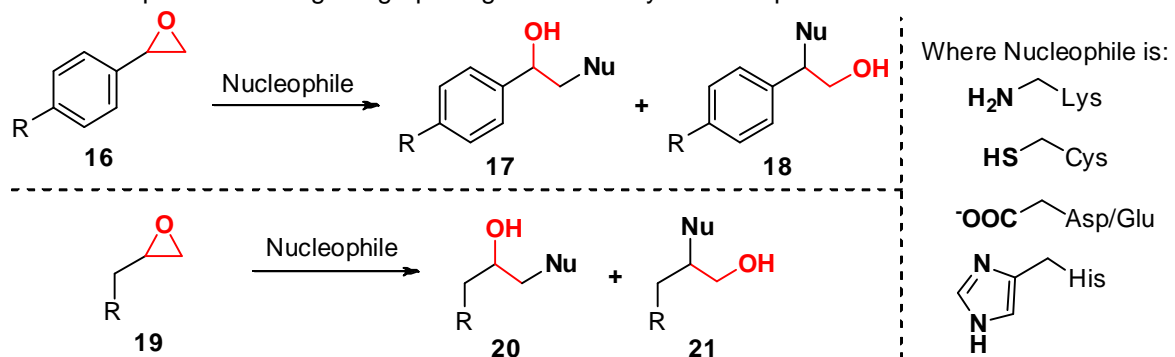


The transient imine (**11**, **14**) formed between the protein and the aldehyde (**10**, **13**) is reduced to a covalent amine bond using a hydride source. For instance, this approach led to the identification of the binding site of the antibiotic bicyclomycin with the *Escherichia coli* (*E. coli*) rho transcription terminator protein.^{296,301,302} The aldehyde **AB** group can, therefore, be utilized to trap a small molecule/protein complex with the **AB&CR** methodology.

2.1.2.1.3. Epoxides

Epoxides are versatile electrophilic groups.³⁰³⁻³⁰⁷ One of the driving forces of the reaction with electron-rich atoms is the release of the epoxide ring strain upon nucleophilic attack.³⁰⁷ In addition to their use as cysteine protease irreversible inhibitors,^{274,308,309} epoxide substrates (**16**, **19**) have been shown to react with the ϵ -amino group of lysines,³¹⁰ the carboxyl group of aspartates³¹¹ and glutamates³¹², and with the imidazole ring of histidines²⁹⁰ to give the corresponding ring-opened adducts (Scheme 6).

Scheme 6. Epoxides undergo ring-opening with a variety of nucleophilic amino acids.



In a recent chemical biology study, Sames and coworkers examined at a panel of diverse electrophiles to construct a chemical probe to specifically target carbonic anhydrase 2 (CA2). Interestingly, the epoxide group was the only **AB** moiety that specifically targeted CA2.²⁹⁰

2.1.2.2. Photoreactive groups

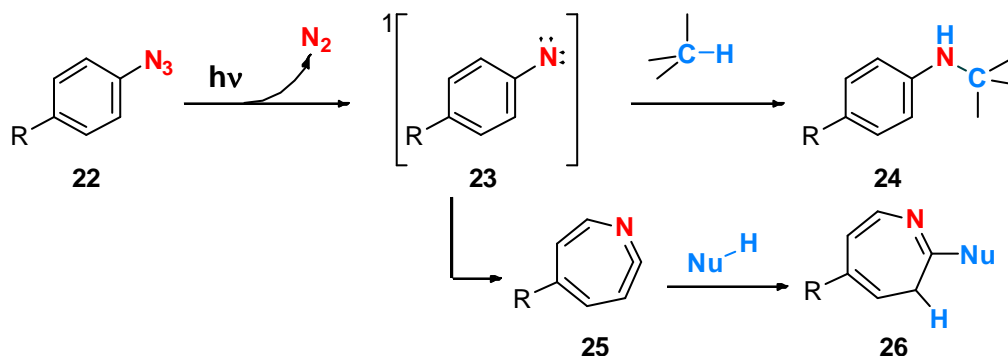
A requirement for electrophilic **AB** groups is the need for a nearby protein nucleophilic moiety in the binding pocket. To overcome this limitation we included in our study several light-activated **AB** groups (**photoAB**). These reactive species can, upon binding to an active site, undergo less restrictive C–H bond insertion reactions to covalently label macromolecules.³¹³

PhotoAB groups have been extensively used in protein modification studies.³¹⁴⁻³¹⁶ Photophores become activated upon irradiation at a specific wavelength. Light triggers the formation of a reactive intermediate capable of undergoing carbon-hydrogen bond insertion or nucleophilic attack. A major advantage of this class of **AB** agents is their lack of reactivity under non-irradiative conditions. Photolabeling experiments may, however, suffer from the reactivity profile of some **photoAB** moieties, their low labeling efficiency, as well as the use of protein-damaging wavelengths.³¹³ Many studies have relied on the use of these light-activated groups for *in vitro* or *ex vivo* experiments.^{263,268,316-320} Aromatic azides, diazirines and benzophenones are commonly used **photoAB** units for biological studies.

2.1.2.2.1. Aromatic azide

Aromatic azides are among the most widely used **photoAB** groups for protein labeling.^{321,317,322,323,296} They can be readily obtained from the corresponding aromatic amine and nitro groups.^{324,325} Irradiation of the Ar-N₃ group (**22**) at an energetic wavelength (254–360 nm) generates a short-lived (few nanoseconds)³²⁶ singlet nitrene (**23**) that reacts with adjacent amino acids (**24**) (Scheme 7).

Scheme 7. Irradiation of **22** leads to the singlet nitrene **23**. The nitrene undergoes C-H bond insertion to give **24** or rearranges to the seven-membered ketimine azepine electrophile **25**. The triplet nitrene is not shown



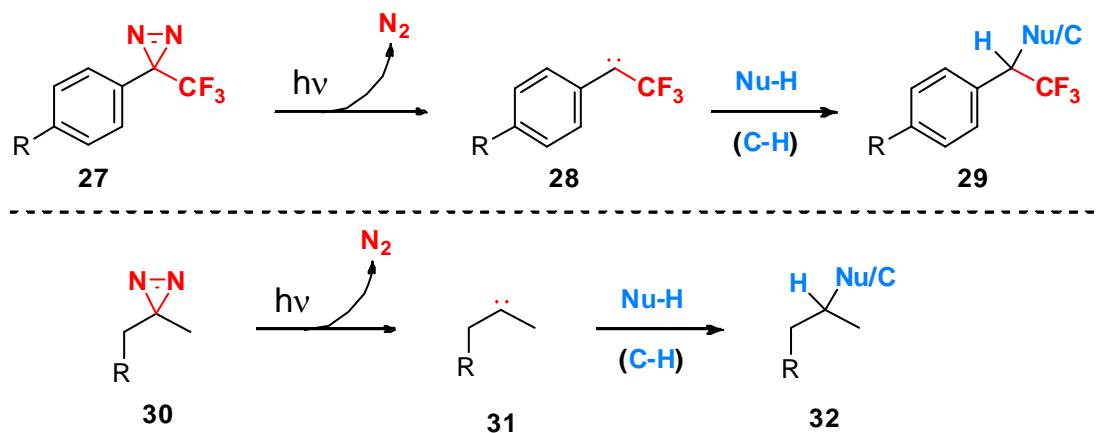
Two side reactions decrease the aryl azide photolabeling yield. The first one is the conversion of the singlet to the ground state triplet nitrene, a species with less value for photoaffinity labeling.³²¹ The second side reaction is the formation of a long-lived (few milliseconds³²⁷) reactive intermediate didehydroazepine **25**.^{313,326,327} The ketenimine moiety in **25** reacts as an **AB** electrophile, and thus may lead to a less specific protein labeling through accessible nucleophilic residues.³¹³ The relative instability of aromatic azides to common reducing agents is also a problem.

Indeed, aryl azides are readily converted to the corresponding aniline upon exposure to dithiothreitol (DTT) and β -mercaptoethanol (BME).^{317,328}

2.1.2.2.2. Diazirines

Diazirines were introduced more than 30 years ago as photoaffinity agents.³¹⁴ Upon irradiation (360 nm), they rearrange into diazo derivatives and/or carbenes (Scheme 8). Further excitation (312 nm) of the diazo intermediate leads to higher levels of the latter species.³¹³ The more pronounced carbene character of diazirines, as well as their stability to reducing, acidic and basic conditions^{267,329} makes these reagents useful for protein modification studies.

Scheme 8. Irradiation of the diazirine moiety (**27**, **30**) generates the corresponding carbene (**28**, **31**) which undergoes nucleophilic attack or C-H bond insertion (**31**, **32**). Only the carbene intermediate is shown.



Two different types of diazirines are generally employed for photolabeling. The trifluoromethylaromatic diazirine (**27**) is the most common in biochemical studies.^{318,330-334} At biologically relevant concentrations (1–1000 μ M), Hatanaka and coworkers showed that irradiating this **photoAB** in buffered aqueous solution at 365

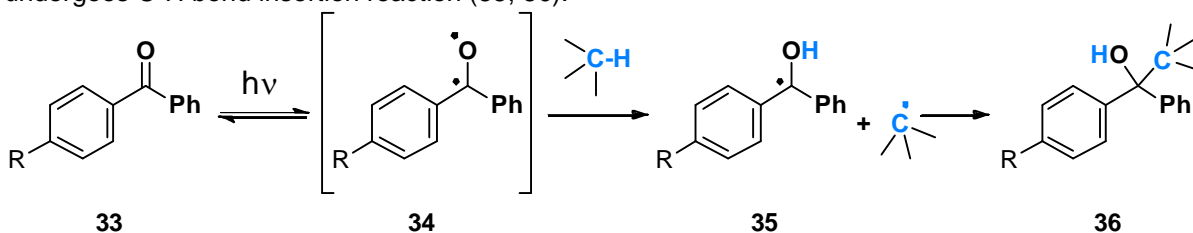
nm (10 min) and 312 nm (1 min) led to full conversion of the diazirine into its corresponding carbene **28**.³³⁵ Used to a lesser extent is the alkyl diazirine photophore **30**.^{268,336,337} The alkyl substituents flanking the diazirine moiety render the resulting carbene **31** less stable than its trifluoromethylaromatic counterpart, thereby reducing the efficiency of the irradiation step.³¹³

Synthetic accessibility is one drawback of this **photoAB** moiety. While the alkyl diazirine is obtained in few steps,^{338,339} the trifluoromethyldiazirine requires up to 10 synthetic transformations.^{333,340,341} The reactive nature of carbenes is also a limitation. Indeed, a tight interaction is required for the short-lived intermediate to efficiently modify macromolecules.

2.1.2.2.3. Benzophenone

The benzophenone is another established **photoAB** for protein labeling (Scheme 9).^{315,318,342,319,320,343-345} Unlike aryl azides and diazirines and their respective nitrene and carbene intermediates, the benzophenone undergoes protein C–H bond insertion via a radical pathway.³⁴⁶ An important feature of this mechanism is that irradiation generates an excited, reactive intermediate (**34**) that returns to its ground state in the absence of a C–H bond substrate.³⁴⁶ This non-destructive equilibrium between the ground and excited state,³⁴⁷ as well as the required correct orientation of the C[•]–O[•] diradical **34** with respect to the C–H bond³⁴² make the benzophenone a highly selective **photoAB** for biological studies.^{313,346,347}

Scheme 9. Excitation of the C=O bond in **33** reversibly leads to an excited diradical **34** that undergoes C-H bond insertion reaction (**35**, **36**).

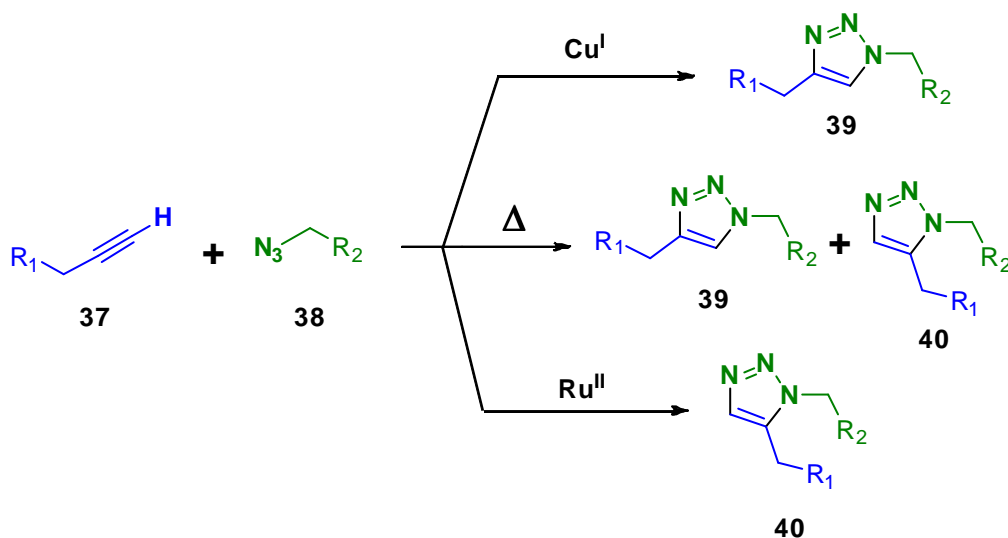


2.1.3. Bioorthogonal groups and click chemistry

1,3-Dipolar cycloadditions have found utility for the construction of a wide variety of heterocycles.³⁴⁸ A copper-catalyzed version of these reactions, the 1,3 alkyne-azide cycloaddition (Scheme 10), has been extensively used in the field of chemical biology and polymer science over the past decade.^{268,276,278,345,349-354}

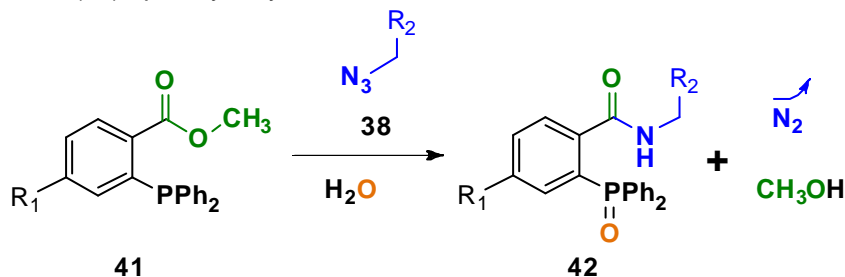
Upon prolonged heating, alkynes and azides are known to form a mixture of 1,4- and 1,5-substituted triazoles.³⁵⁵ However, under metal-catalyzed conditions, the reaction proceeds rapidly. Cu(I)-catalysis gives exclusively the 1,4-regioisomer (**39**), and Ru(II)-catalyzed conditions provide the 1,5-regioisomer (**40**).³⁵⁶ Upon discovery of the Cu(I)-catalyzed azide-alkyne cycloaddition (CuAAC), Sharpless advanced the term of “Click Chemistry” as a concept to designate any organic reaction where reacting partners combine to give a single product and where the process is reliable, quantitative, selective, fast, clean, inexpensive, and environmentally friendly.³⁵⁷ The CuAAC is the prototypical “Click Chemistry” reaction and is now commonly referred to by that name.^{278,349-351}

Scheme 10. Terminal alkynes and azides lead to different triazole regioisomers under different conditions



Along with others, Cravatt and coworkers pioneered the use of this transformation in *in vitro* biological studies and employed CuAAC to identify the target proteins for several small molecules.^{275,345,354,358-360} However, this reaction cannot be extended to cells or living organisms due to the cytotoxicity of Cu(I) and Cu(II) species.³⁶¹ To circumvent this problem other types of copper-free click chemistry reagents have been advanced.

Scheme 11. Staudinger ligation reaction. The phosphorus atom reacts in **41** with an azide (**38**) to form an iminophosphorane intermediate that attacks the Me ester and forms an amide linkage and the phosphine oxide (**42**) upon hydrolysis

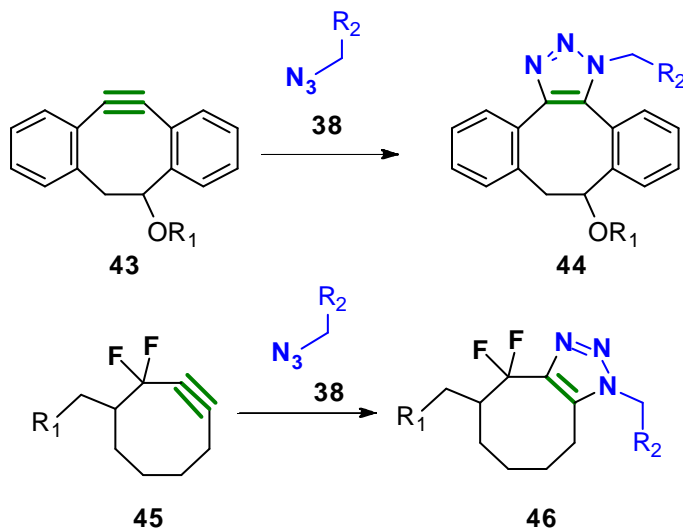


Bertozzi and coworkers have shown that both the Staudinger ligation (Scheme 11) and the strain-promoted azide-alkyne cycloaddition (Scheme 12) are

both suitable reactions to perform “Click Chemistry” in a biological milieu.^{280-282,362-364}

Despite their excellent biocompatibility, both the phosphine and the first generation cyclooctyne suffered from slow kinetics. Recently, progress has been made in the development of more reactive cyclooctyne species.^{352,365,366} Some of these copper-free click reactions have been used to observe biological events in cells and living organisms.^{349,352}

Scheme 12. Two examples of strain-promoted cyclooctyne addition reactions. The strained ring as well as the electronic effects of neighboring groups improve the kinetics of the reaction. Only one of the two triazole regioisomers is drawn.

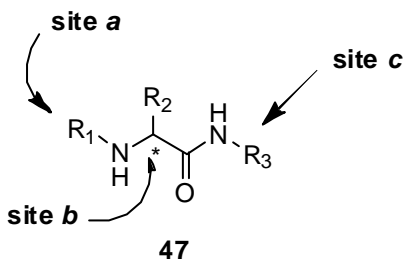


2.2. Structure-activity relationship of FAAs

2.2.1. FAAs

The potent anticonvulsant activity of FAAs (**47**) was discovered by the Kohn laboratory in 1985 and led to a focused SAR study.^{234,367,241,368,237,369,238,370} More than 250 FAAs were prepared and then evaluated at the NINDS ASP and the Eli Lilly Laboratories. Compounds were tested for seizure protection in the MES and scPTZ tests and neurological toxicity in the rotarod test (mice) and behavioral test (rats).

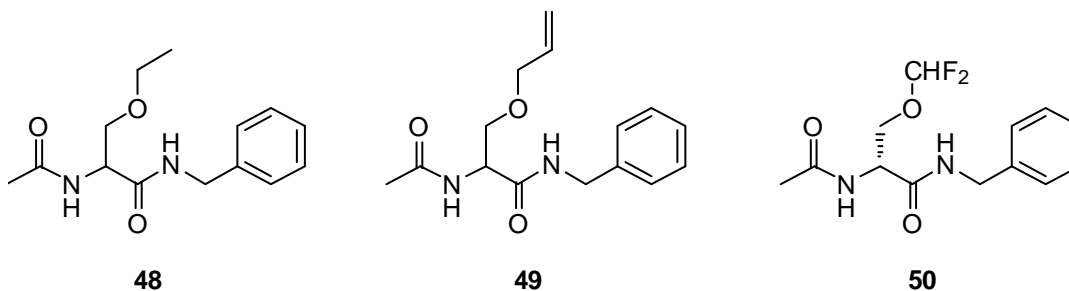
Scheme 13. Structure of FAAs. Different modification sites studied for the SAR of lacosamide are shown.



The SAR study of **47** focused on three different sites (*a*, *b* and *c*, Scheme 13). The optimal substituent for site a was the acetyl group (R₁ = C(O)CH₃). For site c, the requirements were also stringent. Excellent anticonvulsant activity was obtained for an unsubstituted benzyl group (e.g., R₃ = CH₂Ph). Accordingly, most of the SAR study focused on modifications at site b. The Kohn laboratory showed that several compounds containing small aliphatic groups and heteroaromatic groups (*i.e.*, pyridyl, furanyl, oxazolyl) positioned at C(2) displayed significant anticonvulsant activity in the MES seizure test. When a heteroatom was introduced one atom removed from C(2), the seizure protection was comparable with or exceeded that of

phenytoin,^{234,367,241,239} the prototypical antiepileptic agent in the MES-seizure model.³⁷¹ The highest anticonvulsant activities were obtained with oxygen as the heteroatom. The SAR study led to the discovery of lacosamide ($R_2 = \text{CH}_2\text{OCH}_3$). Most important, the SAR study demonstrated that one structural feature was recurrent: the anticonvulsant activity resided in the (*R*)-enantiomer (D-configuration) of the FAAs.

The initial SAR of FAAs concluded with lacosamide's invention. Efforts to explore the impact of the methoxy unit replacement in (*R*)-LCM were hampered by the unavailability of efficient synthetic pathways to the enantiomerically pure derivatives. At the start of our investigation, little was known about the structural tolerance at this site in lacosamide. The Kohn group reported the activities of the racemic *O*-ethyl (*R,S*)-**48** and *O*-allyl (*R,S*)-**49** analogs.²³⁴ Both compounds exhibited significant activities but were 2–8-fold less active than (*R,S*)-**1** in mice (MES $\text{ED}_{50} = 8.3 \text{ mg.kg}^{-1}$ (0.5 h)).²³⁴ Recently, a lacosamide analog was prepared where the OCH_3 moiety was replaced by a OCHF_2 (**50**).³⁷² This fluorinated derivative displayed excellent protection and prolonged duration of action (rat, po) in the MES test ($\text{ED}_{50} = 3.0 \text{ mg.kg}^{-1}$ (0.5 h), 4.2 mg.kg^{-1} (4 h)) when compared with (*R*)-LCM ($\text{ED}_{50} = 1.8 \text{ mg.kg}^{-1}$ (0.5 h), 8.3 mg.kg^{-1} (4 h)) under the same test conditions.³⁷²

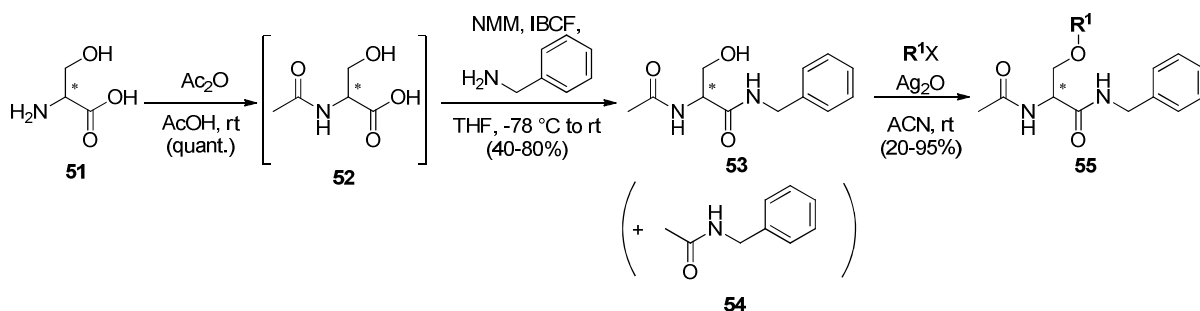


2.2.2. Synthetic approaches to side chain modification

2.2.2.1. Functionalization using O-alkylation

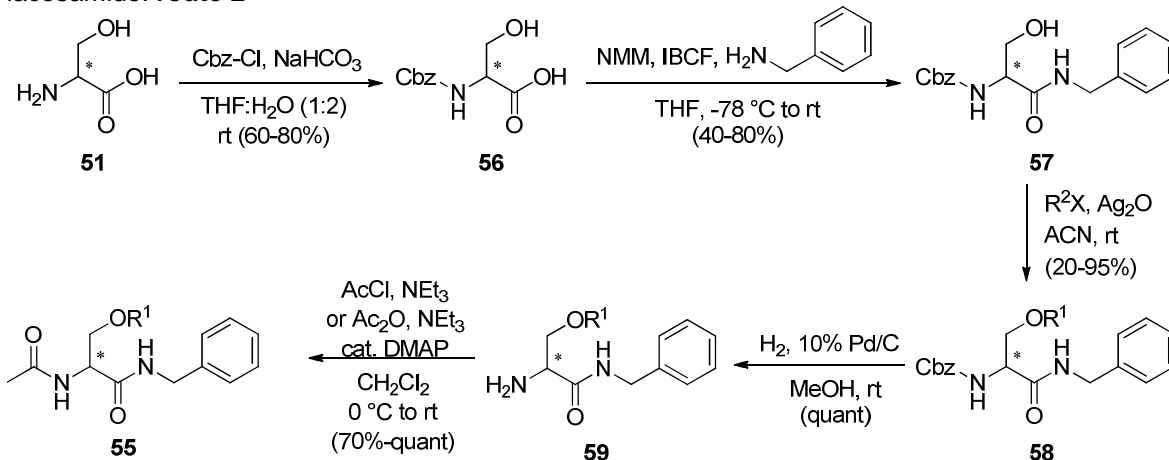
At the beginning of our studies two synthetic routes were available to synthesize enantiomerically pure LCM and LCM analogs. The shortest pathway (Scheme 14, **route 1**) to the AED started with commercial L- or D-serine (**51**). Acetylation with Ac₂O in acetic acid led to the *N*-acetylserine derivative **52** that directly reacted with benzylamine. Benzylamide **53** was then methylated with MeI under basic conditions to provide lacosamide enantiopure derivatives **55**. The need for the complete removal of excess AcOH prior to the amide coupling step was a major limitation of this pathway. Any acetic acid not removed resulted in the side-formation of *N*-acetylbenzylamide (**54**).

Scheme 14. Synthetic pathway to enantiomerically pure O-alkoxysubstituted derivatives of lacosamide: **route 1**



The second pathway (Scheme 15, **route 2**) was analogous to **route 1** except a protection/deprotection step was introduced. Enantiopure *N*-Cbz-serine (**56**) was either purchased or prepared from serine and Cbz-Cl. After amide coupling and methylation, the Cbz group was removed under catalytic hydrogenation conditions

and the free amine **59** acetylated with acetyl chloride or acetic anhydride. The enhanced solubility of *N*-protected serine derivatives in organic solvents made **route 2** more practical than **route 1** despite the increased number of steps. Nonetheless, a drawback to both pathways was the cost of Ag₂O (5 equiv required for the Williamson ether synthesis step). More important, only a narrow range of substituents could be installed at the 3-hydroxy site under alkylating conditions. Reaction yields rapidly dropped as the *O*-methyl group in LCM was increased to ethyl or allyl. Thus, **routes 1** and **2** were only useful to prepare either LCM AB or CR derivatives where the AB or CR moiety was introduced at the *N*-benzylamide position.

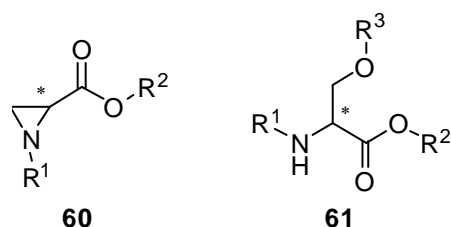


2.2.2.2. Functionalization using aziridine ring-opening, a general approach to

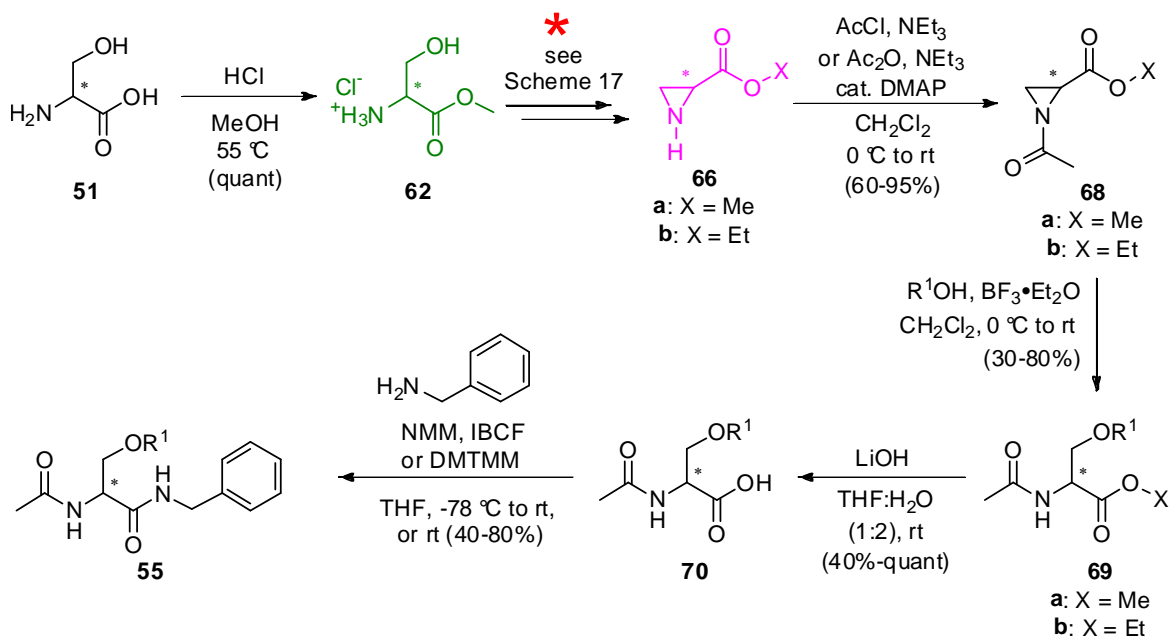
LCM O-substituted derivatives

2.2.2.2.1. Synthesis via *N*-Trt aziridine carboxylate esters

N-Substituted aziridines carboxylate esters (**60**, $R^1 = \text{Ac, Cbz}$) are valuable intermediates in the synthesis of amino acid derivatives.³⁷³⁻³⁸¹ Under Lewis acid-catalyzed conditions, alcohols can add to the strained ring and produce an *O*-substituted serine analog **61** with the same C(2) stereochemistry as its precursor.³⁷⁹



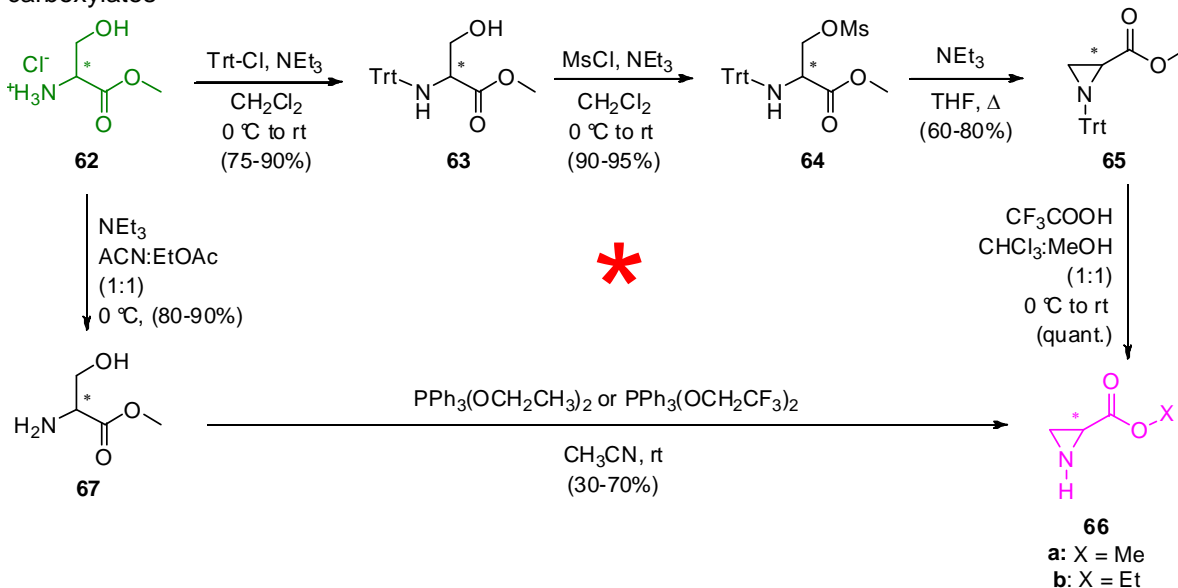
Scheme 16. Synthetic pathway to enantiomerically pure *O*-alkoxysubstituted derivatives of lacosamide: **route 3**



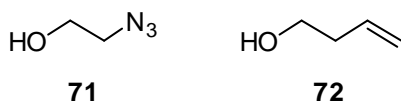
This methodology provided a third pathway (Scheme 16, **route 3**) for the preparation of LCM analogs and the desired AB&CR agents. L or D-Serine methyl

ester hydrochloride (**62**) was purchased or prepared from serine and HCl in MeOH.³⁸² The serine Me ester hydrochloride was successively *N*-tritylated, *O*-mesylated, and heated to reflux under basic conditions to form *N*-Trt-aziridinecarboxylate methyl ester (**65**, X = Me) (Scheme 17).^{375,383} The trityl group was removed using TFA (Scheme 17) and the free aziridine **66a** acetylated with acetyl chloride to yield **68a** (Scheme 16). Ring-opening of **68a** with a variety of alcohols in the presence of $\text{BF}_3 \cdot \text{Et}_2\text{O}$ gave **69a**.³⁷⁸ The *O*-substituted *N*-acetyl serine esters (**69a**, and **69a,b**) were hydrolyzed with LiOH and coupled to benzylamine to provide LCM derivatives **55**.³⁸⁴ The AB&CR agents were synthesized by coupling **70** with various substituted benzylamines. Depending on the nature of the *N*-benzylamide substituent, up to 3 additional steps were necessary to obtain the desired AB&CR compound.

Scheme 17. Different synthetic pathways used to access enantiomerically pure aziridine ester carboxylates



Despite the generality of this approach, two aspects in reaction Scheme 16 hindered our efficient synthesis of the lacosamide agents necessary for animal testing. The first was the generation of large quantities of **68**. The literature sequence^{379,380,383} was time-consuming (4–5 d), labor intensive and the use of the Trt group as shown in Scheme 17 required its removal prior to *N*-acetylation, resulting in only moderate yields of **68a** (~40%). The second experimental roadblock involved the ring-opening of **68a** with select alcohols and the subsequent ester hydrolysis step. We found that the nature of the alcohol influenced the yield of the nucleophilic opening reaction. With 2-azidoethanol (**71**, 3–10 equiv), the reaction proceeded in a 30–40% yield while with 3-buten-1-ol (**72**, 3–5 equiv) it reached 65–70% yield. Furthermore, for water-soluble derivatives of **70**, we obtained poor to moderate recovery after ester hydrolysis and work-up.

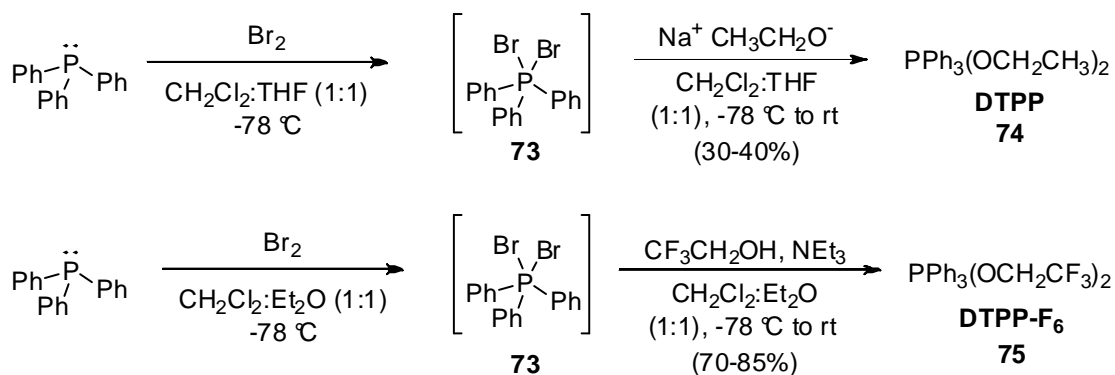


2.2.2.2.2. Synthesis using dialkoxyphosphoranes derivatives

Little could be done to resolve the second roadblock. Efforts to enhance the ring-opening step by increasing the number of equivalents of alcohol did not improve the yields of **69**. We addressed the first issue by employing a more efficient way to access **68**. Evans and coworkers demonstrated the versatility of dialkoxytriphenylphosphoranes ($\text{PPh}_3(\text{OR})_2$) as cyclodehydration reagents to form heterocyclic systems.³⁸⁵⁻³⁸⁹ Using an improved method,³⁸⁷ we prepared

diethoxytriphenylphosphorane ($\text{PPh}_3(\text{OCH}_2\text{CH}_3)_2$, **DTPP**) from PPh_3 , Br_2 , and NaOEt (Scheme 18). Using serine methyl ester **67** and **DTPP** (1.2 equiv), we obtained aziridine **66a,b** as a mixture of methyl/ethyl esters. The reaction proceeded in 24 h, provided good yields (50–70%) of **66a,b** after bulb-to-bulb distillation, and was used to prepare up to 20 g of **68a,b** in a single experiment. We found that the reaction only proceeded if serine methyl ester **67** was first *isolated* as the free amine.³⁸¹ Acetylation of **66a,b** with acetic anhydride and catalytic DMAP afforded pure **68a,b** upon work-up. The remainder of the synthesis proceeded as previously described (Scheme 16).

Scheme 18. Synthetic route to dialkoxytriphenylphosphoranes **DTPP** and **DTPP-F₆**

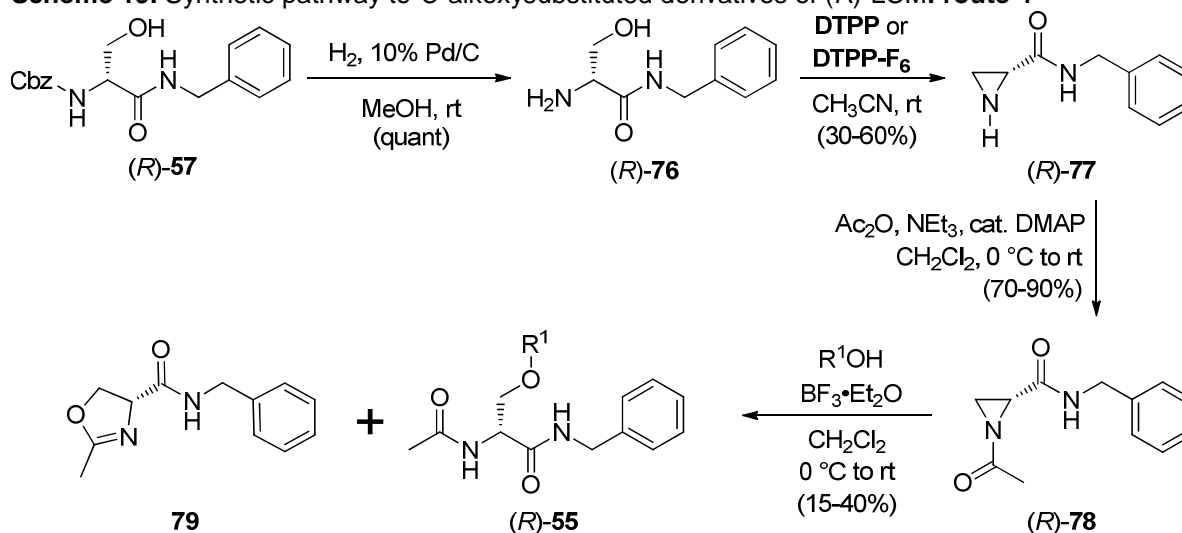


Although useful, **DTPP** proved to be a tedious reagent to prepare on large scale. The procedure required an initial centrifugation step (8000 rpm, 10 min) to remove finely divided NaBr , and 3–4 evaporation/filtration steps to remove $\text{PPh}_3(\text{O})$, a by-product of the reaction.³⁸⁷ Accordingly, we prepared the hexafluoro derivative of **DTPP**, $\text{PPh}_3(\text{OCH}_2\text{CF}_3)_2$, **DTPP-F₆**,³⁹⁰ by replacing NaOEt with a mixture of NEt_3 and $\text{CF}_3\text{CH}_2\text{OH}$ (Scheme 18).³⁹¹ Phosphorane formation proceeded faster and required only filtration and evaporation to yield the pure compound.³⁹¹ Unfortunately,

DTPP-F₆ provided a decreased yield of **66** (25–30%) after bulb-to-bulb transfer compared with **DTPP** (40–70%).

We examined a more convergent synthesis of the desired O-substituted LCM analogs (Scheme 19, **route 4**). Derivative (*R*)-**55** was obtained by catalytic hydrogenation of (*R*)-**57** and reaction with either **DTPP** or **DTPP-F₆** to give aziridine *N*-benzylcarboxamide (*R*)-**77**. Following acetylation, the *N*-acetylaziridine benzylamide (*R*)-**78** was ring-opened with several alcohols (phenol, phenethyl alcohol and 3-butyne-1-ol) to yield the corresponding derivative of (*R*)-LCM. Paralleling the formation of **68-a,b**, greater yields of (*R*)-**77** were obtained with **DTPP** (50–60%) compared with **DTPP-F₆** (30–35%) (Scheme 19, **route 4**).

Scheme 19. Synthetic pathway to O-alkoxysubstituted derivatives of (*R*)-LCM: **route 4**



Several factors, however, made this synthetic route inconvenient. First, the low volatility of the aziridine benzylamide (*R*)-**77** prevented its bulb-to-bulb distillation, thus requiring its purification using silica gel flash chromatography. Second, 2-oxazoline **79** was generated as a by-product in the final step, presumably

through the rearrangement the *N*-acetylaziridine ring under Lewis-acid catalyzed conditions.³⁹² Interestingly, this rearrangement was not observed when using the *N*-acetylaziridine carboxylate ester (Scheme 16, **route 3**). Compound **79** was not readily separated from the final product and complicated the purification of (*R*)-**55** by flash column chromatography. The pure LCM derivatives were only obtained by recrystallization and we were not able to purify 2-oxazoline **79**. Compound **79** was tentatively identified by the characteristic ¹³C resonance for the oxazoline CH₃ group (δ 13–14 ppm)³⁹³ and by HRMS.

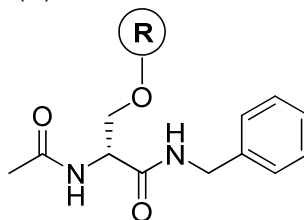
2.2.3. Structure activity relationship of the LCM 3-oxy-substituent

Large quantities of **68** were available using the **DTPP**-mediated aziridine synthesis. Using this new route we were able to explore the lacosamide SAR for the side chain oxy-substituent to identify potential structural constraints that would accompany either AB or CR placement at this site. We used different classes of alcohols to ring-open **68**, and in some instances **78**, and tested the new analogs of (*R*)-LCM at the NINDS ASP for anticonvulsant activity and neurotoxicity.³⁸¹

2.2.3.1. Choice of compounds

With little knowledge of the structural tolerance at this site we designed, synthesized, and tested a series of *O*-substituted derivatives for anticonvulsant activity. We probed for several potential protein/drug interactions. We examined the effect of steric size by replacing the LCM methoxy unit ((*R*)-**1**) by progressively

larger alkoxy groups ((*R*)-**48**, (*R*)-**80**–(*R*)-**82**) (Table 1). We introduced unsaturated aliphatic and aromatic systems ((*R,S*)-**49**, (*R*)-**83**–(*R*)-**88**, (*R*)-**90**, (*R*)-**91**, (*R*)-**98**) to look for potential hydrophobic, π - π , and cationic- π interactions.³⁹⁴ Within this set, we varied the length of the methylene spacer between several of these groups and the 3-oxy site in (*R*)-**55**. Not to limit ourselves to strictly lipophilic interactions, we prepared derivatives containing a polar side chain ((*R*)-**96**, (*R*)-**99**, (*R*)-**100**). These compounds could accept and/or donate a hydrogen bond(s) to a suitable amino acid residue within the putative drug binding pocket(s). Finally, we evaluated LCM oxy-substituted analogs that contained either an AB ((*R*)-**92**–(*R*)-**95**) or a CR group ((*R*)-**84**, (*R*)-**97**). In those cases where little or no anticonvulsant activity was observed for the AB agent, we prepared the corresponding isostere to see if metabolic factors, or structural and electrophysical constraints contributed to the loss of activity.³⁹⁵⁻⁴⁰⁰

Table 1. The Structure Activity Relationship of O-Substituted (*R*)-Lacosamide Derivatives

No.	R	mp (°C)	Mice (ip) ^b				Rat (po) ^c		
			MES, ^d ED ₅₀	6 Hz, ED ₅₀ ^e	Tox, ^f TD ₅₀	PI ^g	MES, ^d ED ₅₀	Tox, ^h TD ₅₀	PI ^g
1 ⁱ	CH ₃	142–143	4.5 [0.5] (3.7 – 5.5)		27 [0.25] (26 – 28)	6.0	3.9 [0.5] (2.6 – 6.2)	>500	>128
1-<i>d</i>₃	CD ₃	142–143					5.2 [0.5] (4.3 – 5.7)	~200	~38
48	CH ₂ CH ₃	129–130	7.9 [0.25] (5.3 – 10)		44 [0.25] (37 – 54)	5.6	5.6 [0.25] (2.5 – 16)	>500	>89
80	CH(CH ₃) ₂	151–153	23 [0.25] (20 – 26)	23 [0.25] (16 – 28)	77 [0.25] (66 – 96)	3.3	8.6 [0.25] (6.9 – 13)	>500	>58
81	C(CH ₃) ₃	126–127	30-100 [0.5]		~300 [0.5]				
82	C ₆ H ₁₁	134–135	100-300 [0.5]		~300 [0.5]		~30 [0.25]	>30	
83	C ₆ H ₅	169–170	100-300 [0.5]		>600 [0.5]				
49 ⁱ	CH ₂ CH=CH ₂ (<i>R,S</i>)	76–77	30–100		30–100				
84 ^j	CH ₂ C≡CH	149	16 [0.25] (13 – 19)	29 [0.5] (21 – 40)	59 [0.25] (55 – 66)		7.9 [0.5] (4.7 – 11)	>500	>63
85 ^k	CH ₂ C≡CCH ₃	149–151	30-100 [0.5]		30-100 [0.5]				
86	CH ₂ C ₆ H ₁₁	143–144	100-300 [0.5]		~300 [0.5]				

87	<chem>CH2C6H5</chem>	145–146	64 [0.25] (56 – 76)		200 [0.25] (160 – 300)	3.2	>30	>30	
88	<chem>CH2CH2CH=CH2</chem>	103–104	30-100 [0.5]		~100 [0.5]		17 [0.5] (13 – 21)	>500	>29
89	<chem>CH2CH2C1CC1</chem>	97–99	46 [0.25] (42 – 50)		85 [0.25] (69 – 105)	1.9	>30	>30	
90	<chem>CH2CH2C#CH</chem>	111–113	30–100 [0.5]		30–100 [0.5]				
91	<chem>CH2CH2C6H5</chem>	90–92	100-300 [0.5]		100-300 [0.5]		>30	>30	
92'	<chem>CH2CH2C1(C)N1</chem>		30-100 [0.5]		100-300 [0.5]		44 [1] (28–65)	>500	>11
93	<chem>CH2CH2C(O)H</chem>	120–121	>300 [0.5]		>300 [0.5]		>100		
94	<chem>CH2CH2C1OC1</chem>	104–110	>300 [0.5]		>300 [0.5]				
95' ⁱ	<chem>CH2CH2NCS</chem>		>300 [0.5]		100-300 [0.5]		<30 [4]	>30 [4]	
96	<chem>CH2CH2NHC(O)CH3</chem>	166–168	>300 [0.5]		>300 [0.5]		>30	>30	
97	<chem>CH2CH2N3</chem>	111–113	100-300 [0.5]	44 [0.25] (32 – 65)			>40 [0.25] (po) 5.7 [0.25] (ip) (3.6 – 8.4)	78 [0.25] (ip) (72 – 83)	>13
98	<chem>CH2CH2N1C=CC1COCH3</chem>	127–129	>300 [0.5]	>100	>300 [0.5]				
99	<chem>CH2CH2OCH3</chem>	109–110	30-100 [0.5]		~300 [0.5]				
100	<chem>(CH2CH2O)2CH3</chem>	48–52	>300 [0.5]	>100	>300 [0.5]		>30	>50	
<hr/> phenytoin ^m			9.5 [2] (8.1–10)		66 [2] (53–72)	6.9	30 [4] (22–39)	"	> 100

phenobarbital ^m	22 [1] (15 – 23)	69 [0.5] (63 – 73)	3.2	9.1 [0.5] (7.6 – 12)	61 [0.5] (44 – 96)	6.7
valproate ^m	270 [0.25] (250 – 340)	430 [0.25] (370 – 450)	1.6	490 [0.5] (350 – 730)	280 [0.5] (190 – 350)	0.6

^a All compounds tested corresponded to the (*R*)-enantiomer except **49**. The compounds were tested through the auspices of the NINDS ASP. ^b The compounds were administered intraperitoneally. ED₅₀ and TD₅₀ values are in milligrams per kilogram. ^c The compounds were administered orally unless otherwise indicated. ED₅₀ and TD₅₀ values are in mg/kg. ^d MES = maximal electroshock seizure test. ^e The 6 Hz test was carried out at 32 mA. ^f TD₅₀ value determined from the rotorod test. ^g PI = protective index (TD₅₀/ED₅₀). ^h Tox = behavioral toxicity. ⁱ Ref.1. ^j Ref.23. ^k Work of Dr. Ki Duk Park. ^l Work of Dr. Christophe Salomé. ^m Porter, R. J.; Cereghino, J J.; Gladding, G. D.; Hessie, B. J.; Kupferberg, H. J.; Scoville, B.; White, B. G.; *Cleveland Clin. Q.* **1984**, 51, 293-305. ⁿ No ataxia observed up to 3000 mg/kg.

2.2.3.2. Pharmacological results

Compounds (*R*)-**1**, (*R*)-**48**, (*R,S*)-**49**, (*R*)-**80**–(*R*)-**100** were tested for anticonvulsant activity at the NINDS ASP using the procedures described by Stables and Kupferberg.⁴⁰¹ The pharmacological data from the MES^{401,402} and 6 Hz⁵⁷ tests are summarized in Table 1 along with clinical AEDs phenytoin,⁴⁰³ valproate,⁴⁰³ and phenobarbital.⁴⁰³ All compounds were administered intraperitoneally (ip) to mice and orally (po) to rats unless otherwise indicated. The table lists the values that were determined to be protective in blocking hind limb extension induced in the MES seizure model from the rodent identification studies. For compounds that showed significant activity, we report the effective dose (50%) (ED₅₀) values obtained in quantitative screening evaluations. Also provided are the median doses for neurological impairment (50%) (TD₅₀) in mice, using the rotorod test,⁷⁵ and the behavioral toxicity effects observed in rats. TD₅₀ values were determined for those compounds exhibiting significant activity in the MES test. The protective index (PI = TD₅₀/ED₅₀) for these analogs are also listed. Select compounds were evaluated in the psychomotor 6 Hz (32 mA) seizure models (mice, ip).⁵⁷ When the derivatives were evaluated in the scPTZ seizure model⁴⁰¹ none provided protection at 300 mg/kg doses at the times (0.5 and 4 h) tested (data not shown). The absence of seizure protection in this assay is a hallmark of FAA activity.^{234,367,241,368,237,369,238,370}

In total, 23 new O-substituted LCM analogs were prepared and evaluated for anticonvulsant activity at the NINDS ASP. We observed a steady increase in activity in mice (ip, [0.25–0.5 h]) as the substituent steric size decreased from cyclohexyl ((*R*)-**82**, ED₅₀ = 100–300 mg.kg⁻¹), phenyl ((*R*)-**83**, ED₅₀ = 100–300 mg.kg⁻¹), and

tert-butyl ((*R*)-**81**, ED₅₀ = 30–100 mg.kg⁻¹), to isopropyl ((*R*)-**80**, ED₅₀ = 23 mg.kg⁻¹), to ethyl ((*R*)-**48**, ED₅₀ = 7.9 mg.kg⁻¹) and to methyl ((*R*)-**1**, ED₅₀ = 4.5 mg.kg⁻¹), indicating that non-bulky 3-oxy substituted groups in (*R*)-**55** analogs provided the highest anticonvulsant activity.³⁸¹ Interestingly, we observed a similar increase in activity as the size of the 3-oxy substituent decreased when the compounds were administered orally to rats, but the range of activities was narrower. For example, the *O*-cyclohexyl derivative (*R*)-**82** exhibited an ED₅₀ of ~30 mg/kg while *O*-isopropyl (*R*)-**80** (ED₅₀ = 5.6 mg/kg), *O*-ethyl (*R*)-**48** (ED₅₀ = 5.2 mg/kg), and *O*-methyl (*R*)-**1** (ED₅₀ = 3.9 mg/kg) all displayed excellent seizure protection. (*R*)-**48** and (*R*)-**80** showed no behavioral neurotoxicity in the rat at the highest dose (500 mg/kg) tested, leading to high PI values for both compounds ((*R*)-**48**: PI >89; (*R*)-**80**: PI >58). When we inserted a methylene group between the cyclohexyl group and 3-oxy site in (*R*)-**82** (ED₅₀ = 100–300 mg/kg) to give (*R*)-**86** (ED₅₀ = 100–300 mg/kg), we observed no improvement in anticonvulsant activity in mice (ip).

Next, we examined the effect of incorporating an unsaturated unit at the 3-oxy site in (*R*)-**55**. When the *O*-phenoxy (*R*)-**83** derivative was evaluated, we observed minimal protection in the MES test in mice (ip) (ED₅₀ = 100–300 mg/kg).³⁸¹ Correspondingly, in mice we found pronounced anticonvulsant activity for other derivatives that contained an unsaturated 3-oxy substituent. The *O*-allyl²³⁴ ((*R,S*)-**49**, ED₅₀ = 30–100 mg/kg), *O*-propargyl ((*R*)-**84**, ED₅₀ = 16 mg/kg),³⁸⁴ and *O*-but-2-ynyl ((*R*)-**85**, ED₅₀ = 30–100 mg/kg) (*R*)-**1** analogs all provided pronounced seizure protection. When the *O*-propargyl ((*R*)-**84**, ED₅₀ = 7.9 mg/kg) and the *O*-but-2-ynyl ((*R*)-**85**, ED₅₀ = 6.4 mg/kg) (*R*)-**55** derivatives were tested in the rat (po) we

observed excellent seizure protection, which was comparable with phenytoin ($ED_{50} = 6.9 \text{ mg/kg}$),⁴⁰³ and no behavioral neurological toxicity at 500 mg/kg. Significantly, the propargyl unit was shown to be a superior CR unit in bioorthogonal Cu(I)-mediated cycloaddition reactions.^{384,276} Our finding that (*R*)-**84** and (*R*)-**85** exhibited excellent activity in the MES seizure model indicated that this CR unit in (*R*)-**1** AB&CR agents would not likely impact the unit's binding to its cognate receptor(s). Inserting a methylene group between the C(3)-oxy site and the phenyl group in *O*-phenoxy (*R*)-**83** ($ED_{50} = 100\text{-}300 \text{ mg/kg}$) to give the *O*-benzyl derivative (*R*)-**87** ($ED_{50} = 64 \text{ mg/kg}$) led to improved seizure protection in mice (ip). These collective findings suggest that beneficial protein interactions with the 3-oxy π -system in (*R*)-**55** existed at the drug binding site(s) responsible for MES-induced seizure protection. This interaction with the 3-oxy site in (*R*)-**55** analogs may offset adverse steric effects introduced when a larger, unsaturated group was included at this position.

We next explored the effect of adding a second methylene unit between the unsaturated unit and the (*R*)-**55** 3-oxy site to determine if the location of the unsaturated site affected anticonvulsant activity. When we added the second methylene group to *O*-propargyl (*R*)-**84** ($ED_{50} = 16 \text{ mg/kg}$) and *O*-benzyl (*R*)-**87** ($ED_{50} = 64 \text{ mg/kg}$) to give *O*-3-butynyl (*R*)-**90** ($ED_{50} = 30\text{--}100 \text{ mg/kg}$) and *O*-2-phenylethyl (*R*)-**91** ($ED_{50} = 100\text{--}300 \text{ mg/kg}$) (*R*)-**55** derivatives, we saw a decrease in anticonvulsant activity in mice (ip). Like the *O*-phenylethyl derivative (*R*)-**91** ($ED_{50} = 100\text{-}300 \text{ mg/kg}$), the *O*-triazolyethyl (*R*)-**98** compound ($ED_{50} = >300 \text{ mg/kg}$) did not display activity at the doses tested. Nonetheless, when tested orally in rats, the *O*-3-butynyl (*R*)-**90** ($ED_{50} = <30 \text{ mg/kg}$) provided appreciable seizure protection.

These results indicated that the site of unsaturation at the 3-oxy site in (*R*)-**55** may be important for anticonvulsant activity. We observed one exception to this pattern, the *O*-allyl ((*R,S*)-**49**, ED₅₀ = 30–100 mg/kg) and the *O*-3-butenyl ((*R*)-**88**, ED₅₀ = 30–100 mg/kg) (*R*)-**55** derivatives showed similar anticonvulsant activity in mice (ip). Like *O*-3-butynyl (*R*)-**90**, the activity of the *O*-3-butenyl (*R*)-**88** derivative improved from mice (ip) (ED₅₀ = 30–100 mg/kg) to rat (po) (ED₅₀ = 17 mg/kg).

The effect of polar substituents at the C(2) site in (*R*)-**55** was assessed by incorporating either an ethylenoxy or an acetamidoethoxy unit two methylene units removed from the 3-oxy site. When we attached one ethylenoxy group to give methyl ether (*R*)-**99**, we observed noticeable seizure protection (ED₅₀ = 30–100 mg/kg). Adding a second ethylenoxy spacer to (*R*)-**99** to give (*R*)-**100** produced no detectable activity under the test conditions (ED₅₀ = >300 mg/kg). Similarly, the acetamidoethyl analog (*R*)-**96** (ED₅₀ = >300 mg/kg) was inactive at the doses tested. The limited data do not allow us to speculate on the factors responsible for the loss of anticonvulsant activity of (*R*)-**96**, (*R*)-**99**, and (*R*)-**100**, and our findings indicated that introducing polar substituents at the 3-oxy site in (*R*)-**55** did not improve seizure protection.

We tested (*R*)-**55** derivatives, (*R*)-**93**–(*R*)-**95**, that contained AB groups at their 3-oxy sites. The electrophilic groups aldehyde (*R*)-**93** (ED₅₀ = >300 mg/kg) and epoxide (*R*)-**94** (ED₅₀ = >300 mg/kg) exhibited no anticonvulsant activity and no neurological toxicity at the doses tested. The lack of neurotoxicity may suggest that the compounds did not cross the blood brain barrier. The aliphatic isothiocyanate (*R*)-**95** was inactive in mice (ED₅₀ = >300 mg/kg), active in rats (ED₅₀ = <30 mg/kg),

but neurologically toxic ($TD_{50} = 30\text{--}100$ mg/kg, mice (ip); $TD_{50} >30$ mg/kg, rat (po)). We suspect that several of these AB groups may have metabolized under the test conditions. Indeed, aldehydes and epoxides are known substrates for a variety of enzymes (e.g., aldehyde reductases, epoxide hydrolases).³⁹⁵⁻⁴⁰⁰ Since we planned to use these AB groups for in vitro experiments where metabolism would less likely be an issue, we evaluated, where possible, the corresponding AB isostere to determine if the steric size of the AB group precluded their use. We were gratified to find that the *O*-but-3-enyl isostere (*R*)-**88** ($ED_{50} = 30\text{--}100$ mg/kg, mice (ip); $ED_{50} = 17$ mg/kg, rat (po)) for aldehyde (*R*)-**93** and the *O*-cyclopropyl isostere (*R*)-**89** ($ED_{50} = 46$ mg/kg, mice (ip)) for epoxide (*R*)-**94** displayed pronounced-to-excellent anticonvulsant activity. Thus, we have not attributed the absence of activity for aldehyde (*R*)-**93** and epoxide (*R*)-**94** to steric factors. Similar to the *O*-cyclopropyl (*R*)-**89**, the photolabile methyldiazirine AB derivative (*R*)-**92** exhibited pronounced animal protection in the MES seizure test ($ED_{50} = 30\text{--}100$ mg/kg, mice (ip); $ED_{50} = 44$ mg/kg, rat (po)).

Of all the *O*-substituted LCM analogs prepared, the CR *O*-azidoethyl (*R*)-**97** was the most intriguing. Its anticonvulsant activity was dependent on the animal, the seizure test, and the route of administration. While (*R*)-**97** displayed poor MES seizure protection in mice (ip) ($ED_{50} = 100\text{--}300$ mg.kg⁻¹), it proved potent in the 6 Hz test when administered to mice by the same route of administration ($ED_{50} = 44$ mg.kg⁻¹, 32 mA stimulation). Furthermore, we observed that (*R*)-**97** exhibited exceptional activity in the MES test in the rat when administered ip ($ED_{50} = 5.7$

mg.kg⁻¹), but that activity dropped with oral administration (MES ED₅₀ >40 mg.kg⁻¹). The TD₅₀ for (*R*)-**97** was 78 mg.kg⁻¹ (rat, po), providing a PI greater than 13.

2.2.3.3. Discussion

The composite SAR documented the stringent structural requirements for the 3-oxy site in (*R*)-**55**. In mice (ip), the *O*-substituent that afforded the best activity was methyl ((*R*)-**1**, ED₅₀ = 4.5 mg.kg⁻¹). Replacing the *O*-methyl group with ethyl ((*R*)-**48**, ED₅₀ = 7.9 mg/kg), isopropyl ((*R*)-**80**, ED₅₀ = 23 mg/kg), *tert*-butyl ((*R*)-**81**, ED₅₀ = 30-100 mg/kg), and cyclohexyl ((*R*)-**82**, ED₅₀ = 100-300 mg/kg) led to a steady drop in anticonvulsant activity in the MES seizure test. The difference in activity for (*R*)-**1**, (*R*)-**48** and (*R*)-**80** diminished in the rat (po) model where the MES ED₅₀ values were below 10 mg/kg. We concluded that including bulky alkyl substituents at the 3-oxy site in (*R*)-**55** adversely affected seizure protection in the MES seizure test.

Inserting one methylene (CH₂) group between the oxygen and the cyclohexyl ring in (*R*)-**82** (ED₅₀ = 100-300 mg/kg) to give (*R*)-**85** (ED₅₀ = 100–300 mg/kg) did not improve activity in mice (ip). However, we observed a significant increase in potency in mice going from *O*-phenyl (*R*)-**83** (ED₅₀ = 100–300 mg/kg) to *O*-benzyl (*R*)-**87** (ED₅₀ = 64 mg/kg). Pronounced-to-excellent activity was also observed for the *O*-allyl (*R,S*)-**49** (ED₅₀ = 30–100 mg/kg) and the *O*-propargyl (*R*)-**84** (ED₅₀ = 16 mg/kg) compounds. Inclusion of an ethylene (CH₂CH₂) spacer between the oxygen and the phenyl groups to provide (*R*)-**91** (ED₅₀ = 100–300 mg/kg) led to a loss of activity, compared with (*R*)-**87** that contained a methylene spacer. A similar activity loss in

mice was observed going from the *O*-propargyl compound (*R*)-**84** (ED₅₀ = 16 mg/kg) to the *O*-3-butynyl derivative (*R*)-**90** (ED₅₀ = 30-100 mg/kg). When several of these compounds were tested in the rat (po), we observed improved anticonvulsant activity (i.e., (*R*)-**84**, (*R*)-**88**, (*R*)-**90**). The pronounced-to-excellent activity in the *O*-benzyl (*R*)-**87** (ED₅₀ = 64 mg/kg), *O*-propargyl (*R*)-**84** (ED₅₀ = 16 mg/kg), *O*-but-2-ynyl (*R*)-**85** (ED₅₀ = 30–100 mg/kg), and racemic *O*-allyl (*R,S*)-**49** (ED₅₀ = 30–100 mg/kg) derivatives suggested that a favorable interaction with the 3-oxy π system in (*R*)-**55** at the target site(s) may foster binding, provided the group was not large and the unsaturated system was correctly positioned at the 3-oxy site.

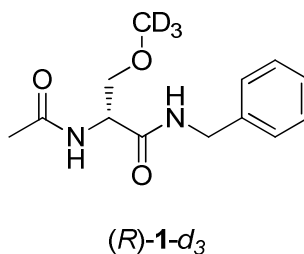
Compounds (*R*)-**96**, (*R*)-**99**, and (*R*)-**100** were prepared to help us determine if potential hydrogen bonding interactions at the 3-oxy site in (*R*)-**55** would affect anticonvulsant activity. Methyl ether (*R*)-**99** contained one ethylenoxy unit at the 3-oxy site and showed significant activity (ED₅₀ = 30–100 mg/kg). Adding a second ethylenoxy unit to give (*R*)-**100** (ED₅₀ = >300 mg/kg) led to a loss of anticonvulsant activity. Replacement of the ethylenoxy moiety in (*R*)-**99** with an acetamidoethoxy group provided (*R*)-**96** (ED₅₀ = >300 mg/kg), which was inactive in the MES seizure test. When (*R*)-**99** was compared with two non-polar analogs, (*R*)-**88** (ED₅₀ = 30–100 mg/kg) and (*R*)-**90** (ED₅₀ = 30–100 mg/kg), we found that it displayed similar anticonvulsant activity. We concluded that introducing additional oxygen and nitrogen substituents at the (*R*)-**55** 3-oxy site did not improve activity. Several factors may be responsible for these whole animal pharmacological findings, such as (*R*)-**55** biodistribution in the brain, metabolism, and drug binding. Our data do not allow us to distinguish these factors but do provide valuable information for

the installation of both AB and CR units in the (*R*)-**1** framework and future drug design efforts.

As part of our (*R*)-**55** 3-oxy SAR study, we prepared several (*R*)-**55** AB agents ((*R*)-**92**–(*R*)-**95**) and (*R*)-**55** CR agents ((*R*)-**84**, (*R*)-**97**). The alkyne (*R*)-**84** and azide (*R*)-**97** CR compounds displayed excellent anticonvulsant activity (ED_{50} = <10 mg/kg) in the rat upon po and ip administration, respectively. These findings supported the use of these CR units in (*R*)-**1** proteomic target searches. Correspondingly, of the four (*R*)-**55** AB agents we prepared, only the diazirinyl (*R*)-**92** showed anticonvulsant activity, modest in mice at ED_{50} = 30–100 mg/kg and in rat at ED_{50} = 44 mg/kg. The three other (*R*)-**55** AB agents, (*R*)-**93**–(*R*)-**95** displayed no anticonvulsant activity in mice (ip) at the highest dose tested (300 mg/kg). When (*R*)-**95** was tested in the rat (po), we observed activity at 30 mg/kg. To test whether the structural size of the AB units in aldehyde (*R*)-**93** and epoxide (*R*)-**94** was responsible for anticonvulsant activity loss in the MES seizure model, we prepared the isosteres (*R*)-**88** and (*R*)-**89**, respectively. When (*R*)-**88** (ED_{50} = 30–100 mg/kg) and (*R*)-**89** (ED_{50} = 46 mg/kg) were evaluated in the MES seizure model in mice, we observed appreciable seizure protection for both compounds, suggesting that other factors, such as metabolism or drug biodistribution in the CNS, were responsible for the inactivity of these (*R*)-**55** AB agents in animals.

Finally, we asked whether the methyl-*d*₃ analog of (*R*)-**1**, (*R*)-**1-d**₃, would display enhanced anticonvulsant activity over (*R*)-**1**. Recently, pharmaceutical companies have prepared deuterated versions (“heavy drugs”) of marketed medicinal agents.⁴⁰⁴ The greater strength of C–D bonds compared with C–H bonds

is predicted to confer increased metabolic stability for the deuterated version of the drug.⁴⁰⁴ Significantly, the major metabolite for (*R*)-**1** in humans is the desmethyl analog (*R*)-**53**.⁴⁰⁵ The metabolic conversion of (*R*)-**1** to (*R*)-**53** has not been attributed to a specific metabolic enzyme.⁴⁰⁶ Nonetheless, (*R*)-**53** accounts for ~30% of the (*R*)-**1** excreted in human urine,²⁰³ and it exhibits little anticonvulsant activity (ED_{50} = 100–300 mg/kg).²³⁴ Accordingly, we reasoned that replacing the 3-oxy methyl group in (*R*)-**1** with the perdeuterated methyl unit to give (*R*)-**1-d**₃ might reduce metabolic processes and thus lead to increased bioavailability of the AED. We prepared (*R*)-**1-d**₃ using a method we reported for (*R*)-**1**⁴⁸ and substituting CD₃I for CH₃I. The deuterated derivative (*R*)-**1-d**₃ (ED_{50} = 5.2 mg/kg) showed an anticonvulsant activity in the rat (po) comparable with (*R*)-**1** (ED_{50} = 3.9 mg/kg), without exceeding it, and exhibited greater neurological toxicity ((*R*)-**1-d**₃, TD_{50} = ~200 mg/kg; (*R*)-**1**, TD_{50} = >500 mg/kg).



2.2.4. Experimental Section

General Methods

Melting points were determined in open capillary tubes using a Thomas-Hoover melting point apparatus and are uncorrected. Infrared spectra (IR) were run on an ATI Mattson Genesis FT-IR spectrometer. Absorption values are expressed in wavenumbers (cm^{-1}). Optical rotations were obtained on a Jasco P-1030 polarimeter at the sodium D line (589 nm) using a 1 dm path length cell and are given in units of $\text{deg cm}^3 \text{g}^{-1} \text{dm}^{-1}$. NMR spectra were obtained at 300 MHz (^1H) and 75 MHz (^{13}C) using TMS as an internal standard. Chemical shifts (δ) are reported in parts per million (ppm) from tetramethylsilane. Low-resolution mass spectra were obtained with a BioToF-II-Bruker Daltonics spectrometer by Drs Matt Crowe and S. Habibi at the University of North Carolina Department of Chemistry. The high-resolution mass spectrum was performed on a Bruker Apex-Q 12 Telsa FTICR spectrometer by Drs Matt Crowe and S. Habibi. Microanalyses were performed by Atlantic Microlab, Inc. (Norcross, GA). Reactions were monitored by analytical thin-layer chromatography (TLC) plates (Aldrich, Cat # Z12272-6) and analyzed with 254 nm light. The reaction mixtures were purified by flash column chromatography using silica gel (Dynamic Adsorbents Inc., Cat #02826-25). All chemicals and solvents were reagent grade and used as obtained from commercial sources without further purification. THF was distilled from blue sodium benzophenone ketyl. Yields reported are for purified products and were not optimized. All compounds were checked by TLC, ^1H and ^{13}C

NMR, MS, and elemental analyses. The TLC, NMR and the analytical data confirmed the purity of the products was $\geq 95\%$.

2.2.4.1. Synthetic procedures

2.2.4.1.1. General procedure for the aziridine ring-opening with alcohols. Method A

To a cooled CH_2Cl_2 solution (ice bath) of **68a,b** or **78** ($[\text{C}] \sim 0.5\text{--}1\text{ M}$) and the appropriate alcohol (1–5 equiv) was added $\text{BF}_3 \cdot \text{Et}_2\text{O}$ (1 equiv) dropwise while stirring. After addition, the mixture was warmed to room temperature and stirred (30 min), and then an equal volume of saturated aqueous NaHCO_3 was added. The reaction was vigorously stirred (15 min) and the organic layer separated. The aqueous layer was extracted with CH_2Cl_2 until no additional product could be detected (TLC analysis). All the organic layers were then combined, dried (Na_2SO_4), and concentrated in vacuo to yield a residue that was either or used directly for the next step, purified by flash column chromatography, or recrystallized from EtOAc and hexanes.

2.2.4.1.2. General procedure for the ester hydrolysis of *N*-acetylserine esters with LiOH. Method B

To a THF solution of serine methyl ester (2 volumes, $[\text{C}] \sim 0.1\text{ M}$) was added an aqueous solution (1 volume) of LiOH (1 equiv). The homogeneous solution was stirred at room temperature (60 min), after which time Et_2O (2 volumes) was added. The aqueous layer was recovered, and washed with Et_2O . The remaining aqueous

layer was acidified (pH \sim 1) by the dropwise addition of aqueous concentrated HCl, saturated with NaCl, and extracted with EtOAc until no further product was detected (TLC analysis). The combined organic layers were combined, dried (Na_2SO_4), and evaporated to an oily residue that was used directly for the next step or recrystallized from EtOAc and hexanes to provide an analytical sample.

2.2.4.1.3. General procedure for the MAC reaction. Method C

To a cooled THF solution ($-78\text{ }^\circ\text{C}$, dry ice/acetone bath) of acid ($[\text{C}] \sim 0.1\text{ M}$) were successively added NMM (1.0 equiv), stirred for 2 min, IBCF (1.0 equiv), stirred for 15 min, and then the desired benzylamine (1.0 equiv). Upon addition the reaction mixture was allowed to warm to room temperature and further stirred (2 h). The salts were filtered and rinsed with THF, and the filtrate was concentrated in vacuo. The residue obtained was purified by flash chromatography, followed by recrystallization from EtOAc and hexanes when necessary.

2.2.4.1.4. General procedure for the DMTMM coupling reaction. Method D

To a THF solution of acid ($[\text{C}] \sim 0.1\text{ M}$) at room temperature was added the desired benzylamine (1.2 equiv). The solution was stirred (5–10 min) until the benzylammonium carboxylate precipitated. With stirring, DMTMM (1.2 equiv) was added all at once, and the resulting suspension was stirred at room temperature (3–12 h). In those cases where a salt did not precipitate, DMTMM was added after 15 min to the solution. The salts were removed by filtration and washed with THF,

and the solvent was removed in vacuo. The residue obtained was purified by flash column chromatography to afford the benzylamide, and then recrystallized from EtOAc and hexanes.

2.2.4.1.5. General procedure for the Swern oxidation reaction. Method E

To a cooled solution (dry ice/acetone bath) of oxalyl chloride (1.3 equiv) in anhydrous CH_2Cl_2 ([C] ~ 0.5 M) was added dropwise a CH_2Cl_2 solution of DMSO (2.6 equiv) ([C] ~ 0.5 M). After stirring at -78°C (15 min) a solution of alcohol (1.0 equiv) in CH_2Cl_2 or a mixture of CH_2Cl_2 and DMSO ([C] ~ 0.5 M) was added dropwise at -78°C and the reaction was stirred at -78°C (1 h). DIEA (5 equiv) was then added dropwise, stirred (20 min), warmed to room temperature and then stirred (30 min). Minimal amounts of aqueous 10% citric acid solution were added to the solution until the pH of the aqueous layer remained acidic (pH ~ 3). The CH_2Cl_2 layer was separated and the aqueous layer extracted with CH_2Cl_2 (~ 6 to 7 volumes) until no more UV visible product was detected (TLC analysis) in the organic layer. The combined organic layers were washed with brine (1 volume), dried (Na_2SO_4), and evaporated to give an oily residue. Recrystallization from EtOAc and hexanes afforded the pure aldehyde.

2.2.4.1.6. General procedure for the Corey-Chaykovsky epoxidation. Method F

Trimethylsulfoxonium iodide (1.2 equiv.) and NaH (60% dispersion in mineral oil, 1.2 equiv.) were suspended in DMSO or DMF ([C] ~ 0.1 M) and stirred under N_2

(1 h) until a clear solution was obtained (**solution A**). The aromatic aldehyde (1.0 equiv) was added at once as a solid and the reaction was stirred at room temperature (12 h). Brine was added (10 volumes) and the aqueous layer was extracted with CH_2Cl_2 until no additional product was detected in the aqueous layer. The combined organic layers were dried (Na_2SO_4), evaporated, and the residue was purified by flash chromatography and recrystallized from EtOAc and hexanes.

2.2.4.1.7. General procedure for the Williamson ether synthesis. Method G

A CH_3CN solution of alcohol ([C] $\sim 0.05\text{--}0.5$ M), Ag_2O (5 equiv) and MeI (10 equiv) was stirred at room temperature (2–3 d). The reaction was filtered through Celite[®], and the solvent was evaporated in vacuo. The residue was purified by silica gel chromatography or used directly for the next step.

2.2.4.1.8. General procedure for the Pd-catalyzed hydrogenation reaction. Method H

A MeOH suspension of the starting material ([C] $\sim 0.01\text{--}0.2$ M) and 10% Pd/C (10% w/w) was vigorously stirred under an atmosphere of H_2 (balloon) at room temperature (16 h). The mixture was filtered through a bed of Celite[®]. The bed was washed with MeOH and CH_2Cl_2 , the washings were collected and evaporated in vacuo. The amine was used without further purification.

2.2.4.1.9. General procedure for the aromatic aldehyde deprotection. Method I

To a THF solution of the protected aldehyde ([C] ~0.1–0.5 M, 2 volumes) was added 1 volume of aqueous 0.1 M HCl. The reaction was stirred at room temperature (15 h) and the THF was removed in vacuo. The remaining aqueous layer was extracted with CH₂Cl₂ until no compound was detectable (TLC analysis). The combined organic layers were washed with brine (1 volume), dried (Na₂SO₄) and evaporated to yield the aldehyde that was purified either by silica gel chromatography or recrystallized from EtOAc and hexanes.

2.2.4.1.10. General Procedure for the *m*-CPBA epoxidation. Method J

A CH₂Cl₂ ([C] ~0.1 M) solution of *m*-CPBA (1.0–1.2 equiv) was stirred in the presence of anhydrous Na₂SO₄ at room temperature (5 min). The starting material was then added at once as a solid (1.0 equiv) and the reaction was allowed to proceed at room temperature (15 h). The Na₂SO₄ was filtered, the solvent removed under vacuum, and the residue purified by silica gel chromatography.

2.2.4.2. Synthesis of *N*-acetylaziridine carboxylate esters and carboxamides

Methyl (2*R*)-1-Tritylaziridine-2-carboxylate ((*R*)-65).³⁸³ D-Serine methyl ester hydrochloride (25.0 g, 161 mmol) was suspended in CH₂Cl₂ (200 mL) and cooled to 0 °C. While stirring, Et₃N (44.8 mL, 322 mmol) was added, followed by the portionwise addition of trityl chloride (44.8 g, 161 mmol). The reaction was stirred at

0 °C (24 h), filtered and the filtrate was successively washed with a 10% aqueous citric acid solution (200 mL) and brine (200 mL), dried (Na₂SO₄), and evaporated to yield 55.1 g of a white foam. The foam was dissolved in CH₂Cl₂ (400 mL), cooled (0 °C) and Et₃N (32 mL, 207 mmol) was added followed by the dropwise addition of mesyl chloride (13.2 mL, 167.6 mmol). The reaction was maintained at 0 °C (40 min), filtered, and the filtrate was washed with a 10% aqueous citric acid solution (400 mL), and brine (400 mL), dried (Na₂SO₄), and evaporated to give 65.0 g of a pale yellow foam. The foam was dissolved in 1,2-dimethoxyethane (110 mL) and Et₃N (44.8 mL, 322 mmol) was added. The solution was heated to reflux (24 h), cooled to room temperature and washed with 10% aqueous citric acid (2 x 250 mL), saturated aqueous sodium bicarbonate (2 x 250 mL), and brine (2 x 250 mL), dried (Na₂SO₄), and evaporated. The crude residue was recrystallized from EtOH to yield 32.2 g (58%) of (*R*)-**65** as a white solid. Pure (*R*)-**65** could also be obtained by SiO₂ chromatography (1/3 hexanes/CHCl₃): mp 124–126 °C (lit.³⁸³ mp 123–125°C); [α]_D²⁵ +91.2° (c 1.0, EtOAc); *R*_f = 0.52 (1/3 hexanes/CHCl₃); ¹H NMR (CDCl₃) δ 1.41 (dd, *J* = 1.8, 7.0 Hz, NCHH'CH), 1.89 (dd, *J* = 3.0, 7.0 Hz, CHC(O)OCH₃), 2.55 (dd, *J* = 1.8, 3.0 Hz, NCHH'CH), 3.75 (s, C(O)OCH₃); ¹³C NMR (CDCl₃) δ 28.7 (NCH₂CH), 31.8 (CHC(O)OCH₃), 52.2 (C(O)OCH₃), 74.5 (NCPH₃), 127.1, 127.8, 129.4, 143.7 (3 C₆H₅), 172.0 (C(O)OCH₃).

Methyl (2*S*)-1-Tritylaziridine-2-carboxylate ((*S*)-65**).**³⁸³ Following the preceding procedure, L-serine methyl ester hydrochloride (25.0 g, 161 mmol), Et₃N (44.8 mL, 322 mmol), trityl chloride (44.8 g, 161 mmol) in CH₂Cl₂ (200 mL), followed by Et₃N

(32 mL, 207 mmol), mesyl chloride (13.2 mL, 167.6 mmol) in CH_2Cl_2 (400 mL), and Et_3N (44.8 mL, 322 mmol) in 1,2-dimethoxyethane (110 mL) gave 30.8 g (56%) of (*S*)-**65** as a white solid upon work-up and recrystallization from EtOH: mp 124–126 °C (lit.³⁸³ mp = 123–125 °C); $[\alpha]_D^{25}$ -90.9° (c 1.0, EtAc); R_f = 0.52 (1/3 hexanes/ CHCl_3); ^1H NMR (CDCl_3) δ 1.41 (dd, J = 1.8, 7.0 Hz, $\text{NCHH}'\text{CH}$), 1.89 (dd, J = 3.0, 7.0 Hz, $\text{CHC}(\text{O})\text{OCH}_3$), 2.55 (dd, J = 1.8, 3.0 Hz, $\text{NCHH}'\text{CH}$), 3.75 (s, $\text{C}(\text{O})\text{OCH}_3$); ^{13}C NMR (CDCl_3) δ 28.7 (NCH_2CH), 31.8 ($\text{CHC}(\text{O})\text{OCH}_3$), 52.2 ($\text{C}(\text{O})\text{OCH}_3$), 74.5 (NCPH_3), 127.1, 127.8, 129.4, 143.7 (3 C_6H_5), 172.0 ($\text{C}(\text{O})\text{OCH}_3$).

(*R*)-Methyl 1-Acetylaziridine-2-carboxylate ((*R*)-68).⁴⁰⁷ Compound (*R*)-**65** (26.0 g, 75.8 mmol) was dissolved in CHCl_3 :MeOH (1:1) (200 mL) and cooled (ice bath). While stirring, TFA (87 mL) was added dropwise and the reaction was stirred at 0 °C (2 h). Solvents were removed in vacuo and the solid residue was dissolved in CH_2Cl_2 (150 mL), cooled (0 °C) and then Et_3N (44.2 mL, 303 mmol) followed by acetyl chloride (5.88 mL, 83.4 mmol) were added dropwise. The reaction was stirred (2 h), filtered, and the filtrate was successively washed with 10% aqueous citric acid (150 mL), saturated aqueous sodium bicarbonate (150 mL), and brine (150 mL). The organic layer was dried (Na_2SO_4) and evaporated. The solid residue was purified using silica gel chromatography (1/4 to 1/1 EtOAc/hexanes) to give 3.60 g (33%) of (*R*)-**68** as a colorless residue: $[\alpha]_D^{25}$ +81.7° (c 1.3, CHCl_3); R_f = 0.41 (1/2 EtOAc/hexanes); ^1H NMR (CDCl_3) δ 2.15 (s, $\text{CH}_3\text{C}(\text{O})$), 2.49 (dd, J = 1.8, 7.0 Hz, $\text{NCHH}'\text{CH}$), 2.56 (dd, J = 3.0, 7.0 Hz, $\text{CHC}(\text{O})\text{OCH}_3$), 3.14 (dd, J = 1.8, 3.0 Hz, $\text{NCHH}'\text{CH}$), 3.78 (s, $\text{C}(\text{O})\text{OCH}_3$); ^{13}C NMR (CDCl_3) δ 23.8 ($\text{CH}_3\text{C}(\text{O})$), 31.0

(NCH₂CH), 34.5 (CHC(O)OCH₃), 53.0 (C(O)OCH₃), 169.0 (CH₃C(O)), 180.6 (C(O)OCH₃).

(S)-Methyl 1-Acetylaziridine-2-carboxylate ((S)-68).⁴⁰⁷ Using the preceding procedure, (S)-65 (17.4 g, 50.7 mmol) in CHCl₃:MeOH (1:1) (150 mL) was reacted with TFA (58 mL) at 0 °C (2 h). The solvents were removed and the residue was dissolved in CH₂Cl₂ (100 mL) and reacted with Et₃N (28.3 mL, 202.8 mmol) and acetyl chloride (3.96 mL, 55.8 mmol). Purification by SiO₂ flash chromatography (1/4 to 1/1 EtOAc/hexanes) afforded 2.50 g (34%) of (S)-68 as a colorless residue: [α]_D²⁵ -81.7° (c 1.3, CHCl₃); *R*_f = 0.41 (1/2 EtOAc/hexanes); ¹H NMR (CDCl₃) δ 2.15 (s, CH₃C(O)), 2.49 (dd, *J* = 1.8, 7.0 Hz, NCHH'CH), 2.56 (dd, *J* = 3.0, 7.0 Hz, CHC(O)OCH₃), 3.14 (dd, *J* = 1.8, 3.0 Hz, NCHH'CH), 3.78 (s, C(O)OCH₃); ¹³C NMR (CDCl₃) δ 23.9 (CH₃C(O)), 31.1 (NCH₂CH), 34.6 (CHC(O)OCH₃), 53.1 (C(O)OCH₃), 169.1 (CH₃C(O)), 180.7 (C(O)OCH₃).

Serine Methyl Ester Free Amine (67).³⁸¹ L or D-Serine methyl ester hydrochloride (62, 1 equiv) was suspended in CH₂Cl₂ ([C] ~1 M) and Et₃N (1.5 equiv) was added. After stirring at room temperature (1 h), the salts were filtered and briefly rinsed with EtOAc, and an equal volume of EtOAc was then added. The mixture was stirred at 0 °C (10 min), the solids filtered, and the solvent reduced in vacuo to one third in volume. The remaining reaction mixture was stirred at 0 °C (10 min), filtered, and the solvent removed. CH₃CN was then used to azeotropically remove excess Et₃N until

it could not be detected. Free amine **67** (80–90% yield) was immediately used in the next step.

(R)-Methyl N-Acetylaziridine-carboxylate ((R)-68a) and (R)-Ethyl N-Acetylaziridine-carboxylate ((R)-68b). To a solution of (*R*)-**67** (41.3 g, 347 mmol) in CH₃CN (500 mL) was added **DTPP** (86% by wt, 142.0 g, 346 mmol). The solution was stirred at room temperature (24 h). The solvent was removed in vacuo, the residue dissolved in minimal amount of CH₂Cl₂ (250 mL), and extracted with aqueous 0.1 M H₂SO₄ until the pH of the aqueous phase remained acidic (3 x 150 mL). The combined aqueous layers were washed with EtOAc (3 x 200 mL), basified (pH ~10) with solid Na₂CO₃, saturated with solid NaCl until the solution became cloudy, and extracted with EtOAc (6 x 200 mL). The combined organic layers were dried (Na₂SO₄) and evaporated to give a crude yellow liquid. Bulb-to-bulb distillation of the liquid at 80 °C under vacuum (6 mm Hg) yielded an approximately 9:1 molar mixture of (*R*)-**66a** and (*R*)-**66b** as a colorless liquid (24.60 g, 69%). The mixture was directly dissolved in CH₂Cl₂ (500 mL) and Et₃N (33.4 mL, 239 mmol) and DMAP (1.46 g, 12 mmol) were successively added. While stirring at room temperature (water bath), Ac₂O (22.6 mL, 239 mmol) was added dropwise (15 min) and the reaction was allowed to proceed at room temperature (45 min). The solution was successively washed with 10% aqueous citric acid (500 mL) and brine (500 mL), dried (Na₂SO₄), and the solvents were removed in vacuo to yield an approximately 9:1 molar mixture of a colorless residue (32.80 g, 94%) that did not require further purification: *R*_f = 0.38 ((*R*)-**68a**), 0.39 ((*R*)-**68b**) (2:1 hexanes/EtOAc). Spectral data

for (*R*)-**68a** (~90% mol. based on ^1H NMR integrations): ^1H NMR (CDCl_3) δ 2.16 (s, $\text{CH}_3\text{C}(\text{O})$), 2.49 (dd, $J = 1.8, 7.0$ Hz, $\text{NCHH}'\text{CH}$), 2.58 (dd, $J = 1.8, 3.0$ Hz, $\text{NCHH}'\text{CH}$), 3.15 (dd, $J = 3.0, 7.0$ Hz, $\text{CHC}(\text{O})\text{OCH}_3$), 3.80 (s, $\text{C}(\text{O})\text{OCH}_3$); ^{13}C NMR (CDCl_3) δ 23.8 ($\text{CH}_3\text{C}(\text{O})$), 31.0 (NCH_2CH), 34.5 ($\text{CHC}(\text{O})\text{OCH}_3$), 52.9 ($\text{C}(\text{O})\text{OCH}_3$), 168.9 ($\text{CH}_3\text{C}(\text{O})$), 180.6 ($\text{C}(\text{O})\text{OCH}_3$); (*R*)-**68a** was not detected by HRMS. Spectral data for (*R*)-**68b** (~10% mol. on ^1H NMR integrations): ^1H NMR (CDCl_3) δ 1.31 (t, $J = 6.9$ Hz, $\text{C}(\text{O})\text{OCH}_2\text{CH}_3$), 4.24 (q, $J = 6.9$ Hz, $\text{C}(\text{O})\text{OCHH}'\text{CH}_3$), 4.25 (q, $J = 6.9$ Hz, $\text{C}(\text{O})\text{OCHH}'\text{CH}_3$), the remaining signals were not detected and are believed to overlap with the ^1H signals for (*R*)-**68a**; ^{13}C NMR (CDCl_3) no ^{13}C signals were detected for (*R*)-**68b**; M_r (+ESI) 180.0631 $[\text{M}+\text{Na}]^+$ (calcd for $\text{C}_7\text{H}_{11}\text{NO}_3\text{Na}^+$ 180.0637).

(*R*)-*N*-Benzyl 2-*N*-(Benzyloxycarbonyl)amino-3-hydroxypropionamide ((*R*)-57**).**²³⁵ Using Method C, Cbz-D-serine ((*R*)-**56**) (5.10 g, 21.3 mmol), NMM (2.3 mL, 21.3 mmol), IBCF (2.8 mL, 21.3 mmol), and benzylamine (2.3 mL, 21.3 mmol) gave (*R*)-**57** (5.33 g, 76%) as a white solid: mp 147–149 °C (lit.²³⁵ mp 147–149 °C); $[\alpha]_D^{25} +4.5^\circ$ (c 1.0, MeOH) (lit.²³⁵ $[\alpha]_D^{25} +4.6^\circ$ (c 2.0, MeOH)); ^1H NMR ($\text{DMSO}-d_6$) δ 3.58 (d, $J = 5.7$ Hz, CH_2), 4.04–4.11 (m, CHCH_2), 4.27 (d, $J = 6.0$ Hz, CH_2N), 4.90–4.95 (m, CH_2OH), 5.02 (s, CH_2O), 7.20–7.38 (m, 10 ArH, $\text{OC}(\text{O})\text{NH}$), 8.32–8.37 (m, $\text{C}(\text{O})\text{NHCH}_2\text{Ph}$).

(*R*)-*N*-Benzyl 2-Amino-3-hydroxypropionamide ((*R*)-76**).**²³⁵ Using Method H, compound (*R*)-**57** (3.00 g, 9.14 mmol) and 10% Pd/C (300 mg) in MeOH (50 mL)

gave (*R*)-**76** (1.75 g, 98%) as a white solid: mp 89–91 °C (lit.²³⁵ mp 88–90 °C); $[\alpha]_D^{25}$ -3.0° (c 1.0; MeOH) (lit.²³⁵ $[\alpha]_D^{25}$ -3.2° (c 0.9; MeOH)); R_f = 0.15 (1/9 MeOH/CHCl₃); ¹H NMR (DMSO-*d*₆) δ 3.31–3.36 (m, CHCH₂OH), 3.40–3.60 (m, CHCH₂OH), 4.29 (d, J = 6.0 Hz, C(O)NHCH₂Ph), 4.78–4.98 (br s, CH₂OH), 7.20–7.32 (m, C₆H₅), 8.34–8.48 (br t, C(O)NHCH₂Ph); ¹³C NMR (CDCl₃) δ 41.9 (NHCH₂Ph), 56.6 (CHCH₂O), 63.7 (CHCH₂OH), 126.7, 127.1, 128.2, 139.4 (C₆H₅), 172.4 (C(O)NHCH₂).

(*R*)-*N*-Benzyl 1-Acetylaziridine-2-carboxamide ((*R*)-78). Compound (*R*)-**76** (1.75 g, 9.1 mmol) was suspended in CH₃CN (20 mL) and while stirring **DTPP** (90% by wt, 3.60 g, 10.01 mmol) was added all at once. The solution became clear within minutes and was then stirred at room temperature (3 h). The solvent was removed in vacuo, and the residue was partitioned between aqueous 0.1 M H₂SO₄ (20 mL) and toluene (20 mL). The toluene layer was extracted with aqueous 0.1 M H₂SO₄ (20 mL). The combined aqueous layers were washed with toluene and basified (pH ~10) by addition of solid K₂CO₃, saturated with NaCl, and then extracted with EtOAc (3 x 40 mL). The combined EtOAc layers were dried (Na₂SO₄), and concentrated to yield 1.47 g (92%) of aziridine (*R*)-**77** as a crude yellow oil. Crude (*R*)-**77** was dissolved in CH₂Cl₂ (80 mL), cooled to 0 °C, and Et₃N (1.71 mL, 10.28 mmol) added. While stirring, AcCl (581 μ L, 8.18 mmol) in CH₂Cl₂ (6 mL) was added dropwise. The reaction was stirred at 0 °C (1 h), and successively washed with aqueous 10% citric acid (100 mL) and brine (100 mL). The organic layer was dried (Na₂SO₄) and evaporated. The residue was purified using flash chromatography (CH₂Cl₂/EtOAc 1:1) and further recrystallized from EtOAc and hexanes to yield 1.12 g of (*R*)-**78**

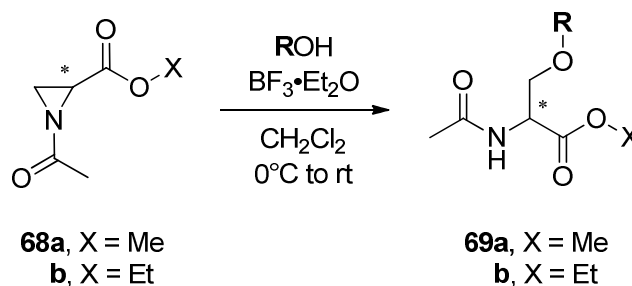
(62% for two steps): mp 82–84 °C (lit.³⁸⁴ mp 82–83 °C); $[\alpha]_D^{25}$ -106.6° (c 1.6; CHCl₃); R_f = 0.44 (1/1 CH₂Cl₂/EtOAc); IR (nujol) 3230, 1660, 1558, 1459, 1390, 1154, 1092 cm⁻¹; ¹H NMR (CDCl₃) δ 2.17 (s, CH₃C(O)N), 2.37 (dd, J = 0.9, 3.0 Hz, NCHH'CH), 2.56 (dd, J = 0.9, 6.3 Hz, NCHH'CH), 3.08 (dd, J = 3.0, 6.3 Hz, NCHH'CH) 4.38–4.50 (m, C(O)NHCH₂Ph), 6.46–6.62 (m, C(O)NHCH₂Ph), 7.20–7.40 (m, C₆H₅); ¹³C NMR (CDCl₃) δ 23.7 (CH₃C(O)), 31.2 (NCH₂CH), 36.4 (NCH₂CH), 43.4 (NHCH₂Ph), 127.7, 127.8, 128.9, 137.8 (C₆H₅), 167.3 (C(O)NHCH₂), 181.5 (CH₃C(O)N); M_r (+ESI) 219.1129 [M+H]⁺ (calcd for C₁₂H₁₄N₂O₂H⁺ 219.1134). Anal. Calcd for C₁₂H₁₄N₂O₂: C, 66.04; H, 6.47; N, 12.84. Found: C, 66.06; H, 6.43; N, 12.73.


Alternate Procedure for (*R*)-*N*-Benzyl 1-Acetylaziridine-2-carboxamide ((*R*)-78).

PPh₃ (100 g, 377 mmol) was dissolved in CH₂Cl₂ (400 mL), cooled at -78 °C (dry ice/acetone) under N₂ and Br₂ (19.3 mL, 380 mmol) was added quickly with a syringe. After stirring at -78 °C (10 min), a solution of CF₃CH₂OH (54.2 mL, 754 mmol) and Et₃N (105 mL, 754 mmol) in Et₂O (300 mL) was added dropwise (15 min). Upon addition, the reaction was allowed to stir and slowly warm up to room temperature (1 h), then quickly filtered using oven-dried glassware, and the solvents were removed in vacuo at room temperature to give **DTPP-F₆** (138 g, 300 mmol, 79%) as a pale beige solid. **DTPP-F₆** was directly added to a suspension of (*R*)-76 (36.6 g, 189 mmol) in CH₃CN (500 mL) and the reaction was stirred at room temperature (15 h). The solvent was removed under vacuum and the solid residue was partitioned between EtOAc (500 mL) and aqueous 0.5 M H₂SO₄ (50 mL). The aqueous layer was recovered and washed with EtOAc (3 x 200 mL), basified using

solid Na_2CO_3 (pH ~10), saturated with NaCl, and extracted with CH_2Cl_2 (5 x 200 mL). The EtOAc and CH_2Cl_2 layers were separately washed with brine (200 mL), combined, dried (Na_2SO_4), and concentrated. The residue was purified using flash chromatography (5/95 MeOH CH_2Cl_2) to give 9.70 g of a crude yellow oil ($R_f = 0.43$, 5/95 MeOH/ CH_2Cl_2) that was dissolved in CH_2Cl_2 (500 mL). While stirring, Et_3N (7.7 mL, 55.0 mmol), DMAP (300 mg, 2.5 mmol) and Ac_2O (5.2 mL, 55.0 mmol) were successively added and the reaction was stirred at room temperature (1 h). The reaction was then washed with aqueous 0.1 M H_2SO_4 (300 mL), brine (200 mL), dried (Na_2SO_4), and the solvents were removed under vacuum. The residue was purified using flash chromatography (EtOAc/ CH_2Cl_2 1/1 to 4/1) to yield (*R*)-**78** as a white solid (5.70 g, 15% overall yield for 2 steps): mp 82–84 °C (lit.³⁸⁴ mp 82–83 °C); $[\alpha]_D^{25} -106.0^\circ$ (c 1.3, CHCl_3); $R_f = 0.44$ (1/1 EtOAc/ CH_2Cl_2); ^1H NMR (CDCl_3) δ 2.18 (s, $\text{CH}_3\text{C}(\text{O})$), 2.37 (d, $J = 3.3$ Hz, $\text{CHH}'(\text{N})\text{CH}$), 2.58 (d, $J = 7.6$ Hz, $\text{CHH}'(\text{N})\text{CH}$), 3.09 (dd, $J = 3.3, 7.6$ Hz, $\text{CH}_2(\text{N})\text{CH}$), 4.38–4.54 (m, $\text{NHCH}_2\text{C}_6\text{H}_5$), 6.42–6.54 (m, $\text{NHCH}_2\text{C}_6\text{H}_5$), 7.20–7.40 (m, $\text{CH}_2\text{C}_6\text{H}_5$); ^{13}C NMR (CDCl_3) δ 23.6 ($\text{CH}_3\text{C}(\text{O})$), 31.4 ($\text{CH}_2(\text{N})\text{CH}$), 36.4 ($\text{CH}_2(\text{N})\text{CH}$), 43.4 (NHCH_2Ph), 127.8, 128.9, 137.6 (C_6H_5), 167.2 ($\text{C}(\text{O})\text{NHCH}_2$), 181.3 ($\text{CH}_3\text{C}(\text{O})\text{N}$), the remaining carbon signal was not detected and is believed to overlap with nearby peaks.

2.2.4.3. Synthesis of *O*-Substituted *N*-Acetylserine Esters



R =	Compound number (a, X = Me, b, X = Et)
Me	101
Et	102
<i>i</i> -Pr	103
<i>t</i> -Bu	104
C ₆ H ₁₁	105
Ph	106
CH ₂ C ₆ H ₁₁	107
CH ₂ CH ₂ CH=CH ₂	108
CH ₂ CH ₂ 	109
CH ₂ CH ₂ OBn	110
CH ₂ CH ₂ CH ₂ OBn	111
CH ₂ CH ₂ N ₃	112
CH ₂ CH ₂ OCH ₃	113
(CH ₂ CH ₂ O) ₂ CH ₃	114

(*R*)-Methyl 2-Acetamido-3-methoxypropionate ((*R*)-101a) and (*R*)-Ethyl 2-Acetamido-3-methoxypropionate ((*R*)-101b). Using Method A, a ~9:1 mixture of (*R*)-**68a** and (*R*)-**68b** (5.46 g, 40.6 mmol) and BF₃•Et₂O (5.1 mL, 40.6 mmol) in MeOH (50 mL) gave 3.95 g (56%) of (*R*)-**101a** and (*R*)-**101b** as a pale yellow residue that turned to a white solid upon concentration under high vacuum: *R*_f = 0.40 ((*R*)-**101a**), 0.42 ((*R*)-**101b**) (5/95 hexanes/EtOAc); IR (CH₂Cl₂ film) 3300, 3062,

2996, 2940, 1743, 1656, 1547, 1444, 1380, 1214, 1119 cm^{-1} . Spectral data for (*R*)-**101a** (approximately 90 mol percent based on ^1H NMR integrations): ^1H NMR (CDCl_3) δ 2.06 (s, $\text{CH}_3\text{C}(\text{O})\text{NH}$), 3.34 (s, OCH_3), 3.61 (dd, $J = 4.0, 9.3$ Hz, $\text{CHCHH}'\text{OCH}_3$), 3.77 (s, $\text{C}(\text{O})\text{OCH}_3$), 3.81 (dd, $J = 4.0, 9.3$ Hz, $\text{CHCHH}'\text{OCH}_3$), 4.75 (app dt, $J = 4.0, 7.8$ Hz, $\text{CHCH}_2\text{OCH}_3$), 6.74 (br d, $J = 7.8$ Hz, $\text{CH}_3\text{C}(\text{O})\text{NH}$); ^{13}C NMR (CDCl_3) δ 22.9 ($\text{CH}_3\text{C}(\text{O})$), 52.4 ($\text{CHCH}_2\text{OCH}_3$ or $\text{C}(\text{O})\text{OCH}_3$), 52.5 ($\text{C}(\text{O})\text{OCH}_3$ or $\text{CHCH}_2\text{OCH}_3$), 59.1 (CH_2OCH_3), 72.2 ($\text{CHCH}_2\text{OCH}_3$), 170.1, 170.8 ($\text{CH}_3\text{C}(\text{O})\text{NH}$, $\text{C}(\text{O})\text{OCH}_3$); M_r (+ESI) 198.0740 $[\text{M}+\text{Na}]^+$ (calcd for $\text{C}_7\text{H}_{13}\text{NO}_4\text{Na}^+$ 198.0742).

Spectral data for (*R*)-**101b** (approximately 10 mol percent based on ^1H NMR integrations): ^1H NMR (CDCl_3) δ 1.29 (t, $J = 7.2$ Hz, $\text{C}(\text{O})\text{OCH}_2\text{CH}_3$) 1.99 (s, $\text{CH}_3\text{C}(\text{O})\text{NH}$), 3.44 (s, OCH_3), 3.92 (dd, $J = 4.0, 9.3$ Hz, $\text{CHCHH}'\text{OCH}_3$), 4.19–4.28 (m, $\text{C}(\text{O})\text{OCH}_2\text{CH}_3$), 6.40–6.50 (br d, $\text{CH}_3\text{C}(\text{O})\text{NH}$), the remaining signals were not detected and are believed to overlap with (*R*)-**101a** signals; ^{13}C NMR signals were not detected for (*R*)-**101b**; M_r (+ESI) 212.0896 $[\text{M}+\text{Na}]^+$ (calcd for $\text{C}_8\text{H}_{15}\text{NO}_4\text{Na}^+$ 212.0899).

(*S*)-Methyl 2-Acetamido-3-(methoxy)propionate ((*S*)-101a) and (*S*)-Ethyl 2-Acetamido-3-(methoxy)propionate ((*S*)-101b). Using Method A, a ~9:1 mixture of (*S*)-**68a** and (*S*)-**68b** (1.50 g, 10 mmol) and $\text{BF}_3 \cdot \text{Et}_2\text{O}$ (1.3 mL, 10 mmol) in MeOH (20 mL) gave upon work-up a mixture of (*S*)-**101a** and (*S*)-**101b** (1.43 g, 80%) as a pale yellow solid that was used without further purification: $R_f = 0.40$ ((*S*)-**101a**), 0.42 ((*S*)-**101b**) (5/95 hexanes/EtOAc); IR (neat) 3287, 3064, 2977, 2877, 1746, 1662, 1542, 1442, 1375, 1296, 1212 cm^{-1} . Spectral data for (*S*)-**101a** (~90% based on ^1H

NMR integrations): ^1H NMR (CDCl_3) δ 2.06 (s, $\text{CH}_3\text{C}(\text{O})$), 3.35 (s, CH_2OCH_3), 3.61 (dd, $J = 3.0, 9.0$ Hz, $\text{CHH}'\text{OCH}_3$), 3.78 (s, $\text{C}(\text{O})\text{OCH}_3$), 3.81 (dd, $J = 3.0, 9.0$ Hz, $\text{CHH}'\text{OCH}_3$), 4.73 (app. dt, $J = 3.0, 7.2$ Hz, CHCH_2O), 6.30–6.40 (br d, NHCHCH_2O); ^{13}C NMR (CDCl_3) δ 23.3 ($\text{CH}_3\text{C}(\text{O})$), 52.8 (CHOCH_2 or $\text{C}(\text{O})\text{OCH}_3$), 59.5 (CH_2OCH_3), 72.5 ($\text{CHCH}_2\text{OCH}_3$), 170.1, 171.0 ($\text{CH}_3\text{C}(\text{O})$, $\text{CHC}(\text{O})\text{OCH}_3$), the remaining signal was not detected and is believed to overlap with nearby peaks; M_r (+ESI) 198.0741 [$\text{M}+\text{Na}]^+$ (calcd for $\text{C}_7\text{H}_{13}\text{NO}_4\text{Na}^+$ 198.0742).

Spectral data for (S)-**101b** (~10% based on ^1H NMR integrations): ^1H NMR(CDCl_3) δ 1.28 (t, $J = 7.2$ Hz, OCH_2CH_3), 3.45 (s, CH_2OCH_3), 4.19–4.28 (m, OCH_2CH_3), the remaining signals were not detected and are believed to overlap with nearby signals or are too small to be detected; ^{13}C NMR signals were not detected for (S)-**14b**; M_r (+ESI) 212.0897 [$\text{M}+\text{Na}]^+$ (calcd for $\text{C}_8\text{H}_{15}\text{NO}_4\text{Na}^+$ 212.0899).

(R)-Methyl 2-Acetamido-3-ethoxypropionate ((R)-102a) and (R)-Ethyl 2-Acetamido-3-ethoxypropionate ((R)-102b). Using Method A, a ~9:1 mixture of (R)-**68a** and (R)-**68b** (1.88 g, 13.0 mmol) and $\text{BF}_3 \cdot \text{Et}_2\text{O}$ (1.63 mL, 13.0 mmol) in EtOH (25 mL) gave 1.34 g (54%) of (R)-**102a** and (R)-**102b** as a pale yellow oil: $R_f = 0.43$ ((R)-**102a**), 0.45 ((R)-**102b**) (5/95 hexanes/EtOAc); IR (neat) 3287, 3064, 2977, 2876, 1745, 1661, 1542, 1442, 1375, 1212, 1119 cm^{-1} . Spectral data for (R)-**102a** (approximately 90 mol percent based on ^1H NMR integrations): ^1H NMR (CDCl_3) δ 1.16 (t, $J = 7.2$ Hz, $\text{CH}_2\text{OCH}_2\text{CH}_3$), 2.06 (s, $\text{CH}_3\text{C}(\text{O})\text{NH}$), 3.50 (q, $J = 7.2$ Hz, $\text{CH}_2\text{OCHH}'\text{CH}_3$), 3.51 (q, $J = 7.2$ Hz, $\text{CH}_2\text{OCHH}'\text{CH}_3$), 3.65 (dd, $J = 4.0, 8.7$ Hz, $\text{CHCHH}'\text{OCH}_2\text{CH}_3$), 3.76 (s, $\text{C}(\text{O})\text{OCH}_3$), 3.84 (dd, $J = 4.0, 8.7$ Hz,

CHCHH'OCH₂CH₃), 4.75 (app dt, $J = 4.0, 7.5$ Hz, CHCH₂OCH₂CH₃), 6.54 (br d, $J = 7.5$ Hz, CH₃C(O)NH); ¹³C NMR (CDCl₃) δ 15.0 (OCH₂CH₃), 23.3 (CH₃C(O)), 52.7 (CHCH₂OCH₃ or C(O)OCH₃), 52.8 (C(O)OCH₃ or CHCH₂OCH₂H₃), 67.1 (CHCH₂OCH₂CH₃), 70.2 (CHCH₂OCH₂CH₃), 170.1, 171.1 (CH₃C(O)NH, C(O)OCH₃); M_r (+ESI) 212.0897 [M+Na]⁺ (calcd for C₈H₁₅NO₄Na⁺ 212.0899).

Spectral data for (*R*)-**102b** (approximately 10 mol percent based on ¹H NMR integrations): ¹H NMR (CDCl₃) δ 1.24 (t, $J = 7.2$ Hz, CH₂OCH₂CH₃ or C(O)OCH₂CH₃), 1.29 (t, $J = 7.2$ Hz, C(O)OCH₂CH₃ or CH₂OCH₂CH₃), 1.99 (s, CH₃C(O)NH), 3.96–4.04 (m, CH₂OCHH'CH₃), 4.19–4.30 (m, C(O)OCH₂CH₃), 6.10–6.22 (br d, $J = 6.8$ Hz, CH₃C(O)NH), the remaining signals were not detected and are believed to overlap with (*R*)-**102a** signals; ¹³C NMR signals were not detected for (*R*)-**102b**; M_r (+ESI) 226.1054 [M+Na]⁺ (calcd for C₉H₁₇NO₄Na⁺ 226.1055).

(*R*)-Methyl 2-Acetamido-3-isopropoxypropionate ((*R*)-103a) and (*R*)-Ethyl 2-Acetamido-3-isopropoxypropionate ((*R*)-103b). Using Method A, a ~9:1 mixture of (*R*)-**68a** and (*R*)-**68b** (3.40 g, 23.5 mmol) and BF₃•Et₂O (2.95 mL, 23.5 mmol) in *i*-PrOH (30 mL) gave 2.98 g (62%) of (*R*)-**103a** and (*R*)-**103b** as a pale yellow oil: $R_f = 0.46$ ((*R*)-**103a**), 0.48 ((*R*)-**103b**) (5/95 hexanes/EtOAc); IR (neat) 3295, 3062, 2972, 2877, 1748, 1663, 1538, 1442, 1375, 1212, 1147 cm⁻¹. Spectral data for (*R*)-**103a** (approximately 90 mol percent based on ¹H NMR integrations): ¹H NMR (CDCl₃) δ 1.10 (d, $J = 6.0$ Hz, CH₂OCHCH₃(C'H₃)), 1.12 (d, $J = 6.0$ Hz, CH₂OCHCH₃(C'H₃)), 2.06 (s, CH₃C(O)NH), 3.55 (hept, $J = 6.0$ Hz, CH₂OCH(CH₃)₂), 3.64 (dd, $J = 3.7, 9.3$ Hz, CHCHH'OCH(CH₃)₂), 3.76 (s, C(O)OCH₃), 3.84 (dd, $J = 3.7, 9.3$ Hz,

CHCHH'OCH(CH₃)₂), 4.72 (app dt, $J = 3.7, 7.2$ Hz, CHCH₂OCH(CH₃)₂), 6.41 (br d, $J = 7.2$ Hz, CH₃C(O)NH); ¹³C NMR (CDCl₃) δ 21.5 (OCHCH₃(C'H₃)), 21.6 (OCHCH₃(C'H₃)), 22.9 (CH₃C(O)), 52.1 (CHCH₂OCH(CH₃)₂ or C(O)OCH₃), 52.6 (C(O)OCH₃ or CHCH₂OCH(CH₃)₂), 67.5 (CHCH₂OCH(CH₃)₂), 70.2 (CHCH₂OCH(CH₃)₂), 169.6, 170.4 (CH₃C(O)NH, C(O)OCH₃); M_r (+ESI) 226.1054 [M+Na]⁺ (calcd for C₉H₁₇NO₄Na⁺ 226.1055).

Spectral data for (*R*)-**103b** (approximately 10% mol based on integrations): ¹H NMR (CDCl₃) δ 1.16 (d, $J = 6.0$ Hz, CH₂OCHCH₃(C'H₃)), 1.21 (d, $J = 6.0$ Hz, CH₂OCHCH₃(C'H₃)), 1.28 (t, $J = 6.0$ Hz, C(O)OCH₂CH₃), 1.99 (s, CH₃C(O)NH), 4.06–4.12 (m, CHCHH'OCH(CH₃)₂), 4.18–4.26 (m, C(O)OCH₂CH₃), 5.95–6.10 (br m, CH₃C(O)NH), the remaining signals were not detected and are believed to overlap with (*R*)-**103a** signals; ¹³C NMR signals were not detected for (*R*)-**103b**; M_r (+ESI) 240.1211 [M+Na]⁺ (calcd for C₁₀H₁₉NO₄Na⁺ 240.1212).

(*R*)-Methyl 2-Acetamido-3-*tert*-butoxypropionate ((*R*)-104a) and (*R*)-Ethyl 2-Acetamido-3-*tert*-butoxypropionate ((*R*)-104b). Using Method A, a mixture of ~9:1 (*R*)-**68a** and (*R*)-**68b** (3.50 g, 24.2 mmol) and BF₃•Et₂O (3.05 mL, 24.2 mmol) in *t*-BuOH (30 mL) gave 2.75 g (52%) of (*R*)-**104a** and (*R*)-**104b** as a pale yellow oil: $R_f = 0.52$ ((*R*)-**104a**), 0.54 ((*R*)-**104b**) (5/95 hexanes/EtOAc); IR (neat) 3298, 3062, 2974, 1749, 1663, 1537, 1370, 1204, 1098 cm⁻¹. Spectral data for (*R*)-**104a** (approximately 95 mol percent based on ¹H NMR integrations): ¹H NMR (CDCl₃) δ 1.14 (s, CH₂OC(CH₃)₃), 2.06 (s, CH₃C(O)NH), 3.56 (dd, $J = 3.0, 9.0$ Hz, CHCHH'OC(CH₃)₃), 3.76 (s, C(O)OCH₃), 3.81 (dd, $J = 3.0, 9.0$ Hz, CHCHH'OC(CH₃)₃), 4.72 (app dt, $J =$

3.0, 7.2 Hz, CHCH₂OC(CH₃)₃), 6.41 (br d, J = 7.2 Hz, CH₃C(O)NH); ¹³C NMR (CDCl₃) δ 22.9 (CH₃C(O)), 27.7 (OC(CH₃)₃), 52.1 (CHCH₂OC(CH₃)₃ or C(O)OCH₃), 53.3 (C(O)OCH₃ or CHCH₂OCH(CH₃)₂), 62.4 (CHCH₂OC(CH₃)₃), 73.8 (CHCH₂OC(CH₃)₃), 170.3, 171.5 (CH₃C(O)NH, C(O)OCH₃); M_r (+ESI) 240.1211 [M+Na]⁺ (calcd for C₁₀H₁₉NO₄Na⁺ 240.1212).

Spectral data for (*R*)-**104b** (approximately 5% mol based on integrations): ¹H NMR (CDCl₃) δ 1.21 (s, CH₂OC(CH₃)₃), 1.99 (s, CH₃C(O)NH), 4.18–4.24 (m, C(O)OCH₂CH₃), 5.95–6.15 (m, CH₃C(O)NH), the remaining signals were not detected and are believed to overlap with (*R*)-**104a** signals or are too small to be detected; ¹³C NMR signals were not detected for (*R*)-**104b**; M_r (+ESI) 254.1368 [M+Na]⁺ (calcd for C₁₁H₂₁NO₄Na⁺ 254.1368).

(*R*)-Methyl 2-Acetamido-3-(cyclohexyloxy)propionate ((*R*)-105a) and (*R*)-Ethyl 2-Acetamido-3-(cyclohexyloxy)propionate ((*R*)-105b). Using Method A, a ~1:1 mixture of (*R*)-**68a** and (*R*)-**68b** (2.70 g, 18.0 mmol), cyclohexanol (6.0 mL, 57 mmol) and BF₃•Et₂O (2.3 mL, 18.3 mmol) in CH₂Cl₂ (20 mL) gave a ~1:1 mixture of (*R*)-**105a** and (*R*)-**105b** (2.18 g, 48%) as a yellow oil after work-up and purification by flash chromatography (1/1 EtOAc/hexanes to EtOAc): R_f = 0.49 ((*R*)-**105a**), 0.51 ((*R*)-**105b**) (5/95 hexanes/EtOAc); IR (neat) 3308, 3061, 2926, 2861, 1747, 1662, 1537, 1447, 1372, 1206, 1106 cm⁻¹; ¹H NMR (CDCl₃) δ 1.18–1.35, 1.42–1.58, 1.62–1.86 (m, OCH(CH₂CH₂)₂CH₂, (*R*)-**105a,b**), 1.28 (t, J = 6.9 Hz, OCH₂CH₃, (*R*)-**105b**), 2.06 (s, CH₃C(O), (*R*)-**105a,b**), 3.18–3.26 (m, OCH(CH₂CH₂)₂CH₂, (*R*)-**105a,b**), 3.66 (dd, J = 3.0, 9.0 Hz, CHH'OCH(CH₂CH₂)₂CH₂, (*R*)-**105a,b**), 3.76 (s, C(O)OCH₃, (*R*)-

105a), 3.88 (dd, $J = 3.0, 9.0$ Hz, CHH'OCH(CH₂CH₂)₂CH₂, (*R*)-**105a,b**), 4.15–4.28 (m, C(O)OCH₂CH₃, (*R*)-**105b**), 4.66–4.78 (m, CHCH₂O, (*R*)-**105a,b**), 6.30–6.40 (br d, CH₃C(O)NH, (*R*)-**105a,b**); ¹³C NMR (CDCl₃) δ 14.3 (C(O)OCH₂CH₃, (*R*)-**105b**), 23.4, 23.9, 24.0, 25.9 (CH₃C(O), OCH(CH₂CH₂)₂CH₂, (*R*)-**105a,b**), 31.9, 32.1 (OCH(CH₂CH₂)₂CH₂, (*R*)-**105a,b**), 52.7, 52.9, 53.0 (CHCH₂OCH₂, (*R*)-**105a,b**, C(O)OCH₃, (*R*)-**105a**), 61.7 (C(O)OCH₂CH₃, (*R*)-**105b**), 67.8, 67.9 (CH₂OCH(CH₂CH₂)₂CH₂, (*R*)-**105a,b**), 78.1 (OCH(CH₂CH₂)₂CH₂, (*R*)-**105a,b**), 170.1, 170.7, 171.2 (CH₃C(O)NH, C(O)OCH₃, (*R*)-**105a,b**), the remaining resonances were not detected and are believed to overlap with nearby signals; M_r (*R*)-**105a** (+ESI) 266.1368 [M+Na]⁺ (calcd for C₁₂H₂₁NO₄Na⁺ 266.1362), (*R*)-**105b** (+ESI) 280.1525 [M+Na]⁺ (calcd for C₁₃H₂₃NO₄Na⁺ 280.1524).

(*R*)-Methyl 2-Acetamido-3-phenoxypropionate ((*R*)-106a) and (*R*)-Ethyl 2-Acetamido-3-phenoxypropionate ((*R*)-106b). Using Method A, a ~3:7 mixture of (*R*)-**68a** and (*R*)-**68b** (2.00 g, 13.1 mmol), phenol (3.95 g, 42.0 mmol) and BF₃•Et₂O (1.6 mL, 13.1 mmol) in CH₂Cl₂ (20 mL) gave 1.4 g (43%) of (*R*)-**106a** and (*R*)-**106b** as a pale yellow residue: $R_f = 0.50$ ((*R*)-**106a**), 0.52 ((*R*)-**106b**) (5/95 hexanes/EtOAc); IR (neat) 3067, 2984, 1743, 1660, 1596, 1541, 1498, 1379, 1296, 1238, 1159 cm⁻¹; Spectral data for (*R*)-**106a** (approximately 30 mol percent based on ¹H NMR integrations): ¹H NMR (CDCl₃) δ 2.06 (s, CH₃C(O)NH), 3.76 (s, C(O)OCH₃), 4.20–4.23 (m, CHCHH'OPh), 4.36–4.43 (m, CHCHH'OPh), 4.68–5.06 (m, CHCH₂OPh), 6.52 (br d, $J = 7.2$ Hz, CH₃C(O)NH), 6.84–6.90 (m, 2 ArH (*o*)), 6.95–7.00 (m, ArH (*p*)), 7.24–7.32 (m, 2 ArH (*m*)); ¹³C NMR (CDCl₃) δ 23.1

(**CH₃C(O)**), 52.4 (**CHCH₂OPh** or **C(O)OCH₃**), 53.0 (**C(O)OCH₃** or **CHCH₂OPh**), 68.1 (**CHCH₂OPh**), 114.8, 121.7, 129.7, 158.4 (**CH₂OPh**), 170.0, 170.1, 170.5 (**CH₃C(O)NH**, **C(O)OCH₃**), additional peaks are believed to be part of (*R*)-**106b** but cannot be precisely attributed; *M_r* (+ESI) 268.0895 [*M*+Na]⁺ (calcd for C₁₂H₁₅NO₄Na⁺ 260.0899).

Spectral data for (*R*)-**106b** (approximately 70 mol percent based on ¹H NMR integrations): ¹H NMR (CDCl₃) δ 1.25 (t, *J* = 7.2 Hz, **C(O)OCH₂CH₃**), 2.06 (s, **CH₃C(O)NH**), 4.20–4.23 (m, **CHCHH'OPh**), 4.24 (q, *J* = 7.2 Hz, **C(O)OCH₂CH₃**), 4.36–4.43 (m, **CHCHH'OPh**), 4.68–5.06 (m, **CHCH₂OPh**), 6.52 (br d, *J* = 7.2 Hz, **CH₃C(O)NH**), 6.84–6.90 (m, 2 ArH (*o*)), 6.95–7.00 (m, ArH (*p*)), 7.24–7.32 (m, 2 ArH (*m*)); ¹³C NMR (CDCl₃) δ 14.3 (**CH₂CH₃**), 23.1 (**CH₃C(O)**), 52.5 (**CHCH₂OPh**), 68.2 (**CHCH₂OPh**), 114.8, 121.7, 129.7, 158.4 (**CH₂OPh**), 170.0, 170.1, 170.5 (**CH₃C(O)NH**, **C(O)OCH₃**), additional peaks are believed to be part of (*R*)-**106a** but cannot be precisely attributed; *M_r* (+ESI) 274.1052 [*M*+Na]⁺ (calcd for C₁₃H₁₇NO₄Na⁺ 274.1055).

(*R*)-Methyl 2-Acetamido-3-(cyclohexylmethoxy)propionate ((*R*)-107a) and (*R*)-Ethyl 2-Acetamido-3-(cyclohexylmethoxy)propionate ((*R*)-107b). Using Method A, a ~1:4 mixture of (*R*)-**68a** and (*R*)-**68b** (3.50 g, 22.7 mmol), cyclohexylmethanol (6.0 mL, 57 mmol) and BF₃•Et₂O (2.3 mL, 18.3 mmol) in CH₂Cl₂ (20 mL) gave a ~1:4 mixture of (*R*)-**107a** and (*R*)-**107b** (2.32 g, 38%) as a yellow oil after work-up and purification by flash chromatography (1/1 EtOAc/hexanes to EtOAc): *R_f* = 0.60 ((*R*)-**107a**), 0.62 ((*R*)-**107b**) (EtOAc); IR (neat) 3438, 3062, 2930, 2858, 1745, 1662,

1537, 1452, 1374, 1206, 1121 cm^{-1} ; ^1H NMR (CDCl_3) δ 0.80–0.95, 1.05–1.38, 1.48–1.80 (m, $\text{CH}_2\text{CH}(\text{CH}_2\text{CH}_2)_2\text{CH}_2$, (*R*)-**107a,b**), 1.28 (t, $J = 6.9$ Hz, OCH_2CH_3 , (*R*)-**107b**), 2.06 (s, $\text{CH}_3\text{C}(\text{O})$, (*R*)-**107a,b**), 3.12–3.30 (m, $\text{OCH}_2\text{CH}(\text{CH}_2\text{CH}_2)_2\text{CH}_2$, (*R*)-**107a,b**), 3.66 (dd, $J = 3.0, 9.6$ Hz, $\text{CHH}'\text{OCH}_2\text{CH}(\text{CH}_2\text{CH}_2)_2\text{CH}_2$, (*R*)-**107a,b**), 3.76 (s, $\text{C}(\text{O})\text{OCH}_3$, (*R*)-**107a**), 3.88 (dd, $J = 3.0, 9.0$ Hz, $\text{CHH}'\text{OCH}_2\text{CH}(\text{CH}_2\text{CH}_2)_2\text{CH}_2$, (*R*)-**107a,b**), 4.22 (q, $J = 6.9$ Hz, $\text{C}(\text{O})\text{OCH}_2\text{CH}_3$, (*R*)-**107b**), 4.68–4.78 (m, CHCH_2O , (*R*)-**107a,b**), 6.28–6.40 (br d, $\text{CH}_3\text{C}(\text{O})\text{NH}$, (*R*)-**107a,b**); ^{13}C NMR (CDCl_3) δ 14.4 ($\text{C}(\text{O})\text{OCH}_2\text{CH}_3$, (*R*)-**107b**), 23.4, 26.0, 26.7 ($\text{CH}_3\text{C}(\text{O})$, $\text{OCH}_2\text{CH}(\text{CH}_2\text{CH}_2)_2\text{CH}_2$, (*R*)-**107a,b**), 30.0, 30.1 ($\text{OCH}_2\text{CH}(\text{CH}_2\text{CH}_2)_2\text{CH}_2$, (*R*)-**107a,b**), 37.9 ($\text{OCH}_2\text{CH}(\text{CH}_2\text{CH}_2)_2\text{CH}_2$, (*R*)-**107a,b**), 52.7, 53.0 ($\text{C}(\text{O})\text{OCH}_3$, (*R*)-**107a**, $\text{CHCH}_2\text{OCH}_2$, (*R*)-**107a,b**), 61.8 ($\text{C}(\text{O})\text{OCH}_2\text{CH}_3$, (*R*)-**107b**), 67.8, 67.9 ($\text{CH}_2\text{OCH}_2\text{CH}(\text{CH}_2\text{CH}_2)_2\text{CH}_2$, (*R*)-**107a,b**), 77.5 ($\text{OCH}_2\text{CH}(\text{CH}_2\text{CH}_2)_2\text{CH}_2$, (*R*)-**107a,b**), 170.0, 170.6 ($\text{CH}_3\text{C}(\text{O})\text{NH}$, $\text{C}(\text{O})\text{OCH}_3$, (*R*)-**107a,b**), the remaining resonances for (*R*)-**107a** were not detected and are believed to overlap with nearby signals or to be too small to be detected; M_r (*R*)-**107a** (+ESI) 280.1525 [$\text{M}+\text{Na}$] $^+$ (calcd for $\text{C}_{13}\text{H}_{23}\text{NO}_4\text{Na}^+$ 280.1524), (*R*)-**107b** (+ESI) 294.1682 [$\text{M}+\text{Na}$] $^+$ (calcd for $\text{C}_{14}\text{H}_{25}\text{NO}_4\text{Na}^+$ 294.1681).

(*R*)-Methyl 2-Acetamido-3-(but-3-enyloxy)propionate ((*R*)-108a) and (*R*)-Ethyl 2-Acetamido-3-(but-3-enyloxy)propionate ((*R*)-108b). Using Method A, a ~3:7 mixture of (*R*)-**68a** and (*R*)-**68b** (3.00 g, 20 mmol), 3-buten-1-ol (3.4 mL, 40 mmol) and $\text{BF}_3 \cdot \text{Et}_2\text{O}$ (2.5 mL, 20 mmol) in CH_2Cl_2 (40 mL) gave a mixture of (*R*)-**108a** and (*R*)-**108b** (3.50 g, 77%) as a pale yellow oil that was used without further purification:

R_f = 0.48 ((*R*)-**108a**), 0.50 ((*R*)-**108b**) (5/95 hexanes/EtOAc); IR (neat) 3302, 3074, 2982, 2935, 2872, 1744, 1663, 1539, 1443, 1374, 1207 cm^{-1} ; ^1H NMR (CDCl_3) δ 2.05 (s, $\text{CH}_3\text{C(O)}$, (*R*)-**108a,b**), 2.24–2.35 ($\text{OCH}_2\text{CH}_2\text{CH}=\text{CH}_2$, (*R*)-**108a,b**), 3.40–3.58 (m, $\text{OCH}_2\text{CH}_2\text{CH}=\text{CH}_2$, (*R*)-**108a,b**), 3.62–3.70 (m, $\text{CHH}'\text{OCH}_2\text{CH}_2$, (*R*)-**108a,b**), 3.76 (s, C(O)OCH_3 , (*R*)-**108a**), 3.72–3.80 (m, $\text{CHH}'\text{OCH}_2\text{CH}_2$, (*R*)-**108a,b**), 4.15–4.28 (m, OCH_2CH_3 , (*R*)-**108b**), 4.58–4.68 (m, CHCH_2O , (*R*)-**108a,b**), 5.00–5.25 (m, $\text{CH}_2\text{CH}=\text{CH}_2$, (*R*)-**108a,b**), 5.69–5.85 (m, $\text{CH}_2\text{CH}=\text{CH}_2$, (*R*)-**108a,b**), 6.50–6.61 (br d, NHCHCH_2O , (*R*)-**108a,b**); ^{13}C NMR (CDCl_3) δ 14.1 (OCH_2CH_3 , (*R*)-**108b**), 23.3 ($\text{CH}_3\text{C(O)}$, (*R*)-**108a,b**), 33.7, 33.8 ($\text{CH}_2\text{CH}_2\text{CH}=\text{CH}_2$, (*R*)-**108a,b**), 52.5, 52.6, 52.7 (C(O)OCH_3 , (*R*)-**108a**, CHOCH_2 , (*R*)-**108a,b**), 61.5 (OCH_2CH_3 , (*R*)-**108b**), 70.3, 70.4, 70.6, 70.7 ($\text{CHCH}_2\text{OCH}_2$, (*R*)-**108a,b**), 116.5 ($\text{CH}_2\text{CH}_2\text{CH}=\text{CH}_2$, (*R*)-**108a,b**), 134.9 ($\text{CH}_2\text{CH}_2\text{CH}=\text{CH}_2$, (*R*)-**108a,b**), 170.0, 170.4, 171.1 ($\text{CH}_3\text{C(O)}$, CHC(O)O , (*R*)-**108a,b**), the remaining signal was not detected and is believed to overlap with nearby peaks. M_r (*R*)-**108a** (+ESI) 254.0794 $[\text{M}+\text{K}]^+$ (calcd for $\text{C}_{10}\text{H}_{17}\text{NO}_4\text{K}^+$ 254.0795), (*R*)-**108b** (+ESI) 252.1211 $[\text{M}+\text{Na}]^+$ (calcd for $\text{C}_{11}\text{H}_{19}\text{NO}_4\text{Na}^+$ 252.1212).

(S)-Methyl 2-Acetamido-3-(but-3-enyloxy)propionate ((S)-108a) and (S)-Ethyl 2-Acetamido-3-(but-3-enyloxy)propionate ((S)-108b). Using Method A, a ~9:1 mixture of (*S*)-**68a** and (*S*)-**68b** (1.50 g, 10 mmol), 3-buten-1-ol (1.3 mL, 17 mmol) and $\text{BF}_3\cdot\text{Et}_2\text{O}$ (1.3 mL, 23 mmol) in CH_2Cl_2 (20 mL) gave a mixture of (*S*)-**108a** and (*S*)-**108b** (550 mg, 25%) as a pale yellow oil after purification by flash chromatography (5/95 hexanes/EtOAc): R_f = 0.48 ((*S*)-**108a**), 0.50 ((*S*)-**108b**) (5/95 hexanes/EtOAc); IR (neat) 3300, 3071, 2944, 2870, 1747, 1662, 1537, 1441, 1372,

1211 cm^{-1} . Spectral data for (S)-**108a** (~90% based on ^1H NMR integrations): ^1H NMR (CDCl_3) δ 2.05 (s, $\text{CH}_3\text{C}(\text{O})$), 2.24–2.35 (m, $\text{OCH}_2\text{CH}_2\text{CH}=\text{CH}_2$), 3.42–3.56 (m, $\text{OCH}_2\text{CH}_2\text{CH}=\text{CH}_2$), 3.62–3.70 (m, $\text{CHH}'\text{OCH}_2\text{CH}_2$), 3.76 (s, $\text{C}(\text{O})\text{OCH}_3$), 3.72–3.80 (m, $\text{CHH}'\text{OCH}_2\text{CH}_2$), 4.68–4.73 (m, CHCH_2O), 5.00–5.12 (m, $\text{CH}_2\text{CH}=\text{CH}_2$), 5.69–5.85 (m, $\text{CH}_2\text{CH}=\text{CH}_2$), 6.30–6.45 (br d, NHCHCH_2O); ^{13}C NMR (CDCl_3) δ 23.3 ($\text{CH}_3\text{C}(\text{O})$), 33.9 ($\text{CH}_2\text{CH}_2\text{CH}=\text{CH}_2$), 52.7 ($\text{C}(\text{O})\text{OCH}_3$ or CHOCH_2), 52.8 (CHOCH_2 or $\text{C}(\text{O})\text{OCH}_3$), 70.4, 70.8 ($\text{CHCH}_2\text{OCH}_2$), 116.7 ($\text{CH}_2\text{CH}_2\text{CH}=\text{CH}_2$), 135.0 ($\text{CH}_2\text{CH}_2\text{CH}=\text{CH}_2$), 170.0, 171.0 ($\text{CH}_3\text{C}(\text{O})$, $\text{CHC}(\text{O})\text{OCH}_3$); M_r no signal was detected for (S)-**108a**.

Spectral data for (S)-**108b** (~10% based on ^1H NMR integrations): ^1H NMR (CDCl_3) δ 1.23–1.35 (m, OCH_2CH_3), 4.18–4.25 (m, OCH_2CH_3), the remaining signals were not detected and are believed to overlap with nearby signals or are too small to be detected; ^{13}C NMR signals were not detected for (S)-**108b**; M_r no signal was detected for (S)-**108b**.

(R)-Methyl 2-Acetamido-3-(2-cyclopropylethoxy)propionate ((R)-109a) and (R)-Ethyl 2-Acetamido-3-(2-cyclopropylethoxy)propionate ((R)-109b). Using Method A, a ~1:1 mixture of (R)-**68a** and (R)-**68b** (2.75 g, 18.3 mmol), 2-cyclopropylethanol (2.2 mL, 22 mmol) and $\text{BF}_3 \cdot \text{Et}_2\text{O}$ (2.3 mL, 18.3 mmol) in CH_2Cl_2 (40 mL) gave a ~1:1 mixture of (R)-**109a** and (R)-**109b** (1.61 g, 37%) as a yellow oil after work-up and purification by flash chromatography (1/1 EtOAc/hexanes to EtOAc): R_f = 0.48 ((R)-**109a**), 0.50 ((R)-**109b**) (5/95 hexanes/EtOAc); IR (neat) 3264, 3071, 2995, 2926, 2869, 1744, 1662, 1537, 1442, 1373, 1210, 1119 cm^{-1} ; ^1H NMR (CDCl_3) δ 0.01–0.08

(m, CH(CHH'CHH'), (*R*)-**109a,b**), 0.38–0.46 (m, CH(CHH'CHH'), (*R*)-**109a,b**), 0.60–0.68 (m, CH(CH₂CH₂), (*R*)-**109a,b**), 1.28 (t, *J* = 6.9 Hz, OCH₂CH₃, (*R*)-**109b**), 1.38–1.45 (m, CH₂CH(CH₂CH₂), (*R*)-**109a,b**), 2.06 (s, CH₃C(O), (*R*)-**109a,b**), 3.40–3.58 (m, OCH₂CH₂CH, (*R*)-**109a,b**), 3.54–3.60 (m, CHH'OCH₂CH₂, (*R*)-**109a,b**), 3.76 (s, C(O)OCH₃, (*R*)-**109a**), 3.82–3.90 (m, CHH'OCH₂CH₂, (*R*)-**109a,b**), 4.30–4.52 (m, C(O)OCH₂CH₃, (*R*)-**109b**), 4.70–4.78 (m, CHCH₂O, (*R*)-**109a,b**), 6.30–6.40 (br d, CH₃C(O)NH, (*R*)-**109a,b**); ¹³C NMR (CDCl₃) δ 4.3 (CH(CH₂CH₂), (*R*)-**109a,b**), 7.9 (CH(CH₂CH₂), (*R*)-**109a,b**), 14.3 (C(O)OCH₂CH₃, (*R*)-**109b**), 23.1 (CH₃C(O), (*R*)-**109a,b**), 34.5, 34.6 (CH₂CH(CH₂CH₂), (*R*)-**109a,b**), 52.7, 52.9, 53.0 (CHCH₂OCH₂, (*R*)-**109a,b**, C(O)OCH₃, (*R*)-**109a**), 61.7 (C(O)OCH₂CH₃, (*R*)-**109b**), 70.6, 70.7, 71.9 (CH₂OCH₂CH₂, (*R*)-**109a,b**), 170.1, 170.6, 171.1 (CH₃C(O)NH, C(O)OCH₃, (*R*)-**109a,b**), the remaining resonances were not detected and are believed to overlap with nearby signals; *M_r* (*R*)-**109a** (+ESI) 252.1212 [M+Na]⁺ (calcd for C₁₁H₁₉NO₄Na⁺ 252.1209), (*R*)-**109b** (+ESI) 266.1368 [M+Na]⁺ (calcd for C₁₂H₂₁NO₄Na⁺ 266.1368).

(S)-Methyl 2-Acetamido-3-(2-(benzyloxy)ethoxy)propionate ((S)-110). Using Method A compound (*S*)-**68a** (600 mg, 4.20 mmol), 2-benzyloxyethanol (775 μL, 5.45 mmol) and BF₃•Et₂O (527 μL, 4.20 mmol) in CH₂Cl₂ (20 mL) gave 600 mg (48%) of (*S*)-**110** as a pale yellow residue after purification by flash chromatography (5/95, cyclohexane/EtOAc): [α]_D²⁵ +33.1° (c 1.0, CHCl₃); *R_f* = 0.43 (5/95 cyclohexane/EtOAc); IR (neat) 3286, 2869, 1744, 1663, 1537, 1446, 1369, 1207; 1111 cm⁻¹; ¹H NMR (CDCl₃) δ 1.97 (s, CH₃C(O)NH), 3.58–3.68 (m, OCH₂CH₂OBn), 3.71 (dd, *J* = 3.3, 8.7 Hz, CHCHH'OCH₂), 3.75 (s, OCH₃), 3.99 (dd, *J* = 3.3, 8.7 Hz,

CHCHH'OCH₂), 4.55 (s, CH₂CH₂OCH₂Ph), 4.74 (app. dt, J = 6.0, 8.7 Hz, CHCH₂O), 6.50 (br d, J = 6.0 Hz, NHCHCH₂O), 7.26–7.40 (m, C₆H₅); ¹³C NMR (CDCl₃) δ 23.0 (CH₃C(O)), 52.5 (CHCH₂O or OCH₃), 52.8 (OCH₃ or CHCH₂O), 69.4, 71.0 (OCH₂CH₂O), 71.1 (CHCH₂O), 73.2 (OCH₂Ph), 127.6, 127.7, 128.4, 138.0 (C₆H₅), 170.0, 170.8 (CHC(O)NH and C(O)OCH₃); M_r (+ESI) 318.1310 [M+Na]⁺ (calcd for C₁₅H₂₁NO₅Na⁺ 318.1317). Anal. Calcd for C₁₅H₂₁NO₅•0.2H₂O: C, 60.27; H, 7.22; N, 4.69. Found: C, 60.14; H, 7.21; N, 4.65.

(*R*)-Methyl 2-Acetamido-3-(3-(benzyloxy)propoxy)propionate ((*R*)-111a) and (*R*)-Ethyl 2-Acetamido-3-(3-(benzyloxy)propoxy)propionate ((*R*)-111b). Using Method A, a ~3:2 mixture of (*R*)-68a and (*R*)-68b (4.26 g, 28.4 mmol), 3-benzyloxypropan-1-ol (12 mL, 75.5 mmol), and BF₃•Et₂O (3.57 mL, 28.4 mmol) in CH₂Cl₂ (200 mL) gave 4.30 g (48%) of a mixture of (*R*)-111a and (*R*)-111b as a pale yellow oil after purification by flash column chromatography (1/9 hexanes/EtOAc): R_f = 0.53 ((*R*)-111a) and 0.55 ((*R*)-111b) (5/95 hexanes/EtOAc); IR (neat) 3306, 3063, 3033, 2941, 2869, 1744, 1665, 1535, 1449, 1372, 1210, 1109 cm⁻¹; ¹H NMR (CDCl₃) δ 1.25 (t, J = 6.9 Hz, OCH₂CH₃, (*R*)-111b), 1.84 (quint, J = 6.3 Hz, OCH₂CH₂CH₂O, (*R*)-111a,b), 1.98 (s, CH₃C(O), (*R*)-111a,b), 3.48–3.58 (m, OCH₂CH₂CH₂O, (*R*)-111a,b), 3.60–3.66 (m, CHH'OCH₂CH₂CH₂, (*R*)-111a,b), 3.71 (s, C(O)OCH₃, (*R*)-111a), 3.86 (dd, J = 3.0, 9.6 Hz, CHH'OCH₂CH₂CH₂, (*R*)-111a,b), 4.18 (q, J = 6.9 Hz, C(O)OCH₂CH₃, (*R*)-111b), 4.48 (s, OCH₂Ph, (*R*)-111a,b), 4.68–4.74 (m, CHCH₂O, (*R*)-111a,b), 6.45–6.56 (m, CH₃C(O)NH, (*R*)-111a,b), 7.24–7.38 (m, C₆H₅, (*R*)-111a,b); ¹³C NMR (CDCl₃) δ 14.1 (C(O)OCH₂CH₃,

(*R*)-**111b**), 23.0, 23.1 ($\text{CH}_3\text{C(O)}$), (*R*)-**111a,b**), 29.7, 29.8 ($\text{OCH}_2\text{CH}_2\text{CH}_2\text{O}$), (*R*)-**111a,b**), 52.4, 52.7, 52.8 ($\text{CHCH}_2\text{OCH}_2$), (*R*)-**111a,b**, C(O)OCH_3 , (*R*)-**111a**), 61.5 (C(O)OCH_2), (*R*)-**111b**), 67.0, 68.5 ($\text{OCH}_2\text{CH}_2\text{CH}_2\text{O}$), (*R*)-**111a,b**), 70.4, 70.5 ($\text{CHCH}_2\text{OCH}_2\text{CH}_2\text{CH}_2$), (*R*)-**111a,b**), 73.0 (OCH_2Ph), (*R*)-**111a,b**), 127.6, 128.4, 138.4 (C_6H_5), (*R*)-**111a,b**), 170.0, 170.3, 170.9 (CHC(O)O , $\text{CH}_3\text{C(O)NH}$), (*R*)-**111a,b**), the remaining aromatic signal and additional signals corresponding to each ester were not detected and are believed to overlap with nearby signals; M_r (*R*)-**111a** (+ESI) 332.1467 $[\text{M}+\text{Na}]^+$ (calcd for $\text{C}_{16}\text{H}_{23}\text{NO}_5\text{Na}^+$ 332.1474), (*R*)-**111b** (+ESI) 346.1624 $[\text{M}+\text{Na}]^+$ (calcd for $\text{C}_{17}\text{H}_{25}\text{NO}_5\text{Na}^+$ 346.1630).

(S)-Methyl 2-Acetamido-3-(3-(benzyloxy)propoxy)propionate ((S)-111a). Using Method A, (*S*)-**68a** (1.00 g, 7.0 mmol), 3-benzyloxypropan-1-ol (1.44 mL, 9.11 mmol), and $\text{BF}_3 \cdot \text{Et}_2\text{O}$ (878 μL , 7.0 mmol) in CH_2Cl_2 (3.5 mL) gave 816 mg (37%) of (*S*)-**111a** as a pale yellow oil after two purifications by flash column chromatography (5/95 hexanes/EtOAc) and (5/95 MeOH/ CHCl_3): $[\alpha]_D^{25} +32.9^\circ$ (c 0.5, CHCl_3); $R_f = 0.53$ (5/95 hexanes/EtOAc); IR (neat) 3294, 3032, 2931, 2867, 1746, 1665, 1535, 1445, 1371, 1212, 1109 cm^{-1} ; ^1H NMR (CDCl_3) δ 1.85 (quint, $J = 6.3$ Hz, $\text{OCH}_2\text{CH}_2\text{CH}_2\text{O}$), 2.00 (s, $\text{CH}_3\text{C(O)}$), 3.48–3.59 (m, $\text{OCH}_2\text{CH}_2\text{CH}_2\text{O}$), 3.63 (dd, $J = 3.0, 9.6$ Hz, $\text{CHH}'\text{OCH}_2\text{CH}_2\text{CH}_2$), 3.73 (s, C(O)OCH_3), 3.86 (dd, $J = 3.0, 9.6$ Hz, $\text{CHH}'\text{OCH}_2\text{CH}_2\text{CH}_2$), 4.50 (s, OCH_2Ph), 4.73 (app dt, $J = 3.0, 7.8$ Hz, CHCH_2O), 6.33 (d, $J = 7.8$ Hz, $\text{CH}_3\text{C(O)NH}$), 7.24–7.38 (m, C_6H_5); ^{13}C NMR (CDCl_3) δ 23.3 ($\text{CH}_3\text{C(O)}$), 29.9 ($\text{OCH}_2\text{CH}_2\text{CH}_2\text{O}$), 52.7 ($\text{CHCH}_2\text{OCH}_2$ or C(O)OCH_3), 52.9 (C(O)OCH_3 or $\text{CHCH}_2\text{OCH}_2$), 67.2, 68.8 ($\text{OCH}_2\text{CH}_2\text{CH}_2\text{O}$), 70.7

(CHCH₂OCH₂CH₂CH₂), 73.2 (OCH₂Ph), 127.7, 127.8, 128.6, 138.6 (C₆H₅), 170.1, 171.1 (CHC(O)OCH₃, CH₃C(O)NH); *M_r* (+ESI) 332.1469 [M+Na]⁺ (calcd for C₁₅H₂₁NO₅Na⁺ 332.1474). Anal. Calcd for C₁₆H₂₃NO₅•0.2H₂O: C, 61.40; H, 7.54; N, 4.48. Found: C, 61.38; H, 7.47; N, 4.48.

(*R*)-Methyl 2-Acetamido-3-(2-azidoethoxy)propionate ((*R*)-112). Using Method A, (*R*)-**68a** (2.35 g, 16.4 mmol), 2-azidoethanol (4.5 mL, 65.6 mmol) and BF₃•Et₂O (1 mL, 8.2 mmol) in CH₂Cl₂ (30 mL) gave 1.56 g (41%) of (*R*)-**112** after purification; [α]²⁵_D +49.1° (c 1.0; EtOAc); *R_f* = 0.47 (EtOAc); IR (neat) 3302, 2948, 2107, 1746, 1668, 1534, 1443 cm⁻¹; ¹H NMR (CDCl₃) δ 2.06 (s, CH₃C(O)NH), 3.23–3.42 (m, CH₂N₃), 3.31–3.64 (m, OCH₂CH₂N₃, CHCHH'OCH₂), 3.78 (s, OCH₃), 3.96 (dd, *J* = 3.0, 9.1 Hz, CHCHH'O), 4.76–4.81 (m, CHCH₂O), 6.30–6.41 (br d, CH₃C(O)NH); ¹³C NMR (CDCl₃) δ 23.2 (CH₃C(O)), 50.0 (OCH₂CH₂N₃), 52.6 (OCH₃ or CHCH₂O), 52.8 (CHCH₂O or OCH₃), 70.9 (CHCH₂O or OCH₂CH₂N₃), 71.1 (OCH₂CH₂N₃ or CHCH₂O), 170.1 (CH₃C(O)NH or C(O)OCH₃), 170.6 (C(O)OCH₃ or CH₃C(O)NH); *M_r* (+ESI) 253.0906 [M+Na]⁺ (calcd for C₈H₁₄N₄O₄Na⁺ 253.0913). No satisfactory elemental analysis was obtained.

(*S*)-Methyl 2-Acetamido-3-(2-azidoethoxy)propionate ((*S*)-112). Using Method A, (*S*)-**68a** (3.30 g, 23 mmol), 2-azidoethanol (6.3 mL, 92 mmol), and BF₃•Et₂O (1.4 mL, 11.5 mmol) in CH₂Cl₂ (115 mL) gave 1.67 g (31%) of (*S*)-**112** as a colorless residue after purification by silica gel chromatography (EtOAc): [α]²⁵_D -48.0° (c 1.0; EtOAc); *R_f* = 0.47 (EtOAc); IR (neat) 3302, 2948, 2107, 1746, 1667, 1534, 1443 cm⁻¹; ¹H

NMR (CDCl₃) δ 2.06 (s, CH₃C(O)NH), 3.23–3.42 (m, CH₂N₃), 3.31–3.64 (m, OCH₂CH₂N₃, CHCHH'OCH₂), 3.78 (s, OCH₃), 3.96 (dd, J = 3.0, 9.1 Hz, CHCHH'O), 4.76–4.81 (m, CHCH₂O), 6.30–6.41 (br d, CH₃C(O)NH); ¹³C NMR (CDCl₃) δ 23.3 (CH₃C(O)), 50.1 (OCH₂CH₂N₃), 52.7 (OCH₃ or CHCH₂O), 52.9 (CHCH₂O or OCH₃), 71.0 (CHCH₂O or OCH₂CH₂N₃), 71.2 (OCH₂CH₂N₃ or CHCH₂O), 170.2, 170.7 (CH₃C(O)NH and C(O)OCH₃); M_r (+ESI) 253.0906 [M+Na]⁺ (calcd for C₈H₁₄N₄O₄Na⁺ 253.0913). No satisfactory elemental analysis was obtained.

(*R*)-Methyl 2-Acetamido-3-(2-methoxyethoxy)propionate ((*R*)-113a) and (*R*)-Ethyl 2-Acetamido-3-(2-methoxyethoxy)propionate ((*R*)-113b). Using Method A, a ~5:95 mixture of (*R*)-**68a** and (*R*)-**68b** (3.50 g, 23 mmol), ethylene glycol monomethyl ether (3.6 mL, 46 mmol) and BF₃•Et₂O (2.9 mL, 23 mmol) in CH₂Cl₂ (40 mL) gave upon work-up a ~5:95 mixture of (*R*)-**113a** and (*R*)-**113b** (4.24 g, 80%) as a pale yellow oil that did not require further purification: R_f = 0.41 ((*R*)-**113a**), 0.43 ((*R*)-**113b**) (EtOAc); IR (neat) 3303, 3061, 2930, 1743, 1668, 1535, 1451, 1374, 1204, 1113 cm⁻¹. Spectral data for (*R*)-**113a**: ¹H and ¹³C NMR signals for (*R*)-**113a** were not detected and are believed to overlap with nearby signals or are too small to be detected; M_r (+ESI) 258.0744 [M+K]⁺ (calcd for C₉H₁₇NO₅K⁺ 258.0744).

Spectral data for (*R*)-**113b** (~95% based on ¹H NMR integrations): ¹H NMR (CDCl₃) δ 1.29 (t, J = 7.2 Hz, OCH₂CH₃), 2.05 (s, CH₃C(O)), 3.37 (s, CH₂OCH₃), 3.49–3.53 (m, CH₂OCH₂CH₂OCH₃ or CH₂OCH₂CH₂OCH₃), 3.59–3.64 (m, CH₂OCH₂CH₂OCH₃ or CH₂OCH₂CH₂OCH₃), 3.73 (dd, J = 3.0, 9.0 Hz, CHH'OCH₂CH₂), 3.94 (dd, J = 3.0, 9.0 Hz, CHH'OCH₂CH₂), 4.22 (d, J = 7.2 Hz,

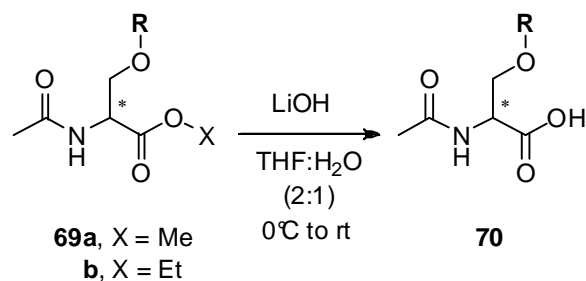
OCH₂CH₃), 4.52 (app. dt, J = 3.0, 7.2 Hz, CHCH₂O), 6.48–6.60 (br d, NHCHCH₂O); ¹³C NMR (CDCl₃) δ 14.3 (OCH₂CH₃), 23.3 (CH₃C(O)), 53.0 (CHC(O)OCH₂), 59.1 (CH₂OCH₃), 61.7 (C(O)OCH₂CH₃), 71.1, 71.3, 71.9 (CHCH₂OCH₂CH₂OCH₃), 170.1, 170.5 (CH₃C(O), CHC(O)OCH₂); M_r (+ESI) 272.0901 [M+K]⁺ (calcd for C₁₀H₁₉NO₅K⁺ 272.0900).

(*R*)-Methyl 2-Acetamido-3-(2-(2-methoxyethoxy)ethoxy)propionate ((*R*)-114a) and (*R*)-Ethyl 2-Acetamido-3-(2-(2-methoxyethoxy)ethoxy)propionate ((*R*)-114b). Using Method A, a ~1:1 mixture of (*R*)-68a and (*R*)-68b (4.5 g, 30.0 mmol), diethyleneglycol monomethyl ether (11.3 g, 94.5 mmol) and BF₃•Et₂O (3.8 mL, 30.0 mmol) in CH₂Cl₂ (30 mL) gave 2.84 g (35%) of (*R*)-114a and (*R*)-114b as a colorless viscous oil: R_f = 0.31 ((*R*)-114a), 0.33 ((*R*)-114b) (EtOAc); IR (neat) 3300, 3063, 2940, 2940, 1744, 1659, 1553, 1446, 1216, 1120 cm⁻¹. Spectral data for (*R*)-114a (approximately 50 mol percent based on ¹H NMR integrations): ¹H NMR (CDCl₃) δ 2.06 (s, CH₃C(O)NH), 3.39 (s, CH₂CH₂OCH₃), 3.52–3.58 (m, CH₂CH₂OCH₃), 3.60–3.64 (m, OCH₂CH₂OCH₂), 3.68–3.74 (m, CHCHH'OCH₂), 3.76 (s, C(O)OCH₃), 3.94 (app. t, J = 4.2, CHCHH'OCH₂), 4.68–4.76 (m, CHCH₂OCH₂), 6.52–6.70 (m, CH₃C(O)NH); ¹³C NMR (CDCl₃) δ 23.1 (CH₃C(O)), 52.6 (CHCH₂OCH₂ or C(O)OCH₃), 52.9, 53.0 (C(O)OCH₃ or CHCH₂OCH₃, (*R*)-114a, CHCH₂OCH₃, (*R*)-114b), 59.2 (CH₂CH₂OCH₃), 70.5, 70.6, 71.1, 71.2, 71.3 (OCH₂CH₂OCH₂CH₂OCH₃), 170.1, 170.4, 170.9 (CH₃C(O)NH, C(O)OCH₃), additional peaks were observed and are believed to be part of (*R*)-114b but cannot

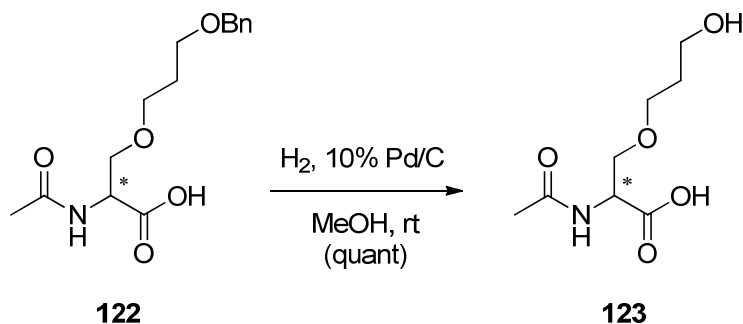
be precisely attributed; Compound **114a** was only detected by HRMS as the acid. M_r (+ESI) found 272.1107 $[M+Na]^+$ (calcd for $C_{10}H_{19}NO_6Na^+$ 272.1110).

Spectral data for (*R*)-**114b** (approximately 50 mol percent based on 1H NMR integrations): 1H NMR ($CDCl_3$) δ 1.28 (t, $J = 7.2$ Hz, $C(O)OCH_2CH_3$), 2.06 (s, $CH_3C(O)NH$), 3.39 (s, $CH_2CH_2OCH_3$), 3.52–3.58 (m, $CH_2CH_2OCH_3$), 3.60–3.64 (m, $OCH_2CH_2OCH_2$), 3.68–3.74 (m, $CHCHH'OCH_2$), 3.97 (app. t, $J = 4.2$, $CHCHH'OCH_2$), 4.22 (t, $J = 7.2$ Hz, $C(O)OCH_2CH_3$), 4.68–4.76 (m, $CHCH_2OCH_2$), 6.52–6.70 (m, $CH_3C(O)NH$); ^{13}C NMR ($CDCl_3$) δ 14.3 ($C(O)OCH_2CH_3$), 23.1 ($CH_3C(O)$), 52.6 ($CHCH_2OCH_2$), 52.9, 53.0 ($C(O)OCH_3$ or $CHCH_2OCH_3$, (*R*)-**114a**, $CHCH_2OCH_3$ (*R*)-**114b**), 70.5, 70.6, 71.1, 71.2, 71.3 ($OCH_2CH_2OCH_2CH_2OCH_3$), 170.1, 170.4, 170.9 ($CH_3C(O)NH$, $C(O)OCH_3$), additional peaks were observed and are believed to be part of (*R*)-**114a** but cannot be precisely attributed; M_r (+ESI) found 300.1421 $[M+Na]^+$ (calcd for $C_{12}H_{23}NO_6Na^+$ 300.1423).

2.2.4.4. Synthesis of *O*-Substituted *N*-Acetylserine Derivatives.



Scheme 20. Synthesis of acid **123** to prepare the side chain aldehyde AB group



R =	Compound number
Me	115
Et	116
<i>i</i> -Pr	117
<i>t</i> -Bu	118
Ph	119
CH ₂ CH ₂ CH=CH ₂	120
CH ₂ CH ₂ OBn	121
CH ₂ CH ₂ CH ₂ OBn	122
CH ₂ CH ₂ CH ₂ OH	123
CH ₂ CH ₂ N ₃	124
(CH ₂ CH ₂ O) ₂ CH ₃	125

(*R*)-2-Acetamido-3-methoxypropionic Acid ((*R*)-115). Using Method B, a mixture of (*R*)-**101a** and (*R*)-**101b** (3.79 g, 21.5 mmol) in THF (210 mL) and LiOH (515 mg, 21.5 mmol) in H₂O (100 mL) gave 1.31 g (38%) of (*R*)-**115** as a white solid after

work-up and recrystallization from EtOAc: mp 108–109°C; $[\alpha]_D^{25}$ -20.9° (c 0.7, MeOH) (lit.²³⁵ $[\alpha]_D^{25}$ -16.9° (c 1.2; MeOH) for a partially racemized sample (~4:1, (*R*):(*S*))); R_f = 0–0.1 (EtOAc); IR (nujol) 3352, 3100–2200, 1746, 1631, 1549, 1459, 1375 cm⁻¹; ¹H NMR (DMSO-*d*₆) δ 1.86 (s, CH₃C(O)), 3.25 (s, CH₂OCH₃), 3.49 (dd, J = 3.9, 10.0 Hz, CHH'OCH₃), 3.63 (dd, J = 6.0, 10.0 Hz CHH'OCH₃), 4.36–4.45 (m, CHCH₂O), 8.20 (d, J = 7.2 Hz, CH₃C(O)NH), 12.7 (s, CO₂H); ¹³C NMR (DMSO-*d*₆) δ 22.3 (CH₃C(O)), 52.1 (CHCH₂OCH₃), 58.3 (OCH₃), 71.8 (CHCH₂OCH₃), 169.4, 171.7 (CHCO₂H, CH₃C(O)NH). M_r (+ESI) 184.0582 [M+Na]⁺ (calcd for C₆H₁₁NO₄Na⁺ 184.0586). Anal. Calcd for C₆H₁₁NO₄: C, 44.72; H, 6.88; N, 8.69. Found: C, 44.75; H, 6.82; N, 8.77.

(*S*)-2-Acetamido-3-(methoxy)propionic Acid ((*S*)-115). Using Method B, a ~9:1 mixture of (*S*)-**101a** and (*S*)-**101b** (1.43 g, 8 mmol) in THF (60 mL) and LiOH (192 mg, 8 mmol) in H₂O (30 mL) gave (*S*)-**115** (470 mg, 37%) upon work-up as a yellow oil that was recrystallized from EtOAc: mp 107–109°C; $[\alpha]_D^{25}$ +20.7° (c 0.5; MeOH); R_f = 0–0.10 (EtOAc); IR (nujol) 3351, 3300–2200 (br), 1746, 1631, 1549, 1459, 1375 cm⁻¹; ¹H NMR (CD₃OD) δ 2.01 (s, CH₃C(O)), 3.35 (s, CH₂OCH₃), 3.61 (dd, J = 3.3, 9.3 Hz, CHH'OCH₃), 3.81 (dd, J = 4.8, 9.3 Hz, CHH'OCH₃), 4.54–4.62 (m, CHCH₂O); ¹³C NMR (CD₃OD) δ 22.5 (CH₃C(O)), 54.2 (CHOCH₂), 59.4 (CH₂OCH₃), 73.2 (CHCH₂OCH₃), 173.3, 173.5 (CH₃C(O), CHC(O)OH); M_r (+ESI) 184.0584 [M+Na]⁺ (calcd for C₆H₁₁NO₄Na⁺ 184.0586). Anal. Calcd for C₆H₁₁NO₄: C, 44.72; H, 6.88; N, 8.69. Found: C, 44.47; H, 6.92; N, 8.46.

(*R*)-2-Acetamido-3-ethoxypropionic Acid ((*R*)-116). Using Method B, a mixture of (*R*)-102a and (*R*)-102b (2.48 g, 13.0 mmol) in THF (130 mL) and LiOH (312 mg, 13.0 mmol) in H₂O (65 mL) gave 1.57 g (69%) of (*R*)-116 as a white solid after work-up and recrystallization from EtOAc: mp 149–151°C; $[\alpha]_D^{25} -31.5^\circ$ (c 0.7, MeOH); $R_f = 0-0.15$ (5/95 hexanes/EtOAc); IR (nujol) 3355, 3300–2100 (br), 1951, 1747, 1630, 1545, 1457, 1374, 1204, 1107 cm⁻¹; ¹H NMR (DMSO-*d*₆) δ 1.09 (t, $J = 6.9$ Hz, OCH₂CH₃), 1.86 (s, CH₃C(O)), 3.39–3.49 (m, CH₂OCH₂CH₃), 3.53 (dd, $J = 4.2, 10.0$ Hz, CHH'OCH₂CH₃), 3.63 (dd, $J = 6.0, 10.0$ Hz, CHH'OCH₂CH₃), 4.36–4.42 (m, CHCH₂O), 8.15 (d, $J = 7.2$ Hz, CH₃C(O)NH), the carboxylic acid proton could not be detected; ¹³C NMR (DMSO-*d*₆) δ 14.9 (OCH₂CH₃), 22.3 (CH₃C(O)), 52.4 (CHCH₂OCH₃), 65.8 (OCH₂CH₃), 69.6 (CHCH₂OCH₂CH₃), 169.4, 171.7 (CHCO₂H, CH₃C(O)NH); M_r (+ESI) 214.0480 [M+K]⁺ (calcd for C₇H₁₃NO₄K⁺ 214.0482). Anal. Calcd for C₇H₁₃NO₄: C, 47.99; H, 7.48; N, 8.00. Found: C, 48.21; H, 7.56; N, 7.95.

(*R*)-2-Acetamido-3-isopropoxypropionic Acid ((*R*)-117). Using Method B, a mixture of (*R*)-103a and (*R*)-103b (2.47 g, 12.0 mmol) in THF (120 mL) and LiOH (288 mg, 12.0 mmol) in H₂O (60 mL) gave 2.15 g (95%) of (*R*)-117 as a white solid after work-up. Recrystallization from EtOAc and hexanes afforded an analytical sample: mp 128–130°C; $[\alpha]_D^{25} -36.5^\circ$ (c 0.6, MeOH); $R_f = 0.05-0.18$ (5/95 hexanes/EtOAc); IR (nujol) 3366, 3300–2100 (br), 1751, 1636, 1548, 1457, 1376, 1328 cm⁻¹; ¹H NMR (DMSO-*d*₆) δ 1.06 (d, $J = 6.0$ Hz, OCHCH₃(C'H₃)), 1.07 (d, $J = 6.0$ Hz, OCHCH₃(C'H₃)), 1.87 (s, CH₃C(O)), 3.49–3.50 (m, CHH'OCH(CH₃)₂), 3.64 (dd, $J = 5.7, 9.9$ Hz, CHH'OCH(CH₃)₂), 4.33–4.40 (m, CHCH₂O), 8.10 (d, $J = 7.2$ Hz,

CH₃C(O)NH), 12.70 (CO₂H); ¹³C NMR (DMSO-*d*₆) δ 21.8 (OCHCH₃(C'H₃)), 21.9 (OCHCH₃(C'H₃), 22.4 (s, CH₃C(O)), 52.6 (CHCH₂OCH(CH₃)₂), 67.4 (CH₂OCH(CH₃)₂), 71.3 (CH₂OCH(CH₃)₂), 169.4, 171.8 (CH₃C(O)NH, CO₂H); *M_r* (+ESI) 212.0897 [M+Na]⁺ (calcd for C₈H₁₅NO₄Na⁺ 212.0899). Anal. Calcd for C₈H₁₅NO₄: C, 50.78; H, 7.99; N, 7.40. Found: C, 50.87; H, 8.02; N, 7.34.

(*R*)-2-Acetamido-3-*tert*-butoxypropionic Acid ((*R*)-118). Using Method B, a mixture of (*R*)-**104a** and (*R*)-**104b** (2.17 g, 9.90 mmol) in THF (100 mL) and LiOH (237 mg, 9.90 mmol) in H₂O (50 mL) gave 1.10 g (55%) of (*R*)-**118** as a white solid after work-up. Recrystallization from EtOAc and hexanes afforded an analytical sample: mp 154–156°C; [α]_D²⁵ -46.7° (c 0.8, MeOH); *R_f* = 0.48 (5/95 hexanes/EtOAc); IR (nujol) 3370, 3300–2100 (br), 1875, 1708, 1613, 1542, 1459, 1371, 1229, 1103 cm⁻¹; ¹H NMR (DMSO-*d*₆) δ 1.11 (s, OC(CH₃)₃), 1.87 (s, CH₃C(O)), 3.47 (dd, *J* = 4.2, 9.3 Hz, CHH'OC(CH₃)₃), 3.60 (dd, *J* = 5.1, 9.3 Hz, CHH'OC(CH₃)₃), 4.30–4.38 (m, CHCH₂O), 8.01 (d, *J* = 7.2 Hz, CH₃C(O)NH), 12.60 (CO₂H); ¹³C NMR (DMSO-*d*₆) δ 22.4 (s, CH₃C(O)), 27.2 (OC(CH₃)₃), 52.8 (CHCH₂OC(CH₃)₃), 61.7 (CH₂OC(CH₃)₃), 72.8 (CHCH₂OC(CH₃)₃), 169.4, 171.9 (CH₃C(O)NH, CO₂H); *M_r* (+ESI) 242.0794 [M+K]⁺ (calcd for C₉H₁₇NO₄K⁺ 242.0795). Anal. Calcd for C₉H₁₇NO₄: C, 53.19; H, 8.43; N, 6.89; Found: C, 53.04; H, 8.49; N, 6.84.

(*R*)-2-Acetamido-3-phenoxypropionic Acid ((*R*)-119). Using Method B, a ~3:7 mixture of (*R*)-**106a** and (*R*)-**106b** (1.4 g, 5.7 mmol), LiOH (142 mg, 5.9 mmol) in

THF:H₂O (80 mL) gave 950 mg (74%) of (*R*)-**119** after recrystallization from EtOAc and hexanes: mp 168–170°C; $[\alpha]_D^{25}$ -91.2° (*c* 0.5, MeOH); R_f = 0–0.15 (1/9 MeOH/CHCl₃); IR (nujol) 3362, 2300–2800 (br), 1950, 1746, 1607, 1551, 1461 cm⁻¹; ¹H NMR (DMSO-*d*₆) δ 1.90 (s, CH₃C(O)), 4.13 (dd, *J* = 3.9, 9.6 Hz, CHH'OPh), 4.37 (dd *J* = 5.1, 9.6 Hz, CHH'OPh), 4.60–4.68 (m, CHCH₂O), 6.88–6.98 (m, 3 ArH), 7.24–7.32 (m, 2 ArH), 8.42 (d, *J* = 7.5 Hz, NHCHCH₂), 12.50–13.00 (m, C(O)OH); ¹³C NMR (DMSO-*d*₆) δ 22.3 (CH₃C(O)), 51.8 (CHCH₂OPh), 67.6 (CH₂OPh), 114.6, 121.0, 129.8, 158.1 (CH₂OPh), 169.5, 171.3 (CH₃C(O)NH, CHC(O)OH); M_r (+ESI) 246.0739 [M+Na]⁺ (calcd for C₁₁H₁₃NO₄Na⁺ 246.0742). Anal. Calcd for C₁₁H₁₃NO₄•0.25 H₂O: C, 58.02; H, 5.98; N, 6.15. Found: C, 58.00; H, 5.98; N, 5.91.

(*R*)-2-Acetamido-3-(but-3-enyloxy)propionic Acid ((*R*)-120**).** Using Method B, a ~3:7 mixture of (*R*)-**108a** and (*R*)-**108b** (3.28 g, 14.6 mmol) in THF (145 mL) and LiOH (350 mg, 14.6 mmol) in H₂O (70 mL) gave (*R*)-**120** (1.90 g, 65%) as a yellow oil that was used without further purification: $[\alpha]_D^{25}$ -21.9° (*c* 0.9; MeOH); R_f = 0.10 (15/85 MeOH/CH₂Cl₂); IR (neat) 3300–2100 (br), 1957, 1735, 1635, 1544, 1432, 1376, 1228, 1118 cm⁻¹; ¹H NMR (CDCl₃) δ 2.09 (s, CH₃C(O)), 2.25–2.37 (m, OCH₂CH₂CH=CH₂), 3.46–3.51 (m, OCH₂CH₂CH=CH₂), 3.69 (dd, *J* = 4.0, 9.0 Hz, CHH'OCH₂), 3.93 (dd, *J* = 4.0, 9.0 Hz, CHH'OCH₂), 4.73 (app dt, *J* = 4.0, 7.7 Hz, CHCH₂O), 5.00–5.22 (m, CH₂CH=CH₂), 5.70–5.85 (m, CH₂CH=CH₂), 6.22 (d, *J* = 7.7 Hz, NHCHCH₂O), 9.80–10.00 (br s, C(O)OH); ¹³C NMR (CDCl₃) δ 23.1 (CH₃C(O)), 33.9 (CH₂CH₂CH=CH₂), 52.9 (CHOCH₂), 70.0, 70.9 (CHCH₂OCH₂), 117.0 (CH₂CH₂CH=CH₂), 134.9 (CH₂CH₂CH=CH₂), 171.5, 173.4 (CH₃C(O),

CHC(O)OH); M_r (+ESI) 224.0897 $[M+Na]^+$ (calcd for $C_9H_{15}NO_4Na^+$ 224.0899). Anal. Calcd for $C_9H_{15}NO_4 \cdot 0.30H_2O$: C, 52.32; H, 7.61; N, 6.78; Found: C, 52.11; H, 7.37; N, 6.77.

(S)-2-Acetamido-3-(but-3-enyloxy)propionic Acid ((S)-120). Using Method B, a ~9:1 mixture of (S)-**108a** and (S)-**108b** (550 mg, 2.5 mmol) in THF (25 mL) and LiOH (61 mg, 2.5 mmol) in H_2O (12 mL) gave (S)-**120** (260 mg, 51%) as a yellow oil that was used without further purification: $[\alpha]_D^{25} +22.2^\circ$ (c 0.5; MeOH); $R_f = 0.10$ (15/85 MeOH/ CH_2Cl_2); IR (neat) 3300–2200 (br), 1953, 1735, 1636, 1547, 1432, 1376, 1227, 1118 cm^{-1} ; 1H NMR ($CDCl_3$) δ 2.01 (s, $CH_3C(O)$), 2.28–2.36 (m, $OCH_2CH_2CH=CH_2$), 3.49–3.52 (m, $OCH_2CH_2CH=CH_2$), 3.68 (dd, $J = 4.0, 9.0$ Hz, $CHH'OCH_2$), 3.93 (dd, $J = 4.0, 9.0$ Hz, $CHH'OCH_2$), 4.73 (app dt, $J = 4.0, 7.7$ Hz, $CHCH_2O$), 5.00–5.25 (m, $CH_2CH=CH_2$), 5.70–5.85 (m, $CH_2CH=CH_2$), 6.52 (d, $J = 7.7$ Hz, $NHCHCH_2O$), 9.10–9.60 (br s, $C(O)OH$); ^{13}C NMR ($CDCl_3$) δ 23.2 ($CH_3C(O)$), 33.9 ($CH_2CH_2CH=CH_2$), 52.8 ($CHOCH_2$), 69.9, 70.9 ($CHCH_2OCH_2$), 117.0 ($CH_2CH_2CH=CH_2$), 134.9 ($CH_2CH_2CH=CH_2$), 171.3, 173.5 ($CH_3C(O)$, $CHC(O)OH$); M_r (+ESI) 224.0901 $[M+Na]^+$ (calcd for $C_9H_{15}NO_4Na^+$ 224.0899). Anal. Calcd for $C_9H_{15}NO_4 \cdot 0.30H_2O$: C, 52.32; H, 7.61; N, 6.78; Found: C, 52.08; H, 7.47; N, 6.88.

(S)-2-Acetamido-3-(2-(benzyloxy)ethoxy)propionic Acid ((S)-121). Using Method B, (S)-**110a** (460 mg, 1.56 mmol) in THF (15 mL) and LiOH (37 mg, 1.56 mmol) in H_2O (7 mL) gave 386 mg (87%) of (S)-**121** as a colorless residue that was used

directly in the next step: $[\alpha]_D^{25} +16.3^\circ$ (c 1.0, CHCl_3); $R_f = 0.05$ (5/95 cyclohexane/EtOAc); IR (neat) 3400–2600 (br), 3322, 1736, 1631, 1541, 1449, 1372, 1214; 1121 cm^{-1} ; ^1H NMR (CDCl_3) δ 1.97 (s, $\text{CH}_3\text{C}(\text{O})\text{NH}$), 3.58–3.80 (m, $\text{OCH}_2\text{CH}_2\text{OBn}$, $\text{CHCHH}'\text{OCH}_2$), 3.95–4.04 (m, $\text{CHCHH}'\text{OCH}_2$), 4.54 (s, OCH_2Ph), 4.68–4.75 (m, $\text{CHCH}_2\text{OCH}_2$), 6.80 (d, $J = 6.1\text{ Hz}$, NHCHCH_2O), 7.22–7.40 (m, C_6H_5), 8.30–8.70 (br s, $\text{C}(\text{O})\text{OH}$); ^{13}C NMR (CDCl_3) δ 23.0 ($\text{CH}_3\text{C}(\text{O})$), 52.9 (CHCH_2O), 69.4, 70.7, 71.0 ($\text{OCH}_2\text{CH}_2\text{O}$ and CHCH_2O), 73.2 (OCH_2Ph), 128.0, 128.6, 137.7 (C_6H_5), 171.3, 172.5 ($\text{CH}_3\text{C}(\text{O})\text{NH}$ and $\text{C}(\text{O})\text{OH}$), the remaining aromatic resonance was not detected and is believed to overlap with nearby signals; M_r (+ESI) 304.1157 $[\text{M}+\text{Na}]^+$ (calcd for $\text{C}_{14}\text{H}_{19}\text{NO}_5\text{Na}^+$ 304.1161).

(*R*)-2-Acetamido-3-(3-(benzyloxy)propoxy)propionic Acid ((*R*)-122). Using Method B, a ~1:1 mixture of (*R*)-111a and (*R*)-111b (4.30 g, 13.6 mmol) in THF (150 mL) and LiOH (325 mg, 13.6 mmol) in H_2O (70 mL) gave 3.63 g (90%) of (*R*)-122 as a viscous yellow oil that was used directly in the next step: $[\alpha]_D^{25} -17.7^\circ$ (c 1.0, MeOH); $R_f = 0.53$ (1/9 MeOH/ CHCl_3); IR (neat) 3500–2200 (br), 1959, 1735, 1630, 1540, 1449, 1373, 1213, 1107 cm^{-1} ; ^1H NMR (CDCl_3) δ 1.85 (quint, $J = 6.0\text{ Hz}$, $\text{OCH}_2\text{CH}_2\text{CH}_2\text{O}$), 2.00 (s, $\text{CH}_3\text{C}(\text{O})$), 3.54 (t, $J = 6.0\text{ Hz}$, $\text{OCH}_2\text{CH}_2\text{CH}_2\text{OBn}$ or $\text{OCH}_2\text{CH}_2\text{CH}_2\text{OBn}$), 3.57 (t, $J = 6.0\text{ Hz}$, $\text{OCH}_2\text{CH}_2\text{CH}_2\text{OBn}$ or $\text{OCH}_2\text{CH}_2\text{CH}_2\text{OBn}$), 3.64 (dd, $J = 3.9, 9.7\text{ Hz}$, $\text{CHH}'\text{OCH}_2\text{CH}_2\text{CH}_2$), 3.86 (dd, $J = 3.3, 9.7\text{ Hz}$, $\text{CHH}'\text{OCH}_2\text{CH}_2\text{CH}_2$), 4.49 (s, OCH_2Ph), 4.65–4.75 (m, CHCH_2O), 6.59 (d, $J = 7.5\text{ Hz}$, $\text{CH}_3\text{C}(\text{O})\text{NH}$), 7.24–7.38 (m, C_6H_5), 9.10–9.50 (m, $\text{C}(\text{O})\text{OH}$); ^{13}C NMR (CDCl_3) δ 23.1 ($\text{CH}_3\text{C}(\text{O})$), 29.7 ($\text{OCH}_2\text{CH}_2\text{CH}_2\text{O}$), 52.9 ($\text{CHCH}_2\text{OCH}_2$), 67.2, 68.9

(OCH₂CH₂CH₂O), 70.2 (CHCH₂OCH₂CH₂CH₂), 73.1 (OCH₂Ph), 127.9, 128.0, 128.6, 138.4 (C₆H₅), 171.3, 173.1 (CHC(O)OH, CH₃C(O)NH); *M_r* (+ESI) 296.1492 [M+H]⁺ (calcd for C₁₅H₂₁NO₅H⁺ 296.1498). Anal. Calcd for C₁₅H₂₁NO₅•0.25H₂O: C, 60.09; H, 7.23; N, 4.67. Found: C, 59.93; H, 7.28; N, 4.67.

(S)-2-Acetamido-3-(3-(benzyloxy)propoxy)propionic Acid ((S)-122). Using Method B, a ~9:1 mixture of (S)-111a and (S)-111b (8.30 g, 26.8 mmol) in THF (250 mL) and LiOH (643 mg, 26.8 mmol) in H₂O (125 mL) gave 5.78 g (73%) of (S)-122 as a viscous yellow oil that was used without further purification: [α]_D²⁵ +17.4° (c 1.0, MeOH); *R_f* = 0.53 (1/9 MeOH/CHCl₃); IR (nujol) 3500–2200 (br), 1962, 1735, 1637, 1545, 1449, 1373, 1216, 1111 cm⁻¹; ¹H NMR (DMSO-*d*₆) δ 1.76 (quint, *J* = 6.9 Hz, OCH₂CH₂CH₂O), 1.87 (s, CH₃C(O)), 3.38–3.52 (m, OCH₂CH₂CH₂O), 3.55 (dd, *J* = 4.2, 13.8 Hz, CHH'OCH₂CH₂CH₂), 3.86 (dd, *J* = 5.8, 13.8 Hz, CHH'OCH₂CH₂CH₂), 4.38–4.44 (m, OCH₂Ph, CHCH₂O), 7.24–7.38 (m, C₆H₅), 8.17 (d, *J* = 8.1 Hz, CH₃C(O)NH), the carboxylic acid proton was not detected; ¹³C NMR (DMSO-*d*₆) δ 22.3 (CH₃C(O)), 29.4 (OCH₂CH₂CH₂O), 52.4 (CHCH₂OCH₂), 66.6, 67.7 (OCH₂CH₂CH₂O), 70.0 (CHCH₂OCH₂CH₂CH₂), 71.9 (OCH₂Ph), 127.3, 127.4, 128.3, 138.7 (C₆H₅), 169.4, 171.8 (CHC(O)OH, CH₃C(O)NH); *M_r* (+ESI) 318.1318 [M+Na]⁺ (calcd for C₁₅H₂₁NO₅Na⁺ 318.1317). Anal. Calcd for C₁₅H₂₁NO₅: C, 61.00; H, 7.17; N, 4.74. Found: C, 60.75; H, 7.26; N, 4.86.

(R)-2-Acetamido-3-(3-hydroxypropoxy)propionic Acid ((R)-123). Using Method H, compound (R)-122 (1.80 g, 6.1 mmol) and 10% Pd/C (150 mg) in MeOH (20 mL)

gave 1.14 g (91%) of (*R*)-**123** as a pale yellow viscous oil that did not require further purification: $[\alpha]^{25}_{\text{D}} -18.2^{\circ}$ (*c* 1.0, MeOH); $R_f = 0.23$ (1/4 MeOH/CHCl₃); IR (neat) 3500–2200 (br), 1958, 1734, 1655, 1547, 1427, 1377, 1232, 1127 cm⁻¹; ¹H NMR (DMSO-*d*₆) δ 1.62 (quint, *J* = 6.3 Hz, OCH₂CH₂CH₂O), 1.86 (s, CH₃C(O)), 3.36–3.50 (m, OCH₂CH₂CH₂O), 3.53 (dd, *J* = 4.2, 9.9 Hz, CHH'OCH₂CH₂CH₂), 3.64 (dd, *J* = 5.4, 9.9 Hz, CHH'OCH₂CH₂CH₂), 4.34–4.44 (m, CHCH₂O), 8.13 (d, *J* = 8.4 Hz, CH₃C(O)NH), the carboxylic acid proton was not detected; ¹³C NMR (DMSO-*d*₆) δ 22.3 (CH₃C(O)), 32.4 (OCH₂CH₂CH₂O), 52.4 (CHCH₂OCH₂), 57.7 (OCH₂CH₂CH₂OH), 67.7 (CHCH₂OCH₂CH₂CH₂), 70.0 (CHCH₂OCH₂CH₂CH₂), 169.3, 171.7 (CHC(O)OH, CH₃C(O)NH); *M_r* (+ESI) 228.0842 [M+Na]⁺ (calcd for C₈H₁₅NO₅Na⁺ 228.0848). Anal. Calcd for C₈H₁₅NO₅•0.15H₂O: C, 46.62; H, 7.42; N, 6.74. Found: C, 46.26; H, 7.42; N, 6.55.

(*S*)-2-Acetamido-3-(3-hydroxypropoxy)propionic Acid ((*S*)-123). Using Method H, compound (*S*)-**122** (4.78 g, 16.2 mmol), 10% Pd/C (400 mg) in MeOH (50 mL) gave (*S*)-**123** as a pale yellow viscous oil that was used directly for next step: $[\alpha]^{25}_{\text{D}} +17.8^{\circ}$ (*c* 1.2, MeOH); $R_f = 0.23$ (1/4 MeOH/CHCl₃); IR (neat) 3500–2200 (br), 1956, 1735, 1654, 1547, 1455, 1376, 1229, 1120 cm⁻¹; ¹H NMR (DMSO-*d*₆) δ 1.62 (quint, *J* = 6.6 Hz, OCH₂CH₂CH₂O), 1.87 (s, CH₃C(O)), 3.34–3.50 (m, OCH₂CH₂CH₂O), 3.55 (dd, *J* = 3.9, 9.9 Hz, CHH'OCH₂CH₂CH₂), 3.64 (dd, *J* = 5.7, 9.9 Hz, CHH'OCH₂CH₂CH₂), 4.34–4.44 (m, CHCH₂O), 8.12 (d, *J* = 8.1 Hz, CH₃C(O)NH), the carboxylic acid proton was not detected; ¹³C NMR (DMSO-*d*₆) δ 22.3 (CH₃C(O)), 32.4 (OCH₂CH₂CH₂O), 52.3 (CHCH₂OCH₂), 57.7 (OCH₂CH₂CH₂OH), 67.8

(CHCH₂OCH₂CH₂CH₂), 69.9 (CHCH₂OCH₂CH₂CH₂), 169.3, 171.7 (CHC(O)OH, CH₃C(O)NH); *M_r* (+ESI) 228.0845 [M+Na]⁺ (calcd for C₈H₁₅NO₅Na⁺ 228.0848). Anal. Calcd for C₈H₁₅NO₅: C, 46.82; H, 7.37; N, 6.83. Found: C, 46.52; H, 7.42; N, 6.73.

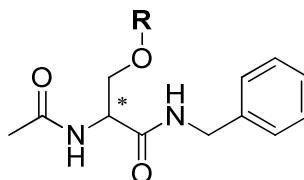
(*R*)-2-Acetamido-3-(2-azidoethoxy)propionic Acid ((*R*)-124). Using Method B, (*R*)-112a (1.56 g, 6.78 mmol) in THF (40 mL) and LiOH (195 mg, 8.14 mmol) in H₂O (20 mL) gave 750 mg (51%) of (*R*)-124 as a white solid upon work-up: mp 99–100 °C; [α]_D²⁵ -12.6° (c 1.8; MeOH); *R_f* = 0.21 (1/9 MeOH/CHCl₃); IR (nujol) 3356, 2119, 1735, 1625, 1547, 1457, 1267, 1232 cm⁻¹; ¹H NMR (CDCl₃) δ 2.07 (s, CH₃C(O)NH), 3.23–3.42 (m, CH₂N₃), 3.60–3.80 (m, OCH₂CH₂N₃, CHCH'HOCH₂), 4.01 (dd, *J* = 3.0, 9.1 Hz, CHCH'HO), 4.76–4.80 (m, CHCH₂O), 6.00–7.00 (m, CO₂H), 6.48 (d, *J* = 7.5 Hz, CH₃C(O)NH); ¹³C NMR (DMSO-*d*₆) δ 22.3 (CH₃C(O)), 49.9 (OCH₂CH₂N₃), 52.2 (CHCH₂O), 69.4 (CHCH₂O or OCH₂CH₂N₃), 70.1 (OCH₂CH₂N₃ or CHCH₂O), 169.4, 171.5 (CH₃C(O)NH, C(O)OH); *M_r* (+ESI) 239.0750 [M+Na]⁺ (calcd for C₇H₁₂N₄O₄Na⁺ 239.0756). Anal. Calcd for C₇H₁₂N₄O₄•0.07EtOAc: C, 39.30; H, 5.69; N, 25.23. Found: C, 39.30; H, 5.73; N, 25.33.


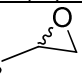
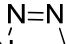
(*S*)-2-Acetamido-3-(2-azidoethoxy)propionic Acid ((*S*)-124). Using Method B, compound (*S*)-112a (1.67 g, 7.26 mmol) in THF (40 mL), and LiOH (209 mg, 8.71 mmol) in H₂O (20 mL) gave a white solid upon work-up and evaporation: mp 99–100 °C; [α]_D²⁵ +12.4° (c 1.3; MeOH); *R_f* = 0.21 (1/9 MeOH/CHCl₃); IR (nujol) 3356, 2119, 1735, 1624, 1547, 1458, 1267, 1233 cm⁻¹; ¹H NMR (DMSO-*d*₆) δ 1.86 (s, CH₃C(O)NH), 3.30–3.45 (m, CH₂N₃), 3.50–3.78 (m, OCH₂CH₂N₃, CHCHH'OCH₂,

CHCH'HO), 4.39–4.48 (m, CHCH₂O), 8.13 (d, $J = 8.1$ Hz, CH₃C(O)NH); ¹³C NMR (DMSO-*d*₆) δ 22.3 (CH₃C(O)), 49.9 (OCH₂CH₂N₃), 52.2 (CHCH₂O), 69.4 (CHCH₂O or OCH₂CH₂N₃), 70.1 (OCH₂CH₂N₃ or CHCH₂O), 169.4, 171.5 (CH₃C(O)NH, C(O)OH); M_r (+ESI) 239.0750 [M+Na]⁺ (calcd for C₇H₁₂N₄O₄Na⁺ 239.0756). Anal. Calcd for C₇H₁₂N₄O₄•0.07EtOAc: C, 39.30; H, 5.69; N, 25.23. Found: C, 39.28; H, 5.71; N, 25.37.

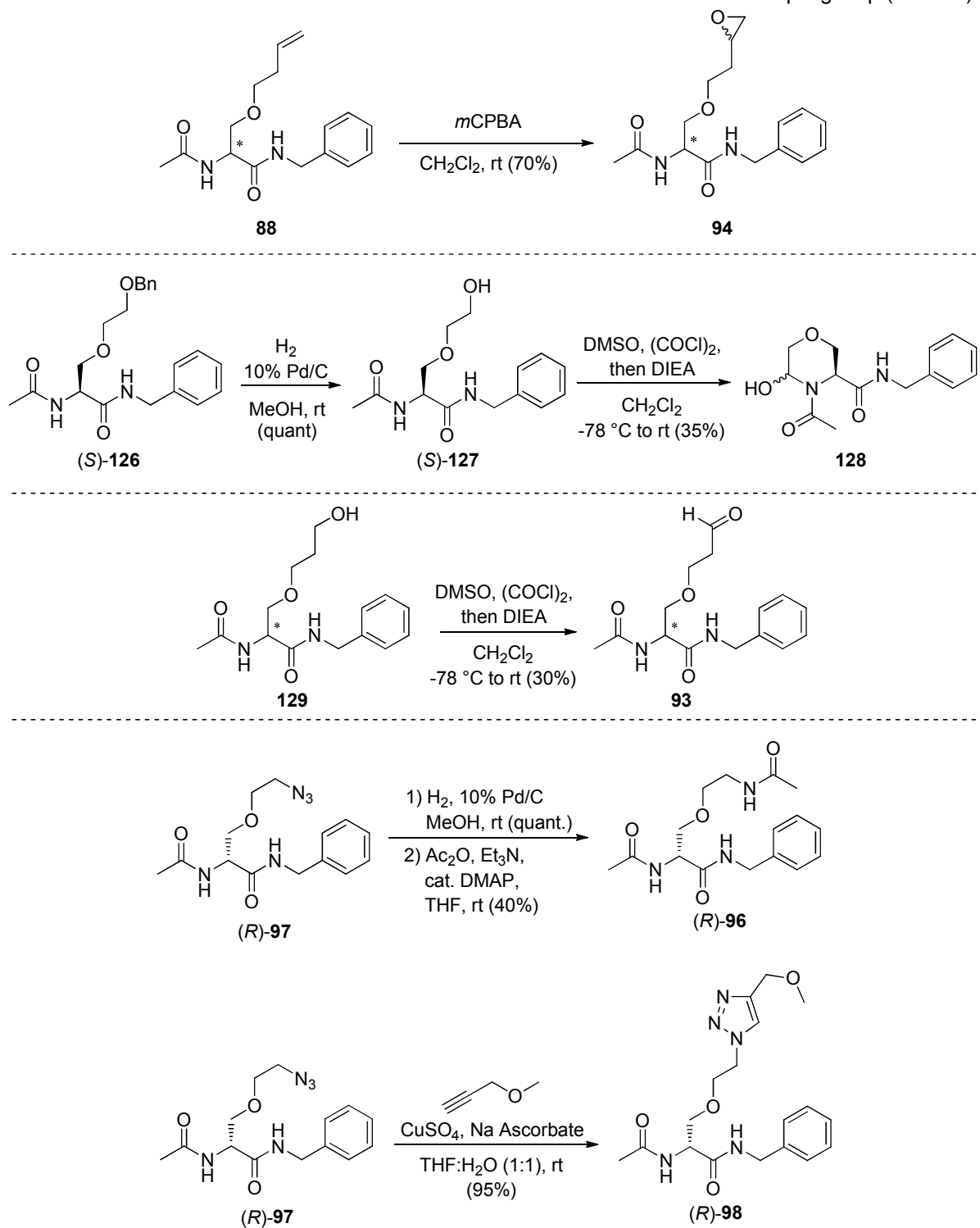
(*R*)-2-Acetamido-3-(2-(2-methoxyethoxy)ethoxy)propionic Acid ((*R*)-125). Using Method B, a ~1:1 mixture of (*R*)-114a and (*R*)-114b (3.85 g, 14.2 mmol), LiOH (376 mg, 15.6 mmol) in THF:H₂O (160 mL) gave 2.44 g (68%) of (*R*)-125 as a colorless viscous oil after work-up: $[\alpha]_D^{25} -38.5^\circ$ (c 1.2, CHCl₃); $R_f = 0-0.11$ (1/9 MeOH/CHCl₃); IR (neat) 3500-2500 (br), 1974, 1731, 1654, 1547, 1103 cm⁻¹; ¹H NMR (CDCl₃) δ 2.08 (s, CH₃C(O)), 3.40 (s, OCH₃), 3.54–3.70 (m, OCH₂CH₂OCH₂CH₂OCH₃), 3.75 (dd, $J = 3.3, 9.7$ Hz, CHH'OCH₂), 3.98 (dd $J = 3.3, 9.7$ Hz, CHH'OCH₂), 4.68–4.78 (m, CHCH₂O), 6.98 (d, $J = 7.8$ Hz, C(O)NHCH), 9.10–9.50 (m, C(O)OH); ¹³C NMR (CDCl₃) δ 22.9 (CH₃C(O)), 53.0 (CHCH₂OCH₂CH₂), 59.0 (OCH₃), 70.3, 70.4, 70.7, 70.8, 72.1 (CH₂OCH₂CH₂OCH₂CH₂O), 171.4, 172.3 (C(O)OH, CH₃C(O)NH); M_r (+ESI) 272.1107 [M+Na]⁺ (calcd for C₁₈H₂₀N₂O₃Na⁺ 272.1110). Anal. Calcd for C₁₀H₉NO₆•0.33H₂O: C, 46.50; H, 7.81; N, 5.42. Found: C, 46.34; H, 7.74; N, 5.46.

2.2.4.5. Synthesis of O-substituted derivatives of lacosamide

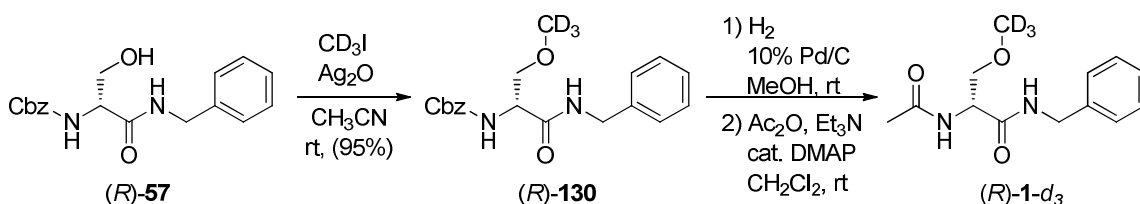


R =	Compound number
Me	1
Et	48
<i>i</i> -Pr	80
<i>t</i> -Bu	81
C ₆ H ₁₁	82
Ph	83
CH ₂ C ₆ H ₁₁	86
CH ₂ Ph	87
CH ₂ CH ₂ CH=CH ₂	88
CH ₂ CH ₂ 	89
CH ₂ CH ₂ C≡CH	90
CH ₂ CH ₂ Ph	91
CH ₂ CH ₂ OBn	126
CH ₂ CH ₂ OH	127
CH ₂ CH ₂ CH ₂ OH	129
CH ₂ CH ₂ C(O)H	93
CH ₂ CH ₂ 	94
CH ₂ CH ₂ NHC(O)CH ₃	96
CH ₂ CH ₂ N ₃	97
 CH ₂ CH ₂ -N=N-CH=CH-CH ₂ OCH ₃	98
CH ₂ CH ₂ OCH ₃	99
(CH ₂ CH ₂ O) ₂ CH ₃	100
CD ₃	1-<i>d</i>₃

Scheme 21. Different reactions used to obtain **55** derivatives after the amide coupling step (**route 3**).



Scheme 22. Synthesis of the deuterated analog of (*R*)-lacosamide (*R*)-1-*d*₃ (**route 1**)



(*R*)-*N*-Benzyl 2-Acetamido-3-methoxypropionamide ((*R*)-1). Using Method D, (*R*)-**115** (100 mg, 0.62 mmol), benzylamine (81 μ L, 0.74 mmol), and DMTMM (205 mg, 0.74 mmol) in anhydrous THF (10 mL) gave 95 mg (61%) of (*R*)-**1** after flash column chromatography (1/9 MeOH/ CHCl_3) and recrystallization from EtOAc: mp 142–143 $^{\circ}\text{C}$ (lit.²³⁵ mp 142–143 $^{\circ}\text{C}$); $[\alpha]_D^{25} +16.1^{\circ}$ (*c* 0.9, MeOH) (lit.²³⁵ $[\alpha]_D^{25} +16.0^{\circ}$ (*c* 1.0; MeOH)); $R_f = 0.47$ (1/9 MeOH/ CHCl_3); ^1H NMR (CDCl_3) δ 2.03 (s, $\text{CH}_3\text{C}(\text{O})$), 3.37 (s, CH_2OCH_3), 3.46 (dd, $J = 7.2, 8.4$ Hz, $\text{CHH}'\text{OCH}_3$), 3.79 (dd $J = 4.2, 8.4$ Hz, $\text{CHH}'\text{OCH}_3$), 4.40–4.52 (m, $\text{NHCH}_2\text{C}_6\text{H}_5$), 4.52–4.60 (m, CHCH_2O), 6.40–6.60 (br m, $\text{CH}_3\text{C}(\text{O})\text{NH}$), 6.78–6.92 (br m, $\text{C}(\text{O})\text{NHCH}_2\text{Ph}$), 7.18–7.38 (m, $\text{NHCH}_2\text{C}_6\text{H}_5$), addition of excess (*R*)-(-)-mandelic acid to a CDCl_3 solution of (*R*)-**1** gave only one signal for the acetyl methyl protons and the methoxy protons, addition of excess (*R*)-(-)-mandelic acid to a CDCl_3 solution of (*S*)-**1** and (*R*)-**1** (1:2 ratio) gave two signals for the acetyl methyl protons (δ 2.023 (*S*) and 2.010 (*R*) ($\Delta\text{ppm} = 0.013$)), and two signals for the methoxy protons (δ 3.311 (*S*) and 3.350 (*R*) ($\Delta\text{ppm} = 0.039$)); ^{13}C NMR (CDCl_3) δ 23.4 ($\text{CH}_3\text{C}(\text{O})$), 43.7 (NHCH_2Ph), 52.6 ($\text{CHCH}_2\text{OCH}_3$), 59.3 (CH_2OCH_3), 71.9 (CH_2OCH_3), 127.6, 127.7, 138.1 ($\text{NHCH}_2\text{C}_6\text{H}_5$), 170.2, 170.5 ($\text{CHC}(\text{O})\text{NH}$, $\text{CH}_3\text{C}(\text{O})\text{NH}$), the remaining aromatic resonance was not detected and is believed to overlap with nearby signals

(*R*)-*N*-Benzyl 2-Acetamido-3-ethoxypropionamide ((*R*)-48). Using Method D, (*R*)-**116** (1.34 g, 7.7 mmol), benzylamine (1.00 mL, 9.2 mmol), and DMTMM (2.54 g, 9.2 mmol) in anhydrous THF (80 mL) gave 1.11 g (46%) of (*R*)-**48** as a white solid after flash column chromatography (8/92 MeOH/CHCl₃) and 2 recrystallizations from EtOAc: mp 129–130°C; $[\alpha]_D^{25}$ -34.1° (c 0.6, CHCl₃); R_f = 0.35 (5/95 MeOH/CHCl₃); IR (nujol) 3283, 1634, 1555, 1456, 1375, 1114 cm⁻¹; ¹H NMR (CDCl₃) δ 1.15 (t, J = 7.2 Hz, OCH₂CH₃), 2.04 (s, CH₃C(O)), 3.44 (dd, J = 8.4, 9.3 Hz, CHH'OCH₂CH₃), 3.48–3.62 (m, OCH₂CH₃), 3.85 (dd J = 4.2, 9.3 Hz, CHH'OCH₂CH₃), 4.40–4.58 (m, CHCH₂OCH₂, NHCH₂C₆H₅), 6.40–6.50 (br d, CH₃C(O)NH), 6.78–6.90 (br t, C(O)NHCH₂Ph), 7.22–7.38 (m, NHCH₂C₆H₅), addition of excess (*R*)-(-)-mandelic acid to a CDCl₃ solution of (*R*)-**48** gave only one signal for the acetyl methyl protons (δ 2.017); ¹³C NMR (CDCl₃) δ 15.1 (OCH₂CH₃), 23.3 (CH₃C(O)), 43.6 (NHCH₂Ph), 52.7 (CHCH₂OCH₂CH₃), 67.0 (CHCH₂OCH₂CH₃), 69.9 (CHCH₂OCH₂CH₃), 127.6, 127.7, 128.7, 138.1 (NHCH₂C₆H₅), 170.3, 170.5 (CHC(O)NH, CH₃C(O)NH); M_r (+ESI) 287.1374 [M+Na]⁺ (calcd for C₁₄H₂₀N₂O₃Na⁺ 287.1372). Anal. Calcd for C₁₄H₂₀N₂O₃: C, 63.62; H, 7.63; N, 10.60. Found: C, 63.62; H, 7.56; N, 10.47.

(*R*)-*N*-Benzyl 2-Acetamido-3-isopropoxypropionamide ((*R*)-80). Using Method D, (*R*)-**117** (1.90 g, 10.0 mmol), benzylamine (1.31 mL, 12.0 mmol), and DMTMM (3.32 g, 12.0 mmol) in anhydrous THF (100 mL) gave 2.01 g (72%) of (*R*)-**80** as a white solid after flash column chromatography (5/95 MeOH/CHCl₃) and recrystallization from EtOAc: mp 151–153°C; $[\alpha]_D^{25}$ -23.4° (c 0.5, CHCl₃); R_f = 0.37 (5/95

MeOH/CHCl₃); IR (nujol) 3280, 3098, 1642, 1555, 1458, 1377, 1298, 1258, 1147 cm⁻¹; ¹H NMR (CDCl₃) δ 1.09 (d, J = 6.0 Hz, OCHCH₃(C'H₃)), 1.13 (d, J = 6.0 Hz, OCHCH₃(C'H₃)), 2.04 (s, CH₃C(O)), 3.40 (app t, J = 8.7 Hz, CHH'OCH(CH₃)₂), 3.63 (hept, J = 6.0 Hz, OCH(CH₃)₂), 3.84 (dd J = 3.9, 8.7 Hz, CHH'OCH(CH₃)₂), 4.38–4.57 (m, CHCH₂OCH, NHCH₂C₆H₅), 6.42–6.50 (br d, CH₃C(O)NH), 6.82–6.94 (br t, C(O)NHCH₂Ph), 7.24–7.38 (m, NHCH₂C₆H₅), addition of excess (*R*)-(-)-mandelic acid to a CDCl₃ solution of (*R*)-**80** gave only one signal for the acetyl methyl protons (δ 2.014); ¹³C NMR (CDCl₃) δ 22.0 (OCHCH₃(C'H₃)), 22.2 (OCHCH₃(C'H₃)), 23.4 (CH₃C(O)), 43.7 (NHCH₂Ph), 52.9 (CHCH₂OCH(CH₃)₂), 67.5 (CH₂OCH(CH₃)₂), 72.7 (CH₂OCH(CH₃)₂), 127.7, 128.8, 138.1 (NHCH₂C₆H₅), 170.5 (CHC(O)NH or CH₃C(O)NH), the remaining aromatic and C(O) peaks were not detected and are believed to overlap with nearby signals; *M_r* (+ESI) 301.1530 [M+Na]⁺ (calcd for C₁₅H₂₂N₂O₃Na⁺ 301.1528). Anal. Calcd for C₁₅H₂₂N₂O₃: C, 64.73; H, 7.97; N, 10.06. Found: C, 64.56; H, 8.00; N, 10.12.

(*R*)-*N*-Benzyl 2-Acetamido-3-*tert*-butoxypropionamide ((*R*)-81**).** Using Method D, (*R*)-**118** (1.10 g, 5.4 mmol), benzylamine (0.71 mL, 6.5 mmol), and DMTMM (1.80 g, 6.5 mmol) in anhydrous THF (50 mL) gave 730 mg (46%) of (*R*)-**81** as a white solid after flash column chromatography (5/95 MeOH/CHCl₃) and recrystallization from EtOAc: mp 126–127°C; [α]_D²⁵ -22.9° (c 0.9, CHCl₃); *R_f* = 0.39 (5/95 MeOH/CHCl₃); IR (nujol) 3280, 3091, 1641, 1550, 1459, 1372, 1246, 1194, 1090 cm⁻¹; ¹H NMR (CDCl₃) δ 1.14 (s, OC(CH₃)₃), 2.04 (s, CH₃C(O)), 3.40 (app t, J = 8.5 Hz, CHH'OC(CH₃)₃), 3.84 (dd J = 4.2, 8.5 Hz, CHH'OC(CH₃)₃), 4.38–4.57 (m,

CHCH₂OC, NHCH₂C₆H₅), 6.40–6.50 (br d, CH₃C(O)NH), 6.80–6.92 (br t, C(O)NHCH₂Ph), 7.23–7.40 (m, NHCH₂C₆H₅), addition of excess (*R*)-(-)-mandelic acid to a CDCl₃ solution of (*R*)-**81** gave only one signal for the acetyl methyl protons (δ 2.009) and the *t*-Bu methyl protons (δ 1.112); ¹³C NMR (CDCl₃) δ 23.4 (CH₃C(O)), 27.6 (OC(CH₃)₃), 43.8 (NHCH₂Ph), 53.2 (CHCH₂OC(CH₃)₃), 61.7 (CH₂OC(CH₃)₃), 74.5 (CH₂OC(CH₃)₃), 127.7, 127.8, 128.8, 138.1 (NHCH₂C₆H₅), 170.3, 170.5 (CHC(O)NH, CH₃C(O)NH); *M_r* (+ESI) 315.1687 [M+Na]⁺ (calcd for C₁₆H₂₄N₂O₃Na⁺ 315.1685). Anal. Calcd for C₁₆H₂₄N₂O₃: C, 65.73; H, 8.27; N, 9.58. Found: C, 65.64; H, 8.08; N, 9.57.

(*R*)-*N*-Benzyl 2-Acetamido-3-(2-cyclohexyloxy)propionamide ((*R*)-82**).** Using Method B, a ~1:1 mixture of (*R*)-**105a** and (*R*)-**105b** (2.10 g, 8.4 mmol) in THF (80 mL) and LiOH (202 mg, 8.4 mmol) in H₂O (40 mL) gave upon work-up the corresponding acid (1.62 g, 7.1 mmol, 84%) as a yellow viscous oil (*M_r* (+ESI) 252.1212 [M+Na]⁺ (calcd for C₁₁H₁₉NO₄Na⁺ 252.1204)) that was directly dissolved in THF (70 mL). Using Method D, addition of benzylamine (930 μ L, 8.5 mmol) and DMTMM (2.4 g, 8.5 mmol) gave (*R*)-**82** as a white solid (1.17 g, 65%) after purification by flash chromatography (1:2 hexanes/EtOAc to 1/9 MeOH/CH₂Cl₂) followed by recrystallization from EtOAc and hexanes: mp 134–135 °C; [α]_D²⁵ -33.5° (c 1.2; CHCl₃); *R_f* = 0.52 (EtOAc); IR (nujol) 3282, 2857, 1641, 1561, 1456, 1375, 1303, 1256 cm⁻¹; ¹H NMR (CDCl₃) δ 1.10–1.34, 1.42–1.88 (m, OCH(CH₂CH₂)₂CH₂), 2.03 (s, CH₃C(O)), 3.24–3.36 (m, OCH(CH₂CH₂)₂CH₂), 3.43 (app. t, *J* = 9.0 Hz, CHH'OCH₂CH), 3.86 (dd, *J* = 3.6, 9.0 Hz, CHH'OCH₂CH), 4.38–4.56 (m, NHCH₂Ph,

CHCH₂O), 6.48–6.58 (br d, CH₃C(O)NH), 6.92–7.02 (br t, NHCH₂Ph), 7.22–7.38 (m, C₆H₅), addition of excess (*R*)-(-)-mandelic acid to a CDCl₃ solution of (*R*)-**82** gave only one signal for the acetyl protons (δ 2.006); ¹³C NMR (CDCl₃) δ 23.4, 23.9, 25.8 (CH₃C(O), OCH(CH₂CH₂)₂CH₂), 32.0, 32.2 (OCH(CH₂CH₂)₂CH₂), 43.8 (NHCH₂Ph), 52.9 (CHCH₂OCH), 67.3 (CH₂OCH(CH₂CH₂)₂CH₂), 78.4 (OCH(CH₂CH₂)₂CH₂), 127.7, 127.8, 128.9, 138.1 (C₆H₅), 170.4 (CH₃C(O)NH, C(O)NHCH₂), the remaining resonance was not detected and is believed to overlap with a nearby signal; *M*_r (+ESI) 341.3 [M+Na]⁺ (calcd for C₁₈H₂₆N₂O₃Na⁺ 341.3). Anal. Calcd for C₁₈H₂₆N₂O₃: C, 67.90; H, 8.23; N, 8.80. Found: C, 67.86; H, 8.12; N, 8.74.

(*R*)-*N*-Benzyl 2-Acetamido-3-phenoxypropionamide (*R*)-83**.** Using Method A, (*R*)-**78** (2.66 g, 12.1 mmol), phenol (5.70 g, 60.6 mmol), and BF₃•Et₂O (1.52 mL, 12.1 mmol) in CH₂Cl₂ (50 mL) gave a crude residue that was recrystallized (3 x) from EtOAc and hexanes to give (*R*)-**83** (340 mg, 8%) as a white solid. The mother liquors from the recrystallization were concentrated and then purified using flash chromatography (5/95 MeOH/CHCl₃). The obtained solid was recrystallized from EtOAc and hexanes to yield an additional 100 mg (3%) of (*R*)-**83** (total yield: 440 mg, 11%): mp 169–170°C; [α]_D²⁵ -18.0° (*c* 0.4, MeOH); *R*_f = 0.52 (5/95 MeOH/CHCl₃); IR (nujol) 3288, 3073, 1687, 1551, 1458, 1375 cm⁻¹; ¹H NMR (CDCl₃) δ 2.03 (s, CH₃C(O)), 4.05 (dd, *J* = 7.5, 9.6 Hz, CHH'OCH₃), 4.37 (dd *J* = 4.2, 9.6 Hz, CHH'OCH₃), 4.40–4.56 (m, NHCH₂C₆H₅), 4.78–4.86 (m, CHCH₂O), 6.66 (d, *J* = 6.0 Hz, CH₃C(O)NH), 6.87 (d, *J* = 7.8 Hz, 3 ArH) 6.98 (t, *J* = 7.8 Hz, 2 ArH), 7.16–7.35 (m, CH₂C₆H₅ and NHCH₂C₆H₅), addition of excess (*R*)-(-)-mandelic acid

to a CDCl₃ solution of (*R*)-**83** gave only one signal for the acetyl protons (δ 1.985); ¹³C NMR (CDCl₃) δ 23.4 (CH₃C(O)), 43.9 (NH₂CH₂C₆H₄), 52.6 (CHCH₂OPh), 67.4 (CH₂OPh), 114.8, 121.9, 127.7, 127.8, 128.9, 129.8, 137.8, 157.9 (2 C₆H₅), 169.5, 170.6 (CHC(O)NH, CH₃C(O)); *M_r* (+ESI) 335.1366 [M+Na]⁺ (calcd for C₁₈H₂₀N₂O₃Na⁺ 335.1372). Anal. Calcd for C₁₈H₂₀N₂O₃: C, 69.21; H, 6.45; N, 8.97; Found: C, 69.29; H, 6.52; N, 9.05.

(*R*)-*N*-Benzyl 2-Acetamido-3-phenoxypropionamide ((*R*)-83) (Alternate procedure). Using Method D, acid (*R*)-**119** (376 mg, 1.68 mmol), benzylamine (219 μ L, 2.02 mmol), and DMTMM (557 mg, 2.02 mmol) in THF (20 mL) gave a (*R*)-**83** as a white solid (305 mg, 58%) after purification by flash chromatography (5/95 MeOH/CHCl₃) and further recrystallization from EtOAc: mp 169–170 °C; [α]_D²⁵ -18.2° (c 1.0, MeOH); *R_f* = 0.52 (5/95 MeOH/CHCl₃); ¹H NMR (CDCl₃) δ 2.06 (s, CH₃C(O)), 4.03 (dd, *J* = 7.5, 9.6 Hz, CHH'OCH₃), 4.42 (dd *J* = 4.2, 9.6 Hz, CHH'OCH₃), 4.36–4.56 (m, NHCH₂C₆H₅), 4.78–4.84 (m, CHCH₂O), 6.53 (d, *J* = 6.0 Hz, CH₃C(O)NH), 6.61–6.71 (br t, C(O)NHCH₂Ph), 6.90 (d, *J* = 7.8 Hz, OC₆H₅), 7.00 (t, *J* = 7.8 Hz, OC₆H₅), 7.20–7.32 (m, CH₂C₆H₅), addition of excess (*R*)-(-)-mandelic acid to a CDCl₃ solution of (*R*)-**83** gave only one signal for the acetyl peak protons (δ 2.002).

(*R*)-*N*-Benzyl 2-Acetamido-3-(2-cyclohexylmethoxy)propionamide ((*R*)-86). Using Method B, a ~1:4 mixture of (*R*)-**107a** and (*R*)-**107b** (2.32 g, 8.6 mmol) in THF (85 mL) and LiOH (207 mg, 8.6 mmol) in H₂O (40 mL) gave upon work-up the corresponding acid (1.88 g, 7.7 mmol, 90%) as a yellow viscous that was directly

dissolved in THF (75 mL). Using Method D, addition of benzylamine (1.0 mL, 9.2 mmol) and DMTMM (2.54 g, 9.2 mmol) gave (*R*)-**86** as a white solid (1.50 g, 59%) after purification by flash chromatography (1/2 hexanes/EtOAc to 1/9 MeOH/CH₂Cl₂) followed by recrystallization from EtOAc and hexanes: mp 143–144 °C; $[\alpha]_D^{25} +6.7^\circ$ (c 1.6; MeOH); $R_f = 0.39$ (5/95 MeOH/CH₂Cl₂); IR (nujol) 3280, 3092, 2861, 1641, 1550, 1459, 1372, 1301, 1247 cm⁻¹; ¹H NMR (CDCl₃) δ 0.74–0.90, 1.00–1.26, 1.40–1.72 (m, OCH₂CH(CH₂CH₂)₂CH₂), 2.02 (s, CH₃C(O)), 3.16–3.32 (m, OCH₂CH(CH₂CH₂)₂CH₂), 3.42 (app. t, $J = 9.0$ Hz, CHH'OCH₂CH), 3.79 (dd, $J = 3.6, 9.0$ Hz, CHH'OCH₂), 4.38–4.50 (m, NHCH₂Ph), 4.51–4.60 (m, CHCH₂O), 6.53 (d, $J = 6.3$ Hz, CH₃C(O)NH), 6.88–7.00 (br t, NHCH₂Ph), 7.22–7.38 (m, C₆H₅), addition of excess (*R*)-(-)-mandelic acid to a CDCl₃ solution of (*R*)-**86** gave only one signal for the acetyl protons (δ 2.008); ¹³C NMR (CDCl₃) δ 23.4 (CH₃C(O)), 25.9, 26.6, OCH₂CH(CH₂CH₂)₂CH₂, 30.0, 30.1 (OCH₂CH(CH₂CH₂)₂CH₂), 38.0 (OCH₂CH(CH₂CH₂)₂CH₂), 43.9 (NHCH₂Ph), 52.5 (CHCH₂OCH₂), 70.2 (CH₂OCH₂CH(CH₂CH₂)₂CH₂), 77.5 (OCH₂CH(CH₂CH₂)₂CH₂), 127.7, 127.8, 128.9, 138.0 (C₆H₅), 170.3, 170.4 (CH₃C(O)NH, C(O)NHCH₂); M_r (+ESI) 355.1998 [M+Na]⁺ (calcd for C₁₉H₂₈N₂O₃Na⁺ 355.1997). Anal. Calcd for C₁₉H₂₈N₂O₃: C, 68.65; H, 8.49; N, 8.43. Found: C, 68.52; H, 8.43; N, 8.38.

(*R*)-*N*-Benzyl 2-Acetamido-3-(benzyloxy)propionamide (*R*)-87. To a stirred suspension of O-benzyl-D-serine (Astatech Inc.) (1.00 g, 5.13 mmol) in a 9:1 THF:H₂O mixture (50 mL) was added Ac₂O (1.45 mL, 15.3 mmol) at room temperature. The reaction became clear within 30 min and was further stirred at

room temperature (3 h). The solvents were removed in vacuo to yield a viscous clear residue (1.22 g, 5.13 mmol, quant.) that was directly dissolved in THF (60 mL). Using Method D, benzylamine (670 μ L, 6.2 mmol) and DMTMM (1.71 g, 6.2 mmol) gave (*R*)-**87** as a white solid (1.55 g, 93% for 2 steps) upon purification by flash chromatography (EtOAc to 1/9 MeOH/CH₂Cl₂): mp 145–146 °C; $[\alpha]_D^{25}$ -28.7° (c 0.7; CHCl₃); R_f = 0.49 (EtOAc); IR (nujol) 3291, 2862, 1635, 1547, 1457, 1375, 1310, 1248 cm⁻¹; ¹H NMR (CDCl₃) δ 2.01 (s, CH₃C(O)), 3.51 (dd, J = 7.8, 9.0 Hz, CHH'OCH₂Ph), 3.90 (dd, J = 4.2, 9.0 Hz, CHH'OCH₂Ph), 4.38–4.64 (m, NHCH₂Ph, OCH₂Ph, CHCH₂O), 6.40–6.52 (br d, CH₃C(O)NH), 6.72–6.84 (br t, NHCH₂Ph), 7.18–7.38 (m, 2 C₆H₅), addition of excess (*R*)-(-)-mandelic acid to a CDCl₃ solution of (*R*)-**87** gave only one signal for the acetyl protons (δ 1.996); ¹³C NMR (CDCl₃) δ 23.4 (CH₃C(O)), 43.9 (NHCH₂Ph), 52.5 (CHCH₂OCH₂), 69.6, 73.8 (CH₂OCH₂Ph), 127.7, 127.8, 128.1, 128.2, 128.6, 128.9, 137.4, 137.9 (2 C₆H₅), 170.1, 170.4 (CH₃C(O)NH, C(O)NHCH₂); M_r (+ESI) 349.2 [M+Na]⁺ (calcd for C₁₉H₂₂N₂O₃Na⁺ 349.2). Anal. Calcd for C₁₉H₂₂N₂O₃: C, 69.92; H, 6.79; N, 8.58. Found: C, 70.30; H, 6.86; N, 8.64.

(*R*)-*N*-Benzyl 2-Acetamido-3-(but-3-enyloxy)propionamide ((*R*)-88**).** Using the Method D, (*R*)-**120** (1.32 g, 6.57 mmol), benzylamine (860 μ L, 7.88 mmol), and DMTMM (2.18 g, 7.88 mmol) gave (*R*)-**88** (1.30 g, 67%) as a white solid after purification by flash chromatography (EtOAc) and further recrystallization from EtOAc and hexanes: mp 103–104 °C; $[\alpha]_D^{25}$ +51.3° (c 0.6; MeOH); R_f = 0.37 (5/95 MeOH/CH₂Cl₂); IR (nujol) 3291, 3099, 1637, 1554, 1456, 1375, 1117 cm⁻¹; ¹H NMR

(CDCl₃) δ 2.03 (s, CH₃C(O)), 2.22–2.36 (m, CH₂CH₂CH=CH₂), 3.40–3.62 (m, CH₂OCH₂CH₂, CHH'OCH₂CH₂), 3.85 (dd, J = 4.2, 9.0 Hz, CHH'OCH₂CH₂), 4.45 (d, J = 7.2 Hz, NHCH₂Ph), 4.48–4.57 (m, CHCH₂O), 4.92–5.06 (m, CH₂CH=CH₂), 5.62–5.74 (m, CH₂CH=CH₂), 6.42–6.56 (m, NHCHCH₂O), 6.84–6.96 (br t, NHCH₂Ph), 7.20–7.36 (m, C₆H₅), addition of excess (*R*)-(-)-mandelic acid to a CDCl₃ solution of (*R*)-**88** gave only one signal for the acetyl protons (δ 2.011 ppm), addition of excess (*R*)-(-)-mandelic acid to a CDCl₃ solution of (*S*)-**88** and (*R*)-**88** in a ~1:2 ratio gave two signals with a relative ~1:2 intensity for the acetyl protons (δ 2.027 ppm (*S*)-**88**, δ 2.014 ppm (*R*)-**88**, (Δ ppm = 0.013)); ¹³C NMR (CDCl₃) δ 23.4 (CH₃C(O)), 34.2 (CH₂CH₂CH=CH₂), 43.8 (NHCH₂Ph), 52.5 (CHC(O)NH), 69.9, 70.6 (CHCH₂OCH₂), 117.0 (CH₂CH₂CH=CH₂), 127.7, 128.9, 135.3, 138.1 (C₆H₅, CH₂CH₂CH=CH₂), 170.2, 170.4 (CH₃C(O), CHC(O)NH), the remaining peak was not detected and is believed to overlap with nearby signals; *M_r* (+ESI) 313.1528 [M+Na]⁺ (calcd for C₁₆H₂₂N₂O₃Na⁺ 313.1528). Anal. Calcd for C₁₆H₂₂N₂O₃: C, 66.18; H, 7.64; N, 9.65. Found: C, 65.98; H, 7.55; N, 9.68.

(S)-*N*-Benzyl 2-Acetamido-3-(but-3-enyloxy)propionamide ((S)-88). Using Method D, (*S*)-**120** (164 mg, 0.87 μ mol), benzylamine (113 μ L, 1.04 mmol), and DMTMM (287 mg, 1.04 mmol) in THF (10 mL) gave (*S*)-**88** (150 mg, 60%) as a white solid after purification by flash chromatography (EtOAc) and further recrystallization from EtOAc and hexanes: mp 103–104 °C; [α]_D²⁵ -50.9° (*c* 0.6; MeOH); *R_f* = 0.37 (5/95 MeOH/CH₂Cl₂); IR (nujol) 3298, 3093, 2861, 1637, 1553, 1455, 1375, 1117 cm⁻¹; ¹H NMR (CDCl₃) δ 2.02 (s, CH₃C(O)), 2.22–2.36 (m, CH₂CH₂CH=CH₂), 3.40–

3.62 (m, CH₂OCH₂CH₂, CHH'OCH₂CH₂), 3.84 (dd, $J = 4.2, 9.0$ Hz, CHH'OCH₂CH₂), 4.45 (d, $J = 7.2$ Hz, NHCH₂Ph), 4.48–4.57 (m, CHCH₂O), 4.92–5.06 (m, CH₂CH=CH₂), 5.62–5.74 (m, CH₂CH=CH₂), 6.48–6.60 (m, NHCHCH₂O), 6.88–7.00 (br t, NHCH₂Ph), 7.20–7.36 (m, C₆H₅), addition of excess (*R*)-(-)-mandelic acid to a CDCl₃ solution of (*S*)-**88** gave only one signal for the acetyl protons (δ 2.026 ppm), addition of excess (*R*)-(-)-mandelic acid to a CDCl₃ solution of (*S*)-**88** and (*R*)-**88** in a ~1:2 ratio gave two signals with a relative ~1:2 intensity for the acetyl protons (δ 2.027 ppm (*S*)-**88**, δ 2.014 ppm (*R*)-**88**, (Δ ppm = 0.013)); ¹³C NMR (CDCl₃) δ 23.2 (CH₃C(O)), 34.1 (CH₂CH₂CH=CH₂), 43.7 (NHCH₂Ph), 52.5 (CHC(O)NH), 69.9, 70.6 (CHCH₂OCH₂), 117.0 (CH₂CH₂CH=CH₂), 127.6, 127.7, 128.8, 134.9, 138.3 (C₆H₅, CH₂CH₂CH=CH₂), 170.2, 170.4 (CH₃C(O), CHC(O)NH); M_r (+ESI) 313.1530 [M+Na]⁺ (calcd for C₁₆H₂₂N₂O₃Na⁺ 313.1528). Anal. Calcd for C₁₆H₂₂N₂O₃: C, 66.18; H, 7.64; N, 9.65. Found: C, 66.27; H, 7.51; N, 9.51.

(*R*)-*N*-Benzyl 2-Acetamido-3-(2-cyclopropylethoxy)propionamide ((*R*)-89**).** Using Method B, a ~1:1 mixture of (*R*)-**109a** and (*R*)-**109b** (1.60 g, 6.6 mmol) in THF (60 mL) and LiOH (158 mg, 6.6 mmol) in H₂O (30 mL) gave upon work-up the corresponding acid (1.27 g, 5.9 mmol, 90%) as a yellow oil (M_r (+ESI) 238.1056 [M+Na]⁺ (calcd for C₁₀H₁₇NO₄Na⁺ 238.1054)) that was directly dissolved in THF (60 mL). Using Method D, addition of benzylamine (740 μ L, 7.13 mmol) and DMTMM (2.0 g, 7.13 mmol) gave (*R*)-**89** as a white solid (1.17 g, 65%) after purification by flash chromatography (1:2 hexanes/EtOAc to 1/9 MeOH/CH₂Cl₂) followed by recrystallization from EtOAc and hexanes: mp 97–99 °C; $[\alpha]_D^{25}$ -32.1° (c 1.5;

MeOH); R_f = 0.52 (EtOAc); IR (nujol) 3292, 2859, 1640, 1549, 1457, 1376, 1303, 1249 cm^{-1} ; ^1H NMR (CDCl_3) δ -0.08–0.01 (m, $\text{CH}(\text{CHH}'\text{CHH}')$), 0.30–0.38 (m, $\text{CH}(\text{CHH}'\text{CHH}')$), 0.50–0.64 (m, $\text{CH}(\text{CH}_2\text{CH}_2)$), 1.32–1.48 (m, $\text{CH}_2\text{CH}(\text{CH}_2\text{CH}_2)$), 2.02 (s, $\text{CH}_3\text{C}(\text{O})$), 3.40–3.62 (m, $\text{OCH}_2\text{CH}_2\text{CH}(\text{CH}_2\text{CH}_2)$, $\text{CHH}'\text{OCH}_2\text{CH}_2$), 3.84 (dd, J = 3.9, 9.0 Hz, $\text{CHH}'\text{OCH}_2\text{CH}_2$), 4.38–4.58 (m, NHCH_2Ph , CHCH_2O), 6.48–6.58 (br d, $\text{CH}_3\text{C}(\text{O})\text{NH}$), 6.90–7.00 (br t, NHCH_2Ph), 7.20–7.36 (m, C_6H_5), addition of excess (*R*)-(-)-mandelic acid to a CDCl_3 solution of (*R*)-**89** gave only one signal for the acetyl protons (δ 2.011); ^{13}C NMR (CDCl_3) δ 4.3, 4.4 ($\text{CH}(\text{CH}_2\text{CH}_2)$), 8.0 ($\text{CH}(\text{CH}_2\text{CH}_2)$), 23.4 ($\text{CH}_3\text{C}(\text{O})$), 34.7 ($\text{CH}_2\text{CH}(\text{CH}_2\text{CH}_2)$), 43.8 (NHCH_2Ph), 52.5 ($\text{CHCH}_2\text{OCH}_2$), 70.1, 71.8 ($\text{CH}_2\text{OCH}_2\text{CH}_2$), 127.7, 128.9, 138.0 (C_6H_5), 170.3, 170.4 ($\text{CH}_3\text{C}(\text{O})\text{NH}$, $\text{C}(\text{O})\text{NHCH}_2$), the remaining resonance was not detected and is believed to overlap with nearby signals; M_r (+ESI) 327.2 [$\text{M}+\text{Na}$] $^+$ (calcd for $\text{C}_{17}\text{H}_{24}\text{N}_2\text{O}_3\text{Na}^+$ 327.2). Anal. Calcd for $\text{C}_{17}\text{H}_{24}\text{N}_2\text{O}_3$: C, 67.08; H, 7.95; N, 9.20. Found: C, 67.06; H, 7.94; N, 9.27.

(*R*)-*N*-Benzyl 2-Acetamido-3-(but-3-ynyloxy)propionamide ((*R*)-90**).** Using Method A, compound (*R*)-**78** (1.14 g, 5.22 mmol), homopropargyl alcohol (2.0 mL, 26.1 mmol), and $\text{BF}_3\cdot\text{Et}_2\text{O}$ (500 μL , 3.97 mmol) in CH_2Cl_2 (30 mL) gave (*R*)-**90** as a white solid (450 mg, 30%) upon work-up, purification by flash chromatography (2/1 EtOAc/ CH_2Cl_2), and subsequent recrystallization from EtOAc and hexanes: mp 120–122 $^\circ\text{C}$; $[\alpha]_D^{25}$ -49.1 $^\circ$ (c 0.8, CHCl_3); R_f = 0.38 (2/1 EtOAc/ CH_2Cl_2); IR (CHCl_3 film) 3088, 2932, 2867, 1746, 1640, 1548, 1449, 1377, 1303, 1243 cm^{-1} ; ^1H NMR (CDCl_3) δ 1.80 (t, J = 2.7 Hz, $\text{CH}_2\text{C}\equiv\text{CH}$), 2.04 (s, $\text{CH}_3\text{C}(\text{O})$), 2.38–2.46 (m, OCH_2CH_2), 3.46–3.74 (m, $\text{CHH}'\text{OCH}_2\text{CH}_2\text{C}\equiv\text{CH}$), 3.90 (dd, J = 3.9, 9.0 Hz,

CHH'OCH₂CH₂C≡CH), 4.38–4.58 (m, NHCH₂C₆H₅, CHCH₂O), 6.48–6.56 (m, NHCHCH₂O), 6.92–7.06 (m, NHCH₂Ph), 7.20–7.38 (m, NHCH₂C₆H₅), addition of excess (*R*)-(-)-mandelic acid to a CDCl₃ solution of (*R*)-**90** gave only one signal for the acetyl protons (δ 2.006); ¹³C NMR (CDCl₃) δ 20.0 (CH₂C≡CH), 23.4 (CH₃C(O)), 43.8 (NH₂CH₂Ph), 52.4 (CHCH₂OCH₂), 69.3, 69.8, 70.0 (CH₂OCH₂CH₂C≡CH), 81.6 (CH₂C≡CH), 127.7, 127.8, 128.9, 138.1 (C₆H₅), 170.1, 170.4 (CHC(O)NH, CH₃C(O)); *M_r* (+ESI) 421.1 [M+Cs]⁺ (calcd for C₁₆H₂₀N₂O₃Cs⁺ 421.1). Anal. Calcd for C₁₆H₂₀N₂O₃: C, 66.65; H, 6.99; N, 9.72. Found: C, 66.38; H, 6.90; N, 9.65.

(*R*)-*N*-Benzyl 2-Acetamido-3-phenethoxypropionamide ((*R*)-91**).** Using Method A, compound (*R*)-**78** (2.0 g, 9.2 mmol), phenethyl alcohol (6.0 mL, 49.2 mmol), and BF₃•Et₂O (1.0 mL, 8.0 mmol) in CH₂Cl₂ (30 mL) gave (*R*)-**91** as a white solid (392 mg, 10%) upon work-up and purification by flash chromatography (2/1 EtOAc/CH₂Cl₂) and recrystallization from EtOAc and hexanes: mp 90–92 °C; [α]_D²⁵ -29.2° (c 0.5, CHCl₃); *R_f* = 0.44 (3/1 EtOAc/CH₂Cl₂); IR (nujol) 3285, 3124, 1639, 1547, 1457, 1375, 1303, 1118 cm⁻¹; ¹H NMR (CDCl₃) δ 1.97 (s, CH₃C(O)), 2.84 (d, *J* = 6.3 Hz, OCH₂CH₂Ph), 3.40 (app d, *J* = 8.1 Hz, CHH'OCH₂CH₂Ph), 3.62–3.92 (m, CHH'OCH₂CH₂Ph), 4.20–4.38 (m, NHCH₂C₆H₅), 4.40–4.50 (m, CHCH₂O), 6.32–6.40 (m, NHCHCH₂O), 6.50–6.62 (m, NHCH₂Ph), 7.12–7.38 (m, CH₂CH₂C₆H₅, NHCH₂C₆H₅), addition of excess (*R*)-(-)-mandelic acid to a CDCl₃ solution of (*R*)-**91** gave only one signal for the acetyl protons (δ 1.988); ¹³C NMR (CDCl₃) δ 23.4 (CH₃C(O)), 36.2 (CH₂CH₂Ph), 43.6 (NH₂CH₂Ph), 52.4 (CHCH₂OCH₂), 70.0, 72.1 (CH₂OCH₂CH₂), 126.6, 127.5, 127.6, 128.7, 128.8, 129.0, 138.2, 139.0 (2 C₆H₅),

170.2, 170.4 (CHC(O)NH, CH₃C(O)); M_r (+ESI) 363.2 [M+Na]⁺ (calcd for C₂₀H₂₄N₂O₃Na⁺ 363.2). Anal. Calcd C₂₀H₂₄N₂O₃: C, 70.56; H, 7.11; N, 8.23. Found: C, 70.40; H, 7.08; N, 8.15.

(S)-N-Benzyl 2-Acetamido-3-(2-(benzyloxy)ethoxy)propionamide ((S)-126).

Using Method D, acid (S)-**121** (386 mg, 1.37 mmol), benzylamine (165 μ L, 1.51 mmol) and DMTMM (418 mg, 1.51 mmol) in THF (14 mL) gave 365 mg (72%) of (S)-**126** as a white solid after purification by silica gel flash chromatography (5/95, MeOH/CHCl₃): mp 86–88 °C, $[\alpha]_D^{25} +30.0^\circ$ (c 1.0, CHCl₃); $R_f = 0.56$ (5/95 MeOH/CHCl₃); IR (nujol) 3284, 1637, 1560 cm⁻¹; ¹H NMR (DMSO-*d*₆) δ 1.86 (s, CH₃C(O)NH), 3.52–3.62 (m, OCH₂CH₂OBn, CHCH₂OCH₂), 4.20–4.38 (m, NHCH₂Ph), 4.46–4.54 (m, OCH₂Ph, CHCH₂OCH₂), 7.19–7.40 (m, 2 C₆H₅), 8.08 (d, $J = 8.1$ Hz, NHCHCH₂O), 8.51 (t, $J = 6.0$ Hz, NHCH₂Ph); ¹³C NMR (DMSO-*d*₆) δ 22.5 (CH₃C(O)), 42.0 (NHCH₂Ph), 52.8 (CHCH₂O), 68.9, 69.8, 70.7 (OCH₂CH₂O, CHCH₂O), 72.0 (OCH₂Ph), 126.6, 126.9, 127.3, 127.4, 128.1, 128.2, 138.4, 139.2 (2 C₆H₅), 169.3, 169.7 (CH₃C(O)NH and C(O)OH); M_r (+ESI) 393.1807 [M+Na]⁺ (calcd for C₂₁H₂₆N₂O₄Na⁺ 393.1790). Anal. Calcd for C₂₁H₂₆N₂O₄•0.1H₂O: C, 67.76; H, 7.09; N, 7.53. Found: C, 67.57; H, 7.08; N, 7.90.

(S)-N-Benzyl 2-Acetamido-3-(2-hydroxyethoxy)propionamide ((S)-127). Using Method H, (S)-**126** (347 mg, 0.94 mmol), and 5% Pd/C (100 mg) in MeOH (12 mL) gave a residue that was purified using SiO₂ flash chromatography (5/95 MeOH/CHCl₃) to yield (S)-**127** as a colorless residue that slowly turned into a white

solid (193 mg, 73%): mp 100–102 °C, $[\alpha]_D^{25}$ -15.9° (c 0.2; MeOH); R_f = 0.28 (5/95 MeOH/CHCl₃); IR (neat) 3400–3000 (br), 2928, 1650, 1542, 1456, 1373 cm⁻¹; ¹H NMR (CDCl₃) δ 1.98 (s, CH₃C(O)NH), 3.20 (br s, CH₂OH), 3.52–3.78 (m, OCH₂CH₂OH, CHCHH'OCH₂), 3.82–3.88 (CHCHH'OCH₂), 4.38–4.50 (m, NHCH₂Ph), 4.60–4.68 (m, CHCH₂OCH₂), 6.84 (d, J = 7.2 Hz, NHCHCH₂O), 7.21–7.40 (m, C₆H₅, NHCH₂Ph); ¹³C NMR (CDCl₃) δ 22.5 (CH₃C(O)), 42.0 (NHCH₂Ph), 52.9 (CHCH₂O), 61.7 (CH₂OH), 70.4 (OCH₂CH₂), 72.8 (CHCH₂O), 127.7, 128.9, 138.1 (C₆H₅), 170.3 (CH₃C(O)NH or C(O)OH), 170.9 (C(O)OH or CH₃C(O)NH), the remaining aromatic resonance was not detected and is believed to overlap with nearby peaks; M_r (+ESI) 303.1314 [M+Na]⁺ (calcd for C₁₄H₂₀N₂O₄Na⁺ 303.1321). Anal. Calcd for C₁₄H₂₀N₂O₄•0.25H₂O: C, 59.04; H, 7.25; N, 9.84. Found: C, 58.80; H, 7.40; N, 9.99.

(3S)-*N*-Benzyl 4-Acetyl-5-hydroxymorpholine-3-carboxamide (S)-128. Using Method E, (COCl)₂ (63 μ L, 732 μ mol) in CH₂Cl₂ (1 mL), DMSO (105 μ L, 1.46 mmol) in CH₂Cl₂ (1 mL) and (S)-**127** (189 mg, 665 μ mol) in CH₂Cl₂ (10 mL) followed by DIEA (580 μ L, 3.325 mmol) gave after work-up a residue that was purified using flash chromatography (6/94 MeOH/CHCl₃) to yield 53 mg (28%) of (S)-**128** a white solid : mp 146–148 °C, $[\alpha]_D^{25}$ -18.8° (c 0.9; MeOH); R_f = 0.26 (5/95 MeOH/CHCl₃); IR (CH₂Cl₂ film) 3400–3000 (br), 3283, 3102, 1646, 1575, 1460, 1403, 1133, 1056 cm⁻¹; ¹H NMR (DMSO-*d*₆) δ 2.17 (s, CH₃C(O)N), 3.53 (dd, J = 2.1, 12.0 Hz, CH(OH)CH₂OCHH'), 3.65 (dd, J = 4.3, 12.3 Hz CH(OH)CHH'), 3.80 (d, J = 12.0 Hz, CH(OH)CHH'), 4.07 (d, J = 12.3 Hz, CH(OH)CH₂OCHH'), 4.34 (app. d, J = 6.0 Hz,

NHCH₂Ph), 4.69 (d, J = 4.3 Hz, CHCH₂OCH₂), 5.14 (br d, J = 8.1 Hz, NCH(OH)CH₂O), 7.00 (d, J = 8.1 Hz, NCH(OH)CH₂O), 7.20–7.36 (m, C₆H₅), 8.98 (t, J = 6.0 Hz, NHCH₂Ph); ¹³C NMR (DMSO-*d*₆) δ 20.4 (CH₃C(O)), 42.5 (NHCH₂Ph), 53.1 (CHCH₂O), 68.1 (CHCH₂OCH₂), 71.7 (OCH₂CH(OH)N), 73.2 (OCH₂CH(OH)N), 126.9, 127.0, 128.4, 138.5 (C₆H₅), 172.1 (CH₃C(O)N or C(O)NHCH₂), 172.5 (C(O)NHCH₂ or CH₃C(O)N); M_r (+ESI) 301.1157 [M+Na]⁺ (calcd for C₁₄H₁₈N₂O₄Na⁺ 301.1164). Anal. Calcd for C₁₄H₁₈N₂O₄: C, 60.42; H, 6.52; N, 10.07. Found: C, 60.12; H, 6.55; N, 9.81.

(*R*)-*N*-Benzyl 2-Acetamido-3-(3-hydroxypropoxy)propionamide ((*R*)-129**).** Using Method D, acid (*R*)-**123** (1.07 g, 5.22 mmol), benzylamine (0.68 mL, 6.26 mmol), and DMTMM (1.73 g, 6.26 mmol) in anhydrous THF (50 mL) gave 1.34 g (87%) of (*R*)-**129** as a white solid after flash column chromatography (8/92 MeOH/CHCl₃): mp 90–92 °C; [α]_D²⁵ +8.0° (c 1.0, MeOH); R_f = 0.38 (8/92 MeOH/CHCl₃); IR (CH₂Cl₂ film) 3313, 3059, 2932, 2876, 1660, 1532, 1454, 1374, 1266, 1118 cm⁻¹; ¹H NMR (CDCl₃) δ 1.76 (quint, J = 6.0 Hz, OCH₂CH₂CH₂O), 1.98 (s, CH₃C(O)), 3.56 (dd, J = 6.6, 9.3 Hz, CHH'OCH₂CH₂CH₂), 3.58–3.68 (m, OCH₂CH₂CH₂O), 3.78 (dd, J = 3.9, 9.3 Hz, CHH'OCH₂CH₂CH₂), 4.36–4.52 (m, NHCH₂Ph), 4.60–4.65 (m, CHCH₂O), 6.76 (d, J = 7.2 Hz, CH₃C(O)NH), 7.20–7.38 (m, C₆H₅, C(O)NHCH₂); ¹³C NMR (CDCl₃) δ 23.1 (CH₃C(O)), 32.1 (OCH₂CH₂CH₂O), 43.6 (NHCH₂Ph), 52.7 (CHCH₂OCH₂), 60.3 (OCH₂CH₂CH₂OH), 69.3 (CHCH₂OCH₂CH₂CH₂), 70.6 (CHCH₂OCH₂CH₂CH₂), 127.5, 127.7, 128.8, 138.1 (C₆H₅), 170.3, 170.9 (CHC(O)NH, CH₃C(O)NH); M_r (+ESI) 317.1477 [M+Na]⁺ (calcd for C₁₅H₂₂N₂O₄Na⁺

317.1477). Anal. Calcd for $C_{15}H_{22}N_2O_4 \cdot 0.15H_2O$: C, 60.65; H, 7.57; N, 9.43. Found: C, 60.40; H, 7.56; N, 9.67.

(S)-N-Benzyl 2-Acetamido-3-(3-hydroxypropoxy)propionamide ((S)-129). Using Method D, acid (S)-**123** (1.52 g, 7.41 mmol), benzylamine (0.97 mL, 8.9 mmol), and DMTMM (2.46 g, 8.9 mmol) in anhydrous THF (75 mL) gave 1.51 g (69%) of (S)-**129** as a white solid after flash column chromatography (8/92 MeOH/ $CHCl_3$). The solid contained an unidentified impurity (~20 mol percent based on 1H NMR integrations) that co-eluted using different solvent systems and could not be removed by recrystallization: mp 87–90 °C; $[\alpha]_D^{25} -7.5^\circ$ (c 1.0, MeOH); $R_f = 0.38$ (8/92 MeOH/ $CHCl_3$); IR (nujol) 3300–2600 (br), 3278, 1638, 1553, 1458, 1375, 1306, 1245, 1123 cm^{-1} ; 1H NMR ($CDCl_3$) δ 1.75 (quint, $J = 5.7$ Hz, $OCH_2CH_2CH_2O$), 1.98 (s, $CH_3C(O)$), 2.44–2.60 (br s, CH_2OH), 3.53 (dd, $J = 6.9, 9.6$ Hz, $CHH'OCH_2CH_2CH_2$), 3.36–3.50 (m, $OCH_2CH_2CH_2O$), 3.80 (dd, $J = 4.2, 9.6$ Hz, $CHH'OCH_2CH_2CH_2$), 4.35–4.51 (m, $NHCH_2Ph$), 4.58–4.66 (m, $CHCH_2O$), 6.74 (d, $J = 6.9$ Hz, $CH_3C(O)NH$), 7.20–7.40 (m, C_6H_5 , $C(O)NHCH_2$); ^{13}C NMR ($CDCl_3$) δ 23.3 ($CH_3C(O)$), 32.1 ($OCH_2CH_2CH_2O$), 43.7 ($NHCH_2Ph$), 52.7 ($CHCH_2OCH_2$), 60.6 ($OCH_2CH_2CH_2OH$), 69.5 ($CHCH_2OCH_2CH_2CH_2$), 70.6 ($CHCH_2OCH_2CH_2CH_2$), 127.7, 127.8, 128.8, 138.0 (C_6H_5), 170.2, 170.7 ($CHC(O)NH$, $CH_3C(O)NH$); M_r (+ESI) 317.1478 $[M+Na]^+$ (calcd for $C_{15}H_{22}N_2O_4Na^+$ 317.1477).

(R)-N-Benzyl 2-Acetamido-3-(3-oxopropoxy)propionamide ((R)-93). Using Method E, alcohol (R)-**129** (1.20 g, 4.08 mmol) in CH_2Cl_2 (12 mL), $(COCl)_2$ (432 μL ,

4.92 mmol) in CH₂Cl₂ (12 mL), DMSO (720 μL, 9.84 mmol) in CH₂Cl₂ (24 mL), and DIEA (3.55 mL, 14.4 mmol) gave 506 mg (39%) of (*R*)-**93** as white needles after recrystallization from EtOAc: mp 120–121 °C; [α]_D²⁵ -22.1° (*c* 0.9, CHCl₃); *R*_f = 0.34 (5/95 MeOH/CHCl₃); IR (CH₂Cl₂ film) 3306, 3057, 1724, 1662, 1523, 1374, 1266, 1119 cm⁻¹; ¹H NMR (CDCl₃) δ 2.04 (s, CH₃C(O)), 2.60–2.80 (m, CH₂C(O)H), 3.48 (dd, *J* = 7.5, 9.3 Hz, CHCHH'OCH₂CH₂), 3.70–3.78 (m, CH₂OCHH'CH₂C(O)H), 3.80–3.87 (m, CH₂OCHH'CH₂C(O)H), 3.90 (dd, *J* = 3.6, 9.3 Hz, CHCHH'OCH₂CH₂), 4.46 (d, *J* = 6.0 Hz, NHCH₂Ph), 4.51–4.58 (m, CHCH₂O), 6.61 (d, *J* = 6.3 Hz, CH₃C(O)NH), 6.85–7.04 (br t, C(O)NHCH₂), 7.22–7.38 (m, C₆H₅), 9.71 (t, *J* = 1.4 Hz, C(O)H), addition of excess (*R*)-(-)-mandelic acid to a CDCl₃ solution of (*R*)-**93** gave only one signal for the acetyl methyl protons and the aldehyde proton, addition of excess (*R*)-(-)-mandelic acid to a CDCl₃ solution of (*S*)-**93** and (*R*)-**93** (1:3 ratio) gave two signals for the acetyl methyl protons (δ 2.032 (*S*) and 2.018 (*R*) (Δ ppm = 0.014)), and two signals for the aldehyde protons (δ 9.658 (*S*) and 9.680 (*R*) (Δ ppm = 0.022)); ¹³C NMR (CDCl₃) δ 23.4 (CH₃C(O)), 43.8, 43.9 (OCH₂CH₂C(O)H, NHCH₂Ph), 52.4 (CHCH₂OCH₂), 64.5 (OCH₂CH₂C(O)H), 70.4 (CHCH₂OCH₂CH₂C(O)H), 127.6, 127.7, 128.8, 138.3 (C₆H₅), 170.0, 170.6 (CHC(O)NH, CH₃C(O)NH), 200.9 (C(O)H); *M*_r (+ESI) 315.1323 [M+Na]⁺ (calcd for C₁₅H₂₀N₂O₄Na⁺ 315.1321). Anal. Calcd for C₁₅H₂₀N₂O₄: C, 61.63; H, 6.90; N, 9.58. Found: C, 61.34; H, 6.94; N, 9.42.

(S)-N-Benzyl 2-Acetamido-3-(3-oxopropoxy)propionamide ((S)-93). Using Method E, compound (*S*)-**129** (1.50 g, 5.10 mmol) in CH₂Cl₂ (10 mL), (COCl)₂ (580

μL , 6.63 mmol) in CH_2Cl_2 (20 mL), DMSO (941 μL , 6.63 mmol) in CH_2Cl_2 (10 mL), and DIEA (4.44 mL, 25.5 mmol) gave 757 mg (49%) of (S)-**93** as white needles after recrystallization from EtOAc: mp 120–121 $^\circ\text{C}$; $[\alpha]_{\text{D}}^{25} +22.0^\circ$ (c 1.0, CHCl_3); $R_f = 0.34$ (5/95 MeOH/ CHCl_3); IR (CHCl_3 film) 3306, 3057, 2984, 2922, 2875, 1724, 1662, 1523, 1373, 1265, 1119 cm^{-1} ; ^1H NMR (CDCl_3) δ 2.02 (s, $\text{CH}_3\text{C}(\text{O})$), 2.60–2.80 (m, $\text{CH}_2\text{C}(\text{O})\text{H}$), 3.49 (dd, $J = 7.2, 9.6$ Hz, $\text{CHCHH}'\text{OCH}_2\text{CH}_2$), 3.69–3.78 (m, $\text{CH}_2\text{OCHH}'\text{CH}_2\text{C}(\text{O})\text{H}$), 3.78–3.85 (m, $\text{CH}_2\text{OCHH}'\text{CH}_2\text{C}(\text{O})\text{H}$), 3.88 (dd, $J = 3.9, 9.6$ Hz, $\text{CHCHH}'\text{OCH}_2\text{CH}_2$), 4.45 (d, $J = 5.7$ Hz, NHCH_2Ph), 4.56 (app dt, $J = 3.9, 7.2$ Hz, CHCH_2O), 6.68 (d, $J = 7.2$ Hz, $\text{CH}_3\text{C}(\text{O})\text{NH}$), 6.90–7.21 (br t, $\text{C}(\text{O})\text{NHCH}_2$), 7.20–7.38 (m, C_6H_5), 9.70 (t, $J = 1.4$ Hz, $\text{C}(\text{O})\text{H}$), addition of excess (R)-(-)-mandelic acid to a CDCl_3 solution of (S)-**93** gave only one signal for the acetyl methyl protons and the aldehyde proton, addition of excess (R)-(-)-mandelic acid to a CDCl_3 solution of (S)-**93** and (R)-**93** (~1:3 ratio) gave two signals for the acetyl methyl protons (δ 2.032 (S) and 2.018 (R) ($\Delta\text{ppm} = 0.014$)), and two signals for the aldehyde protons (δ 9.658 (S) and 9.680 (R) ($\Delta\text{ppm} = 0.022$)); ^{13}C NMR (CDCl_3) δ 23.3 ($\text{CH}_3\text{C}(\text{O})$), 43.7, 43.8 ($\text{OCH}_2\text{CH}_2\text{C}(\text{O})\text{H}$, NHCH_2Ph), 52.4 ($\text{CHCH}_2\text{OCH}_2$), 64.5 ($\text{OCH}_2\text{CH}_2\text{C}(\text{O})\text{H}$), 70.4 ($\text{CHCH}_2\text{OCH}_2\text{CH}_2\text{C}(\text{O})\text{H}$), 127.6, 127.7, 128.8, 138.2 (C_6H_5), 170.0, 170.6 ($\text{CHC}(\text{O})\text{NH}$, $\text{CH}_3\text{C}(\text{O})\text{NH}$), 200.9 ($\text{C}(\text{O})\text{H}$); M_r (+ESI) 315.1325 $[\text{M}+\text{Na}]^+$ (calcd for $\text{C}_{15}\text{H}_{20}\text{N}_2\text{O}_4\text{Na}^+$ 315.1321). Anal. Calcd for $\text{C}_{15}\text{H}_{20}\text{N}_2\text{O}_4$: C, 61.63; H, 6.90; N, 9.58. Found: C, 61.71; H, 7.01; N, 9.52.

(2R)-N-Benzyl 2-Acetamido-3-(2-(oxiran-2-yl)ethoxy)propionamide ((R)-94)
(mixture of diastereomers). Using Method J, (R)-**88** (320 mg, 1.10 mmol), Na_2SO_4

(50 mg) and *m*CPBA (77% wt, 420 mg, 1.88 mmol) in CH₂Cl₂ (3 mL) gave (*R*)-**94** (265 mg, 72%) as a ~1:1 mixture of diastereoisomers after purification by flash chromatography (15/85 acetone/EtOAc): mp 104–110 °C; [α]_D²⁵ -29.6° (c 0.3; CHCl₃); *R*_f = 0.31 (15/85 acetone/EtOAc); IR (nujol) 3292, 1637, 1545, 1457, 1376, 1127 cm⁻¹; ¹H NMR (CDCl₃) δ 1.52–1.64 (m, CH₂CHH'CH(O)CH₂), 1.86–2.00 (m, CH₂CHH'CH(O)CH₂), 2.03, 2.04 (s, CH₃C(O)), 2.41–2.46 (m, CH₂CH₂CH(O)CHH'), 2.66–2.71 (m, CH₂CH₂CH(O)CHH'), 2.82–2.96 (m, CH₂CH₂CH(O)CH₂), 3.44–3.52 (m, CHH'OCH₂CH₂), 3.54–3.76 (m, CH₂OCH₂CH₂), 3.84–3.93 (m, CHH'OCH₂CH₂), 4.39–4.52 (m, NHCH₂Ph), 4.50–4.58 (m, CHCH₂O), 6.56–6.68 (m, NHCHCH₂O), 6.88–6.98, 6.99–7.08 (m, NHCH₂Ph), 7.22–7.36 (m, C₆H₅), addition of excess (*R*)-(-)-mandelic acid to a CDCl₃ solution of (*R*)-**94** gave only one set of signals for the acetyl protons (δ 2.015 and 2.022 ppm), addition of excess (*R*)-(-)-mandelic acid to a CDCl₃ solution of (*S*)-**94** and (*R*)-**94** in a ~1:3 ratio gave two sets of signals with a relative ~1:3 intensity for the acetyl protons (δ 2.028 and 2.022 ppm (*S*)-**94**, δ 2.015 and 2.008 ppm (*R*)-**94**); ¹³C NMR (CDCl₃) δ 23.4 (CH₃C(O)), 32.4, 32.6 (CH₂CH₂CH(O)CH₂), 43.8 (NHCH₂Ph), 46.7 (CH₂CH₂CH(O)CH₂), 50.3, 50.4, 52.6, 52.7 (CHC(O)NH, CH₂CH₂CH(O)CH₂), 68.5, 68.8, 69.9, 70.1 (CHCH₂OCH₂), 127.6, 127.7, 128.8, 128.9, 138.2, 138.3 (C₆H₅), 170.2, 170.6 (CH₃C(O), CHC(O)NH), the remaining peaks were not detected and are believed to overlap with nearby signals; *M*_r (+ESI) 329.1478 [M+Na]⁺ (calcd for C₁₆H₂₂N₂O₄Na⁺ 329.1477). Anal. Calcd for C₁₆H₂₂N₂O₄: C, 62.73; H, 7.24; N, 9.14. Found: C, 62.92; H, 7.37; N, 9.07.

(2S)-N-Benzyl 2-Acetamido-3-(2-(oxiran-2-yl)ethoxy)propionamide ((S)-94)

(mixture of diastereomers). Using Method J, (S)-**88** (100 mg, 0.35 mmol), Na₂SO₄ (25 mg) and *m*CPBA (77% wt, 131 mg, 0.59 mmol) in CH₂Cl₂ (3 mL) yielded (S)-**94** (76 mg, 72%) as a ~1:1 mixture of diastereoisomers: mp 104–109 °C; [α]_D²⁵ +31.3° (c 1.4; CHCl₃); *R*_f = 0.31 (15/85 acetone/EtOAc); IR (nujol) 3281, 3062, 1638, 1547, 1457, 1376, 1127 cm⁻¹; ¹H NMR (CDCl₃) δ 1.52–1.64 (m, CH₂CHH'CH(O)CH₂), 1.84–1.96 (m, CH₂CHH'CH(O)CH₂), 2.00, 2.01 (s, CH₃C(O)), 2.40–2.46 (m, CH₂CH₂CH(O)CHH'), 2.65–2.71 (m, CH₂CH₂CH(O)CHH'), 2.82–2.96 (m, CH₂CH₂CH(O)CH₂), 3.44–3.52 (m, CHH'OCH₂CH₂), 3.54–3.72 (m, CH₂OCH₂CH₂), 3.81–3.90 (m, CHH'OCH₂CH₂), 4.36–4.52 (m, NHCH₂Ph), 4.53–4.61 (m, CHCH₂O), 6.70–6.80 (m, NHCHCH₂O), 7.04–7.11, 7.12–7.21 (2 br t, NHCH₂Ph), 7.22–7.36 (m, C₆H₅), addition of excess (*R*)-(-)-mandelic acid to a CDCl₃ solution of (S)-**94** gave only one set of signals for the acetyl protons (δ 2.026 and 2.031 ppm), addition of excess (*R*)-(-)-mandelic acid to a CDCl₃ solution of (S)-**94** and (*R*)-**94** in a ~1:3 ratio gave two sets of signals with a relative ~1:3 intensity for the acetyl protons (δ 2.028 and 2.022 ppm (S)-**94**, δ 2.015 and 2.008 ppm (*R*)-**94**); ¹³C NMR (CDCl₃) δ 23.3 (CH₃C(O)), 32.4, 32.6 (CH₂CH₂CH(O)CH₂), 43.7 (NHCH₂Ph), 46.7 (CH₂CH₂CH(O)CH₂), 50.3, 50.4, 52.6, 52.7 (CHC(O)NH, CH₂CH₂CH(O)CH₂), 68.4, 68.7, 70.0, 70.2 (CHCH₂OCH₂), 127.5, 127.6, 127.7, 128.7, 128.8, 138.3 (C₆H₅), 170.2, 170.5 (CH₃C(O), CHC(O)NH), the remaining peaks were not detected and are believed to overlap with nearby signals; *M*_r (+ESI) 329.1479 [M+Na]⁺ (calcd for C₁₆H₂₂N₂O₄Na⁺ 329.1477). Anal. Calcd for C₁₆H₂₂N₂O₄: C, 62.73; H, 7.24; N, 9.14. Found: C, 62.94; H, 7.34; N, 9.12.

(*R*)-*N*-Benzyl 2-Acetamido-3-(2-acetamidoethoxy)propionamide ((*R*)-96). Using Method H, (*R*)-97 (1.14 g, 3.7 mmol) and 10% Pd/C (100 mg) in MeOH (25 mL) gave upon filtration and evaporation a residue that was dissolved in CH₂Cl₂ (50 mL). Et₃N (570 μ L, 4.1 mmol), DMAP (1 mg, catalytic), and Ac₂O (390 μ L, 4.1 mmol) were then successively added and the reaction was stirred at room temperature (30 min), filtered, and the solvents were removed under vacuum. The crude residue was purified by flash chromatography (1/9 MeOH/CH₂Cl₂) to give an oily residue that was dissolved in warm THF (25 mL). The white solid that precipitated upon cooling was filtered to give (*R*)-96 (490 mg, 40% overall yield for two steps): mp 166–168 °C; $[\alpha]_D^{25} +11.7^\circ$ (c 0.6, MeOH); $R_f = 0.30$ (5/95 MeOH/CH₂Cl₂); IR (nujol) 3494, 3089, 3288, 2861, 1637, 1554, 1456, 1372, 1290 cm⁻¹; ¹H NMR (DMSO-*d*₆) δ 1.79, 1.88 (s, 2 CH₃C(O)), 3.10–3.24 (m, OCH₂CH₂NHAc), 3.36–3.46 (m, OCH₂CH₂NHAc), 3.52–3.64 (m, CHCH₂OCH₂), 4.29 (d, $J = 7.0$ Hz, NHCH₂C₆H₅), 4.42–4.52 (m, CHCH₂O), 7.20–7.36 (m, CH₂C₆H₅), 7.80–7.88 (m, NHCH₂Ph or NHCH₂CH₂), 8.07 (d, $J = 7.0$ Hz, NHCHCH₂), 8.50 (t, $J = 6.0$ Hz, NHCH₂CH₂ or NHCH₂Ph); ¹³C NMR (DMSO-*d*₆) δ 22.6 (2 CH₃C(O)), 38.3 (CH₂CH₂NHAc), 42.0 (NH₂CH₂Ph), 52.7 (CHCH₂OCH₂), 69.1, 70.3 (CH₂OCH₂CH₂), 126.6, 126.9, 128.2, 139.3 (C₆H₅), 169.3, 169.4, 169.7 (CHC(O)NH, 2 CH₃C(O)), the remaining signal was not detected and is believed to overlap with nearby peaks; M_r (+ESI) 344.2 [M+Na]⁺ (calcd for C₁₆H₂₃N₃O₄Na⁺ 344.2). Anal. Calcd for C₁₆H₂₃N₃O₄: C, 59.80; H, 7.21; N, 13.08. Found: C, 59.63; H, 7.16; N, 12.94.

(*R*)-*N*-Benzyl 2-Acetamido-3-(2-azidoethoxy)propionamide ((*R*)-97**).** Using Method D, (*R*)-**124** (950 mg, 4.4 mmol), benzylamine (622 μ L, 5.7 mmol), and DMTMM (1.58 g, 5.7 mmol) in THF (50 mL) gave 715 mg (53%) of (*R*)-**97** as a white solid after SiO₂ chromatography column (4/96 MeOH/CHCl₃) followed by recrystallization from EtOAc: mp 111–113 °C; $[\alpha]_D^{25} +12.0^\circ$ (c 1.0; MeOH); $R_f = 0.51$ (5/95 MeOH/CHCl₃); IR (nujol) 3139, 2107, 1635, 1547 cm⁻¹; ¹H NMR (CDCl₃) δ 1.98 (s, CH₃C(O)NH), 3.32–3.43 (m, OCH₂CH₂N₃), 3.50–3.56 (m, CHCHH'OCH₂), 3.58–3.75 (m, OCH₂CH₂N₃), 3.88–3.96 (m, CHCHH'OCH₂), 4.39–4.51 (m, NHCH₂Ph), 4.52–4.58 (m, CHCH₂OCH₂), 6.55–6.65 (br d, NHCHCH₂O), 6.76–6.86 (m, NHCH₂Ph), 7.21–7.35 (C₆H₅), addition of excess (*R*)-(-)-mandelic acid to a CDCl₃ solution of (*R*)-**97** gave only one signal for the acetyl protons, addition of excess (*R*)-(-)-mandelic acid to a CDCl₃ solution of (*S*)-**97** and (*R*)-**97** (1:2 ratio) gave two signals for the acetyl protons (δ 2.006 (*S*) and 1.993 (*R*) (Δ ppm = 0.013)); ¹³C NMR (CDCl₃) δ 23.4 (CH₃C(O)), 43.9 (NHCH₂Ph), 50.9 (CH₂N₃), 52.7 (CHCH₂O), 70.3 (OCH₂CH₂N₃ or CHCH₂O), 70.4 (CHCH₂O or OCH₂CH₂N₃), 127.7, 128.9, 138.0 (C₆H₅), 169.8, 170.9 (CH₃C(O)NH and C(O)NHCH₂), the remaining aromatic resonance was not detected and is believed to overlap with nearby signals; M_r (+ESI) 328.1380 [M+Na]⁺ (calcd for C₁₄H₁₉N₅O₃Na⁺ 328.1386). Anal. Calcd for C₁₄H₁₉N₅O₃: C, 55.07; H, 6.27; N, 22.94. Found: C, 54.85; H, 6.27; N, 22.94.

(*S*)-*N*-Benzyl 2-Acetamido-3-(2-azidoethoxy)propionamide ((*S*)-97**).** Using Method D, acid (*S*)-**124** (1.08 g, 5 mmol), benzylamine (600 μ L, 5.5 mmol) and DMTMM (1.52 g, 5.5 mmol) in THF (50 mL) gave 854 mg (56%) of (*S*)-**97** as a white

solid after silica gel chromatography (4/96 MeOH/CHCl₃) followed by recrystallization from EtOAc and hexanes: mp 111–113 °C; [α]_D²⁵ -12.1° (c 1.0; MeOH); *R*_f = 0.51 (5/95 MeOH/CHCl₃); IR (nujol) 3139, 2107, 1635, 1547 cm⁻¹; ¹H NMR (CDCl₃) δ 1.98 (s, CH₃C(O)NH), 3.32–3.43 (m, OCH₂CH₂N₃), 3.50–3.56 (m, CHCHH'OCH₂), 3.58–3.75 (m, OCH₂CH₂N₃), 3.88–3.96 (m, CHCHH'OCH₂), 4.39–4.51 (m, NHCH₂Ph), 4.52–4.58 (m, CHCH₂OCH₂), 6.42–6.52 (br d, NHCHCH₂O), 6.74–6.84 (br t, NHCH₂Ph), 7.21–7.35 (C₆H₅), addition of excess (*R*)-(-)-mandelic acid to a CDCl₃ solution of (*S*)-**97** gave only one signal for the acetyl protons, addition of excess (*R*)-(-)-mandelic acid to a CDCl₃ solution of (*S*)-**97** and (*R*)-**97** (1:2 ratio) gave two signals for the acetyl protons (δ 2.006 (*S*) and 1.993 (*R*) (Δ ppm = 0.013)); ¹³C NMR (CDCl₃) δ 23.4 (CH₃C(O)), 43.9 (NHCH₂Ph), 50.9 (CH₂N₃), 52.7 (CHCH₂O), 70.3 (OCH₂CH₂N₃ or CHCH₂O), 70.4 (CHCH₂O or OCH₂CH₂N₃), 127.7, 128.9, 138.0 (C₆H₅), 169.8, 170.9 (CH₃C(O)NH and C(O)NHCH₂), the remaining aromatic resonance was not detected and is believed to overlap with nearby signals; *M*_r (+ESI) 328.1380 [M+Na]⁺ (calcd for C₁₄H₁₉N₅O₃Na⁺ 328.1386). Anal. Calcd for C₁₄H₁₉N₅O₃: C, 55.07; H, 6.27; N, 22.94. Found: C, 55.16; H, 6.28; N, 22.91.

(*R*)-*N*-Benzyl 2-Acetamido-3-(2-(4-(methoxymethyl)-1*H*-1,2,3-triazol-1-yl)ethoxy)propionamide ((*R*)-98**).** Compound (*R*)-**97** (400 mg, 1.3 mmol) was dissolved in a THF:H₂O (1:1, 50 mL) and while stirring, methyl propargyl ether (1.0 mL, 11.8 mmol), sodium ascorbate (25 mg, 0.13 mmol), and CuSO₄ (3 mg, 0.01 mmol) were successively added. The reaction was stirred at room temperature (24 h), and saturated aqueous NaHCO₃ (100 mL) was added. The aqueous layer was

extracted with CH₂Cl₂ (2 x 100 mL), the combined organic layers were washed with brine (100 mL) and filtered over a Celite[®] bed. Removal of solvents in vacuo gave an off-white solid that was purified by flash chromatography (1/9 MeOH/CH₂Cl₂) to yield (*R*)-**98** (470 mg, 96%) as a crystalline solid: mp 127–129 °C; [α]_D²⁵ +1.8° (c 0.34; MeOH); *R*_f = 0.49 (1/9 MeOH/CH₂Cl₂); IR (nujol) 3296, 2861, 1641, 1545, 1457, 1377, 1143, 1095 cm⁻¹; ¹H NMR (CDCl₃) δ 2.00 (s, CH₃C(O)), 3.38 (s, CH₂OCH₃), 3.50 (dd, *J* = 6.5, 9.6 Hz, CHH'OCH₂CH₂), 3.76–3.85 (m, OCH₂CH₂N(N)CH), 3.92 (dd, *J* = 4.2, 9.6 Hz, CHH'OCH₂CH₂), 4.34–4.51 (m, NHCH₂Ph, OCH₂CH₂N(N)CH, CH₂OCH₃), 6.63 (d, *J* = 6.6 Hz, NHCHC(O)), 7.00–7.10 (br t, NHCH₂Ph), 7.18–7.35 (m, C₆H₅), 7.52 (s, NCHC(N)), addition of excess (*R*)-(-)-mandelic acid to a CDCl₃ solution of (*R*)-**98** gave only one signal for the acetyl protons (δ 1.995); ¹³C NMR (CDCl₃) δ 23.2 (CH₃C(O)), 43.7 (NHCH₂Ph), 50.0 (CH₂N(N)CH), 52.9 (CHC(O)NH), 58.6 (CH₂OCH₃), 66.0 (OCH₂CH₂N), 69.4, 70.5 (CHCH₂OCH₂, CH₂OCH₃), 123.8 (NCHC(N)), 127.6, 127.7, 128.8, 138.3 (C₆H₅), 145.3 (NCHC(N)), 169.7, 170.8 (CH₃C(O), CHC(O)NH); *M*_r (+ESI) 398.1806 [M+Na]⁺ (calcd for C₁₈H₂₅N₅O₄Na⁺ 398.1804). Anal. Calcd for C₁₈H₂₅N₅O₄: C, 57.59; H, 6.71; N, 18.65. Found: C, 57.34; H, 6.72; N, 18.49.

(*R*)-*N*-Benzyl 2-Acetamido-3-(2-methoxyethoxy)propionamide ((*R*)-99**).** Using Method B, a ~5:95 mixture of (*R*)-**113a** and (*R*)-**113b** (4.00 g, 17.4 mmol) in THF (170 mL) and LiOH (415 mg, 17.3 mmol) in H₂O (80 mL) gave 1.10 g (31%, 5.36 mmol) of a crude viscous yellow oil upon work-up (*M*_r (+ESI) 228.0848 [M+Na]⁺ (calcd for C₈H₁₅NO₅Na⁺ 228.0848)). Using Method D, the oil was directly dissolved

in THF (60 mL) and then benzylamine (732 μL , 6.7 mmol) followed by DMTMM (1.90 g, 6.7 mmol) were added. Purification by flash chromatography (1/9 hexanes/EtOAc to 1/9 MeOH/ CH_2Cl_2) followed by recrystallization from EtOAc and hexanes afforded (*R*)-**99** (750 mg, 45%) as a white solid: mp 109–110 $^\circ\text{C}$; $[\alpha]_D^{25} +10.3^\circ$ (c 0.5; MeOH); $R_f = 0.43$ (1/9 MeOH/ CH_2Cl_2); IR (CH_2Cl_2 film) 3427, 3306, 3058, 2998, 1741, 1664, 1528, 1454, 1372, 1267, 1206, 1107, 1028 cm^{-1} ; ^1H NMR (CDCl_3) δ 2.02 (s, $\text{CH}_3\text{C}(\text{O})$), 3.18 (s, CH_2OCH_3), 3.43–3.53 (m, $\text{CHH}'\text{OCH}_2$, $\text{OCH}_2\text{CH}_2\text{OCH}_3$ or $\text{OCH}_2\text{CH}_2\text{OCH}_3$), 3.62–3.78 (m, $\text{OCH}_2\text{CH}_2\text{OCH}_3$ or $\text{OCH}_2\text{CH}_2\text{OCH}_3$), 3.85 (dd, $J = 4.2, 9.6$ Hz, $\text{CHH}'\text{OCH}_2\text{CH}_2$), 4.37–4.51 (m, NHCH_2Ph), 4.52–4.58 (m, CHCH_2O), 6.65 (d, $J = 6.6$ Hz, $\text{NHCHC}(\text{O})$), 7.21–7.38 (m, $\text{NHCH}_2\text{C}_6\text{H}_5$, C_6H_5), addition of excess (*R*)-(-)-mandelic acid to a CDCl_3 solution of (*R*)-**99** gave only one signal for the acetyl protons (δ 1.997); ^{13}C NMR (CDCl_3) δ 23.4 ($\text{CH}_3\text{C}(\text{O})$), 43.8 (NHCH_2Ph), 51.9 ($\text{CHC}(\text{O})\text{NH}$), 58.8 ($\text{CH}_2\text{CH}_2\text{OCH}_3$), 69.4, 70.5 ($\text{CHCH}_2\text{OCH}_2$, CH_2OCH_3), 127.6, 127.7, 128.8, 138.2 (C_6H_5), 170.2, 170.4 ($\text{CH}_3\text{C}(\text{O})$, $\text{CHC}(\text{O})\text{NH}$), the remaining signal was not detected and is believed to overlap with nearby peaks; M_r (+ESI) 317.1478 $[\text{M}+\text{Na}]^+$ (calcd for $\text{C}_{15}\text{H}_{22}\text{N}_2\text{O}_4\text{Na}^+$ 317.1477). Anal. Calcd for $\text{C}_{15}\text{H}_{22}\text{N}_2\text{O}_4$: C, 61.21; H, 7.53; N, 9.52; Found: C, 61.38; H, 7.36; N, 9.44.

(*R*)-*N*-Benzyl 2-Acetamido-3-(2-(2-methoxyethoxy)ethoxy)propionamide ((*R*)-100**).** Using Method D, (*R*)-**125** (1.67 g, 6.70 mmol), benzylamine (876 μL , 8.04 mmol) and DMTMM (2.22 g, 8.04 mmol) in THF (70 mL) gave a residue that was purified twice by flash chromatography (5/95 MeOH/ CHCl_3) to yield (*R*)-**100** (1.20 g, 53%) as a yellow oil that progressively turned to an amorphous solid after 3 d under

vacuum: mp 48–52 °C; $[\alpha]_D^{25} +7.7^\circ$ (c 1.2, MeOH); $R_f = 0.51$ (5/95 MeOH/CHCl₃); IR (neat) 3313, 3072, 2921, 2358, 2245, 1657, 1538, 1103 cm⁻¹; ¹H NMR (CDCl₃) δ 2.02 (s, CH₃C(O)), 3.26 (s, OCH₃), 3.39–3.80 (m, CHH'OCH₂CH₂OCH₂CH₂OCH₃), 4.05 (dd, $J = 3.9$ Hz, 9.9 Hz, CHH'OCH₂CH₂O), 4.48 (d, $J = 6.0$ Hz, NHCH₂C₆H₅), 4.54–4.62 (m, CHCH₂O), 6.77 (d, $J = 6.0$ Hz, NHCH₂C₆H₅), 7.20–7.39 (m, C₆H₅), addition of excess (*R*)-(-)-mandelic acid to a CDCl₃ solution of (*R*)-**100** gave only one signal for the acetyl peak protons (δ 1.998); ¹³C NMR (CDCl₃) δ 23.4 (CH₃C(O)), 43.7 (NH₂CH₂C₆H₄), 52.5 (CHCH₂OCH₂CH₂), 59.0 (OCH₃), 70.4, 70.5, 70.6, 71.9 (OCH₂CH₂OCH₂CH₂O), 127.5, 127.7, 128.8, 137.8 (C₆H₅), 170.3, 170.4 (CHC(O)NH, CH₃C(O)), the remaining methylene signal was not detected and is believed to overlap with nearby signals; M_r (+ESI) 361.1743 [M+Na]⁺ (calcd for C₁₇H₂₆N₂O₅Na⁺ 361.1739). Anal. Calcd for C₁₇H₂₆N₂O₅•0.33 H₂O: C, 58.77; H, 7.83; N, 8.06. Found: C, 58.59; H, 7.88; N, 8.10.

(*R*)-*N*-Benzyl 2-*N*-(Benzyloxycarbonyl)amino-3-(methoxy-*d*₃)propionamide ((*R*)-130**).** Using Method G, compound (*R*)-**57** (1.40 g, 4.4 mmol), Ag₂O (5.00 g, 21.5 mmol) and CD₃I (2.7 mL, 43.5 mmol) in CH₃CN (40 mL) gave (*R*)-**130** as a white solid (1.50 g, 96%) upon purification by flash silica gel chromatography (2/98 MeOH/CH₂Cl₂): mp 130–131 °C; $[\alpha]_D^{25} -25.2^\circ$ (c 0.6, CHCl₃); $R_f = 0.52$ (3/97 MeOH/CH₂Cl₂); IR (CHCl₃ film) 3021, 1719, 1675, 1501, 1326, 1217, 1131, 1073 cm⁻¹; ¹H NMR (CDCl₃) δ 3.48 (dd, $J = 6.3, 9.0$ Hz, CHH'OCD₃), 3.84 (dd, $J = 3.9, 9.0$ Hz, CHH'OCD₃), 4.30–4.40 (CHCH₂O), 4.46 (d, $J = 5.7$ Hz, NHCH₂C₆H₅), 5.10 (s, PhCH₂OC(O)), 5.64–5.78 (m, NHCHCH₂O), 6.70–6.80 (m, NHCH₂Ph), 7.20–7.38

(m, 2 C₆H₅); ¹³C NMR (CDCl₃) δ 43.8 (NH₂CH₂Ph), 54.6 (CHCH₂OCH₂), 57.8–59.0 (m, OCD₃), 67.4 (PhCH₂OC(O)), 72.1 (CH₂OCD₃), 127.7, 128.3, 128.4, 128.6, 128.8, 128.9, 136.3, 138.1 (2 C₆H₅), 156.3 (OC(O)NH), 170.1 (CHC(O)NH); *M*_r (+ESI) [M+Na]⁺ 368.2 (calcd for C₁₉H₁₉D₃N₂O₄Na⁺ 368.2). Anal. Calcd for C₁₉H₁₉D₃N₂O₃: C, 66.07; H, 6.41; N, 8.11. Found: C, 66.05; H, 6.39; N, 8.04.

(*R*)-*N*-Benzyl 2-Acetamido-3-(methoxy-*d*₃)propionamide ((*R*)-1-*d*₃). Using Method H, (*R*)-**130** (1.5 g, 4.25 mmol) and 10% Pd/C (200 mg) in MeOH (50 mL) gave after evaporation an oily residue that was directly dissolved in CH₂Cl₂ (50 mL). While stirring Et₃N (590 μL, 4.25 mmol), DMAP (25 mg, 212 μmol) and Ac₂O (400 μL, 4.25 mmol) were successively added and the reaction was stirred at room temperature (1 h). The organic layer was washed with aqueous 0.1 M H₂SO₄ (20 mL). The aqueous layer was extracted with CH₂Cl₂ (4 x 20 mL). The organic layers were combined, washed with brine (50 mL), dried (Na₂SO₄), and the solvents were removed under vacuum. The obtained solid was recrystallized from EtOAc and hexanes to give (*R*)-1-*d*₃ as a white solid (888 mg, 82% over 2 steps): mp 142–143 °C; [α]_D²⁵ +16.0° (c 0.7, MeOH); *R*_f = 0.31 (5/95 MeOH/CH₂Cl₂); IR (nujol) 3300, 3064, 2859, 1635, 1549, 1457, 1376, 1313, 1230, 1132 cm⁻¹; ¹H NMR (CDCl₃) δ 1.97 (s, CH₃C(O)), 3.47 (dd, *J* = 6.6, 9.0 Hz, CHH'OCD₃), 3.84 (dd, *J* = 4.0, 9.0 Hz, CHH'OCD₃), 4.34–4.52 (m, NHCH₂C₆H₅), 4.62 (dt, *J* = 4.0, 6.6 Hz, CHCH₂O), 6.72 (d, *J* = 7.0 Hz, NHCHCH₂O), 7.05–7.16 (m, NHCH₂Ph), 7.20–7.38 (m, C₆H₅), addition of excess (*R*)-(-)-mandelic acid to a CDCl₃ solution of (*R*)-1-*d*₃ gave only one signal for the acetyl protons (δ 2.011); ¹³C NMR (CDCl₃) δ 23.0 (CH₃C(O)), 43.4 (NH₂CH₂Ph), 52.5

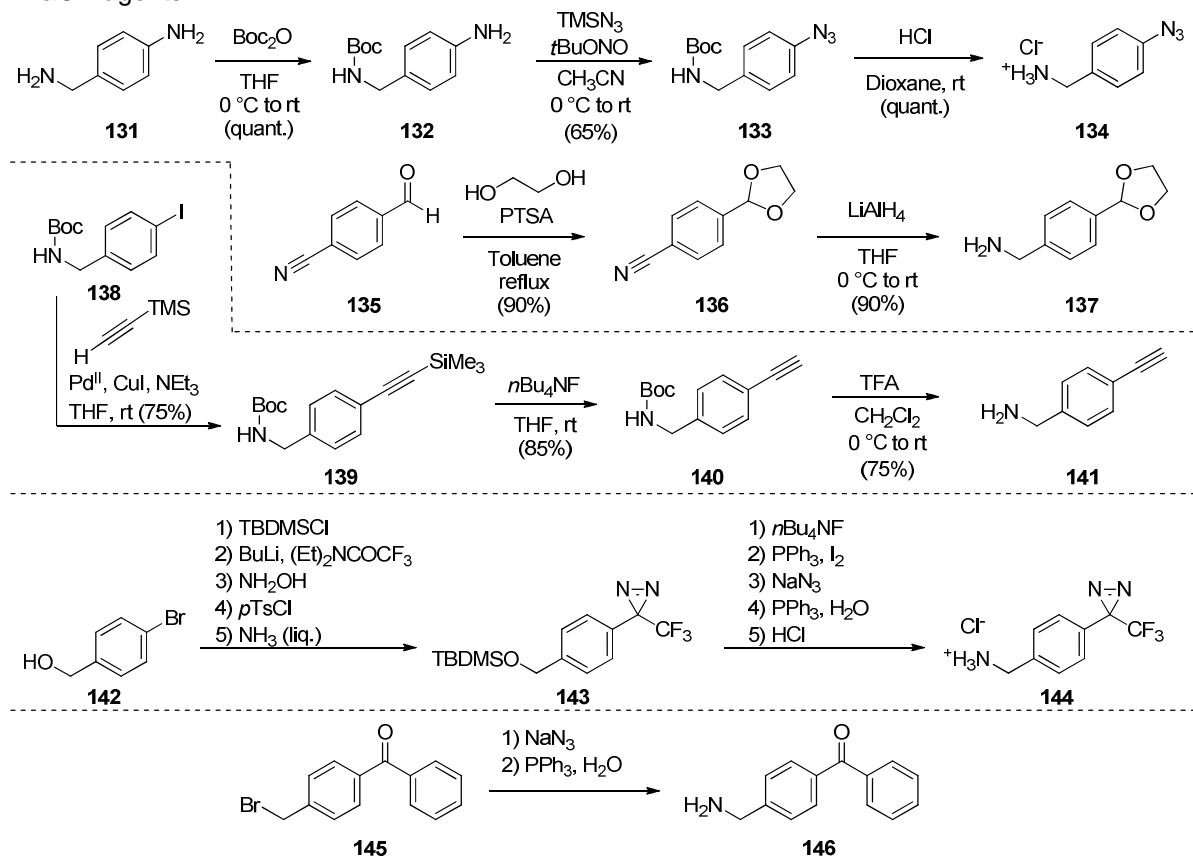
(CHCH₂OCD₃), 58.1 (app quint, $J = 21.6$ Hz, OCD₃), 71.8 (CH₂OCD₃), 127.4, 128.6, 137.9 (C₆H₅), 170.0, 170.3 (CH₃C(O), CHC(O)NH), the remaining signal was not detected and is believed to overlap with nearby peaks; M_r (+ESI) 276.1 [M+Na]⁺ (calcd for C₁₃H₁₅D₃N₂O₃Na⁺ 276.1). Anal. Calcd for C₁₃H₁₅D₃N₂O₃: C, 61.64; H, 7.16; N, 11.06. Found: C, 61.60; H, 7.10; N, 10.99.

2.3. Synthesis of a molecular toolkit for use in chemical biology studies

2.3.1. Synthetic strategies to different AB, CR and AB&CR derivatives

To allow efficient synthesis of AB, CR and AB&CR derivatives we constructed a series of functionalized benzylamines (**134**, **137**, **141**, **144**, **146**, Scheme 23) using protection/deprotection strategies. Upon removal of the protecting group, the benzylamine was either stored in a cold, dry environment under Ar or directly coupled with select enantiomerically pure acids.

Scheme 23. Synthetic routes to *para*-substituted benzylamines used in the synthesis of AB, CR and AB&CR agents



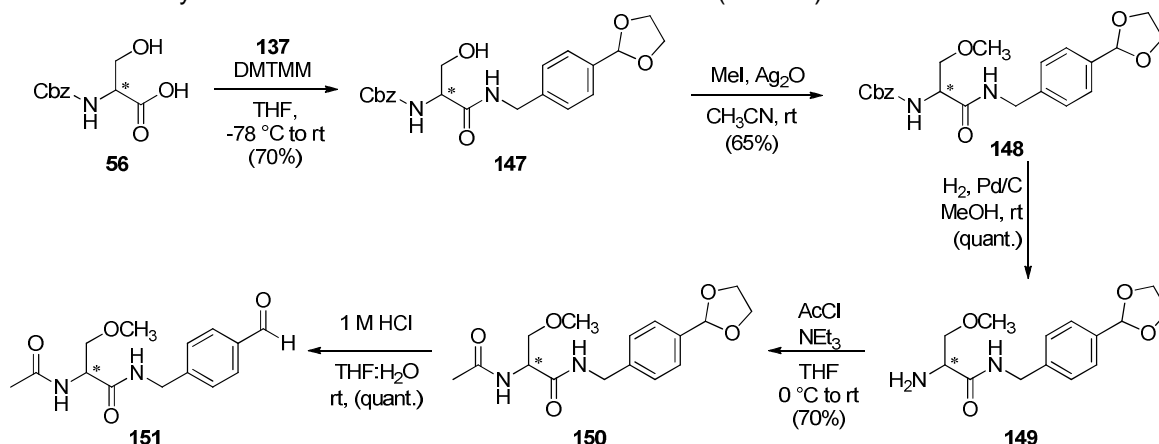
Commercially available 4-aminobenzylamine (**131**) was protected using di-*tert*-butyl dicarbonate to give **132**, and then the aniline moiety was converted to the azide using *tert*-butyl nitrite and trimethylsilylazide in a Sandmeyer-type reaction.³²⁵ Deprotecting the Boc group with HCl yielded 4-azidobenzylammonium hydrochloride (**134**). To introduce the aromatic aldehyde and aromatic epoxide AB groups, commercial 4-cyanobenzaldehyde (**135**) was condensed with ethylene glycol and catalytic *p*TSA to protect the aldehyde moiety, and the cyano group was reduced with LiAlH₄ in THF to afford benzylamine **137**.⁴⁰⁸ The aldehyde was deprotected after the amide coupling step.⁴⁰⁹ The alkynyl benzylamine **141** was prepared from Boc-protected benzylamine **138** that was coupled with trimethylsilyl acetylene using a Sonogashira reaction (*work of Dr. Christophe Salomé*). The TMS protecting group in **139** was removed with tetrabutylammonium fluoride, and the Boc group deprotected with trifluoroacetic acid to yield benzylamine **141** as the trifluoroacetate salt. Benzylamine **141** degraded over time in a dry, refrigerated environment and was only stable for prolonged times (-20 °C, up to 6 months) as the Boc and TMS protected intermediate **139**. Finally, the benzylamine containing the trifluoromethyldiazirine was synthesized in 10 steps using the following sequence of reactions (*work of Dr. Christophe Salomé*): commercial 4-bromobenzyl alcohol (**142**) was protected with a *tert*-butyldimethylsilyl group. The O-TBDMS intermediate was reacted with *n*-BuLi and diethylamide trifluoroacetate to give the trifluoromethylaryl ketone. The ketone was condensed with hydroxylamine and the resulting oxime tosylated with *p*TsCl. Treatment with liquid ammonia generated the desired photoAB moiety (**143**). The TBDMS group was then removed by fluoridolysis and the hydroxyl

group converted to the iodo derivative under Mitsunobu conditions. Nucleophilic substitution with sodium azide followed by Staudinger reduction and treatment with HCl gave benzylammonium hydrochloride **144**. Finally, the 4-aminomethylbenzophenone was prepared by reacting commercial 4-bromomethylbenzophenone (**145**) with sodium azide and reducing the benzyl azide under Staudinger conditions to yield benzylamine **146** (*work of Dr. Christophe Salomé*).

2.3.1.1. Introduction of aldehyde AB groups

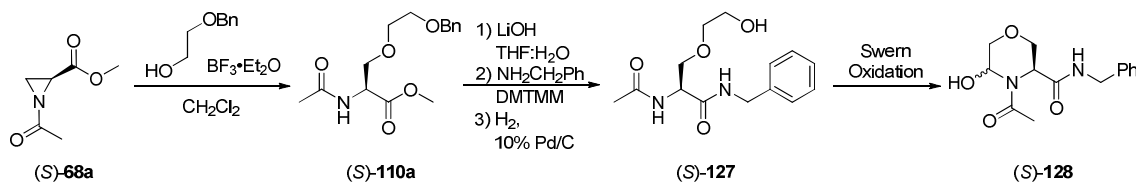
We initiated our study with compound **151**, that bore an C(O)H AB group at the *N*-benzylamide *para* position. The synthesis proceeded via **route 1** shown in Scheme 14.⁴⁰⁸ *N*-Cbz-protected L- or D- serine (**56**) was coupled with **137** using the DMTMM method to give **147**.^{234,236} The side chain hydroxyl group was alkylated using MeI and Ag₂O,^{234,236} the Cbz-protecting group removed by hydrogenolysis (10% Pd/C), and the amine then acetylated using acetyl chloride.^{234,236} Finally, removal of the dioxolanyl protecting group under aqueous acidic conditions⁴⁰⁹ yielded enantiomerically pure compounds (*R*)-**151** and (*S*)-**151** (Scheme 24).

Scheme 24. Synthesis of the lacosamide AB derivative **151** (**route 1**).



To introduce the aldehyde on the C(2) side chain we first ring-opened (*S*)-**68a** with commercial 2-benzyloxyethanol (Scheme 25). The ester was hydrolyzed, coupled with benzylamine and the *O*-benzyl protecting group was removed under hydrogenation conditions to give alcohol (*S*)-**127**. To our surprise, Swern oxidation (oxalyl chloride, DMSO, then DIEA)⁴¹⁰ of (*S*)-**127** gave the six-membered cyclized hemiaminal isomer **128** with no trace of the expected product.

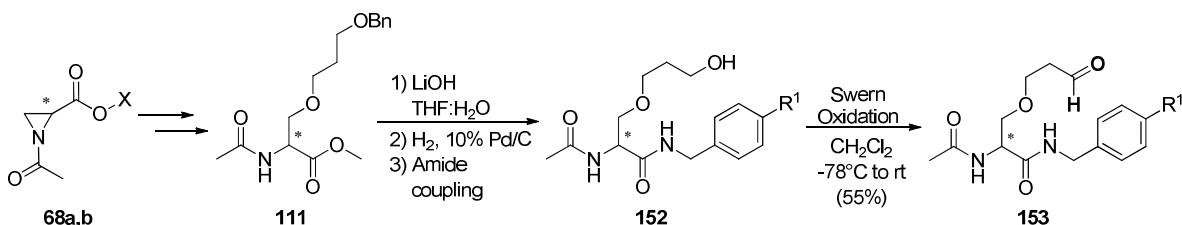
Scheme 25. First attempt to synthesize the side chain aldehyde AB group (**route 3**).



Accordingly, we increased by one the length of the carbon chain to entropically disfavor ring cyclization (6-membered vs. 7-membered rings).⁴¹¹ Ring-opening of **68a,b** with commercial 3-benzyloxypropanol, followed by ester hydrolysis, removal of the benzyl protecting group, and coupling of the acid with the

desired benzylamine gave **152** (Scheme 26). Swern oxidation of the side chain hydroxyl group yielded the desired enantiomerically pure aldehyde **153**.

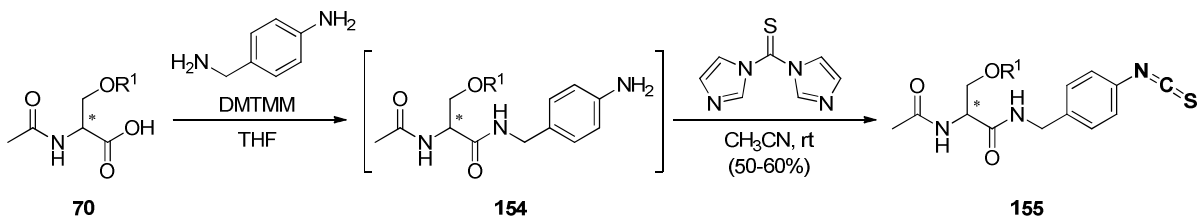
Scheme 26. Synthesis of the side chain aldehyde AB group (**route 3**)



2.3.1.2. Introduction of isothiocyanate AB groups

Using **route 3**, we prepared the desired *O*-substituted *N*-acetylserine benzylamide derivative **155** containing an isothiocyanate moiety at the *N*-benzylamide *para* position from acid **70**. After amide coupling with 4-aminobenzylamine, the aniline was reacted with diimidazolylthionocarbonate (DITC) to form the aromatic isothiocyanate AB&CR analog **155** (Scheme 27).

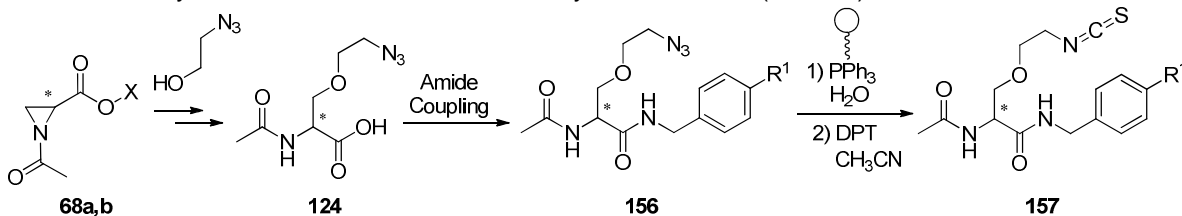
Scheme 27. Synthesis of aromatic isothiocyanate AB&CR derivatives (**route 3**)



To introduce the NCS group on the C(2) side chain, **68a** was ring-opened with 2-azidoethanol under $\text{BF}_3 \cdot \text{Et}_2\text{O}$ -catalyzed conditions, hydrolyzed, coupled with the

desired benzylamine and reacted with polymer-supported triphenylphosphine (Fluka, cat. # 93094). Reaction of the obtained amine with di-(2-pyridyl) thionocarbonate (DPT) gave the alkyl isothiocyanate derivative **157** (Scheme 28, *work of Dr. Christophe Salomé*).

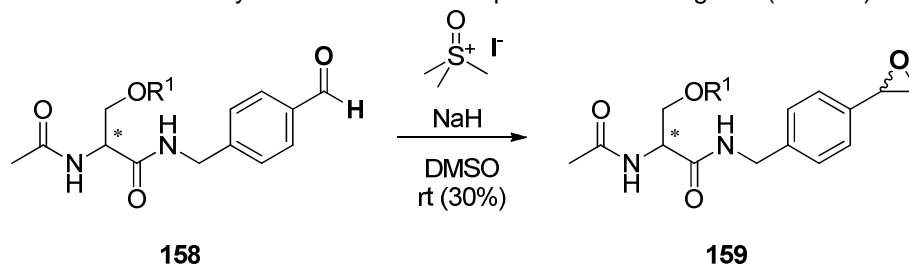
Scheme 28. Synthesis of the side chain isothiocyanate AB&CR (**route 3**)



2.3.1.3. Introduction of epoxide AB groups

With aryl aldehyde **158** in hand, we used the conjugate base of trimethylsulfoxonium iodide (Corey-Chaykovsky reagent) to form the corresponding epoxides **159** in one step (Scheme 29).⁴¹²

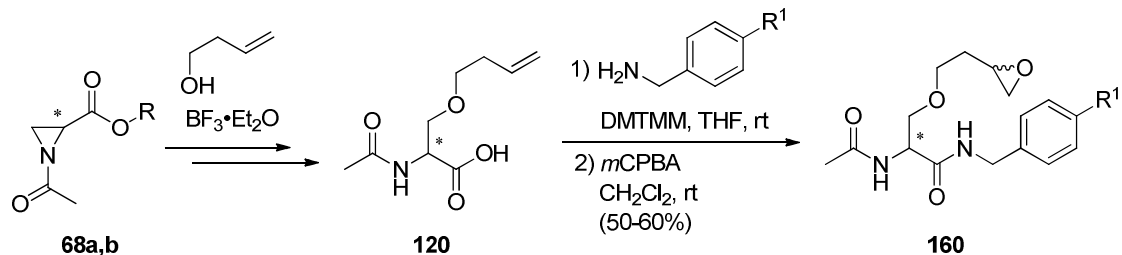
Scheme 29. Synthesis of aromatic epoxide AB&CR agents (**route 3**)



To introduce the epoxide on the C(2) side chain, we ring opened **68-a,b** with commercial 3-buten-1-ol. Saponification of the esters gave enantiopure acid **120**.

Subsequent coupling with the required benzylamine and epoxidation with *meta*-chloroperbenzoic acid (*m*CPBA) gave the diastereomeric epoxide **160** with the desired C(2) configuration (Scheme 30).⁴¹³

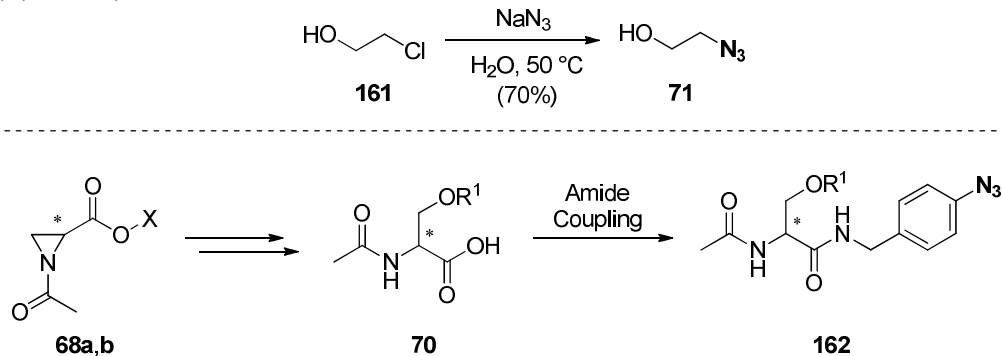
Scheme 30. Synthesis of the side chain epoxide AB&CR agents (**route 3**)



2.3.1.4. Introduction of azide CR groups

Benzylammonium hydrochloride **134** was coupled with various carboxylic acids to introduce the azide CR/photoAB on the phenyl ring (**162**, Scheme 31, bottom). To introduce the azide on the C(2) side chain, we prepared 2-azidoethanol (**71**) from 2-chloroethanol (**161**) and NaN_3 ⁴¹⁴ (Scheme 31, top) and used the established sequence to form the FAA **156** (see Scheme 28).

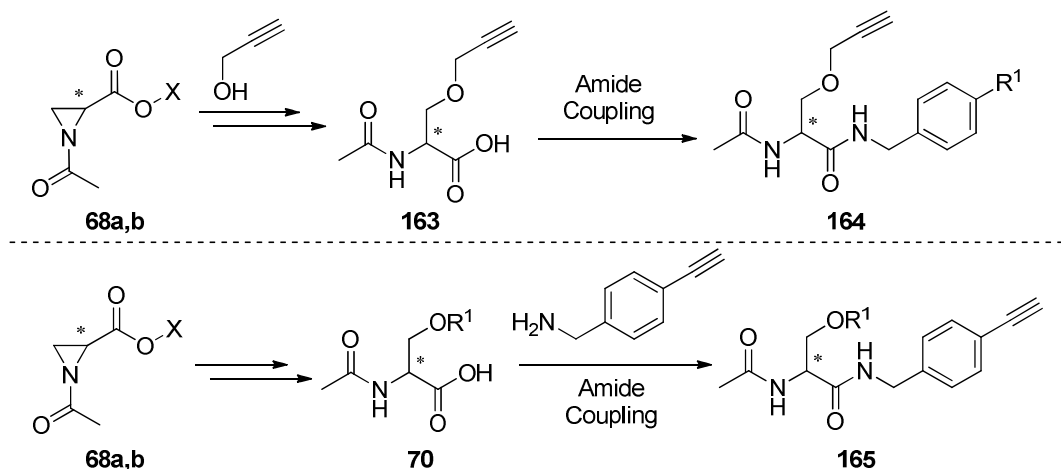
Scheme 31. Synthesis of 2-azidoethanol (top) and AB&CR agents bearing an aromatic azide (bottom) (**route 3**)



2.3.1.5. Introduction of alkyne CR groups

The alkyne CR was introduced on the lacosamide C(2) side-chain by ring-opening **68a,b** with propargyl alcohol and following **route 3** to benzylamide **164** (Scheme 32, top). For the CR agents bearing the *para*-substituted alkyne, carboxylic acid **70** was treated with benzylamine **141** using an amide coupling reaction (Scheme 32, bottom).

Scheme 32. Synthesis of the alkyne-containing AB&CR agents (**route 3**)

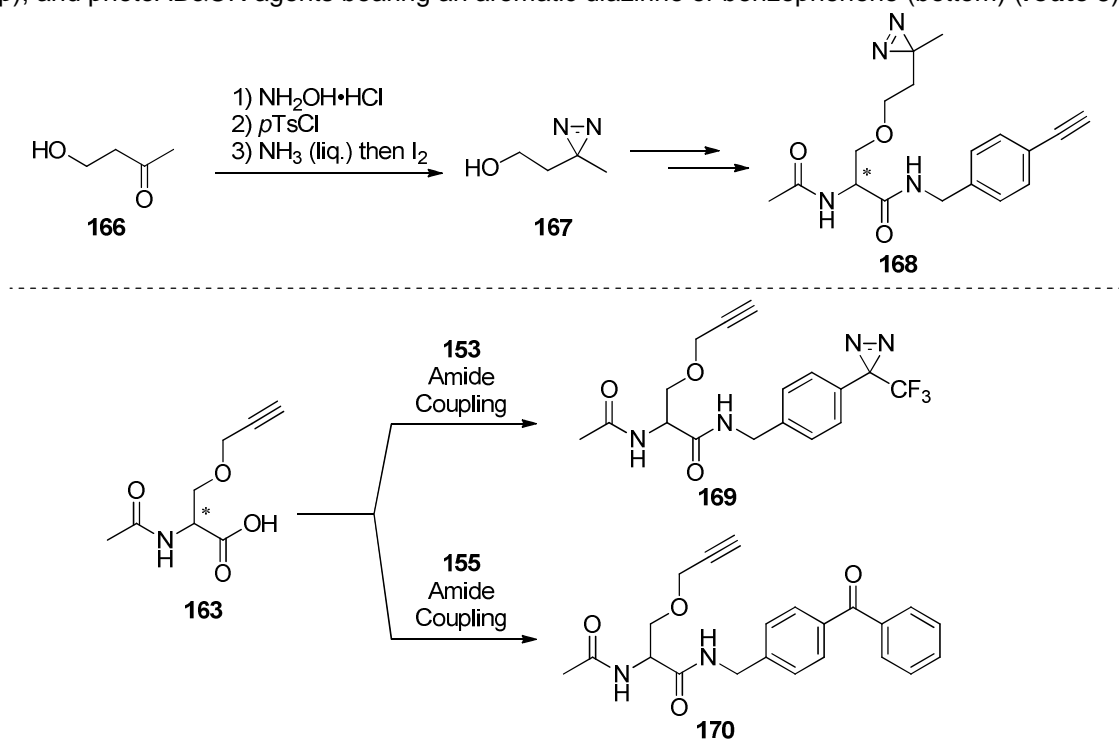


2.3.1.6. Introduction of diazirine and benzophenone photoAB groups (*work of Dr. Christophe Salomé*)

The trifluoromethylaromatic diazirine was introduced by coupling acid **163** with benzylamine **144**. For the C(2) side chain alkyl diazirine, 4-hydroxybutan-2-one (**166**) was condensed with hydroxylamine and the resulting oxime successively tosylated and reacted with liquid ammonia and iodine (Scheme 33, top). Methyl diazirinyl alcohol **167** was then reacted with **68** to give **168** after ester hydrolysis and amide coupling. The esters were hydrolyzed and coupled with

benzylamine **150** to provide the desired AB&CR derivative. Finally, 4-aminomethylbenzophenone **146** was coupled with acid **163** to provide AB&CR agent **170** (Scheme 33, bottom).

Scheme 33. Synthesis of 2-(3-methyl-3*H*-diazirin-3-yl)ethanol and the corresponding AB&CR agent (top), and photoAB&CR agents bearing an aromatic diazirine or benzophenone (bottom) (**route 3**)



2.3.1.7. Summary

A comprehensive list of all the AB&CR agents synthesized and used for chemical biology studies is given in Figure 9. All molecules were prepared stereoisomerically pure at the C(2) following the previously described synthetic schemes. Compounds **172** and **181** were synthesized by Dr Ki Duk Park, and compounds **168**, **169**, **170**, and **177** were synthesized by Dr Christophe Salomé.

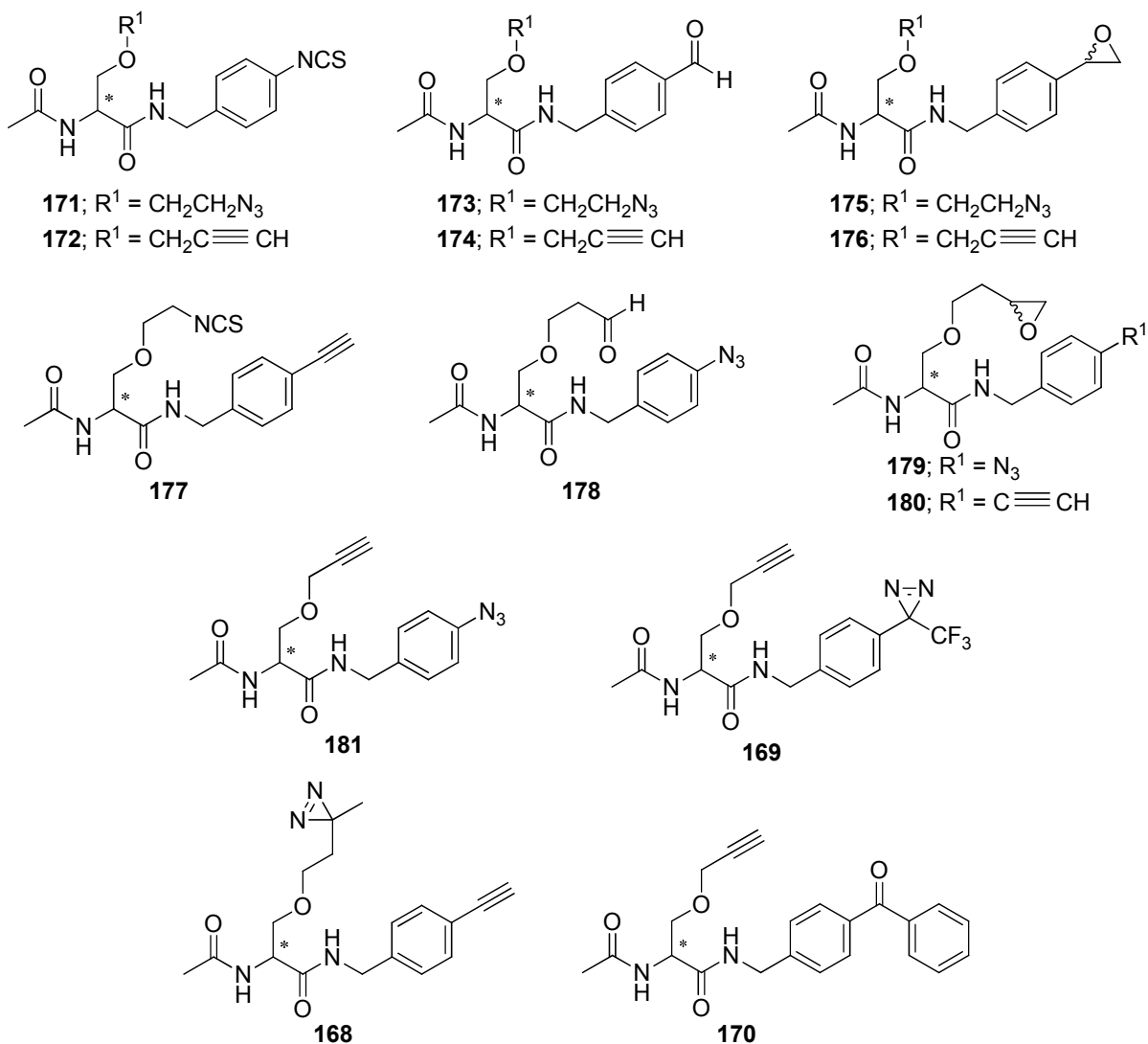


Figure 9. Structures of the different AB&CR agents synthesized for chemical biology studies.

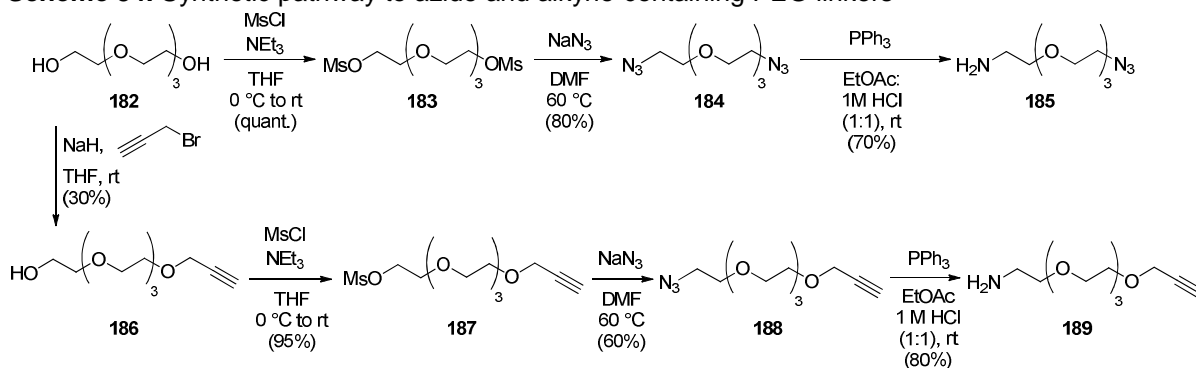
2.3.2. Biotin and fluorescent alkyne and azide Probes

Two sets of Probes were constructed for chemical biology studies. The first set contained a biotin unit appended to the CR group. This set of Probes was used for isolating putative target proteins from the rat brain lysate. The biotinylated proteins were captured using Streptavidin beads, washed, eluted, resolved on SDS PAGE gel and analyzed by mass spectrometry. Although ideal for purifying

drug/protein complexes,^{415,258,416} biotin/streptavidin-based purification is a time-consuming process. Therefore, we prepared the corresponding set of Probes containing a tetramethylrhodamine fluorophore (TAMRA). Incorporation of the TAMRA moiety readily permitted protein detection by in-gel fluorescence.

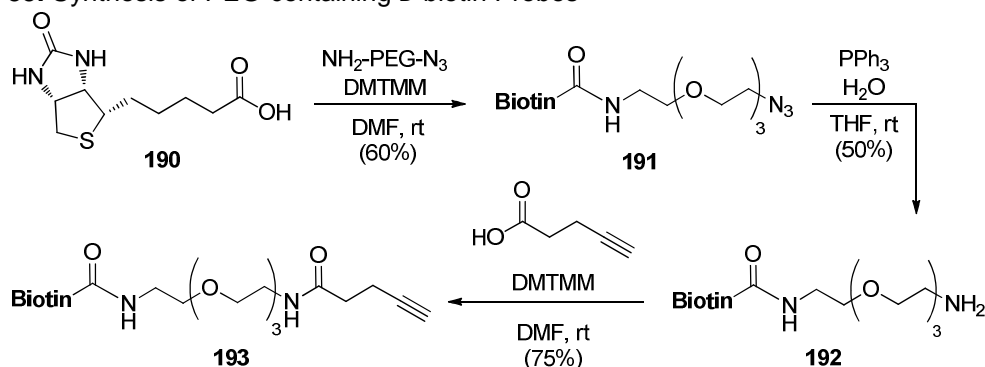
For both Probes we chose to include a polyethyleneglycol (PEG) spacer for two reasons. The first one was to improve the water solubility of the molecule and the second to minimize adverse protein (*i.e.* Streptavidin)/Probe interactions. To synthesize these, we first constructed the polyethylene glycol (PEG) moieties (Scheme 34). Commercial tetraethylene glycol (**182**) was reacted with MsCl (2 equiv) to form the di-mesylate intermediate **183**, and then treated with NaN₃ (2 equiv) to form diazido tetraethyleneglycol **184**.⁴¹⁷ Amine **185** was obtained by a mono-reduction of diazide **184** using a Staudinger reaction in a biphasic solvent system.⁴¹⁷ The PEG moiety of the alkyne Probe was constructed in a similar fashion. Tetraethylene glycol was reacted with NaH and propargyl bromide (1 equiv).^{418,419} The hydroxyl group was mesylated, displaced with NaN₃, and reduced under Staudinger conditions to yield amine **189**.

Scheme 34. Synthetic pathway to azide and alkyne-containing PEG linkers

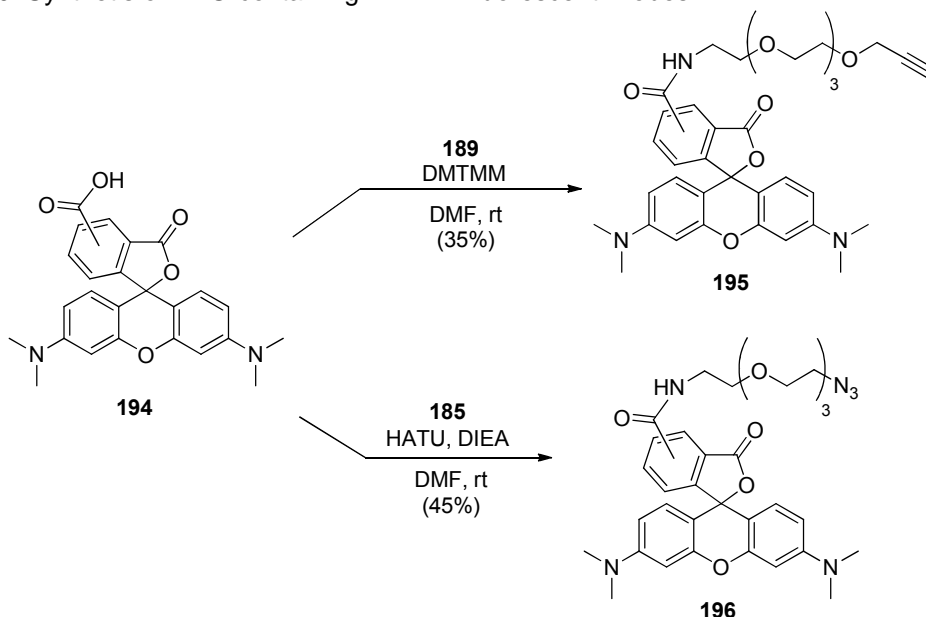


Biotin Probe **193** was prepared by linking commercial D-biotin (**190**) with **185** using an amide coupling reaction (DMTMM) to yield biotin-PEG-N₃ Probe **191**. The azide was reduced with PPh₃ and H₂O and the resulting amine **192** was coupled (DMTMM) with 4-pentynoic acid to yield biotin-PEG-alkyne Probe **193** (Scheme 35). Both amines **185** and **189** were readily coupled with 5,6-carboxytetramethylrhodamine to give fluorescent Probes TAMRA-PEG-N₃ **196** and TAMRA-PEG-alkyne **195**, respectively (Scheme 36).

Scheme 35. Synthesis of PEG-containing D-biotin Probes



Scheme 36. Synthesis of PEG-containing TAMRA fluorescent Probes



2.3.3. Experimental Section

2.3.3.1. Synthesis of *para*-substituted benzylamines

***Tert*-butyl 4-Azidobenzylcarbamate (133).**³²⁴ To a cooled (ice bath) THF solution (40 mL) of 4-aminobenzylamine (1.00 g, 8.2 mmol) was slowly added a solution of Boc₂O (1.8 g, 8.2 mmol) in THF (10 mL). The reaction was stirred at room temperature (15 h) and the THF was evaporated to give **132** as a pale yellow solid (1.86 g, quant.) that was directly dissolved in CH₃CN (25 mL) and cooled (ice bath). While stirring, *t*-BuONO (1.5 mL, 12.6 mmol) and TMSN₃ (132 μ L, 1 mmol) were added and the reaction was vigorously stirred at 0 °C until bubbling was observed (10–20 min). More TMSN₃ (1.2 mL, 9 mmol) was then added dropwise at 0 °C and the reaction stirred at room temperature (14 h). The solvent was evaporated and the residue purified by flash chromatography (CH₂Cl₂) to give **133** as an orange oil (1.33 g, 65%) that slowly turned to yellow crystals: mp 58–60 °C; *R*_f = 0.33 (CH₂Cl₂); ¹H NMR (CDCl₃) δ 1.45 (s, C(CH₃)₃), 4.24–4.28 (m, NHCH₂C₆H₄), 4.90–5.10 (m, NHCH₂C₆H₄), 6.96 (d, *J* = 8.4 Hz, 2 ArH), 7.25 (d, *J* = 8.4 Hz, 2 ArH); ¹³C NMR (CDCl₃) δ 28.5 (C(CH₃)₃), 44.2 (NHCH₂C₆H₄), 79.7 (C(CH₃)₃), 119.3, 129.0, 136.0, 139.1 (C₆H₄), 156.0 (OC(O)NH).

4-Azidobenzylammonium Hydrochloride (134). Compound **133** (7.17 g, 28.9 mmol) was dissolved in a 4 M HCl dioxane solution (25 mL, 100 mmol). The reaction was stirred at room temperature (12 h) and the resulting salt was filtered, and rinsed with Et₂O to give hydrochloride **134** (5.23 g, 98%) as a light beige solid: mp 80–82 °C; *R*_f = 0–0.1 (1/9 MeOH/CH₂Cl₂); ¹H NMR (DMSO-*d*₆) δ 3.99 (d, *J* = 5.1 Hz,

CH₂C₆H₄), 7.14–7.18, 7.54–7.58 (m, CH₂C₆H₄), 8.25–8.80 (m, NH₃⁺); ¹³C NMR (DMSO-*d*₆) δ 41.5 (CH₂C₆H₄), 119.2, 130.9, 131.0, 139.5 (C₆H₄); **134** was not detected by mass spectrometry. Anal. Calcd for C₇H₉N₄Cl: C, 45.54; H, 4.91; N, 30.35; Cl, 19.20. Found: C, 45.78; H, 5.02; N, 30.18; Cl, 19.37.

4-(1,3-Dioxolan-2-yl)benzonitrile (136).⁴⁰⁸ To a toluene solution (150 mL) of (4-cyano)benzaldehyde (**135**, 15.00 g, 108.8 mmol) was added ethylene glycol (23.9 mL, 435.1 mmol) and *p*TSA (21 mg, 0.11 mmol). The reaction solution was heated to reflux with a Dean-Stark apparatus until H₂O ceased forming (15 h), and then cooled to room temperature. The reaction was washed with aqueous saturated NaHCO₃ (150 mL) and brine (150 mL). The organic layer was concentrated in vacuo to give a pale yellow residue that was recrystallized from Et₂O and hexanes to yield 17.20 g of **135** (90%) as white flakes: mp 44–45 °C (lit.⁴⁰⁸ mp = 39–40 °C); *R*_f = 0.55 (CHCl₃); ¹H NMR (CDCl₃) δ 4.02–4.14 (m, OCH₂CH₂O), 5.84 (s, OCHO), 7.58 (d, *J* = 9.0 Hz, 2 ArH), 7.66 (d, *J* = 9.0 Hz, 2 ArH); ¹³C NMR (CDCl₃) δ 65.6 (OCH₂CH₂O), 102.6 (OCHO), 113.0 (ArC), 118.7 (C≡N), 127.3 (2 ArC), 132.4 (2 ArC), 143.3 (ArC).

(4-(1,3-Dioxolan-2-yl)phenyl)methanamine (137).⁴⁰⁸ A THF solution (60 mL) of **136** (23.12 g, 132 mmol) was added dropwise to a stirred THF solution of 1.0 M LiAlH₄ (400 mL, 400 mmol) at 0 °C. The reaction solution was stirred at 0 °C (15 min) and progressively turned yellow. It was further stirred at room temperature (15 h) and the excess LiAlH₄ was quenched by cooling the reaction (0 °C) and successively adding H₂O (12 mL), 15% aqueous NaOH (6 mL), and H₂O (12 mL).

dropwise. The mixture was stirred at room temperature (2 h) and filtered. The solid residue was rinsed CH_2Cl_2 and the combined organic layers were evaporated to give 21.80 g (92%) of **137** as a slightly yellow residue that did not require further purification: $R_f = 0.20\text{--}0.44$ (5/95 MeOH/ CHCl_3); ^1H NMR (CDCl_3) δ 1.43 (s, NH_2), 3.85 (s, CH_2NH_2), 3.96–4.16 (m, $\text{OCH}_2\text{CH}_2\text{O}$), 5.79 (s, $\text{OC}(\text{H})\text{O}$), 7.31 (d, $J = 8.1$ Hz, 2 ArH), 7.43 (d, $J = 8.1$ Hz, 2 ArH); ^{13}C NMR (CDCl_3) δ 46.4 ($\text{NH}_2\text{CH}_2\text{C}_6\text{H}_4$), 65.6 ($\text{OCH}_2\text{CH}_2\text{O}$), 103.7 ($\text{OC}(\text{H})\text{O}$), 126.8, 127.3, 136.5, 144.6 (C_6H_4).

tert-Butyl 4-(Ethyne)benzylcarbamate (140).⁴²⁰ To a THF solution (130 mL) of compound **139** (4.10 g, 13.5 mmol) was added TBAF (1 M in THF, 28 mL, 28 mmol) in one portion and the reaction was stirred at room temperature (4 h). CH_2Cl_2 (150 mL) and 10% aqueous citric acid (100 mL) were added. The aqueous layer was extracted with CH_2Cl_2 (2 x 50 mL). All of the CH_2Cl_2 layers were washed with brine (200 mL), dried (Na_2SO_4), and evaporated to dryness. The dark brown residue obtained was purified by flash chromatography (15/85 EtOAc/hexanes) to yield **140** as a pale orange solid (2.70 g, 85%): mp 82–83 °C (lit.⁴²⁰ mp 82 °C); $R_f = 0.47$ (15/85 acetone/EtOAc); ^1H NMR (CDCl_3) δ 1.46 (s, $(\text{CH}_3)_3\text{COC}(\text{O})\text{NH}$), 3.06 (s, $\text{ArC}\equiv\text{CH}$), 4.31 (d, $J = 6.0$ Hz, $\text{C}(\text{O})\text{NHCH}_2$), 4.80–4.92 (m, $\text{C}(\text{O})\text{NHCH}_2$), 7.23 (d, $J = 9.1$ Hz, 2 ArH), 7.45 (d, $J = 9.1$ Hz, 2 ArH); ^{13}C NMR (CDCl_3) δ 28.6 ($(\text{CH}_3)_3\text{C}(\text{O})$), 44.6 ($\text{C}(\text{O})\text{NHCH}_2$), 77.4 ($\text{ArC}\equiv\text{CH}$), 79.9 ($(\text{CH}_3)_3\text{CO}$), 83.6 ($\text{ArC}\equiv\text{CH}$), 121.2, 127.5, 132.6, 140.0 (C_6H_4), 156.0 ($\text{OC}(\text{O})\text{NH}$).

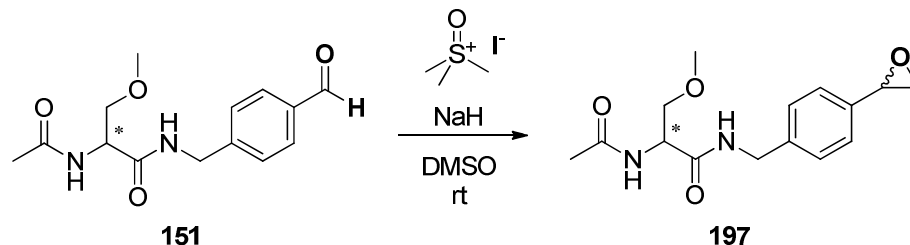
4-(Ethynyl)benzylamine (141).⁴²⁰ Compound **140** (1.20 g, 5.2 mmol) was dissolved in CH₂Cl₂ (50 mL) and TFA (10 mL) was added. The dark brown solution was stirred at room temperature (1 h), after which time it was concentrated in vacuo. Saturated aqueous NaHCO₃ (100 mL) was added to the residue, and the emulsion was vigorously stirred until no more gas evolved. CH₂Cl₂ (50 mL) was added and the organic layer was separated. The aqueous layer was further extracted with CH₂Cl₂ (3 x 50 mL). All the organic layers were combined, washed with brine (100 mL), dried (Na₂SO₄), and evaporated to yield amine **140** as a dark brown oil (510 mg, 75%) that was used immediately in the next step.

Dimethoxytriazine N-Methylmorpholinium Hydrochloride (DMTMM).⁴²¹

Chlorodimethoxytriazine (CDMT) (25.00 g, 142 mmol) was suspended in THF (1 L) and while stirring NMM (17.3 mL, 157 mmol) was added. The suspension was stirred at room temperature (3 h) and filtered. The white solid was rinsed with THF and dried to yield 32.50 g (83%) of DMTMM that required no further purification: mp 121–123 °C (lit.⁴²¹ mp 116–117 °C); ¹H NMR (CD₃OD) δ 3.54 (s, N⁺CH₃), 3.78–3.95, 4.02–4.10, 4.51–4.58 (N⁺(CH₂CH₂)₂O), 4.17 (s, 2 OCH₃); ¹³C NMR (CDCl₃) δ 56.6 (N⁺CH₃), 57.7 (N⁺(CH₂CH₂)₂O), 61.5 (2 OCH₃), 63.4 ((N⁺(CH₂CH₂)₂O), 172.1, 175.6 (2 COCH₃).

2.3.3.2. Synthesis of lacosamide AB derivatives

Scheme 37. Synthesis of the AB derivative **197** bearing the epoxide at the benzylamide *para* position.



(*R*)-*N*-(4-(1,3-Dioxolan-2-yl)benzyl)

2-*N*-(Benzyloxycarbonyl)amino-3-

hydroxypropionamide ((*R*)-147**).** Using Method D, Cbz-D-serine (6.18 g, 25.85 mmol), **137** (5.09 g, 28.44 mmol) and DMTMM (7.86 g, 28.44 mmol) in THF (400 mL) gave 5.56 g (54%) of (*R*)-**147** as a white solid after recrystallization of the crude material from CHCl₃. Purification of the mother liquors by silica gel chromatography (6/93.5/0.5 MeOH/CHCl₃/NEt₃) yielded an additional 1.86 g (18%) (total yield: 7.42 g, 72%): mp 129–131 °C; [α]_D²⁵ +2.9° (c 1.0, MeOH); *R*_f = 0.37 (5/95 MeOH/CHCl₃); IR (nujol) 3288, 1689, 1642, 1540, 1459 cm⁻¹; ¹H NMR (DMSO-*d*₆) δ 3.53–3.59 (m, CHCH₂O), 3.88–4.13 (m, OCH₂CH₂O, CHCH₂O), 4.30 (d, *J* = 5.7 Hz, NHCH₂C₆H₄), 4.90 (t, *J* = 5.4 Hz, CH₂OH), 5.04 (s, C₆H₅CH₂O), 5.69 (s, OC(H)O), 7.19–7.42 (m, C₆H₅, C₆H₄), 8.44 (t, *J* = 5.7 Hz, NHCH₂C₆H₄), the carbamate NH was not detected; ¹³C NMR (DMSO-*d*₆) δ 41.9 (NHCH₂C₆H₄), 57.4 (CHCH₂OH), 61.7 (C₆H₅CH₂O), 64.8 (OCH₂CH₂O), 65.5 (CHCH₂OH), 102.7 (OC(H)O), 126.2, 126.8, 127.7, 127.8, 128.3, 136.5, 137.0, 140.4, (C₆H₅, C₆H₄) 155.9 (OC(O)NH), 170.2 (CHC(O)NH); *M*_r (+ESI) 423.1531 [M+Na]⁺ (calcd for C₂₁H₂₄N₂O₆Na⁺ 423.1532). Anal. Calcd for C₂₁H₂₄N₂O₆: C, 62.99; H, 6.04; N, 7.00. Found: C, 63.00; H, 6.03; N, 6.97.

(S)-N-(4-(1,3-Dioxolan-2-yl)benzyl)**2-N-(Benzyloxycarbonyl)amino-3-**

hydroxypropionamide ((S)-147). Using Method D and following the preceding procedure, benzylamine **137** (5.09 g, 28.44 mmol), Cbz-L-serine (6.18 g, 25.85 mmol) and DMTMM (7.86 g, 28.44 mmol) in THF (500 mL) gave 5.66 g (55%) of (S)-**147** after recrystallization from CHCl₃ and an additional 1.78 g (17%) after purification of mother liquors (total yield: 7.44 g, 72%): mp 129–131°C; [α]_D²⁵ -2.9° (c 1.0, MeOH); *R*_f = 0.37 (5/95 MeOH/CHCl₃); IR (nujol) 3288, 1689, 1642, 1540, 1459 cm⁻¹; ¹H NMR (DMSO-*d*₆) δ 3.53–3.59 (m, CHCH₂O), 3.88–4.13 (m, OCH₂CH₂O, CHCH₂O), 4.30 (d, *J* = 5.7 Hz, NHCH₂C₆H₄), 4.82–4.97 (br s, CH₂OH). 5.04 (s, C₆H₅CH₂O), 5.69 (s, OC(H)O), 7.19–7.42 (m, C₆H₅, C₆H₄), 8.44 (t, *J* = 5.7 Hz, NHCH₂C₆H₄), the carbamate NH could not be detected; ¹³C NMR (CD₃OD) δ 44.0 (NHCH₂C₆H₄), 58.9 (CHCH₂OH), 63.4 (C₆H₅CH₂O), 66.4 (OCH₂CH₂O), 68.0 (CHCH₂OH), 104.9 (OC(H)O), 128.0, 128.4, 129.1, 129.2, 129.6, 138.2, 138.5, 141.0 (C₆H₅), 158.6 (OC(O)NH), 173.2 (CHC(O)NH); *M*_r (+ESI) 423.1525 [M+Na]⁺ (calcd for C₂₁H₂₄N₂O₆Na⁺ 423.1532). Anal. Calcd for C₂₁H₂₄N₂O₆: C, 62.99; H, 6.04; N, 7.00. Found: C, 62.86; H, 6.05; N, 7.06.

(R)-N-(4-(1,3-Dioxolan-2-yl)benzyl)**2-N-(Benzyloxycarbonyl)amino-3-**

methoxypropionamide ((R)-148). Using Method G, (R)-**147** (5.56 g 13.9 mmol), Ag₂O (16.19 g, 69.5 mmol) and MeI (8.66 mL, 139 mmol) gave a pale yellow residue after filtration and evaporation. Et₂O (50 mL) was added to the residue and (R)-**148** (3.95 g, 69%) was recovered as a white solid after filtration: mp 118–119°C; [α]_D²⁵ +1.5° (c 1.0, MeOH); *R*_f = 0.57 (5/95 MeOH/CHCl₃); IR (nujol) 3298, 1690, 1645,

1542 cm⁻¹; ¹H NMR (CDCl₃) δ 3.34 (s, CH₂OCH₃), 3.47 (dd, *J* = 6.6, 9.3 Hz, CHH'OCH₃), 3.82 (dd *J* = 3.8, 9.3 Hz, CHH'OCH₃), 4.01–4.15 (m, OCH₂CH₂O), 4.08–4.18 (br m, CHCH'H), 4.45 (d, *J* = 5.7 Hz, NHCH₂C₆H₄), 5.10 (s, C₆H₅CH₂O), 5.73 (br d, *J* = 5.7 Hz, OC(O)NH), 5.78 (s, OC(H)O), 6.61–6.74 (m, NHCH₂C₆H₄), 7.26 (d, *J* = 7.8 Hz, 2 ArH), 7.31–7.39 (m, C₆H₅), 7.42 (d, *J* = 7.8 Hz, 2 ArH); ¹³C NMR (CDCl₃) δ 43.4 (NH₂CH₂C₆H₄), 54.5 (CHCH₂O), 59.3 (CH₂OCH₃), 65.5 (OCH₂CH₂O), 67.4 (C₆H₅CH₂O), 72.2 (CH₂OCH₃), 103.6 (OC(H)O), 127.0, 127.7, 128.3, 128.4, 128.7, 136.2, 137.4, 139.1 (C₆H₅, C₆H₄), 156.3 (OC(O)NH), 170.0 (CHC(O)NH); *M_r* (+ESI) 437.1687 [M+Na]⁺ (calcd for C₂₂H₂₆N₂O₆Na⁺ 437.1689). Anal. Calcd for C₂₂H₂₆N₂O₆•0.25H₂O: C, 63.07; H, 6.38; N, 6.69. Found: C, 63.18; H, 6.38; N, 6.70.

(*S*)-*N*-(4-(1,3-Dioxolan-2-yl)benzyl) 2-*N*-(Benzyloxycarbonyl)amino-3-methoxypropionamide ((*S*)-148**).** Using Method G and following the preceding procedure, (*S*)-**147** (5.66 g, 14.2 mmol), Ag₂O (16.54 g, 71.0 mmol) and MeI (8.84 mL, 142.0 mmol) in CH₃CN (100 mL) gave 3.91 g (67%) of (*S*)-**148** as a white powder after precipitation of the residue with Et₂O (150 mL): mp 118–119°C; [α]_D²⁵ -1.5° (c 1.0, MeOH); *R_f* = 0.57 (5/95 MeOH/CHCl₃); IR (film) 3424, 3055, 2986, 1723, 1678 cm⁻¹; ¹H NMR (CDCl₃) δ 3.36 (s, CH₂OCH₃), 3.47 (dd, *J* = 6.6, 9.3 Hz, CHH'OCH₃), 3.87 (dd *J* = 3.8, 9.3 Hz, CHH'OCH₃), 4.01–4.15 (m, OCH₂CH₂O), 4.28–4.38 (m, CHCH'H), 4.48 (d, *J* = 5.7 Hz, NHCH₂C₆H₄), 5.12 (s, C₆H₅CH₂O), 5.61–5.70 (m, OC(O)NH), 5.80 (s, OCHO), 6.61–6.74 (m, NHCH₂C₆H₄), 7.22–7.48 (m, C₆H₅, C₆H₄), 8.44 (t, *J* = 5.7 Hz, NHCH₂C₆H₄); ¹³C NMR (CDCl₃) δ 43.5

(NH₂CH₂C₆H₄), 54.5 (CHCH₂OCH₃), 59.3 (CH₂OCH₃), 65.5 (OCH₂CH₂O), 67.5 (C₆H₅CH₂O), 72.2 (CH₂OCH₃), 103.7 (OC(H)O), 127.1, 127.7, 128.4, 128.5, 128.8, 136.2, 137.5, 139.1 (C₆H₅, C₆H₄), 156.3 (OC(O)NH), 170.1 (CHC(O)NH); *M_r* (+ESI) 437.1681 [M+Na]⁺ (calcd for C₂₂H₂₆N₂O₆Na⁺ 437.1689). Anal. Calcd for C₂₂H₂₆N₂O₆•0.25H₂O: C, 63.07; H, 6.38; N, 6.69. Found: C, 63.09; H, 6.37; N, 6.64.

(*R*)-*N*-(4-(1,3-Dioxolan-2-yl)benzyl) 2-Acetamido-3-methoxypropionamide ((*R*)-150**).** Using Method H, (*R*)-**148** (3.75 g, 9.1 mmol), and 10% Pd/C (700 mg) in MeOH (50 mL) gave 2.54 g (100%) of a yellow oily residue that was directly dissolved in THF (100 mL). After cooling (ice bath), Et₃N (1.26 mL, 9.07 mmol) and AcCl (0.644 mL, 9.07 mmol) were successively added. The reaction was stirred at room temperature (1 h) filtered and evaporated. Recrystallization of the residue from EtOAc and hexanes gave 1.67 g (57%) of (*R*)-**150** as a pale beige solid: mp 138–139°C; [α]_D²⁵ +13.0° (c 1.0, MeOH); *R_f* = 0.39 (5/95 MeOH/CHCl₃); IR (nujol) 3281, 3090, 1638, 1546, 1458 cm⁻¹; ¹H NMR (CDCl₃) δ 1.97 (s, CH₃C(O)), 3.35 (s, CH₂OCH₃), 3.45 (dd, *J* = 6.9, 9.0 Hz, CHH'OCH₃), 3.73 (dd *J* = 4.2, 9.0 Hz, CHH'OCH₃), 4.01–4.15 (m, OCH₂CH₂O), 4.20–4.55 (m, NHCH₂C₆H₄), 4.60 (app. dt, *J* = 4.2, 6.9 Hz, CHCH₂O), 5.80 (s, OC(H)O), 6.76 (d, *J* = 6.9 Hz, CH₃C(O)NH), 7.14 (t, *J* = 5.7 Hz, NHCH₂C₆H₄), 7.25 (d, *J* = 7.8 Hz, 2 ArH), 7.42 (d, *J* = 7.8 Hz, 2 ArH), addition of excess (*R*)-(-)-mandelic acid to a CDCl₃ solution of (*R*)-**150** gave only one signal for the acetyl methyl protons and the methoxy protons, addition of excess (*R*)-(-)-mandelic acid to a CDCl₃ solution of (*S*)-**150** and (*R*)-**150** (~1:2 ratio) gave two signals for the acetyl methyl protons (δ 2.021 (*S*) and 2.008 (*R*) (Δppm = 0.013) and

two signals for the methoxy protons (δ 3.317 (*S*) and 3.351 (*R*) (Δ ppm = 0.034)) in a ~1:2 ratio; ^{13}C NMR (CDCl_3) δ 23.2 ($\text{CH}_3\text{C}(\text{O})$), 43.3 ($\text{NH}_2\text{CH}_2\text{C}_6\text{H}_4$), 52.7 (CHCH_2O), 59.2 (CH_2OCH_3), 65.4 ($\text{OCH}_2\text{CH}_2\text{O}$), 72.0 (CH_2OCH_3), 103.6 ($\text{OC}(\text{H})\text{O}$), 126.9, 127.6, 137.2, 139.2 (C_6H_4), 170.2 ($\text{CHC}(\text{O})\text{NH}$ or $\text{CH}_3\text{C}(\text{O})$), 170.6 ($\text{CH}_3\text{C}(\text{O})$ or $\text{CHC}(\text{O})\text{NH}$): M_r (+ESI) 345.1424 [$\text{M}+\text{Na}$] $^+$ (calcd for $\text{C}_{16}\text{H}_{22}\text{N}_2\text{O}_5\text{Na}^+$ 345.1426). Anal. Calcd for $\text{C}_{16}\text{H}_{22}\text{N}_2\text{O}_5$: C, 59.61; H, 6.88; N, 8.69. Found: C, 59.51; H, 6.90; N, 8.58.

(*S*)-*N*-(4-(1,3-Dioxolan-2-yl)benzyl) 2-Acetamido-3-methoxypropionamide ((*S*)-150**).** Using Method H and following the preceding procedure compound (*S*)-**148** (3.81 g, 9.2 mmol), 10% Pd/C (700 mg) in MeOH (50 mL) and Et_3N (1.28 mL, 9.18 mmol) and AcCl (650 μL , 9.18 mmol) in THF (100 mL) gave 1.70 g (57%) of (*S*)-**150** as a light brown solid after recrystallization from EtOAc and hexanes: mp 138–139 $^\circ\text{C}$; $[\alpha]_D^{25}$ -13.0 $^\circ$ (c 1.0, MeOH); R_f = 0.39 (5/95 MeOH/ CHCl_3); IR (nujol) 3281, 3084, 1638, 1546, 1458 cm^{-1} ; ^1H NMR (CDCl_3) δ 2.03 (s, $\text{CH}_3\text{C}(\text{O})$), 3.38 (s, CH_2OCH_3), 3.43 (dd, J = 7.5, 9.0 Hz, $\text{CHH}'\text{OCH}_3$), 3.80 (dd J = 3.7, 9.0 Hz, $\text{CHH}'\text{OCH}_3$), 4.01–4.15 (m, $\text{OCH}_2\text{CH}_2\text{O}$), 4.40–4.50 (m, $\text{NHCH}_2\text{C}_6\text{H}_4$), 4.54 (app. dt, J = 3.7, 7.5 Hz, CHCH_2), 5.80 (s, $\text{OC}(\text{H})\text{O}$), 6.45 (d, J = 6.6 Hz, $\text{CH}_3\text{C}(\text{O})\text{NH}$), 6.78–6.82 (m, $\text{N}(\text{H})\text{CH}_2\text{C}_6\text{H}_4$), 7.27 (d, J = 7.8 Hz, 2 ArH), 7.45 (d, J = 7.8 Hz, 2 ArH), addition of excess (*R*)-(-)-mandelic acid to a CDCl_3 solution of (*S*)-**150** gave only one signal for the the acetyl peak protons and the methoxy protons, addition of excess (*R*)-(-)-mandelic acid to a CDCl_3 solution of (*S*)-**150** and (*R*)-**150** (~1:2 ratio) gave two signals for the acetyl methyl protons (δ 2.021 (*S*) and 2.008 (*R*) (Δ ppm = 0.013)

and two signals for the methoxy protons (δ 3.317 (S) and 3.351 (R) (Δ ppm = 0.034)) in a ~1:2 ratio; ^{13}C NMR (CDCl_3) δ 23.4 ($\text{CH}_3\text{C}(\text{O})$), 43.5 ($\text{NH}_2\text{CH}_2\text{C}_6\text{H}_4$), 52.6 (CHCH_2O), 59.3 (CH_2OCH_3), 65.5 ($\text{OCH}_2\text{CH}_2\text{O}$), 71.8 (CH_2OCH_3), 103.7 ($\text{OC}(\text{H})\text{O}$), 127.0, 127.7, 137.5, 139.1 (C_6H_4), 170.2, 170.5 ($\text{CHC}(\text{O})\text{NH}$, $\text{CH}_3\text{C}(\text{O})$); M_r (+ESI) 345.1421 $[\text{M}+\text{Na}]^+$ (calcd for $\text{C}_{16}\text{H}_{22}\text{N}_2\text{O}_5\text{Na}^+$ 345.1426). Anal. Calcd for $\text{C}_{16}\text{H}_{22}\text{N}_2\text{O}_5$: C, 59.61; H, 6.88; N, 8.69. Found: C, 59.50; H, 6.90; N, 8.56.

(R)-N-(4-Formylbenzyl) 2-Acetamido-3-methoxypropionamide ((R)-151). Using Method I, compound (R)-**150** (1.62 g, 5.03 mmol) and aqueous HCl in a THF:H₂O solution (2:1, 30 mL) gave 930 mg (66%) of (R)-**151** after work-up and recrystallization from EtOAc and hexanes. Mother liquors were purified by silica gel flash chromatography (MeOH/ CHCl_3 5/95) and yielded another 336 mg (24%) of the desired product (total yield: 1.27 g (90%)): mp 132–133°C; $[\alpha]_D^{25}$ -10.4° (c 1.0, CHCl_3); R_f = 0.40 (5/95 MeOH/ CHCl_3); IR (nujol) 3288, 3073, 1687, 1637, 1551, 1458, 1375 cm^{-1} ; ^1H NMR (CDCl_3) δ 2.04 (s, $\text{CH}_3\text{C}(\text{O})$), 3.40 (s, CH_2OCH_3), 3.46 (dd, J = 7.5 Hz, 9.6 Hz, $\text{CHH}'\text{OCH}_3$), 3.83 (dd J = 4.2 Hz, 9.6 Hz, $\text{CHH}'\text{OCH}_3$), 4.48–4.64 (m, $\text{NHCH}_2\text{C}_6\text{H}_4$, CHCH_2), 6.45 (d, J = 6.6 Hz, $\text{CH}_3\text{C}(\text{O})\text{NH}$), 6.99–7.15 (m, $\text{NHCH}_2\text{C}_6\text{H}_4$), 7.42 (d, J = 8.1 Hz, 2 ArH), 7.85 (d, J = 8.1 Hz, 2 ArH), 9.99 (s, $\text{C}(\text{O})\text{H}$), addition of excess (R)-(-)-mandelic acid to a CDCl_3 solution of (R)-**151** gave only one signal for the the acetyl peak protons and the methoxy protons, addition of excess (R)-(-)-mandelic acid to a CDCl_3 solution of (S)-**151** and (R)-**151** (~1:2 ratio) gave two signals for the acetyl methyl protons (δ 2.037 (S) and 2.023 (R) (Δ ppm = 0.014) in a ~1:2 ratio, and two signals for the methoxy protons (δ 3.317 (S) and

3.351 (*R*) (Δ ppm = 0.034)) in a ~1:2 ratio; ^{13}C NMR (CDCl_3) δ 23.4 ($\text{CH}_3\text{C}(\text{O})$), 43.4 ($\text{NH}_2\text{CH}_2\text{C}_6\text{H}_4$), 52.7 (CHCH_2O), 59.4 (CH_2OCH_3), 71.7 (CH_2OCH_3), 128.0, 130.3, 135.9, 145.2 (C_6H_4), 170.5, 170.6 ($\text{CHC}(\text{O})\text{NH}$, $\text{CH}_3\text{C}(\text{O})$), 192.0 ($\text{C}(\text{O})\text{H}$); M_r (+ESI) 301.1161 $[\text{M}+\text{Na}]^+$ (calcd for $\text{C}_{14}\text{H}_{18}\text{N}_2\text{O}_4\text{Na}^+$ 301.1164). Anal. Calcd for $\text{C}_{14}\text{H}_{18}\text{N}_2\text{O}_4$: C, 60.42; H, 6.52; N, 10.07. Found: C, 60.13; H, 6.49; N, 9.91.

(*R*)-*N*-(4-Formylbenzyl) 2-Acetamido-3-methoxypropionamide ((*R*)-151)

(alternate procedure). Using Method D, (*R*)-115 (500 mg, 3.1 mmol), 137 (668 mg, 3.7 mmol) and DMTMM (1.030 g, 3.7 mmol) gave a pale yellow residue after filtration and evaporation. Using Method I, the crude benzylamide and aqueous HCl in a THF:H₂O solution (2:1, 30 mL) gave (*R*)-151 (633 mg, 73%) as a white solid after work-up and silica gel chromatography: mp 131–133°C; $[\alpha]_D^{25}$ -10.3° (*c* 1.0, CHCl_3); R_f = 0.40 (5/95 MeOH/ CHCl_3); ^1H NMR (CDCl_3) δ 2.02 (s, $\text{CH}_3\text{C}(\text{O})$), 3.38 (s, CH_2OCH_3), 3.48 (app t, J = 9.0 Hz, $\text{CHH}'\text{OCH}_3$), 3.75 (dd J = 4.6, 9.0 Hz, $\text{CHH}'\text{OCH}_3$), 4.45–4.70 (m, $\text{NHCH}_2\text{C}_6\text{H}_4$, CHCH_2O), 6.24–6.40 (m, $\text{CH}_3\text{C}(\text{O})\text{NH}$), 6.78–6.95 (m, $\text{NHCH}_2\text{C}_6\text{H}_4$), 7.42 (d, J = 8.3 Hz, 2 ArH), 7.82 (d, J = 8.3 Hz, 2 ArH), 9.92 (s, $\text{C}(\text{O})\text{H}$); ^{13}C NMR (CDCl_3) δ 23.3 ($\text{CH}_3\text{C}(\text{O})$), 43.3 ($\text{NH}_2\text{CH}_2\text{C}_6\text{H}_4$), 52.8 ($\text{CHCH}_2\text{OCH}_3$), 59.3 (CH_2OCH_3), 71.8 (CH_2OCH_3), 127.9, 130.3, 135.7, 145.2 (C_6H_4), 170.4, 170.5 ($\text{CHC}(\text{O})\text{NH}$, $\text{CH}_3\text{C}(\text{O})$), 192.1 ($\text{C}(\text{O})\text{H}$).

(*S*)-*N*-(4-Formylbenzyl) 2-Acetamido-3-methoxypropionamide ((*S*)-151). Using Method I, compound (*S*)-150 (1.65 g, 5.12 mmol) and aqueous HCl in THF:H₂O (2:1, 30 mL) gave 1.17 g of (*S*)-151 as a white solid after recrystallization (EtOAc) and

silica gel chromatography (5/95 MeOH/CHCl₃): mp 132–133°C; [α]_D²⁵ +10.4° (c 1.0, CHCl₃); *R*_f = 0.40 (5/95 MeOH/CHCl₃); IR (nujol) 3288, 1687, 1642, 1549, 1458, 1375 cm⁻¹; ¹H NMR (CDCl₃) δ 1.96 (s, CH₃C(O)), 3.36 (s, CH₂OCH₃), 3.53 (dd, *J* = 6.0, 9.3 Hz, CHH'OCH₃), 3.75 (dd *J* = 5.1, 9.3 Hz, CHH'OCH₃), 4.38–4.58 (m, NHCH₂C₆H₄), 4.71 (app. dt, *J* = 5.1, 6.0 Hz, CHCH₂O), 7.03 (d, *J* = 7.8 Hz, NHCH₂C₆H₄), 7.38 (d, *J* = 8.4 Hz, 2 ArH), 7.68 (t, *J* = 5.4 Hz, CH₃C(O)NH), 7.77 (d, *J* = 8.4 Hz, 2 ArH), 9.93 (s, C(O)H), addition of excess (*R*)-(-)-mandelic acid to a CDCl₃ solution of (*S*)-**151** gave only one signal for the methoxy protons and the acetyl peak protons, addition of excess (*R*)-(-)-mandelic acid to a CDCl₃ solution of (*S*)-**151** and (*R*)-**151** (~1:2 ratio) gave two signals for the acetyl methyl protons (δ 2.037 (*S*) and 2.023 (*R*) (Δ ppm = 0.014), in a ~1:2 ratio and two signals for the methoxy protons (δ 3.346 (*S*) and 3.377 (*R*) (Δ ppm = 0.031)) in a ~1:2 ratio; ¹³C NMR (CDCl₃) δ 23.0 (CH₃C(O)), 43.1 (NH₂CH₂C₆H₄), 52.8 (CHCH₂O), 59.1 (CH₂OCH₃), 72.0 (CH₂OCH₃), 127.7, 130.0, 135.5, 145.3 (C₆H₄), 170.5, 170.7 (CHC(O)NH, CH₃C(O)), 192.0 (C(O)H); *M*_r (+ESI) 301.1158 [M+Na]⁺ (calcd for C₁₄H₁₈N₂O₄Na⁺ 301.1164). Anal. Calcd for C₁₄H₁₈N₂O₄: C, 60.42; H, 6.52; N, 10.07. Found: C, 60.40; H, 6.57; N, 9.90.

(*S*)-*N*-(4-Formylbenzyl) 2-Acetamido-3-methoxypropionamide ((*S*)-151**)**

(Alternate Procedure). Using Method D, (*S*)-**115** (200 mg, 1.24 mmol), **137** (267 mg, 1.49 mmol), and DMTMM (412 mg, 1.49 mmol) in THF (12 mL), followed by aqueous HCl in THF:H₂O (2:1, 20 mL) gave (*S*)-**151** (160 mg, 46%) as a white solid after work-up, purification by silica gel chromatography and recrystallization from

EtOAc: mp 132–133 °C; $[\alpha]_D^{25} +10.2^\circ$ (c 1.0, CHCl₃); $R_f = 0.40$ (5/95 MeOH/CHCl₃); ¹H NMR (CDCl₃) δ 2.02 (s, CH₃C(O)), 3.38 (s, CH₂OCH₃), 3.48 (app t, $J = 9.0$ Hz, CHH'OCH₃), 3.75 (dd $J = 4.6, 9.0$ Hz, CHH'OCH₃), 4.45–4.62 (m, NHCH₂C₆H₄), 4.60–4.68 (m, CHCH₂O), 6.62 (d, $J = 8.1$ Hz, CH₃C(O)NH), 7.15–7.25 (br t, NHCH₂C₆H₄), 7.42 (d, $J = 8.1$ Hz, 2 ArH), 7.82 (d, $J = 8.4$ Hz, 2 ArH), 9.96 (s, C(O)H); ¹³C NMR (CDCl₃) δ 23.3 (CH₃C(O)), 43.3 (NH₂CH₂C₆H₄), 52.8 (CHCH₂OCH₃), 59.3 (CH₂OCH₃), 71.9 (CH₂OCH₃), 127.9, 130.3, 135.7, 145.2 (C₆H₄), 170.5, 170.6 (CHC(O)NH, CH₃C(O)), 192.0 (C(O)H).

(2*R*)-*N*-(4-(Oxiran-2-yl)benzyl) 2-Acetamido-3-methoxypropionamide ((*R*)-197)

(mixture of diastereomers). Using Method F, (*R*)-151 (720 mg, 2.57 mmol) and solution A (DMSO, 30.0 mL, [C]= 0.1 M, 3 mmol) gave (*R*)-197 (312 mg, 42%) as a white solid after work-up and purification by flash chromatography (15/85 acetone/EtOAc): mp 131–138 °C; $[\alpha]_D^{25} -19.0^\circ$ (c 0.6; CHCl₃); $R_f = 0.36$ (5/95 MeOH/CH₂Cl₂); IR (nujol) 3279, 1636, 1547, 1458, 1376, 1130 cm⁻¹; ¹H NMR (CDCl₃) δ 2.01 (s, CH₃C(O)), 2.77 (dd, $J = 2.4, 5.6$ Hz, CH(O)CHH'), 3.14 (dd, $J = 4.2, 5.6$ Hz, CH(O)CHH'), 3.37 (s, CH₂OCH₃), 3.40–3.62 (dd, $J = 7.4, 9.0$ Hz, CHH'OCH₃), 3.76 (dd, $J = 4.2, 9.0$ Hz, CHH'OCH₃), 3.84 (dd, $J = 2.4, 4.2$ Hz, CH(O)CH₂), 4.38–4.52 (m, NHCH₂C₆H₄), 4.53–4.62 (m, CHCH₂O), 6.52 (d, $J = 7.0$ Hz, NHCHCH₂O), 6.86–6.92 (m, NHCH₂C₆H₄), 7.24 (s, C₆H₄), addition of excess (*R*)-(-)-mandelic acid to a CDCl₃ solution of (*R*)-197 gave only one signal for the acetyl protons (δ 2.008 ppm) and one signal for the methoxy protons (δ 3.356 ppm), addition of excess (*R*)-(-)-mandelic acid to a CDCl₃ solution of (*S*)-197 and (*R*)-197

in a ~1:2 ratio gave two signals with a relative ~1:2 intensity for both the acetyl protons (δ 2.027 ppm (*S*)-**197**, δ 2.011 ppm (*R*)-**197**, (Δ ppm = 0.016)) and the methoxy protons (δ 3.331 ppm (*S*)-**197**, δ 3.357 ppm (*R*)-**197**, (Δ ppm = 0.026)); ^{13}C NMR (CDCl_3) δ 23.4 ($\text{CH}_3\text{C}(\text{O})$), 43.4 ($\text{NHCH}_2\text{C}_6\text{H}_4$), 51.4, 52.3, 52.6 ($\text{CHC}(\text{O})\text{NH}$, $\text{CH}(\text{O})\text{CH}_2$), 59.3 (CH_2OCH_3), 71.9 ($\text{CHCH}_2\text{OCH}_3$), 126.0, 127.8, 137.1, 138.2 (C_6H_4), 170.2, 170.5 ($\text{CH}_3\text{C}(\text{O})$, $\text{CHC}(\text{O})\text{NH}$); M_r (+ESI) 315.1323 [$\text{M}+\text{Na}$] $^+$ (calcd for $\text{C}_{15}\text{H}_{19}\text{N}_2\text{O}_4\text{Na}^+$ 315.1321). Anal. Calcd for $\text{C}_{15}\text{H}_{19}\text{N}_2\text{O}_4$: C, 61.63; H, 6.90; N, 9.58; Found: C, 61.53; H, 6.85; N, 9.44.

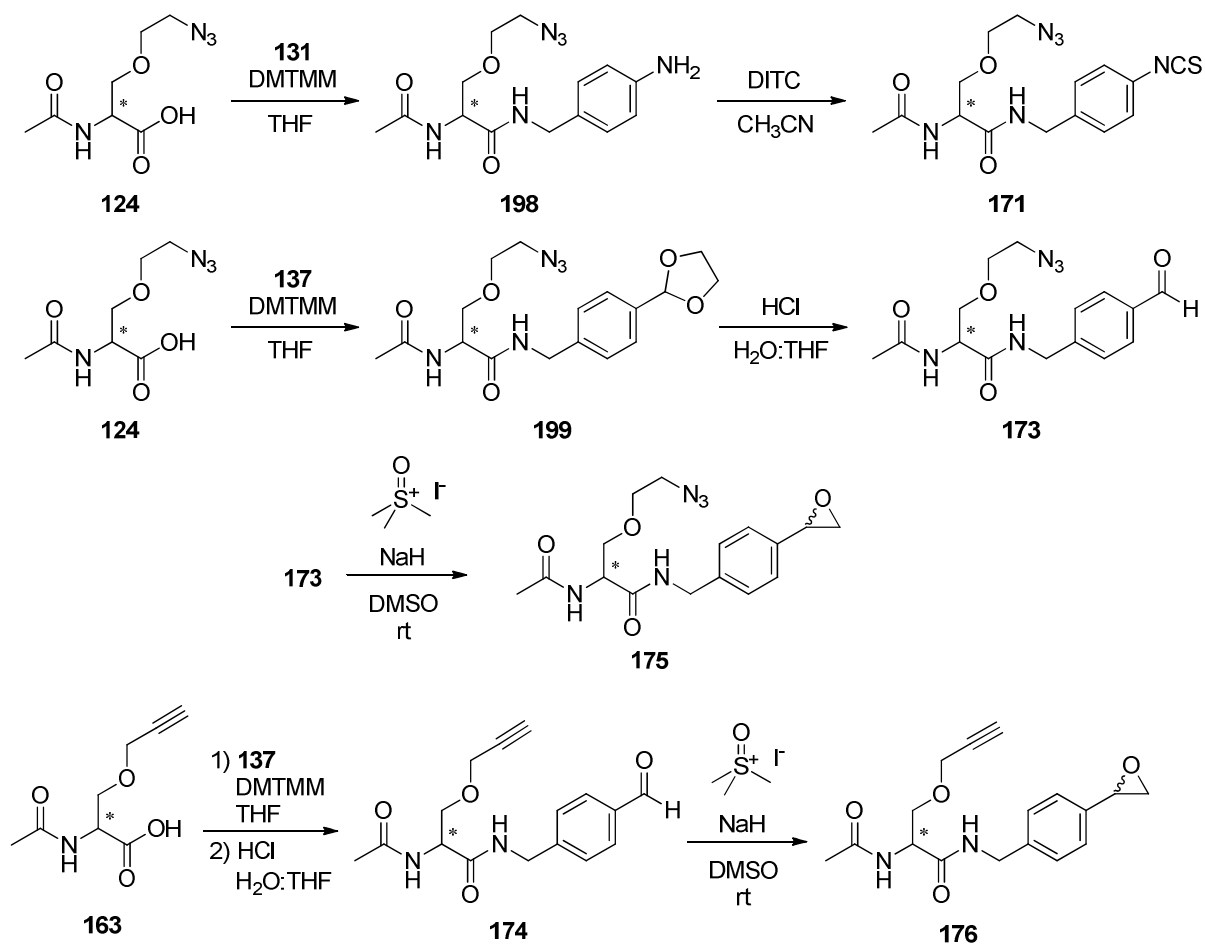
(2*S*)-*N*-(4-(Oxiran-2-yl)benzyl) 2-Acetamido-3-methoxypropionamide ((*S*)-197**) (mixture of diastereomers).** Using Method F, compound (*S*)-**151** (160 mg, 0.58 mmol) and solution A (DMSO, 6.9 mL, $[\text{C}] = 0.1 \text{ M}$, 0.69 mmol) gave (*S*)-**197** (60 mg, 36%) as a white solid after work-up and purification by flash chromatography (15/85 acetone/EtOAc): mp 130–139 °C; $[\alpha]_D^{25} +17.7^\circ$ (c 1.4; CHCl_3); $R_f = 0.36$ (5/95 MeOH/ CH_2Cl_2); IR (nujol) 3281, 1636, 1547, 1458, 1376, 1130 cm^{-1} ; ^1H NMR (CDCl_3) δ 2.00 (s, $\text{CH}_3\text{C}(\text{O})$), 2.77 (dd, $J = 2.4, 5.6 \text{ Hz}$, $\text{CH}(\text{O})\text{CHH}'$), 3.14 (dd, $J = 4.2, 5.6 \text{ Hz}$, $\text{CH}(\text{O})\text{CHH}'$), 3.36 (s, CH_2OCH_3), 3.45 (dd, $J = 7.4, 9.0 \text{ Hz}$, $\text{CHH}'\text{OCH}_3$), 3.76 (dd, $J = 4.2, 9.0 \text{ Hz}$, $\text{CHH}'\text{OCH}_3$), 3.84 (dd, $J = 2.4, 4.2 \text{ Hz}$, $\text{CH}(\text{O})\text{CH}_2$), 4.34–4.52 (m, $\text{NHCH}_2\text{C}_6\text{H}_4$), 4.53–4.64 (m, CHCH_2O), 6.58–6.68 (br d, NHCHCH_2O), 6.98–7.08 (m, $\text{NHCH}_2\text{C}_6\text{H}_4$), 7.23 (s, C_6H_4), addition of excess (*R*)-(-)-mandelic acid to a CDCl_3 solution of (*S*)-**197** gave only one signal for the acetyl protons (δ 2.030 ppm) and one signal for the methoxy protons (δ 3.328 ppm), addition of excess (*R*)-(-)-mandelic acid to a CDCl_3 solution of (*S*)-**197** and (*R*)-**197** in a ~1:2 ratio gave two

signals with a relative ~1:2 intensity for the acetyl protons (δ 2.027 ppm (S)-**197**, δ 2.011 ppm (R)-**197**, (Δ ppm = 0.016)) and the methoxy protons (δ 3.331 ppm (S)-**197**, δ 3.357 ppm (R)-**197**, (Δ ppm = 0.026)); ^{13}C NMR (CDCl_3) δ 23.3 ($\text{CH}_3\text{C}(\text{O})$), 43.7 ($\text{NHCH}_2\text{C}_6\text{H}_4$), 51.3, 52.3, 52.7 ($\text{CHC}(\text{O})\text{NH}$, $\text{CH}(\text{O})\text{CH}_2$), 59.2 (CH_2OCH_3), 72.0 ($\text{CHCH}_2\text{OCH}_3$), 126.0, 127.7, 137.0, 138.2 (C_6H_4), 170.2, 170.6 ($\text{CH}_3\text{C}(\text{O})$, $\text{CHC}(\text{O})\text{NH}$); M_r (+ESI) 315.1322 $[\text{M}+\text{Na}]^+$ (calcd for $\text{C}_{15}\text{H}_{19}\text{N}_2\text{O}_4\text{Na}^+$ 315.1321). Anal. Calcd for $\text{C}_{15}\text{H}_{19}\text{N}_2\text{O}_4$: C, 61.63; H, 6.90; N, 9.58. Found: C, 61.81; H, 7.01; N, 9.47.

2.3.3.3. Synthesis of lacosamide AB&CR derivatives

2.3.3.3.1. Derivatives bearing the CR group on the C(2) side chain

Scheme 38. Structure of the different intermediates and chemical reactions used in the synthesis of AB&CR agents **171**, **173**, **174**, **175** and **176**.



(R)-N-(4-Aminobenzyl) 2-Acetamido-3-(2-azidoethoxy)propionamide ((R)-198).

Using Method D, acid (R)-**124** (2.25 g, 10.4 mmol), 4-aminobenzylamine (1.52 g, 12.5 mmol) and DMTMM (3.46 g, 12.5 mmol) in THF (200 mL) gave 1.40 g (42%) of a dark brown residue *that was normally directly used in the next step*. Recrystallization from CHCl₃ and hexanes yielded a white solid that rapidly turned

brown when exposed to light or air: mp 98–99 °C; $[\alpha]_D^{25} +12.8^\circ$ (c 0.5; MeOH); $R_f = 0.36$ (5/95 MeOH/CHCl₃); IR (nujol) 3314, 3205, 2107, 1628, 1522, 1457, 1374, 1285 cm⁻¹; ¹H NMR (DMSO-*d*₆) δ 1.85 (s, CH₃C(O)NH), 3.30–3.40 (m, CH₂N₃), 3.52–3.64 (m, OCH₂CH₂N₃, CHCH₂OCH₂), 4.08 (d, $J = 6.0$ Hz, C(O)NHCH₂Ph), 4.44–4.56 (m, CHCH₂O), 4.95 (s, C₆H₄NH₂), 6.48 (d, $J = 8.7$ Hz, 2 ArH), 6.88 (d, $J = 8.7$ Hz, 2 ArH), 8.02 (d, $J = 8.4$ Hz, CH₃C(O)NH), 8.29 (t, $J = 6.0$ Hz, C(O)NHCH₂Ph); ¹³C NMR (DMSO-*d*₆) δ 22.5 (CH₃C(O)), 41.8 (NHCH₂Ph), 49.8 (CH₂N₃), 52.4 (CHCH₂O), 69.1 (OCH₂CH₂N₃ or CHCH₂O), 70.4 (CHCH₂O or OCH₂CH₂N₃), 113.5, 125.9, 128.0, 147.4 (C₆H₄), 169.8, 169.2 (CH₃C(O)NH, C(O)NHCH₂); M_r (+ESI) 321.1671 [M+H]⁺ (calcd for C₁₄H₂₀N₆O₃H⁺ 321.1675). Efforts to obtain satisfactory elemental analyses were unsuccessful.

(*R*)-*N*-(4-Isothiocyanatobenzyl) 2-Acetamido-3-(2-azidoethoxy)propionamide ((*R*)-171). Compound (*R*)-198 (715 mg, 2.23 mmol) was dissolved in CH₃CN (40 mL) and DITC (90%, 510 mg, 2.57 mmol) was added all at once. The reaction solution was stirred at room temperature (1 h), the solvent was removed in vacuo, and the residue was purified using flash chromatography (5/95 MeOH/CHCl₃) and then recrystallized from EtOAc to yield 502 mg (62%) of an off-white solid: mp 142–143 °C; $[\alpha]_D^{25} -28.6^\circ$ (c 0.8; CHCl₃); $R_f = 0.45$ (1/9 acetone/EtOAc); IR (nujol) 3276, 2181, 2114, 1631, 1547, 1459, 1374, 1285 cm⁻¹; ¹H NMR (CDCl₃) δ 2.05 (s, CH₃C(O)NH), 3.30–3.50 (m, CH₂N₃), 3.55 (dd, $J = 7.5, 9.3$ Hz, CHCHH'OCH₂), 3.62–3.80 (m, OCH₂CH₂N₃), 3.95 (dd, $J = 4.0, 9.3$ Hz, CHCHH'OCH₂), 4.46 (d, $J = 6.0$ Hz, C(O)NHCH₂Ph), 4.54–4.60 (m, CHCH₂O), 6.45 (br d, $J = 6.2$ Hz,

CH₃C(O)NH), 6.84–6.92 (br t, C(O)NHCH₂Ph), 7.18–7.22 (m, 2 ArH), 7.23–7.29 (m, 2 ArH), addition of excess (*R*)-(-)-mandelic acid to a CDCl₃ solution of (*R*)-**171** gave only one signal for the acetyl protons (δ 2.019), addition of excess (*R*)-(-)-mandelic acid to a CDCl₃ solution of (*S*)-**171** and (*R*)-**171** (~1:2 ratio) gave two signals for the acetyl methyl protons (δ 2.033 (*S*) and 2.020 (*R*) (Δ ppm = 0.013)) in a ~1:2 ratio; ¹³C NMR (CDCl₃) δ 23.2 (CH₃C(O)), 41.0 (NHCH₂Ph), 50.7 (CH₂N₃), 52.4 (CHCH₂O), 70.0 (OCH₂CH₂N₃ or CHCH₂O), 70.3 (CHCH₂O or OCH₂CH₂N₃), 125.9, 128.6, 130.5 (3 ArC), 135.6 (NCS), 137.4 (1 ArC), 169.8, 169.2 (CH₃C(O)NH, C(O)NHCH₂); *M*_r (+ESI) 363.1236 [M+H]⁺ (calcd for C₁₅H₁₈N₆O₃SH⁺ 363.1239). Anal. Calcd for C₁₅H₁₈N₆O₃S: C, 49.71; H, 5.01; N, 23.19; S, 8.85. Found: C, 49.55; H, 4.91; N, 23.13; S, 8.63.

(*S*)-*N*-(4-Isothiocyanatobenzyl) 2-Acetamido-3-(2-azidoethoxy)propionamide ((*S*)-171**).** Using Method D, acid (*S*)-**124** (1.61 g, 7.52 mmol), 4-aminobenzylamine (1.02 mL, 9.03 mmol), and DMTMM (2.50 g, 9.03 mmol) in anhydrous THF (200 mL) gave after evaporation a brown residue to which EtOAc (100 mL) was added. After stirring (5 min) the insoluble materials were filtered, and rinsed with EtOAc. The filtrate was concentrated to yield a dark orange oily residue (2.38 g (crude)) (*M*_r (+ESI) 343.1496 [M+H]⁺ (calcd for C₁₄H₂₀N₆O₃Na⁺ 343.1495)). The residue was dissolved in CH₃CN (20 mL) and DITC (90%, 1.58 g, 7.90 mmol) was added at once. After stirring at room temperature (3 h), the reaction was concentrated in vacuo and the crude material was purified by flash column chromatography (5/95 MeOH/CHCl₃) and then recrystallized from EtOAc and hexanes to yield 706 mg (26% overall yield)

of (*S*)-**171** as an off-white solid: mp 142–143 °C; $[\alpha]_D^{25} +28.5^\circ$ (c 1.0; CHCl₃); R_f = 0.45 (1/9 acetone/EtOAc); IR (nujol) 3280, 2177, 2108, 1637, 1548, 1452, 1374, 1293 cm⁻¹; ¹H NMR (CDCl₃) δ 2.01 (s, CH₃C(O)NH), 3.28–3.48 (m, CH₂N₃), 3.55 (dd, J = 7.2, 9.3 Hz, CHCHH'OCH₂), 3.62–3.78 (m, OCH₂CH₂N₃), 3.91 (dd, J = 4.0, 9.3 Hz, CHCHH'OCH₂), 4.43 (d, J = 6.0 Hz, C(O)NHCH₂Ph), 4.56–4.62 (m, CHCH₂O), 6.56 (br d, J = 6.2 Hz, CH₃C(O)NH), 6.84–6.92 (br t, J = 6.0 Hz, C(O)NHCH₂Ph), 7.14–7.20 (m, 2 ArH), 7.22–7.28 (m, 2 ArH), addition of excess (*R*)-(-)-mandelic acid to a CDCl₃ solution of (*S*)-**171** gave only one signal for the acetyl protons (δ 2.032), addition of excess (*R*)-(-)-mandelic acid to a CDCl₃ solution of (*S*)-**171** and (*R*)-**171** (~1:2 ratio) gave two signals for the acetyl methyl protons (δ 2.033 (*S*) and 2.020 (*R*) (Δ ppm = 0.013)) in a ~1:2 ratio; ¹³C NMR (CDCl₃) δ 23.3 (CH₃C(O)), 43.2 (NHCH₂Ph), 50.9 (CH₂N₃), 52.7 (CHCH₂O), 70.3 (OCH₂CH₂N₃ or CHCH₂O), 70.4 (CHCH₂O or OCH₂CH₂N₃), 126.1, 128.8, 130.6 (3 ArC), 135.8 (NCS), 137.6 (1 ArC), 170.0, 170.7 (CH₃C(O)NH, C(O)NHCH₂); M_r (+ESI) 363.1241 [M+H]⁺ (calcd for C₁₅H₁₈N₆O₃SH⁺ 363.1239). Anal. Calcd for C₁₅H₁₈N₆O₃S: C, 49.71; H, 5.01; N, 23.19; S, 8.85. Found: C, 49.86; H, 5.07; N, 23.10; S, 8.75.

(*R*)-*N*-(4-(1,3-Dioxolan-2-yl)benzyl)

2-Acetamido-3-(2-

azidoethoxy)propionamide ((*R*)-199**).** Using Method D, acid (*R*)-**124** (400 mg, 1.87 mmol), benzylamine **137** (402 mg, 2.24 mmol), and DMTMM (620 mg, 2.24 mmol) in anhydrous THF (20 mL) gave 628 mg (89%) of (*R*)-**199** as a white solid after flash column chromatography (10/89.5/0.5 MeOH/CHCl₃/NEt₃). An analytical sample was obtained by recrystallization from EtOAc and hexanes: mp 112–113 °C; $[\alpha]_D^{25} -23.9^\circ$

(c 0.9; CHCl₃); R_f = 0.47 (10/89.5/0.5 MeOH/CHCl₃/NEt₃); IR (nujol) 3288, 3071, 2134, 1634, 1544, 1457, 1382, 1305, 1236, 1126 cm⁻¹; ¹H NMR (CDCl₃) δ 2.02 (s, CH₃C(O)NH), 3.24–3.46 (m, CH₂N₃), 3.55 (dd, J = 7.2, 9.3 Hz, CHCHH'OCH₂), 3.60–3.74 (m, OCH₂CH₂N₃), 3.91 (dd, J = 4.0, 9.3 Hz, CHCHH'OCH₂), 4.00–4.16 (m, OCH₂CH₂O), 4.40–4.54 (m, C(O)NHCH₂Ph), 4.56–4.62 (m, CHCH₂O), 5.79 (s, OCH(O)), 6.51 (d, J = 6.9 Hz, CH₃C(O)NH), 6.81–6.87 (br t, C(O)NHCH₂Ar), 7.28 (d, J = 8.1 Hz, 2 ArH), 7.44 (d, J = 8.1 Hz, 2 ArH), addition of excess (*R*)-(-)-mandelic acid to a CDCl₃ solution of (*R*)-**199** gave only one signal for the acetyl protons, addition of excess (*R*)-(-)-mandelic acid to a CDCl₃ solution of (*S*)-**199** and (*R*)-**199** (~1:2 ratio) gave two signals for the acetyl methyl protons (δ 2.028 (*S*) and 2.018 (*R*) (Δ ppm = 0.010)) in a ~1:2 ratio; ¹³C NMR (CDCl₃) δ 23.3 (CH₃C(O)), 43.6 (NHCH₂Ph), 50.8 (CH₂N₃), 52.7 (CHCH₂O), 65.5 (OCH₂CH₂O), 70.3 (OCH₂CH₂N₃ or CHCH₂O), 70.4 (CHCH₂O or OCH₂CH₂N₃), 103.6 (OCH(O)), 127.0, 127.7, 137.5, 139.1 (C₆H₄), 169.8, 170.6 (CH₃C(O)NH, C(O)NHCH₂); M_r (+ESI) 400.1601 [M+Na]⁺ (calcd for C₁₇H₂₃N₅O₅Na⁺ 400.1597). Anal. Calcd for C₁₇H₂₃N₅O₅: 54.10; H, 6.14; N, 18.56. Found: C, 54.30; H, 6.09; N, 18.36.

(*S*)-*N*-(4-(1,3-Dioxolan-2-yl)benzyl)

2-Acetamido-3-(2-

azidoethoxy)propionamide ((*S*)-199**). Using Method D, acid (*S*)-**124** (400 mg, 1.87 mmol), benzylamine **137** (402 mg, 2.24 mmol), and DMTMM (620 mg, 2.24 mmol) in anhydrous THF (20 mL) gave 518 mg (73%) of (*S*)-**199** as a white solid after flash column chromatography (10/89.5/0.5 MeOH/CHCl₃/NEt₃). An analytical sample was obtained by recrystallization from EtOAc and hexanes: mp 112–113 °C; [α]_D²⁵ +23.9°**

(*c* 1.2; CHCl₃); *R_f* = 0.47 (10/89.5/0.5 MeOH/CHCl₃/NEt₃); IR (nujol) 3281, 3078, 2133, 1634, 1544, 1457, 1380, 1307, 1236, 1126 cm⁻¹; ¹H NMR (CDCl₃) δ 2.01 (s, CH₃C(O)NH), 3.24–3.44 (m, CH₂N₃), 3.55 (dd, *J* = 7.2, 9.0 Hz, CHCHH'OCH₂), 3.60–3.76 (m, OCH₂CH₂N₃), 3.91 (dd, *J* = 4.0, 9.0 Hz, CHCHH'OCH₂), 4.00–4.18 (m, OCH₂CH₂O), 4.40–4.54 (m, C(O)NHCH₂Ph), 4.54–4.60 (m, CHCH₂O), 5.79 (s, OCH(O)), 6.51 (d, *J* = 6.6 Hz, CH₃C(O)NH), 6.84–6.94 (br t, C(O)NHCH₂Ar), 7.28 (d, *J* = 8.1 Hz, 2 ArH), 7.44 (d, *J* = 8.1 Hz, 2 ArH), addition of excess (*R*)-(-)-mandelic acid to a CDCl₃ solution of (*S*)-**199** gave only one signal for the acetyl protons, addition of excess (*R*)-(-)-mandelic acid to a CDCl₃ solution of (*S*)-**199** and (*R*)-**199** (~1:2 ratio) gave two signals for the acetyl methyl protons (δ 2.028 (*S*) and 2.018 (*R*) (Δppm = 0.010)) in a ~1:2 ratio; ¹³C NMR (CDCl₃) δ 23.3 (CH₃C(O)), 43.5 (NHCH₂Ph), 50.8 (CH₂N₃), 52.6 (CHCH₂O), 65.5 (OCH₂CH₂O), 70.3 (OCH₂CH₂N₃ or CHCH₂O), 70.4 (CHCH₂O or OCH₂CH₂N₃), 103.6 (OCH(O)), 127.0, 127.7, 137.5, 139.1 (C₆H₄), 169.8, 170.6 (CH₃C(O)NH, C(O)NHCH₂); *M_r* (+ESI) 400.1600 [M+Na]⁺ (calcd for C₁₇H₂₃N₅O₅Na⁺ 400.1597). Anal. Calcd for C₁₇H₂₃N₅O₅: 54.10; H, 6.14; N, 18.56. Found: C, 54.35; H, 6.20; N, 18.54.

(*R*)-*N*-(4-Formylbenzyl) 2-Acetamido-3-(2-azidoethoxy)propionamide ((*R*)-173**).**

Using Method I, (*R*)-**199** (280 mg, 0.74 mmol) and aqueous HCl in a THF:H₂O solution (2:1, 15 mL) gave 141 mg (57%) of (*R*)-**173** after work-up and recrystallization from EtOAc: mp 107–109 °C; [α]_D²⁵ -21.3° (*c* 1.1; CHCl₃); *R_f* = 0.45 (5/95 MeOH/CHCl₃); IR (nujol) 3277, 3080, 2860, 2106, 1699, 1638, 1550, 1456, 1378, 1304, 1131 cm⁻¹; ¹H NMR (CDCl₃) δ 2.06 (s, CH₃C(O)NH), 3.30–3.38 (m,

CH₂N₃), 3.59 (dd, $J = 7.2, 9.0$ Hz, CHCHH'OCH₂), 3.64–3.82 (m, OCH₂CH₂N₃), 3.97 (dd, $J = 4.0, 9.0$ Hz, CHCHH'OCH₂), 4.52–4.64 (m, C(O)NHCH₂Ph, CHCH₂O), 6.40–6.50 (br d, CH₃C(O)NH), 6.90–7.00 (br t, C(O)NHCH₂Ph), 7.43 (d, $J = 8.1$ Hz, 2 ArH), 7.85 (d, $J = 8.1$ Hz, 2 ArH), 10.01 (s, ArC(O)H), addition of excess (*R*)-(-)-mandelic acid to a CDCl₃ solution of (*R*)-**173** gave only one signal for the acetyl protons, addition of excess (*R*)-(-)-mandelic acid to a CDCl₃ solution of (*S*)-**173** and (*R*)-**173** (~2:1 ratio) gave two signals for the acetyl methyl protons (δ 2.043 (*S*) and 2.032 (*R*) (Δ ppm = 0.011)) in a ~2:1 ratio; ¹³C NMR (CDCl₃) δ 23.3 (CH₃C(O)), 43.4 (NHCH₂Ph), 50.8 (CH₂N₃), 52.7 (CHCH₂O), 70.3 (OCH₂CH₂N₃ or CHCH₂O), 70.5 (CHCH₂O or OCH₂CH₂N₃), 128.0, 130.3, 135.8, 145.1 (C₆H₄), 170.2, 170.7 (CH₃C(O)NH, C(O)NHCH₂), 192.0 (ArC(O)H); M_r (+ESI) 356.1341 [M+Na]⁺ (calcd for C₁₅H₁₉N₅O₄Na⁺ 356.1335). Anal. Calcd for C₁₅H₁₉N₅O₄: C, 54.05; H, 5.75; N, 21.01. Found: C, 54.30; H, 5.74; N, 20.73.

(*S*)-*N*-(4-Formylbenzyl) 2-Acetamido-3-(2-azidoethoxy)propionamide ((*S*)-173**).**

Using Method I, (*S*)-**199** (256 mg, 0.68 mmol) and aqueous HCl in a THF:H₂O solution (2:1, 15 mL) yielded 110 mg (48%) of (*S*)-**173** after work-up and recrystallization from EtOAc: mp 107–109 °C; [α]_D²⁵ +21.3° (c 1.8; CHCl₃); R_f = 0.45 (5/95 MeOH/CHCl₃); IR (nujol) 3273, 3082, 2860, 2106, 1699, 1639, 1550, 1455, 1377, 1303, 1221 cm⁻¹; ¹H NMR (CDCl₃) δ 2.03 (s, CH₃C(O)NH), 3.28–3.44 (m, CH₂N₃), 3.60 (dd, $J = 6.9, 9.0$ Hz, CHCHH'OCH₂), 3.62–3.80 (m, OCH₂CH₂N₃), 3.92 (dd, $J = 4.0, 9.0$ Hz, CHCHH'OCH₂), 4.50–4.58 (m, C(O)NHCH₂Ar), 4.60–4.68 (m, CHCH₂O), 6.57 (d, $J = 6.9$ Hz, CH₃C(O)NH), 7.10–7.20 (br t, C(O)NHCH₂Ph), 7.43

(d, $J = 8.1$ Hz, 2 ArH), 7.83 (d, $J = 8.1$ Hz, 2 ArH), 9.98 (s, ArC(O)H), addition of excess (*R*)-(-)-mandelic acid to a CDCl₃ solution of (*S*)-**173** gave only one signal for the acetyl protons, addition of excess (*R*)-(-)-mandelic acid to a CDCl₃ solution of (*S*)-**173** and (*R*)-**173** (~2:1 ratio) gave two signals for the acetyl methyl protons (δ 2.043 (*S*) and 2.032 (*R*) (Δ ppm = 0.011)) in a ~2:1 ratio; ¹³C NMR (CDCl₃) δ 23.3 (CH₃C(O)), 43.4 (NHCH₂Ph), 50.8 (CH₂N₃), 52.7 (CHCH₂O), 70.3 (OCH₂CH₂N₃ or CHCH₂O), 70.5 (CHCH₂O or OCH₂CH₂N₃), 128.0, 130.3, 135.8, 145.1 (C₆H₄), 170.2, 170.7 (CH₃C(O)NH, C(O)NHCH₂), 192.0 (ArC(O)H); M_r (+ESI) 356.1338 [M+Na]⁺ (calcd for C₁₅H₁₉N₅O₄Na⁺ 356.1335). Anal. Calcd for C₁₅H₁₉N₅O₄: C, 54.05; H, 5.75; N, 21.01. Found: C, 54.45; H, 5.81; N, 20.66.

(2*R*)-*N*-(4-(Oxiran-2-yl)benzyl) 2-Acetamido-3-(2-azidoethoxy)propionamide ((*R*)-175**) (mixture of diastereomers).** Using Method F, solution A (DMF, 7.5 mL, [C]= 0.2 M, 1.5 mmol) and (*R*)-**173** (410 mg, 1.23 mmol) gave (*R*)-**175** (80 mg, 19%) as a white solid after purification by flash chromatography (15/85 acetone/EtOAc): mp 91–98°C; [α]_D²⁵ -24.6° (c 0.4; CHCl₃); R_f = 0.38 (1/9 acetone/EtOAc); IR (CHCl₃ film) 3288, 3107, 2924, 2867, 2104, 1638, 1541, 1448, 1378, 1124 cm⁻¹; ¹H NMR (CDCl₃) δ 1.99 (s, CH₃C(O)), 2.76 (dd, $J = 2.4, 5.6$ Hz, CH(O)CHH'), 3.13 (dd, $J = 4.0, 5.6$ Hz, CH(O)CHH'), 3.24–3.44 (m, OCH₂CH₂N₃), 3.52–3.68 (m, OCH₂CH₂N₃, CHH'OCH₂), 3.83 (dd, $J = 2.4, 4.0$ Hz, CH(O)CHH'), 3.88 (dd, $J = 4.5, 9.2$ Hz, CHH'OCH₂), 4.43 (d, $J = 7.2$ Hz, NHCH₂C₆H₄), 4.58–4.64 (m, CHCH₂O), 6.65 (d, $J = 7.2$ Hz, NHCHCH₂O), 7.10–7.18 (br t, NHCH₂C₆H₄), 7.23 (s, C₆H₄), addition of excess (*R*)-(-)-mandelic acid to a CDCl₃ solution of (*R*)-**175** gave only one signal for

the acetyl protons (δ 2.024 ppm), addition of excess (*R*)-(-)-mandelic acid to a CDCl_3 solution of (*S*)-**175** and (*R*)-**175** in a ~1:5 ratio gave two signals with a relative ~1:5 intensity for the acetyl protons (δ 2.030 ppm (*S*)-**175**, δ 2.020 ppm (*R*)-**175**, (Δ ppm = 0.010)), at 300 MHz, we were not able to detect individual peaks for the two diastereomers; ^{13}C NMR (CDCl_3) δ 23.3 ($\text{CH}_3\text{C}(\text{O})$), 43.5 ($\text{NHCH}_2\text{C}_6\text{H}_4$), 50.8, 51.3, 52.3, 52.6 ($\text{CHC}(\text{O})\text{NH}$, $\text{CH}(\text{O})\text{CH}_2$, CH_2N_3), 70.3, 70.4 ($\text{CH}_2\text{OCH}_2\text{CH}_2\text{N}_3$), 126.0, 127.9, 137.1, 138.1 (C_6H_4), 169.9, 170.6 ($\text{CH}_3\text{C}(\text{O})$, $\text{CHC}(\text{O})\text{NH}$), at 75 MHz, we were not able to detect individual peaks for the two diastereomers; M_r (+ESI) 370.1491 [$\text{M}+\text{Na}$] $^+$ (calcd for $\text{C}_{16}\text{H}_{21}\text{N}_5\text{O}_4\text{Na}^+$ 370.1491). Anal. Calcd for $\text{C}_{16}\text{H}_{21}\text{N}_5\text{O}_4$: 55.32; H, 6.09; N, 20.16. Found: C, 55.36; H, 6.16; N, 20.00.

(2*S*)-*N*-(4-(Oxiran-2-yl)benzyl) 2-Acetamido-3-(2-azidoethoxy)propionamide ((*S*)-175**) (mixture of diastereomers).** Using Method F, solution A (DMF, 7.5 mL, [C]= 0.2 M, 1.5 mmol) and (*S*)-**173** (334 mg, 1.00 mmol) gave (*S*)-**175** (71 mg, 20%) as a white solid after purification by flash chromatography (15/85 acetone/EtOAc): mp 92–98°C; $[\alpha]_D^{25} +25.5^\circ$ (c 1.0; CHCl_3); R_f = 0.38 (1/9 acetone/EtOAc); IR (CHCl_3 film) 3311, 3061, 2928, 2874, 2105, 1652, 1530, 1445, 1375, 1121 cm^{-1} ; ^1H NMR (CDCl_3) δ 1.99 (s, $\text{CH}_3\text{C}(\text{O})$), 2.76 (dd, J = 2.4, 5.6 Hz, $\text{CH}(\text{O})\text{CHH}'$), 3.12 (dd, J = 4.0, 5.6 Hz, $\text{CH}(\text{O})\text{CHH}'$), 3.22–3.44 (m, $\text{OCH}_2\text{CH}_2\text{N}_3$), 3.52–3.64 (m, $\text{CHH}'\text{OCH}_2\text{CH}_2\text{N}_3$), 3.82 (dd, J = 2.4, 4.0 Hz, $\text{CH}(\text{O})\text{CHH}'$), 3.84 (dd, J = 4.5, 9.2 Hz, $\text{CHH}'\text{OCH}_2\text{CH}_2\text{N}_3$), 4.42 (d, J = 7.2 Hz, $\text{NHCH}_2\text{C}_6\text{H}_4$), 4.58–4.64 (m, CHCH_2O), 6.71 (d, J = 7.2 Hz, NHCHCH_2O), 7.10–7.18 (br t, $\text{NHCH}_2\text{C}_6\text{H}_4$), 7.23 (s, C_6H_4), addition of excess (*R*)-(-)-mandelic acid to a CDCl_3 solution of (*S*)-**175** gave only one signal

for the acetyl protons (δ 2.030 ppm), addition of excess (*R*)-(-)-mandelic acid to a CDCl₃ solution of (*S*)-**175** and (*R*)-**175** in a ~1:5 ratio gave two signals with a relative ~1:5 intensity for the acetyl protons (δ 2.030 ppm (*S*)-**175**, δ 2.020 ppm (*R*)-**175**, (Δ ppm = 0.010)), at 300 MHz, we were not able to detect individual peaks for the two diastereomers; ¹³C NMR (CDCl₃) δ 23.2 (**CH₃C(O)**), 43.4 (**NHCH₂C₆H₄**), 50.7, 51.3, 52.2, 52.6 (**CHC(O)NH**, **CH(O)CH₂CH₂N₃**), 70.3, 70.4 (**CH₂OCH₂CH₂N₃**), 125.9, 127.8, 137.0, 138.1 (**C₆H₄**), 169.9, 170.6 (**CH₃C(O)**, **CHC(O)NH**), at 75 MHz, we were not able to detect individual peaks for the two diastereomers; *M_r* (+ESI) 370.1491 [M+Na]⁺ (calcd for C₁₆H₂₁N₅O₄Na⁺ 370.1491). Anal. Calcd for C₁₆H₂₁N₅O₄: 55.32; H, 6.09; N, 20.16. Found: C, 55.63; H, 6.23; N, 19.98.

(*R*)-*N*-(4-Formylbenzyl) 2-Acetamido-3-(prop-2-ynyloxy)propionamide ((*R*)-174**).**

(initially prepared by Dr. Ki-Duk Park) Using Method D, acid (*R*)-**163** (480 mg, 2.6 mmol), amine **137** (550 mg, 3.12 mmol) and DMTMM (862 mg, 3.12 mmol) in THF (30 mL) gave a crude yellow residue upon work-up. Using Method I, direct hydrolysis of the residue with HCl in a THF:H₂O solution (2:1, 20 mL) gave (*R*)-**174** as a white solid (382 mg, 49%, two steps) upon work-up and purification by flash chromatography: mp 142–144 °C; [α]_D²⁵ -9.3° (c 0.3, CHCl₃); *R_f* = 0.51 (1/9 MeOH/CH₂Cl₂); ¹H NMR (CDCl₃) δ 2.04 (s, **CH₃C(O)**), 2.48 (t, *J* = 2.4 Hz, **CH₂C≡CH**), 3.67 (dd, *J* = 7.2, 9.0 Hz, **CHH'OCH₂**), 3.95 (dd *J* = 4.2, 9.0 Hz, **CHH'OCH₂**), 4.12–4.28 (m, **OCH₂C≡CH**), 4.47–4.68 (m, **NHCH₂C₆H₄**, **CHCH₂O**), 6.42 (d, *J* = 6.4 Hz, **CH₃C(O)NH**), 6.90–7.00 (m, **NHCH₂C₆H₄**), 7.43 (d, *J* = 8.3 Hz, 2 **ArH**), 7.84 (d, *J* = 8.3 Hz, 2 **ArH**), 10.00 (s, **C(O)H**), addition of excess (*R*)-(-)-

mandelic acid to a CDCl₃ solution of (*R*)-**174** gave only one signal for the acetyl protons (δ 2.029) and the propargyl proton (δ 2.610), addition of excess (*R*)-(-)-mandelic acid to a CDCl₃ solution of (*S*)-**174** and (*R*)-**174** in a ~2:1 ratio gave two signals with a relative ~2:1 intensity for the acetyl protons (δ 2.040 (*S*)-**174**, δ 2.030 (*R*)-**174**) and the propargyl protons (δ 2.469 (*S*), δ 2.434 (*R*)); ¹³C NMR (CDCl₃) δ 23.4 (CH₃C(O)), 43.5 (NH₂CH₂C₆H₄), 52.8 (CHCH₂OCH₃), 58.9 (CH₂OCH₂C≡CH), 69.2 (CH₂OCH₂C≡CH), 75.7 (CH₂C≡CH), 79.0 (CH₂C≡CH), 128.0, 130.3, 135.8, 145.1 (C₆H₄), 170.2, 170.7 (CHC(O)NH, CH₃C(O)), 192.0 (C(O)H).

(*S*)-*N*-(4-Formylbenzyl) 2-Acetamido-3-(prop-2-ynyloxy)propionamide ((*S*)-174**).**

Using Method D, acid (*S*)-**163** (480 mg, 2.6 mmol), amine **137** (550 mg, 3.12 mmol) and DMTMM (862 mg, 3.12 mmol) in THF (30 mL) gave a crude yellow residue upon work-up. Using Method I, the residue was reacted with aqueous HCl in THF:H₂O (2:1, 20 mL) to give (*S*)-**174** as a white solid (382 mg, 49%, two steps) upon work-up and silica gel flash chromatography (1/2 CH₂Cl₂/EtOAc to 1/9 MeOH/CH₂Cl₂): mp 142–144 °C; [α]_D²⁵ +9.1° (c 0.3, CHCl₃); *R*_f = 0.51 (1/9 MeOH/CH₂Cl₂); IR (nujol) 3442, 3372, 3288, 2856, 2111, 1687, 1635, 1554, 1457, 1375, 1108 cm⁻¹; ¹H NMR (CDCl₃) δ 2.05 (s, CH₃C(O)), 2.48 (t, *J* = 2.4 Hz, CH₂C≡CH), 3.67 (dd, *J* = 7.2 Hz, 9.0 Hz, CHH'OCH₂), 3.96 (dd, *J* = 4.2, 9.0 Hz, CHH'OCH₂), 4.14–4.30 (m, OCH₂C≡CH), 4.48–4.66 (m, NHCH₂C₆H₄, CHCH₂O), 6.42 (d, *J* = 6.4 Hz, CH₃C(O)NH), 6.82–6.92 (m, NHCH₂C₆H₄), 7.44 (d, *J* = 8.3 Hz, 2 ArH), 7.85 (d, *J* = 8.3 Hz, 2 ArH), 10.00 (s, C(O)H), addition of excess (*R*)-(-)-mandelic acid to a CDCl₃ solution of (*S*)-**174** gave only one signal for the acetyl protons (δ 2.040) and the

propargyl proton (δ 2.469), addition of excess (*R*)-(-)-mandelic acid to a CDCl_3 solution of (*S*)-**174** and (*R*)-**174** in a ~2:1 ratio gave two signals with a relative ~2:1 intensity for the acetyl protons (δ 2.040 (*S*), δ 2.030 (*R*)) and the propargyl protons (δ 2.469 (*S*), δ 2.434 (*R*)); ^{13}C NMR (CDCl_3) δ 23.4 ($\text{CH}_3\text{C}(\text{O})$), 43.4 ($\text{NH}_2\text{CH}_2\text{C}_6\text{H}_4$), 52.8 ($\text{CHCH}_2\text{OCH}_3$), 58.9 ($\text{CH}_2\text{OCH}_2\text{C}\equiv\text{CH}$), 69.2 ($\text{CH}_2\text{OCH}_2\text{C}\equiv\text{CH}$), 75.7 ($\text{CH}_2\text{C}\equiv\text{CH}$), 79.0 ($\text{CH}_2\text{C}\equiv\text{CH}$), 128.0, 130.3, 135.8, 145.1 (C_6H_4), 170.2, 170.7 ($\text{CHC}(\text{O})\text{NH}$, $\text{CH}_3\text{C}(\text{O})$), 192.0 ($\text{C}(\text{O})\text{H}$); M_r (+ESI) 325.1 $[\text{M}+\text{Na}]^+$ (calcd for $\text{C}_{16}\text{H}_{18}\text{N}_2\text{O}_4\text{Na}^+$ 325.1). Anal. Calcd for $\text{C}_{16}\text{H}_{18}\text{N}_2\text{O}_4$: C, 63.56; H, 6.00; N, 9.27. Found: C, 63.34; H, 5.91; N, 9.20.

(2*R*)-*N*-(4-(Oxiran-2-yl)benzyl) 2-Acetamido-3-(prop-2-ynyloxy)propionamide ((*R*)-176**) (mixture of diastereomers).** Using Method F, solution A (DMSO, $[\text{C}] = 0.1$ M, 11.7 mL, 1.2 mmol) and (*R*)-**174** (410 mg, 1.23 mmol) gave (*R*)-**176** (80 mg, 19%) as a white solid after purification by flash chromatography (15/85 acetone/EtOAc): mp 131–136 °C; $[\alpha]_D^{25} +3.2^\circ$ (c 0.5; MeOH); $R_f = 0.30$ (8/92 acetone/EtOAc); IR (nujol) 3283, 3061, 2109, 1634, 1544, 1458, 1375, 1306, 1096 cm^{-1} ; ^1H NMR (CD_3CN) δ 1.94 (s, $\text{CH}_3\text{C}(\text{O})$), 2.72–2.80 (m, $\text{CH}_2\text{C}\equiv\text{CH}$, $\text{CH}(\text{O})\text{CHH}'$), 3.08 (dd, $J = 4.0, 5.8$ Hz, $\text{CH}(\text{O})\text{CHH}'$), 3.63 (dd, $J = 4.8, 9.0$ Hz, $\text{CHH}'\text{OCH}_2\text{C}\equiv\text{CH}$), 3.80–3.88 (m, $\text{CH}(\text{O})\text{CHH}'$, $\text{CHH}'\text{OCH}_2\text{C}\equiv\text{CH}$), 4.09–4.22 (m, $\text{CH}_2\text{OCH}_2\text{C}\equiv\text{CH}$), 4.34 (d, $J = 6.0$ Hz, $\text{NHCH}_2\text{C}_6\text{H}_4$), 4.38–4.44 (m, CHCH_2O), 6.76–6.86 (br d, NHCHCH_2O), 7.18–7.28 (m, $\text{NHCH}_2\text{C}_6\text{H}_4$), at 300 MHz, we were not able to detect individual peaks for the two diastereomers; ^{13}C NMR (CD_3CN) δ 23.1 ($\text{CH}_3\text{C}(\text{O})$), 43.2 ($\text{NHCH}_2\text{C}_6\text{H}_4$), 51.6, 52.6, 54.4, 59.1 ($\text{CHC}(\text{O})\text{NH}$, $\text{CH}(\text{O})\text{CH}_2$, $\text{OCH}_2\text{C}\equiv\text{CH}$),

70.5 ($\text{CH}_2\text{OCH}_2\text{C}\equiv\text{CH}$), 76.2 ($\text{CH}_2\text{OCH}_2\text{C}\equiv\text{CH}$), 80.5 ($\text{CH}_2\text{OCH}_2\text{C}\equiv\text{CH}$), 126.7, 128.3, 137.8, 140.3 (C_6H_4), 170.7, 171.2 ($\text{CH}_3\text{C}(\text{O})$, $\text{CHC}(\text{O})\text{NH}$), at 75 MHz, we were not able to detect individual peaks for the two diastereomers; M_r (+ESI) 339.1 $[\text{M}+\text{Na}]^+$ (calcd for $\text{C}_{17}\text{H}_{20}\text{N}_2\text{O}_4\text{Na}^+$ 339.1). Anal. Calcd for $\text{C}_{17}\text{H}_{20}\text{N}_2\text{O}_4$: C, 64.54; H, 6.37; N, 8.86. Found: C, 64.38; H, 6.35; N, 8.65.

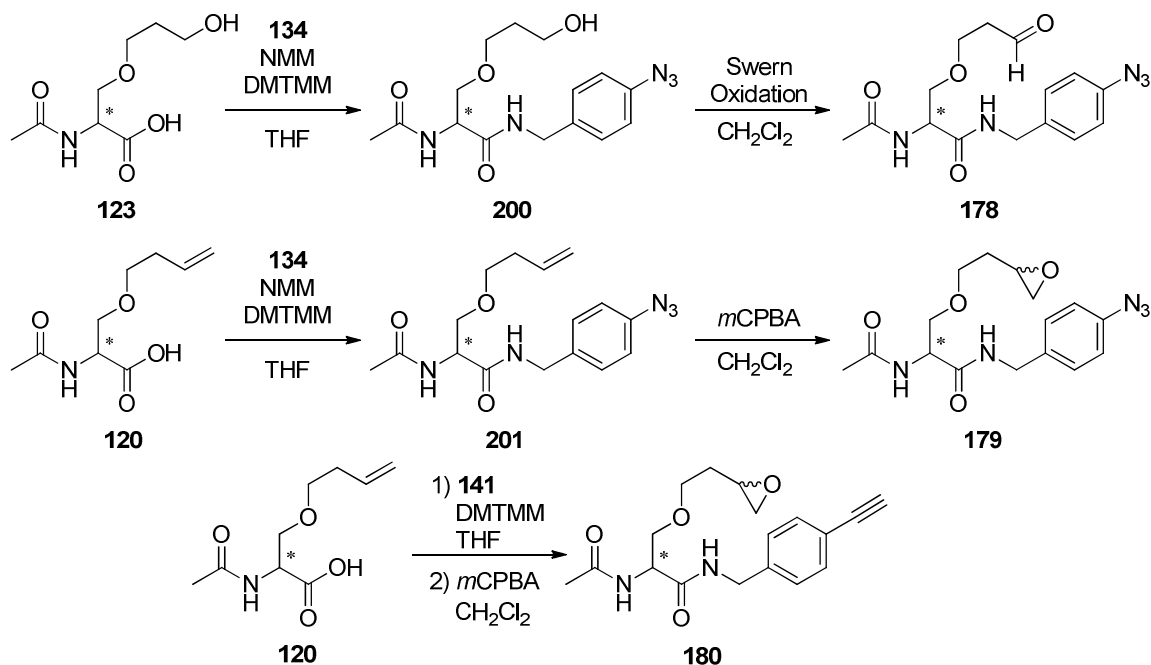
((2S)-N-(4-Oxiran-2-yl)benzyl) 2-Acetamido-3-(prop-2-ynyloxy)propionamide ((S)-176) (mixture of diastereomers). Using Method F, (S)-174 and solution A (DMSO, 17.8 mL, $[\text{C}] = 0.1 \text{ M}$, 1.78 mmol) gave (S)-176 as a white solid (90 mg, 26%) after purification by flash chromatography (15/85 acetone/EtOAc): mp 132–138 °C; $[\alpha]_{\text{D}}^{25} -3.1^\circ$ (c 0.3; MeOH); $R_f = 0.30$ (8/92 acetone/EtOAc); IR (nujol) 3412, 3277, 3138, 2874, 2109, 1633, 1544, 1458, 1375, 1306, 1096 cm^{-1} ; ^1H NMR (CD_3CN) δ 1.94 (s, $\text{CH}_3\text{C}(\text{O})$), 2.73–2.80 (m, $\text{CH}_2\text{C}\equiv\text{CH}$, $\text{CH}(\text{O})\text{CHH}'$), 3.08 (dd, $J = 4.0, 5.8 \text{ Hz}$, $\text{CH}(\text{O})\text{CHH}'$), 3.63 (dd, $J = 4.8, 9.0 \text{ Hz}$, $\text{CHH}'\text{OCH}_2\text{C}\equiv\text{CH}$), 3.80–3.88 (m, $\text{CH}(\text{O})\text{CHH}'$, $\text{CHH}'\text{OCH}_2\text{C}\equiv\text{CH}$), 4.08–4.21 (m, $\text{CH}_2\text{OCH}_2\text{C}\equiv\text{CH}$), 4.34 (d, $J = 6.0 \text{ Hz}$, $\text{NHCH}_2\text{C}_6\text{H}_4$), 4.39–4.47 (m, CHCH_2O), 6.76–6.88 (br d, NHCHCH_2O), 7.17–7.28 (m, $\text{NHCH}_2\text{C}_6\text{H}_4$), at 300 MHz, we were not able to detect individual peaks for the two diastereomers; ^{13}C NMR (CD_3CN) δ 23.1 ($\text{CH}_3\text{C}(\text{O})$), 43.2 ($\text{NHCH}_2\text{C}_6\text{H}_4$), 51.6, 52.7, 54.4, 59.1 ($\text{CHC}(\text{O})\text{NH}$, $\text{CH}(\text{O})\text{CH}_2$, $\text{OCH}_2\text{C}\equiv\text{CH}$), 70.5 ($\text{CH}_2\text{OCH}_2\text{C}\equiv\text{CH}$), 76.2 ($\text{CH}_2\text{OCH}_2\text{C}\equiv\text{CH}$), 80.5 ($\text{CH}_2\text{OCH}_2\text{C}\equiv\text{CH}$), 126.7, 128.3, 137.8, 140.3 (C_6H_4), 170.7, 171.2 ($\text{CH}_3\text{C}(\text{O})$, $\text{CHC}(\text{O})\text{NH}$), at 75 MHz, we were not able to detect individual peaks for the two diastereomers; M_r (+ESI) 339.1 $[\text{M}+\text{Na}]^+$ (calcd for

C₁₇H₂₀N₂O₄Na⁺ 339.1). Anal. Calcd for C₁₇H₂₀N₂O₄: C, 64.54; H, 6.37; N, 8.86.

Found: C, 64.63; H, 6.40; N, 8.76.

2.3.3.3.2. Derivatives bearing the CR group on the aromatic ring

Scheme 39. Structure of the different intermediates and chemical reactions used in the synthesis of AB&CR agents **178**, **179**, and **180**.



(*R*)-*N*-(4-Azidobenzyl) 2-Acetamido-3-(3-hydroxypropoxy)propionamide ((*R*)-200**).** Using Method D, acid (*R*)-**123** (1.00 g, 4.90 mmol), benzylamine hydrochloride **134** (1.07 g, 5.80 mmol), NMM (640 μ L, 5.80 mmol), and DMTMM (1.60 g, 5.80 mmol) in anhydrous THF (100 mL) gave 1.20 g (73%) of (*R*)-**200** as a white solid after flash column chromatography (1/9 MeOH/CHCl₃). The solid slowly turned light yellow upon exposure to light: mp 127–130 °C; [α]_D²⁵ +46.3° (c 0.9, MeOH); *R*_f = 0.57 (1/9 MeOH/CHCl₃); IR (nujol) 3400–2700 (br), 3282, 3085, 2119, 1638, 1552,

1459, 1378, 1296, 1127 cm^{-1} ; ^1H NMR ($\text{DMSO-}d_6$) δ 1.63 (quint, $J = 6.3$ Hz, $\text{OCH}_2\text{CH}_2\text{CH}_2\text{O}$), 1.87 (s, $\text{CH}_3\text{C}(\text{O})$), 3.38–3.48 (m, $\text{OCH}_2\text{CH}_2\text{CH}_2\text{OH}$), 3.48–3.56 (m, $\text{CH}_2\text{OCH}_2\text{CH}_2\text{CH}_2\text{OH}$), 4.19–4.34 (m, NHCH_2Ph), 4.40 (t, $J = 5.1$ Hz, CH_2OH), 4.40–4.48 (m, CHCH_2O), 7.06 (d, $J = 8.4$ Hz, 2 ArH), 7.28 (d, $J = 8.4$ Hz, 2 ArH), 8.05 (d, $J = 7.8$ Hz, $\text{CH}_3\text{C}(\text{O})\text{NH}$), 8.51 (t, $J = 5.7$ Hz, $\text{C}(\text{O})\text{NHCH}_2$); ^{13}C NMR ($\text{DMSO-}d_6$) δ 22.5 ($\text{CH}_3\text{C}(\text{O})$), 32.5 ($\text{OCH}_2\text{CH}_2\text{CH}_2\text{O}$), 41.4 (NHCH_2Ph), 52.8 ($\text{CHCH}_2\text{OCH}_2$), 57.7 ($\text{OCH}_2\text{CH}_2\text{CH}_2\text{OH}$), 67.6 ($\text{CHCH}_2\text{OCH}_2\text{CH}_2\text{CH}_2$), 70.3 ($\text{CHCH}_2\text{OCH}_2\text{CH}_2\text{CH}_2$), 118.8, 128.6, 136.4, 137.7 (C_6H_4), 169.4, 169.8 ($\text{CHC}(\text{O})\text{NH}$, $\text{CH}_3\text{C}(\text{O})\text{NH}$); M_r (+ESI) 358.1494 $[\text{M}+\text{Na}]^+$ (calcd for $\text{C}_{15}\text{H}_{21}\text{N}_5\text{O}_4\text{Na}^+$ 358.1491). Anal. Calcd for $\text{C}_{15}\text{H}_{21}\text{N}_5\text{O}_4 \cdot 0.43\text{H}_2\text{O}$: C, 52.51; H, 6.42; N, 20.37. Found: C, 52.90; H, 6.30; N, 19.99.

(S)-N-(4-Azidobenzyl) 2-Acetamido-3-(3-hydroxypropoxy)propionamide ((S)-200). Using Method D, acid (S)-**123** (260 mg, 1.27 mmol), benzylamine hydrochloride **134** (281 mg, 1.52 mmol), NMM (167 μL , 1.52 mmol), and DMTMM (420 mg, 1.52 mmol) in anhydrous THF (13 mL) gave 327 mg (77%) of (S)-**200** as a white solid after flash column chromatography (1/9 MeOH/ CHCl_3). The solid slowly turned light yellow upon exposure to light: mp 127–130 $^\circ\text{C}$; $[\alpha]_D^{25}$ -46.1 $^\circ$ (c 1.1, MeOH); R_f = 0.57 (1/9 MeOH/ CHCl_3); IR (nujol) 3400–2700 (br), 3282, 3084, 2119, 1638, 1552, 1459, 1377, 1296, 1127 cm^{-1} ; ^1H NMR ($\text{DMSO-}d_6$) δ 1.63 (quint, $J = 6.3$ Hz, $\text{OCH}_2\text{CH}_2\text{CH}_2\text{O}$), 1.87 (s, $\text{CH}_3\text{C}(\text{O})$), 3.38–3.48 (m, $\text{OCH}_2\text{CH}_2\text{CH}_2\text{OH}$), 3.48–3.56 (m, $\text{CH}_2\text{OCH}_2\text{CH}_2\text{CH}_2\text{OH}$), 4.19–4.34 (m, NHCH_2Ph), 4.40 (t, $J = 5.1$ Hz, CH_2OH), 4.40–4.48 (m, CHCH_2O), 7.06 (d, $J = 8.7$ Hz, 2 ArH), 7.28 (d, $J = 8.7$ Hz, 2

ArH), 8.05 (d, $J = 7.8$ Hz, CH₃C(O)NH), 8.51 (t, $J = 5.7$ Hz, C(O)NHCH₂); ¹³C NMR (DMSO-*d*₆) δ 22.5 (CH₃C(O)), 32.5 (OCH₂CH₂CH₂O), 41.4 (NHCH₂Ph), 52.8 (CHCH₂OCH₂), 57.7 (OCH₂CH₂CH₂OH), 67.6 (CHCH₂OCH₂CH₂CH₂), 70.3 (CHCH₂OCH₂CH₂CH₂), 118.8, 128.6, 136.4, 137.7 (C₆H₄), 169.4, 169.8 (CHC(O)NH, CH₃C(O)NH); M_r (+ESI) 358.1494 [M+Na]⁺ (calcd for C₁₅H₂₁N₅O₄Na⁺ 358.1491). Anal. Calcd for C₁₅H₂₁N₅O₄: C, 53.72; H, 6.31; N, 20.88. Found: C, 53.73; H, 6.32; N, 20.76.

(*R*)-*N*-(4-Azidobenzyl) 2-Acetamido-3-(3-oxopropoxy)propionamide ((*R*)-178**).**

Using Method E, alcohol (*R*)-**200** (1.20 g, 3.56 mmol) in a 2:1 CH₂Cl₂:DMSO mixture (12 mL), (COCl)₂ (406 μ L, 4.65 mmol) in CH₂Cl₂ (12 mL), DMSO (660 μ L, 9.30 mmol) in CH₂Cl₂ (24 mL), and DIEA (3.1 mL, 17.8 mmol) gave 663 mg (56%) of (*R*)-**178** as a white solid after recrystallization from EtOAc: mp 120–122 °C; [α]_D²⁵ -18.3° (*c* 2.4, CHCl₃); R_f = 0.68 (1/9 MeOH/CHCl₃); IR (CHCl₃ film) 3293, 3109, 2859, 2108, 1712, 1635, 1563, 1457, 1384, 1293 cm⁻¹; ¹H NMR (CDCl₃) δ 2.02 (s, CH₃C(O)), 2.60–2.80 (m, CH₂C(O)H), 3.48 (dd, $J = 7.5, 9.6$ Hz, CHCHH'OCH₂CH₂), 3.70–3.78 (m, CH₂OCHH'CH₂C(O)H), 3.78–3.90 (m, CH₂OCHH'CH₂C(O)H), 3.86 (dd, $J = 3.9, 9.6$ Hz, CHCHH'OCH₂CH₂), 4.40 (d, $J = 6.0$ Hz, NHCH₂Ar), 4.52–4.62 (m, CHCH₂O), 6.73 (d, $J = 6.6$ Hz, CH₃C(O)NH), 6.84–7.02 (m, 2 ArH), 7.15–7.20 (m, C(O)NHCH₂, 2 ArH), 9.72 (t, $J = 1.4$ Hz, C(O)H), addition of excess (*R*)-(-)-mandelic acid to a CDCl₃ solution of (*R*)-**178** gave only one signal for the acetyl methyl protons and the aldehyde proton, addition of excess (*R*)-(-)-mandelic acid to a CDCl₃ solution of (*S*)-**178** and (*R*)-**178** (~1:3 ratio) gave two signals for the acetyl methyl

protons (δ 2.027 (*S*) and 2.010 (*R*) (Δ ppm = 0.017)) in a ~1:3 ratio, and two signals for the aldehyde protons (δ 9.671 (*S*) and 9.698 (*R*) (Δ ppm = 0.027)) in a ~1:3 ratio; ^{13}C NMR (CDCl_3) δ 23.3 ($\text{CH}_3\text{C}(\text{O})$), 43.0, 43.7 ($\text{OCH}_2\text{CH}_2\text{C}(\text{O})\text{H}$, NHCH_2Ar), 52.4 ($\text{CHCH}_2\text{OCH}_2$), 64.5 ($\text{OCH}_2\text{CH}_2\text{C}(\text{O})\text{H}$), 70.4 ($\text{CHCH}_2\text{OCH}_2\text{CH}_2\text{C}(\text{O})\text{H}$), 119.3, 129.2, 135.1, 139.3 (C_6H_4), 170.1, 170.6 ($\text{CHC}(\text{O})\text{NH}$, $\text{CH}_3\text{C}(\text{O})\text{NH}$), 201.0 ($\text{C}(\text{O})\text{H}$); M_r (+ESI) 334.1518 $[\text{M}+\text{H}]^+$ (calcd for $\text{C}_{15}\text{H}_{19}\text{N}_5\text{O}_4\text{H}^+$ 334.1515). Anal. Calcd for $\text{C}_{15}\text{H}_{19}\text{N}_5\text{O}_4$: C, 54.05; H, 5.75; N, 21.01. Found: C, 53.90; H, 5.77; N, 20.86.

(*S*)-*N*-(4-Azidobenzyl) 2-Acetamido-3-(3-oxopropoxy)propionamide ((*S*)-178**).**

Using Method E, alcohol (*S*)-**200** (327 mg, 0.98 mmol) in a 2:1 CH_2Cl_2 :DMSO mixture (5 mL), $(\text{COCl})_2$ (127 μL , 1.46 mmol) in CH_2Cl_2 (5 mL), DMSO (207 μL , 2.92 mmol) in CH_2Cl_2 (10 mL), and DIEA (848 μL , 4.87 mmol) gave 188 mg (58%) of (*S*)-**178** as an off-white solid after work-up and recrystallization from EtOAc: mp 120–122 $^\circ\text{C}$; $[\alpha]_D^{25} +18.1^\circ$ (c 1.1, CHCl_3); R_f = 0.68 (1/9 MeOH/ CHCl_3); IR (CHCl_3 film) 3293, 3108, 2859, 2108, 1712, 1635, 1552, 1457, 1384, 1293 cm^{-1} ; ^1H NMR (CDCl_3) δ 2.04 (s, $\text{CH}_3\text{C}(\text{O})$), 2.62–2.82 (m, $\text{CH}_2\text{C}(\text{O})\text{H}$), 3.48 (dd, J = 7.5, 9.3 Hz, $\text{CHCHH}'\text{OCH}_2\text{CH}_2$), 3.70–3.78 (m, $\text{CH}_2\text{OCHH}'\text{CH}_2\text{C}(\text{O})\text{H}$), 3.80–3.88 (m, $\text{CH}_2\text{OCHH}'\text{CH}_2\text{C}(\text{O})\text{H}$), 3.89 (dd, J = 3.9, 9.3 Hz, $\text{CHCHH}'\text{OCH}_2\text{CH}_2$), 4.42 (d, J = 6.0 Hz, NHCH_2Ar), 4.50–4.58 (m, CHCH_2O), 6.64 (d, J = 6.3 Hz, $\text{CH}_3\text{C}(\text{O})\text{NH}$), 6.94–7.20 (m, 2 ArH), 7.04–7.14 (m, $\text{C}(\text{O})\text{NHCH}_2$), 7.22–7.30 (m, 2 ArH), 9.73 (t, J = 1.4 Hz, $\text{C}(\text{O})\text{H}$), addition of excess (*R*)-(-)-mandelic acid to a CDCl_3 solution of (*S*)-**178** gave only one signal for the acetyl methyl protons and the aldehyde proton, addition of excess (*R*)-(-)-mandelic acid to a CDCl_3 solution of (*S*)-**178** and (*R*)-**178**

(~1:3 ratio) gave two signals for the acetyl methyl protons (δ 2.027 (*S*) and 2.010 (*R*) (Δ ppm = 0.017)) in a ~1:3 ratio, and two signals for the aldehyde protons (δ 9.671 (*S*) and 9.698 (*R*) (Δ ppm = 0.027)) in a ~1:3 ratio; ^{13}C NMR (CDCl_3) δ 23.4 ($\text{CH}_3\text{C}(\text{O})$), 43.1, 43.8 ($\text{OCH}_2\text{CH}_2\text{C}(\text{O})\text{H}$, NHCH_2Ar), 52.3 ($\text{CHCH}_2\text{OCH}_2$), 64.5 ($\text{OCH}_2\text{CH}_2\text{C}(\text{O})\text{H}$), 70.3 ($\text{CHCH}_2\text{OCH}_2\text{CH}_2\text{C}(\text{O})\text{H}$), 119.4, 129.3, 135.1, 139.4 (C_6H_4), 170.0, 170.6 ($\text{CHC}(\text{O})\text{NH}$, $\text{CH}_3\text{C}(\text{O})\text{NH}$), 200.9 ($\text{C}(\text{O})\text{H}$); M_r (+ESI) 334.1520 $[\text{M}+\text{H}]^+$ (calcd for $\text{C}_{15}\text{H}_{19}\text{N}_5\text{O}_4\text{H}^+$ 334.1515). Anal. Calcd for $\text{C}_{15}\text{H}_{19}\text{N}_5\text{O}_4$: C, 54.05; H, 5.75; N, 21.01. Found: C, 54.15; H, 5.80; N, 20.75.

(*R*)-*N*-(4-Azidobenzyl) 2-Acetamido-3-(but-3-enyloxy)propionamide ((*R*)-201**).**

Using Method D, (*R*)-**120** (300 mg, 1.50 mmol), benzylamine hydrochloride **134** (330 mg, 1.79 mmol), NMM (200 μL , 1.79 mmol), and DMTMM (495 mg, 1.79 mmol) in THF (15 mL) gave (*R*)-**201** (280 mg, 56%) as a pale yellow solid after purification by flash chromatography (EtOAc) and further recrystallization from EtOAc and hexanes: mp 116–118 $^{\circ}\text{C}$; $[\alpha]_{\text{D}}^{25} +42.4^{\circ}$ (c 0.6; MeOH); R_f = 0.38 (5/95 MeOH/ CH_2Cl_2); IR (nujol) 3285, 3093, 2124, 1640, 1551, 1458, 1378, 1127 cm^{-1} ; ^1H NMR (CDCl_3) δ 2.03 (s, $\text{CH}_3\text{C}(\text{O})$), 2.22–2.36 (m, $\text{CH}_2\text{CH}_2\text{CH}=\text{CH}_2$), 3.40–3.62 (m, $\text{CH}_2\text{OCH}_2\text{CH}_2$, $\text{CHH}'\text{OCH}_2\text{CH}_2$), 3.85 (dd, J = 4.2, 9.0 Hz, $\text{CHH}'\text{OCH}_2\text{CH}_2$), 4.42 (d, J = 7.2 Hz, NHCH_2Ph), 4.44–4.54 (m, CHCH_2O), 4.94–5.08 (m, $\text{CH}_2\text{CH}=\text{CH}_2$), 5.62–5.78 (m, $\text{CH}_2\text{CH}=\text{CH}_2$), 6.45 (d, J = 7.2 Hz, NHCHCH_2O), 6.84–6.96 (m, NHCH_2Ph), 6.99 (d, J = 8.7 Hz, 2 ArH), 7.25 (d, J = 8.7 Hz, 2 ArH), addition of excess (*R*)-(-)-mandelic acid to a CDCl_3 solution of (*R*)-**201** gave only one signal for the acetyl protons (δ 2.011 ppm), addition of excess (*R*)-(-)-mandelic acid to a CDCl_3 solution of (*S*)-**201**

and (*R*)-**201** in a ~3:1 ratio gave two signals with a relative ~3:1 intensity for the acetyl protons (δ 2.019 ppm (*S*), δ 2.011 ppm (*R*), (Δ ppm = 0.008)); ^{13}C NMR (CDCl_3) δ 23.5 ($\text{CH}_3\text{C}(\text{O})$), 34.2 ($\text{CH}_2\text{CH}_2\text{CH}=\text{CH}_2$), 43.2 (NHCH_2Ph), 52.5 ($\text{CHC}(\text{O})\text{NH}$), 69.8, 70.6 ($\text{CHCH}_2\text{OCH}_2$), 117.0 ($\text{CH}_2\text{CH}_2\text{CH}=\text{CH}_2$), 119.5, 129.2, 134.9, 135.3, 139.6 (C_6H_4 , $\text{CH}_2\text{CH}_2\text{CH}=\text{CH}_2$), 170.3, 170.5 ($\text{CH}_3\text{C}(\text{O})$, $\text{CHC}(\text{O})\text{NH}$); M_r (+ESI) 354.1542 $[\text{M}+\text{Na}]^+$ (calcd for $\text{C}_{16}\text{H}_{21}\text{N}_5\text{O}_3\text{Na}^+$ 354.1542). Anal. Calcd for $\text{C}_{16}\text{H}_{21}\text{N}_5\text{O}_3$: C, 57.99; H, 6.39; N, 21.13. Found: C, 58.08; H, 6.30; N, 21.00.

(*S*)-*N*-(4-Azidobenzyl) 2-Acetamido-3-(but-3-enyloxy)propionamide ((*S*)-201**).**

Using Method D, (*S*)-**120** (164 mg, 0.87 μmol), benzylammonium hydrochloride **134** (192 mg, 1.04 mmol), NMM (114 μL , 1.04 mmol), and DMTMM (287 mg, 1.04 mmol) in THF (10 mL) gave (*S*)-**201** (150 mg, 60%) as an off-white solid after purification by flash chromatography (EtOAc) and further recrystallization from EtOAc and hexanes: mp 116–118 $^\circ\text{C}$; $[\alpha]_D^{25}$ -42.1 $^\circ$ (c 0.6; MeOH); R_f = 0.38 (5/95 MeOH/ CH_2Cl_2); IR (nujol) 3278, 3091, 2123, 1640, 1551, 1458, 1378, 1127 cm^{-1} ; ^1H NMR (CDCl_3) δ 2.03 (s, $\text{CH}_3\text{C}(\text{O})$), 2.22–2.36 (m, $\text{CH}_2\text{CH}_2\text{CH}=\text{CH}_2$), 3.40–3.62 (m, $\text{CH}_2\text{OCH}_2\text{CH}_2$, $\text{CHH}'\text{OCH}_2\text{CH}_2$), 3.85 (dd, J = 4.2, 9.0 Hz, $\text{CHH}'\text{OCH}_2\text{CH}_2$), 4.42 (d, J = 7.2 Hz, NHCH_2Ph), 4.44–4.54 (m, CHCH_2O), 4.94–5.08 (m, $\text{CH}_2\text{CH}=\text{CH}_2$), 5.62–5.78 (m, $\text{CH}_2\text{CH}=\text{CH}_2$), 6.45 (d, J = 7.2 Hz, NHCHCH_2O), 6.84–6.96 (m, NHCH_2Ph), 6.99 (d, J = 8.7 Hz, 2 ArH), 7.25 (d, J = 8.7 Hz, 2 ArH), addition of excess (*R*)-(-)-mandelic acid to a CDCl_3 solution of (*S*)-**201** gave only one signal for the acetyl protons (δ 2.011 ppm), addition of excess (*R*)-(-)-mandelic acid to a CDCl_3 solution of (*S*)-**201** and (*R*)-**201** in a ~3:1 ratio gave two signals with a relative ~3:1 intensity for the

acetyl protons (δ 2.019 ppm (S), δ 2.011 ppm (R), (Δ ppm = 0.008)); ^{13}C NMR (CDCl_3) δ 23.4 ($\text{CH}_3\text{C}(\text{O})$), 34.2 ($\text{CH}_2\text{CH}_2\text{CH}=\text{CH}_2$), 43.2 (NHCH_2Ph), 52.5 ($\text{CHC}(\text{O})\text{NH}$), 69.8, 70.6 ($\text{CHCH}_2\text{OCH}_2$), 117.1 ($\text{CH}_2\text{CH}_2\text{CH}=\text{CH}_2$), 119.5, 129.2, 135.0, 135.3, 139.5 (C_6H_4 , $\text{CH}_2\text{CH}_2\text{CH}=\text{CH}_2$), 170.3, 170.5 ($\text{CH}_3\text{C}(\text{O})$, $\text{CHC}(\text{O})\text{NH}$); M_r (+ESI) 354.1536 $[\text{M}+\text{Na}]^+$ (calcd for $\text{C}_{16}\text{H}_{21}\text{N}_5\text{O}_3\text{Na}^+$ 354.1542). Anal. Calcd for $\text{C}_{16}\text{H}_{21}\text{N}_5\text{O}_3$: C, 57.99; H, 6.39; N, 21.13. Found: C, 58.09; H, 6.52; N, 20.85.

(2R)-N-(4-Azidobenzyl) 2-Acetamido-3-(2-(oxiran-2-yl)ethoxy)propionamide ((R)-179) (mixture of diastereomers). Using Method J, (R)-201 (80 mg, 0.24 mmol), Na_2SO_4 (15 mg) and *m*CPBA (77% wt, 176 mg, 0.41 mmol) in CH_2Cl_2 (3 mL) gave (R)-179 (54 mg, 65%) as a mixture of diastereoisomers after purification by flash chromatography (15/85 acetone/EtOAc): mp 105–112 °C; $[\alpha]_D^{25}$ -15.3° (c 0.6; CHCl_3); R_f = 0.33 (15/85 acetone/EtOAc); IR (nujol) 3281, 2123, 1639, 1553, 1459, 1378, 1126 cm^{-1} ; ^1H NMR (CDCl_3) δ 1.50–1.64 (m, $\text{CH}_2\text{CHH}'\text{CH}(\text{O})\text{CH}_2$), 1.92–2.02 (m, $\text{CH}_2\text{CHH}'\text{CH}(\text{O})\text{CH}_2$), 2.03, 2.04 (s, $\text{CH}_3\text{C}(\text{O})$), 2.42–2.50 (m, $\text{CH}_2\text{CH}_2\text{CH}(\text{O})\text{CHH}'$), 2.66–2.74 (m, $\text{CH}_2\text{CH}_2\text{CH}(\text{O})\text{CHH}'$), 2.84–2.98 (m, $\text{CH}_2\text{CH}_2\text{CH}(\text{O})\text{CHH}'$), 3.42–3.52 (m, $\text{CHH}'\text{OCH}_2\text{CH}_2$), 3.54–3.76 (m, $\text{CH}_2\text{OCH}_2\text{CH}_2$), 3.84–3.94 (m, $\text{CHH}'\text{OCH}_2\text{CH}_2$), 4.34–4.48 (m, $\text{NHCH}_2\text{C}_6\text{H}_4$), 4.48–4.58 (m, CHCH_2O), 6.58–6.70 (2 br d, NHCHCH_2O), 6.96 (m, 2 ArH, $\frac{1}{2}$ $\text{NHCH}_2\text{C}_6\text{H}_4$), 7.08–7.18 (m, $\frac{1}{2}$ $\text{NHCH}_2\text{C}_6\text{H}_4$), 7.23 (d, J = 8.2 Hz, 2 ArH), addition of excess (R)-(-)-mandelic acid to a CDCl_3 solution of (R)-179 gave only one set of signals for the acetyl protons (δ 2.025 and 2.017 ppm), addition of excess (R)-(-)-mandelic acid to a CDCl_3 solution of (S)-179 and (R)-179 in a ~2:3 ratio gave two sets of signals with a

relative ~2:3 intensity for the acetyl protons (δ 2.037 and 2.029 ppm (S), δ 2.030 and 2.019 ppm (R)); ^{13}C NMR (CDCl_3) δ 23.4 ($\text{CH}_3\text{C}(\text{O})$), 32.4, 32.6 ($\text{CH}_2\text{CH}_2\text{CH}(\text{O})\text{CH}_2$), 43.2 ($\text{NHCH}_2\text{C}_6\text{H}_4$), 46.7 ($\text{CH}_2\text{CH}_2\text{CH}(\text{O})\text{CH}_2$), 50.5, 50.7, 52.6, 52.7 ($\text{CHC}(\text{O})\text{NH}$, $\text{CH}_2\text{CH}_2\text{CH}(\text{O})\text{CH}_2$), 68.6, 68.9, 69.8, 70.0 ($\text{CHCH}_2\text{OCH}_2$), 119.3, 119.4, 129.3, 135.1, 135.2 (C_6H_4), 170.3, 170.6 ($\text{CH}_3\text{C}(\text{O})$, $\text{CHC}(\text{O})\text{NH}$), the remaining peaks were not detected and are believed to overlap with nearby signals; M_r (+ESI) 370.1491 [$\text{M}+\text{Na}$] $^+$ (calcd for $\text{C}_{16}\text{H}_{21}\text{N}_5\text{O}_4\text{Na}^+$ 370.1491). No satisfactory elemental analysis was obtained for (R)-**179**. The ^1H NMR indicated low levels (<10%) of an additional unidentified compound.

(2S)-N-(4-Azidobenzyl) 2-Acetamido-3-(2-(oxiran-2-yl)ethoxy)propionamide ((S)-179) (mixture of diastereomers). Using Method J, (S)-**201** (100 mg, 0.30 mmol), Na_2SO_4 (25 mg) and *m*-CPBA (77% wt, 131 mg, 0.59 mmol) in CH_2Cl_2 (3 mL) gave (S)-**179** (85 mg, 81%) as a mixture of diastereoisomers after purification by flash chromatography (15/85 acetone/EtOAc): mp 106–112 $^\circ\text{C}$; $[\alpha]_D^{25} +18.8^\circ$ (c 0.6; CHCl_3); $R_f = 0.33$ (15/85 acetone/EtOAc); IR (nujol) 3279, 2122, 1640, 1550, 1459, 1378, 1127 cm^{-1} ; ^1H NMR (CDCl_3) δ 1.50–1.64 (m, $\text{CH}_2\text{CHH}'\text{CH}(\text{O})\text{CH}_2$), 1.84–1.96 (m, $\text{CH}_2\text{CHH}'\text{CH}(\text{O})\text{CH}_2$), 2.02, 2.03 (s, $\text{CH}_3\text{C}(\text{O})$), 2.42–2.48 (m, $\text{CH}_2\text{CH}_2\text{CH}(\text{O})\text{CHH}'$), 2.66–2.74 (m, $\text{CH}_2\text{CH}_2\text{CH}(\text{O})\text{CHH}'$), 2.82–2.98 (m, $\text{CH}_2\text{CH}_2\text{CH}(\text{O})\text{CHH}'$), 3.44–3.52 (m, $\text{CHH}'\text{OCH}_2\text{CH}_2$), 3.54–3.72 (m, $\text{CH}_2\text{OCH}_2\text{CH}_2$), 3.82–3.90 (m, $\text{CHH}'\text{OCH}_2\text{CH}_2$), 4.34–4.50 (m, $\text{NHCH}_2\text{C}_6\text{H}_4$), 4.50–4.60 (m, CHCH_2O), 6.66–6.76 (m, NHCHCH_2O), 6.96 (d, $J = 8.2$ Hz, 2 ArH), 7.06–7.14 (m, 0.5 $\text{NHCH}_2\text{C}_6\text{H}_4$), 7.18–7.28 (m, 2 ArH, 0.5 $\text{NHCH}_2\text{C}_6\text{H}_4$), addition of excess (R)-(-)-

mandelic acid to a CDCl₃ solution of (S)-**179** gave only one set of signals for the acetyl protons (δ 2.040 and 2.032 ppm), addition of excess (R)-(-)-mandelic acid to a CDCl₃ solution of (S)-**179** and (R)-**179** in a ~2:3 ratio gave two sets of signals with a relative ~2:3 intensity for the acetyl protons (δ 2.037 and 2.029 ppm (S), δ 2.030 and 2.019 ppm (R)); ¹³C NMR (CDCl₃) δ 23.3 (CH₃C(O)), 32.4, 32.6 (CH₂CH₂CH(O)CH₂), 43.1 (NHCH₂C₆H₄), 46.6, 46.7 (CH₂CH₂CH(O)CH₂), 50.5, 50.6, 52.6, 52.7 (CHC(O)NH, CH₂CH₂CH(O)CH₂), 68.5, 68.8, 69.8, 70.1 (CHCH₂OCH₂), 119.3, 119.4, 129.2, 135.1, 135.2, 139.3 (C₆H₄), 170.2, 170.5, 170.6 (CH₃C(O), CHC(O)NH) the remaining peaks were not detected and are believed to overlap with nearby signals; *M_r* (+ESI) 370.1494 [M+Na]⁺ (calcd for C₁₆H₂₁N₅O₄Na⁺ 370.1491). No satisfactory elemental analysis was obtained for (S)-**179**. The ¹H NMR indicated low levels (<10%) of an additional unidentified compound.

(2R)-N-(4-Ethynylbenzyl) 2-Acetamido-3-(2-(oxiran-2-yl)ethoxy)propionamide ((R)-180) (~1:1 mixture of diastereomers). Using Method D, (R)-**120** (350 mg, 1.74 mmol), 4-ethynylbenzylamine (272 mg, 2.08 mmol), DMTMM (575 mg, 2.08 mmol) in THF (40 mL) gave a residue that was directly used for the next step. Using Method J, Na₂SO₄ (500 mg) and *m*CPBA (70% by wt., 447 mg, 1.88 mmol) in CH₂Cl₂ (25 mL) were added to give (R)-**180** as a white solid (252 mg, 43% for two steps) after flash chromatography (1/9 to 3/7 acetone/EtOAc) and recrystallization from EtOAc and hexanes: mp 130–136 °C; [α]_D²⁵ -19.2° (c 0.8; CHCl₃); *R_f* = 0.36 (15/85 acetone/EtOAc); IR (nujol) 3275, 3069, 1638, 1550, 1458, 1375, 1298, 1256, 1130 cm⁻¹; ¹H NMR (CDCl₃) δ 1.50–1.64 (m, CH₂CHH'CH(O)CH₂), 1.90–2.04 (m,

CH₂CHH'CH(O)CH₂), 2.03, 2.04 (s, CH₃C(O)), 2.42–2.48 (m, CH₂CH₂CH(O)CHH'), 2.66–2.74 (m, CH₂CH₂CH(O)CHH'), 2.82–2.98 (m, CH₂CH₂CH(O)CHH'), 3.07 (s, ArC≡CH), 3.42–3.52 (m, CHH'OCH₂CH₂), 3.54–3.76 (m, CH₂OCH₂CH₂), 3.84–3.92 (m, CHH'OCH₂CH₂), 4.38–4.50 (m, NHCH₂C₆H₄), 4.51–4.58 (m, CHCH₂O), 6.60–6.72 (m, NHCHCH₂O), 7.02–7.12 (m, 0.5 NHCH₂C₆H₄), 7.14–7.25 (m, 2 ArH, 0.5 NHCH₂C₆H₄), 7.40–7.48 (d, *J* = 8.0 Hz, 2 ArH), addition of excess (*R*)-(-)-mandelic acid to a CDCl₃ solution of (*R*)-**180** gave only one set of signals for the acetyl protons (δ 2.019 and 2.010 ppm), addition of excess (*R*)-(-)-mandelic acid to a CDCl₃ solution of (*S*)-**180** and (*R*)-**180** in a ~1:2 ratio gave two sets of two signals with a relative ~1:2 intensity for the acetyl protons (δ 2.030 and 2.023 ppm (*S*); δ 2.017 and 2.009 ppm (*R*)); ¹³C NMR (CDCl₃) δ 23.4 (CH₃C(O)), 32.4, 32.6 (CH₂CH₂CH(O)CH₂), 43.4 (NHCH₂C₆H₄), 46.7 (CH₂CH₂CH(O)CH₂), 50.5, 50.6, 52.6, 52.7 (CHC(O)NH, CH₂CH₂CH(O)CH₂), 68.6, 68.9, 69.8, 70.1 (CHCH₂OCH₂), 77.5 (ArC≡CH), 83.5 (ArC≡CH), 121.3, 121.4, 127.6, 132.5, 132.6, 139.1, 139.3 (C₆H₄), 170.3, 170.5, 170.6 (CH₃C(O), CHC(O)NH), the remaining signals were not detected and are believed to overlap with nearby peaks; *M_r* (+ESI) 353.1 [M+Na]⁺ (calcd for C₁₈H₂₂N₂O₄Na⁺ 353.1). Anal. Calcd for C₁₈H₂₂N₂O₄: C, 65.44; H, 6.71; N, 8.48. Found: C, 64.76; H, 6.61; N, 8.19.

(2*S*)-*N*-(4-Ethynylbenzyl) 2-Acetamido-3-(2-(oxiran-2-yl)ethoxy)propionamide ((*S*)-180**) (~1:1 mixture of diastereomers).** Using Methods D and J, and following the preceding procedure, (*S*)-**120** (348 mg, 1.73 mmol), amine **141** (272 mg, 2.08 mmol), and DMTMM (575 mg, 2.08 mmol) in THF (40 mL), followed by *m*CPBA

(70% by wt., 447 mg, 1.88 mmol), Na₂SO₄ (500 mg) in CH₂Cl₂ (25 mL) gave (S)-**180** as a white solid (152 mg, 26% for two steps) after work-up, purification by flash chromatography (1/9 to 3/7 acetone/EtOAc) and recrystallization from EtOAc and hexanes: mp 130–136 °C; [α]_D²⁵ +18.7° (c 0.5; CHCl₃); *R*_f = 0.36 (15/85 acetone/EtOAc); IR (nujol) 3281, 3193, 3072, 2861, 1638, 1551, 1458, 1376, 1297, 1256, 1130 cm⁻¹; ¹H NMR (CDCl₃) δ 1.50–1.64 (m, CH₂CHH'CH(O)CH₂), 1.90–2.04 (m, CH₂CHH'CH(O)CH₂), 2.03, 2.04 (s, CH₃C(O)), 2.42–2.48 (m, CH₂CH₂CH(O)CHH'), 2.68–2.74 (m, CH₂CH₂CH(O)CHH'), 2.82–2.98 (m, CH₂CH₂CH(O)CHH'), 3.07 (s, ArC \equiv CH), 3.42–3.52 (m, CHH'OCH₂CH₂), 3.54–3.76 (m, CH₂OCH₂CH₂), 3.84–3.92 (m, CHH'OCH₂CH₂), 4.38–4.50 (m, NHCH₂C₆H₄), 4.51–4.58 (m, CHCH₂O), 6.58–6.72 (m, NHCHCH₂O), 7.02–7.12 (m, 0.5 NHCH₂C₆H₄), 7.14–7.25 (m, 2 ArH, 0.5 NHCH₂C₆H₄), 7.40–7.48 (d, *J* = 8.0 Hz, 2 ArH), addition of excess (*R*)-(-)-mandelic acid to a CDCl₃ solution of (S)-**180** gave only one set of signals for the acetyl protons (δ 2.030 and 2.023 ppm), addition of excess (*R*)-(-)-mandelic acid to a CDCl₃ solution of (S)-**180** and (*R*)-**180** in a ~1:2 ratio gave two sets of two signals with a relative ~1:2 intensity for the acetyl protons (δ 2.030 and 2.023 ppm (*S*); δ 2.017 and 2.009 ppm (*R*)); ¹³C NMR (CDCl₃) δ 23.4 (CH₃C(O)), 32.4, 32.6 (CH₂CH₂CH(O)CH₂), 43.4 (NHCH₂C₆H₄), 46.7 (CH₂CH₂CH(O)CH₂), 50.5, 50.6, 52.6, 52.7 (CHC(O)NH, CH₂CH₂CH(O)CH₂), 68.6, 68.9, 69.8, 70.1 (CHCH₂OCH₂), 77.5 (ArC \equiv CH), 83.5 (ArC \equiv CH), 121.4, 127.6, 132.5, 132.6, 139.1, 139.3 (C₆H₄), 170.3, 170.6 (CH₃C(O), CHC(O)NH), additional signals were not detected and are believed to overlap with nearby peaks; *M*_r (+ESI)

353.1 $[M+Na]^+$ (calcd for $C_{18}H_{22}N_2O_4Na^+$ 353.1). Anal. Calcd for $C_{18}H_{22}N_2O_4$: C, 65.44; H, 6.71; N, 8.48. Found: C, 65.17; H, 6.58; N, 8.28.

2.3.3.4. Synthesis of biotin and fluorescent Probes

1,11-Diazido-3,6,9-trioxaundecane (184).⁴¹⁷ To a cooled (ice bath) CH_2Cl_2 solution (250 mL) of tetraethylene glycol (10.30 g, 52.9 mmol) and Et_3N (16.5 mL, 60.8 mmol) was added $MsCl$ (9.16 mL, 60.8 mmol) dropwise. The reaction was then stirred at room temperature (2 h), the salts filtered, and the CH_2Cl_2 layer washed with aqueous 10% citric acid (250 mL) and brine (250 mL). The organic layer was dried (Na_2SO_4) and evaporated to yield tetraethyleneglycol dimesylate (**183**) as a yellow liquid residue (18.70 g, quant.). Dimesylate **183** was dissolved in DMF (50 mL) and NaN_3 (8.65 g, 133 mmol) was added. The solution was stirred at 80 °C (12 h) and cooled to room temperature. H_2O (450 mL) was added to the DMF and the mixture was extracted with Et_2O (8 x 50 mL). The organic layers were combined, dried (Na_2SO_4), and evaporated to yield **184** (10.74 g, 83%) as a pale yellow liquid that was used directly in the next step: R_f = 0.23 (2/1 hexanes/ $EtOAc$); 1H NMR ($CDCl_3$) δ 3.39 (t, J = 5.1 Hz, 2 CH_2N_3), 3.65–3.70 (m, 6 OCH_2); ^{13}C NMR ($CDCl_3$) δ 50.9 ($OCH_2CH_2N_3$), 70.2 ($OCH_2CH_2N_3$), 70.9 (2 OCH_2CH_2O).

1-Amino-11-azido-3,6,9-trioxaundecane (185).⁴¹⁷ Compound **184** (1.52 g, 6.22 mmol) was dissolved in a mixture of $EtOAc$ (50 mL) and aqueous 1 M HCl (10 mL). PPh_3 (1.94 g, 7.40 mmol) was added and the reaction was vigorously stirred (12 h). The aqueous layer was separated, extracted with $EtOAc$ (4 x 50 mL), basified (pH

~11) with solid K_2CO_3 , saturated with NaCl, and extracted with CH_2Cl_2 (6 x 30 mL) to yield **185** (950 mg, 70%) as a colorless residue that was used without further purification: R_f = 0.18 (1/9 MeOH/ $CHCl_3$); 1H NMR ($DMSO-d_6$) δ 2.74 (t, J = 5.4 Hz, CH_2NH_2), 3.36–3.46 (m, CH_2N_3 , $CH_2CH_2NH_2$), 3.48–3.62 (m, 2 OCH_2CH_2O , $CH_2CH_2N_3$), 3.84–4.08 (m, CH_2NH_2); ^{13}C NMR ($DMSO-d_6$) δ 40.5 (CH_2NH_2), 50.0 ($OCH_2CH_2N_3$), 69.2, 69.5, 69.6, 69.7, 69.8, 71.3 (6 OCH_2).

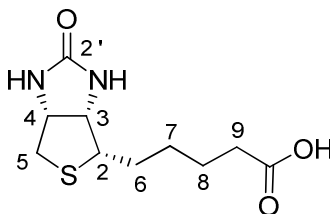
3,6,9,12-Tetraoxapentadec-14-yn-1-ol (186).⁴¹⁸ To a cooled (ice bath) THF solution (50 mL) of tetraethylene glycol (2.00 g, 10.3 mmol) was added NaH (60% suspension in oil, 272 mg, 11.34 mmol). After stirring at 0 °C (15 min), propargyl bromide (80% wt in toluene, 1.68 mL, 11.34 mmol) was added dropwise at 0 °C, the suspension warmed to room temperature and stirred (1 h). The salts were removed by filtration, the filtrate was concentrated in vacuo and purified by flash chromatography to yield **186** as a colorless oil (642 mg, 27%): R_f = 0.58 (1/9 MeOH/ $CHCl_3$); 1H NMR ($CDCl_3$) δ 2.44 (t, J = 2.2 Hz, OCH_2CCH), 2.68 (t, J = 6.3 Hz, CH_2OH), 3.58–3.64 (m, CH_2OH), 3.64–3.76 (m, 3 CH_2OCH_2 , CH_2OCH_2CCH), 4.21 (d, J = 2.2 Hz, CH_2CCH); ^{13}C NMR ($CDCl_3$) δ 58.6 (CH_2CCH), 61.9 (CH_2OH), 69.3, 70.5, 70.6, 70.7, 70.8, 70.9, 72.7 (7 OCH_2), 74.7 (CH_2CCH), 79.8 (CH_2CCH).

1-Azido-3,6,9,12-tetraoxapentadec-14-yne (188). To a cooled (0 °C) THF solution (25 mL) of **186** (624 mg, 2.69 mmol), Et_3N (450 μ L, 3.22 mmol) was added mesyl chloride (250 μ L, 3.22 mmol) dropwise. After stirring at room temperature (45 min), the salts were filtered, and the filtrate concentrated in vacuo. The residue was

dissolved in CH₂Cl₂ (25 mL), successively washed with aqueous 10% citric acid (25 mL) and brine (25 mL), dried (Na₂SO₄) and evaporated to dryness. The crude mesylated product **187** (788 mg, 2.54 mmol, 94%) was directly dissolved in DMF (10 mL). NaN₃ was added (214 mg, 3.3 mmol) and the reaction was heated at 60 °C (18 h). The reaction was cooled, H₂O (90 mL) was added and the mixture was extracted with Et₂O (3 x 100 mL). The combined organic layers were successively washed with H₂O (2 x 50 mL), brine (50 mL), and dried (Na₂SO₄). The solvents were removed under vacuum to yield **188** as pale yellow oil (400 mg, 61%) that was used without further purification: *R*_f = 0.46 (5/95 MeOH/CH₂Cl₂); IR (neat) 3251, 2869, 2106, 1454, 1531, 1293, 1107 cm⁻¹; ¹H NMR (CDCl₃) δ 2.44 (t, *J* = 2.2 Hz, OCH₂CCH), 3.41 (t, *J* = 5.1 Hz, CH₂N₃), 3.62–3.74 (m, 3 CH₂OCH₂, CH₂OCH₂CCH), 4.21 (d, *J* = 2.2 Hz, CH₂CCH); ¹³C NMR (CDCl₃) δ 50.9 (CH₂N₃), 58.6 (CH₂CCH), 69.3, 70.2, 70.5, 70.6, 70.7, 70.8, 70.9 (7 OCH₂), 74.7 (CH₂CCH), 79.8 (CH₂CCH); *M*_r (+ESI) 296.1012 [M+K]⁺ (calcd for C₁₁H₁₉N₃O₄K⁺ 296.1013).

3,6,9,12-Tetraoxapentadec-14-yn-1-amine (189). Azide **188** (355 mg, 1.38 mmol) was dissolved in THF (20 mL) and PPh₃ (724 mg, 2.74 mmol) was added. After dissolution, H₂O (1 mL) was added and the reaction was stirred at room temperature (12 h). The solvents were removed in vacuo, the residue was dissolved in aqueous 0.1 M HCl (20 mL), and washed with CH₂Cl₂ (6 x 80 mL) and EtOAc (2 x 100 mL). The aqueous layer was evaporated to dryness and the remaining salts were suspended in CH₂Cl₂ (25 mL), vigorously stirred (5 min), and filtered. The cake was extensively rinsed with CH₂Cl₂, and the combined organic fractions were evaporated

to yield **189** (247 mg, 77%) as a hygroscopic pale yellow oil that did not require further purification: $R_f = 0\text{--}0.10$ (1/9 MeOH/CH₂Cl₂); IR (neat) 3367, 2870, 2112, 1661, 1596, 1457, 1353, 1294, 1250 cm⁻¹; ¹H NMR (CDCl₃) δ 1.38–1.56 (br s, CH₂NH₂), 2.44 (t, $J = 2.2$ Hz, OCH₂CCH), 2.87 (t, $J = 5.4$ Hz, CH₂NH₂), 3.51 (t, $J = 5.4$ Hz, CH₂CH₂NH₂), 3.60–3.75 (m, 2 CH₂OCH₂, CH₂OCH₂CCH, CH₂OCH₂CH₂NH₂), 4.21 (d, $J = 2.2$ Hz, CH₂CCH); ¹³C NMR (CDCl₃) δ 42.0 (CH₂NH₂), 58.6 (CH₂CCH), 69.3, 70.5, 70.6, 70.7, 70.8, 73.7 (6 OCH₂), 74.7 (CH₂CCH), 79.8 (CH₂CCH), the remaining signal was not detected and is believed to overlap with nearby peaks; M_r (+ESI) 232.1547 [M+H]⁺ (calcd for C₁₁H₂₁NO₄H⁺ 232.1549). Anal. Calcd for C₁₁H₂₁NO₄•0.35H₂O: C, 55.60; H, 9.21; N, 5.89; Found: C, 55.34; H, 8.95; N, 6.26.



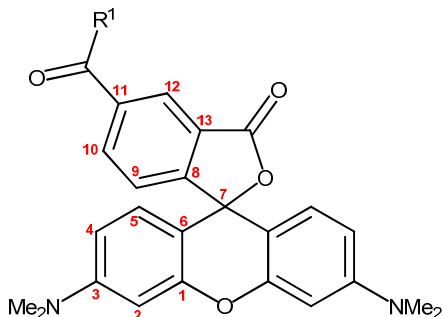
Biotin-PEG-azide (191).⁴¹⁸ Using Method D, amine **185** (415 mg, 1.9 mmol), D-biotin (464 mg, 1.9 mmol) and DMTMM (525 mg, 1.9 mmol) in DMF (20 mL) were stirred at room temperature (12 h). The DMF was removed in vacuo and the residue directly purified using flash chromatography (1/9 MeOH/CHCl₃) to yield biotin-PEG-azide **191** as an off-white solid (523 mg, 62%): mp 118–119 °C; $R_f = 0.40$ (1/9 MeOH/CHCl₃); ¹H NMR (CD₃OD) δ 1.45 (q, $J = 7.2$ Hz, C(6)H₂), 1.50–1.80 (m, C(7)H₂, C(8)H₂), 2.22 (t, $J = 7.2$ Hz, C(9)H₂), 2.70 (d, $J = 12.6$ Hz, C(5)HH'), 2.92 (dd, $J = 4.8, 12.6$ Hz, C(5)HH'), 3.18–3.25 (m, C(2)H), 3.32–3.45 (m, NHCH₂CH₂,

CH₂N₃), 3.55 (t, J = 5.7 Hz, NHCH₂CH₂O), 3.59–3.71 (m, 2 OCH₂CH₂O, OCH₂CH₂N₃), 4.30 (dd, J = 4.8, 7.8 Hz, C(3)H), 4.49 (ddd, J = 0.9, 4.8, 7.8 Hz, C(4)H); ¹³C NMR (CD₃OD) δ 27.0 (C(6)), 29.6, 29.9 (C(7), C(8)), 36.9 (C(9)), 40.6 (NHCH₂CH₂O), 41.2 (C(5)), 51.9 (OCH₂CH₂N₃), 57.1 (C(2)), 61.8 (C(4)), 63.5 (C(3)), 70.7 (NHCH₂CH₂O), 71.3, 71.4, 71.6, 71.7, 71.8 (2 OCH₂CH₂O, OCH₂CH₂N₃), 166.3 (C(2')), 176.3 (C(O)NHCH₂).

Biotin-PEG-amine (192).⁴²² Compound **191** (235 mg, 0.53 mmol) was suspended in THF (5 mL), and PPh₃ (208 mg, 0.79 mmol) was added. After 15 min stirring, H₂O (2 mL) was added and the reaction was stirred at room temperature (24 h). Aqueous 1 M HCl was added (5 mL) to the reaction and the mixture was washed with EtOAc (3 x 20 mL). The aqueous layer was basified (pH ~11) with K₂CO₃, saturated with NaCl, and then extracted with EtOAc (5 x 20 mL) and CH₂Cl₂ (5 x 20 mL). The aqueous layer was concentrated in vacuo and the residual salts triturated repeatedly with CH₂Cl₂ and filtered. The combined organic layers were evaporated to yield **192** (110 mg, 50%) as a colorless residue that did not require further purification: $[\alpha]^{25}_{\text{D}} +40.4^\circ$ (c 1.6, CH₂Cl₂); R_f = 0.15 (1/4 MeOH/CHCl₃); ¹H NMR (CD₃OD) δ 1.58 (q, J = 7.2 Hz, C(6)H₂), 1.66–1.92 (m, C(7)H₂, C(8)H₂), 2.36 (t, J = 7.2 Hz, C(9)H₂), 2.84 (d, J = 12.6 Hz, C(5)HH'), 2.92 (br t, J = 5.1 Hz, OCH₂CH₂NH₂), 3.07 (dd, J = 4.8, 12.6 Hz, C(5)HH'), 3.30–3.39 (m, C(2)H), 3.50 (t, J = 5.1 Hz, C(O)NHCH₂), 3.62–3.71 (m, NHCH₂CH₂O, OCH₂CH₂NH₂), 3.72–3.84 (m, 2 OCH₂CH₂O, OCH₂CH₂N₃), 4.44 (dd, J = 4.8, 7.8 Hz, C(3)H), 4.49 (ddd, J = 0.6, 4.8, 7.8 Hz, C(4)H); ¹³C NMR (CD₃OD) δ 26.8 (C(6)), 29.5, 29.7 (C(7), C(8)), 36.7 (C(9)), 40.6 (NHCH₂CH₂O), 41.2 (C(5)),

42.1 (OCH₂CH₂NH₂), 51.9 (OCH₂CH₂N₃), 57.1 (**C**(2)), 61.8 (**C**(4)), 63.5 (**C**(3)), 70.7 (NHCH₂CH₂O), 71.2, 71.5, 71.6 (3 OCH₂), 73.5 (OCH₂CH₂NH₂), 166.0 (**C**(2')), 176.0 (**C**(O)NHCH₂), the remaining methylene signal was not detected and is believed to overlap with a nearby peak; *M_r* (+ESI) 419.2324 [M+H]⁺ (calcd for C₁₈H₃₄N₄O₅SH⁺ 419.2328).

Biotin-PEG-alkyne (193).⁴²³ Using Method D, amine **192** (96 mg, 229 μmol), 4-pentynoic acid (27 mg, 275 μmol) and DMTMM (76 mg, 275 μmol) in THF (5 mL) gave compound **193** (85 mg, 75%) as a white solid after silica gel flash chromatography (1/9 MeOH/CHCl₃): mp 108–110 °C; [α]_D²⁵ +25.3° (c 1.1, CHCl₃); *R_f* = 0.47 (1/9 MeOH/CHCl₃); ¹H NMR (CD₃OD) δ 1.45 (q, *J* = 7.2 Hz, C(6)H₂), 1.50–1.80 (m, C(7)H₂, C(8)H₂), 2.22 (t, *J* = 7.2 Hz, C(9)H₂), 2.29 (t, *J* = 2.6 Hz, CH₂C≡CH), 2.35–2.50 (m, CH₂CH₂C≡CH), 2.70 (d, *J* = 12.6 Hz, C(5)HH'), 2.92 (dd, *J* = 4.8, 12.6 Hz, C(5)HH'), 3.18–3.25 (m, C(2)H), 3.32–3.42 (m, NHCH₂CH₂O, OCH₂CH₂NH), 3.55 (app. t, *J* = 5.1 Hz, NHCH₂CH₂O, OCH₂CH₂NH), 3.59–3.71 (m, OCH₂CH₂O), 4.30 (dd, *J* = 4.8, 7.8 Hz, C(3)H), 4.49 (ddd, *J* = 0.6, 4.8, 7.8 Hz, C(4)H); ¹³C NMR (CD₃OD) δ 15.9 (CH₂CCH), 27.0 (**C**(6)), 29.6, 29.9 (**C**(7), **C**(8)), 36.1 (CH₂CH₂C≡CH) 36.9 (**C**(9)), 40.5, 40.6 (NHCH₂CH₂O, OCH₂CH₂NH), 41.2 (**C**(5)), 51.9 (OCH₂CH₂N₃), 57.1 (**C**(2)), 61.8 (**C**(4)), 63.5 (**C**(3)), 70.7 (NHCH₂CH₂O), 71.3, 71.4, 71.6, 71.7, 71.8 (2 OCH₂CH₂O, OCH₂CH₂N₃), 83.7 (**C**≡CH) 166.3 (**C**(2')), 176.3 (**C**(O)NHCH₂), the remaining alkyne carbon resonance was not detected. *M_r* (+ESI) 522.2407 [M+Na]⁺ (calcd for C₂₃H₃₈N₄O₆SN⁺ 522.2410).



TAMRA-PEG-alkyne (195). Using Method D, 5-carboxytetramethylrhodamine (20 mg, 47 μ mol), compound **189** (14 mg, 61 μ mol), and DMTMM (17 mg, 61 μ mol) in DMF (500 μ L) gave **195** as a dark pink residue (10 mg, 33%) after purification by preparative TLC (5/95 to 15/85 MeOH/CH₂Cl₂): R_f = 0.25 (1/9 MeOH/CH₂Cl₂); ¹H NMR (CD₃OD) δ 2.85 (t, J = 2.4 Hz, OCH₂CCH), 3.30 (s, 2 N(CH₃)₂), 3.60–3.80 (m, 3 CH₂OCH₂, NHCH₂), 4.17 (d, J = 2.4 Hz, CH₂CCH), 6.92–7.08 (m, 2 C(4)H, 2 C(2)H), 7.13–7.28 (m, 2 C(5)H), 7.41 (d, J = 8.7 Hz, C(9)H), 8.09 (d, J = 8.7 Hz, C(10)H), 8.60–8.75 (br s, C(12)H); ¹³C NMR (CD₃OD) δ 41.0 (2 N(CH₃)₂), 41.3 (C(O)NHCH₂), 59.2 (CH₂CCH), 70.2, 70.7, 71.4, 71.5, 71.6, 71.7, 71.8 (7 OCH₂), 76.1 (CH₂CCH), 80.8 (CH₂CCH), 97.5, 115.0, 115.2, 129.9, 131.0, 132.7, 137.3, 158.9, 159.2, 162.3, 169.4 (TAMRA), the remaining signals were not detected; M_r (+ESI) 644.2968 [M+H]⁺ (calcd for C₃₆H₄₁N₃O₈H⁺ 644.2972).

TAMRA-PEG-azide (196). 5,6-Carboxy-TAMRA (25 mg, 58 μ mol) and amine **185** (12.6 mg, 70 μ mol) were dissolved in DMF (300 μ L) and EDCI (13 mg, 70 μ mol), DMAP (1 mg, catalytic), DIEA (12 μ L, 70 μ mol) were successively added. After stirring at room temperature (1 d), the DMF was evaporated and the residue purified by silica gel chromatography (1/9 to 1/3 MeOH/CH₂Cl₂) to yield 16 mg (44%) of **196**

as a deep purple solid: $R_f = 0.25$ (1/9 MeOH/CH₂Cl₂); ¹H NMR (CD₃OD) δ 3.20–3.40 (m, CH₂N₃, 2 N(CH₃)₂), 3.50–3.80 (m, 3 CH₂OCH₂, NHCH₂), 6.92–7.08, 7.20–7.30, 7.38–7.42, 7.72–7.76, 8.05–8.20, 8.55–8.60 (m, 2 C(4)H, 2 C(2)H, 2 C(5)H, C(9)H, C(10)H, C(12)H); ¹³C NMR (CD₃OD) δ 40.4, 41.0, 41.3 (2 N(CH₃)₂, C(O)NHCH₂), 51.9 (CH₂N₃), 70.7, 71.3, 71.5, 71.7, 71.8 (5 OCH₂), 97.4, 108.4, 115.1, 115.3, 130.2, 131.2, 132.7, 132.9, 137.3, 137.5, 159.0, 159.2, 163.1, 169.2 (TAMRA), the remaining signals were not detected; M_r (+ESI) 631.2876 [M+H]⁺ (calcd for C₃₃H₃₈N₆O₇H⁺ 631.2881).

CHAPTER 3

PROTEIN CHEMISTRY IN THE EYE OF THE CHEMIST

SAR studies demonstrated that placement of AB&CR moieties at the 3-oxy site and the 4'-benzylamide positions in (*R*)-LCM did not lead to significant loss of anticonvulsant activity in the MES test. In those cases where an electrophilic AB agent was inactive, the activity of the corresponding isostere suggested that the AB group could be used in *in vitro* experiments, where metabolism is less likely an issue. With these molecular tools at hand, we advanced to the biological questions of this project. In the following sections, general methods to prepare a protein lysate from animal tissues are presented, along with the protein purification methods used in these studies. These methods are detailed, discussed and explained from the perspective of an organic chemist learning how to manipulate large molecules of complexity. Considerations concerning click chemistry in a biological setting are also discussed.

3.1. General procedures for rat brain fractionation

Differential centrifugation is a widely used method to separate subcellular compartments from a given tissue.⁴²⁴⁻⁴²⁷ It is usually preferred to use freshly prepared tissue samples, by sacrificing the animal and removing the organs

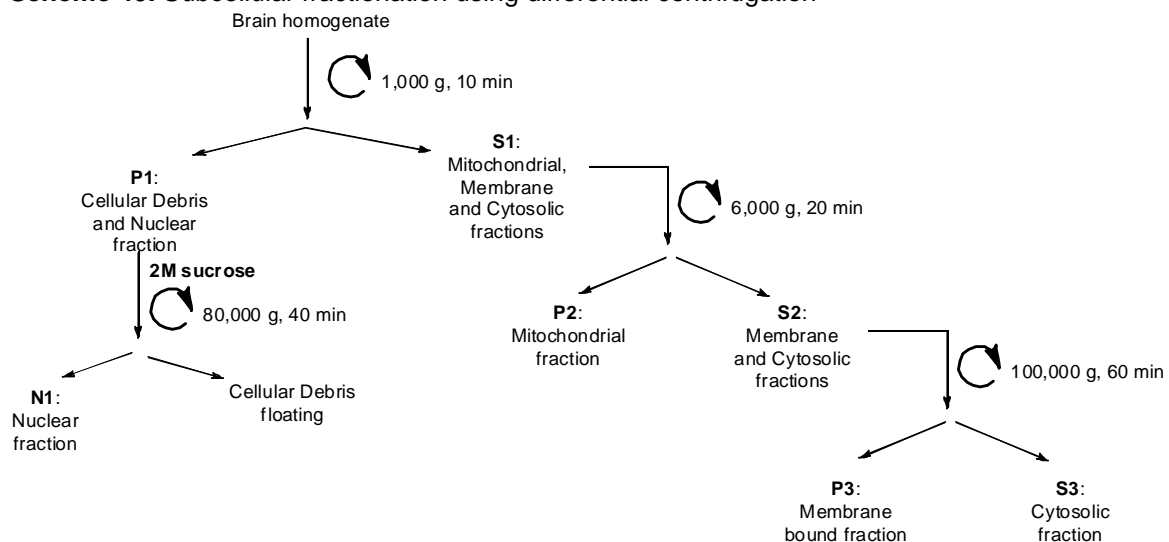
immediately before subcellular fractionation.⁴²⁴ This ensures minimal subcellular cross-contamination that may arise from freeze/thaw cycles-induced compartment leakage. In our case, the purchased rat brains (6-7 weeks old, 200–300 g, male Sprague-Dawley rats, Rockland Immunochemicals or Pel-Freez Biologicals) were frozen in liquid nitrogen upon decapitation. The brains were shipped and received in dry ice, stored at -80 °C and thawed prior to fractionation.

The first tissue preparation step involves homogenizing the tissue in an appropriate homogenization buffer at 4 °C. A key component in the buffer used is sucrose (280–320 mM), and serves as a molecular cushion to prevent the disruption of membranes (nucleus and organelles) by osmotic shock. Dounce homogenizers (glass/glass or glass/Teflon) are generally preferred to electric grinder or sonicators as they constitute a gentler way to disrupt tissues by shearing, leaving the bigger organelles intact. The clearance of the Dounce homogenizer is critical as a fitting too tight will lead to rupture of intracellular compartments and subcellular cross-contamination.

After grinding the tissue in a homogenization buffer the resulting crude homogenate can undergo several differential centrifugation steps to yield different subcellular compartments. The homogenization buffer typically includes a given buffer (5–50 mM Tris or HEPES [pH 7.4–8.0]), 320 mM sucrose, 5 mM MgCl₂ (improves stability of nuclei), and protease inhibitors. Generally, protease inhibitors were included in the different buffers to prevent proteolytic degradation that occurs as soon as the tissue is thawed. Accordingly, the following inhibitors were used for our studies. PMSF (paramethylsulfonyl fluoride) is an irreversible serine protease

inhibitor (working concentration 1 mM, 100 X stock solution in ethanol). PMSF hydrolyzes quickly in aqueous solutions, and should therefore be dissolved right before the homogenization step. E-64 (*N*-(trans-epoxysuccinyl)-L-leucine 4-guanidinobutylamide) is an epoxide containing tripeptide mimic that acts as an irreversible and selective inhibitor of cysteine proteases but does not inactivate proteins containing reactive cysteine groups (working concentration 10 μ M, 100 X stock in water). Pepstatin-A is a peptide analog that acts as a reversible inhibitor of aspartyl proteases. Because of the reversible nature of the inhibitor, the lysate studied should be resupplemented with pepstatin-A after a dialysis step, and before storing the lysate at -80 $^{\circ}$ C (working concentration 1 μ M, 100 X stock in DMSO). TPEN (*N,N,N',N'*-Tetrakis(2-pyridylmethyl)ethylenediamine) is a tight chelator of Zn^{2+} ($\text{pK}_d = 15.2$ at pH 7.6)⁴²⁸ that prevents activation of zinc metalloproteases. As for Pepstatin A, this inhibitor should be resupplemented after a small molecule removing step such as dialysis (working concentration 1 μ M, 100 X stock in ethanol).

Scheme 40. Subcellular fractionation using differential centrifugation



For our studies using rat brains, we utilized the following lysate preparation protocol (Scheme 40). All the following steps were carried out at 4 °C. The protocol was adapted from literature procedures.^{424-426,429}

3.1.1. The nuclear fraction (N1)

N1 is obtained by centrifugating the crude homogenate at low speed (1,000 g) and comes with all the cellular debris. The supernatant (**S1**) is pulled for further separation. The pellet is rinsed 2 or 3 times with homogenization buffer and then resuspended in a high sucrose buffer (~4 to 5 times the approximate volume of the pellet), consisting of a given buffer (5–50 mM Tris or HEPES, pH 7.4), 2 M sucrose, and 5 mM MgCl₂. This suspension is then carefully and slowly layered on top of another high sucrose gradient (2 M) in an ultracentrifuge tube and spun at 80,000 g for 30–40 min. An optional step can be included at this stage that entails filtering the suspension through several layers of cheese cloth or gauze to remove most of the cellular debris, allowing the following step to be cleaner. While it is recommended that sucrose gradient separations be conducted with a swing bucket rotor, it was found that a fixed-angle rotor works fine for this procedure. Upon centrifugation (80,000 g, 35 min), the cellular debris (if not removed by filtration) is found floating at the surface of the tube due to the buoyancy of the solution, while pure nuclei, visible as a white fluffy cloud-like aggregate are pelleted at the bottom of the tube. Nuclei can be recovered by gently removing the supernatant with a pipette, and then the nuclear aggregate is rinsed one time with homogenization buffer (5 mL per rat brain nuclear fraction) to remove the sucrose.

Nuclei are generally lysed under hypertonic conditions (high salt) that cause the disruption of the nuclear membrane. A typical nuclear lysis buffer includes a given buffer (5-50 mM Tris or HEPES [pH 7.4–8.0]), 400–500 mM NaCl, 1.5 mM MgCl_2 , 10–20% glycerol, and protease inhibitors. A high salt concentration and the presence of glycerol are critical to maintain proper folding of nuclear soluble proteins (mimics the high protein density inside the nucleus) as its removal by dialysis causes ~70% of nuclear proteins to precipitate. Nuclei are resuspended in the lysis buffer and can be sheared by 10 syringe passages through a 18 or 20 gauge needle. The suspension is gently rocked at 4 °C for 30 min. The DNA is then found floating at the surface as a white viscous material and removed with a pipette tip. Centrifugation at 14,000 rpm at 4 °C yields a soluble nuclear fraction as a supernatant and a nuclear membrane fraction as a pellet. The pellet is resuspended in a buffer typically consisting of a given buffer (5–50 mM, Tris or HEPES [pH 7.4–8.0]), 1.5 mM MgCl_2 , 100 mM KCl, 10–20% glycerol and 0.5%–1% of a desired non-ionic detergent (Triton X-100, β -Dodecylmatoside, Zwittergent 3-10) and gently rocked at 4 °C for another 30 min. Centrifugation at 14,000 rpm for 10 min provides a solubilized membrane fraction. The fractions are stored at -80 °C and the pellet is discarded.

The soluble nuclear fraction should be resuspended in the smallest possible volume of nuclear lysis buffer and diluted with 4 volumes of lysis buffer depleted in NaCl to reduce the salt concentration to 100 mM NaCl to permit subsequent chemical biology experiments. Final protein concentration should be ideally 1–2 mg.mL^{-1} .

3.1.2. The mitochondrial fraction (P2)

P2 is obtained by centrifugation of the **S1** supernatant at 6,000 g. The supernatant **S2** is pulled for further purification. The mitochondrial fraction is comprised of mitochondria as well as the major cellular organelles (Golgi apparatus). The brain mitochondrial fraction is visible as a dark brown pellet and is lysed by osmotic shock with a hypotonic buffer (low salt). A typical mitochondrial lysis buffer includes a low concentration of buffer (5 mM Tris or 10 mM HEPES, pH 7.4) and protease inhibitors. The suspension is then gently rocked for 30 min at 4 °C and spun at 9,000 g for 30 min. The supernatant is then supplemented to a “normal” buffer concentration (5–50 mM Tris or HEPES, pH 7.4) and 50 mM NaCl. The pellet is then resuspended in a given buffer (5–50 mM Tris or HEPES, pH 7.4) containing 100 mM KCl and 0.5–1% of a desired detergent and gently rocked for 30 min at 4 °C. Centrifugation at 9,000 g for 30 min provides a solubilized mitochondrial membrane fraction. The fractions are stored at -80 °C and the pellet is discarded.

3.1.3. The membrane fraction (P3)

P3 is obtained by centrifugation of the **S2** supernatant. Centrifuging at 100,000 g or more for 1 h provides the membrane fractions, also called microsomal fraction. Supernatant **S3** is pulled. The pellet obtained is resuspended in a given buffer (5–50 mM Tris or HEPES, pH 7.4), 100 mM KCl, 0.5%–1% of a desired detergent, and 15% glycerol and protease inhibitors, and then gently rocked for 30 min at 4 °C and centrifuged at 14,000 rpm (15 min) to provide a solubilized membrane fraction. The fraction is stored at -80 °C and the pellet is discarded.

3.1.4. The cytoplasmic fraction (S3)

S3 contains the soluble, cytoplasmic proteins. Typically, approximately 40 mg of total cytoplasmic protein (Bradford Assay) are obtained per rat brain. The lysate (~20 mL per brain) is then dialyzed at 4 °C for 2 h against 3 L of a given buffer (5–50 mM Tris or HEPES, pH 7.4) containing 50 mM NaCl, changing the buffer after 1 h. Upon dialysis, the cytoplasmic fraction is resupplemented to 10 μ M pepstatin A and 1 μ M TPEN and stored at -80 °C.

3.2. Ammonium sulfate fractionation

Ammonium sulfate (AMS) fractionation is a widely used protein fractionation method^{426,430-432} that uses the ability of high ionic concentrations to negate electrostatic repulsive charges on the solvent-exposed regions of a protein, leading to protein aggregation and precipitation. All proteins possess a specific AMS concentration range between which they progressively precipitate. That range is likely to change if the protein undergoes a conformational change, and therefore both pH and ligand binding can affect the needed AMS value for precipitation.

In contrast with protein denaturing precipitating conditions (trichloroacetic acid/acetone), AMS precipitation is non-denaturing and is very often the first step utilized in protein purification protocols or enrichment methods from a complex mixture. The protein pellet obtained from a given AMS fraction can be readily redissolved (1 to 10 min) by letting it stand in a desired buffer (5–50 mM HEPES or

Tris). If further protein purification is needed, it may be necessary to remove the excess AMS present in solution by dialysis, particularly if the following step involves ion exchange chromatography. A high amount of residual AMS present in a sample can be detrimental to S or Q Sepharose[®] fractionation as it will interact with the support's charged chemical groups and reduce their availability for proteins.

As a general trend, we observed that a slight majority of proteins that precipitated at low AMS saturation were of medium to high molecular weight (40–100 kDa) while a higher percentage lower molecular weight proteins (10–40 kDa) were found to precipitate in the higher AMS cut (>60–70%). Also, we did not observe proteins precipitating before ~15% AMS saturation. This information is important for the use of Phenyl Sepharose[®]. We also noticed an interesting pH-dependency in the AMS fractionation studies. At low levels (<30% AMS saturation), we found that as we lowered pH values from 8.5 to 7.5 to 6.5 we saw a general increase in the relative amounts of proteins that precipitate and it appeared that with decreasing pH we saw a buildup of large MW protein in the precipitate. At high AMS levels (>60–70%), as the pH of the buffer was decreased from 8.5 to 7.5 to 6.5 we observed the opposite trend. At high pH (8.5) we detected higher amounts of protein with pH 7.5 and 6.5.

AMS can be added either as a solution (aqueous AMS saturated solution, 4.1 M at room temperature) or as a solid. While it is easier to add a known precise volume (adding one volume of aqueous saturated AMS brings the solution to 50% saturation) this method becomes impractical at high AMS saturation (e.g., 9 volumes are required to bring a solution to 90% saturation) since it requires the use of larger

containers or multiple small containers. Moreover this method dilutes the proteins in solution and therefore increases the risk that the protein will not precipitate. Generally our experiments were carried out using AMS as a fractionation method employing liquid AMS up to 65-70% saturation (adding ~2 volumes of AMS_{sat}) and using solid AMS to saturate from 70 up to 95%. The amount of solid added was calculated using online software (<http://www.encorbio.com/protocols/AM-SO4.htm>) that takes into account the specific volume of AMS added to the solution.

A typical experiment involves the following protocol. A given volume of aqueous saturated AMS is added to the protein solution to bring the solution to the desired saturation, and the sample is gently mixed. The solution is allowed to stand at room temperature for 5 min and then centrifuged at 14,000 rpm for 4 min. The supernatant is transferred to another tube, and the process is repeated using the same procedure to obtain another protein AMS cut. Fractionation conducted in this way allowed the whole lysate to be “cut” in 5-6 different fractions within 90 min, including all the equilibration, centrifugation and supernatant transfer steps. The different cuts are hereon referred to as MXXYY, which designate the fraction that precipitate between XX% and YY% AMS saturation.

3.3. Ion exchange chromatography

Ion exchange resins are useful tools in protein purification and many different types have been developed. Protein ion exchange chromatography relies on the ability of proteins to form non-covalent electrostatic interactions between charged

amino acids and complementarily charged chemical groups covalently attached to a solid matrix.⁴³³

In this method, the protein solution is incubated with the pre-equilibrated ion exchange resin under low salt conditions (equilibration buffer, typically 50 mM NaCl). Once proteins are adsorbed on the resin, the flow-through is either discarded or kept for further studies. The flow-through contains proteins that do not bind to the resin under these experimental conditions. The beads are then extensively washed with the equilibration buffer to remove unbound proteins present within the interstitial volume of the resin beads. The beads' interstitial volume is called the dead volume. Proteins are then eluted off the resin with increasing salt (typically NaCl) concentrations (elution buffers). The increasing ionic strength of the buffer (salt) progressively displaces macromolecules from the resin and leads to the gradual protein release from the beads. Other constituents can be included in the equilibration, washing and elution buffers in addition to the salt, such as organic type molecules (non-ionic or zwitterionic detergents) when fractionating membrane bound proteins, or inorganic species (Ca^{2+} , Mg^{2+}) to enhance stability of certain proteins.

A typical equilibration buffer contains 50 mM NaCl, and as a general trend for a cytoplasmic lysate, proteins generally start to elute off the column at ~150 mM NaCl, which is near the physiological concentration of NaCl.⁴³⁴ By 350–500 mM NaCl, almost all the proteins have come off the beads employed in this study, Q-Sepharose® and S-Sepharose®.

Elution fractions can be assayed for protein concentration, and also resolved on a SDS PAGE gel, knowing though that high salt concentration may be

detrimental to proper electrophoretic migration. The sample may also be used directly for a reaction (*i.e.* click chemistry) or for further protein purification. Before the next step it may be necessary to remove or lower the salt concentration either by a desalting column or by dialysis.

In our studies, the ion exchange resins were Q-Sepharose[®] Fast-Flow (quaternary ammonium group) for anion exchange and S-Sepharose[®] Fast-Flow (sulphonate group) for cation exchange (GE Healthcare). For most proteins, the pI (isoelectric point) is below pH 7,⁴³⁵ therefore a majority of proteins are negatively charged at physiological pH. Consequently, in a cytoplasmic lysate Q-Sepharose will bind a greater number of proteins than S-Sepharose at pH 7.4. In addition, since proteins are more positively charged at lower pH, and more negatively charged at higher pH, more proteins are anticipated to adsorb to S-Sepharose[®] and Q-Sepharose[®] under acidic and basic conditions, respectively.

Protein fractionation of the soluble cytoplasmic rat brain lysate was first carried out at two different pH values to identify differences in fractionation patterns. We found that S-Sepharose[®] chromatography was more sensitive to pH change (different fractionation patterns at pH 6.5 vs 8.5) than Q-Sepharose[®]. We also observed that the relative amount of protein that bind to S-Sepharose at pH 8.5 was low. These findings led us to combine these two types of ion-exchange chromatographies by adsorbing the lysate at pH 6.5 on S-Sepharose[®] and then adsorbing the unbound fraction on Q-Sepharose[®] without modifying the pH. Since more proteins typically bind to S-Sepharose[®] at pH 6.5 rather than 8.5, this provided an added benefit for the selective elution of proteins with various salt concentrations.

Therefore, we found it unnecessary to start the fractionation at pH 8.5 using S-Sepharose®.

While Sepharose® columns are mostly used for large scale protein purifications involving several different types of columns, they can also be used on small scale to purify or simply enrich a protein. A practical, small scale fractionation experiment with Sepharose® is to use Spin Filter tubes (650 μ L capacity) with a polymer type filter to hold the resin bed. Ideally, experiments should be carried out at 4 °C. Equilibration and elution buffers should be freshly prepared and chilled on ice prior to their use.

In general, in our experiments we used 1 mg of total protein (cytoplasmic lysate) for 100 μ L (termed Column Volume, CV) of Fast-Flow® Sepharose (GE Healthcare, 50% slurry of beads in 20% EtOH). To preequilibrate the beads, the 20% EtOH is first removed by gravity or centrifugation at low speed (2,000 rpm, 5 sec when using Spin Filters) and the beads are washed with ice-chilled ddH₂O (2 x 10 CV) followed by the equilibration buffer (2 x 10 CV). On small scale, low speed centrifugation can be used to accelerate the process. It should be recognized that high speed (>5000 rpm, table-top centrifuge) can damage the beads' solid support. This general procedure was developed as a starting point for our studies of the whole lysate, and we expect that this protocol will be optimized when studying and purifying a specific protein.

On small scale experiments (20 μ L to 200 μ L beads, 50 μ L to 2000 μ L protein solution), the protein solution is tumbled with the beads (1–5 min). The flow-through is then recovered and the resin bed washed with 10 CV of equilibration buffer. To

elute the proteins, 5 CV of the desired elution buffer is added to the washed resin bed and gently swirled for 10–15 sec. The eluted fraction is then recovered by low speed centrifugation. 5–10 CV of the same elution buffer are then added to the beads to wash remaining bound proteins and centrifuged. The flow-through is discarded, and the next salt elution step can take place.

Sepharose type resins are useful in purifying or enriching a given pool of proteins based on electrostatic charges. Its other important role is to concentrate dilute samples, since the amount of resin used is proportional to the amount of protein that can be bound and not the protein concentration.

The main limitations of this method are the general setup, and the recovery of the different fractions. Also, when combining S and Q Sepharose together, while it is possible to adsorb and selectively elute approximately 60-70% of all the proteins present in the lysate, nearly 30-40% of the proteins remain unfractionated under various pH conditions (pH range from 6.5 to 8.5). Thus, it may be necessary to combine this method with other fractionation methods to obtain sufficiently pure material of select proteins.

Another type of Sepharose used in protein purification is the Phenyl Sepharose[®] Fast-Flow (GE Healthcare) type resin that allows proteins to be purified based on hydrophobic interactions. Chemical groups present on the beads of Phenyl Sepharose[®] include linear carbon chains ending with a phenyl group. In order to properly fractionate proteins by Phenyl Sepharose[®], the protein mixture first needs to be adjusted to a certain AMS saturation (15% for a cytoplasmic lysate). This step will shield off the solvent accessible electronic charges of the protein, thus

maximizing interactions of the protein's hydrophobic residues with the Phenyl Sepharose. The purification methodology for Phenyl Sepharose[®] is similar to the one employed for S and Q Sepharose[®], except the proteins are eluted off by progressively decreasing the AMS concentration of the buffer. This decrease frees the protein's electronic charges and releases the proteins from the hydrophobic matrix. The main disadvantage of this fractionation method is the necessity to dialyze the samples upon elution to remove the AMS.

3.4. Click chemistry

Click chemistry was performed using slightly modified conditions from those of Cravatt and co-workers.^{276,345,359} Copper sulfate pentahydrate ($\text{CuSO}_4 \cdot 5\text{H}_2\text{O}$) was used as the source of Cu^{2+} , and tris(2-carboxylethyl)phosphine hydrochloride (TCEP) was used as the reducing agent to generate the Cu(I) species. Earlier work by Sharpless and Finn have shown that the addition of an appropriate Cu(I) ligand in the click reaction increases the yield of this cycloaddition step by stabilizing the Cu(I) species in aqueous solutions and by catalyzing the click chemistry reaction.^{279,284,436,437} When performing click chemistry between labeled proteins and a fluorescent- or a biotin-containing probe, the different ratios of compounds are critical to obtain a correct signal to noise ratio of product versus background labeling. Therefore, for one equivalent of alkyne or azide-containing Probe the following quantities of reagents were used.

25 equiv of CuSO_4 : When the azide-alkyne cycloaddition is done under organic reaction conditions, the reaction only requires a catalytic amount of Cu(I) (5-

10% mol vs the alkyne or azide). In our proteomics studies, the reaction was performed in aqueous buffered solutions and required the use of a high amount of CuSO_4 (25 equiv vs fluorescent probe). This is necessary if we are to detect a fluorescent signal within 1 h. Apart from the fluorescent or biotin probe, the CuSO_4 stock solution is the only component of the click chemistry reaction which does not need to be prepared freshly prior to using.

12.5 equiv of TCEP (50% mol vs Cu^{2+}). The theoretically optimal ratio should be 25 equiv since TCEP reacts stoichiometrically with CuSO_4 . However, it was found that for a 1 h click chemistry reaction, there is no significant difference between 50% mol and 100% mol (25 equiv) of TCEP vs Cu^{2+} . Further increasing the TCEP vs Cu^{2+} ratio to 200% mol (50 equiv) resulted in an increase in background fluorescence. In experiments using sodium ascorbate (Na Asc) as the reducing agent, we did observe a slightly lower fluorescence signal compared with similar conditions using TCEP (data not shown). TCEP stock solution in water should be prepared prior to the experiment.

2.5 equiv (10% mol vs Cu^{2+}) of Cu(I)-chelating ligand: tris[(1-benzyl-1*H*-1,2,3-triazol-4-yl)methyl]amine (TBTA) has been advanced by Sharpless and coworkers as a ligand of choice to perform click chemistry reactions in biological systems. The main disadvantage of TBTA remains its poor solubility in water. Water-soluble Cu(I) chelators, such as sulfobathophenanthroline (SBP), have recently been introduced as useful accelerating ligands for click chemistry.⁴³⁸ Reports indicate that this ligand is more sensitive to oxidation than TBTA.⁴³⁹ When comparing SBP with TBTA, we found that click chemistry with SBP gave rise to fluorescent signals in the no drug

control experiments that were as intense as the signal from the AB&CR-labeled proteins. This problem was not encountered when using TBTA as a ligand. We, therefore, opted to use TBTA. The theoretically optimal ratio of Cu(I) to ligand varied from 1:1 to 1:2 depending on the nature of the ligand. In the case of TBTA, 2 molecules of ligand are required to form the full complex with one Cu(I). We found that click chemistry performed with 200% mol of TBTA vs Cu²⁺ gave a higher fluorescence background when compared with only 10% mol TBTA vs Cu²⁺. These findings were in agreement with published results from the Cravatt group.²⁷⁶ As for TCEP, TBTA should also be prepared just prior to performing the click chemistry.

In initial experiments, the click chemistry was executed by adding given volumes of stock solutions in the following order: fluorescent probe, CuSO₄, TBTA, and TCEP. To combine 3 addition steps to one, we found it possible and more convenient to prepare a 10 x solution of premixed CuSO₄, TBTA and TCEP (termed 10X Cu(I) mix) and then add the appropriate volume to the protein solution containing the fluorescent probe. The 10X Cu(I) mix was prepared so that upon dilution the percentage (v/v) of organic solvents present in the reaction remained below 5%.

A typical click chemistry experiment of a lysate mixture modified with a lacosamide AB&CR agent involved the following (based on a 20 μ M Probe final concentration). The fluorescent probe **195** or **196** (20 μ M final concentration, stock solution in water) was first added to the modified protein solution. Next, a prepared 100 μ L of 10X Cu(I) mix in a transparent tube was added. The Cu(I) mix was prepared by sequentially adding 10 μ L of 50 mM aqueous CuSO₄, and then 40 μ L of

625 μ M TBTA (in a 1/4 DMSO/*t*BuOH mixture). The TBTA in the binary stock solution should be made fresh by first dissolving the solid in 1/5 of the final volume of DMSO, and adding 4/5 of the final volume of *t*BuOH. Solubilizing TBTA directly in a 1/4 DMSO/*t*BuOH mixture takes much longer. Upon mixing the Cu^{2+} and the TBTA stocks together, the solution turns cloudy quickly. At low CuSO_4 concentrations, the suspension looks white, while at higher concentrations it looks light blue (Cu^{2+} complex). To the suspension is then added 50 μ L of freshly prepared 5 mM aqueous TCEP. Immediately upon mixing, the cloudy solution becomes clear and turns pale yellow, characteristic of a Cu(I)-complex. The 10X Cu(I) mix is diluted 10-fold by adding to the protein mixture and homogenized by vortexing. All the additions should be performed relatively quickly (5–10 min). A 10X Cu(I) mix should not be left at room temperature for more than 1 h. When many samples are involved, the use of a multi-channel pipettor is recommended. In our experiments, we found it unnecessary to rotate the tubes while performing click chemistry on soluble (cytoplasmic) proteins. Samples are then let to stand at room temperature for 1 h, and SDS loading buffer is added to stop the reaction and then boiled (75 $^{\circ}\text{C}$ for 4 min) and resolved on SDS PAGE gel.

CHAPTER 4

SCREENING THE RAT BRAIN CYTOPLASMIC FRACTION

4.1. The use of epoxide-based AB&CR molecules as selective labeling agents

4.1.1. Rationale

Early experiments with AB&CR agents **171** and **172** showed that the isothiocyanate (NCS) group led to appreciable non-specific protein labeling that gave complex in-gel fluorescence band patterns. The gel patterns made it difficult to identify unique targets associated with lacosamide function and almost impossible to identify potential targets that are present in low abundance in the lysate. We hypothesized that by using a less reactive AB group, we would observe diminished protein adduction and an increased selectivity of target modification within the proteome. Recently, the epoxide AB was shown to selectively target certain classes of proteases in lysate experiments prepared from whole cells or organ tissue.^{273,309,358} This apparent selectivity was, however, biased by the inherent affinity of protease cysteine residues for epoxide electrophiles. Interestingly, in a comparative study of various protein affinity labels, the aliphatic epoxide was able to selectively modify carbonic anhydrase 2 (CA2) without reacting with abundant or reactive enzymes (i.e., bovine serum albumin (BSA), protein kinase A (PKA),

glyceraldehyde-3-phosphate dehydrogenase (GAPDH)).²⁹⁰ Optimal labeling conditions for epoxide adduction labeling were 20 h at room temperature.²⁹⁰

While aromatic epoxides differ from their aliphatic counterparts in terms of chemical reactivity,³⁰⁷ they can also be used as protein labeling agents.^{440,441} Accordingly, to increase our chances of target protein capture, we screened the proteome with AB&CR agents containing an epoxide moiety at two different positions, where the aliphatic and aromatic epoxide groups were located on the side chain of the molecule (**179**, **180**) and the benzylamide 4'-position (**175**, **176**), respectively.

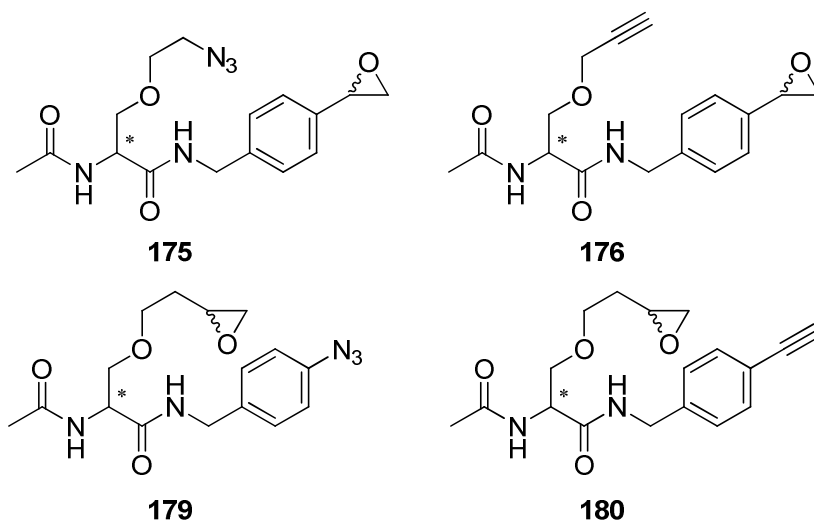


Figure 10. Structures of epoxide-based AB&CR agents used in the rat brain cytoplasmic fraction screening

4.1.2. Labeling and fractionation experiments of cytoplasmic proteins

Rat brain cytoplasmic lysate (**S3**) was prepared as previously described. Screening was initially performed using both enantiomers of **175**, **179**, and Probe **195** for visualization and later with (*R*) and (*S*) enantiomers of **176**, **180**, and Probe

196 (Figure 10, Figure 11). Starting with 200–300 μL of lysate ($\sim 2 \text{ mg.mL}^{-1}$) at the desired pH (6.5, 7.5, or 8.5), AB&CR compounds were allowed to react at room temperature (20 h),²⁹⁰ and then the reaction mixture was fractionated with AMS. Recovered pellets were dissolved in 25 mM HEPES buffer (pH 7.5) and click chemistry (20 μM), CuSO_4 (25 equiv), TCEP (12.5 equiv), and TBTA^{436,442,437} (200% vs. Cu^{2+}) was performed using compound **195**. The molar ratio of TBTA vs Cu^{2+} was reduced in later experiments (5% vs Cu^{2+}) since the higher molar ratio led to high fluorescence backgrounds, as observed by Cravatt and coworkers.^{276,359} Samples were then resolved on SDS PAGE gel (8, 10, or 12.5%), scanned for fluorescence (532 nm excitation; 580 nm emission), and stained with Coomassie Brilliant Blue or silver stain for total protein quantification.

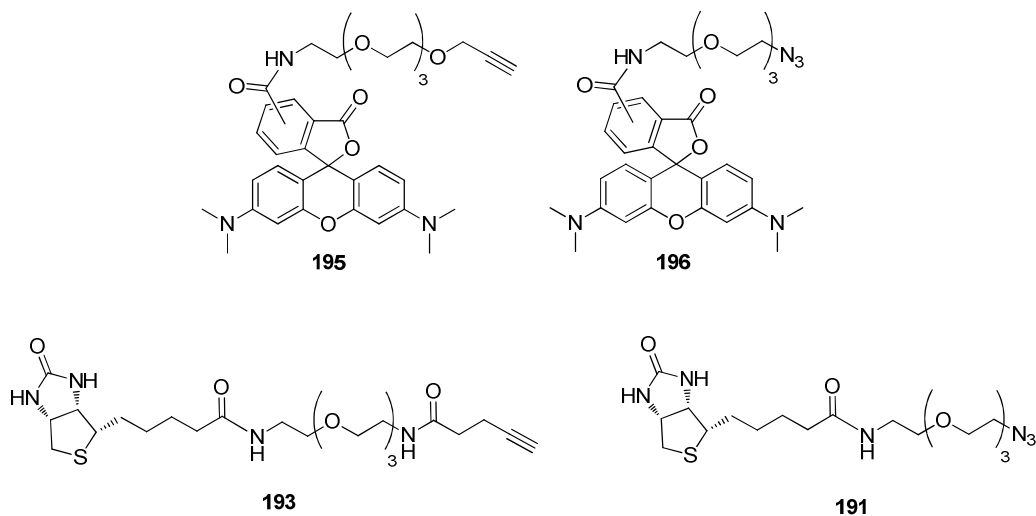


Figure 11. Structures of the different Probes used to react with the CR groups after protein labeling.

4.1.3. Identification of a protein of interest in the soluble fraction

The first experiment was carried out at two different concentrations of AB&CR agent (*R*)-**175** and (*R*)-**179** (50 μ M and 5 μ M), and fractions **M1030**, **M4050**, **M5058**, **M5865**, **M6590** were recovered then treated with **195** under Cu(I)-catalyzed conditions ("clicked"). Fluorescent labeling proved to be relatively high at 50 μ M of AB&CR agent (*R*)-**179**, while only one protein in the **M4050** and the **M5058** fractions showed notable labeling at 5 μ M. The protein was labeled by (*R*)-**179** and not by (*R*)-**175** (Figure 12). Analysis of the other AMS cuts (**M0040** and **M6590**) showed no bands that were selectively labeled by our AB&CR agents (data not shown).

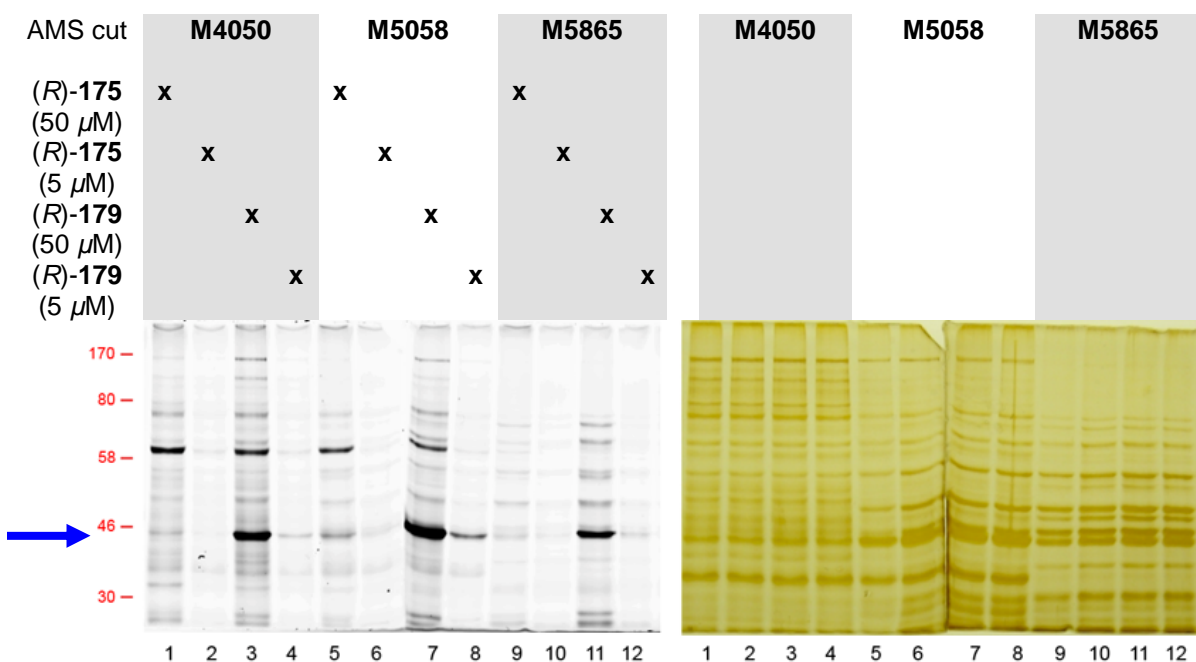


Figure 12. 6% SDS-PAGE gel of rat brain cytoplasmic AMS cuts containing a protein of interest labeled by (*R*)-**179** but not (*R*)-**175**. Cytoplasmic lysate samples (~300 μ g total protein) were labeled with (*R*)-**179** and (*R*)-**175** at 5 or 50 μ M at room temperature (20 h), fractionated with AMS, clicked with Probe **195**, and resolved. Left picture: in-gel fluorescence scan (ex.: 532 nm, em.: 580 nm); right picture: corresponding silver stain. Lanes 1–4: **M4050**; lanes 5–8: **M5058**; lanes 9–12: **M5865**. Lanes 1, 5, 9: (*R*)-**175** (50 μ M); lanes 2, 6, 10: (*R*)-**175** (5 μ M); lanes 3, 7, 11: (*R*)-**179** (50 μ M); lanes 4, 8, 12: (*R*)-**179** (5 μ M). Approximate molecular weight markers (kDa) are shown in red on the left.

A similar experiment with (*R*)-**179** at 50 μ M showed that the protein (~45 kDa) precipitated in the **M4065** fraction. However, it was possible to obtain a cleaner AMS cut containing the majority of the protein using the **M4555** cut. In a subsequent experiment, we found that this protein, enriched in **M4555**, could further be purified using Q-Sepharose® (HEPES, pH 8.0) upon elution between 200 and 300 mM NaCl at pH 8.0 (Figure 13). This experiment also demonstrated that (*R*)-**179** gave preferential labeling over (*S*)-**179**, while giving a solution highly enriched in the protein of interest. Utilizing this purification procedure, the protein was resolved on SDS PAGE gel (8%), Coomassie stained, excised, and sent for mass spectrometric (MS) analysis at the Michael Barber Centre for Mass Spectrometry (University of Manchester).

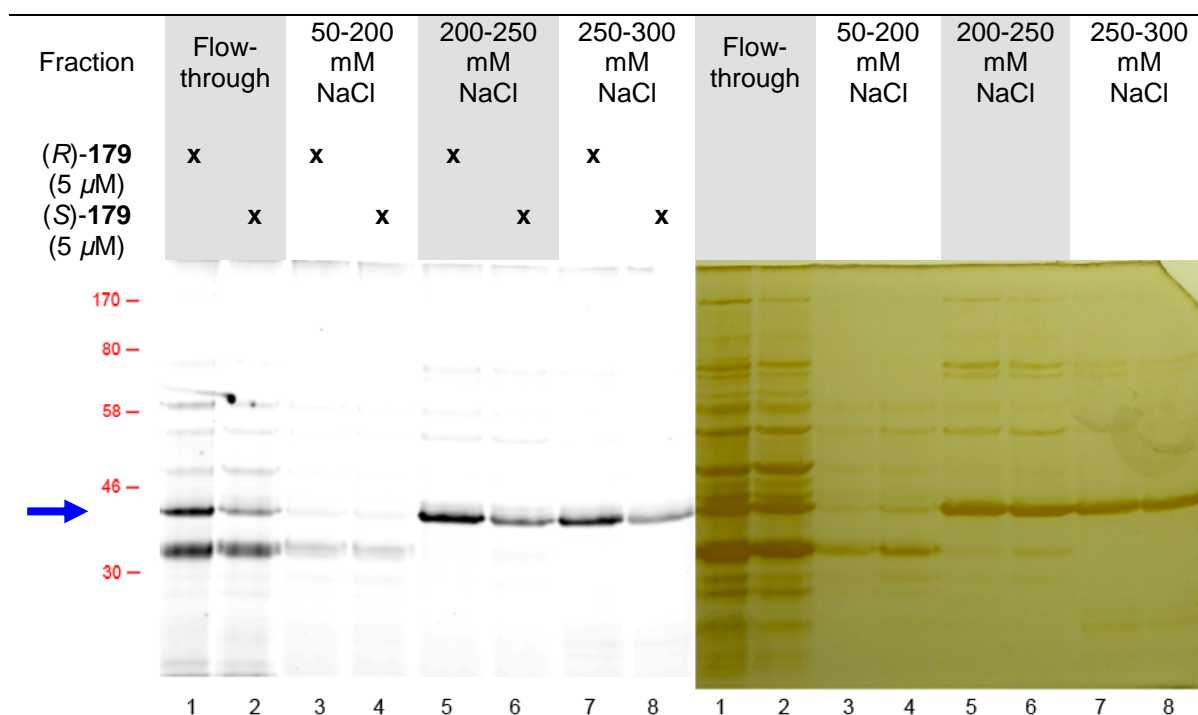


Figure 13. 8% SDS-PAGE gel of rat brain cytoplasmic preferentially labeled by (*R*)-**179** over (*S*)-**179**. Cytoplasmic lysate samples (~300 μ g total protein) were labeled with (*R*)-**179** and (*S*)-**179** at 5 μ M at room temperature (20 h), the **M4555** cut was recovered and further fractionated on Q-Sepharose® (pH 8.0). The flow-through, and elution fractions (50–200 mM NaCl, 200–250 mM NaCl, 250–300 mM NaCl) were recovered, clicked with Probe **195**, and resolved. Left picture: in-gel fluorescence scan

(ex.: 532 nm, em.: 580 nm), a small fraction of the labeled protein did not bind to the resin (lanes 1, 2); right picture: corresponding silver stain. Lanes 1,2: **M4555** Q-Sepharose® flow-through, lanes 3,4: 50–200 mM NaCl elution fraction, lanes 5,6: 200–250 mM NaCl elution fractions, lanes 7,8: 250–300 mM NaCl elution fractions. Lanes 1, 3, 5, 7: (*R*)-**179** (5 μ M); lanes 2, 4, 6, 8: (*S*)-**179** (5 μ M). Approximate molecular weight markers (kDa) are shown in red on the left.

4.2. Brain-type creatine kinase B (CKB)

The protein of interest was identified by mass spectrometry as brain-type creatine kinase (CKB). Mass spectral analysis of similarly cut gel bands from other experiments led to an approximate coverage of 60% of the enzyme sequence. These experiments did not reveal the modified residue on CKB. Table 2 provides representative tryptic fragments identified by MS.

Table 2. Representative list of the CKB tryptic digests identified from the fractionated cytoplasmic lysate

Creatine kinase B-type OS=Rattus norvegicus					
Observed	Mr(expt)	Mr(calc)	Miss	Score	Peptide
759.2673	758.26	758.3347	0	35	R.DWPDAR.G
439.7338	877.453	877.5021	1	43	K.FSEVLKR.L
524.175	1046.3354	1046.543	0	54	K.LLIEMEQR.L + Oxidation (M)
569.7446	1137.4746	1137.5601	1	43	K.GGNMKEVFTR.F
616.7395	1231.4644	1231.6085	0	49	K.DLFDPIIEDR.H
652.323	1302.6314	1302.7183	0	60	K.VLTPELYAELR.A
750.8008	1499.587	1499.7694	0	78	R.FCTGLTQIETLFK.S
801.8158	1601.617	1601.826	0	76	K.LAVEALSSLDGDLSGR.Y
836.3497	1670.6848	1670.8416	0	65	K.TFLVWINEEDHLR.V
841.8837	1681.7528	1681.8345	0	50	R.LEQQQPIDDLMPAQK.-
924.8934	1847.7722	1847.9703	0	110	R.LGFSEVELVQMVDGVK.L
982.9081	1963.8016	1963.9236	0	75	R.GTGGVDTAAGGVFDVSNADR.L
707.6211	2119.8415	2120.0247	1	77	K.RGTGGVDTAAGGVFDVSNADR.L
729.2628	2184.7666	2184.9534	0	53	R.FPAEDEFDLSSHNNHMAK.V
819.0059	2453.9959	2454.1386	1	34	K.LRFPAEDEFDLSSHNNHMAK.V
839.9778	2516.9116	2517.1619	0	56	K.TDLNPDNLQGGDDLDPNYVLSSR.V

4.2.1. CKB is selectively labeled by epoxide-based AB&CR agents

Analogous experiments conducted using the AB&CR agents **176** and **180** (1–10 μ M) containing the alkyne CR moiety and azide Probe **196** (10–50 μ M) showed a

reduced level of background fluorescence (Figure 15). We observed a similar reduced level of background protein labeling using azide Probe **196** compared with the alkyne Probe **195** in the *absence* of AB&CR agents. Finally, a slight reduction in background signal was observed between reactions where click chemistry was conducted with 5% TBTA vs Cu²⁺ compared with 200% TBTA vs Cu²⁺ (Figure 14).

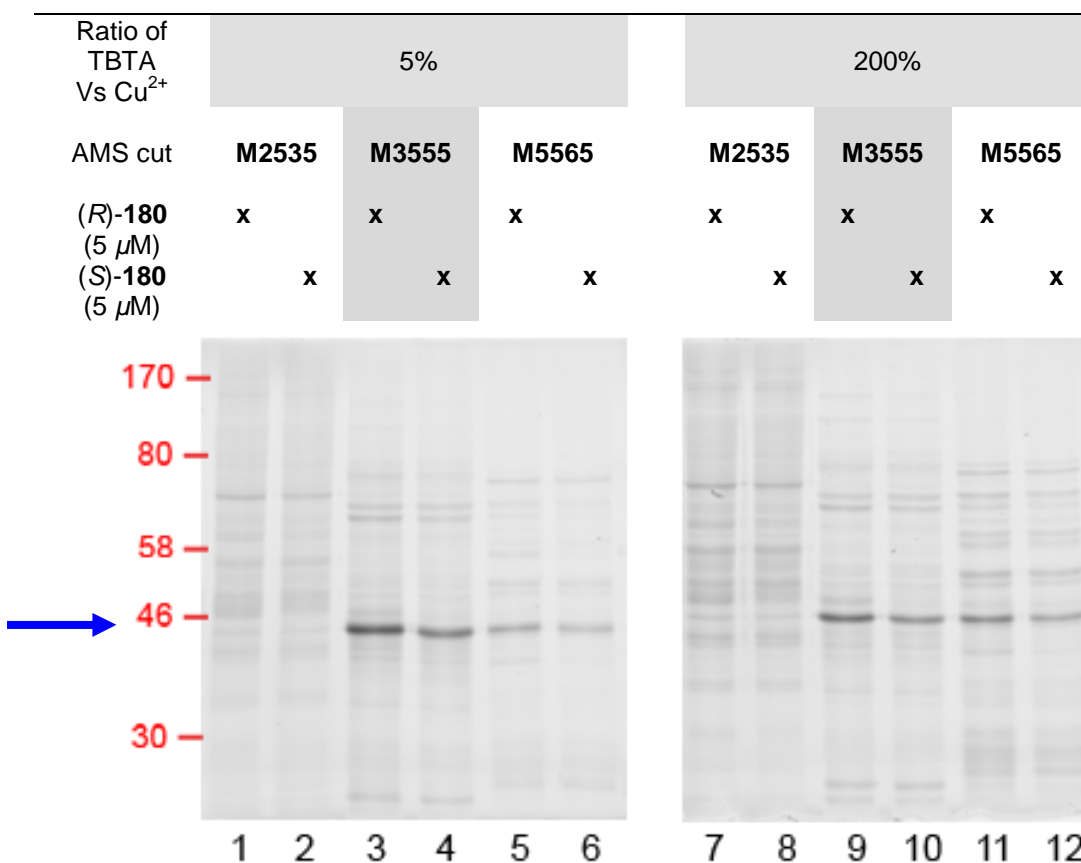


Figure 14. In-gel fluorescence scan of the brain cytoplasmic lysate (6% SDS-PAGE gel). Cytoplasmic lysate samples (~300 μ g total protein) were labeled with (*R*)-**180** and (*S*)-**180** at 5 μ M at room temperature (20 h), and fractionated using AMS. For each AMS cut recovered, the sample was split in half. The first half was clicked using a 5% TBTA vs Cu²⁺ ratio and the second half with 200% TBTA vs Cu²⁺ ratio. The samples were resolved, and scanned for fluorescence. Left gel (lanes 1–6): click chemistry was performed using a 5% TBTA vs Cu²⁺ ratio; right gel: (lanes 7–12): click chemistry was performed using a 200% TBTA vs Cu²⁺ ratio. Lanes 1, 3, 5, 7, 9, 11: (*R*)-**180** (5 μ M); Lanes 2, 4, 6, 8, 10, 12: (*S*)-**180** (5 μ M); Lanes 1, 2, 7, 8: **M2535**; lanes 3, 4, 9, 10: **M3555**; lanes 5, 6, 11, 12: **M5565**. CKB (blue arrow) is present in the **M3555** cut. Approximate molecular weight marker (kDa) are shown in red on the left

To confirm that CKB was specifically labeled by compound (*R*)-**179**, the cytoplasmic brain lysate (500 μ L, 1 mg total protein) was incubated with either DMSO (control) or 10 μ M (*R*)-**179** at room temperature (20 h). AMS fraction **M4555** was recovered, which was subsequently fractionated on Q-Sepharose[®] (pH 8.0) and the fraction eluting between 200 and 300 mM NaCl (HEPES, pH 8.0) was recovered. Click chemistry was performed using Probe **193** (20 μ M) at room temperature (1 h) and each reaction was then incubated with Streptavidin beads (50 μ L beads) that were pre-rinsed with 5 x 1 mL washing buffer (150 mM NaCl, 50 mM HEPES, pH 7.5) by tumbling at room temperature (1 h). The beads were centrifuged at 2000 rpm on a table-top centrifuge (30 sec), and the supernatant was removed. For each reaction the resin was then successively washed with 3 x 1 mL washing buffer, 3 x 1 mL washing buffer supplemented to 0.2% SDS, 3 x 1 mL aqueous 6 M urea, and 5 x 1 mL washing buffer. The beads were sent for MS analysis using off-the-beads trypsinization.⁴⁴³ No proteins were found in the DMSO control sample, whereas only fragments of CKB were identified in the AB&CR sample, confirming that CKB was specifically labeled with (*R*)-**179** (Table 3)

Table 3. List of peptides identified after trypsin digestion of Streptavidin beads for the cytoplasmic sample treated with 10 μ M (*R*)-**179**. No peptides were identified after off-the-beads digestion from the DMSO treated sample.

Creatine kinase B-type OS=<i>Rattus norvegicus</i>					
Observed	Mr(expt)	Mr(calc)	Miss	Score	Peptide
516.23	1030.4454	1030.5481	0	38	K.LLIEMEQR.L
801.86	1601.7054	1601.826	0	84	K.LAVEALSSLDGDLGR.Y
841.89	1681.7654	1681.8345	0	59	R.LEQGQPIDDLMPAQK.-
924.93	1847.8454	1847.9703	0	88	R.LGFSEVELVQMVVDGVK.L

4.2.2. Competition experiments with (*R*)-LCM and a known CKB inhibitor

Protein modification experiments using agent **180** reproducibly showed that CKB was preferentially labeled by (*R*)-**180** compared with (*S*)-**180** and that (*R*)-**176** did not modify the protein. However, (*R*)-**180** labeling experiments in the presence of excess (*R*)-**1** (100–5000 equiv) led, in most cases, to no reduction in the fluorescence intensity signal of the ~43 kDa band (Figure 15, blue arrow). In only one out of the 9 competition experiments did we see a reduction of the intensity of the fluorescent band labeled by (*R*)-**180** by (*R*)-LCM. This finding indicated (*R*)-LCM did not compete with (*R*)-**180** protein adduction. Nonetheless, other findings suggested a direct interaction between (*R*)-LCM and CKB (see Section 4.2.6).

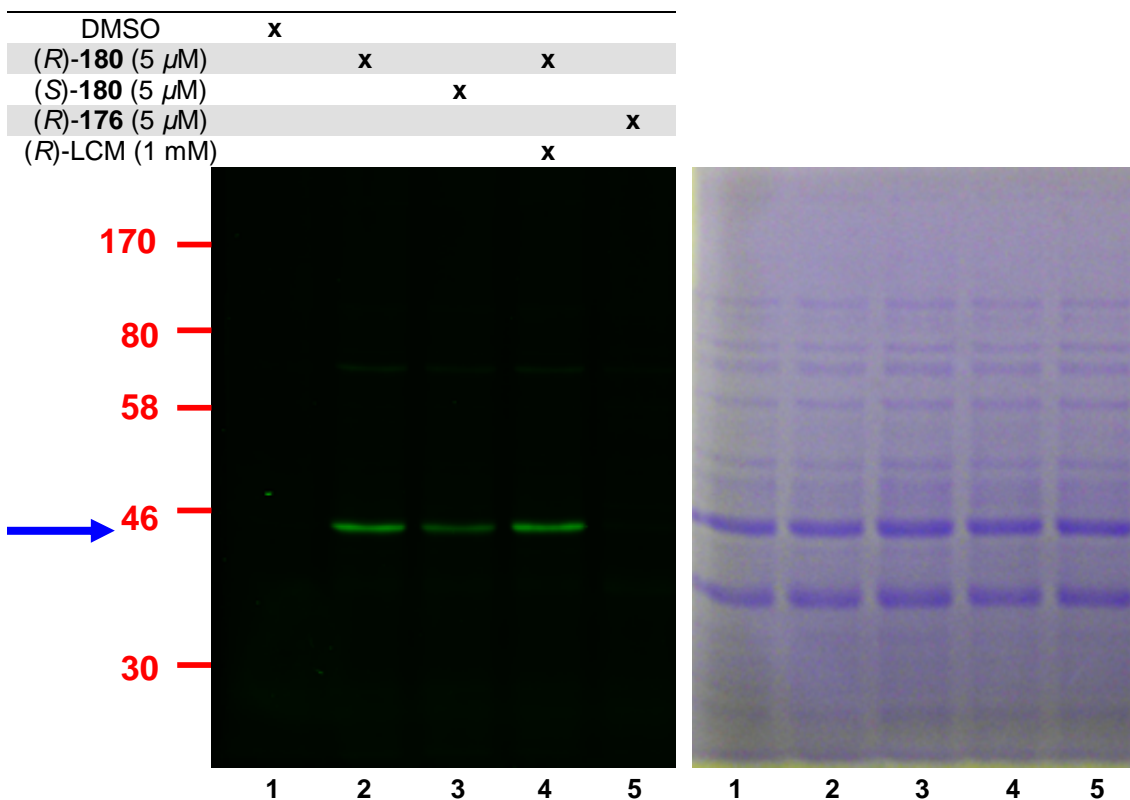


Figure 15. 8% SDS-PAGE gel of the cytoplasmic lysate **M4555** cut. Left picture: fluorescence scan; right picture: corresponding Coomassie stain. Samples (~200 μ g total protein) were incubated at

room temperature (20 h) with the appropriate AB&CR agent or control, and fractionated with AMS. M4555 was recovered, click chemistry was performed using Probe **196**, and samples were resolved and scanned. Lane 1: DMSO; lane 2: (*R*)-**180** (5 μ M); lane 3: (*S*)-**180** (5 μ M); lane 4: (*R*)-**180** (5 μ M) + (*R*)-LCM (1 mM); lane 5: (*R*)-**176** (5 μ M). Approximate molecular weight markers (kDa) are shown in red on the left.

Next, we preincubated (5 min) the lysate with 2,4-dinitrofluorobenzene (DNFB, 10–20 μ M), a known suicide inhibitor of CKB,⁴⁴⁴⁻⁴⁴⁶ and then treated the lysate with (*R*)-**180** at room temperature (18 h). We observed a marked reduction (>50%, quantified with ImageJ[®]) in fluorescence intensity of the CKB containing band, after AMS fractionation (**M4555**) and click chemistry. By comparison, a more modest decrease in CKB-specific reduction (~10%) in the signal intensity was detected when DNFB was added after reaction of (*R*)-**180** with the lysate at room temperature (18 h). Interestingly, incubation with DNFB at room temperature (18 h) led to a shift in the AMS fraction of CKB, with a larger population of the protein now precipitating below 45% AMS saturation. This finding suggested that CKB underwent a protein conformational change upon DNFB modification. The DNFB findings were interesting and suggested that DNFB and (*R*)-**180** may interact at or near the same site. However, our observation that the protein likely underwent conformational change upon DNFB labeling raised several alternative explanations for the reduced (*R*)-**180** labeling with DNFB treatment. Among these, is that the CKB conformational change may have reduced either the efficiency of AB adduction or the extent of modification of the CR group of (*R*)-**180** with Probe **196** by click chemistry. Accordingly, the reduced fluorescence intensity could potentially be due to a combination of several factors. First, DNFB and (*R*)-**180** may label the same residue. Second, DNFB may have induced a conformational change of the protein resulting

in a reduction in (*R*)-**180** labeling. Third, a protein conformational change may have reduced the efficiency of the click chemistry reaction. Nonetheless, this set of experiments suggested the possibility that Cys283, the established residue modified by DNFB,⁴⁴⁴⁻⁴⁴⁶ was covalently modified by (*R*)-**180**.

4.2.3. Possible significance of CKB as a target for epilepsy

CKB is a ~43 kDa cytoplasmic dimeric protein responsible for catalyzing the dephosphorylation of phosphocreatine to generate ATP, and is mainly localized in inhibitory neurons.^{447,448} Importantly, this reaction represents the fastest way for a cell to generate ATP, using phosphocreatine as an energy buffer.⁴⁴⁹ Many studies have shown the physiological importance of CKB in seizures and it has been established that the CKB reaction rate dramatically increases during a seizure, where brain levels of phosphocreatine decrease up to 50%.⁴⁴⁹⁻⁴⁵² This quick generation of ATP is required for fueling and maintaining the high-energy demand of the seizure.⁴⁵⁰⁻⁴⁵² Thus, it is possible that an inhibitor of CKB may act as a preventive agent by suppressing the seizure's energetic pathway. More recently, CKB has been shown to activate the K⁺-Cl⁻-cotransporter 2 (KCC2) in GABAergic neurons.^{453,444} KCC2 has been implicated in playing a crucial role in maintaining homeostasis of the neuron and dictating the inhibitory or excitatory role of GABA in developing neurons.¹¹⁷ It has been recently found that some forms of epilepsy lead to dramatic changes in the expression profiles and the physiological properties of KCC2.^{117,119,454,118} CKB knockout mice (CKB^{-/-}) have been generated and are viable while displaying a mild phenotype, a gradual hearing loss, due to the abundance and

important role played by CKB in cochlear cells.⁴⁵⁵ More interestingly, CKB^{-/-} mice have been shown to have a higher seizure threshold in the ipPTZ seizure test when compared with normal mice.⁴⁵⁶

4.2.4. Creatine Kinase B activity assay

To further explore whether CKB was a potential target for (*R*)-**1** we determined if (*R*)-LCM, (*S*)-LCM and other derivatives could modulate the activity of the purified enzyme. Thus, we cloned, overexpressed and purified human His-tagged CKB in *E. coli* following literature procedures^{457,458} and used the CKB activity assay to verify the functional integrity of the enzyme.

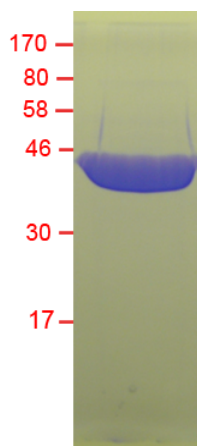
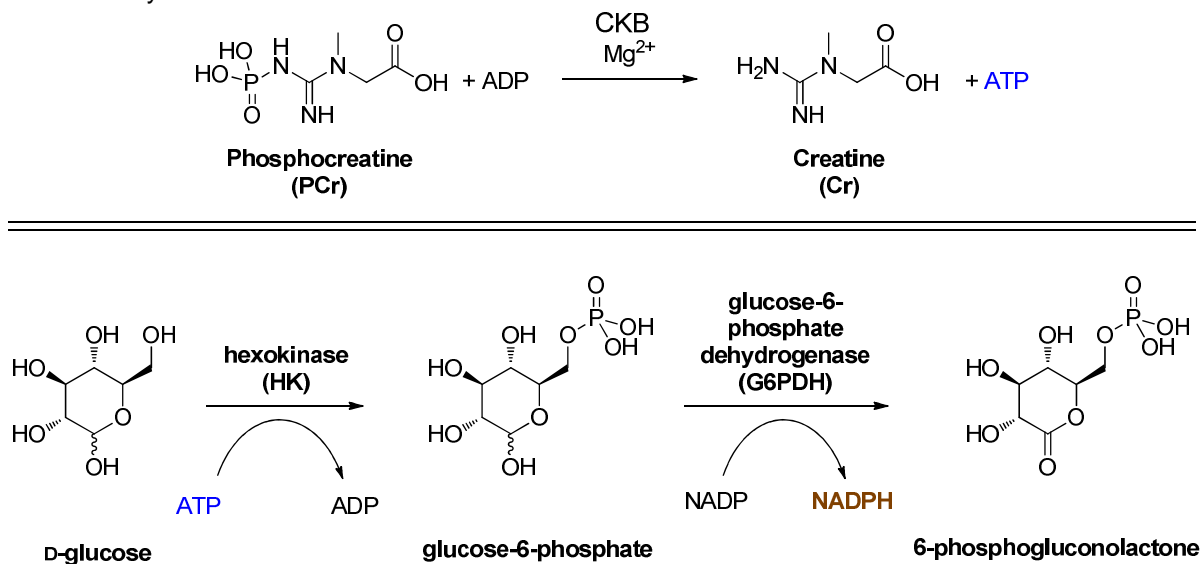


Figure 16. 12.5% SDS-PAGE gel Coomassie stain of overexpressed purified human CKB enzyme after His-tag, AMS, and Q-Sepharose[®] fractionation. Cloning and overexpression protocols can be found in the Experimental Section. Approximate molecular weight markers (kDa) are shown in red on the left.

To do so, we used a validated and widely used CKB coupled enzymatic assay.^{446,459,460} The CKB activity assay was first performed using a commercial source of enzyme (human CKB, cat # 10-663-45059, GenWay Biotech, San Diego, CA), and later using purified overexpressed human CKB from *E. coli* (Figure 16, see

Sections 4.6.7 and 4.6.8 for experimental details). In addition we first used a commercial CK activity assay kit (BioAssay Systems, cat # ECPK-100, Hayward, CA) and later utilized an in house assay using commercially available reagents.^{446,459,460} In this coupled assay, CKB catalyzes the transfer of a phosphate group from phosphocreatine to ADP, generating creatine and ATP (Scheme 41, top). The latter is used by hexokinase (HK) to convert D-glucose to glucose-6-phosphate, which is employed, in turn, by glucose-6-phosphate dehydrogenase (G6PDH), using NADP as a cofactor. NADPH, the reduced form of NADP, absorbs at 340 nm and 360 nm (Scheme 41, bottom).

Scheme 41. Chemical reactions used in the CKB activity assay. Top: CKB-catalyzed generation of ATP. Bottom: coupled enzymatic reactions used in the activity assay. NADPH is quantified by measuring the absorbance at either 340 or 360 nm. The amount of NADPH generated is proportional to the activity CKB.



We compared the enzymatic activities of commercial CKB with the overexpressed purified CKB (Figure 17). The activities were virtually identical, and

both enzymes were completely inhibited by pre-incubation with 10 μ M DNFB at room temperature (10 min). The amount of NADPH produced is directly proportional to the activity of CKB. In early experiments, equipment availability (HTS 7000 Plus Bio Assay Reader, Perkin Elmer) led us to monitor reactions by measuring the optical density (OD) at the sub-optimal 360 nm wavelength. The theoretically optimal 340 nm wavelength was used in later experiments using a different instrument (POLARstar OPTIMA, BMG Labtech).

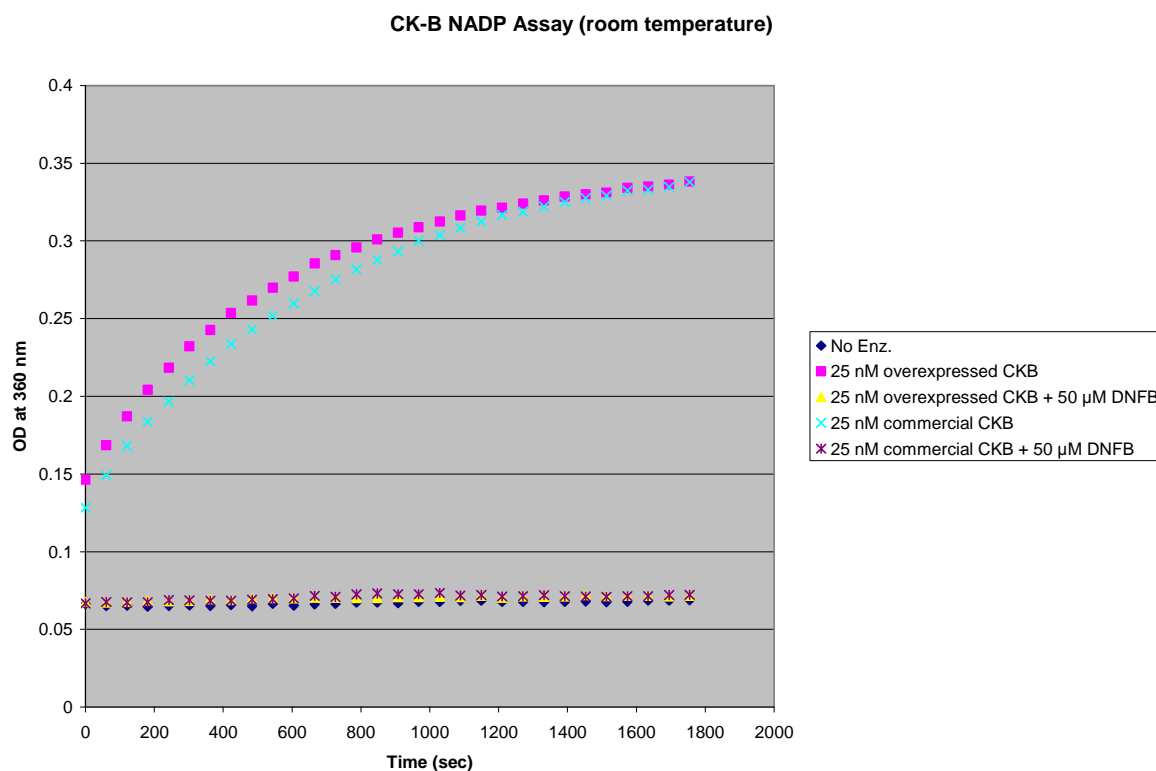


Figure 17. Comparison of enzymatic activities of human commercial CKB and overexpressed CKB. The coupled assay was conducted at room temperature and OD₃₆₀ was plotted versus time. Legend is shown on the right.

4.2.5. Identification of modification sites of CKB

An (*R*)-**180** adduction experiment was conducted using overexpressed, purified human His-tagged CKB to determine which amino acid residue was modified by (*R*)-**180**. The buffer used for the labeling experiment was 100 mM MES (pH 6.5), containing 100 μ M TCEP and a final concentration of 5% DMSO (v/v). One sample (0.5 mg) was incubated with no drug (control), and one with 500 μ M of (*R*)-**180**. The samples were then resolved on 8% SDS-PAGE denaturing gel, the gel was Coomassie stained, and the band corresponding to CKB excised and sent for MS analysis.

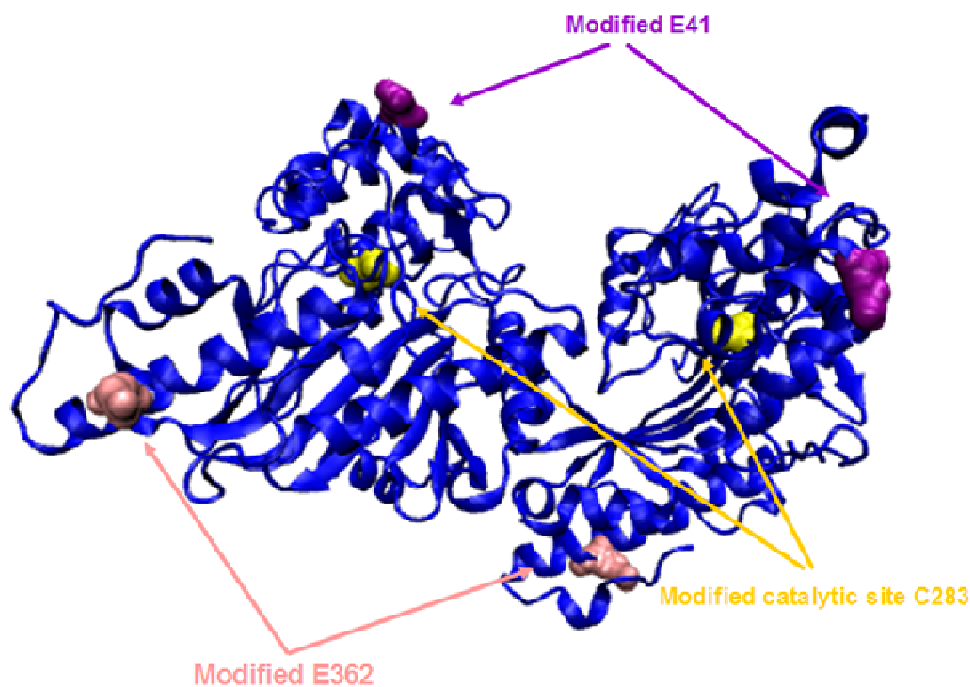


Figure 18. Crystal structure of human CKB (PDB ID: 3B6R). The protein dimer is represented in blue, and the modified residues identified from MS experiments are highlighted. Purified human CKB (~250 μ g) was labeled with 500 μ M (*R*)-**180** at room temperature (20 h), the protein was resolved on SDS-PAGE gel (8%), the gel was Coomassie stained and the ~43 kDa band corresponding to CKB was excised. Tryptic digests of the protein led to the identification of three residues. C283 (yellow) is a key amino acid for catalysis, while E362 (pink) and E41 (purple) are located on the protein surface. The figure was prepared by Ms. Onrapak Reamtong.

In the labeled enzyme sample, three residues were modified by the (*R*)-**180** epoxide AB group: C283, E41, and E362, but the extent of labeling of each residue could not be determined. The two glutamate residues are located on the surface of the enzyme, while C283 is a critical catalytic residue. D340, another key CKB catalytic residue,⁴⁶¹ was not modified under these conditions (Figure 18). The control reaction showed no evidence of amino acid modification.

A dose-dependent experiment was performed where a buffered solution of CKB (~200 μ g per reaction) in 100 mM MES (pH 6.5), 5% DMSO, 100 μ M TCEP was incubated at room temperature (20 h) with no drug, and 50, 500, 5000 μ M of (*R*)-**180**. After labeling, an aliquot of each reaction was used in the CKB enzymatic assay (50 nM final concentration of enzyme). The remaining sample was equally split in two. One sample was dialyzed twice (1 h) against 3 L of double-distilled (dd) H₂O, lyophilized and sent on dry ice for MS analysis of the intact protein. The other sample was dialyzed twice (1 h) against 1.5 L of 50 mM MES (pH 6.5) and 100 μ M TCEP. A 20 μ L aliquot was used to perform click chemistry with Probe **196**. The remaining volume was snap-frozen (dry ice/acetone bath) and sent on dry ice for MS analysis.

Sample preparation proved to be critical for the detection of the intact protein. Only the samples that had undergone dialysis against ddH₂O and lyophilization gave a detectable signal. The CKB activity assay results showed an approximate correlation between the proportion of adducted protein and the inhibition of the enzyme. At 50 μ M of (*R*)-**180**, the CKB enzymatic activity was virtually identical to

that of the unmodified enzyme (Figure 19) and no adduct could be detected by MS analysis (MW 44668 and MW 44710) (Figure 20). Interestingly, CKB appeared as a ~1:1 doublet at MW 44668 and MW 44710. The difference between the two signals (42 Da) likely corresponds to protein *N*-acetylation. We are unsure of the source and location of the acetyl residue, but have tentatively attributed this phenomenon to the CKB overexpression in *E. coli* where acetylation processes can occur.^{462,463}

At 500 μM , the enzymatic activity was reduced by ~60%, and approximately 33% of the enzyme, based on the MS peak intensities, corresponded to a (*R*)-**180** mono-adduct (330 Da modification: MW 44999 and MW 45040) with the rest matching the unmodified enzyme (MW of (*R*)-**180**: 330 Da).

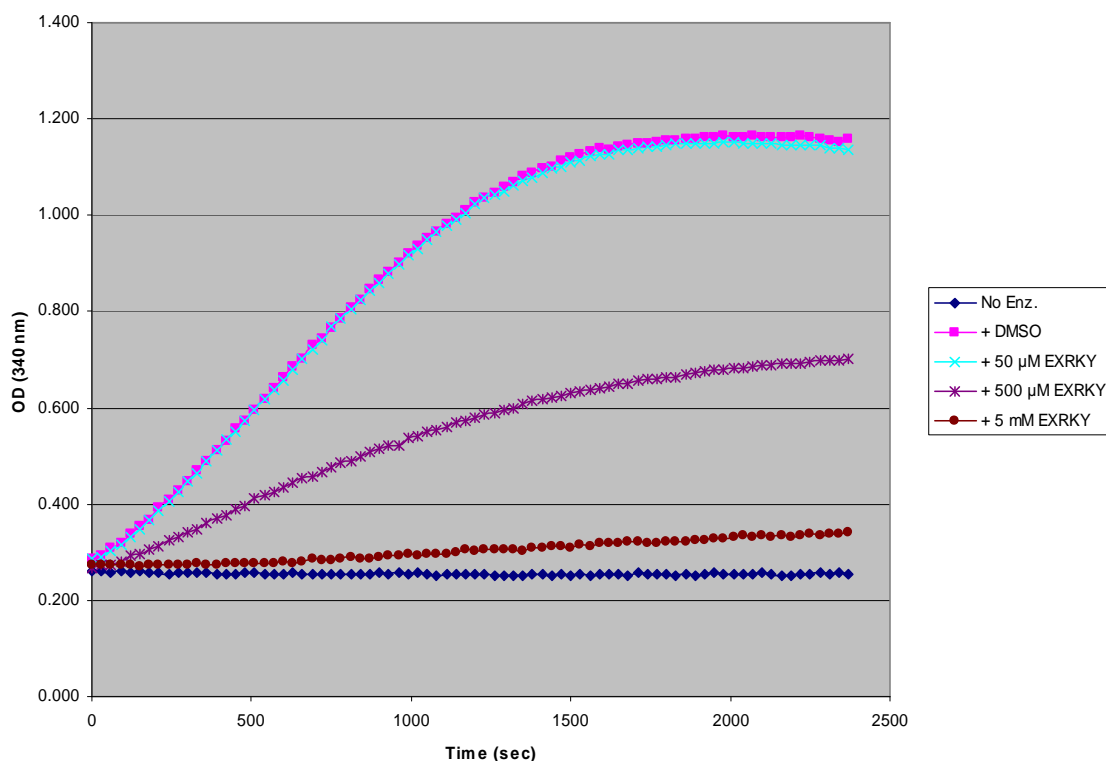


Figure 19. CKB enzymatic inhibition assay with (*R*)-**180** (abbreviated EXRKY). CKB samples were treated at room temperature (20 h) with DMSO, 50 μM , 500 μM , or 5 mM (*R*)-**180**. The assay was performed using an enzyme final concentration of 25 nM.

At 5 mM, the CKB activity was reduced ~95% and no MS peak characteristic of the unmodified enzyme could be observed. The major species in this sample was the (*R*)-**180** CKB mono-adduct (MW 45001 and MW 45042) and trace levels of a (*R*)-**180** di-adduct (MW 45330 and MW 45372). The evidence of a di-adduct may explain, in part, the three different modified residues observed in the tryptic digestion experiments.

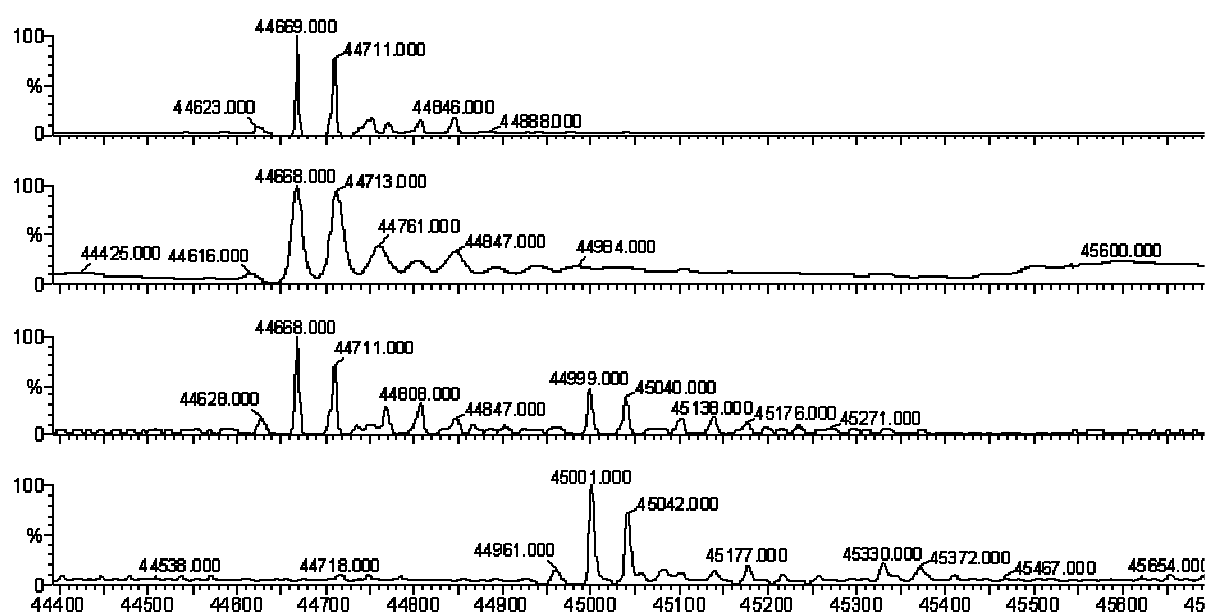


Figure 20. MS analysis of intact CKB (~50 μg) modified with (*R*)-**180** at different concentrations. Samples were incubated with DMSO or the AB&CR agent at room temperature (20 h), dialyzed against ddH₂O, lyophilized, and analyzed. CKB samples were treated with the following conditions, top to bottom: DMSO, 50 μM (*R*)-**180**, 500 μM (*R*)-**180**, 5 mM (*R*)-**180**.

The in-gel fluorescence experiment showed no adduction in the DMSO treated CKB sample, and a dose-dependent increase in the fluorescence intensity with samples modified with 50, 500 and 5000 μM of (*R*)-**180** (Figure 21, [blue arrow](#)). We reduced the sensitivity of the fluorescence scanner for this gel (PMT 300) in order to have non-saturating fluorescence levels.

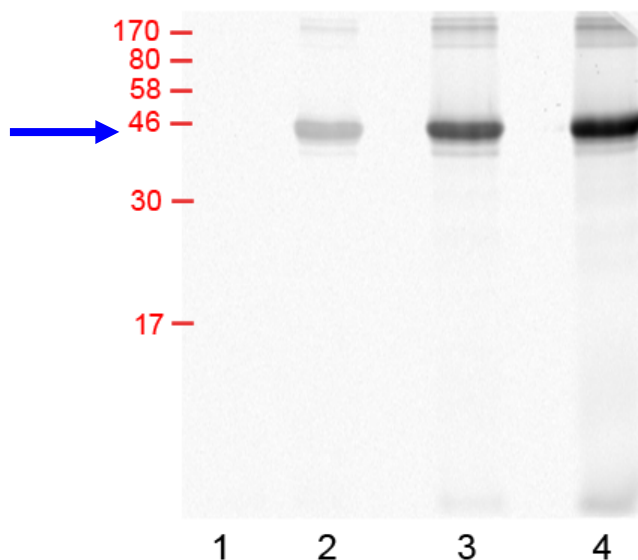


Figure 21. Fluorescence scan (very low sensitivity, PMT 300) of CKB samples treated with various concentrations of (*R*)-**180**. Samples were incubated with DMSO or (*R*)-**180** at room temperature (20 h), dialyzed against HEPES buffer (pH 7.5), clicked with Probe **196** and resolved on 15% SDS-PAGE gel. Lane 1: DMSO treated; lane 2: (*R*)-**180** (50 μ M); lane 3: (*R*)-**180** (500 μ M); lane 4: (*R*)-**180** (5 mM). The Coomassie stain of the gel showed equal amounts of protein per well (picture not shown). Approximate molecular weight markers are shown in red on the left.

The correlation of the MS data with the levels of CKB enzymatic inhibition was not exact. We found that the enzyme activity was reduced by ~60% in samples that showed ~33% of a (*R*)-**180** mono-adduct. Several factors may have accounted for this difference. One of these is the potentially different ionization properties of the CKB unmodified, (*R*)-**180** mono-adduct and (*R*)-**180** di-adduct samples in the mass spectrometer. Taken together, the results strongly suggest that the inhibitory activity of (*R*)-**180** is mediated by a covalent modification of Cys283. In addition, the strong in-gel fluorescent signal obtained at 50 μ M of (*R*)-**180** combined with the absence of a detectable MS signal for the (*R*)-**180** mono-adduct (Figure 20) and no detectable loss of enzymatic activity (Figure 19) indicated that very low adduction levels (<1%) are sufficient to generate an intense signal in the in-gel experiments. These findings provide an insight into the sensitivity of this proteomic method.

4.2.6. Interaction of lacosamide with CKB

Most CKB labeling competition experiments using the rat cytoplasmic lysate or the purified enzyme with (*R*)-**180** (1–10 μ M) in the presence of excess (*R*)- or (*S*)-LCM (100 to 5000 equiv) at room temperature (20 h) led to no reduction in fluorescence intensity of labeled CKB. These findings raised concerns since protein adduction by (*R*)-**180** should be competitively blocked by excess (*R*)-LCM. Accordingly, we asked whether CKB activity was inhibited by (*R*)-LCM.

Intriguingly, our first experiments conducted using purified CKB, showed that (*R*)-LCM inhibited the enzyme at therapeutically relevant concentrations (IC_{50} ~20–50 μ M), while (*S*)-LCM had no effect up to 500 μ M. The IC_{50} value of (*R*)-LCM, however, fluctuated with the amount of enzyme used per reaction. Furthermore, inhibition was only observed if the enzyme was pre-incubated with the drug for 10 min prior to starting the kinetic assay measurement. Noteworthy, incubation of (*R*)-LCM with a CKB sample containing 1 mM DTT led to no detectable inhibition of the enzyme.

The protective effect of DTT led us to hypothesize that the batch of (*R*)-LCM used was contaminated with trace amounts of a heavy metal and that this metal led to enzyme inactivation.^{464,465} Significantly, the (*R*)-LCM sample used in these studies employed Ag₂O in the final synthetic step for (*R*)-**1** (**route 1**, see Section 2.2.2.1, Scheme 14). To confirm this hypothesis, we separately tested the effects of TPEN, a known heavy-metal chelator, on the enzyme. At 10 μ M, TPEN did not have any inhibitory activity on CKB. When CKB (2 nM) was pre-incubated with 200 μ M (*R*)-LCM, the enzyme was fully inhibited. However, in the presence of 10 μ M TPEN, (*R*)-

LCM (200 and 500 μM) had no appreciable effect on the activity of the enzyme. Further supporting these results was the lack of activity of *O*-ethoxy (*R*)-**48**, which possesses anticonvulsant activity similar to (*R*)-LCM in the MES test,⁴⁶⁶ and that was prepared using a heavy-metal-free synthetic route (**route 3**, see Section 2.2.2.2, Scheme 16).⁴⁶⁶ Taking advantage of the large quantity of CKB that was available, we evaluated the binding affinity between CKB and (*R*)-LCM using isothermal titration calorimetry (ITC). In these experiments, highly concentrated stocks of CKB (5–10 mg.mL^{-1} , 115–230 μM) were dialyzed (2 x 2 h) against given equilibration buffers (phosphate buffer, pH 6.5 or 7.5, including TCEP or BME as reducing agent, in either the presence or absence of DMSO (5%)).

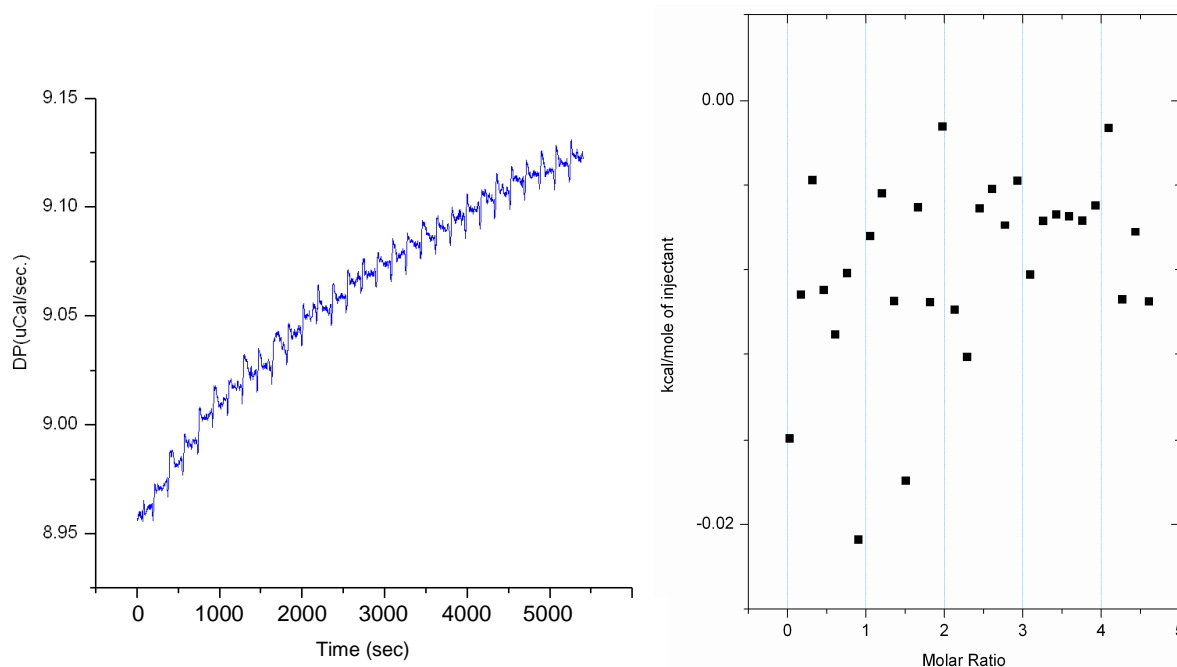


Figure 22. Left picture: ITC trace of the interaction between CKB and (*R*)-LCM. The purified enzyme (200 μM) was dialyzed (3 h) against 50 mM phosphate buffer (pH 7.4) containing 100 μM TCEP. The enzyme was then titrated with a 5 mM solution of (*R*)-LCM dissolved in the dialysis buffer. Right picture: corresponding integrated heat plot showing no correlation between the kcal.mol^{-1} of injectant and the molar ratio of the enzyme to the ligand. Machine settings are detailed in the Experiment Section.

The equilibration buffer of the second dialysis was then used to prepare the stock of (*R*)-LCM (20–25 times the protein concentration, 2.3–6.0 mM). Under no conditions was any significant binding affinity observed (Figure 22). The integrity of the enzyme was assessed by the CKB kinetic assay prior to beginning the ITC measurement. We concluded that CKB is selectively adducted by (*R*)-**180** in a complex protein lysate, but it is not a binding partner of (*R*)-**1**.

4.3. Photoaffinity labeling of the cytoplasmic lysate

Following our studies with epoxide-based AB&CR agents **175**, **179**, **176**, and **180**, other pairs of (*R*)- and (*S*)-AB&CR agents were employed to screen the rat brain soluble proteome (Figure 23).

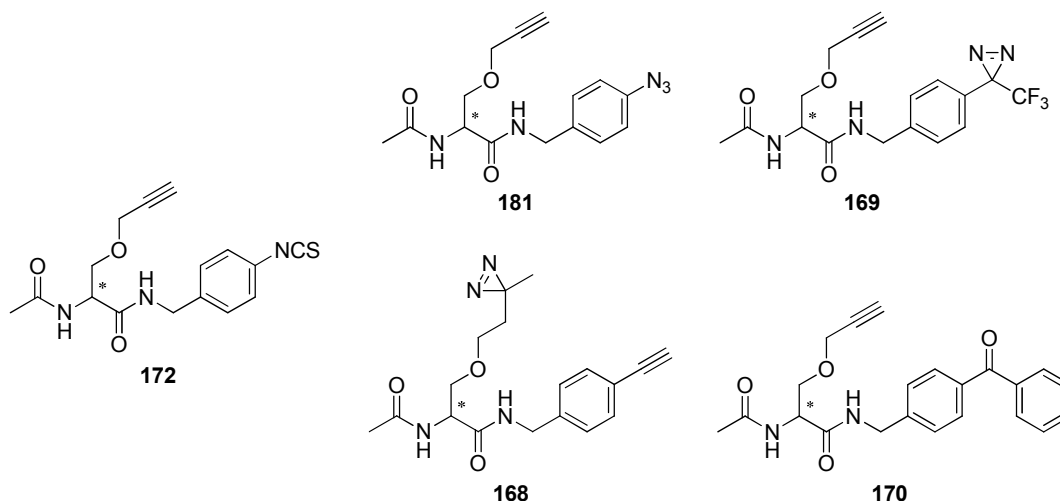


Figure 23. Structures of electrophilic AB&CR agents **172**, and photoAB&CR agents **181**, **169**, **168**, and **170** used in the screening of the rat brain cytoplasmic lysate.

One lesson learnt from the CKB experiments was that enantiospecific labeling of a protein should not be the sole criterion to identify potential targets. Instead, dose-

dependent and enantiospecific competition with (*R*)-LCM should serve as major experimental criteria for target identification. In addition, electrophilic AB groups can introduce a bias in the proteome search since they react with specific nucleophilic residues. Accordingly, the proteomic search was expanded to include a suite of photoAB&CR agents **181**, **169**, **168**, and **170** (Figure 23), and to rely primarily on competition experiments to select target(s) of interest. AB&CR agent **172** was used as a reference to compare the reactivity of the different photoAB&CR derivatives.

Following previously described protocols, we screened the rat brain cytoplasmic lysate with compounds **172**, **181**, **169**, **168**, and **170** using AMS to fractionate proteins. Each photoAB&CR agent was irradiated under specific conditions (see Experimental Section). After irradiation, the content of each well was recovered and AMS fractionation followed by click chemistry with fluorescent Probe **196** was performed. We screened the cytoplasmic lysate with AB&CR agent (*R*)-**172** (1 μ M, 15 min at rt, pH 7.4) and photoAB&CR agents **181**, **169**, **168**, and **170** (1 μ M) in the presence or absence of excess (*R*)-LCM (1 mM). Under these conditions, no protein of interest could be identified where the fluorescent labeling was diminished in the presence of excess (*R*)-LCM (1000 equiv) (Figure 24, Figure 25).

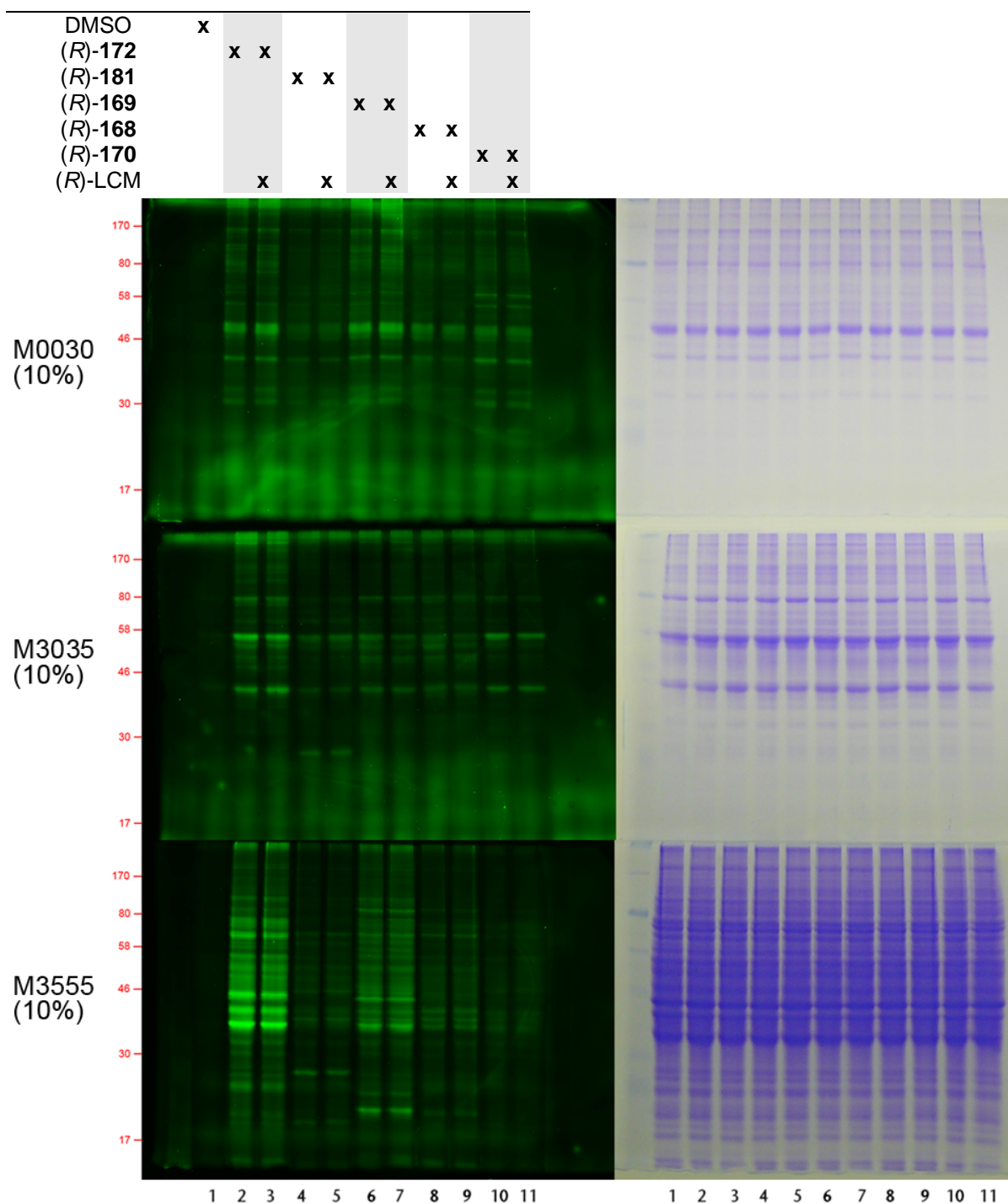


Figure 24. Left: in-gel fluorescence of different AMS cut from the cytoplasmic lysate after labeling with various AB&CR agents. Right: Corresponding Coomassie stains. Top to bottom: **M0030** (10% SDS-PAGE gel); **M3035** (10%); **M3555** (10%). Lane 1: DMSO; lane 2: (*R*)-172 (1 μ M); lane 3: (*R*)-172 (1 μ M) + (*R*)-LCM (1 mM); lane 4: (*R*)-181 (1 μ M); lane 5: (*R*)-181 (1 μ M) + (*R*)-LCM (1 mM); lane 6: (*R*)-169 (1 μ M); lane 7: (*R*)-169 (1 μ M) + (*R*)-LCM (1 mM); lane 8: (*R*)-168 (1 μ M); lane 9: (*R*)-168 (1 μ M) + (*R*)-LCM (1 mM); lane 10: (*R*)-170 (1 μ M); lane 11: (*R*)-170 (1 μ M) + (*R*)-LCM (1 mM). Approximate molecular weight marker (kDa) are shown in red on the left.

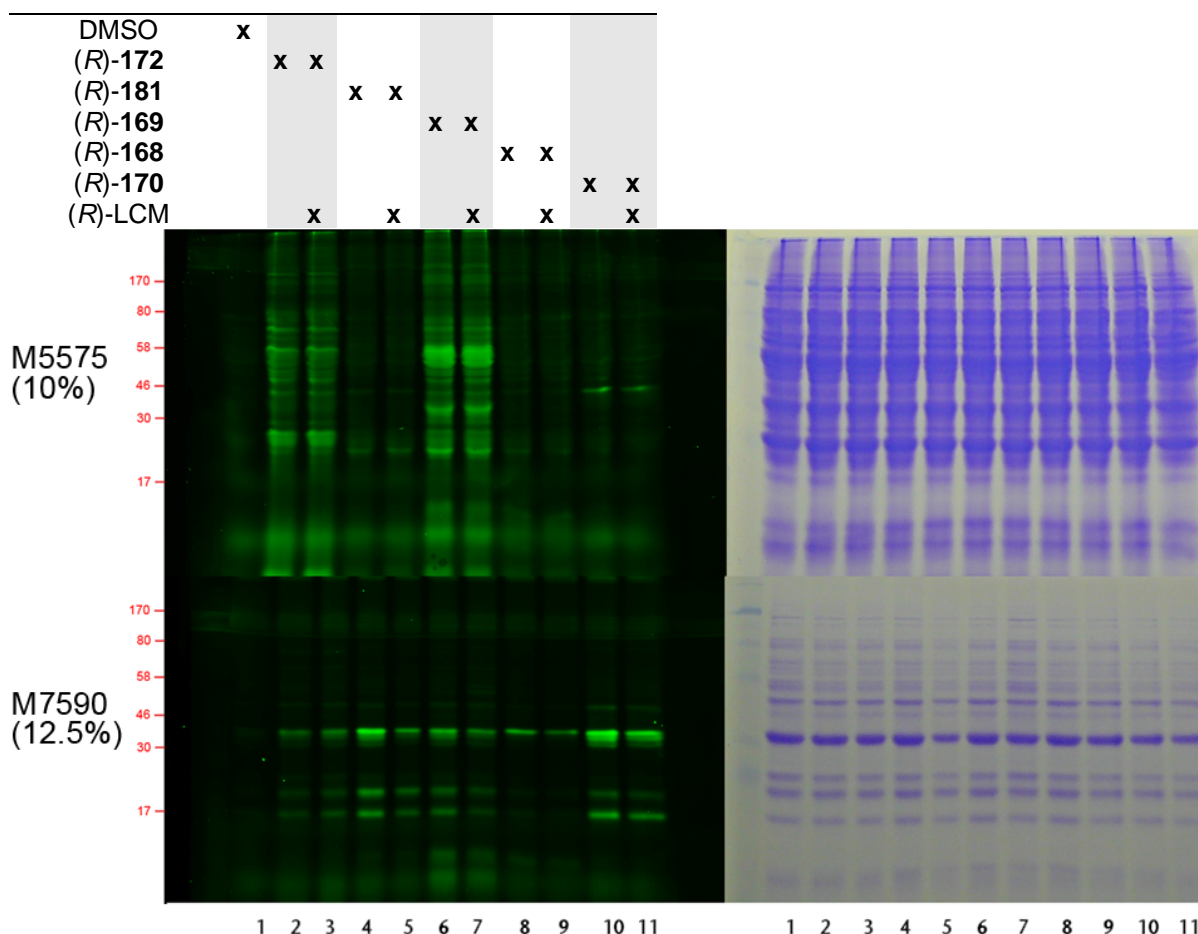


Figure 25. Left: in-gel fluorescence of different AMS cut from the cytoplasmic lysate after labeling with various AB&CR agents. Right: Corresponding Coomassie stains. Top to bottom: **M5570** (12.5%); **M7090** (12.5%). Lane 1: DMSO; lane 2: (R)-172 (1 μ M); lane 3: (R)-172 (1 μ M) + (R)-LCM (1 mM); lane 4: (R)-181 (1 μ M); lane 5: (R)-181 (1 μ M) + (R)-LCM (1 mM); lane 6: (R)-169 (1 μ M); lane 7: (R)-169 (1 μ M) + (R)-LCM (1 mM); lane 8: (R)-168 (1 μ M); lane 9: (R)-168 (1 μ M) + (R)-LCM (1 mM); lane 10: (R)-170 (1 μ M); lane 11: (R)-170 (1 μ M) + (R)-LCM (1 mM). Approximate molecular weight marker (kDa) are shown in red on the left.

4.3.1. A potential protein target for (S)-LCM

We did not identify a protein that was selectively competed with an excess of (R)-LCM using AB&CR agents (R)-172, (R)-181, (R)-169, (R)-168, and (R)-170. However, we found a ~25 kDa cytoplasmic protein that was selectively adducted by a (S)-AB&CR agent. The protein was first identified in two different AMS fractions (**M3045** and **M4555**) and solely labeled by (S)-169 (Figure 26). Interestingly, ^1H

NMR analysis of the (S)-**169** sample used showed that it was contaminated with an impurity. Nonetheless, despite the lowered concentration of (S)-**169** compared with (R)-**169** in this experiment, (S)-**169** gave a stronger fluorescence labeling while producing minimal non-specific protein labeling (Figure 26, [blue arrow](#)).

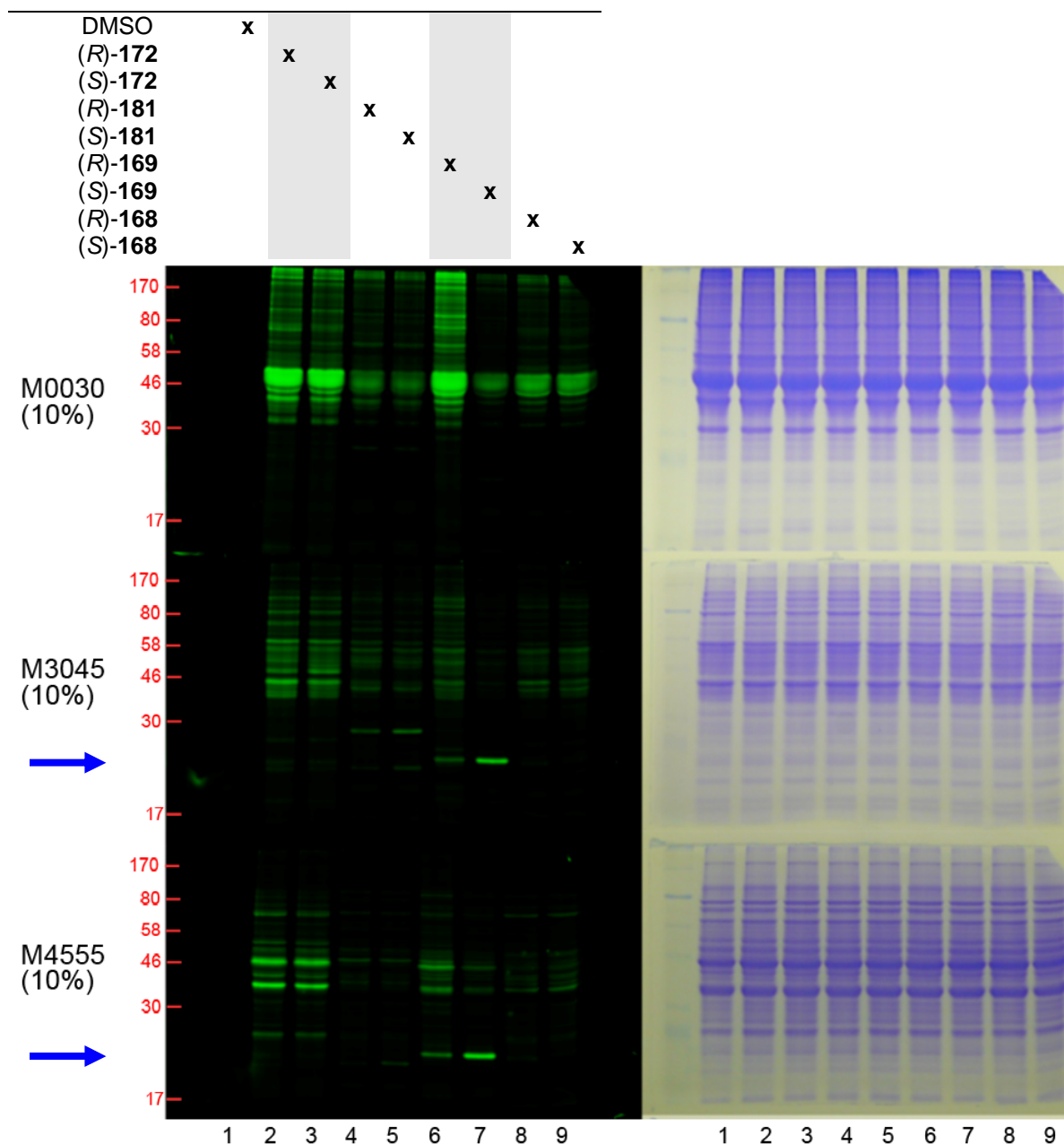


Figure 26. Left: in-gel fluorescence of different AMS cuts (**M0030**, **M3045**, **M4555**) from the cytoplasmic lysate after labeling with various AB&CR agents. Right: Corresponding Coomassie stains. The different AMS cuts corresponding to each gel are shown on the left, along with the percentage of SDS-PAGE gel between parentheses. Lane 1: DMSO; lane 2: (R)-**172** (5 μ M); lane 3:

(*S*)-**172** (5 μ M); lane 4: (*R*)-**181** (5 μ M); lane 5: (*S*)-**181** (5 μ M); lane 6: (*R*)-**169** (5 μ M); lane 7: (*S*)-**169** (5 μ M); lane 8: (*R*)-**168** (5 μ M); lane 9: (*S*)-**168** (5 μ M). An impurity was present in the (*S*)-**169** sample (lane 7), leading to a lower effective AB&CR concentration. Approximate molecular weight markers (kDa) are shown in red on the left.

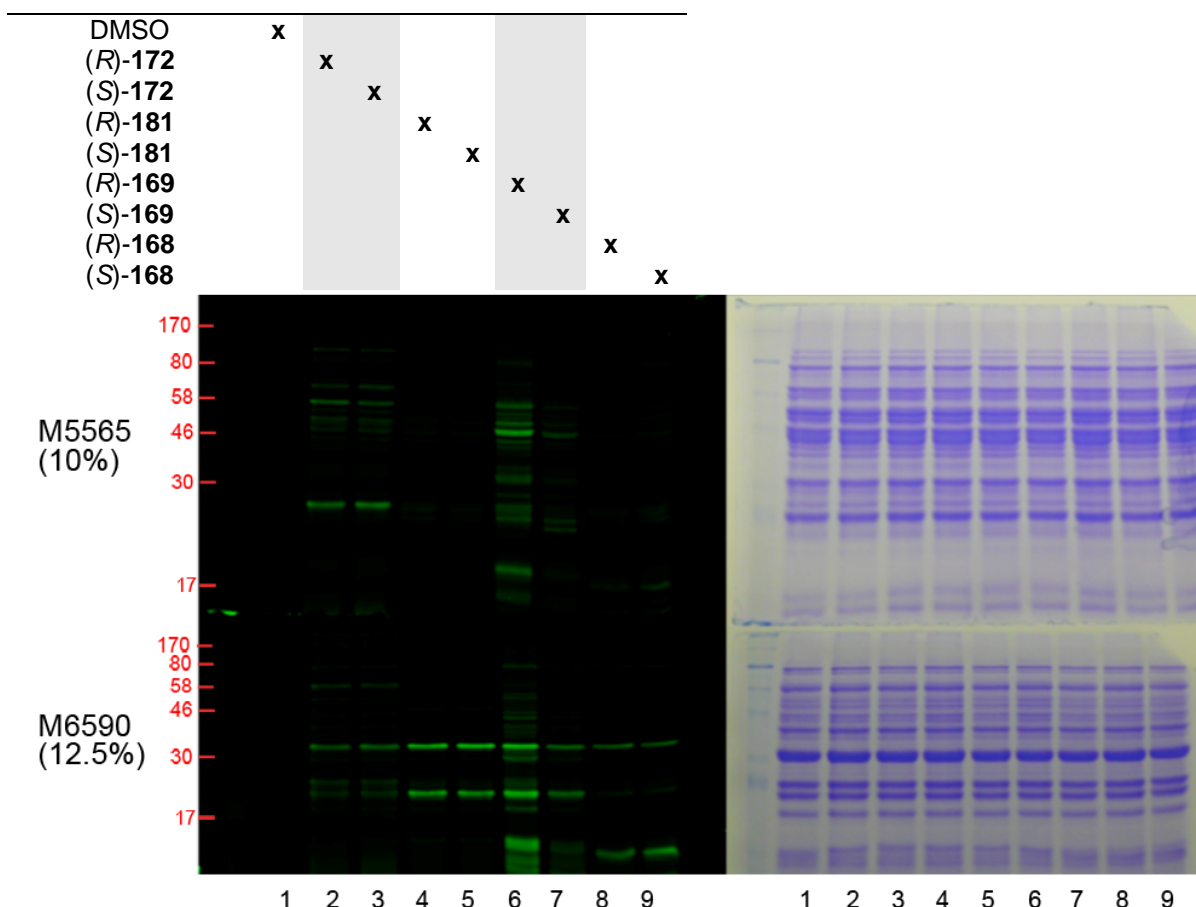


Figure 27. Left: in-gel fluorescence of different AMS cuts (**M5565**, **M6590**) from the cytoplasmic lysate after labeling with various AB&CR agents. Right: Corresponding Coomassie stains. The different AMS cuts corresponding to each gel are shown on the left, along with the percentage of SDS-PAGE gel between parentheses. Lane 1: DMSO; lane 2: (*R*)-**172** (5 μ M); lane 3: (*S*)-**172** (5 μ M); lane 4: (*R*)-**181** (5 μ M); lane 5: (*S*)-**181** (5 μ M); lane 6: (*R*)-**169** (5 μ M); lane 7: (*S*)-**169** (5 μ M); lane 8: (*R*)-**168** (5 μ M); lane 9: (*S*)-**168** (5 μ M). An impurity was present in the (*S*)-**169** sample (lane 7), leading to a lower effective AB&CR concentration. Approximate molecular weight markers (kDa) are shown in red on the left.

We repeated the experiment with repurified (*S*)-**169**, and found that the protein of interest could be enriched in a refined AMS cut (**M3555**) and did not adsorb on S-Sepharose[®], or Q-Sepharose[®] at pH 7.5. We saw a dose-dependent competition of the fluorescent signal with increasing concentrations of (*S*)-LCM

(100–1000 equiv). At 1000 equiv. of (S)-LCM, the (S)-**169** fluorescent signal disappeared, while a 1000-fold excess of (R)-LCM had little to no effect (Figure 28).

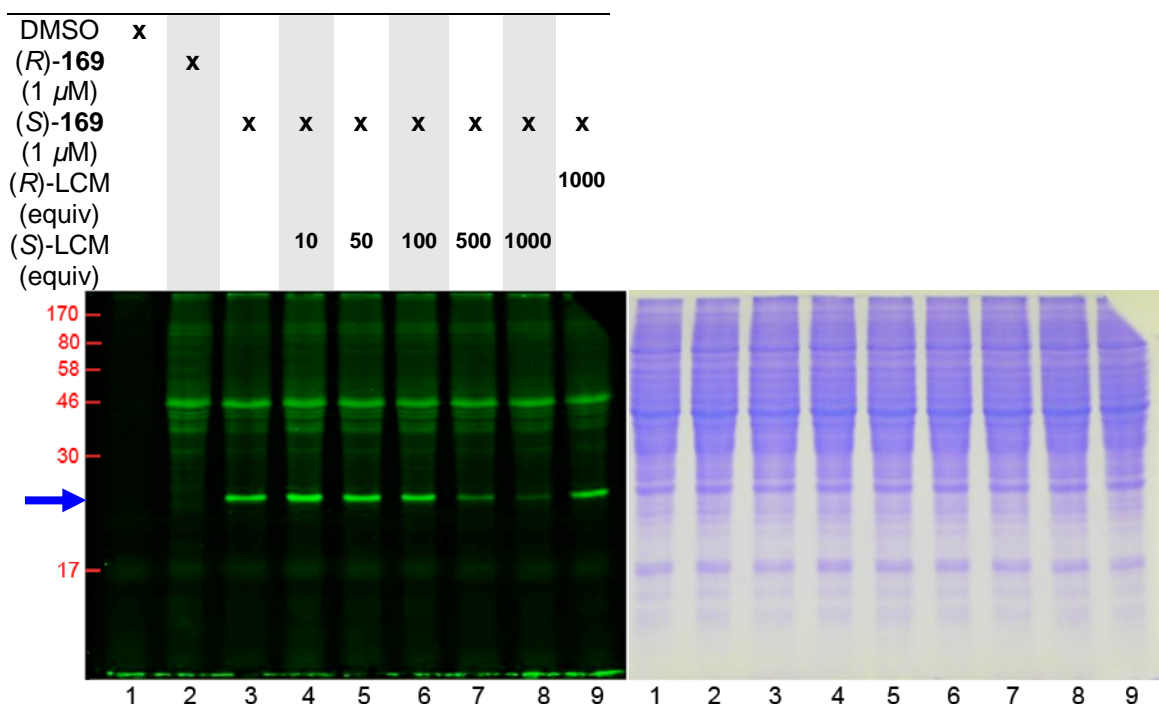


Figure 28. 12.5% SDS-PAGE gel of the rat cytoplasmic **M3555** cut. Left: in-gel fluorescence scan; right: corresponding Coomassie stain. Dose-dependant and enantioselective competition of the protein targeted by (S)-LCM. Rat cytoplasmic lysate was labeled with DMSO, (R)-**169**, and (S)-**169** in the presence or absence of (R)-LCM and (S)-LCM. Lane 1: DMSO; lane 2: (R)-**169** (1 μ M); lane 3: (S)-**169** (1 μ M); lane 4: (S)-**169** (1 μ M) + 10 μ M (S)-LCM; lane 5: (S)-**169** (1 μ M) + (S)-LCM (50 μ M); lane 6: (S)-**169** (1 μ M) + (S)-LCM (100 μ M); lane 7: (S)-**169** (1 μ M) + (S)-LCM (500 μ M); lane 8: (S)-**169** (1 μ M) + (S)-LCM (1 mM); lane 9: (S)-**169** (1 μ M) + (R)-LCM (1 mM). Approximate molecular weight markers (kDa) are shown in red on the left.

Next, we tried to optimize conditions for biotin purification of the ~25 kDa protein by conducting a dose-dependent labeling experiment. However, we observed that while the extent of protein non-specific labeling increased with increasing (S)-**169** concentrations, the intensity of the ~25 kDa fluorescent signal rapidly reached a plateau between 5–10 μ M (Figure 29). This finding suggested that the protein's extent of modification was maximal around 5 μ M of (S)-**169**, and led us to hypothesize that, given the level of fluorescence intensity observed on the gels,

the ~25 kDa protein was present in low abundance in the lysate. In summary, a 1 μ M concentration of (S)-**169** gave minimal non-specific protein labeling while providing a strong specific signal for the protein of interest.

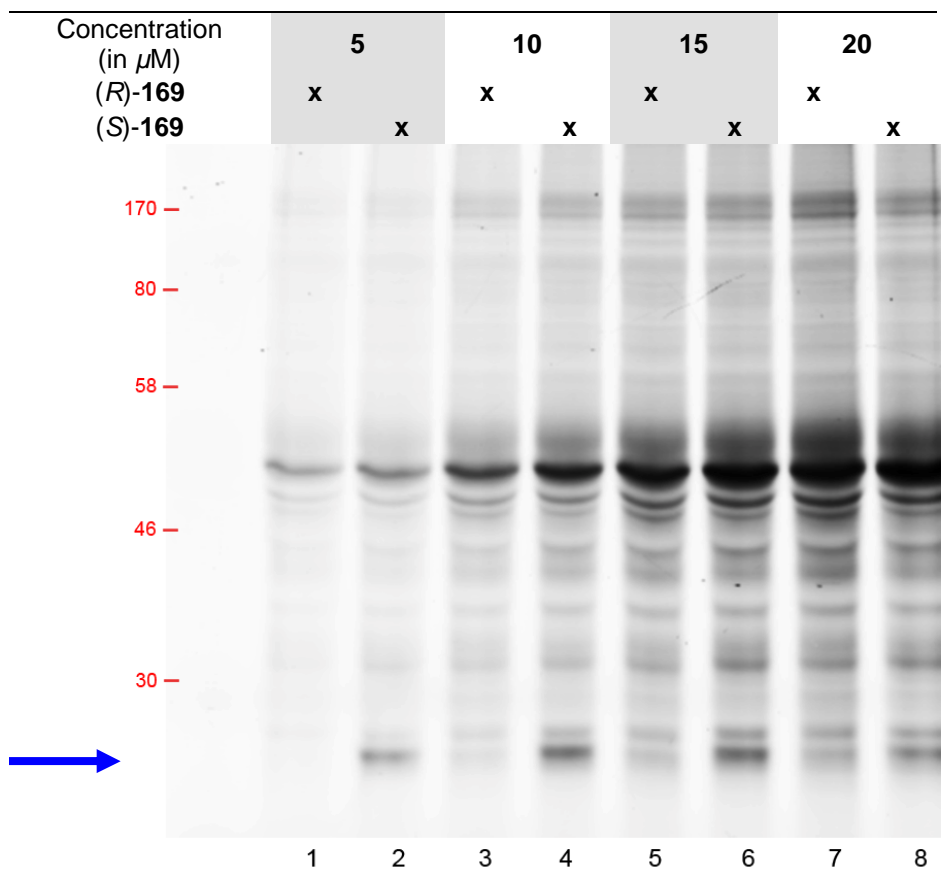


Figure 29. Fluorescence scan of the cytoplasmic AMS cut **M3555** after labeling with (R)-**169** or (S)-**169** at various concentrations (10% SDS-PAGE gel) and click chemistry with **196**. Lane 1: (R)-**169** (5 μ M); lane 2: (S)-**169** (5 μ M); lane 3: (R)-**169** (10 μ M); lane 4: (S)-**169** (10 μ M); lane 5: (R)-**169** (15 μ M); lane 6: (S)-**169** (15 μ M); lane 7: (R)-**169** (20 μ M); lane 8: (S)-**169** (20 μ M). The Coomassie stain (picture not shown) indicated equal amounts of protein loaded per well. Approximate molecular weight markers (kDa) are shown in red on the left.

4.3.2. Enrichment procedure for the ~25 kDa protein

Recognizing the low level of expression of the ~25 kDa protein, we implemented our protocol using two enrichment steps. First, we increased the molecular weight cut-off (MWCO) of the dialysis membrane used to dialyze the S3

supernatant in the lysate preparation. Using a MWCO of ~14 kDa instead of ~5–6 kDa led to the recovery of ~35 mg of cytoplasmic protein per rat brain instead of ~40 mg. Second, we included a pH-dependent protein precipitation step to further enrich the (S)-LCM target. Initially, we briefly (15 sec) lowered the pH of the lysate from 7.4 to either 5.5 (40 mM MES buffer), 5.0, or 4.5 (40 mM acetate buffer) after the photolabeling step. Denatured proteins were pelleted by centrifugation (14,000 rpm, 3 min), and the supernatant was readjusted to pH 7.4 by adding HEPES (pH 7.4) to 80 mM. AMS fractionation was subsequently performed, the **M3555** cut was clicked with Probe **196** and the gels were resolved and scanned for fluorescence. Gratifyingly, the fluorescence intensity levels corresponding to our protein of interest were not affected by the lysate acidification step (pH 4.5), while the Coomassie stain showed a strong reduction in the total amount of protein on the gel (data not shown). We further refined these conditions by precipitating proteins under even more acidic conditions. Using the same protocol, we precipitated proteins at pH 4.0, 3.5 (40 mM formate buffer) and pH 3.0 (40 mM citrate buffer). After AMS fractionation (pH 7.4) and click chemistry, we found that the protein was still unaffected after treatment at pH 4.0 and 3.5, while the Coomassie stain showed a more pronounced reduction in the total amount of protein. At pH 3.0, however, the fluorescent signal corresponding to the ~25 kDa protein disappeared (Figure 30). These combined steps (dialysis, acid precipitation, and AMS fractionation) led to the removal of ~90% of total cytoplasmic proteins (~10-fold enrichment, based on protein concentration measurement using the Bradford assay). We then endeavored to identify the ~25 kDa protein by performing a large scale biotin purification

experiment. The cytoplasmic S3 fraction from 3 rat brains was dialyzed through a 14 kDa MWCO membrane, and split into three equal volumes (9 mL, ~35 mg total protein per reaction).

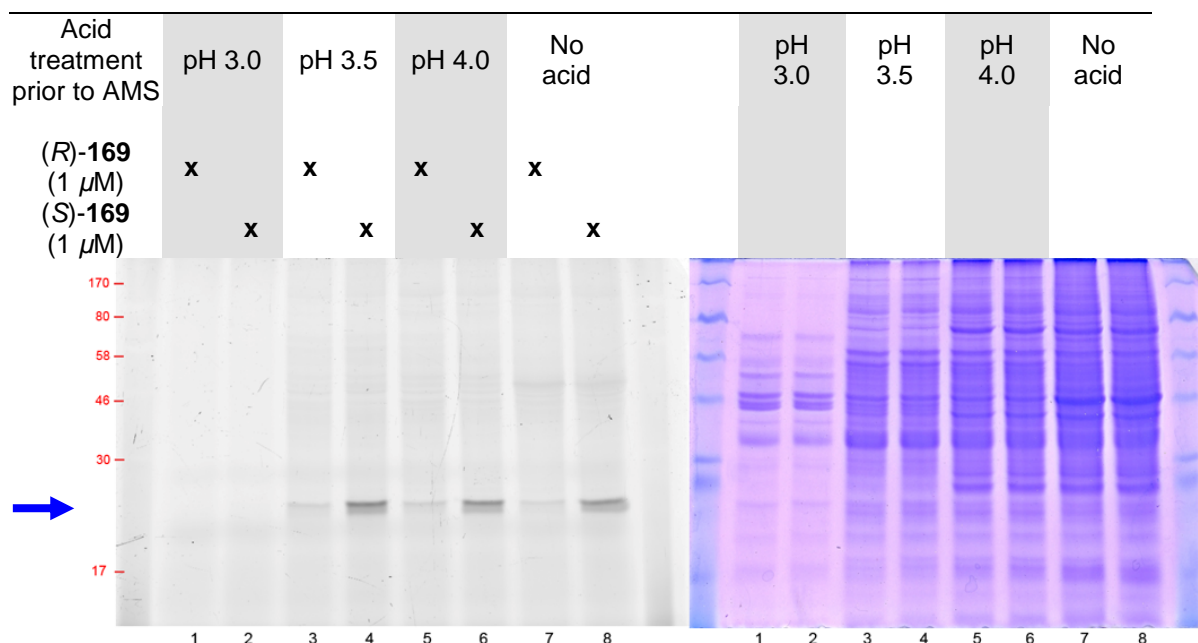


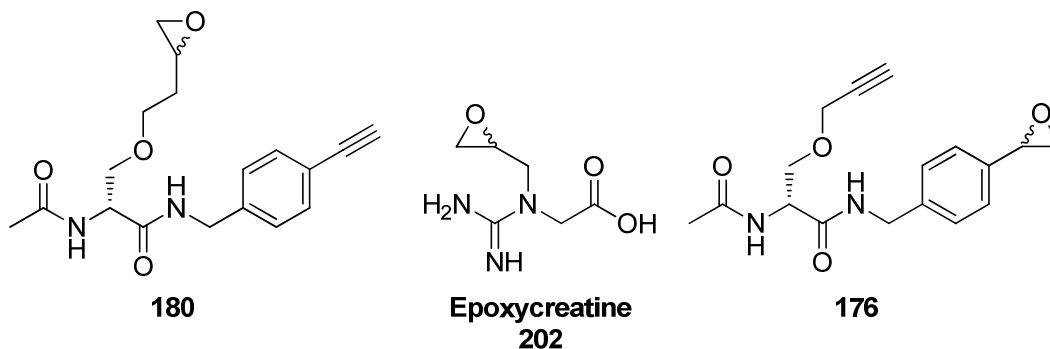
Figure 30. 10% SDS-PAGE gel of the rat brain cytoplasmic lysate **M3555** labeled with 1 μ M (*R*)-**169** or (*S*)-**169**. Left picture: fluorescence scan; right picture: corresponding Coomassie stain. Lanes 1, 3, 5, 7: 1 μ M (*R*)-**169**; lanes 2, 4, 6, 8: 1 μ M (*S*)-**169**. Lanes 1,2: proteins were precipitated at pH 3.0 prior to AMS fractionation; lanes 3,4: at pH 3.5; lanes 5,6: at pH 4.0; lanes 7,8: no acid treatment was performed before AMS fractionation. Approximate molecular weight markers (kDa) are shown in red on the left.

Each reaction (DMSO control, (*R*)-**169** (1 μ M), and (*S*)-**169** (1 μ M)) was plated into a 6-well plate (1.5 mL per well) and irradiated at 4 $^{\circ}$ C (10 min at 365 nm, 1 min at 312 nm). The contents of each well was then recovered and brought to pH 3.5 by addition of 1 M formate buffer (pH 3.5) to provide a 40 mM formate solution. The reactions were mixed (10 sec) and centrifuged (5,500 g, 5 min). The supernatant was transferred to a new tube (50 mL), the pH adjusted to pH 7.4 by addition of 1 M HEPES buffer (pH 7.4) up to 80 mM, and the solution was brought to 35% AMS

saturation by addition of liquid saturated AMS (54% of solution volume). After mixing (5 min), the suspension was centrifuged (5,500 g, 5 min), the supernatant was transferred to a new tube and brought to 55% AMS with saturated aqueous AMS (64% of initial solution volume). After mixing (5 min), and centrifugation (5,500 g, 5 min) the supernatant was discarded, and the residual liquid on the side of the tube carefully wiped without touching the pellet. For each reaction, the pellet was resuspended in 3 mL of 50 mM NaCl, 25 mM HEPES (pH 7.4) and click chemistry was performed with 20 μ M of biotin Probe **196** (1 h). Each reaction was supplemented to 0.1% SDS, dialyzed overnight against 50 mM NaCl, 25 mM HEPES buffer (pH 7.4), and tumbled with streptavidin beads for 30 min. Beads were then sequentially washed with 50 mM NaCl, 25 mM HEPES (pH 7.4) supplemented to 0.2% SDS (120 CV), 8 M urea (120 CV), and 50 mM NaCl, 25 mM HEPES (pH 7.4) (120 CV). The streptavidin beads were then boiled (95 °C, 15 min) in the presence of 2X SDS loading buffer, resolved on 10% SDS PAGE gel and silver stained. Traces of proteins were present in the DMSO control, while the lanes corresponding to (*R*)-**169** and (*S*)-**169** contained identical, low levels of protein despite using an extended silver stain developing time (>5 min, no picture available). The low recovery of the ~25 kDa band and our finding that the (*S*)-**169** reaction did not provide measurably enhanced levels of adduction compared with (*R*)-**169** did not warrant our MS analysis of this band, and we abandoned our efforts to identify this (*S*)-LCM interacting protein.

4.4. Discussion

Epoxide-containing AB&CR agent (*R*)-**180** and (*S*)-**180** proved highly selective at labeling CKB in a complex lysate. In addition we observed that the enzyme was preferentially labeled by (*R*)-**180** over (*S*)-**180**, and that the aromatic epoxide-containing AB&CR agent (*R*)-**176** did not adduct CKB. Mass spectrometric experiments strongly suggested that the principal CKB amino acid residue modified by (*R*)-**180** was Cys283, a catalytic residue crucial for enzymatic activity. However, no direct interaction between (*R*)-LCM and CKB was observed using fluorescence competition experiments, enzymatic inhibition assay, or ITC experiments. We have tentatively attributed the lack of correlation between the CKB selective, enantiospecific labeling by (*R*)-**180** and its binding with (*R*)-LCM to several reasons. First, epoxide electrophiles are prone to react with cysteine residues.^{274,308,309}



In this regard, the selective modification of CKB by aliphatic epoxide (*R*)-**180** compared with aromatic epoxide (*R*)-**176** may be rationalized by the report that epoxycrreatine **202**, is a known rabbit muscle-type creatine kinase (CKM) epoxide inhibitor.⁴⁶⁷ CKM shares an 80% identity with CKB and possesses the conserved catalytic site in humans, rats and rabbits that is seen in CKB. Epoxide **202** is known to modify Cys 282 of rabbit CKM, the CKB Cys283 homolog,⁴⁶⁷ and (*R*)-**180** and

202 have structural features in common. They both possess an aliphatic epoxide moiety in proximity of an amino acid backbone. Among several other possibilities, one can hypothesize that this combination of pharmacophores in both (*R*)-**180** and epoxycreatine, but unmet in (*R*)-**176**, is required for the cysteine residue nucleophilic attack. Thus, only a small fragment of the lacosamide framework in (*R*)-**180** may be sufficient for binding and covalent modification of CKB, while the lack of an epoxide moiety in (*R*)-LCM results in a loss of interaction with CKB (Figure 22), and the absence of (*R*)-LCM competition for (*R*)-**180** modification of CKB in the in-gel fluorescence experiments (Figure 15). We have tentatively attributed compound **180**'s (*R*)- vs (*S*)- labeling selectivity to a greater binding affinity with the CKB **180** binding pocket.

Consistent with our hypothesis, epoxide-based AB&CR agents **175**, **179**, **176** and **180** all displayed high labeling selectivity that mirrored their expected low reactivity profiles. However, the extended reaction time (20 h) needed for epoxide adduction raises concerns that protein denaturation may have occurred during this reaction time. While a robust enzyme such as CKB remains functional over a long time, other proteins of interest in the lysate may denature quickly. This concern suggests that an ideal balance should be reached where the AB agent is sufficiently reactive over a moderate time period, but not too reactive leading to nonspecific adduction, to maximize chances of capturing potential targets.

We also screened the rat brain cytoplasmic fraction using the suite of photoAB&CR agents **181**, **169**, **168** and **170** and compared them with the NCS-containing agent **172**. We observed that the 4 photoAB moieties and the NCS AB all

displayed very different reactivity profiles at 1 μ M (Figure 24, Figure 25) at 4 $^{\circ}$ C. The isothiocyanate group (15 min incubation, pH 7.4) and the trifluoromethylaromatic diazirine (10 min at 365 nm, 1 min at 312 nm) gave fluorescence signals with comparable intensities, yet with different labeling patterns. Aromatic azide (*R*)-**181** (10 min at 365 nm), methyldiazirine (*R*)-**168** (30 min at 365 nm, 1 min at 312 nm), and benzophenone (*R*)-**170** (1 h at 365 nm) all displayed lower adduction levels compared with (*R*)-**172** and (*R*)-**169**, and yet gave different protein labeling profiles. Unlike the three other photoAB&CR agents, we found that the protein labeling efficiency of the aromatic azide photoAB was highly temperature-dependent. At a 1 μ M concentration, photoAB (*R*)-**181** went from a low fluorescence intensity (4 $^{\circ}$ C) comparable to that of benzophenone (*R*)-**170**, to a strong fluorescent signal (room temperature) that was greater than isothiocyanate (*R*)-**172** and aromatic diazirine (*R*)-**169** under the same conditions (data not shown). These findings emphasize the need to use the largest possible variety of affinity labels to maximize the chances of identifying a drug target in a complex protein environment. Despite the number of affinity labels (7) used in this proteomic search, we were not able to identify a selectively labeled protein whose fluorescent signal was competed by an excess amount of (*R*)-LCM.

Interestingly, a parallel study conducted in the laboratory using a mouse brain cytoplasmic lysate (*work of Dr Ki Duk Park*) showed that isothiocyanate-containing AB&CR **172** labeled CRMP2,³⁸⁴ a ~62 kDa putative binding partner of (*R*)-LCM.²³³ The extent of protein labeling was ~2-fold higher with (*R*)-**172** when compared with (*S*)-**172**.³⁸⁴ Nonetheless, using our screening conditions, we did not observe any ~62

kDa protein that was preferentially labeled by (*R*)-**172** over (*S*)-**172** (Figure 24, Figure 25). Many possibilities may account for this difference. The animal used in the protocol should not, in principle, greatly influence the results given the fact that (*R*)-LCM is potent in both the mouse and the rat against MES-induced seizures. Perhaps more important, the amino acid sequences of the mouse and rat CRMP2 proteins are virtually identical. However, the two lysate preparations greatly differ and are likely the source of disparities observed. Significantly, the mouse brain cytoplasm was obtained by homogenizing the rat brain in plain HEPES buffer (50 mM, pH 7.4) that was not supplemented in sucrose, or protease inhibitors, and was used directly to conduct labeling experiments after centrifugation (100,000 g, 1 h). In contrast, the rat brain homogenate was prepared using literature established protocols,⁴²⁴⁻⁴²⁷ using a buffer system (HEPES, 25 mM, pH 7.4) supplemented to 320 mM sucrose and 4 different protease inhibitors (see Section 3.1). Additionally, the rat cytosolic lysate obtained after centrifugation was extensively dialyzed (2 buffer changes) against 100 volumes HEPES buffer (25 mM, pH 7.4, supplemented to 50 mM NaCl). These three major differences may result in very different protein environments and therefore different screening conditions. Importantly, the absence of sucrose may result in some intracellular organelle leakage during homogenization, thus increasing the complexity of the lysate, and the lack of protease inhibitors may lead to some extent of protease degradation. In addition, the absence of a dialysis step will lead to the presence in the lysate of a variety of secondary messenger molecules⁴⁶⁸⁻⁴⁷¹ that might influence protein conformation.

We did, however, identify a soluble protein modified exclusively by (S)-**169**. This ~25 kDa soluble protein precipitated in the **M3555** AMS cut (pH 7.4) (Figure 28), and did not adsorb on S-Sepharose[®] (pH 4.5 or pH 7.5) or Q-Sepharose[®] (pH 7.5) (data not shown). Fluorescence labeling experiments showed a highly selective labeling by (S)-**169** over (R)-**169**, and the fluorescent signal of (S)-**169** disappeared in a dose-dependent manner with excess (S)-LCM, but not (R)-LCM (Figure 28). Use of a strongly acidic workup (~pH 3.5) did not cause the protein of interest to precipitate while ~50% of all the proteins present in the cytoplasmic lysate were denatured and precipitated. Dose-dependent labeling experiments with (S)-**169** showed that the relatively weak fluorescent signal of the ~25 kDa protein rapidly (5–10 μ M) reached a plateau at 5–10 μ M concentrations, while further increasing the photoAB&CR concentration (up to 20 μ M) only resulted in a pronounced labeling of abundant proteins. This finding suggested that the protein was present in low abundance in the cytoplasmic protein lysate. Thus, we used a combination of protein dialysis (MWCO ~14 kDa), brief acidic treatment (pH 3.5), and AMS fractionation which resulted in a ~10-fold enrichment of the protein. The lysate was treated with DMSO, 1 μ M (R)-**169**, and 1 μ M (S)-**169**, irradiated, and each reaction was fractionated with AMS as described in the Experimental Section (see Sections 4.6.2 and 4.6.3). After click chemistry with biotin Probe **191**, dialysis, and streptavidin capture, the streptavidin-bound proteins were stringently washed, and eluted using SDS loading buffer. Traces of proteins were found in the DMSO control, while higher, yet minute amounts of proteins were present in samples treated with (R)-**169** and (S)-**169**. Both agents gave virtually identical protein profiles and did not mirror

the fluorescence scan previously observed (Figure 30). Even after *prolonged* developing, the silver stain did not show any ~25 kDa protein present in higher abundance in the (S)-**169** reaction compared with the (R)-**169** reaction. Thus, despite the use of acid and AMS fractionations and large amounts of protein per reaction (S3 fraction from one rat brain, ~35 mg per reaction, 3 rat brains), we were not able to isolate a protein band of interest after biotin purification. We concluded that the level of expression of this protein targeted (S)-LCM was too low for us to identify using the employed methodology.

4.5. Conclusions

Screening the rat brain cytoplasmic fraction with a large panel of AB&CR agents yielded a potential, low abundance protein targeted by (S)-LCM, but no protein selectively modified by our (R)-LCM AB&CR derivatives. While many factors may have been responsible for our lack of target identification in the cytoplasmic lysate, one likely explanation is the subcellular localization of the drug target. Indeed, membrane-bound proteins such as VGICs, LGICs, neurotransmitter transporters are key targets for many AEDs. Therefore, we advanced to the next step by interrogating the membrane-bound proteome.

4.6. Experimental Section

4.6.1. Preparation of the rat brain cytoplasmic lysate

Frozen male Sprague Dawley stripped rat brains (6–8 weeks old, Pel-Freez Biologicals, cat # 56999, or Rockland Immunochemicals, cat # RT-T081, 1.5–1.8 g per whole brain) were thawed on ice at 4 °C until soft, finely minced with razor blades and homogenized (10 mL buffer per gram of wet tissue) using a glass/Teflon Dounce homogenizer in 320 mM sucrose 25 mM HEPES buffer (pH 7.4) (supplemented with 1 mM PMSF, 10 μ M E-64, 10 μ M Pepstatin A, and 1 μ M TPEN) by 10–15 up-and-down strokes by hand, taking 20 sec to complete one stroke. The homogenate was centrifuged at 4 °C (100,000 g, 50 min), the supernatant was dialyzed twice (1 h) against 3 L of 25 mM HEPES (pH 7.4), 50 mM NaCl using a Spectra/Por[®] dialysis membrane (MWCO 3,500; Spectrum Laboratories Inc., cat # 132720) and stored at -80 °C until use for up to 2 months.

4.6.2. Cytoplasmic protein labeling with AB&CR agents

The following AB&CR agents were incubated as follows prior to fractionation (AMS and/or ion exchange chromatography). Epoxide AB&CR agents **175**, **179**, **176** and **180** (1–10 μ M, 2% (v/v) DMSO final concentration) were incubated with the cytoplasmic lysate (pH 7.4) at room temperature (20 h). The lysate then underwent fractionation and click chemistry. PhotoAB&CR molecules were irradiated as follows: **181**, 10 min at 365 nm; **169**, 10 min at 365 nm then 1 min at 312 nm; **168**, 30 min at 365 nm, then 1 min at 312 nm; **170**, 60 min at 365 nm. On small scale (100 μ L

reactions), photolabeling was carried out at 4 °C in clear 96-well plates (BD Falcon®). Larger scale experiments were conducted using 6-well plates (1.0–1.5 mL per well). Two types of UV lamps were used to irradiate samples (365 nm; 312 nm: Spectroline, Longlife™ Filter), and were positioned 1 cm above the well. A maximum of 2 rows (2 x 12 wells) were irradiated at the same time when using 96-well plates and 1 row (1 x 3 wells) when performing large scale experiments.

Competition experiments were conducted by pre-incubating the lysate with an excess amount of (*R*)- or (*S*)-LCM for 5 min (500–1500 equiv) at room temperature prior to starting the labeling experiment.

4.6.3. General procedure for lysate fractionation

The rat brain lysate (100–200 µL reactions, 2–3 mg.mL⁻¹) was incubated with the desired AB&CR agents and AMS fractionation and ion exchange chromatography were performed as described in Section 3.2. Typical AMS cuts recovered were **M0030**, **M3045**, **M4555**, **M5565**, and **M6590**. The first 4 AMS cuts (0 to 65% saturation) were obtained by liquid addition of a saturated AMS solution at room temperature (65% ~2 initial volumes of sat. AMS added). After mixing, the solution was let to stand for 5 min and centrifuged (14,000 rpm, rt, 3 min). The last cut was obtained by addition of solid AMS. AMS pellets were redissolved in 25 mM HEPES (pH 7.4) and click chemistry was performed.

For ion exchange chromatography, the resin (S-Sepharose or Q-Sepharose, ~10 µL resin for 100 µg of total protein) was pre-equilibrated with the desired buffer, typically HEPES buffer supplemented with 50 mM NaCl, and the lysate was added

to the resin. After a short incubation (30 sec), the flow-through was recovered, and the resin rinsed with 10 CV of equilibration buffer. At pH 7.4, typical elution fractions recovered on both S-Sepharose[®] and Q-Sepharose[®] were 50–200 mM NaCl, 200–250 mM NaCl, 250–300 mM NaCl and 300–350 mM NaCl and click chemistry was performed on the eluates.

4.6.4. Click chemistry

Click chemistry was performed as described in Section 3.4. Fluorescent Probes **195** or **196**, and biotin Probes **193** or **191** were added to the fractionated lysate samples (20 μ M), typically in PCR 8-tube strips (volume 250 μ L). 10X Cu(I) mix was freshly prepared by sequentially adding (for 100 μ L) 10 μ L of 25 mM CuSO₄ (aqueous), 40 μ L of 625 μ M TBTA (in 1:4 DMSO:*t*-BuOH), and 50 μ L of 5 mM TCEP HCl (aqueous), and added to each sample at a 1/10 dilution. Samples were gently mixed and let stand at room temperature (1 h). SDS-loading buffer was added to samples, and then the samples were heated at 75 °C (5 min) and resolved on SDS PAGE gels (6–12.5%).

4.6.5. ITC experiments

ITC experiments were conducted at 25 °C (Microcal[™], VP-ITC microcalorimeter). The CKB enzyme (100–200 μ M, ~2.5 mL) was dialyzed against the desired buffer (1.5 L) for at least 3 h, and a solution of (*R*)-LCM in the dialysis

buffer (2–5 mM) was prepared. In a typical ITC experiment, the enzyme was titrated with (*R*)-LCM, using the following conditions.

Experimental parameters: total number of injections: 30; cell temperature: 25 °C; reference power: 10 $\mu\text{Cal.s}^{-1}$; initial delay: 60 s; stirring speed: 490 rpm.

Injection parameters: initial injection volume: 2 μL , duration: 4 s, spacing: 120 s, filter period: 2 s; injections: 10 μL , duration 20 s, spacing: 180 s.

4.6.6. Creatine Kinase B enzymatic assay

The components of the coupled enzymatic assay were as follows.

(A) CKB (GenWay Biotech cat # 10-663-45059): Commercial human CKB, tag-free. The overexpressed and purified human CKB was prepared according to literature procedures and contains a C-terminus His-tag (see Sections 4.6.7 and 4.6.8).⁴⁵⁷

(B) Hexokinase (HK) (Sigma cat # H4502): Catalyzes the transfer of a phosphate group from ATP to D-glucose to form glucose-6-phosphate (G6P)

(C) Glucose 6-Phosphate Dehydrogenase (G6PDH) from *leuconostoc mesenteroides* (Sigma cat # G5885): Catalyzes the oxidation of G6P to 6-phosphogluconolactone using NADP as a cofactor and generating NADPH. The absorbance of the solution is measured at 340 nm.

(D) Phosphocreatine (Sigma cat # P7936), ADP (Sigma cat # 01897), $\text{Mg}(\text{OAc})_2$ (Sigma cat # M5661), D-glucose (Sigma cat # G7528), NADP (Sigma cat # N5755), DTT and MES. For assays where a complex lysate is used as a source of

creatine kinase, it may be necessary to include 10 mM AMP to stop myokinase activity.⁴⁴⁶ AMP is not utilized in this assay.

The assay was conducted in 96-well plates using 150/200 μL total volume for each reaction either at room temperature (Plate reader: HTS 7000 Plus Bio Assay Reader, Perkin Elmer) or at 37 $^{\circ}\text{C}$ (Plate reader: POLARstar OPTIMA, BMG Labtech). HK was prepared as a 100 X stock in 100 mM MES buffer (pH 6.5) and stored at -20 $^{\circ}\text{C}$. HK can sustain many freeze/thaw cycles without losing activity. G6PDH was prepared as a 1000 X stock in 50 mM phosphate buffer (pH 7.2), 200 mM NaCl, and 1 mM EDTA, and stored at 4 $^{\circ}\text{C}$. Phospho creatine (PCr), ADP, D-glucose, $\text{Mg}(\text{OAc})_2$, and DTT were prepared as 50 X stock solutions in 100 mM MES (pH 6.5) separately, and stored at -20 $^{\circ}\text{C}$. To prepare a 10 X assay buffer mix, one volume of each of the 50 X stock solutions were mixed. When preparing 50 X stocks (concentrated solutions in MES buffer), the specific volumes of the solids were taken into account if the concentration of the stock solution was greater than 300 mM. NADP 10 X solutions were prepared prior to performing the assay and stored at -20 $^{\circ}\text{C}$. The NADP stock solutions did not undergo more than 2–3 freeze-thaw cycles. MES buffer (pH 6.5) was used at a 100 mM working concentration to dissolve all reagents and q.s. reactions to 150 or 200 μL .

For a typical CKB assay having a reaction volume of 200 μL reaction, CKB was used at 5–50 nM final concentration (MW = 43,466 Da, His-tagged CKB).

100 μL of 10 nM CKB (2 X)

4 μL of 500 mM DTT (50 X in 100 mM MES (pH 6.5))

4 μL of 1 M D-glucose (50 X in 100 mM MES (pH 6.5))

4 μL of 500 mM $\text{Mg}(\text{OAc})_2$ (50 X in 100 mM MES (pH 6.5))
 4 μL of 500 mM PCr (50 X in 100 mM MES (pH 6.5))
 4 μL of 50 mM ADP (50 X in 100 mM MES (pH 6.5))
 0.2 μL of 1000 U.mL^{-1} G6PDH (1000 X in 200 mM NaCl, 1 mM EDTA, 50 mM phosphate buffer (pH 7.2))
 2 μL of 50 U.mL^{-1} HK (100 X in 100 mM MES (pH 6.5))
 20 μL of 3 to 4 mM NADP.
 53.8 μL of 100 mM MES (pH 6.5)

4.6.7. Cloning of CK-B

Cloning and overexpression of CKB was performed following literature procedures.^{457,458} The CKB gene was first PCR-amplified from a human brain cDNA library (Liu lab) using the following conditions (Table 4) and established primers.^{457,458}

5'-ATTGCCCATATGCCCTTCTCCAACAGC-3' (**Nde1 site**)

5'-ATACCGCTCGAGTCATTTCTGGGCAGG-3' (**Xho1 site**)

The following conditions were used for the PCR amplification. 1st denaturation step: 95 °C (5 min); 2nd denaturation step: 95 °C (20 sec); annealing step: 60 °C (15 sec); extension step: 72 °C (1 min); repeat from 2nd denaturation step: 30 cycles; final extension step: 72 °C (10 min).

Table 4. Components used for the PCR amplification of the CKB gene from a human cDNA library

Component	Volume	Final Concentration
10 X buffer for KOD DNA Polymerase	5 μL	1X
25 mM MgSO_4	3 μL	1.5 mM
dNTPs (2 mM each)	5 μL	0.2 mM (each)
DEPC-treated water	35.3 μL	
Sense (5') primer (50 μM)	0.4 μL	0.4 μM
Anti-Sense (3') primer (50 μM)	0.4 μL	0.4 μM
Template DNA	0.5 μL	
KOD DNA polymerase (2.5 U/ μL)	0.4 μL	0.02 U/ μL
Total reaction volume	50 μL	

The obtained CKB PCR product ($23 \text{ ng} \cdot \mu\text{L}^{-1}$) and pET28a vector were digested using Nde1 and Xho1 restriction enzymes at 37°C (3.5 h). The enzymes were heat-inactivated at 65°C (20 min) and the samples were resolved on a low melting point agarose gel (1%). Digested products were excised from the gel (visualization with UV irradiation) and extracted following QIAGEN Quick Spin DNA extraction protocol.

The digestion products were used for ligation using a T4 DNA ligase using either a DNA:vector ratio of 3:1 or a DNA:vector ratio of 1:1. Amounts were calculated using an online software (www.promega.com/biomath) based on concentrations of $9.0 \text{ ng} \cdot \mu\text{L}^{-1}$ of 1.1 kb DNA and $33 \text{ ng} \cdot \mu\text{L}^{-1}$ of 5.3 kb vector (Table 5).

Table 5. Components used for the ligation reaction between CKB and pET28a vector digested products

Conditions	3:1 DNA:vector	1:1 DNA:vector
Vector	5 μL	5 μL
CKB DNA	2.4 μL	0.8 μL
10 X buffer T4 ligase	1 μL	1 μL
DEPC H_2O	0.6 μL	2.2 μL
T4 DNA ligase	1 μL	1 μL

The reactions were incubated at 16 °C (18 h), ligation reaction products (5 µL) were transformed into TOP10 competent cells, and colonies were grown overnight (37 °C) on LB agar plates supplemented with kanamycin (50 µg.mL⁻¹). Colony PCR was performed using T7 promoter (sequence: 5' TAA TAC GAC TCA CTA TAG GG 3') and terminator (5' TGC TAG TTA TTG CTC AGC GGT 3') primers to check for correct insertion of the gene of interest. Three colonies positive for insertion were grown on a 5-mL culture scale and the plasmid was purified using commercial plasmid purification kits (QIAGEN, cat # 27104). Each purified plasmid was transformed into the expression cell line Rosetta 21 (Novagen®, cat # 69450) (+ chloramphenicol, 34 µg.mL⁻¹), grown overnight on LB agar (+ kanamycin, 50 µg.mL⁻¹, + chloramphenicol, 34 µg.mL⁻¹) and a single colony of each was used to grow a 5-mL culture of bacteria. Each culture was supplemented to 25% glycerol and stored at -80 °C for future use. Sequencing (UNC-CH Genome Analysis Facility) showed one of the three CK-B plasmids contained a point mutation (K177R), while the other two plasmids were mutation-free. One of the mutation-free plasmids was used for protein overexpression.

4.6.8. Overexpression and purification of CK-B

A 1.5 L LB culture of CKB expressing *E. coli* was grown to OD₆₀₀ ~0.6 by shaking at 37 °C. The culture was then cooled to room temperature, induced with 1 mM isopropyl β-D-1-thiogalactopyranoside (IPTG) and vigorously stirred with a magnetic stirring bar (1000 rpm) at room temperature (15 h). The cells were then harvested by centrifugation at 5000 rpm at 4 °C (10 min), and the pellet

resuspended in lysis buffer (10 mL per gram of wet pellet, 300 mM NaCl, 50 mM HEPES (pH 7.5)) supplemented with 5% (w/v) glycerol, 1 mM PMSF, and 0.5% (w/v) lysozyme. After rotating at 4 °C (30 min), the cells were disrupted by sonication on ice at 4 °C (7 x 1 min bursts, 30 sec pauses) and the suspension was centrifuged at 5000 rpm at 4 °C (15 min). The supernatant was adsorbed on a cobalt-resin (TALON resin, BD Biosciences, cat # 635504) for His-tag purification. The resin was washed with the lysis buffer supplemented with 10 mM imidazole (10 CV) and eluted with lysis buffer supplemented with 250 mM imidazole (5 CV). The eluted fraction was purified by AMS fractionation and **M4070** was recovered. The AMS pellet was resuspended in 50 mM MES (pH 6.5), and 100 mM NaCl, dialyzed against the same buffer (1 h) and fractionated on Q-Sepharose[®] equilibrated with 100 mM NaCl 50 mM MES buffer (pH 6.5). The resin was washed with the equilibration buffer (10 CV) and a homogeneous solution of CK-B (~100 mg of protein) was obtained by eluting with 200 mM NaCl 50 mM MES buffer (pH 6.5). The enzyme was then precipitated with AMS (**M0070**) and stored (-20 °C) either as an AMS pellet, or as a high-concentration stock in 100 mM MES buffer (pH 6.5) supplemented with 1 mM DTT and 20% (v/v) glycerol. Under these conditions, no detectable loss of activity was observed for up to 2 months.

CHAPTER 5

MEMBRANE-BOUND FRACTION SCREENING

We extensively screened the cytoplasmic fraction with different electrophilic and photoactivated AB&CR and did not identify a potential target protein displaying dose-dependent competition with (*R*)-LCM. Therefore, we turned to membrane-bound, subcellular fractions within the rat brain proteome to search for potential lacosamide targets. Membrane-associated proteins can be studied without solubilization as heterogeneous microsomes formed after tissue homogenization. Alternatively, they can be solubilized with a variety of commercially available detergents. Solubilized membranous proteins may then be enriched or purified by ion-exchange resin fractionation, provided that the equilibration and elution buffers are supplemented with the desired detergent.

5.1. Using non-denaturing detergents to solubilize membrane-bound proteins

Detergents, or surfactants, used in membrane protein biology are small molecules capable of forming micelles that serve as a water-soluble membrane-like environment for proteins. The specificity of these molecules lies in their amphiphilic character, and they are typically linear molecules with one hydrophilic head and one lipophilic tail. Other types of detergents exist, which are termed “facial amphiphiles”

and possess one polar and one non-polar surface area.^{472,473} Surfactants come in several classes: cationic, anionic, neutral and zwitterionic. Ionic detergents (*i.e.*, with a net negative or positive charge) strongly interact with protein charged residues and can lead to a loss of protein structure. Anionic and cationic detergents are therefore considered denaturing. On the other hand, neutral and zwitterionic surfactants have been used as mild solubilizing agents to purify membrane-bound proteins while maintaining their activity.^{429,474,475} Nonetheless, the use of a non-denaturing detergent does not guarantee the proper solubilization, folding, or stability of a protein.⁴⁷⁶⁻⁴⁷⁸

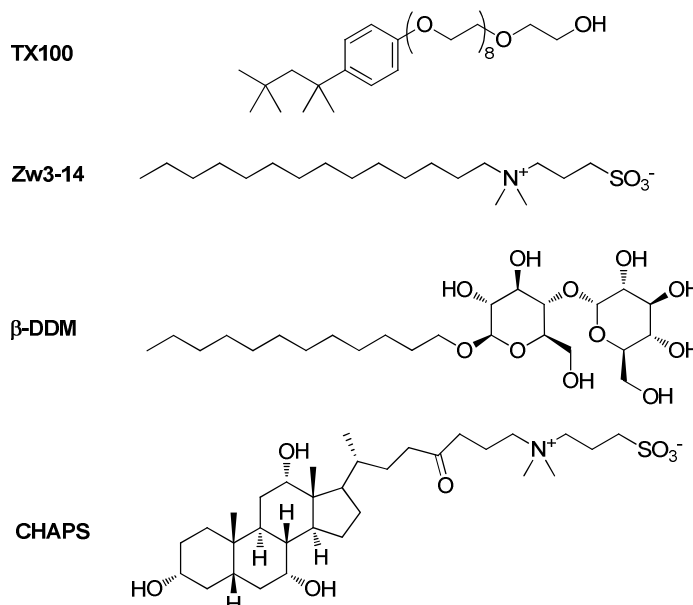


Figure 31. Structure of non-ionic and zwitterionic detergents used in our study of the membrane proteome.

One important physicochemical constant of a given detergent is the critical micellar concentration (CMC), which is the concentration at which it will start forming micelles. A given surfactant can, therefore, only solubilize membrane proteins at a

concentration greater or equal to its CMC. For our studies, we used a small panel of structurally-diverse, non-denaturing detergents to solubilize a wide range of membrane-bound proteins. Triton X-100 (TX100), β -dodecylmaltoside (β -DDM), 3-(*N,N*-dimethylmyristylammonio)propanesulfonate (zwittergent 3-14, Zw3-14), and CHAPS (Figure 31) are commonly used surfactants for the solubilization and study of functional membrane proteins.⁴⁷⁹⁻⁴⁸²

5.1.1. Preparation of detergent-solubilized membrane extract from rat brain

In our initial approach, we recovered the heavy-membrane fraction (P2) and the light-membrane fraction (P3) after homogenization of the rat brain (Scheme 40). The organelles contained in the P2 fraction were hypo-osmotically lysed, and the membrane fraction was recovered by centrifugation at 6,000 g (15 min) and the supernatant discarded. In other preparations, we directly centrifuged the S1 supernatant at 100,000 g (1 h) to obtain a combined P2+P3 pellet containing the whole membrane fraction of the brain. This combined pellet was also subjected to hypotonic lysis to discard the soluble content of intracellular organelles.

In a typical preparation, both membrane materials (P2+P3) was resuspended in isotonic buffer, such as 25 mM HEPES (pH 7.4) containing 150 mM NaCl, in separate tubes at 4 °C with a total protein concentration of $\sim 5 \text{ mg.mL}^{-1}$ (Bradford assay), and each suspension was then supplemented with a detergent at a specific concentration (*i.e.*, (w/v): 1% TX100, 0.5% β -DDM, 0.5% Zw3-14, 1% CHAPS). The suspensions were gently rocked for 15 min at 4 °C and centrifuged at 100,000 g for 1 h. The pellet was discarded and the homogeneous supernatant containing

detergent-solubilized membrane proteins was used to perform labeling and click chemistry.

Membrane proteins fractionation was performed at pH 7.5 using sequential S and Q Sepharose[®] and by supplementing the equilibration and elution buffers with the following concentrations of surfactant: 1% for TX100, 0.5% for β -DDM, 0.1% for Zw3-14, and 1% for CHAPS. For solutions containing greater than 0.5% Zw3-14, the addition of SDS loading buffer to the high salt (>250 mM NaCl) eluted fraction led to a highly viscous solution that impeded proper electrophoretic resolution. Furthermore, the Zw3-14-solubilized protein solutions were not kept for an extended period of time at 0–4 °C since the surfactant is water-insoluble at this temperature. Failure to do so led to protein sample precipitation. Finally, the Zw3-14 samples could be frozen at -80 °C without any special procedure but were thawed quickly (*i.e.*, by immersion in a water bath at room temperature) to avoid loss of proteins. Following this procedure, we did not observe any significant precipitation in our samples.

5.1.2. Solubilized membrane fraction screening

Following the previously described protocol, we screened the rat, detergent-solubilized, membrane-bound proteome using both enantiomers of photoAB&CR agents **181**, **169**, **168**, **170** and where (*R*)-LCM and (*S*)-LCM served as competing agents. The irradiation conditions for the photolabeling step were identical to those described in Section 4.6.2. When Sepharose[®] fractionation was used after the labeling step, membrane fractions were resolved on SDS-PAGE gel (minigel size, ~8

cm high). Alternatively, when no fractionation was performed, samples were resolved using a larger (~20 cm high) SDS-PAGE gel system (Protean II XL cell, Bio Rad) to provide a better protein separation.

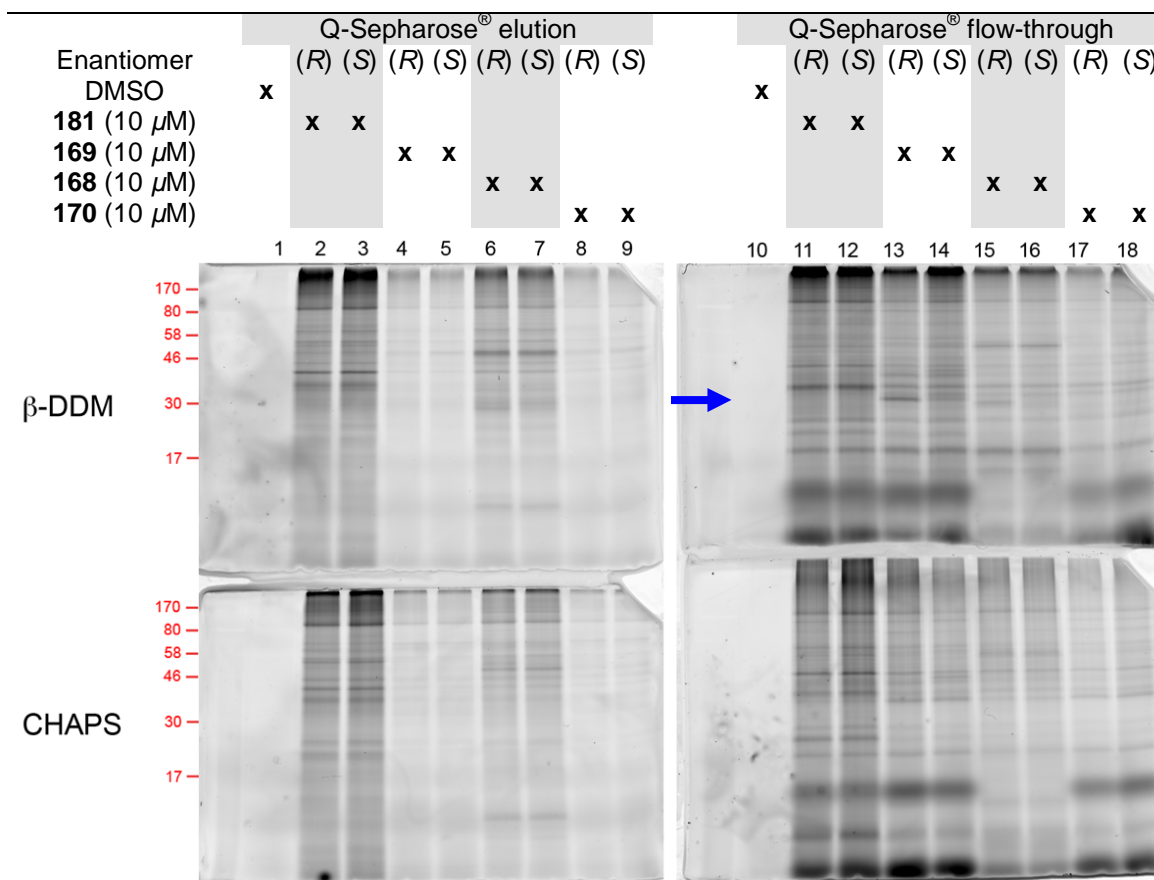


Figure 32. 12.5% SDS PAGE gel of the detergent-solubilized (β -DDM, or CHAPS) membrane fraction (P2+P3) labeled with photoAB&CR agents **181**, **169**, **168**, and **170**. The lysate (~200 μ g total protein) was irradiated at 4 $^{\circ}$ C under the appropriate conditions and each reaction was fractionated using Q-Sepharose[®] (equilibrated with 25 mM HEPES (pH 7.4), 50 mM NaCl, supplemented with β -DDM or CHAPS). The flow-through (lanes 10–18) was recovered, the beads were rinsed with equilibration buffer, and eluted with 350 mM NaCl (lanes 1–9). Each fraction was then clicked with Probe **196**, resolved, and scanned for fluorescence. Lane 1, 10: DMSO control; lane 2, 11: (R)-**181** (10 μ M); lane 3, 12: (S)-**181** (10 μ M); lane 4, 13: (R)-**169** (10 μ M); lane 5, 14: (S)-**169** (10 μ M); lane 6, 15: (R)-**168** (10 μ M); lane 7, 16: (S)-**168** (10 μ M); lane 8, 17: (R)-**170** (10 μ M); lane 9, 18: (S)-**170** (10 μ M). The Coomassie stain (picture not shown) showed equal amounts of protein loaded in each gel. Approximate molecular weight markers (kDa) are shown in red on the left.

TX100; blue numbers: β -DDM; red numbers: CHAPS. Solubilized proteins were labeled as follows. Lane 1: (*R*)-**169** (10 μ M); lane 2: (*S*)-**169** (10 μ M); lane 3: (*R*)-**169** (10 μ M) + (*R*)-LCM (10 mM); lane 4: (*R*)-**169** (10 μ M) + (*S*)-LCM (10 mM). After photolabeling (10 min 365 nm, 1 min 312 nm), each reaction was passed through pre-equilibrated S-Sepharose[®] (pH 7.4) and Q-Sepharose[®] (pH 7.4) supplemented with the appropriate detergent. The flow-through was then clicked with fluorescent Probe **203** and resolved. Approximate molecular weight markers (kDa) are shown in red on the left.

Using this approach, no potential lacosamide interacting proteins were identified that showed (*R*)- vs (*S*)-AB&CR specificity *and* displayed labeling dose-dependent competition with excess (*R*)-LCM. (Figure 33, Figure 34). Nonetheless, some bands were found to be specifically labeled by one photoAB group versus the other three. A few detergent-specific protein candidates were found to show near complete selectivity for the (*R*)-AB&CR versus the (*S*)-AB&CR agent (Figure 32, [blue arrow](#)), but failed to show any selective competition with a 1000–3000-fold excess of either (*R*)- or (*S*)-LCM. For example, we observed a ~30 kDa protein (Figure 32, [blue arrow](#)) that was selectively labeled by (*R*)-**169** over (*S*)-**169** at 10 μ M. The protein was enriched in the β -DDM soluble fraction, and did not adsorb to S or Q Sepharose[®] (pH 7.4). This protein, however, did not display any fluorescence signal competition in the presence of excess (*R*)-LCM (1000 equiv, Figure 33). In addition, the overall fluorescence level of selectively labeled proteins was not intense, indicating either a low binding affinity with the AB&CR agent, a low expression level of the protein, a low level of recovered functional protein, a low efficiency for protein adduction or a combination of these factors.

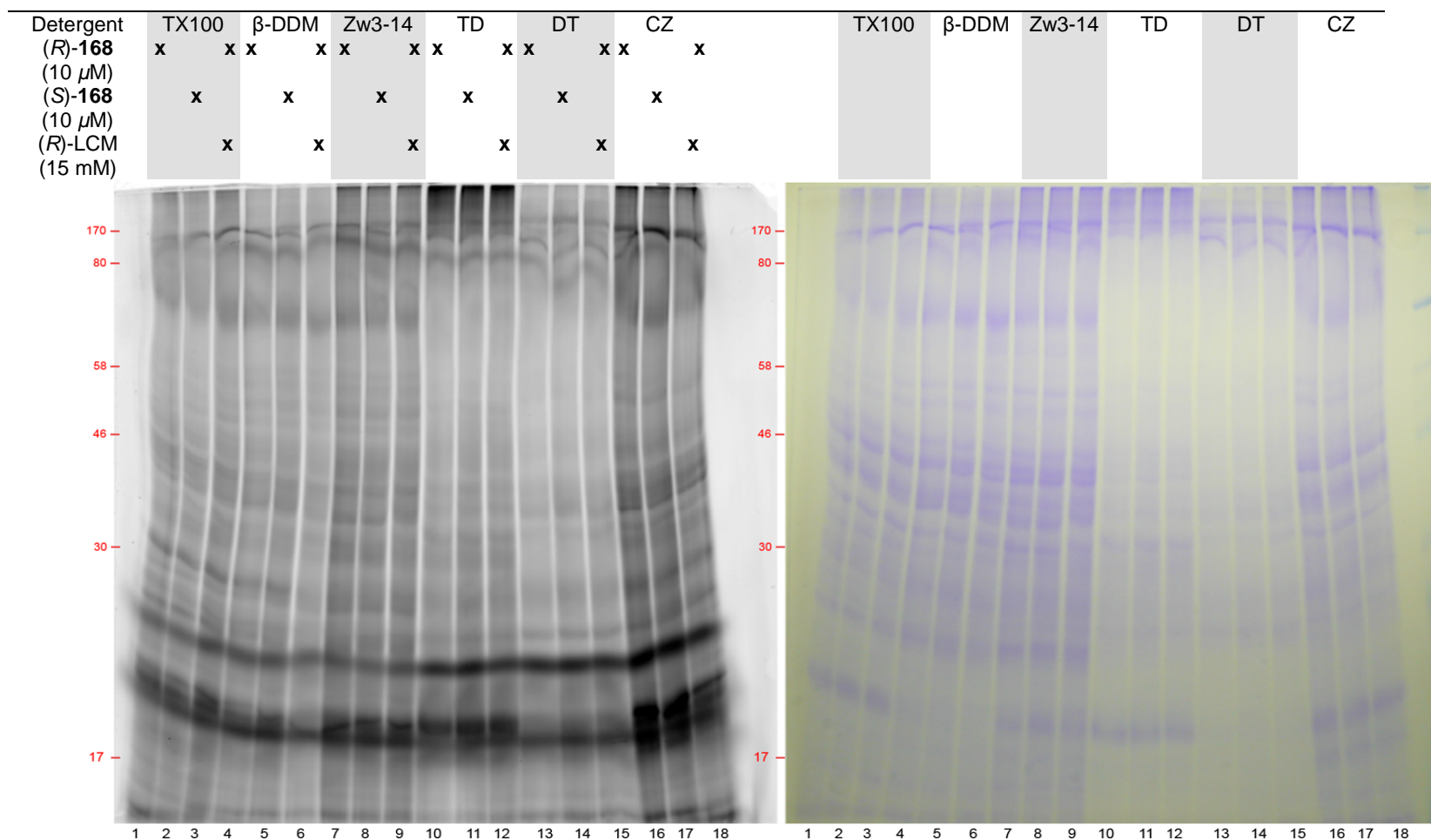


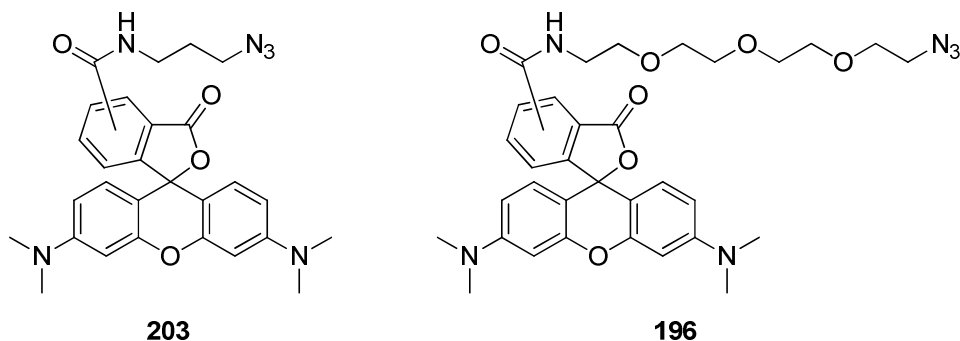
Figure 34. 10% SDS-PAGE gel (large size) of the membrane fraction (P2+P3) solubilized with a single detergent or sequentially-solubilized with two different surfactants. Left: fluorescence scan; right: corresponding Coomassie stain. Lanes 1–3: TX100 solubilized; lanes 4–6: β -DDM solubilized; lanes 7–9: Zw3-14 solubilized; lanes 10–12: the TX100 insoluble pellet was solubilized with β -DDM; lanes 13–15: the β -DDM insoluble pellet was solubilized with TX100; lanes 16–18: the CHAPS insoluble pellet was solubilized in Zw3-14. Lanes 1, 4, 7, 10, 13, 16: (*R*)-**168** (5 μ M); lanes 2, 5, 8, 11, 14, 17: (*S*)-**168** (5 μ M); lanes 3, 6, 9, 12, 15, 18: (*R*)-**168** (5 μ M) + (*R*)-LCM (10 mM). Reactions were photolabeled (30 min 365 nm, 1 min 312 nm), clicked with Probe **196**, and resolved. Approximate molecular weight markers (kDa) are shown in red on the left.

Recognizing the complexity of the protein mixture, we also implemented another fractionation protocol using sequential detergent solubilization. The membrane material was first solubilized with a given surfactant, centrifuged, and the supernatant was discarded. The remaining pellet was solubilized in another detergent, centrifuged, and the supernatant was used for screening. The total protein stain (Coomassie blue or silver stain) showed diverse solubilization patterns for each detergent or combinations of detergents used (Figure 34). Three combinations were used and included β -DDM solubilization of the TX100 insoluble pellet (termed “TD”), the reverse combination (termed “DT”), and Zw3-14 solubilization of the CHAPS insoluble pellet (termed “CZ”). Unfortunately, no membrane lysate preparation yielded any potentially interesting protein band that met our selection criteria.

5.1.3. Interactions between fluorescent Probes and detergent molecules

Our studies showed direct interactions between the fluorescent Probes and detergent molecules. For example, click chemistry with PEG-containing Probe **196** proceeded smoothly in the presence of detergents lacking a PEG chain (β -DDM, Zw3-14, CHAPS), while the fluorescent labeling intensity was dramatically reduced in the presence of TX-100. This difference in click chemistry did not occur when the C3-azide Probe **203** was used for click chemistry. We suspect that this difference is due to the polyethylene glycol chain (containing 3 ethylenoxy units) in **196** that is likely solvated by the PEG chain in TX-100 (8–10 units), thus diminishing the Probe **196**'s ability to participate in the click chemistry reaction. We expect that these

findings would also apply to biotin purification experiments, where a biotin Probe such as **191** would likely behave similarly with TX-100 molecules and provide lower product recovery yields.



We observed one experimental complication using the C3 Probe **203** and all the detergents. We found an intense smear close to the protein migration front (Figure 33, **green arrow**) in the gel that was not washed away by several rinses with ddH₂O. Use of Probe **196** in place of Probe **203** eliminated this problem.

5.2. Screening whole membrane extracts for potential targets

The results using a detergent-based approach, suggested that treatment with surfactants may have been detrimental to the integrity of potential target proteins. Therefore, we decided to further pursue our interrogation of the proteome by using *unsolubilized* whole rat brain membrane extracts. We also tried to maintain a membrane environment as close as possible to native conditions and used a physiological-like buffer solution to conduct our photo-labeling experiments (Locke's buffer: 154 mM NaCl, 5.6 mM KCl, 2.3 mM CaCl₂, 1.0 mM MgCl₂, 3.8 mM NaHCO₃, 5 mM D-glucose, 5 mM HEPES (pH 7.2)).^{483,484} Importantly, in our previous study, no special care was taken when freezing the material for storage. It has been

demonstrated that one single freeze-thaw cycle can lead to a near-complete loss of activity for some proteins.⁴⁸⁵ Therefore, we also included a protocol that used a slow, cryopreserving method to freeze and store samples. After preparation, the samples were suspended to $\sim 1 \text{ mg.mL}^{-1}$ in Locke's buffer supplemented to 10 mg.mL^{-1} bovine serum albumin (BSA) and 10% DMSO (solution termed "cryobuffer").⁴⁸⁵

5.2.1. Rationale for the synaptosomal fraction screening

Homogenization of animal tissue leads to the shearing of different organelle structures. When brain tissue is used, pre-synaptic buttons are pinched at the end of the axon and close themselves to form pre-synaptic membrane vesicles.^{486,487} These subcellular structures are termed synaptosomes, and are widely used as a model to study synaptic proteins or neurotransmission mechanisms.⁴⁸⁸⁻⁴⁹¹ Given the fact that several AEDs target proteins are located at the pre-synaptic level (TGB,²⁰¹ LVT,²¹⁰ gabapentin (GBP)⁴⁹²), we screened the synaptosomes for potential LCM targets.

Synaptosomes are usually recovered by centrifugation of the S1 supernatant at 15,000 g for 20 min (Scheme 40).^{486,487,493,208,494} The pellet recovered at that speed also contains other organelles such as mitochondria and is, therefore, often referred to as the "crude synaptosomal fraction".⁴⁹⁵ A typical enrichment procedure for synaptosomes involves further centrifugating the pellet through a sucrose density gradient.^{485-487,208,209} Due to their specific buoyancy, synaptosomes are recovered at the interface of two specific sucrose layers. Such a procedure, though, requires a swing-bucket ultracentrifuge rotor,^{485-487,208,209} which was unavailable for our studies.

We used an alternative approach based on phase partitioning, which takes advantage of the differences between the physicochemical properties of mitochondrial and synaptic membranes (Figure 35).^{496,497} The method uses a biphasic system composed of two types of polymers: PEG-4000 (Sigma-Aldrich, cat # 81240), a polyethylene glycol polymer with an average molecular weight of 4000 g.mol⁻¹, and dextran 500 (Spectrum Chemicals, cat # D1004), a D-glucose glycopolymer with an average molecular weight of 500,000 g.mol⁻¹.

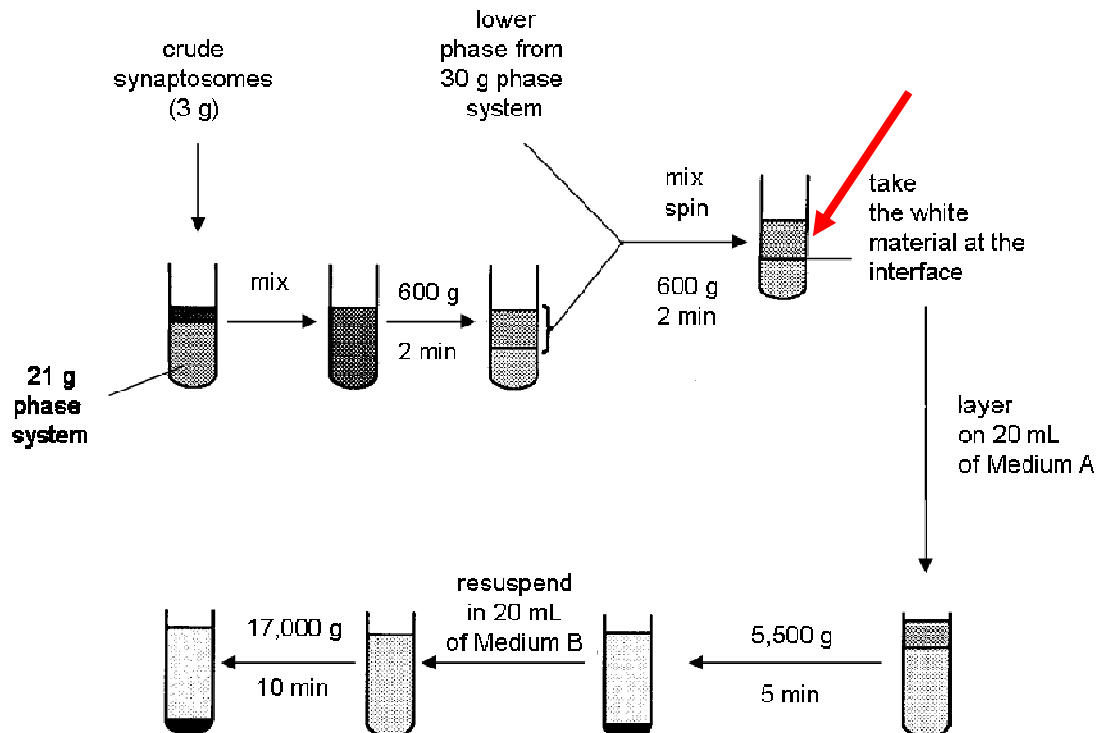


Figure 35. General approach to the purification of synaptosomes by phase partitioning. Experimental details are given in the Experimental Section. The red arrow indicates the procedure's step where differences were observed compared with the literature protocol. The figure was reproduced and modified from Ref.⁴⁹⁶

The two immiscible phases, a PEG-rich and a dextran-rich, are then mixed with the crude pellet and centrifuged at low speed to separate the layers. Synaptosomes are

recovered in the PEG-rich phase and then subjected to a similar, second round of purification to yield an enriched synaptosomal pellet. Utilizing this phase partitioning method, we observed one experimental difference between the synaptosomes preparation we used and the literature protocol (see Section 5.5.2).⁴⁹⁶ After the second purification step, which uses a fresh lower phase from a 30-g phase system, the layer termed “final upper phase” did not contain any synaptosomal particles floating in the layer as described (Figure 35, red arrow).⁴⁹⁶ Instead, a large amount of white material was found at the interface between the two layers. This material was collected with a pipette and directly pelleted at 17,000 g. The procedure yield was ~6 mg of synaptosomal protein per rat brain (~1.5 g wet tissue). To verify if the difference in the procedure was not detrimental to the preparation, we performed a Western blot of the enriched synaptosomes using an antibody raised against synaptosomal-associated protein 25 (SNAP-25), and using the crude rat brain homogenate as a positive control. In addition we also probed for the presence of mitochondrial proteins, using an antibody against the mitochondrial marker cytochrome c oxidase subunit IV (COX IV) (Figure 36). Mitochondria should have been removed during the preparation. Western blot analysis showed that, indeed, SNAP-25 was present in the membrane material recovered (Figure 36, left panel). The anti COX IV antibody was not functional and we could not, therefore, ascertain the absence of mitochondrial proteins (Figure 36, right panel). However, these results gave us confidence that the enrichment procedure worked correctly.

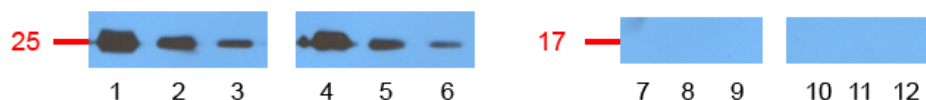


Figure 36. Western blot of the crude brain homogenate and synaptosomes. Proteins SNAP-25 (~25 kDa, synaptosomes) and COX IV (~17 kDa, mitochondria) antibodies were used as subcellular markers. Lanes 1–6: anti SNAP-25; lanes 7–14: anti COX IV. Lanes 1–3, 7–9: crude brain homogenate; lanes 4–6, 10–12: synaptosomes. Lanes 1, 7: ~10 μ g of crude homogenate protein per lane; lanes 2, 8: ~1 μ g; lanes 3, 9: ~0.1 μ g; lanes 4, 10: ~2 μ g of synaptosomal proteins per lane; lanes 5, 11: ~0.2 μ g; lanes 6, 12: ~0.02 μ g. Gels were transferred to nitrocellulose membranes and blocked with 5% milk in TBST. The rabbit polyclonal antibody against SNAP-25 was diluted 1:1000 in 5% milk in TBST and incubated at room temperature (1h). The rabbit polyclonal antibody against COX IV was diluted 1:750 in 5% milk in TBST and incubated at 4 °C (15 h). Both membranes were then probed with donkey anti rabbit IgG, horseradish peroxidase (HRP)-linked, diluted 1:1000 in 5% milk in TBST at room temperature (1 h) and developed (ECLplus). Developing time: SNAP-25: 1 min; COX IV: 15 min. Approximate molecular weight markers (kDa) are shown in red on the left.

5.2.2. Screening the synaptosomal and microsomal fractions

Following the previously established protocol, we screened the synaptosomal fraction using both enantiomers of compounds **181**, **169**, **168**, **170**, and (*R*)- and (*S*)-LCM as competing reagents. On small scale, unsolubilized proteins were dispensed in Locke's buffer (100 μ L per well) after removing the cryobuffer and washing the pellet. PhotoAB&CR agents and competing reagents were added (5% (v/v) DMSO) and the suspension was incubated at 4 °C (10 min) prior to irradiation. After the photolabeling step, the content of each well was transferred to a tube, and centrifuged at 14,000 rpm at 4 °C (5 min). At this stage, several procedures were examined. Pelleted samples were either solubilized in non-denaturing detergents (β -DDM, Zw3-14, CHAPS) or in HEPES buffer (pH 7.4) supplemented to 1% SDS, and then "clicked" with Probe **196** (Method A). Alternatively, click chemistry was performed on the unsolubilized membrane pellet, after which the suspension was successively pelleted, rinsed with HEPES buffer (pH 7.4), spun down, solubilized

with a non-denaturing or denaturing detergent, centrifuged, and the supernatant was resolved on SDS-PAGE gel (Method B).

In the initial experiments, we used the set of photoAB&CR agents **181**, **169**, **168**, **170** to screen the unsolubilized membrane proteome as previously described (see Section 4.3). Using the synaptosomal preparation, we photolabeled proteins with 10 μ M of the appropriate (*R*)-AB&CR and (*S*)-AB&CR agents. In addition, the synaptosomal preparation was irradiated with 10 μ M (*R*)-AB&CR in the presence of 15 mM (*R*)-LCM.

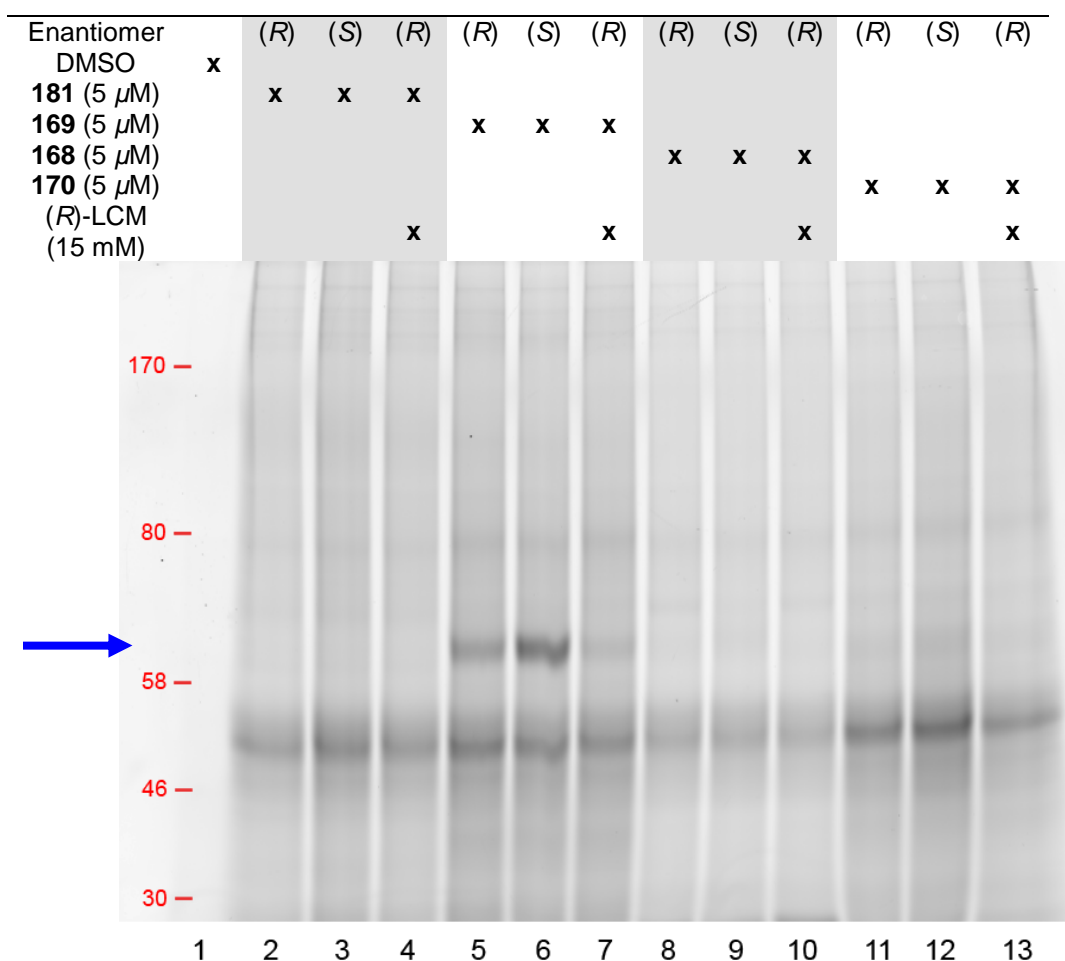


Figure 37. Fluorescence scan of the synaptosomal fraction screened with photoAB&CR agents **181**, **169**, **168**, and **180** (6%SDS PAGE gel). Whole synaptosomal extracts ($\sim 0.2 \text{ mg.mL}^{-1}$ in Locke's

buffer) were irradiated, the pellet was rinsed, dissolved in 25 mM HEPES (pH 7.4) supplemented with 1% SDS, clicked with Probe **196** and resolved. Lane 1: DMSO control; lane 2: (*R*)-**181** (5 μ M); lane 3: (*S*)-**181** (5 μ M); lane 4: (*R*)-**181** (5 μ M) + (*R*)-LCM (15 mM); lane 5: (*R*)-**169** (5 μ M); lane 6: (*S*)-**169** (5 μ M); lane 7: (*R*)-**169** (5 μ M) + (*R*)-LCM (15 mM); lane 8: (*R*)-**168** (5 μ M); lane 9: (*S*)-**168** (5 μ M); lane 10: (*R*)-**168** (5 μ M) + (*R*)-LCM (15 mM); lane 11: (*R*)-**170** (5 μ M); lane 12: (*S*)-**170** (5 μ M); lane 13: (*R*)-**170** (5 μ M) + (*R*)-LCM (15 mM). The Coomassie stain (picture not shown) showed equal amounts of protein loaded in each lane. Approximate molecular weight markers (kDa) are shown in red on the left.

Using Method A and SDS as a detergent, we observed a potential band of interest at ~60 kDa (Figure 37, [blue arrow](#)). This protein was exclusively labeled by (*R*)-**169** and (*S*)-**169**, with a pronounced preference for (*S*)-**169** and the presence of 1,500 equiv of (*R*)-LCM gave a pronounced reduction in the fluorescence intensity of the band.

We found that click chemistry in the presence of 1% SDS led to lower levels of fluorescence when compared with the three non-denaturing detergents β -DDM, Zw3-14, and CHAPS. All three detergents appeared to solubilize the protein of interest, as shown by the strong fluorescent band around 60 kDa on SDS-PAGE gels (Figure 38, [blue arrow](#)). Zw3-14 and β -DDM solubilized the protein equally well, while using CHAPS gave a slightly reduced fluorescent intensity. The amount of total protein solubilized with detergents decreased as follows: Zw3-14, β -DDM, CHAPS. We, therefore, chose to use β -DDM as it provided an adequate balance between its ability to provide a high recovery of the fluorescent signal and its solubilizing properties. The insoluble pellets corresponding to each detergent were then dissolved in 1% SDS (treatments termed “DS”, “ZS”, “CS”, for β -DDM, Zw3-14, and CHAPS, respectively).

In later experiments, we also screened the microsomal fraction (see Section 3.1, Scheme 40) to refine the subcellular localization of the ~60 kDa protein. Thus, in

the same lysate preparation, we isolated rat brain synaptosomes and microsomes, and stored them under identical conditions using the cryobuffer. When screening the two membrane fractions under heterogeneous conditions, we found the ~60 kDa protein characteristic signal in both subcellular compartments (Figure 39). Using Method B, we found that the protein was preferentially labeled by (S)-**169** over (R)-**169**. However, a 3000-fold excess of (R)-LCM led to a strong reduction of fluorescence intensity when compared to (S)-LCM. Intriguingly, both signals from (R)-**169** and (S)-**169** were more affected by (R)-LCM than by (S)-LCM.

Several attempts were made to identify this protein by biotin purification. These efforts were unfruitful, while we observed some intriguing findings. First, when we used Method B to screen the microsomal fraction, the protein pellet after the click chemistry step could be solubilized in β -DDM. Fluorescence scans showed that the protein of interest was efficiently extracted in this detergent (data not shown). The corresponding Coomassie stain, however, showed that this protein was the predominant protein present in the entire gel, whereas all other proteins were only solubilized with denaturing conditions (1% SDS, Figure 39). These results contrasted with the high solubilization properties of β -DDM under native conditions (Method A, Figure 38). On large scale (~1 mg of membrane protein), the strong Coomassie stained band corresponding to ~60 kDa was excised and analyzed by MS (Figure 40). Serum albumin was identified as the likely major constituent in this band (Table 6)

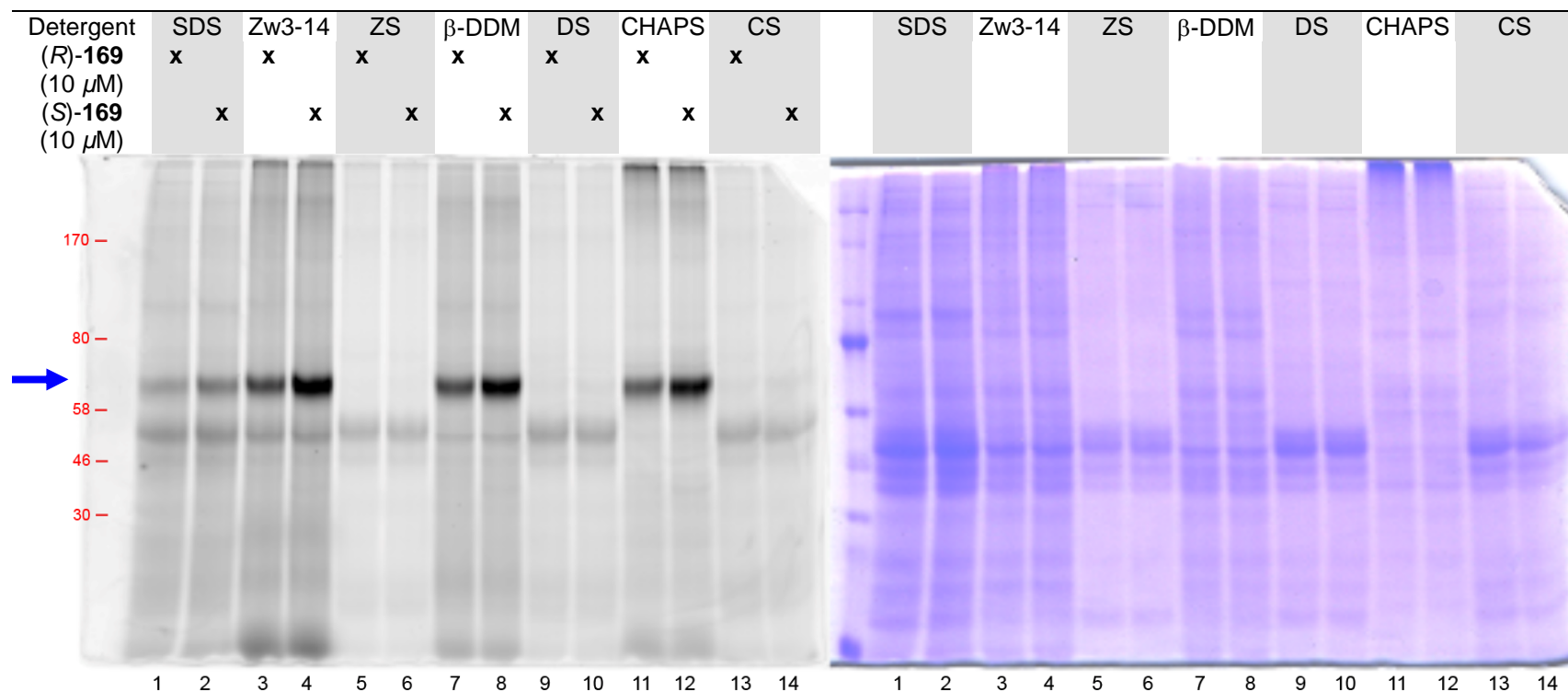


Figure 38. 10% SDS-PAGE gel of the synaptosomal fraction labeled with (*R*)-**169** and (*S*)-**169**. Left: fluorescence scan; right: corresponding Coomassie stain. Whole membrane extracts were irradiated in the presence of the photoAB&CR, solubilized with various detergents and the solubilized material was clicked with Probe **196** and resolved. Lanes 1, 3, 5, 7, 9, 11, 13: (*R*)-**169** (10 μ M); lanes 2, 4, 6, 8, 10, 12, 14: (*S*)-**169** (10 μ M). After photolabeling, membrane extracts were solubilized in detergent-supplemented HEPES buffer (pH 7.4) as follows. Lanes 1,2: 1% SDS; lanes 3, 4: 0.5% Zw3-14; lanes 5, 6: 0.5% Zw3-14 insoluble pellet solubilized in 1% SDS; lanes 7, 8: 0.5% β -DDM; lanes 9, 10: 0.5% β -DDM insoluble pellet solubilized in 1% SDS; lanes 11, 12: CHAPS; lanes 13, 14: CHAPS insoluble pellet solubilized in 1% SDS. Approximate molecular weight markers (kDa) are shown in red on the left.

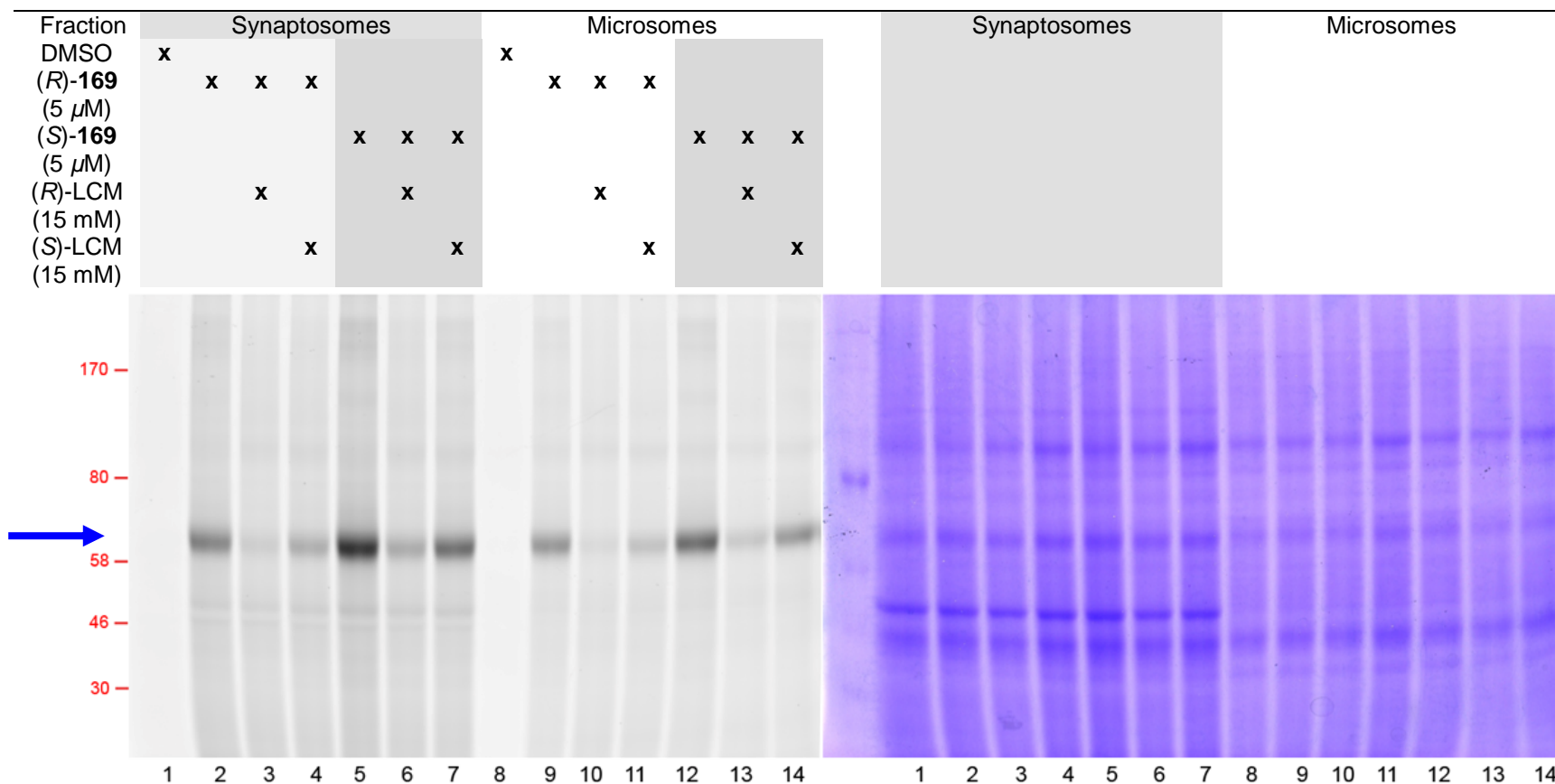


Figure 39. 8% SDS-PAGE gels of the intact membrane-bound fraction after photolabeling, click chemistry with **196** using Method B and 1% SDS 25 mM HEPES (pH 7.4). Left: fluorescence scan; right: corresponding Coomassie stain. Lanes 1–7: synaptosomal fraction; Lanes 8–14: microsomal fraction. Lanes 1, 8: DMSO; lanes 2, 9: (*R*)-**169** (5 μ M); lanes 3, 10: (*R*)-**169** (5 μ M) + (*R*)-LCM (15 mM); lanes 4, 11: (*R*)-**169** (5 μ M) + (*S*)-LCM (15 mM); lanes 5, 12: (*S*)-**169** (5 μ M); lanes 6, 13: (*S*)-**169** (5 μ M) + (*R*)-LCM (15 mM); lanes 7, 14: (*S*)-**169** (5 μ M) + (*S*)-LCM (15 mM). Approximate molecular markers (kDa) are shown in red on the left.

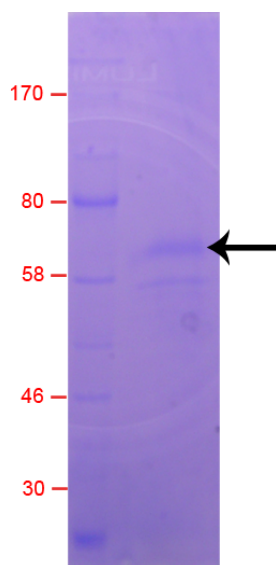


Figure 40. Coomassie stain of the enriched protein of interest (8% SDS-PAGE gel). Starting from 1.5 mg of total microsomal protein, the membrane lysate was irradiated in the presence of 10 μ M (*R*)-**169**, pelleted, rinsed, and clicked with biotin Probe **191** using Method B. After click chemistry, the membrane material was pelleted, rinsed with HEPES buffer and solubilized in 1% β -DDM 25 mM HEPES (pH 7.4). The suspension was centrifuged and the supernatant was resolved on a SDS-PAGE gel and Coomassie stained. The predominant band (black arrow) was excised and sent for MS analysis (see table below). Approximate molecular weight markers (kDa) are shown in red on the left.

Table 6. Representative list of tryptic fragments identified in the Coomassie stained band corresponding to ~60 kDa. Additional tryptic fragments corresponding to limbic system-associated protein (LSAMP) and brain acid soluble protein 1 (BASP1) were also identified.

Serum albumin			
Observed	Miss	Score	Peptide
486.7543	0	49	K.QTALAELVK.H
550.7948	1	47	K.KQTALAELVK.H
575.2831	0	37	K.LVQEVTDFAK.T
633.7795	0	64	R.FPNAEFAEITK.L
720.3389	0	59	K.APQVSTPTLVEAAR.N
733.339	0	72	K.LGEYGFQNAVLVR.Y

Second, the ~60 kDa protein's characteristic fluorescence signal was not observed when we used an aliquot of a freshly prepared microsomal fraction (Figure 41, [blue arrow](#)). However, when experiments were conducted on the cryopreserved material from the same preparation, the signal was again observed (data not shown). These findings indicated that BSA, the protein present at a high

concentration in the cryobuffer (10 mg.mL^{-1}) was likely targeted by (S)-**169** and to a lesser degree by (R)-**169**.

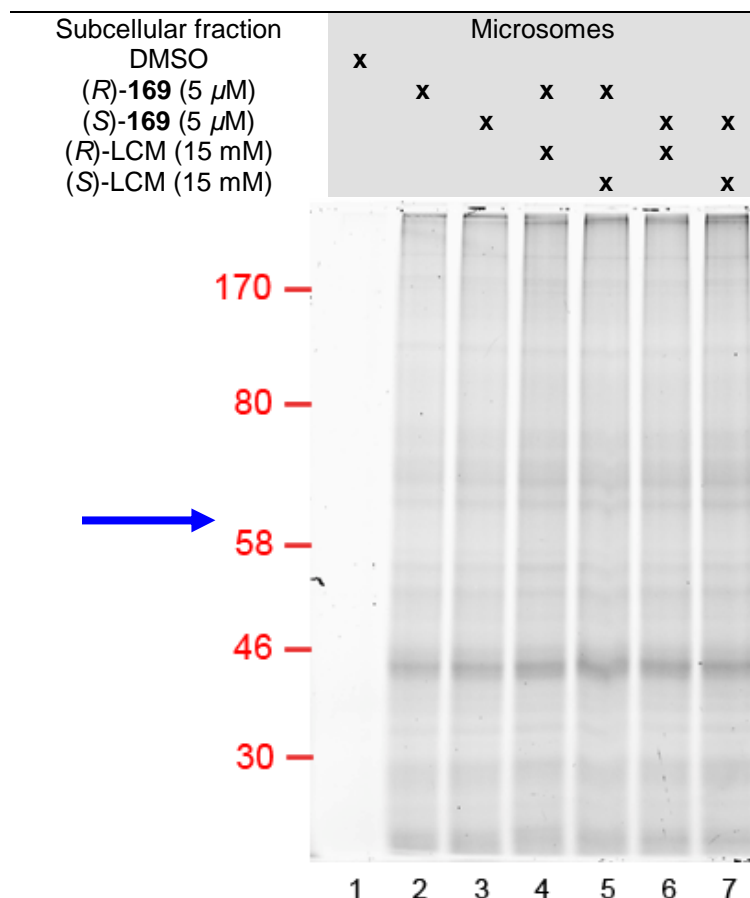


Figure 41. In-gel fluorescence scan of freshly prepared (non cryopreserved) microsomal fraction from the rat brain. Membrane extracts were incubate with photoAB&CR **169**, clicked with Probe **196** using Method B, and resolved (8% SDS PAGE gel). Lane 1: DMSO; lane 2: (R)-**169** (5 μM); lane 3: (S)-**169** (5 μM); lane 4: (R)-**169** (5 μM) + (R)-LCM (15 mM); lane 5: (R)-**169** (5 μM) + (S)-LCM (15 mM); lane 6: (S)-**169** (5 μM) + (R)-LCM (15 mM); lane 7: (S)-**169** (5 μM) + (S)-LCM (15 mM). No specific fluorescence signal was detected around 60 kDa under these conditions. The Coomassie stain (picture not shown) indicated equal amounts of protein loaded per lane. Approximate molecular weight markers (kDa) are shown in red on the left.

The serum albumin fragments identified in Table 6 could not be solely attributed to *Rattus norvegicus* and may have possibly originated from several other species, including *Bos taurus*. Photolabeling experiments conducted on pure BSA and human

serum albumin (HSA) was consistent with this hypothesis (Figure 42), although differences between (*R*)-**169** and (*S*)-**169** labeling were far less pronounced when using the *isolated* protein. Competition with (*R*)-LCM was also dramatically reduced from a fluorescent signal almost abolished with 3000-fold excess of (*R*)-LCM in the whole membrane lysate (Figure 39, lanes 2 and 3) to a barely detectable change with 5000-fold excess of (*R*)-LCM using the purified protein (Figure 42, lanes 2 and 4). Nonetheless, AB&CR **169** selectively labeled BSA and HSA while **181**, **168**, and **170** did not (Figure 43, [blue arrow](#)), thus mirroring the different photoAB labeling profiles observed in Figure 37. The differences observed in the two competition experiments (Figure 39, Figure 42) were surprising and have been tentatively attributed to a change of conformation due to the dissimilarity between the two protein environments.

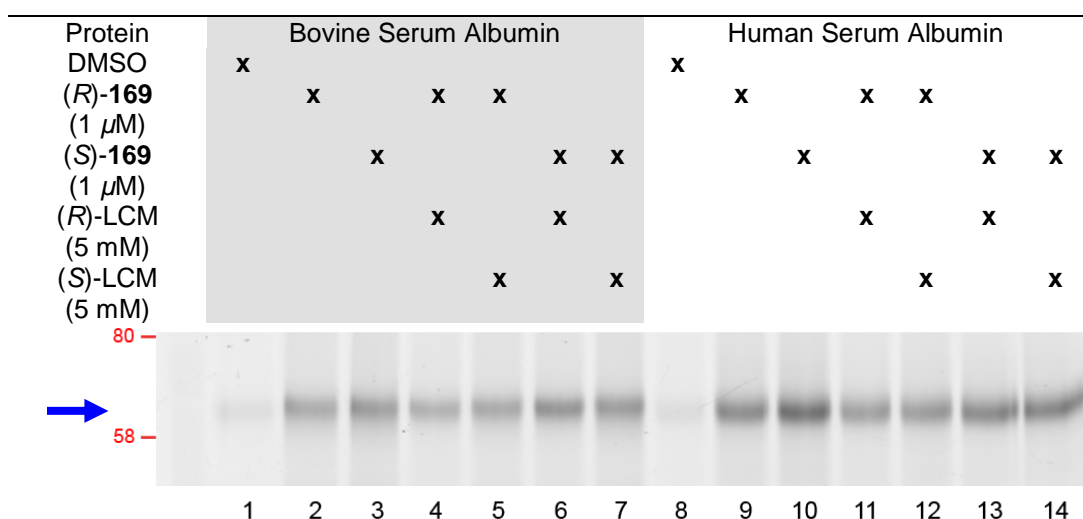


Figure 42. In-gel fluorescence scan of purified BSA and HSA labeled with photoAB&CR agent **169**. Purified proteins were solubilized (0.2 mg.mL^{-1}) in 25 mM HEPES (pH 7.4) containing 150 mM NaCl, photolabeled, clicked with Probe **196**, and resolved ($\sim 200 \text{ ng}$ of protein were loaded per lane). Lanes 1–7: BSA; lanes 8–14: HSA. Lanes 1, 8: DMSO; lanes 2, 9: (*R*)-**169** (1 μ M); lanes 3, 10: (*S*)-**169** (1 μ M); lanes 4, 11: (*R*)-**169** (1 μ M) + (*R*)-LCM (5 mM); lanes 5, 12: (*R*)-**169** (1 μ M) + (*S*)-LCM (5 mM); lanes 6, 13: (*S*)-**169** (1 μ M) + (*R*)-LCM (5 mM); lanes 7, 14: (*S*)-**169** (1 μ M) + (*S*)-LCM (5 mM). The

Coomassie stain (picture not shown), showed equal protein loading in each lane. Approximate molecular weight marker (kDa) are shown in red on the left.

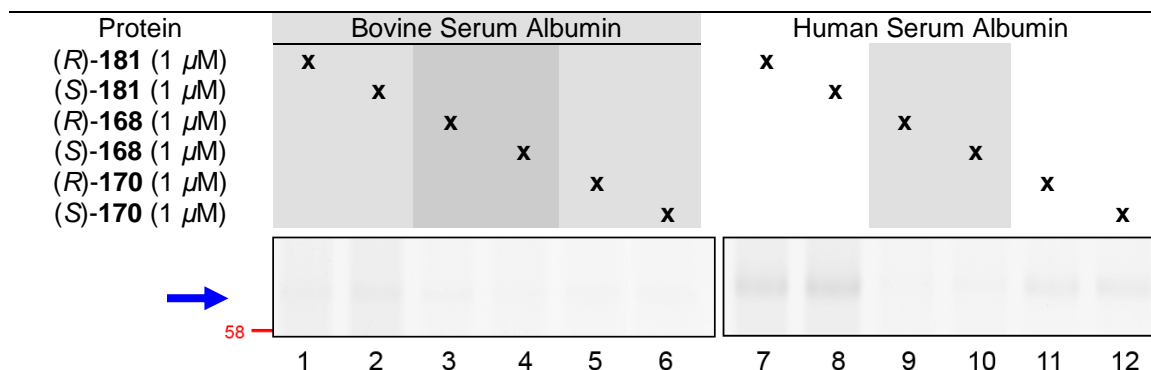


Figure 43. In-gel fluorescence scan of purified BSA and HSA labeled with photoAB&CR agent **181**, **168**, and **170**. Purified proteins were solubilized (0.2 mg.mL^{-1}) in 25 mM HEPES (pH 7.4) containing 150 mM NaCl, photolabeled, clicked with Probe **196**, and resolved ($\sim 200 \text{ ng}$ of protein were loaded per lane). Lanes 1–6: BSA; lanes 7–12: HSA. Lanes 1, 7: (*R*)-**181** (1 μ M); lanes 2, 8: (*S*)-**181** (1 μ M); lanes 3, 9: (*R*)-**168** (1 μ M); lanes 4, 10: (*S*)-**168** (1 μ M); lanes 5, 11: (*R*)-**180** (1 μ M); lanes 6, 12: (*S*)-**180** (1 μ M). The Coomassie stain (picture not shown), showed equal protein loading in each lane. Approximate molecular weight marker (kDa) are shown in red on the left.

5.3. Discussion

The rat membrane-bound proteome was screened under a variety of conditions with the suite of photoAB&CR agents **181**, **169**, **168**, and **170**. Our first attempt at identifying potential LCM targets took advantage of the variety of commercially available non-denaturing detergents. Recognizing the complexity of the membrane proteome, we chose to use four structurally diverse surfactants to solubilize different sets membrane-bound proteins. Indeed, each detergent displayed pronounced differences in the solubilized protein patterns (Figure 33, Figure 34, Figure 38). For example, only CHAPS was found to efficiently solubilize very high molecular weight proteins ($>300 \text{ kDa}$). Overall, TX100 (1%), β -DDM (0.5%), and Zw3-14 (0.5%) solubilized comparable amounts of protein (Bradford assay) that appeared greater than CHAPS (1%). We hypothesized that a wide range of

solubilization conditions would result in higher chances of identifying a potential target protein. Importantly, this non-denaturing solubilization protocol allowed us to use ion-exchange chromatography to deconvolute the membrane lysate. Another technique employed in this study was the use of a larger sized SDS PAGE electrophoresis system. Using longer SDS PAGE gels (~20 cm height) provided a greater separation of the different membrane proteins present in the lysate (15–250 kDa, Figure 34). We also gained in sensitivity by loading increased amounts of protein per well. The downside of the approach, however, was the prolonged gel migration times (from 50 min for mini-gels to 4 h for the larger gels) and the fact that some protein patterns were deformed or appeared smeared on the gel.

Using these screening conditions, we identified a few proteins displaying a strong (*R*) vs (*S*) selectivity for the photoAB&CR molecule by in-gel fluorescence. The overall order of reactivity for **181**, **169**, **168**, and **170** with the membrane fraction was slightly different than that observed for the cytoplasmic fraction screening. Under identical irradiation conditions (see Section 4.6.2), we observed for the membrane fraction that generally the aromatic azide **181** and alkyl diazirine **168** provided the most intense signals, followed by aromatic diazirine **169**, and benzophenone **170**. Nonetheless, these differences varied within different fractionation cuts (Q-Sepharose elution, left gels, and Q-Sepharose flow-through, right gels). By comparison, in the cytosolic fraction, **181** was more reactive, followed by **169**, **168** and **170**, and less disparities in reactivity were observed within different AMS cuts. Differences in the photoAB&CR reactivity profiles between the cytoplasmic and solubilized membrane fractions have been tentatively attributed, in

part, to differences in the inherent nature of proteins present in each subcellular fraction. The fluorescent signals in the membrane fraction were, however, not intense, and unaffected by an excess of competing (*R*)-LCM during the photolabeling step. In addition, the low-intensity fluorescent labeling observed for proteins specifically labeled suggested several potential problems. Among these are that (1) the protein labeled may have been present only at low levels in the lysate; (2) the photoAB&CR agent may only bind weakly to the protein; (3) the efficiency of the photolabeling step was low; (4) the detergent may have only solubilized a partial amount of membrane-bound protein; and (5) the detergent may have partially denatured the protein. A combination of these reasons may also explain the absence of protein targets that were strongly labeled in the membrane fractions. Indeed, some membrane-bound proteins cannot be easily solubilized or remain properly folded upon action of a detergent.⁴⁹⁸⁻⁵⁰⁰

Thus, we also screened the membrane-bound proteome under more native conditions. First, we changed from a simple HEPES-based buffer previously used to the more physiologically relevant Locke's buffer. Second, we took additional care in the handling of the freshly prepared membrane extracts by adding a slow cooling step in a cryobuffer prior to storage at -80 °C. The cryobuffer used was Locke's buffer supplemented to 10% (v/v) DMSO and 1% (w/v) BSA and has been demonstrated to enhance the stability of sensitive membrane synaptosomal proteins.⁴⁸⁵ Using this protocol, we prepared and screened intact synaptosomal and microsomal fractions with the photoAB&CR agents **181**, **169**, **168**, and **170**. We took advantage of a convenient phase-partitioning fractionation method⁴⁹⁶ to quickly

enrich for synaptosomes from the P2 fraction of the rat brain. However, in our hands, we observed a difference in the synaptosome preparation. The literature method indicated that the synaptosomes would be present in the upper layer after the second purification step (Figure 35, **red arrow**).⁴⁹⁶ Instead, we observed abundant white particles present at the interface between the two layers and assumed them to be the enriched synaptosomes. To check the integrity of the membrane extracts, we probed for the presence of a synaptosomal marker, SNAP-25, using an antibody and showed that the protein the material isolated after fractionation was enriched in SNAP-25 (Figure 36). We also probed the isolated synaptosomes for a mitochondrial marker (COX IV) to confirm that the protein isolated was not cross-contaminated with mitochondria, using the crude brain homogenate as a positive control. However, the antibody purchased was not functional and this secondary control was not pursued further. Recovery yields of synaptosomes (~6 mg per rat brain, 3–4 mg per gram of wet tissue) were in agreement with yields obtained using other literature procedures.^{501,493,502}

Using this new screening condition and utilizing the same irradiating conditions, we observed another difference in the reactivity profile of photoAB&CR derivatives. In the intact membrane photolabeling, aromatic azide **181**, aromatic diazine **169** and benzophenone **170** displayed a similar non-specific labeling profile whereas the photolabeled products from aliphatic diazine **168** were less intense (Figure 37). However, we identified a ~60 kDa protein targeted in the synaptosomal fraction, which was exclusively labeled by aromatic diazine **169**, and displayed a strong (*S*) vs (*R*) preference (Figure 37, Figure 38). Interestingly, both (*R*)-**169** and (*S*)-**169**

were competed by an excess of (*R*)-LCM, and to a lesser extent by (*S*)-LCM (Figure 39). The preference for (*S*)-**169** over (*R*)-**169** in the labeling step was intriguing, especially in view of the competition experiments. Indeed, the competition results suggested that (*R*)-LCM bound to that protein stronger than (*S*)-LCM. This (*S*)- vs (*R*)- preference for **169** has been tentatively attributed to an increased labeling efficiency of (*S*)-**169** due to a more ideally positioned amino acid residue, despite a potentially lower binding affinity when compared to (*R*)-**169**. We observed the presence of the same molecular weight protein in the microsomal fraction. The fluorescent signal observed for this photoadduction was intense (Figure 38, left panel) and did not correlate with the amount of total protein (Figure 38, right panel) present in the lane, thus suggesting a specific photolabeling. Attempts to purify this protein using a biotin purification experiment did not provide us with definitive identification of the protein but suggested that the putative interacting partner of (*R*)-LCM was likely serum albumin (Figure 40, Table 6). Supporting this hypothesis was the disappearance of the characteristic ~60 kDa fluorescent signal when we used a freshly prepared brain microsomal extract (e.g., without BSA present) to perform the assay (Figure 41). The fluorescent signal returned when the same extract was stored using the slow cooling step in the presence of cryobuffer. A photolabeling experiment using pure BSA and HSA showed that serum albumin was indeed selectively labeled by photoAB&CR agent **169** (Figure 42), and not by **181**, **168**, and **170** (Figure 43). However, we observed notable differences when labeling was performed on the protein by itself. The difference in fluorescence intensity between (*R*)-**169** and (*S*)-**169** was greatly reduced, and competition with a large excess of

(*R*)-LCM (5000 equiv) had almost no effect on (*R*)-**169** or (*S*)-**169**'s fluorescent signals (Figure 42). We have hypothesized that the conformational states of serum albumin could be different in an isolated setting and in a complex hydrophobic environment, and that this difference could affect the AB&CR modification. Nonetheless, this finding indicates that lacosamide has an inherent binding affinity for serum albumin, a finding that has been previously observed for numerous marketed drugs.⁵⁰³⁻⁵⁰⁶

5.4. Conclusions

We screened the membrane-bound proteome with photoAB&CR agents using a variety of screening conditions. The search yielded one protein of interest for which the AB&CR **169**'s fluorescent labeling displayed enantiospecific competition with (*R*)-LCM over (*S*)-LCM. This protein has been tentatively identified as bovine serum albumin, a component of the cryobuffer for membrane extract storage. The labeling specificity was greatly reduced when either purified BSA or HSA was used for the experiment in buffer alone. While the therapeutic relevance of serum albumin for lacosamide overall function is unknown, we did not pursue this lead because the literature did not provide a rationale to link SA to epilepsy.

The identification of SA in our proteomic screening protocol suggested that the AB&CR methodology worked, in part, in that we were able to identify a medium-to-low affinity binding partner of (*R*)-LCM from a complex protein environment. Significantly, we do not assert that lacosamide function is intimately connected with SA binding. Rather, our finding suggests that lacosamide possesses an inherent,

modest binding affinity to serum albumin. If this is the case, SA sequestration of LCM may indirectly affect the AED's function by modulating the serum concentration of lacosamide and its biodistribution in the CNS.

5.5. Experimental Section

5.5.1. Preparation of the solubilized membrane lysate

The whole rat brain homogenate (320 mM sucrose, 25 mM HEPES (pH 7.4), supplemented with protease inhibitors 1 mM PMSF, 10 μ M E-64, 10 μ M pepstatin A, 1 μ M TPEN) was centrifuged at 1,500 g (10 min). The supernatant (S1) was pulled and centrifuged at the desired speed. Centrifugation at 15,000 g (20 min) yielded the P2 fraction (heavy membrane), and a S2 supernatant that was centrifuged at 100,000 g (50 min) to yield a P3 fraction (light membrane). Alternatively, the S1 supernatant could also be centrifuged directly at 100,000 g to yield a combined P2+P3 membrane fraction. The pellet (P2, P3, or P2+P3) was hypoosmotically lysed by resuspension in 10 mM HEPES buffer (pH 7.4) on ice (20 min) and centrifuged at 15,000 g (20 min, P2) or 100,000 g (50 min, P3, P2+P3). The supernatant was discarded, and the pellets resuspended in 25 mM HEPES, 150 mM NaCl to a total protein concentration of 4–5 mg.mL⁻¹. The desired supernatant was added at the desired concentration (1% TX100, 0.5% β -DDM, 0.5% Zw3-14, 1% CHAPS), the suspension gently rocked at 4 °C (20 min) and centrifuged at 15,000 g (20 min, P2) or 100,000 g (50 min, P3, P2+P3). The supernatant was used as the detergent-solubilized membrane fraction for screening.

5.5.2. Protocol for the enrichment of synaptosomes by phase partitioning

Synaptosomes were prepared following a literature procedure.⁴⁹⁶ One day prior to the experiment, the two phase systems (termed 21-g and 30-g (g for grams)) were prepared and stored at 4 °C. Because biomolecules are very sensitive to small changes in polymer concentrations, all solutions were prepared by weighing the different reagents. The stock solution of PEG-4000 (40% w/w) was prepared by accurately weighing 40.0 g of PEG-4000 and made up to 100.0 g with ddH₂O. The dextran-500 was prepared at least 2 days in advance. For a 20.0% (w/w) stock, a ~35% (w/w) solution was prepared by layering 35 g of dextran over 65 g of water. The highly viscous solution was heated in a water bath (40–50 °C) while gently stirring until all the polymer was dissolved (~30 min). The solution was then dialyzed against ddH₂O (15 h) and transferred to a *weighed* container. The following was only carried out if no air bubbles were present in the viscous liquid. A known amount of dextran solution (~2 g) was precisely diluted to 10 mL with ddH₂O and the optical rotation was measured with a polarimeter. Using the specific rotation of dextran 500 ($[\alpha]_D^{25} = +199^\circ\text{g.dm.mL}^{-1}$),⁵⁰⁷ the exact concentration was determined and the stock solution was adjusted to 20.0% (w/w) by addition of ddH₂O. Care was taken to gently swirl the solution and avoid creating air bubbles.

The two stock solutions described were used as follows. The 21-g phase system was prepared in a 50 mL plastic centrifuge tube by weighing 7.680 g of 20.0% (w/w) dextran 500, 3.840 g of 40.0% PEG-4000, 6.720 g of 1 M sorbitol, 600 mg of 200 mM potassium phosphate (pH 7.4), 300 mg of 10 mM potassium EDTA,

and 1.860 g of ddH₂O. For convenience in later experiments, all volumes were increased by 20%. The 21-g solution was mixed and stored at 4 °C.

The 30-g phase system was prepared by weighing 9.600 g of 20.0% dextran 500, 4.800 g of 40.0% PEG-4000, 9.600 g of 1 M sorbitol, 750 mg of 200 mM potassium phosphate (pH 7.4), 375 mg of 10 mM potassium EDTA and 4.875 g of ddH₂O. After mixing well, the phase system was allowed to settle at room temperature until two phases appeared. The process could be accelerated by low speed centrifugation (1,500 g, 3 min). The lower phase was collected without disturbing the interface and stored at 4 °C (fresh lower phase).

The following buffers were used in the preparation of rat brains. Homogenization was carried out using 320 mM sucrose, 1 mM potassium EDTA, 10 mM Tris HCl (pH 7.4) (buffer A), supplemented with protease inhibitors (PMSF 1 mM, E-64 10 µM, Pepstatin A 10 µM, TPEN 1 µM). Resuspension of the synaptosomal pellet was carried out in 320 mM sorbitol, 0.1 mM potassium EDTA, and 5 mM potassium phosphate (pH 7.4) (buffer B).

Starting with 4 rat brains, homogenization was conducted as described in Section 3.1 using 15 mL buffer A per rat brain: The crude homogenate was centrifuged at 1,500 g (5 min), the supernatant (S1) was transferred to a new tube and the pellet was discarded.

The S1 fraction was centrifuged at 1,500 g (5 min), to give a cleaner supernatant (S1-clean) and the pellet was discarded.

The S1-clean fraction was centrifuged at 17,000 g (10 min), the supernatant (S2) was kept aside and later centrifuged at 100,000 g (50 min) to provide the microsomal fraction (P3) and the cytoplasmic fraction (S3).

The pellet (P2, crude synaptosomal pellet) was resuspended in 30 mL of buffer B and centrifuged at 12,000 g (10 min) and the supernatant was discarded.

The pellet was resuspended in a minimal amount of buffer B. Three grams of resuspension were precisely weighed in a conical tube and were added to one 21-g phase system, creating a 24-g phase system. Typically, one 21-g phase system was used for 2 rat brains.

The 24-g phase was mixed by 20 inversions and centrifuged at 600 g (2 min). The upper phase was carefully transferred to a tube containing 9 mL of fresh lower phase from the 30-g phase system. The new phase system was mixed by 20 inversions and centrifuged at 600 g (2 min). The final upper phase and the interface was layered on 20 mL of buffer A and centrifuged at 17,000 g (10 min). The pellet was rinsed with Locke's buffer, and then resuspended in cryobuffer for storage.

5.5.3. Photolabeling of the membrane fraction

The detergent-solubilized membrane lysate was photolabeled like the cytoplasmic lysate. Briefly, 100 μ L (~200 μ g total protein) aliquots of detergent-solubilized membrane lysate were dispensed in 96-well plates and irradiated under the appropriate conditions (see Section 4.6.2).

For the photolabeling of intact synaptosomes and microsomes, the extracts were rinsed from cryobuffer (see Section 5.5.5) and resuspended in Locke's buffer

(154 mM NaCl, 5.6 mM KCl, 2.3 mM CaCl₂, 1.0 mM MgCl₂, 3.8 mM NaHCO₃, 5 mM D-glucose, 5 mM HEPES (pH 7.2))^{483,484} to a total protein concentration of 0.1–0.2 mg.mL⁻¹. Small scale experiments were conducted in 100 μ L reaction volume in a 96-well plate. Photolabeling was performed at 4 °C with photoAB&CR **181**, **169**, **168**, and **170** as previously described.

5.5.4. Click chemistry on intact labeled membrane proteins (Methods A and B)

After photolabeling, the content of each well was transferred to an 1.5 mL Eppendorf tube, spun down (14,000 rpm, 10 min), resuspended in 200 μ L 25 mM HEPES (pH 7.4), spun down again (14,000 rpm, 10 min), and the washing process was carried out one more time.

Using Method A, the pellet was resuspended in 30–50 μ L of 25 mM HEPES buffer (pH 7.4) supplemented to the desired concentration of detergent (5 min) and centrifuged (14,000 rpm, 10 min). Click chemistry with the desired Probe was performed on the supernatant as previously described (see Section 4.6.4).

Using Method B, the pellet was resuspended in 30–50 μ L of 25 mM HEPES buffer (pH 7.4), the desired Probe and click chemistry reagents were added, and the suspension was tumbled at room temperature (1 h). Each tube was spun down (14,000 rpm, 10 min) and the supernatant was discarded. The pellet in each tube was rinsed twice with 200 μ L of 25 mM HEPES buffer (pH 7.4). The final pellet was resuspended in 30–50 μ L 25 mM HEPES buffer (pH 7.4) supplemented to 1% SDS (5 min) and spun down (14,000 rpm, 10 min). SDS loading buffer was then added to the supernatant and the proteins resolved on SDS-PAGE gel.

5.5.5. Protocol for the cryopreservation step

The slow cooling step⁴⁸⁵ was performed as follows. A thick-wall (~4–5 cm) Styrofoam box was filled halfway with loosely packed cheesecloth. The tubes were placed in the center of the box and more cheesecloth was added on top of the samples. The Styrofoam container was closed and allowed to cool in a dry ice chest at least 5 h before transferring the slowly frozen samples to a -80 °C freezer box. Before performing the labeling experiment, samples were quickly brought to room temperature using a water bath (37 °C). The samples were then spun down (14,000 rpm, 4 °C, 5–10 min), the cryobuffer was discarded and the pellet resuspended in Locke's buffer. These steps were repeated once, and the final pellet was resuspended to a protein concentration of ~0.1–0.2 mg.mL⁻¹ (10–20 µg in 100 µL) in Locke's buffer.

CHAPTER 6

CONCLUSIONS AND FUTURE DIRECTIONS

In this research project, we have designed, synthesized, and evaluated a series of molecular tools to identify the biological targets of the antiepileptic drug lacosamide. Over the course of our study, we have extended the structure activity relationship of LCM at the 3-oxy site, and the *N*-benzylamide 4' position. Based on the SAR results, we have constructed a series of LCM AB&CR analogs to interrogate the rat brain proteome and identify potential binding partners of LCM.

Using up to 11 LCM AB&CR derivatives, we have screened the brain soluble and membrane-bound proteome. We took advantage of several established protein purification methods and subcellular fractionation protocols to reduce the complexity of the brain proteome. Following this approach, we were not able to identify a protein target with a therapeutic relevance to epilepsy. Nonetheless, our methodology allowed the identification of some proteins that were stereospecifically adducted by either (*R*)-AB&CR or (*S*)-AB&CR derivatives. In some instances, the protein displayed a labeling dose-dependent competition with excess (*R*)-LCM or (*S*)-LCM. Among these were creatine kinase B, serum albumin, and a ~25 kDa cytosolic protein in too low abundance for us to identify. These results have not allowed us to further define the mechanism of action of lacosamide.

Our overall findings exemplified two potential limitations in the use of the AB&CR methodology to identify protein targets of small molecules. First, the methodology may not allow the pull-down capture of proteins expressed at low levels, although the in-gel fluorescence approach is sensitive enough to allow their detection. Second, and perhaps most important, is that the method used can only yield an interacting partner, and no guarantee exists that the adducted protein is a biomolecule with therapeutic relevance to epilepsy. Following is a general discussion on this project's observations and learnt lessons, as well as potential shortcomings of our drug target identification method. Comparisons with the work of other groups are presented, where applicable. For each section, possible suggestions for future work are highlighted.

6.1. The importance of the lysate source

The handling of the animal tissue is a crucial step in the preparation of a lysate. In our study, we used a commercial source of rat brains that were frozen on dry ice prior to overnight shipment, and stored upon arrival at -80 °C. Ideally, the animal should have been sacrificed prior to brain homogenization, as potential proteins of interest may have been denatured by a single freeze-thaw step.⁴²⁴ Lacosamide is able to prevent MES-induced seizures in healthy rodents and the protein targeted by this AED likely is present in the rat brain. Nonetheless, it is possible that the expression levels of this protein are too low to detect. Thus, it may be helpful to prepare a whole brain protein lysate from animals that have been undergone MES-seizure or 6 Hz treatment prior to sacrifice. Indeed, the protein(s)

targeted by (*R*)-LCM may be upregulated in the early events or during the course of a seizure.

Along the same line, screening the rat brain proteome of healthy animals with our AB&CR analogs would, if successful, only lead to identification of protein(s) involved in the development of artificially-induced seizures (*i.e.* implicated in *epileptic* pathways). In light of the unique pharmacological profile of (*R*)-LCM and notably its activity against kindled seizures, screening the brain proteome of kindled animals may lead to the identification of proteins implicated in *epileptogenic* pathways. These proteins and their biological pathways still remain to be discovered, and together this information would provide invaluable insights into the pathology of epileptic disorders. These could potentially translate into “cures” for epileptic patients. Similarly, using genetically modified animals (Frings and DBA/2 mouse models) as a source of brain tissue, would enhance the diversity of proteins screened, and thus the chances of identifying key macromolecules implicated in audiogenic or reflex epilepsy pathways.

6.2. Other subcellular fractions and proteins for screening

Our study focused on the cytosolic and membrane fractions. Other rat brain subcellular compartments yet to be screened include the mitochondria (soluble and membrane fraction) and the nucleus (nuclear membrane and nucleoplasm). Attempts to isolate nuclei from rat brain were unsuccessful, as the traditional sucrose gradient procedure requires a swing-bucket ultracentrifuge.^{508-510,425} In addition, brain nuclei are reported to be more fragile than other organs' nuclei.⁵¹⁰

Several findings support the importance of nuclear proteins in epileptic pathways. A recent publication indicates that drastic changes in the brain nucleus occur during a seizure, from increased protein activity to histone modifications.⁵¹¹ It is interesting to note that curcumin, an established histone acetyltransferase (HAT) inhibitor,⁵¹² has protective effects in a variety of animal seizure models including chemoconvulsant-induced kindled seizures.^{66,513,514} In addition, the established AED VPA has been shown to have a direct inhibitory activity against histone deacetylases (HDAC).⁵¹⁵ However, the pharmacological relationship between HDAC inhibition and the antiepileptic or neuroprotective effects of VPA still remains to be validated.

Ion channels are extensively, and rightfully, studied for interactions with AEDs. Nonetheless, some currently emerging drugs (RGB, 2DG) do not interact with any epilepsy-related VGIC, LGIC, neurotransmitter transporter, or neurotransmitter degradative enzyme. These observations should encourage researchers to probe for different biological mechanisms and to approach epilepsy from a less electrophysiological perspective. The reemergence of the ketogenic diet as a front line treatment for refractory epilepsy^{222,221} and the advancement of 2DG^{224,212} in clinical trials suggest a trend to tackle epileptic syndromes from the energetic standpoint. In this regard, and despite its lack of interaction with (*R*)-LCM, it would be interesting to determine if small molecule CKB inhibitors have a protective effect on seizures. Indeed, the CKB-catalyzed phosphotransfer reaction is the fastest way for a cell to generate ATP.⁴⁴⁹ Studies have shown the physiological importance of CKB in seizures and that the enzyme's reaction rate dramatically increases during a seizure, while brain levels of PCr decrease by up to 50%.⁴⁴⁹⁻⁴⁵² This quick

generation of ATP is required for fueling and maintaining the high-energy demand of the seizure.⁴⁵⁰⁻⁴⁵² Inhibitors of CKB may, therefore, act as preventive agents by suppressing the seizure's energetic pathway.

6.3. Drug target identification methods

Advantages and drawbacks of electrophilic and photo-activated affinity labels used in this study have already been highlighted. We took advantage of a variety of AB moieties with different reactivity profiles to cover a wide spectrum of potential amino acid modification sites. Experimental observations from our research project show distinct protein labeling patterns for each AB moiety and support the rationale for the use of a wide range of affinity labels. Significantly, all the “selectively modified” proteins we observed in our experiments (e.g., proteins showing enantiospecific labeling but not necessarily displaying competition with either (*R*)-LCM or (*S*)-LCM) were only labeled by one AB moiety. For example, serum albumin (Figure 37) and the protein targeted by (*S*)-LCM (Figure 26) were only identified with the trifluoromethyl aromatic diazirine photoAB **169**. Other proteins in the membrane-bound fraction were exclusively labeled by the alkyl methyldiazirinyI photoprobe **168** (Figure 32, Figure 33). These findings support the idea that identification of unknown proteins using an affinity label/pulldown strategy is a delicate task that requires multiple approaches. In this regard, it is impossible to have a universal affinity label.

Whether or not click chemistry is involved, activity-based protein profiling (ABPP) has developed into a powerful proteomic method. ABPP involves the use of electrophilic moieties (e.g., phenylsulfonates,³⁵⁹ epoxides,^{358,309} beta-lactones,⁵¹⁶ or

fluorophosphonates⁵¹⁷) to establish the reactivity profile of specific enzymes or identify new macromolecular entities that interact with specific AB moieties. In that sense, ABPP may be viewed as a drug target discovery method where the drug target is a *reactive enzyme* and possesses activated nucleophilic residues prone to react with the AB. Using this method, proteases⁵¹⁸ implicated in cancer and bacterial signaling pathways have been identified.^{519-521,517} The ABPP ligands preferentially target small molecule binding sites or spatially related sites, because the enzyme's reactive residue is located within this pocket.

By comparison, in an epilepsy drug target discovery project such as ours, the biological target is more likely to be a membrane-bound or soluble protein where the AED binding site *does not possess reactive amino acids*. Rather than utilizing substrate-processing catalytic binding sites, AEDs seem to interact at sites modulating protein conformation. In these cases, photoactivated ligands may be more appropriate tools to covalently modify the target via a non-nucleophilic residue, and therefore be more suited for receptor binding site identification. For example, the use of the aromatic azide photoAB led to the identification of the binding site of LVT,²⁰⁸ and photoreactive analogs of tetrodotoxin (TTX) and saxitoxin (STX) helped identify key regions for VGSCs function.⁵²²

Finally, we did not identify any specific labeling of VGSCs, an established binding partner for (*R*)-LCM. It is, however, possible that our lysate preparation did not yield functional Na⁺ channel. Indeed, extensive purification studies by Catterall and coworkers have demonstrated the extreme sensitivity of these proteins to detergent solubilization or proteases.^{429,427} Thus, it would be interesting to use our

array of photoAB&CR agents on oocytes overexpressing VGSCs to potentially identify the channel's binding region critical for slow inactivation.¹³⁵ In addition, it would also be interesting to use a complementary screening approach to the whole brain lysate. One could, for example, use a variety of readily available neuronal and glial cell lines to screen the AB&CR agents. These less complex protein sources may increase our chances of biological target capture.

REFERENCES

- (1) *Fundamental Neuroscience*; Squire, L.R.; Bloom, F.; McConnell, S.; Roberts, J.; Spitzer, N.; Zigmond, M., Eds.; 2nd ed.; Academic Press, 2003.
- (2) Stone, T. W. *Neuropharmacology*; Biochemical & Medicinal Chemistry Series; W.H. Freeman Spektrum: Oxford, 1995.
- (3) Golgi, C. Sulla struttura della sostanza grigia del cervello. *Gazzetta Medica Italiana. Lombardia* **1873**, 244-246.
- (4) Ramón y Cajal, S. ¿Neuronismo o reticularismo? Las pruebas objetivas de la unidad anatómica de las células nerviosas. *Arch. Neurobiol.* **1933**, 1-144.
- (5) Ramón y Cajal, S. Estructura de los centros nerviosos de las aves. *Rev. Trimest. Histol. Norm. Patol.* **1888**, 1-10.
- (6) Golgi, C. The impossible interview with the man of the hidden biological structures. Interview by Paolo Mazzarello. *J. Hist. Neurosci.* **2006**, 15, 318-325.
- (7) Williams, R. W.; Herrup, K. The control of neuron number. *Annu. Rev. Neurosci.* **1988**, 11, 423-453.
- (8) Stiefel, K. M.; Sejnowski, T. J. Mapping function onto neuronal morphology. *J. Neurophysiol.* **2007**, 98, 513-526.
- (9) Cooper, J. R.; Bloom, F. E.; Roth, R. H. *The Biochemical Basis of Neuropharmacology*, 7th ed.; Oxford University Press: New York, 1996.
- (10) Allen, N. J.; Barres, B. A. Neuroscience: Glia — more than just brain glue. *Nature* **2009**, 457, 675-677.
- (11) Allen, N. J.; Barres, B. A. Signaling between glia and neurons: focus on synaptic plasticity. *Curr. Opin. Neurobiol.* **2005**, 15, 542-548.
- (12) Barres, B. A. The mystery and magic of glia: a perspective on their roles in health and disease. *Neuron* **2008**, 60, 430-440.
- (13) Nave, K.; Trapp, B. D. Axon-glial signaling and the glial support of axon function. *Annu. Rev. Neurosci.* **2008**, 31, 535-561.
- (14) Wang, D. D.; Bordey, A. The astrocyte odyssey. *Prog. Neurobiol.* **2008**, 86, 342-367.

- (15) Sah, P.; McLachlan, E. M. Potassium currents contributing to action potential repolarization and the afterhyperpolarization in rat vagal motoneurons. *J. Neurophysiol.* **1992**, *68*, 1834-1841.
- (16) Hauser, W. A.; Annegers, J. F.; Kurland, L. T. Prevalence of epilepsy in Rochester, Minnesota: 1940-1980. *Epilepsia* **1991**, *32*, 429-445.
- (17) Fisher, R. S.; van Emde Boas, W.; Blume, W.; Elger, C.; Genton, P.; Lee, P.; Engel, J. Epileptic seizures and epilepsy: definitions proposed by the International League Against Epilepsy (ILAE) and the International Bureau for Epilepsy (IBE). *Epilepsia* **2005**, *46*, 470-472.
- (18) Guidelines for epidemiologic studies on epilepsy. Commission on epidemiology and prognosis, International League Against Epilepsy. *Epilepsia* **1993**, *34*, 592-596.
- (19) ILAE commission report. The epidemiology of the epilepsies: future directions. International League Against Epilepsy. *Epilepsia* **1997**, *38*, 614-618.
- (20) Proposal for revised classification of epilepsies and epileptic syndromes. Commission on Classification and Terminology of the International League Against Epilepsy. *Epilepsia* **1989**, *30*, 389-399.
- (21) World Health Organization | Epilepsy. (<http://www.who.int/topics/epilepsy/en/>).
- (22) Begley, C. E.; Lairson, D. R.; Reynolds, T. F.; Coan, S. Early treatment cost in epilepsy and how it varies with seizure type and frequency. *Epilepsy Res.* **2001**, *47*, 205-215.
- (23) Begley, C. E.; Famulari, M.; Annegers, J. F.; Lairson, D. R.; Reynolds, T. F.; Coan, S.; Dubinsky, S.; Newmark, M. E.; Leibson, C.; So, E. L.; Rocca, W. A. The cost of epilepsy in the United States: an estimate from population-based clinical and survey data. *Epilepsia* **2000**, *41*, 342-351.
- (24) Begley, C. E.; Annegers, J. F.; Lairson, D. R.; Reynolds, T. F.; Hauser, W. A. Cost of epilepsy in the United States: a model based on incidence and prognosis. *Epilepsia* **1994**, *35*, 1230-1243.
- (25) CDC - Epilepsy. (<http://cdc.gov/epilepsy/>).
- (26) Proposal for revised clinical and electroencephalographic classification of epileptic seizures. From the Commission on Classification and Terminology of the International League Against Epilepsy. *Epilepsia* **1981**, *22*, 489-501.
- (27) Wallace, R. H.; Scheffer, I. E.; Parasivam, G.; Barnett, S.; Wallace, G. B.; Sutherland, G. R.; Berkovic, S. F.; Mulley, J. C. Generalized epilepsy with

- febrile seizures plus: mutation of the sodium channel subunit SCN1B. *Neurology* **2002**, 58, 1426-1429.
- (28) Anticonvulsant Screening Program: National Institute of Neurological Disorders and Stroke (NINDS). (<http://www.ninds.nih.gov/research/asp/>).
 - (29) Chabolla, D. R. Characteristics of the epilepsies. *Mayo Clin. Proc.* **2002**, 77, 981-990.
 - (30) Theodore, W. H.; Porter, R. J.; Albert, P.; Kelley, K.; Bromfield, E.; Devinsky, O.; Sato, S. The secondarily generalized tonic-clonic seizure: A videotape analysis. *Neurology* **1994**, 44, 1403.
 - (31) Panayiotopoulos, C. P.; Chroni, E.; Daskalopoulos, C.; Baker, A.; Rowlinson, S.; Walsh, P. Typical absence seizures in adults: clinical, EEG, video-EEG findings and diagnostic/syndromic considerations. *J. Neurol. Neurosurg. Psychiatr.* **1992**, 55, 1002-1008.
 - (32) Towne, A. R.; Pellock, J. M.; Ko, D.; DeLorenzo, R. J. Determinants of mortality in status epilepticus. *Epilepsia* **1994**, 35, 27-34.
 - (33) Hauser, W. A. Status epilepticus: epidemiologic considerations. *Neurology* **1990**, 40, 9-13.
 - (34) Lindsay, J. M. M. Genetics and epilepsy: a model from critical path analysis. *Epilepsia* **1971**, 12, 47-54.
 - (35) Lang, E. S.; Andruchow, J. E. What is the preferred first-line therapy for status epilepticus? *Ann. Emerg. Med.* **2006**, 48, 98-100.
 - (36) Wasterlain, C. G.; Fujikawa, D. G.; Penix, L.; Sankar, R. Pathophysiological mechanisms of brain damage from status epilepticus. *Epilepsia* **1993**, 34, S37-S53.
 - (37) Pitkänen, A.; Nissinen, J.; Nairismägi, J.; Lukasiuk, K.; Gröhn, O. H. J.; Miettinen, R.; Kauppinen, R. Progression of neuronal damage after status epilepticus and during spontaneous seizures in a rat model of temporal lobe epilepsy. *Prog. Brain Res.* **2002**, 135, 67-83.
 - (38) Macdonald, R. L. Antiepileptic drug actions. *Epilepsia* **1989**, 30 Suppl 1, S19-28; discussion S64-8.
 - (39) Stahl, S. M. Psychopharmacology of anticonvulsants: do all anticonvulsants have the same mechanism of action? *J. Clin. Psychiatry* **2004**, 65, 149-50.
 - (40) Porter, R. J. New antiepileptic agents: strategies for drug development. *Lancet* **1990**, 336, 423-424.

- (41) McDowell, J. Epilepsy. *Mod. Drug Discovery* **2004**, 7, 21-23.
- (42) Ragsdale, D. S.; Scheuer, T.; Catterall, W. A. Frequency and voltage-dependent inhibition of type IIA Na⁺ channels, expressed in a mammalian cell line, by local anesthetic, antiarrhythmic, and anticonvulsant drugs. *Mol. Pharmacol.* **1991**, 40, 756-765.
- (43) Gee, N. S.; Brown, J. P.; Dissanayake, V. U.; Offord, J.; Thurlow, R.; Woodruff, G. N. The novel anticonvulsant drug, gabapentin (Neurontin), binds to the alpha2delta subunit of a calcium channel. *J. Biol. Chem.* **1996**, 271, 5768-5776.
- (44) Fielding, S.; Hoffmann, I. Pharmacology of anti-anxiety drugs with special reference to clobazam. *Br. J. Clin. Pharmacol.* **1979**, 7 Suppl 1, 7S-15S.
- (45) Caccia, S.; Carli, M.; Garattini, S.; Poggesi, E.; Rech, R.; Samanin, R. Pharmacological activities of clobazam and diazepam in the rat: relation to drug brain levels. *Arch. Int. Pharmacodyn. Ther.* **1980**, 243, 275-283.
- (46) Barzaghi, F.; Fournex, R.; Mantegazza, P. Pharmacological and toxicological properties of clobazam (1-phenyl-5-methyl-8-chloro-1,2,4,5-tetrahydro-2,4-diketo-3H-1,5-benzodiazepine), a new psychotherapeutic agent. *Arzneimittelforschung* **1973**, 23, 683-686.
- (47) McCorry, D.; Chadwick, D.; Marson, A. Current drug treatment of epilepsy in adults. *Lancet Neurol.* **2004**, 3, 729-735.
- (48) Duncan, J. S. The promise of new antiepileptic drugs. *Br. J. Clin. Pharmacol.* **2002**, 53, 123-131.
- (49) Bauer, J.; Reuber, M. Medical treatment of epilepsy. *Expert Opin. Emerg. Drugs* **2003**, 8, 457-467.
- (50) Mattson, R. H.; Cramer, J. A.; Collins, J. F.; Smith, D. B.; Delgado-Escueta, A. V.; Browne, T. R.; Williamson, P. D.; Treiman, D. M.; McNamara, J. O.; McCutchen, C. B. Comparison of carbamazepine, phenobarbital, phenytoin, and primidone in partial and secondarily generalized tonic-clonic seizures. *N. Engl. J. Med.* **1985**, 313, 145-151.
- (51) Pellock, J. M.; Willmore, L. J. A rational guide to routine blood monitoring in patients receiving antiepileptic drugs. *Neurology* **1991**, 41, 961-964.
- (52) Stables, J. P.; Kupferberg, H. J. The NIH Anticonvulsant Drug Development (ADD) Program: preclinical anticonvulsant screening project.
- (53) Sarkisian, M. R. Overview of the current animal models for human seizure and epileptic disorders. *Epilepsy Behav.* **2001**, 2, 201-216.

- (54) Fisher, R. S. Animal models of the epilepsies. *Brain Res. Rev.* **1989**, *14*, 245-278.
- (55) Krall, R. L.; Penry, J. K.; White, B. G.; Kupferberg, H. J.; Swinyard, E. A. Antiepileptic Drug Development: II. Anticonvulsant drug screening. *Epilepsia* **1978**, *19*, 409-428.
- (56) Swinyard, E. A.; Brown, W. C.; Goodman, L. S. Comparative assays of antiepileptic drugs in mice and rats. *J. Pharmacol. Exp. Ther.* **1952**, *106*, 319-330.
- (57) Barton, M. E.; Klein, B. D.; Wolf, H. H.; White, H. S. Pharmacological characterization of the 6 Hz psychomotor seizure model of partial epilepsy. *Epilepsy Res.* **2001**, *47*, 217-227.
- (58) Brown, W. C.; Schiffman, D. O.; Swinyard, E. A.; Goodman, L. S. Comparative assay of an antiepileptic drugs by psychomotor seizure test and minimal electroshock threshold test. *J. Pharmacol. Exp. Ther.* **1953**, *107*, 273-283.
- (59) Barton, M. E.; Peters, S. C.; Shannon, H. E. Comparison of the effect of glutamate receptor modulators in the 6 Hz and maximal electroshock seizure models. *Epilepsy Res.* **2003**, *56*, 17-26.
- (60) White, H.; Johnson, M.; Wolf, H.; Kupferberg, H. The early identification of anticonvulsant activity: role of the maximal electroshock and subcutaneous pentylenetetrazol seizure models. *Ital. J. Neurol. Sci.* **1995**, *16*, 73-77.
- (61) Adler, M. W.; Lin, C. H.; Keinath, S. H.; Braverman, S.; Geller, E. B. Anticonvulsant action of acute morphine administration in rats. *J. Pharmacol. Exp. Ther.* **1976**, *198*, 655-660.
- (62) el Hamdi, G.; de Vasconcelos, A. P.; Vert, P.; Nehlig, A. An experimental model of generalized seizures for the measurement of local cerebral glucose utilization in the immature rat. I. Behavioral characterization and determination of lumped constant. *Dev. Brain Res.* **1992**, *69*, 233-242.
- (63) Mandhane, S. N.; Aavula, K.; Rajamannar, T. Timed pentylenetetrazol infusion test: A comparative analysis with s.c.PTZ and MES models of anticonvulsant screening in mice. *Seizure* **2007**, *16*, 636-644.
- (64) Erakovic, V.; Zupan, G.; Varljen, J.; Laginja, J.; Simonic, A. Lithium plus pilocarpine induced status epilepticus -- biochemical changes. *Neurosci. Res.* **2000**, *36*, 157-166.
- (65) Leite, J. P.; Cavalheiro, E. A. Effects of conventional antiepileptic drugs in a model of spontaneous recurrent seizures in rats. *Epilepsy Res.* **1995**, *20*, 93-104.

- (66) Sng, J. C. G.; Taniura, H.; Yoneda, Y. Histone modifications in kainate-induced status epilepticus. *Eur. J. Neurosci.* **2006**, 23, 1269-1282.
- (67) Turski, W. A.; Cavalheiro, E. A.; Calderazzo-Filho, L. S.; Kleinrok, Z.; Czuczwar, S. J.; Turski, L. Injections of picrotoxin and bicuculline into the amygdaloid complex of the rat: an electroencephalographic, behavioural and morphological analysis. *Neuroscience* **1985**, 14, 37-53.
- (68) Frings, H.; Frings, M.; Kivert, A. Behavior patterns of the laboratory mouse under auditory stress. *J. Mammal.* **1951**, 32, 60-76.
- (69) Steinlein, O. K. Genetic mechanisms that underlie epilepsy. *Nat. Rev. Neurosci.* **2004**, 5, 400-408.
- (70) Skradski, S. L.; Clark, A. M.; Jiang, H.; White, H.; Fu, Y.; Ptáček, L. J. A novel gene causing a Mendelian audiogenic mouse epilepsy. *Neuron* **2001**, 31, 537-544.
- (71) Chapman, A. G.; Croucher, M. J.; Meldrum, B. S. Evaluation of anticonvulsant drugs in DBA/2 mice with sound-induced seizures. *Arzneimittelforschung* **1984**, 34, 1261-1264.
- (72) Lothman, E.; Williamson, J. Closely spaced recurrent hippocampal seizures elicit two types of heightened epileptogenesis: a rapidly developing, transient kindling and a slowly developing, enduring kindling. *Brain Res.* **1994**, 649, 71-84.
- (73) Racine, R. J. Modification of seizure activity by electrical stimulation. II. Motor seizure. *Electroencephalogr. Clin. Neurophysiol.* **1972**, 32, 281-294.
- (74) Brandt, C.; Ebert, U.; Löscher, W. Epilepsy induced by extended amygdala-kindling in rats: lack of clear association between development of spontaneous seizures and neuronal damage. *Epilepsy Res.* **2004**, 62, 135-156.
- (75) Dunham, N. W.; Miya, T. S. A note on a simple apparatus for detecting neurological deficit in rats and mice. *J. Am. Pharm. Assoc., Sci. Ed.* **1957**, 46, 208-209.
- (76) Errington, A. C.; Stöhr, T.; Lees, G. Voltage gated ion channels: targets for anticonvulsant drugs. *Curr. Top. Med. Chem.* **2005**, 5, 15-30.
- (77) Rogawski, M. A.; Loscher, W. The neurobiology of antiepileptic drugs. *Nat. Rev. Neurosci.* **2004**, 5, 553-564.
- (78) Ragsdale, D. S.; Avoli, M. Sodium channels as molecular targets for antiepileptic drugs. *Brain Res. Rev.* **1998**, 26, 16-28.

- (79) Catterall, W. A. From ionic currents to molecular mechanisms: the structure and function of voltage-gated sodium channels. *Neuron* **2000**, 26, 13-25.
- (80) Catterall, W. A.; Goldin, A. L.; Waxman, S. G. International Union of Pharmacology. XLVII. Nomenclature and structure-function relationships of voltage-gated sodium channels. *Pharmacol. Rev.* **2005**, 57, 397-409.
- (81) Heinemann, S. H.; Terlau, H.; Stühmer, W.; Imoto, K.; Numa, S. Calcium channel characteristics conferred on the sodium channel by single mutations. *Nature* **1992**, 356, 441-443.
- (82) Catterall, W. A. Cellular and molecular biology of voltage-gated sodium channels. *Physiol. Rev.* **1992**, 72, S15-48.
- (83) Qu, Y.; Curtis, R.; Lawson, D.; Gilbride, K.; Ge, P.; DiStefano, P. S.; Silos-Santiago, I.; Catterall, W. A.; Scheuer, T. Differential modulation of sodium channel gating and persistent sodium currents by the beta1, beta2, and beta3 subunits. *Mol. Cell. Neurosci.* **2001**, 18, 570-580.
- (84) Isom, L.; Catterall, W. A. Na⁺ channel subunits and Ig domains. *Nature* **1996**, 307-308.
- (85) Ceulemans, B. P. G. M.; Claes, L. R. F.; Lagae, L. G. Clinical correlations of mutations in the SCN1A gene: from febrile seizures to severe myoclonic epilepsy in infancy. *Pediatr. Neurol.* **2004**, 30, 236-243.
- (86) Sugawara, T.; Tsurubuchi, Y.; Fujiwara, T.; Mazaki-Miyazaki, E.; Nagata, K.; Montal, M.; Inoue, Y.; Yamakawa, K. Nav1.1 channels with mutations of severe myoclonic epilepsy in infancy display attenuated currents. *Epilepsy Res.* **2003**, 54, 201-207.
- (87) Sugawara, T.; Tsurubuchi, Y.; Agarwala, K. L.; Ito, M.; Fukuma, G.; Mazaki-Miyazaki, E.; Nagafuji, H.; Noda, M.; Imoto, K.; Wada, K.; Mitsudome, A.; Kaneko, S.; Montal, M.; Nagata, K.; Hirose, S.; Yamakawa, K. A missense mutation of the Na⁺ channel alpha II subunit gene Na(v)1.2 in a patient with febrile and afebrile seizures causes channel dysfunction. *Proc. Natl. Acad. Sci. U.S.A.* **2001**, 98, 6384-6389.
- (88) Patton, D. E.; West, J. W.; Catterall, W. A.; Goldin, A. L. Amino acid residues required for fast Na(+)-channel inactivation: charge neutralizations and deletions in the III-IV linker. *Proc. Natl. Acad. Sci. U.S.A.* **1992**, 89, 10905-10909.
- (89) Goldin, A. L. Mechanisms of sodium channel inactivation. *Curr. Opin. Neurobiol.* **2003**, 13, 284-290.
- (90) Mitrovic, N.; George, A. L.; Horn, R. Role of domain 4 in sodium channel slow inactivation. *J. Gen. Physiol.* **2000**, 115, 707-718.

- (91) Struyk, A. F.; Cannon, S. C. Slow inactivation does not block the aqueous accessibility to the outer pore of voltage-gated Na channels. *J. Gen. Physiol.* **2002**, *120*, 509-516.
- (92) Ong, B. H.; Tomaselli, G. F.; Balser, J. R. A structural rearrangement in the sodium channel pore linked to slow inactivation and use dependence. *J. Gen. Physiol.* **2000**, *116*, 653-662.
- (93) Catterall, W. A.; Perez-Reyes, E.; Snutch, T. P.; Striessnig, J. International Union of Pharmacology. XLVIII. Nomenclature and structure-function relationships of voltage-gated calcium channels. *Pharmacol. Rev.* **2005**, *57*, 411-425.
- (94) Dolphin, A. C. A short history of voltage-gated calcium channels. *Br. J. Pharmacol.* **2006**, *147 Suppl 1*, S56-62.
- (95) Llinás, R.; Sugimori, M.; Lin, J. W.; Cherksey, B. Blocking and isolation of a calcium channel from neurons in mammals and cephalopods utilizing a toxin fraction (FTX) from funnel-web spider poison. *Proc. Natl. Acad. Sci. U.S.A.* **1989**, *86*, 1689-1693.
- (96) Nakagawa, T.; Yuan, J. Cross-talk between two cysteine protease families: activation of caspase-12 by calpain in apoptosis. *J. Cell Biol.* **2000**, *150*, 887-894.
- (97) Berridge, M. J. Inositol trisphosphate and calcium signalling. *Nature* **1993**, 315-325.
- (98) Dubovsky, S.; Murphy, J.; Christiano, J.; Lee, C. The calcium second messenger system in bipolar disorders: data supporting new research directions. *J. Neuropsych. Clin. Neurosci.* **1992**, *4*, 3-14.
- (99) Mattson, M. P.; Chan, S. L. Calcium orchestrates apoptosis. *Nat. Cell Biol.* **2003**, *5*, 1041-1043.
- (100) Ghosh, A.; Greenberg, M. Calcium signaling in neurons: molecular mechanisms and cellular consequences. *Science* **1995**, *268*, 239-247.
- (101) Kohn, E. C.; Alessandro, R.; Spoonster, J.; Wersto, R. P.; Liotta, L. A. Angiogenesis: role of calcium-mediated signal transduction. *Proc. Natl. Acad. Sci. U.S.A.* **1995**, *92*, 1307-1311.
- (102) Sieghart, W.; Fuchs, K.; Tretter, V.; Ebert, V.; Jechlinger, M.; Höger, H.; Adamiker, D. Structure and subunit composition of GABAA receptors. *Neurochem. Int.* **1999**, *34*, 379-385.
- (103) Olsen, R. W.; Sieghart, W. International Union of Pharmacology. LXX. Subtypes of gamma-aminobutyric acid(A) receptors: classification on the

- basis of subunit composition, pharmacology, and function. Update. *Pharmacol. Rev.* **2008**, *60*, 243-260.
- (104) Chebib, M.; Johnston, G. A. GABA-Activated ligand gated ion channels: medicinal chemistry and molecular biology. *J. Med. Chem.* **2000**, *43*, 1427-1447.
 - (105) Olsen, R. W.; Sieghart, W. GABA A receptors: subtypes provide diversity of function and pharmacology. *Neuropharmacology* **2009**, *56*, 141-148.
 - (106) Collingridge, G. L.; Olsen, R. W.; Peters, J.; Spedding, M. A nomenclature for ligand-gated ion channels. *Neuropharmacology* **2009**, *56*, 2-5.
 - (107) Johnston, G. A. GABAA receptor pharmacology. *Pharmacol. Ther.* **1996**, *69*, 173-198.
 - (108) Kananura, C.; Haug, K.; Sander, T.; Runge, U.; Gu, W.; Hallmann, K.; Rebstock, J.; Heils, A.; Steinlein, O. K. A splice-site mutation in GABRG2 associated with childhood absence epilepsy and febrile convulsions. *Arch. Neurol.* **2002**, *59*, 1137-1141.
 - (109) Cossette, P.; Liu, L.; Brisebois, K.; Dong, H.; Lortie, A.; Vanasse, M.; Saint-Hilaire, J.; Carmant, L.; Verner, A.; Lu, W.; Tian Wang, Y.; Rouleau, G. A. Mutation of GABRA1 in an autosomal dominant form of juvenile myoclonic epilepsy. *Nat. Genet.* **2002**, *31*, 184-189.
 - (110) Rimvall, K.; Martin, D. L. The level of GAD67 protein is highly sensitive to small increases in intraneuronal gamma-aminobutyric acid levels. *J. Neurochem.* **1994**, *62*, 1375-1381.
 - (111) Borden, L. A.; Smith, K. E.; Hartig, P. R.; Branchek, T. A.; Weinshank, R. L. Molecular heterogeneity of the gamma-aminobutyric acid (GABA) transport system. Cloning of two novel high affinity GABA transporters from rat brain. *J. Biol. Chem.* **1992**, *267*, 21098-21104.
 - (112) De Biasi, S.; Vitellaro-Zuccarello, L.; Brecha, N. C. Immunoreactivity for the GABA transporter-1 and GABA transporter-3 is restricted to astrocytes in the rat thalamus. A light and electron-microscopic immunolocalization. *Neuroscience* **1998**, *83*, 815-828.
 - (113) Borden, L. A. GABA transporter heterogeneity: pharmacology and cellular localization. *Neurochem. Int.* **1996**, *29*, 335-356.
 - (114) Lasiter, P. S.; Kachele, D. L. Organization of GABA and GABA-transaminase containing neurons in the gustatory zone of the nucleus of the solitary tract. *Brain Res. Bull.* **1988**, *21*, 623-636.

- (115) Ben-Ari, Y. Excitatory actions of GABA during development: the nature of the nurture. *Nat. Rev. Neurosci.* **2002**, 3, 728-739.
- (116) Rivera, C.; Voipio, J.; Kaila, K. Two developmental switches in GABAergic signalling: the K⁺-Cl⁻ cotransporter KCC2 and carbonic anhydrase CAVII. *J. Physiol.* **2005**, 562, 27-36.
- (117) Rivera, C.; Voipio, J.; Payne, J. A.; Ruusuvuori, E.; Lahtinen, H.; Lamsa, K.; Pirvola, U.; Saarma, M.; Kaila, K. The K⁺/Cl⁻ co-transporter KCC2 renders GABA hyperpolarizing during neuronal maturation. *Nature* **1999**, 397, 251-255.
- (118) Palma, E.; Amici, M.; Sobrero, F.; Spinelli, G.; Di Angelantonio, S.; Ragozzino, D.; Mascia, A.; Scoppetta, C.; Esposito, V.; Miledi, R.; Eusebi, F. Anomalous levels of Cl⁻ transporters in the hippocampal subiculum from temporal lobe epilepsy patients make GABA excitatory. *Proc. Natl. Acad. Sci. U.S.A.* **2006**, 103, 8465-8468.
- (119) Huberfeld, G.; Wittner, L.; Clemenceau, S.; Baulac, M.; Kaila, K.; Miles, R.; Rivera, C. Perturbed chloride homeostasis and GABAergic signaling in human temporal lobe epilepsy. *J. Neurosci.* **2007**, 27, 9866-9873.
- (120) Mayer, M. L. Glutamate receptor ion channels. *Curr. Opin. Neurobiol.* **2005**, 15, 282-288.
- (121) Moldrich, R. X.; Chapman, A. G.; De Sarro, G.; Meldrum, B. S. Glutamate metabotropic receptors as targets for drug therapy in epilepsy. *Eur. J. Pharmacol.* **2003**, 476, 3-16.
- (122) Dingledine, R.; Borges, K.; Bowie, D.; Traynelis, S. F. The glutamate receptor ion channels. *Pharmacol. Rev.* **1999**, 51, 7-61.
- (123) Yuzaki, M. The delta2 glutamate receptor: 10 years later. *Neurosci. Res.* **2003**, 46, 11-22.
- (124) Paoletti, P.; Neyton, J. NMDA receptor subunits: function and pharmacology. *Curr. Opin. Pharmacol.* **2007**, 7, 39-47.
- (125) Song, I.; Huganir, R. L. Regulation of AMPA receptors during synaptic plasticity. *Trends Neurosci.* **2002**, 25, 578-588.
- (126) Kuner, T.; Wollmuth, L. P.; Karlin, A.; Seeburg, P. H.; Sakmann, B. Structure of the NMDA receptor channel M2 segment inferred from the accessibility of substituted cysteines. *Neuron* **1996**, 17, 343-352.
- (127) Verdoorn, T. A.; Burnashev, N.; Monyer, H.; Seeburg, P. H.; Sakmann, B. Structural determinants of ion flow through recombinant glutamate receptor channels. *Science* **1991**, 252, 1715-1718.

- (128) Olney, J. W. Brain lesions, obesity, and other disturbances in mice treated with monosodium glutamate. *Science* **1969**, *164*, 719-721.
- (129) Lankiewicz, S.; Marc Luetjens, C.; Truc Bui, N.; Krohn, A. J.; Poppe, M.; Cole, G. M.; Saido, T. C.; Prehn, J. H. Activation of calpain I converts excitotoxic neuron death into a caspase-independent cell death. *J. Biol. Chem.* **2000**, *275*, 17064-17071.
- (130) Manev, H.; Favaron, M.; Guidotti, A.; Costa, E. Delayed increase of Ca²⁺ influx elicited by glutamate: role in neuronal death. *Mol. Pharmacol.* **1989**, *36*, 106-112.
- (131) Fujikawa, D. G. Prolonged seizures and cellular injury: understanding the connection. *Epilepsy Behav.* **2005**, *7 Suppl 3*, S3-11.
- (132) Merritt, H. H.; Putnam, T. J. Landmark article Sept 17, 1938: Sodium diphenyl hydantoinate in the treatment of convulsive disorders. By H. Houston Merritt and Tracy J. Putnam. *JAMA* **1984**, *251*, 1062-1067.
- (133) Poupaert, J. H.; Vandervorst, D.; Guiot, P.; Moustafa, M. M.; Dumont, P. Structure-activity relationships of phenytoin-like anticonvulsant drugs. *J. Med. Chem.* **1984**, *27*, 76-78.
- (134) Brodie, M. J.; Dichter, M. A. Antiepileptic Drugs. *N. Engl. J. Med.* **1996**, *334*, 168-175.
- (135) Errington, A. C.; Stöhr, T.; Heers, C.; Lees, G. The investigational anticonvulsant lacosamide selectively enhances slow inactivation of voltage-gated sodium channels. *Mol. Pharmacol.* **2008**, *73*, 157-69.
- (136) Rho, J. M.; Sankar, R. The pharmacologic basis of antiepileptic drug action. *Epilepsia* **1999**, *40*, 1471-1483.
- (137) McLean, M. J.; Macdonald, R. L. Multiple actions of phenytoin on mouse spinal cord neurons in cell culture. *J. Pharmacol. Exp. Ther.* **1983**, *227*, 779-789.
- (138) Taylor, C. P.; Meldrum, B. S. Na⁺ channels as targets for neuroprotective drugs. *Trends Pharmacol. Sci.* **1995**, *16*, 309-316.
- (139) Okuma, T.; Kishimoto, A. A history of investigation on the mood stabilizing effect of carbamazepine in Japan. *Psychiatry Clin. Neurosci.* **1998**, *52*, 3-12.
- (140) McLean, M. J.; Macdonald, R. L. Carbamazepine and 10,11-epoxycarbamazepine produce use- and voltage-dependent limitation of rapidly firing action potentials of mouse central neurons in cell culture. *J. Pharmacol. Exp. Ther.* **1986**, *238*, 727-738.

- (141) Willow, M.; Gonoj, T.; Catterall, W. A. Voltage clamp analysis of the inhibitory actions of diphenylhydantoin and carbamazepine on voltage-sensitive sodium channels in neuroblastoma cells. *Mol. Pharmacol.* **1985**, *27*, 549-558.
- (142) Kuo, C. C.; Chen, R. S.; Lu, L.; Chen, R. C. Carbamazepine inhibition of neuronal Na⁺ currents: quantitative distinction from phenytoin and possible therapeutic implications. *Mol. Pharmacol.* **1997**, *51*, 1077-1083.
- (143) Hough, C. J.; Irwin, R. P.; Gao, X. M.; Rogawski, M. A.; Chuang, D. M. Carbamazepine inhibition of N-methyl-D-aspartate-evoked calcium influx in rat cerebellar granule cells. *J. Pharmacol. Exp. Ther.* **1996**, *276*, 143-149.
- (144) Coulter, D. A.; Huguenard, J. R.; Prince, D. A. Characterization of ethosuximide reduction of low-threshold calcium current in thalamic neurons. *Ann. Neurol.* **1989**, *25*, 582-593.
- (145) Coulter, D. A.; Huguenard, J. R.; Prince, D. A. Differential effects of petit mal anticonvulsants and convulsants on thalamic neurones: calcium current reduction. *Br. J. Pharmacol.* **1990**, *100*, 800-806.
- (146) Snead III, O. C. Basic mechanisms of generalized absence seizures. *Ann. Neurol.* **1995**, *37*, 146-157.
- (147) Gomora, J. C.; Daud, A. N.; Weiergräber, M.; Perez-Reyes, E. Block of cloned human T-type calcium channels by succinimide antiepileptic drugs. *Mol. Pharmacol.* **2001**, *60*, 1121-1132.
- (148) Meunier, H.; Carraz, G.; Meunier, Y. Propriétés pharmacodynamiques de l'acide n-dipropylacétique. 1er mémoire: propriétés antiépileptiques. *Thérapie* **1963**, 435-438.
- (149) Carraz, G.; Fau, R.; Chateau, R.; Bonnin, J. Communication à propos des premiers essais cliniques sur l'activité anti-épileptique de l'acide n-dipropylacétiques (sel de Na). *Ann. Med. Psychol.* **1964**, 577-585.
- (150) Löscher, W. Basic pharmacology of valproate: a review after 35 years of clinical use for the treatment of epilepsy. *CNS Drugs* **2002**, *16*, 669-694.
- (151) McLean, M. J.; Macdonald, R. L. Sodium valproate, but not ethosuximide, produces use- and voltage-dependent limitation of high frequency repetitive firing of action potentials of mouse central neurons in cell culture. *J. Pharmacol. Exp. Ther.* **1986**, *237*, 1001-1011.
- (152) Albus, H.; Williamson, R. Electrophysiologic analysis of the actions of valproate on pyramidal neurons in the rat hippocampal slice. *Epilepsia* **1998**, *39*, 124-139.

- (153) Willow, M.; Kuenzel, E. A.; Catterall, W. A. Inhibition of voltage-sensitive sodium channels in neuroblastoma cells and synaptosomes by the anticonvulsant drugs diphenylhydantoin and carbamazepine. *Mol. Pharmacol.* **1984**, *25*, 228-234.
- (154) Francis, J.; Burnham, W. M. [3H]Phenytoin identifies a novel anticonvulsant-binding domain on voltage-dependent sodium channels. *Mol. Pharmacol.* **1992**, *42*, 1097-1103.
- (155) Coulter, D. A.; Huguenard, J. R.; Prince, D. A. Characterization of ethosuximide reduction of low-threshold calcium current in thalamic neurons. *Ann. Neurol.* **1989**, *25*, 582-593.
- (156) Kelly, K. M.; Gross, R. A.; Macdonald, R. L. Valproic acid selectively reduces the low-threshold (T) calcium current in rat nodose neurons. *Neurosci. Lett.* **1990**, *116*, 233-238.
- (157) Davis, R.; Peters, D. H.; McTavish, D. Valproic acid. A reappraisal of its pharmacological properties and clinical efficacy in epilepsy. *Drugs* **1994**, *47*, 332-372.
- (158) Nau, H.; Löscher, W. Valproic acid: brain and plasma levels of the drug and its metabolites, anticonvulsant effects and gamma-aminobutyric acid (GABA) metabolism in the mouse. *J. Pharmacol. Exp. Ther.* **1982**, *220*, 654-659.
- (159) Wikinski, S. I.; Acosta, G. B.; Rubio, M. C. Valproic acid differs in its in vitro effect on glutamic acid decarboxylase activity in neonatal and adult rat brain. *Gen. Pharmacol.* **1996**, *27*, 635-638.
- (160) Olkkola, K. T.; Ahonen, J. In *Modern Anesthetics*; Schüttler, J.; Schwilden, H., Eds.; Springer: Berlin, Heidelberg, 2008; Vol. 182, pp. 335-360.
- (161) Bateson, A. N. Basic pharmacologic mechanisms involved in benzodiazepine tolerance and withdrawal. *Curr. Pharm. Des.* **2002**, *8*, 5-21.
- (162) Walker, M. Status epilepticus: an evidence based guide. *Brit. Med. J.* **2005**, *331*, 673-677.
- (163) Mandrioli, R.; Mercolini, L.; Raggi, M. A. Benzodiazepine metabolism: an analytical perspective. *Curr. Drug Metab.* **2008**, *9*, 827-844.
- (164) Sieghart, W. GABAA receptors: ligand-gated Cl⁻ ion channels modulated by multiple drug-binding sites. *Trends Pharmacol. Sci.* **1992**, *13*, 446-450.
- (165) Macdonald, R. L.; Olsen, R. W. GABAA receptor channels. *Annu. Rev. Neurosci.* **1994**, *17*, 569-602.

- (166) Twyman, R. E.; Rogers, C. J.; Macdonald, R. L. Differential regulation of gamma-aminobutyric acid receptor channels by diazepam and phenobarbital. *Ann. Neurol.* **1989**, *25*, 213-220.
- (167) Polc, P. Electrophysiology of benzodiazepine receptor ligands: multiple mechanisms and sites of action. *Prog. Neurobiol.* **1988**, *31*, 349-423.
- (168) Taft, W. C.; DeLorenzo, R. J. Micromolar-affinity benzodiazepine receptors regulate voltage-sensitive calcium channels in nerve terminal preparations. *Proc. Natl. Acad. Sci. U.S.A* **1984**, *81*, 3118-3122.
- (169) McLean, M. J.; Macdonald, R. L. Benzodiazepines, but not beta carbolines, limit high frequency repetitive firing of action potentials of spinal cord neurons in cell culture. *J. Pharmacol. Exp. Ther.* **1988**, *244*, 789-795.
- (170) Heller, A. J.; Chesterman, P.; Elwes, R. D.; Crawford, P.; Chadwick, D.; Johnson, A. L.; Reynolds, E. H. Phenobarbitone, phenytoin, carbamazepine, or sodium valproate for newly diagnosed adult epilepsy: a randomised comparative monotherapy trial. *J. Neurol. Neurosurg. Psychiatr.* **1995**, *58*, 44-50.
- (171) Frankenburg, F. R.; Tohen, M.; Cohen, B. M.; Lipinski, J. F. Long-term response to carbamazepine: a retrospective study. *J. Clin. Psychopharm.* **1988**, *8*, 130-132.
- (172) Iivanainen, M.; Savolainen, H. Side effects of phenobarbital and phenytoin during long-term treatment of epilepsy. *Acta Neurol. Scand., Suppl.* **1983**, *97*, 49-67.
- (173) Baxter, M. G.; Miller, A. A.; Webster, R. A. Some studies on the convulsant action of folic acid. *Br. J. Pharmacol.* **1973**, *48*, 350P-351P.
- (174) Obbens, E. A.; Hommes, O. R. The epileptogenic effects of folate derivatives in the rat. *J. Neurol. Sci.* **1973**, *20*, 223-229.
- (175) Rogawski, M. A.; Porter, R. J. Antiepileptic drugs: pharmacological mechanisms and clinical efficacy with consideration of promising developmental stage compounds. *Pharmacol. Rev.* **1990**, *42*, 223-286.
- (176) Miller, A. A.; Wheatley, P.; Sawyer, D. A.; Baxter, M. G.; Roth, B. Pharmacological studies on lamotrigine, a novel potential antiepileptic drug: I. Anticonvulsant profile in mice and rats. *Epilepsia* **1986**, *27*, 483-489.
- (177) Cheung, H.; Kamp, D.; Harris, E. An in vitro investigation of the action of lamotrigine on neuronal voltage-activated sodium channels. *Epilepsy Res.* **1992**, *13*, 107-112.

- (178) Xie, X.; Lancaster, B.; Peakman, T.; Garthwaite, J. Interaction of the antiepileptic drug lamotrigine with recombinant rat brain type IIA Na⁺ channels and with native Na⁺ channels in rat hippocampal neurones. *Pflug. Arch. Eur. J. Phy.* **1995**, *430*, 437-446.
- (179) Curia, G.; Biagini, G.; Perucca, E.; Avoli, M. Lacosamide: a new approach to target voltage-gated sodium currents in epileptic disorders. *CNS Drugs* **2009**, *23*, 555-568.
- (180) Lang, D. G.; Wang, C. M.; Cooper, B. R. Lamotrigine, phenytoin and carbamazepine interactions on the sodium current present in N4TG1 mouse neuroblastoma cells. *J. Pharmacol. Exp. Ther.* **1993**, *266*, 829-835.
- (181) Lees, G.; Leach, M. J. Studies on the mechanism of action of the novel anticonvulsant lamotrigine (Lamictal) using primary neurological cultures from rat cortex. *Brain Res.* **1993**, *612*, 190-199.
- (182) Kuo, C. C. A common anticonvulsant binding site for phenytoin, carbamazepine, and lamotrigine in neuronal Na⁺ channels. *Mol. Pharmacol.* **1998**, *54*, 712-721.
- (183) Shank, R. P.; Maryanoff, B. E. Molecular pharmacodynamics, clinical therapeutics, and pharmacokinetics of topiramate. *CNS Neurosci. Ther.* **2008**, *14*, 120-142.
- (184) Maryanoff, B. E.; Nortey, S. O.; Gardocki, J. F.; Shank, R. P.; Dodgson, S. P. Anticonvulsant O-alkyl sulfamates. 2,3:4,5-Bis-O-(1-methylethylidene)-beta-D-fructopyranose sulfamate and related compounds. *J. Med. Chem.* **1987**, *30*, 880-887.
- (185) Maryanoff, B. E. Sugar sulfamates for seizure control: discovery and development of topiramate, a structurally unique antiepileptic drug. *Curr. Top. Med. Chem.* **2009**, *9*, 1049-1062.
- (186) Shank, R. P.; Gardocki, J. F.; Vaught, J. L.; Davis, C. B.; Schupsky, J. J.; Raffa, R. B.; Dodgson, S. J.; Nortey, S. O.; Maryanoff, B. E. Topiramate: preclinical evaluation of structurally novel anticonvulsant. *Epilepsia* **1994**, *35*, 450-460.
- (187) DeLorenzo, R. J.; Sombati, S.; Coulter, D. A. Effects of topiramate on sustained repetitive firing and spontaneous recurrent seizure discharges in cultured hippocampal neurons. *Epilepsia* **2000**, *41 Suppl 1*, S40-44.
- (188) Gibbs, J. W.; Sombati, S.; DeLorenzo, R. J.; Coulter, D. A. Cellular actions of topiramate: blockade of kainate-evoked inward currents in cultured hippocampal neurons. *Epilepsia* **2000**, *41 Suppl 1*, S10-16.

- (189) White, H. S.; Brown, S. D.; Woodhead, J. H.; Skeen, G. A.; Wolf, H. H. Topiramate enhances GABA-mediated chloride flux and GABA-evoked chloride currents in murine brain neurons and increases seizure threshold. *Epilepsy Res.* **1997**, *28*, 167-179.
- (190) Swinyard, E. A.; Sofia, R. D.; Kupferberg, H. J. Comparative anticonvulsant activity and neurotoxicity of felbamate and four prototype antiepileptic drugs in mice and rats. *Epilepsia* **1986**, *27*, 27-34.
- (191) Pisani, A.; Stefani, A.; Siniscalchi, A.; Mercuri, N. B.; Bernardi, G.; Calabresi, P. Electrophysiological actions of felbamate on rat striatal neurones. *Br. J. Pharmacol.* **1995**, *116*, 2053-2061.
- (192) White, H. S.; Wolf, H. H.; Swinyard, E. A.; Skeen, G. A.; Sofia, R. D. A neuropharmacological evaluation of felbamate as a novel anticonvulsant. *Epilepsia* **1992**, *33*, 564-572.
- (193) Taglialatela, M.; Ongini, E.; Brown, A. M.; Di Renzo, G.; Annunziato, L. Felbamate inhibits cloned voltage-dependent Na⁺ channels from human and rat brain. *Eur. J. Pharmacol.* **1996**, *316*, 373-377.
- (194) Kume, A.; Greenfield, L. J.; Macdonald, R. L.; Albin, R. L. Felbamate inhibits [3H]t-butylbicycloorthobenzoate (TBOB) binding and enhances Cl⁻ current at the gamma-aminobutyric AcidA (GABAA) receptor. *J. Pharmacol. Exp. Ther.* **1996**, *277*, 1784-1792.
- (195) Rho, J. M.; Donevan, S. D.; Rogawski, M. A. Mechanism of action of the anticonvulsant felbamate: opposing effects on N-methyl-D-aspartate and gamma-aminobutyric acidA receptors. *Ann. Neurol.* **1994**, *35*, 229-234.
- (196) McCabe, R. T.; Wasterlain, C. G.; Kucharczyk, N.; Sofia, R. D.; Vogel, J. R. Evidence for anticonvulsant and neuroprotectant action of felbamate mediated by strychnine-insensitive glycine receptors. *J. Pharmacol. Exp. Ther.* **1993**, *264*, 1248-1252.
- (197) Suzdak, P. D.; Jansen, J. A. A review of the preclinical pharmacology of tiagabine: a potent and selective anticonvulsant GABA uptake inhibitor. *Epilepsia* **1995**, *36*, 612-626.
- (198) Takahashi, K.; Miyoshi, S.; Kaneko, A.; Copenhagen, D. R. Actions of nipecotic acid and SKF89976A on GABA transporter in cone-driven horizontal cells dissociated from the catfish retina. *Jpn. J. Physiol.* **1995**, *45*, 457-473.
- (199) Braestrup, C.; Nielsen, E. B.; Sonnewald, U.; Knutsen, L. J.; Andersen, K. E.; Jansen, J. A.; Frederiksen, K.; Andersen, P. H.; Mortensen, A.; Suzdak, P. D. (R)-N-[4,4-bis(3-methyl-2-thienyl)but-3-en-1-yl]nipecotic acid binds with high affinity to the brain gamma-aminobutyric acid uptake carrier. *J. Neurochem.* **1990**, *54*, 639-647.

- (200) Borden, L. A.; Murali Dhar, T. G.; Smith, K. E.; Weinshank, R. L.; Branchek, T. A.; Gluchowski, C. Tiagabine, SK&F 89976-A, CI-966, and NNC-711 are selective for the cloned GABA transporter GAT-1. *Eur. J. Pharmacol.* **1994**, *269*, 219-224.
- (201) Brodie, M. J. Tiagabine pharmacology in profile. *Epilepsia* **1995**, *36 Suppl 6*, S7-S9.
- (202) Klitgaard, H. Levetiracetam: the preclinical profile of a new class of antiepileptic drugs? *Epilepsia* **2001**, *42*, 13-18.
- (203) Bialer, M.; Johannessen, S. I.; Kupferberg, H. J.; Levy, R. H.; Loiseau, P.; Perucca, E. Progress report on new antiepileptic drugs: a summary of the Sixth Eilat Conference (EILAT VI). *Epilepsy Res.* **2002**, *51*, 31-71.
- (204) Yan, H.; Ji-qun, C.; Ishihara, K.; Nagayama, T.; Serikawa, T.; Sasa, M. Separation of antiepileptogenic and antiseizure effects of levetiracetam in the spontaneously epileptic rat (SER). *Epilepsia* **2005**, *46*, 1170-1177.
- (205) Löscher, W.; Hönack, D.; Rundfeldt, C. Antiepileptogenic effects of the novel anticonvulsant levetiracetam (ucb L059) in the kindling model of temporal lobe epilepsy. *J. Pharmacol. Exp. Ther.* **1998**, *284*, 474-479.
- (206) Brandt, C.; Glien, M.; Gastens, A. M.; Fedrowitz, M.; Bethmann, K.; Volk, H. A.; Potschka, H.; Löscher, W. Prophylactic treatment with levetiracetam after status epilepticus: lack of effect on epileptogenesis, neuronal damage, and behavioral alterations in rats. *Neuropharmacology* **2007**, *53*, 207-221.
- (207) Rogawski, M. A.; Bazil, C. W. New molecular targets for antiepileptic drugs: alpha(2)delta, SV2A, and K(v)7/KCNQ/M potassium channels. *Curr. Neurol. Neurosci. Rep.* **2008**, *8*, 345-352.
- (208) Lambeng, N.; Gillard, M.; Vertongen, P.; Fuks, B.; Chatelain, P. Characterization of [3H]ucb 30889 binding to synaptic vesicle protein 2A in the rat spinal cord. *Eur. J. Pharmacol.* **2005**, *520*, 70-76.
- (209) Lynch, B. A.; Lambeng, N.; Nocka, K.; Kensel-Hammes, P.; Bajjalieh, S. M.; Matagne, A.; Fuks, B. The synaptic vesicle protein SV2A is the binding site for the antiepileptic drug levetiracetam. *Proc. Natl. Acad. Sci. U.S.A.* **2004**, *101*, 9861-9866.
- (210) Kaminski, R. M.; Matagne, A.; Leclercq, K.; Gillard, M.; Michel, P.; Kenda, B.; Talaga, P.; Klitgaard, H. SV2A protein is a broad-spectrum anticonvulsant target: functional correlation between protein binding and seizure protection in models of both partial and generalized epilepsy. *Neuropharmacology* **2008**, *54*, 715-720.

- (211) Kasteleijn-Nolst Trenité, D. G. A.; Genton, P.; Parain, D.; Masnou, P.; Steinhoff, B. J.; Jacobs, T.; Pigeolet, E.; Stockis, A.; Hirsch, E. Evaluation of brivaracetam, a novel SV2A ligand, in the photosensitivity model. *Neurology* **2007**, 69, 1027-1034.
- (212) Bialer, M.; Johannessen, S. I.; Levy, R. H.; Perucca, E.; Tomson, T.; White, H. S. Progress report on new antiepileptic drugs: A summary of the Ninth Eilat Conference (EILAT IX). *Epilepsy Res.* **2009**, 83, 1-43.
- (213) Rostock, A.; Tober, C.; Rundfeldt, C.; Bartsch, R.; Engel, J.; Polymeropoulos, E. E.; Kutscher, B.; Löscher, W.; Hönack, D.; White, H. S.; Wolf, H. H. D-23129: a new anticonvulsant with a broad spectrum activity in animal models of epileptic seizures. *Epilepsy Res.* **1996**, 23, 211-223.
- (214) Tober, C.; Rostock, A.; Rundfeldt, C.; Bartsch, R. D-23129: a potent anticonvulsant in the amygdala kindling model of complex partial seizures. *Eur. J. Pharmacol.* **1996**, 303, 163-169.
- (215) Main, M. J.; Cryan, J. E.; Dupere, J. R.; Cox, B.; Clare, J. J.; Burbidge, S. A. Modulation of KCNQ2/3 potassium channels by the novel anticonvulsant retigabine. *Mol. Pharmacol.* **2000**, 58, 253-262.
- (216) Rundfeldt, C. The new anticonvulsant retigabine (D-23129) acts as an opener of K⁺ channels in neuronal cells. *Eur. J. Pharmacol.* **1997**, 336, 243-249.
- (217) Gutman, G. A.; Chandy, K. G.; Grissmer, S.; Lazdunski, M.; McKinnon, D.; Pardo, L. A.; Robertson, G. A.; Rudy, B.; Sanguinetti, M. C.; Stühmer, W.; Wang, X. International Union of Pharmacology. LIII. Nomenclature and molecular relationships of voltage-gated potassium channels. *Pharmacol. Rev.* **2005**, 57, 473-508.
- (218) Tatulian, L.; Brown, D. A. Effect of the KCNQ potassium channel opener retigabine on single KCNQ2/3 channels expressed in CHO cells. *J. Physiol. (Lond.)* **2003**, 549, 57-63.
- (219) Rundfeldt, C.; Netzer, R. The novel anticonvulsant retigabine activates M-currents in Chinese hamster ovary-cells transfected with human KCNQ2/3 subunits. *Neurosci. Lett.* **2000**, 282, 73-76.
- (220) Garriga-Canut, M.; Schoenike, B.; Qazi, R.; Bergendahl, K.; Daley, T. J.; Pfender, R. M.; Morrison, J. F.; Ockuly, J.; Stafstrom, C.; Sutula, T.; Roopra, A. 2-Deoxy-D-glucose reduces epilepsy progression by NRSF-CtBP-dependent metabolic regulation of chromatin structure. *Nat. Neurosci.* **2006**, 9, 1382-1387.
- (221) Kinsman, S. L.; Vining, E. P.; Quaskey, S. A.; Mellits, D.; Freeman, J. M. Efficacy of the ketogenic diet for intractable seizure disorders: review of 58 cases. *Epilepsia* **1992**, 33, 1132-1136.

- (222) Hartman, A. L.; Gasior, M.; Vining, E. P. G.; Rogawski, M. A. The neuropharmacology of the ketogenic diet. *Pediatr. Neurol.* **2007**, *36*, 281-292.
- (223) Huttenlocher, P. R. Ketonemia and seizures: metabolic and anticonvulsant effects of two ketogenic diets in childhood epilepsy. *Pediatr. Res.* **1976**, *10*, 536-540.
- (224) Stafstrom, C. E.; Ockuly, J. C.; Murphree, L.; Valley, M. T.; Roopra, A.; Sutula, T. P. Anticonvulsant and antiepileptic actions of 2-deoxy-D-glucose in epilepsy models. *Ann. Neurol.* **2009**, *65*, 435-447.
- (225) de Silva, M.; MacArdle, B.; McGowan, M.; Hughes, E.; Stewart, J.; Neville, B. G.; Johnson, A. L.; Reynolds, E. H. Randomised comparative monotherapy trial of phenobarbitone, phenytoin, carbamazepine, or sodium valproate for newly diagnosed childhood epilepsy. *Lancet* **1996**, *347*, 709-713.
- (226) Nakane, Y.; Okuma, T.; Takahashi, R.; Sato, Y.; Wada, T.; Sato, T.; Fukushima, Y.; Kumashiro, H.; Ono, T.; Takahashi, T.; Aoki, Y.; Kazamatsuri, H.; Inami, M.; Komai, S.; Seino, M.; Miyakoshi, M.; Tanimura, T.; Hazama, H.; Kawahara, R.; Otsuki, S.; Hosokawa, K.; Inanaga, K.; Nakazawa, Y.; Yamamoto, K. Multi-institutional study on the teratogenicity and fetal toxicity of antiepileptic drugs: a report of a collaborative study group in Japan. *Epilepsia* **1980**, *21*, 663-680.
- (227) Perucca, E. Clinically relevant drug interactions with antiepileptic drugs. *Br.J. Clin. Pharmacol.* **2006**, *61*, 246-255.
- (228) Almeida, L.; Soares-da-Silva, P. Eslicarbazepine acetate (BIA 2-093). *Neurotherapeutics* **2007**, *4*, 88-96.
- (229) Dam, M.; Ekberg, R.; Løyning, Y.; Waltimo, O.; Jakobsen, K. A double-blind study comparing oxcarbazepine and carbamazepine in patients with newly diagnosed, previously untreated epilepsy. *Epilepsy Res.* **1989**, *3*, 70-76.
- (230) Mello, L. E.; Cavaleiro, E. A.; Tan, A. M.; Kupfer, W. R.; Pretorius, J. K.; Babb, T. L.; Finch, D. M. Circuit mechanisms of seizures in the pilocarpine model of chronic epilepsy: cell loss and mossy fiber sprouting. *Epilepsia* **1993**, *34*, 985-995.
- (231) Ikegaya, Y. Abnormal targeting of developing hippocampal mossy fibers after epileptiform activities via L-type Ca²⁺ channel activation in vitro. *J. Neurosci.* **1999**, *19*, 802-812.
- (232) Parent, J. M.; Elliott, R. C.; Pleasure, S. J.; Barbaro, N. M.; Lowenstein, D. H. Aberrant seizure-induced neurogenesis in experimental temporal lobe epilepsy. *Ann. Neurol.* **2006**, *59*, 81-91.

- (233) Beyreuther, B. K.; Freitag, J.; Heers, C.; Krebsfänger, N.; Scharfenecker, U.; Stöhr, T. Lacosamide: a review of preclinical properties. *CNS Drug Rev.* **2007**, *13*, 21-42.
- (234) Choi, D.; Stables, J. P.; Kohn, H. Synthesis and anticonvulsant activities of N-benzyl-2-acetamidopropionamide derivatives. *J. Med. Chem.* **1996**, *39*, 1907-1916.
- (235) Andurkar, S. V.; Stables, J. P.; Kohn, H. Synthesis and anticonvulsant activities of (R)-(O)-methylserine derivatives. *Tet. Asymmetry* **1998**, *9*, 3841-3854.
- (236) Andurkar, S. V.; Stables, J. P.; Kohn, H. The anticonvulsant activities of N-benzyl 3-methoxypropionamides. *Bioorg. Med. Chem.* **1999**, *7*, 2381-2389.
- (237) Conley, J. D.; Kohn, H. Functionalized DL-amino acid derivatives. Potent new agents for the treatment of epilepsy. *J. Med. Chem.* **1987**, *30*, 567-574.
- (238) Kohn, H.; Conley, J. D.; Leander, J. D. Marked stereospecificity in a new class of anticonvulsants. *Brain Res.* **1988**, *457*, 371-375.
- (239) Kohn, H.; Sawhney, K. N.; LeGall, P.; Conley, J. D.; Robertson, D. W.; Leander, J. D. Preparation and anticonvulsant activity of a series of functionalized alpha-aromatic and alpha-heteroaromatic amino acids. *J. Med. Chem.* **1990**, *33*, 919-926.
- (240) Kohn, H.; Sawhney, K. N.; Bardel, P.; Robertson, D. W.; Leander, J. D. Synthesis and anticonvulsant activities of alpha-heterocyclic alpha-acetamido-N-benzylacetamide derivatives. *J. Med. Chem.* **1993**, *36*, 3350-3360.
- (241) Bardel, P.; Bolanos, A.; Kohn, H. Synthesis and anticonvulsant activities of alpha-acetamido-N-benzylacetamide derivatives containing an electron-deficient alpha-heteroaromatic substituent. *J. Med. Chem.* **1994**, *37*, 4567-4571.
- (242) Wolf, H. H.; White, H. S.; Franklin, M. R.; Skeen, G. A.; Woodhead, J. H. The early evaluation of anticonvulsant drugs (Contract No. N01-NS-4-2311): The profile of anticonvulsant activity and minimal toxicity of ADD 234037 in mice and rats. Epilepsy Branch, Neurological Disorders Program, National Institute of Neurological Disorders and Stroke **1996**.
- (243) Errington, A. C.; Coyne, L.; Stöhr, T.; Selve, N.; Lees, G. Seeking a mechanism of action for the novel anticonvulsant lacosamide. *Neuropharmacology* **2006**, *50*, 1016-1029.

- (244) Beydoun, A.; D'Souza, J.; Hebert, D.; Doty, P. Lacosamide: pharmacology, mechanisms of action and pooled efficacy and safety data in partial-onset seizures. *Expert Rev. Neurother.* **2009**, 9, 33-42.
- (245) Hovinga, C. A. Novel anticonvulsant medications in development. *Expert Opin. Investig. Drugs* **2002**, 11, 1387-1406.
- (246) Hovinga, C. A. SPM-927 (Schwarz Pharma). *IDrugs* **2003**, 6, 479-485.
- (247) Beyreuther, B. K.; Stöhr, T.; Freitag, J. Method for Identifying CRMP Modulators. WO 2008/000512.
- (248) Wang, S.; Sim, T. B.; Kim, Y.; Chang, Y. Tools for target identification and validation. *Curr. Opin. Chem. Biol.* **2004**, 8, 371-377.
- (249) Burdine, L.; Kodadek, T. Target identification in chemical genetics: the (often) missing link. *Chem. Biol.* **2004**, 11, 593-597.
- (250) Allen, J. J.; Lazerwith, S. E.; Shokat, K. M. Bio-orthogonal affinity purification of direct kinase substrates. *J. Am. Chem. Soc.* **2005**, 127, 5288-5289.
- (251) Schreiber, S. L. Chemical genetics resulting from a passion for synthetic organic chemistry. *Bioorg. Med. Chem.* **1998**, 6, 1127-1152.
- (252) Schreiber, S. L. Small molecules: the missing link in the central dogma. *Nat. Chem. Biol.* **2005**, 1, 64-66.
- (253) Alaimo, P. J.; Shogren-Knaak, M. A.; Shokat, K. M. Chemical genetic approaches for the elucidation of signaling pathways. *Curr. Opin. Chem. Biol.* **2001**, 5, 360-367.
- (254) Bishop, A.; Buzko, O.; Heyeck-Dumas, S.; Jung, I.; Kraybill, B.; Liu, Y.; Shah, K.; Ulrich, S.; Witucki, L.; Yang, F.; Zhang, C.; Shokat, K. M. Unnatural ligands for engineered proteins: new tools for chemical genetics. *Annu. Rev. Biophys. Biomol. Struct.* **2000**, 29, 577-606.
- (255) Meisner, N.; Hintersteiner, M.; Uhl, V.; Weidemann, T.; Schmied, M.; Gstach, H.; Auer, M. The chemical hunt for the identification of drugable targets. *Curr. Opin. Chem. Biol.* **2004**, 8, 424-431.
- (256) Doyle, D. F.; Braasch, D. A.; Jackson, L. K.; Weiss, H. E.; Boehm, M. F.; Mangelsdorf, D. J.; Corey, D. R. Engineering orthogonal ligand-receptor pairs from "near drugs". *J. Am. Chem. Soc.* **2001**, 123, 11367-11371.
- (257) De Felipe, K. S.; Carter, B. T.; Althoff, E. A.; Cornish, V. W. Correlation between ligand-receptor affinity and the transcription readout in a yeast three-hybrid system. *Biochemistry* **2004**, 43, 10353-10363.

- (258) Hussey, S. L.; Muddana, S. S.; Peterson, B. R. Synthesis of a beta-estradiol-biotin chimera that potently heterodimerizes estrogen receptor and streptavidin proteins in a yeast three-hybrid system. *J. Am. Chem. Soc.* **2003**, *125*, 3692-3693.
- (259) SenGupta, D. J.; Zhang, B.; Kraemer, B.; Pochart, P.; Fields, S.; Wickens, M. A three-hybrid system to detect RNA-protein interactions in vivo. *Proc. Natl. Acad. Sci. U.S.A.* **1996**, *93*, 8496-8501.
- (260) Schena, M.; Shalon, D.; Davis, R. W.; Brown, P. O. Quantitative monitoring of gene expression patterns with a complementary DNA microarray. *Science* **1995**, *270*, 467-470.
- (261) Fire, A.; Xu, S.; Montgomery, M. K.; Kostas, S. A.; Driver, S. E.; Mello, C. C. Potent and specific genetic interference by double-stranded RNA in *Caenorhabditis elegans*. *Nature* **1998**, *391*, 806-811.
- (262) Campbell, D. A.; Szardenings, A. K. Functional profiling of the proteome with affinity labels. *Curr. Opin. Chem. Biol.* **2003**, *7*, 296-303.
- (263) Dormán, G.; Prestwich, G. D. Using photolabile ligands in drug discovery and development. *Trends Biotechnol.* **2000**, *18*, 64-77.
- (264) Burke, T. R.; Jacobson, A. E.; Rice, K. C.; Silverton, J. V.; Simonds, W. F.; Streaty, R. A.; Klee, W. A. Probes for narcotic receptor mediated phenomena. 12. cis-(+)-3-Methylfentanyl isothiocyanate, a potent site-directed acylating agent for delta opioid receptors. Synthesis, absolute configuration, and receptor enantioselectivity. *J. Med. Chem.* **1986**, *29*, 1087-1093.
- (265) Morse, K. L.; Fournier, D. J.; Li, X.; Grzybowska, J.; Makriyannis, A. A novel electrophilic high affinity irreversible probe for the cannabinoid receptor. *Life Sci.* **1995**, *56*, 1957-1962.
- (266) Atlas, D.; Plotek, Y.; Miskin, I. An affinity label for alpha 2-adrenergic receptors in rat brain. *Eur. J. Biochem.* **1982**, *126*, 537-541.
- (267) Brunner, J.; Senn, H.; Richards, F. M. 3-Trifluoromethyl-3-phenyldiazirine. A new carbene generating group for photolabeling reagents. *J. Biol. Chem.* **1980**, *255*, 3313-3318.
- (268) MacKinnon, A.; Garrison, J.; Hegde, R.; Taunton, J. Photo-leucine incorporation reveals the target of a cyclodepsipeptide inhibitor of cotranslational translocation. *J. Am. Chem. Soc.* **2007**, *129*, 14560-14561.
- (269) Goetz, D. H.; Choe, Y.; Hansell, E.; Chen, Y. T.; McDowell, M.; Jonsson, C. B.; Roush, W. R.; McKerrow, J.; Craik, C. S. Substrate specificity profiling and identification of a new class of inhibitor for the major protease of the SARS coronavirus. *Biochemistry* **2007**, *46*, 8744-8752.

- (270) Votta, B. J.; Levy, M. A.; Badger, A.; Bradbeer, J.; Dodds, R. A.; James, I. E.; Thompson, S.; Bossard, M. J.; Carr, T.; Connor, J. R.; Tomaszek, T. A.; Szewczuk, L.; Drake, F. H.; Veber, D. F.; Gowen, M. Peptide aldehyde inhibitors of cathepsin K inhibit bone resorption both in vitro and in vivo. *J. Bone Miner. Res.* **1997**, *12*, 1396-1406.
- (271) Zhang, H.; Zhang, H.; Kemnitzer, W.; Tseng, B.; Cinatl, J.; Michaelis, M.; Doerr, H.; Cai, S. Design and synthesis of dipeptidyl glutaminy fluoromethyl ketones as potent severe acute respiratory syndrome coronavirus (SARS-CoV) inhibitors. *J. Med. Chem.* **2006**, *49*, 1198-1201.
- (272) Costanzo, M. J.; Almond, H. R.; Hecker, L. R.; Schott, M. R.; Yabut, S. C.; Zhang, H.; Andrade-Gordon, P.; Corcoran, T. W.; Giardino, E. C.; Kauffman, J. A.; Lewis, J. M.; de Garavilla, L.; Haertlein, B. J.; Maryanoff, B. E. In-depth study of tripeptide-based alpha-ketoheterocycles as inhibitors of thrombin. Effective utilization of the S1' subsite and its implications to structure-based drug design. *J. Med. Chem.* **2005**, *48*, 1984-2008.
- (273) Sadaghiani, A. M.; Verhelst, S. H. L.; Gocheva, V.; Hill, K.; Majerova, E.; Stinson, S.; Joyce, J. A.; Bogoy, M. Design, synthesis, and evaluation of in vivo potency and selectivity of epoxysuccinyl-based inhibitors of papain-family cysteine proteases. *Chem. Biol.* **2007**, *14*, 499-511.
- (274) Demarcus, M.; Ganadu, M. L.; Mura, G. M.; Porcheddu, A.; Quaranta, L.; Reginato, G.; Taddei, M. Small ring constrained peptidomimetics. Synthesis of epoxy peptidomimetics, inhibitors of cysteine proteases. *J. Org. Chem.* **2001**, *66*, 697-706.
- (275) Cravatt, B. F.; Wright, A. T.; Kozarich, J. W. Activity-based protein profiling: from enzyme chemistry to proteomic chemistry. *Annu. Rev. Biochem.* **2008**, *77*, 383-414.
- (276) Speers, A. E.; Cravatt, B. F. Profiling enzyme activities in vivo using click chemistry methods. *Chem. Biol.* **2004**, *11*, 535-546.
- (277) Sieber, S. A.; Niessen, S.; Hoover, H. S.; Cravatt, B. F. Proteomic profiling of metalloprotease activities with cocktails of active-site probes. *Nat. Chem. Biol.* **2006**, *2*, 274-281.
- (278) Whiting, M.; Muldoon, J.; Lin, Y.; Silverman, S. M.; Lindstrom, W.; Olson, A. J.; Kolb, H. C.; Finn, M. G.; Sharpless, K. B.; Elder, J. H.; Fokin, V. V. Inhibitors of HIV-1 protease by using in situ click chemistry. *Angew. Chem. Int. Ed.* **2006**, *45*, 1435-1439.
- (279) Wang, Q.; Chan, T.; Hilgraf, R.; Fokin, V.; Sharpless, K.; Finn, M. Bioconjugation by copper(I)-catalyzed azide-alkyne [3 + 2] cycloaddition. *J. Am. Chem. Soc.* **2003**, *125*, 3192-3193.

- (280) Agard, N. J.; Baskin, J. M.; Prescher, J. A.; Lo, A.; Bertozzi, C. R. A comparative study of bioorthogonal reactions with azides. *ACS. Chem. Biol.* **2006**, *1*, 644-648.
- (281) Rabuka, D.; Hubbard, S. C.; Laughlin, S. T.; Argade, S. P.; Bertozzi, C. R. A chemical reporter strategy to probe glycoprotein fucosylation. *J. Am. Chem. Soc.* **2006**, *128*, 12078-12079.
- (282) Prescher, J. A.; Bertozzi, C. R. Chemistry in living systems. *Nat. Chem. Biol.* **2005**, *1*, 13-21.
- (283) Jessani, N.; Cravatt, B. F. The development and application of methods for activity-based protein profiling. *Curr. Opin. Chem. Biol.* **2004**, *8*, 54-59.
- (284) Rostovtsev, V. V.; Green, L. G.; Fokin, V. V.; Sharpless, K. B. A stepwise Huisgen cycloaddition process: copper(I)-catalyzed regioselective "ligation" of azides and terminal alkynes. *Angew. Chem. Int. Ed.* **2002**, *41*, 2596-2599.
- (285) Brouwer, A. J.; Bunschoten, A.; Liskamp, R. M. Synthesis and evaluation of chloromethyl sulfoxides as a new class of selective irreversible cysteine protease inhibitors. *Bioorg. Med. Chem.* **2007**, *15*, 6985-6993.
- (286) Linton, S. D.; Aja, T.; Armstrong, R. A.; Bai, X.; Chen, L.; Chen, N.; Ching, B.; Contreras, P.; Diaz, J.; Fisher, C. D.; Fritz, L. C.; Gladstone, P.; Groessl, T.; Gu, X.; Herrmann, J.; Hirakawa, B. P.; Hoglen, N. C.; Jahangiri, K. G.; Kalish, V. J.; Karanewsky, D. S.; Kodandapani, L.; Krebs, J.; McQuiston, J.; Meduna, S. P.; Nalley, K.; Robinson, E. D.; Sayers, R. O.; Sebring, K.; Spada, A. P.; Ternansky, R. J.; Tomaselli, K. J.; Ullman, B. R.; Valentino, K. L.; Weeks, S.; Winn, D.; Wu, J. C.; Yeo, P.; Zhang, C. First-in-class pan caspase inhibitor developed for the treatment of liver disease. *J. Med. Chem.* **2005**, *48*, 6779-6782.
- (287) Ghosh, S. S.; Said-Nejad, O.; Roestamadj, J.; Mobashery, S. The first mechanism-based inactivators for angiotensin-converting enzyme. *J. Med. Chem.* **1992**, *35*, 4175-4179.
- (288) Evans, M. J.; Saghatelian, A.; Sorensen, E. J.; Cravatt, B. F. Target discovery in small-molecule cell-based screens by in situ proteome reactivity profiling. *Nat. Biotechnol.* **2005**, *23*, 1303-1307.
- (289) Powers, J. C.; Asgian, J. L.; Ekici, O. D.; James, K. E. Irreversible inhibitors of serine, cysteine, and threonine proteases. *Chem. Rev.* **2002**, *102*, 4639-4750.
- (290) Chen, G.; Heim, A.; Riether, D.; Yee, D.; Milgrom, Y.; Gawinowicz, M.; Sames, D. Reactivity of functional groups on the protein surface: development of epoxide probes for protein labeling. *J. Am. Chem. Soc.* **2003**, *125*, 8130-8133.

- (291) Miller, L.; Phillips, M.; Reisler, E. Polymerization of actin modified with fluorescein isothiocyanate. *Eur. J. Biochem.* **1988**, *174*, 23-29.
- (292) Bayer, E. A.; Zalis, M. G.; Wilchek, M. 3-(N-maleimido-propionyl) biocytin: A versatile thiol-specific biotinylating reagent. *Anal. Biochem.* **1985**, *149*, 529-536.
- (293) Kim, M. J.; Kim, H. J.; Kim, J. M.; Kim, B.; Han, S. H.; Cha, G. S. Homogeneous assays for riboflavin mediated by the interaction between enzyme-biotin and avidin-riboflavin conjugates. *Anal. Biochem.* **1995**, *231*, 400-406.
- (294) Konecsni, T.; Kilár, F. Monitoring of the conjugation reaction between human serum transferrin and fluorescein isothiocyanate by capillary electrophoresis. *J. Chromatogr. A* **2004**, *1051*, 135-139.
- (295) Weber, P.; Ohlendorf, D.; Wendoloski, J.; Salemme, F. Structural origins of high-affinity biotin binding to streptavidin. *Science* **1989**, *243*, 85-88.
- (296) Cho, H.; Park, H.; Zhang, X.; Riba, I.; Gaskell, S.; Widger, W.; Kohn, H. Design, syntheses, and evaluations of bicyclomycin-based Rho inactivators. *J. Org. Chem.* **1997**, *62*, 5432-5440.
- (297) Aliau, S.; Mattras, H.; Richard, E.; Borgna, J. Cysteine 530 of the human estrogen receptor α is the main covalent attachment site of 11 β -(aziridinylalkoxyphenyl)estradiols. *Biochemistry* **1999**, *38*, 14752-14762.
- (298) Casalotti, S. O.; Kozikowski, A. P.; Fauq, A.; Tückmantel, W.; Krueger, K. E. Design of an irreversible affinity ligand for the phencyclidine recognition site on N-methyl-D-aspartate-type glutamate receptors. *J. Pharmacol. Exp. Ther.* **1992**, *260*, 21-28.
- (299) Jentoft, N.; Dearborn, D. G. In *Enzyme Structure Part I*; Academic Press, 1983; Vol. 91, pp. 570-579.
- (300) Dirksen, A.; Dawson, P. E. Rapid oxime and hydrazone ligations with aromatic aldehydes for biomolecular labeling. *Bioconjugate Chem.* **2008**, *19*, 2543-2548.
- (301) Riba, I.; Gaskell, S. J.; Cho, H.; Widger, W. R.; Kohn, H. Evidence for the location of bicyclomycin binding to the Escherichia coli transcription termination factor Rho. *J. Biol. Chem.* **1998**, *273*, 34033-34041.
- (302) Vincent, F.; Widger, W. R.; Openshaw, M.; Gaskell, S. J.; Kohn, H. 5a-formylbicyclomycin: studies on the bicyclomycin-Rho interaction. *Biochemistry* **2000**, *39*, 9067-9076.

- (303) Blum, S. A.; Walsh, P. J.; Bergman, R. G. Epoxide-opening and group-transfer reactions mediated by monomeric zirconium imido complexes. *J. Am. Chem. Soc.* **2003**, *125*, 14276-14277.
- (304) Das, B.; Reddy, V. S.; Tehseen, F.; Krishnaiah, M. Catalyst-free highly regio- and stereoselective ring opening of epoxides and aziridines with sodium azide using poly(ethylene glycol) as an efficient reaction medium. *Synthesis* **2007**, *5*, 666-668.
- (305) Fan, R.; Hou, X. Efficient ring-opening reaction of epoxides and aziridines promoted by tributylphosphine in water. *J. Org. Chem.* **2003**, *68*, 726-730.
- (306) Jacobsen, E. N. Asymmetric catalysis of epoxide ring-opening reactions. *Accounts Chem. Res.* **2000**, *33*, 421-431.
- (307) Parker, R. E.; Isaacs, N. S. Mechanisms of epoxide reactions. *Chem. Rev.* **1959**, *59*, 737-799.
- (308) Barrett, A. J.; Kembhavi, A. A.; Brown, M. A.; Kirschke, H.; Knight, C. G.; Tamai, M.; Hanada, K. L-trans-Epoxysuccinyl-leucylamido(4-guanidino)butane (E-64) and its analogues as inhibitors of cysteine proteinases including cathepsins B, H and L. *Biochem. J.* **1982**, *201*, 189-198.
- (309) Greenbaum, D.; Medzihradszky, K. F.; Burlingame, A.; Bogoy, M. Epoxide electrophiles as activity-dependent cysteine protease profiling and discovery tools. *Chem. Biol.* **2000**, *7*, 569-581.
- (310) Gratzer, P. F.; Santerre, J. P.; Lee, J. M. Modulation of collagen proteolysis by chemical modification of amino acid side-chains in acellularized arteries. *Biomaterials* **2004**, *25*, 2081-2094.
- (311) Legler, G.; Harder, A. Amino acid sequence at the active site of beta-glucosidase A from bitter almonds. *BBA-Enzymology* **1978**, *524*, 102-108.
- (312) Schray, K. J.; O'Connell, E. L.; Rose, I. A. Inactivation of muscle triose phosphate isomerase by D- and L-glycidol phosphate. *J. Biol. Chem.* **1973**, *248*, 2214-2218.
- (313) A. Fleming, S. Chemical reagents in photoaffinity labeling. *Tetrahedron* **1995**, *51*, 12479-12520.
- (314) Smith, R. A. G.; Knowles, J. R. Aryldiazirines. Potential reagents for photolabeling of biological receptor sites. *J. Am. Chem. Soc.* **1973**, *95*, 5072-5073.
- (315) Pitts, J. N.; Johnson, H. W.; Kuwana, T. Structural effects in the photochemical processes of ketones in solution. *J. Phys. Chem.* **1962**, *66*, 2456-2461.

- (316) Brems, D. N.; Rilling, H. C. Photoaffinity labeling of the catalytic site of prenyltransferase. *Biochemistry* **1979**, *18*, 860-864.
- (317) Evans, R. K.; Haley, B. E. Synthesis and biological properties of 5-azido-2'-deoxyuridine 5'-triphosphate, a photoactive nucleotide suitable for making light-sensitive DNA. *Biochemistry* **1987**, *26*, 269-276.
- (318) Hatanaka, Y.; Ishiguro, M.; Hashimoto, M.; Gastinel, L. N.; Nakagomi, K. A model of photoprobe docking with beta1,4-galactosyltransferase identifies a possible carboxylate involved in glycosylation steps. *Bioorg. Med. Chem. Lett.* **2001**, *11*, 411-413.
- (319) Ballell, L.; Scherpenzeel, M. V.; Buchalova, K.; Liskamp, R. M. J.; Pieters, R. J. A new chemical probe for the detection of the cancer-linked galectin-3. *Org. Biomol. Chem.* **2006**, *4*, 4387-4394.
- (320) John, B.; Kumar, E. R.; Lala, A. K. Depth-dependent analysis of membranes using benzophenone-based phospholipids. *Biophys. Chem.* **2000**, *87*, 37-42.
- (321) Watt, D. S.; Kawada, K.; Leyva, E.; Platz, M. S. Exploratory photochemistry of iodinated aromatic azides. *Tet. Lett.* **1989**, *30*, 899-902.
- (322) Sani, B. P.; Wille, J. J.; Dawson, M. I.; Hobbs, P. D.; Bupp, J.; Rhee, S.; Chao, W. R.; Dorsky, A.; Morimoto, H. Biologically active aromatic retinoids bearing azido photoaffinity-labeling groups and their binding to cellular retinoic acid-binding protein. *Chem. Biol. Interact.* **1990**, *75*, 293-304.
- (323) MacLeod, K. J.; Vasilyeva, E.; Merdek, K.; Vogel, P. D.; Forgac, M. Photoaffinity labeling of wild-type and mutant forms of the yeast V-ATPase A subunit by 2-azido-[(32)P]ADP. *J. Biol. Chem.* **1999**, *274*, 32869-32874.
- (324) Liu, Q.; Tor, Y. Simple conversion of aromatic amines into azides. *Org. Lett.* **2003**, *5*, 2571-2572.
- (325) Barral, K.; Moorhouse, A.; Moses, J. Efficient conversion of aromatic amines into azides: A one-pot synthesis of triazole linkages. *Org. Lett.* **2007**, *9*, 1809-1811.
- (326) Mandel, S.; Liu, J.; Hadad, C. M.; Platz, M. S. Study of singlet and triplet 2,6-difluorophenylnitrene by time-resolved infrared spectroscopy. *J. Phys. Chem.* **2005**, *109*, 2816-2821.
- (327) Shields, C. J.; Chrisope, D. R.; Schuster, G. B.; Dixon, A. J.; Poliakoff, M.; Turner, J. J. Photochemistry of aryl azides: detection and characterization of a dehydroazepine by time-resolved infrared spectroscopy and flash photolysis at room temperature. *J. Am. Chem. Soc.* **1987**, *109*, 4723-4726.

- (328) Staros, J. V.; Bayley, H.; Standring, D. N.; Knowles, J. R. Reduction of aryl azides by thiols: Implications for the use of photoaffinity reagents. *Biochem. Biophys. Res. Co.* **1978**, *80*, 568-572.
- (329) Nakashima, H.; Hashimoto, M.; Sadakane, Y.; Tomohiro, T.; Hatanaka, Y. Simple and versatile method for tagging phenyldiazirine photophores. *J. Am. Chem. Soc.* **2006**, *128*, 15092-15093.
- (330) Kuroda, T.; Suenaga, K.; Sakakura, A.; Handa, T.; Okamoto, K.; Kigoshi, H. Study of the interaction between actin and antitumor substance aplyronine A with a novel fluorescent photoaffinity probe. *Bioconjugate Chem.* *17*, 524-529.
- (331) Hashimoto, M.; Komano, T.; Nabeta, K.; Hatanaka, Y. Stereoselective synthesis of (E)- and (Z)-beta-bromostyrene containing trifluoromethyldiazirine for photoaffinity labeling. *Chem. Pharm. Bull.* **2005**, *53*, 140-142.
- (332) Burgermeister, W.; Nassal, M.; Wieland, T.; Helmreich, E. J. A carbene-generating photoaffinity probe for beta-adrenergic receptors. *Biochim. Biophys. Acta* **1983**, *729*, 219-228.
- (333) Bongo, N. B.; Tomohiro, T.; Hatanaka, Y. Synthesis and evaluation of novel photoreactive [alpha]-amino acid analog carrying acidic and cleavable functions. *Bioorg. Med. Chem. Lett.* **2009**, *19*, 80-82.
- (334) Otto, J. C.; Smith, W. L. Photolabeling of prostaglandin endoperoxide H synthase-1 with 3-trifluoro-3-(m-[125I]iodophenyl)diazirine as a probe of membrane association and the cyclooxygenase active site. *J. Biol. Chem.* **1996**, *271*, 9906-9910.
- (335) Hashimoto, M.; Hatanaka, Y. Practical conditions for photoaffinity labeling with 3-trifluoromethyl-3-phenyldiazirine photophore. *Anal. Biochem.* **2006**, *348*, 154-156.
- (336) Tanaka, Y.; Kohler, J. J. Photoactivatable crosslinking sugars for capturing glycoprotein interactions. *J. Am. Chem. Soc.* **2008**, *130*, 3278-3279.
- (337) Stoll, G.; Voges, R.; Gerok, W.; Kurz, G. Synthesis of a metabolically stable modified long-chain fatty acid salt and its photolabile derivative. *J. Lipid Res.* **1991**, *32*, 843-857.
- (338) Husain, S. S.; Forman, S. A.; Kloczewiak, M. A.; Addona, G. H.; Olsen, R. W.; Pratt, M. B.; Cohen, J. B.; Miller, K. W. Synthesis and properties of 3-(2-hydroxyethyl)-3-n-pentyldiazirine, a photoactivable general anesthetic. *J. Med. Chem.* **1999**, *42*, 3300-3307.

- (339) Shigdel, U. K.; Zhang, J.; He, C. Diazirine-based DNA photo-cross-linking probes for the study of protein-DNA interactions. *Angew. Chem. Int. Ed.* **2008**, *47*, 90-93.
- (340) Stromgaard, K.; Saito, D. R.; Shindou, H.; Ishii, S.; Shimizu, T.; Nakanishi, K. Ginkgolide derivatives for photolabeling studies: preparation and pharmacological evaluation. *J. Med. Chem.* **2002**, *45*, 4038-4046.
- (341) Nassal, M. 4-(1-Azi-2,2,2-trifluoroethyl)benzoic acid, a highly photolabile carbene generating label readily fixable to biochemical agents. *Liebigs Ann. Chem.* **1983**, *1983*, 1510-1523.
- (342) Kawamura, A.; Hindi, S.; Mihai, D. M.; James, L.; Aminova, O. Binding is not enough: flexibility is needed for photocrosslinking of Lck kinase by benzophenone photoligands. *Bioorg. Med. Chem.* **2008**, *16*, 8824-8829.
- (343) Shen, R.; Inoue, T.; Forgac, M.; Porco, J. A. Synthesis of photoactivatable acyclic analogues of the lobatamides. *J. Org. Chem.* **2005**, *70*, 3686-92.
- (344) van Scherpenzeel, M.; van der Pot, M.; Arnusch, C. J.; Liskamp, R. M.; Pieters, R. J. Detection of galectin-3 by novel peptidic photoprobes. *Bioorg. Med. Chem. Lett.* **2007**, *17*, 376-378.
- (345) Salisbury, C. M.; Cravatt, B. F. Optimization of activity-based probes for proteomic profiling of histone deacetylase complexes. *J. Am. Chem. Soc.* **2008**, *130*, 2184-2194.
- (346) Dorman, G.; Prestwich, G. D. Benzophenone photophores in biochemistry. *Biochemistry* **1994**, *33*, 5661-5673.
- (347) Weber, P. J.; Beck-Sickinger, A. G. Comparison of the photochemical behavior of four different photoactivatable probes. *J. Pept. Res.* **1997**, *49*, 375-383.
- (348) Huisgen, R. Centenary lecture - 1,3-Dipolar cycloadditions. *Proc. Chem. Soc.* **1961**, 357-369.
- (349) Baskin, J. M.; Prescher, J. A.; Laughlin, S. T.; Agard, N. J.; Chang, P. V.; Miller, I. A.; Lo, A.; Codelli, J. A.; Bertozzi, C. R. Copper-free click chemistry for dynamic in vivo imaging. *Proc. Natl. Acad. Sci. U.S.A.* **2007**, *104*, 16793-16797.
- (350) Ladmiral, V.; Mantovani, G.; Clarkson, G. J.; Cauet, S.; Irwin, J. L.; Haddleton, D. M. Synthesis of neoglycopolymers by a combination of "Click Chemistry" and living radical polymerization. *J. Am. Chem. Soc.* **2006**, *128*, 4823-4830.

- (351) Moses, J. E.; Moorhouse, A. D. The growing applications of click chemistry. *Chem. Soc. Rev.* **2007**, 36, 1249-1262.
- (352) Ning, X.; Guo, J.; Wolfert, M. A.; Boons, G. Visualizing metabolically labeled glycoconjugates of living cells by copper-free and fast Huisgen cycloadditions. *Angew. Chem. Int. Ed.* **2008**, 47, 2253-2255.
- (353) Tornøe, C. W.; Christensen, C.; Meldal, M. Peptidotriazoles on solid phase: [1,2,3]-triazoles by regiospecific copper(I)-catalyzed 1,3-dipolar cycloadditions of terminal alkynes to azides. *J. Org. Chem.* **2002**, 67, 3057-3064.
- (354) Link, A. J.; Tirrell, D. A. Cell surface labeling of *Escherichia coli* via copper(I)-catalyzed [3+2] cycloaddition. *J. Am. Chem. Soc.* **2003**, 125, 11164-11165.
- (355) Tsy-pin, G. I.; Timofeeva, T. N.; Mel'nikov, V. V.; Gidasov, B. V. Structure and reactivity of aliphatic azido compounds. IV. Isomeric 1,2,3-triazoles in the cycloaddition of aliphatic azides with phenylacetylene and propargyl alcohol. *Zh. Org. Khim.* **1975**, 11, 1395-1400.
- (356) Zhang, L.; Chen, X.; Xue, P.; Sun, H. H. Y.; Williams, I. D.; Sharpless, K. B.; Fokin, V. V.; Jia, G. Ruthenium-catalyzed cycloaddition of alkynes and organic azides. *J. Am. Chem. Soc.* **2005**, 127, 15998-15999.
- (357) Kolb, H. C.; Finn, M. G.; Sharpless, K. B. Click Chemistry: diverse chemical function from a few good reactions. *Angew. Chem. Int. Ed.* **2001**, 40, 2004-2021.
- (358) Drahl, C.; Cravatt, B. F.; Sorensen, E. J. Protein-reactive natural products. *Angew. Chem. Int. Ed.* **2005**, 44, 5788-5809.
- (359) Speers, A. E.; Adam, G. C.; Cravatt, B. F. Activity-based protein profiling in vivo using a copper(I)-catalyzed azide-alkyne [3 + 2] cycloaddition. *J. Am. Chem. Soc.* **2003**, 125, 4686-4687.
- (360) Weerapana, E.; Speers, A. E.; Cravatt, B. F. Tandem orthogonal proteolysis-activity-based protein profiling (TOP-ABPP) — a general method for mapping sites of probe modification in proteomes. *Nat. Protoc.* **2007**, 2, 1414-1425.
- (361) Cortizo, M.; Lorenzo de Mele, M. Cytotoxicity of copper ions released from metal. *Biol. Trace Elem. Res.* **2004**, 102, 129-141.
- (362) Agard, N. J.; Prescher, J. A.; Bertozzi, C. R. A strain-promoted [3 + 2] azide-alkyne cycloaddition for covalent modification of biomolecules in living systems. *J. Am. Chem. Soc.* **2004**, 126, 15046-15047.
- (363) Laughlin, S. T.; Agard, N. J.; Baskin, J. M.; Carrico, I. S.; Chang, P. V.; Ganguli, A. S.; Hangauer, M. J.; Lo, A.; Prescher, J. A.; Bertozzi, C. R.

- Metabolic labeling of glycans with azido sugars for visualization and glycoproteomics. *Method. Enzymol.* **2006**, 415, 230-250.
- (364) Saxon, E.; Bertozzi, C. R. Cell surface engineering by a modified Staudinger reaction. *Science* **2000**, 287, 2007-2010.
- (365) van Berkel, S. S.; Dirks, A. T.; Debets, M. F.; van Delft, F. L.; Cornelissen, J. J. L. M.; Nolte, R. J. M.; Rutjes, F. P. J. T. Metal-free triazole formation as a tool for bioconjugation. *ChemBiochem* **2007**, 8, 1504-1508.
- (366) Codelli, J. A.; Baskin, J. M.; Agard, N. J.; Bertozzi, C. R. Second-generation difluorinated cyclooctynes for copper-free Click Chemistry. *J. Am. Chem. Soc.* **2008**, 130, 11486-11493.
- (367) Kohn, H.; Sawhney, K. N.; LeGall, P.; Robertson, D. W.; Leander, J. D. Preparation and anticonvulsant activity of a series of functionalized alpha-heteroatom-substituted amino acids. *J. Med. Chem.* **1991**, 34, 2444-2452.
- (368) Cortes, S.; Liao, Z. K.; Watson, D.; Kohn, H. Effect of structural modification of the hydantoin ring on anticonvulsant activity. *J. Med. Chem.* **1985**, 28, 601-606.
- (369) Kohn, H.; Conley, J. D. New antiepileptic agents. *Chem. Br.* **1988**, 231-234.
- (370) Kohn, H.; Sawhney, K. N.; Robertson, D. W.; Leander, J. D. Anticonvulsant properties of N-substituted alpha,alpha-diamino acid derivatives. *J. Pharm. Sci.* **1994**, 83, 689-691.
- (371) Levy, M. A.; Mattson, R. H.; Meldrum, B. *Antiepileptic Drugs*; 4th ed.; Raven Press: New York, 1995.
- (372) Higgins, G. A.; Isaac, M.; Slassi, A.; Xin, T. Fluorinated compounds. WO/2007/076306 **2007**.
- (373) Axelsson, B. S.; O'Toole, K. J.; Spencer, P. A.; Young, D. W. Versatile synthesis of stereospecifically labelled D-amino acids via labelled aziridines-preparation of (2R,3S)-[3-2H1]- and (2R,3R)-[2,3-2H2]-serine; (2S,2[prime or minute]S,3S,3[prime or minute]S)-[3,3[prime or minute]-2H2]- and (2S,2[prime or minute]S,3R,3[prime or minute]R)-[2,2[prime or minute],3,3[prime or minute]-2H4]-cystine; and (2S,3S)-[3-2H1-] and (2S,3R)-[2,3-2H2]-[small beta]-chloroalanine. *J. Chem. Soc., Perkin Trans. 1* **1994**, 807-815.
- (374) Baldwin, J. E.; Adlington, R. M.; Robinson, N. G. Nucleophilic ring opening of aziridine-2-carboxylates with Wittig reagents; an enantioefficient synthesis of unsaturated amino acids. *J. Chem. Soc., Chem. Commun.* **1987**, 153-155.

- (375) Bělohradský, M.; Ridvan, L.; Závada, J. Synthesis of homochiral acyclic mono- and bis (alpha-amino acids) with oligo(oxyethylene) chains. *Collect. Czech. Chem. Commun.* **2003**, 68, 1319-1328.
- (376) Galonic, D. P.; van der Donk, W. A.; Gin, D. Y. Site-selective conjugation of thiols with aziridine-2-carboxylic acid-containing peptides. *J. Am. Chem. Soc.* **2004**, 126, 12712-12713.
- (377) Kato, S.; Harada, H.; Morie, T. Efficient synthesis of (6R)-6-amino-1-methyl-4-(3-methylbenzyl)hexahydro-1H-1,4-diazepine from methyl (2R)- and (2S)-1-benzyloxycarbonylaziridine-2-carboxylates. *J. Chem. Soc., Perkin Trans. 1* **1997**, 3219-3226.
- (378) Lee, T.; Bryan Jones, J. Probing enzyme stereospecificity. Evaluation of beta-alkoxy-alpha-amino acids with two stereocenters as inhibitors of serine proteases. *Tetrahedron* **1995**, 51, 7331-7346.
- (379) Nakajima, K.; Oda, H.; Okawa, K. Studies on 2-aziridinecarboxylic acid. IX. convenient synthesis of optically active S-alkylcysteine, threo-S-alkyl-β-methylcysteine, and lanthionine derivatives via the ring-opening reaction of aziridine by several thiols. *Bull. Chem. Soc. Jpn.* **1983**, 56, 520-522.
- (380) Nakajima, K.; Neya, M.; Yamada, S.; Okawa, K. Studies on 2-aziridinecarboxylic acid. VI. Synthesis of beta-alkoxy-alpha-amino acids via ring-opening reaction of aziridine. *Bull. Chem. Soc. Jpn.* **1982**, 55, 3049-3050.
- (381) Morieux, P.; Stables, J. P.; Kohn, H. Synthesis and anticonvulsant activities of N-benzyl (2R)-2-acetamido-3-oxysubstituted propionamide derivatives. *Bioorg. Med. Chem.* **2008**, 16, 8968-8975.
- (382) Ressurreicao, A. S. M.; Bordessa, A.; Civera, M.; Belvisi, L.; Gennari, C.; Piarulli, U. Synthesis and conformational studies of peptidomimetics containing a new bifunctional diketopiperazine scaffold acting as a β-hairpin inducer. *J. Org. Chem.* **2008**, 73, 652-660.
- (383) Larsson, U.; Carlson, R. Synthesis of amino acids with modified principal properties 2: amino acids with polar side chains. *Acta Chem. Scand.* **1994**, 48, 511-516.
- (384) Park, K. D.; Morieux, P.; Salomé, C.; Cotten, S. W.; Reamtong, O.; Evers, C.; Gaskell, S. J.; Stables, J. P.; Liu, R.; Kohn, H. Lacosamide isothiocyanate-based agents: novel agents to target and identify lacosamide receptors. *J. Med. Chem.* **2009**, 52, 6897-6911.
- (385) Kelly, J. W.; Anderson, N. L.; Evans, S. A. Cyclodehydration of N- and C-substituted β-amino alcohols to the corresponding aziridines with diethoxytriphenylphosphorane. *J. Org. Chem.* **1986**, 51, 95-97.

- (386) Kelly, J. W.; Evans, S. A. Regioselective phosphoranylation and cyclodehydration of triols with diethoxytriphenylphosphorane. *J. Am. Chem. Soc.* **1986**, *108*, 7681-7685.
- (387) Mathieu-Pelta, I.; Evans, S. A. A new and improved preparation of acyclic sigma-dialkoxyposphoranes. *J. Org. Chem.* **1994**, *59*, 2234-2237.
- (388) Murray, W. T.; Kelly, J. W.; Evans, S. A. Synthesis of substituted 1,4-oxathianes. Mechanistic details of diethoxytriphenylphosphorane and triphenylphosphine/tetrachloromethane-promoted cyclodehydrations and carbon-13 NMR spectroscopy. *J. Org. Chem.* **1987**, *52*, 525-529.
- (389) Robinson, P. L.; Kelly, J. W.; Evans, S. A. The synthetic utility of dioxyposphoranes in organic synthesis. *Phosphorus Sulfur* **1986**, *26*, 15-24.
- (390) Kubota, T.; Miyashita, S.; Kitazume, T.; Ishikawa, N. Novel synthetic reactions using bis(2,2,2-trifluoroethoxy)triphenylphosphorane. *J. Org. Chem.* **1980**, *45*, 5052-5057.
- (391) Yang, Z. Bis(fluoroalkoxy)triphenylphosphorane: a new reagent for the preparation of fluorinated ketals. *J. Org. Chem.* **1995**, *60*, 5696-5698.
- (392) Cardillo, G.; Gentilucci, L.; Gianotti, M.; Tolomelli, A. Microwave-assisted ring expansion of N-acetyl 3'-unsubstituted aziridine in the presence of Lewis acids. *Tetrahedron* **2001**, *57*, 2807-2812.
- (393) Choi, D.; Kohn, H. Trimethylsilyl halides: Effective reagents for the synthesis of beta-halo amino acid derivatives. *Tet. Lett.* **1995**, *36*, 7011-7014.
- (394) Gallivan, J. P.; Dougherty, D. A. Cation-pi interactions in structural biology. *Proc. Natl. Acad. Sci. U.S.A.* **1999**, *96*, 9459-9464.
- (395) Daly, A. K.; Mantle, T. J. The kinetic mechanism of the major form of ox kidney aldehyde reductase with D-glucuronic acid. *Biochem. J.* **1982**, *205*, 381-388.
- (396) Whittle, S. R.; Turner, A. J. Effects of the anticonvulsant sodium valproate on gamma-aminobutyrate and aldehyde metabolism in ox brain. *J. Neurochem.* **1978**, *31*, 1453-1459.
- (397) Rane, A.; Peng, D. Phenytoin enhances epoxide metabolism in human fetal liver cultures. *Drug Metab. Dispos.* **1985**, *13*, 382-385.
- (398) Marshall, A. D.; Caldwell, J. Influence of modulators of epoxide metabolism on the cytotoxicity of trans-anethole in freshly isolated rat hepatocytes. *Food Chem. Toxicol.* **1992**, *30*, 467-473.

- (399) Morisseau, C.; Hammock, B. D. Epoxide hydrolases: mechanisms, inhibitor designs, and biological roles. *Annu. Rev. Pharmacol. Toxicol.* **2005**, *45*, 311-313.
- (400) Greenfield, N. J.; Pietruszko, R. Two aldehyde dehydrogenases from human liver. Isolation via affinity chromatography and characterization of the isozymes. *Biochim. Biophys. Acta* **1977**, *483*, 35-45.
- (401) Stables, J. P.; Kupferberg, H. G. *Molecular and Cellular Targets for Antiepileptic Drugs*; Avoli, M.; Avanzini, G.; Tanganelli, P., Eds.; John Libbey: London, 1977.
- (402) Krall, R. L.; Penry, J. K.; Kupferberg, H. J.; Swinyard, E. A. Antiepileptic Drug Development: I. History and a program for progress. *Epilepsia* **1978**, *19*, 393-407.
- (403) Porter, R. J.; Cereghino, J. J.; Gladding, G. D.; Hessie, B. J.; Kupferberg, H. J.; Scoville, B.; White, B. G. Antiepileptic drug development program. *Cleveland Clin. Q.* **1984**, *51*, 293-305.
- (404) Yarnell, A. T. Heavy-hydrogen drugs turn heads, again. *Chem. Eng. News* **2009**, *87*, 36-39.
- (405) Stöhr, T.; Kupferberg, H. J.; Stables, J. P.; Choi, D.; Harris, R. H.; Kohn, H.; Walton, N.; White, H. S. Lacosamide, a novel anti-convulsant drug, shows efficacy with a wide safety margin in rodent models for epilepsy. *Epilepsy Res.* **2007**, *74*, 147-154.
- (406) *Assessment Report for Vimpat*, European Medicines Agency, 2008.
- (407) Davoli, P.; Forni, A.; Moretti, I.; Prati, F. Stereochemistry of nucleophilic ring-opening reactions of optically active N-acetyl-2-methoxycarbonylaziridine. *Tet. Asymmetry* **1995**, *6*, 2011-2016.
- (408) Herre, S.; Steinle, W.; Rück-Braun, K. Synthesis of photoswitchable hemithioindigo-based omega-amino acids and application in Boc-based peptide assembly. *Synthesis* **2005**, *19*, 3297-3300.
- (409) Grieco, P. A.; Nishizawa, M.; Oguri, T.; Burke, S. D.; Marinovic, N. Sesquiterpene lactones: total synthesis of (+)-vernolepin and (+)-vernomenin. *J. Am. Chem. Soc.* **1977**, *99*, 5773-5780.
- (410) Mancuso, A. J.; Brownfain, D. S.; Swern, D. J. Structure of the dimethyl sulfoxide-oxalyl chloride reaction product. Oxidation of heteroaromatic and diverse alcohols to carbonyl compounds. *J. Org. Chem.* **1979**, *44*, 4148-4150.
- (411) Casadei, M. A.; Galli, C.; Mandolini, L. Ring-closure reactions. 22. Kinetics of cyclization of diethyl (omega-bromoalkyl)malonates in the range of 4- to 21-

- membered rings. Role of ring strain. *J. Am. Chem. Soc.* **1984**, *106*, 1051-1056.
- (412) Ewing, D. F.; Len, C.; Mackenzie, G.; Ronco, G.; Villa, P. Facile separation of chiral 1,3-dihydrobenzo[c]furan derivatives using a -xylose moiety as a protecting group. *Tet. Asymmetry* **2000**, *11*, 4995-5002.
- (413) Madhushaw, R.; Li, C.; Shen, K.; Hu, C.; Liu, R. Tungsten-promoted [3+2]- and [3+3]-cycloaddition of epoxides with alkynes. A facile enantiospecific synthesis of bicyclic lactones. *J. Am. Chem. Soc.* **2001**, *123*, 7427-7428.
- (414) Pfändler, H. R.; Weimar, V. Synthesis of racemic ethanolamine plasmalogen. *Synthesis* **1996**, *11*, 1345-1349.
- (415) Rybak, J.; Scheurer, S. B.; Neri, D.; Elia, G. Purification of biotinylated proteins on streptavidin resin: A protocol for quantitative elution. *Proteomics* **2004**, *4*, 2296-2299.
- (416) Pazy, Y.; Kulik, T.; Bayer, E. A.; Wilchek, M.; Livnah, O. Ligand Exchange between Proteins. Exchange of Biotin and Biotin Derivatives between Avidin and Streptavidin. *J. Biol. Chem.* **2002**, *277*, 30892-30900.
- (417) Iyer, S. S.; Anderson, A. S.; Reed, S.; Swanson, B.; Schmidt, J. G. Synthesis of orthogonal end functionalized oligoethylene glycols of defined lengths. *Tet. Lett.* **2004**, *45*, 4285-4288.
- (418) Sun, X.; Stabler, C.; Cazalis, C.; Chaikof, E. Carbohydrate and protein immobilization onto solid surfaces by sequential Diels-Alder and azide-alkyne cycloadditions. *Bioconjugate Chem.* **2006**, *17*, 52-57.
- (419) Polito, L.; Monti, D.; Caneva, E.; Delnevo, E.; Russo, G.; Prosperi, D. One-step bioengineering of magnetic nanoparticles via a surface diazo transfer/azide-alkyne click reaction sequence. *Chem. Commun.* **2008**, 621-623.
- (420) Lee, J.; Kang, S.; Lim, J.; Choi, H.; Jin, M.; Toth, A.; Pearce, L. V.; Tran, R.; Wang, Y.; Szabo, T.; Blumberg, P. M. N-[4-(Methylsulfonylamino)benzyl]thiourea analogues as vanilloid receptor antagonists: analysis of structure-activity relationships for the '[C-Region]'. *Bioorg. Med. Chem.* **2004**, *12*, 371-385.
- (421) Kunishima, M.; Kawachi, C.; Monta, J.; Terao, K.; Iwasaki, F.; Tani, S. 4-(4,6-dimethoxy-1,3,5-triazin-2-yl)-4-methyl-morpholinium chloride: an efficient condensing agent leading to the formation of amides and esters. *Tetrahedron* **1999**, *55*, 13159-13170.

- (422) McReynolds, K. D.; Bhat, A.; Conboy, J. C.; Saavedra, S. S.; Gervay-Hague, J. Non-natural glycosphingolipids and structurally simpler analogues bind HIV-1 recombinant Gp120. *Bioorg. Med. Chem.* **2002**, *10*, 625-637.
- (423) Punna, S.; Kaltgrad, E.; Finn, M. G. "Clickable" agarose for affinity chromatography. *Bioconjugate Chem.* **2005**, *16*, 1536-1541.
- (424) Cox, B.; Emili, A. Tissue subcellular fractionation and protein extraction for use in mass-spectrometry-based proteomics. *Nat. Protoc.* **2006**, *1*, 1872-1878.
- (425) Sporn, M. B.; Wanko, T.; Dingman, W. The isolation of cell nuclei from rat brain. *J. Cell Biol.* **1962**, *15*, 109-120.
- (426) Schindler, J.; Lewandrowski, U.; Sickmann, A.; Friauf, E.; Gerd Nothwang, H. Proteomic analysis of brain plasma membranes isolated by affinity two-phase partitioning. *Mol. Cell. Proteomics* **2006**, *5*, 390-400.
- (427) Hartshorne, R. P.; Catterall, W. A. The sodium channel from rat brain. Purification and subunit composition. *J. Biol. Chem.* **1984**, *259*, 1667-75.
- (428) Outten, C. E.; O'Halloran, T. V. Femtomolar sensitivity of metalloregulatory proteins controlling zinc homeostasis. *Science* **2001**, *292*, 2488-2492.
- (429) Messner, D. J.; Catterall, W. A. The sodium channel from rat brain. Role of the beta 1 and beta 2 subunits in saxitoxin binding. *J. Biol. Chem.* **1986**, *261*, 211-215.
- (430) Weisenberg, R. C. Microtubule formation in vitro in solutions containing low calcium concentrations. *Science* **1972**, *177*, 1104-1105.
- (431) Stupp, Y.; Yoshida, T.; Paul, W. E. Determination of antibody-hapten equilibrium constants by an ammonium sulfate precipitation technique. *J. Immunol.* **1969**, *103*, 625-627.
- (432) Gilman, A. G. A protein binding assay for adenosine 3':5'-cyclic monophosphate. *Proc. Natl. Acad. Sci. U.S.A.* **1970**, *67*, 305-312.
- (433) GE Healthcare Affinity chromatography, principles and methods. **2007**.
- (434) Maeda, S.; Nagasawa, S. Effect of sodium chloride concentration on fluid-phase assembly and stability of the C3 convertase of the classical pathway of the complement system. *Biochem J.* **1990**, *271*, 749-754.
- (435) E. Gianazza; P.G. Righetti Size and charge distribution of macromolecules in living systems. *J. Chromatogr.* **1980**, 1-8.

- (436) Rodionov, V. O.; Presolski, S. I.; Díaz, D. D.; Fokin, V. V.; Finn, M. G. Ligand-accelerated Cu-catalyzed azide-alkyne cycloaddition: a mechanistic report. *J. Am. Chem. Soc.* **2007**, *129*, 12705-12712.
- (437) Rodionov, V. O.; Presolski, S. I.; Gardinier, S.; Lim, Y.; Finn, M. G. Benzimidazole and related ligands for Cu-catalyzed azide-alkyne cycloaddition. *J. Am. Chem. Soc.* **2007**, *129*, 12696-12704.
- (438) Lewis, W.; Magallon, F.; Fokin, V.; Finn, M. Discovery and characterization of catalysts for azide-alkyne cycloaddition by fluorescence quenching. *J. Am. Chem. Soc.* **2004**, *126*, 9152-9153.
- (439) Gupta, S. S.; Raja, K. S.; Kaltgrad, E.; Strable, E.; Finn, M. G. Virus-glycopolymer conjugates by copper(I) catalysis of atom transfer radical polymerization and azide-alkyne cycloaddition. *Chem. Commun.* **2005**, 4315-4317.
- (440) Pelkonen, O.; Nebert, D. W. Metabolism of polycyclic aromatic hydrocarbons: etiologic role in carcinogenesis. *Pharmacol. Rev.* **1982**, *34*, 189-222.
- (441) Klinman, J. P. Probes of mechanism and transition-state structure in the alcohol dehydrogenase reaction. *Crit. Rev. Biochem.* **1981**, *10*, 39-78.
- (442) Rodionov, V. O.; Fokin, V. V.; Finn, M. G. Mechanism of the ligand-free CuI-catalyzed azide-alkyne cycloaddition reaction. *Angew. Chem. Int. Ed.* **2005**, *44*, 2210-2215.
- (443) Speers, A. E.; Cravatt, B. F. A tandem orthogonal proteolysis strategy for high-content chemical proteomics. *J. Am. Chem. Soc.* **2005**, *127*, 10018-10019.
- (444) Inoue, K.; Yamada, J.; Ueno, S.; Fukuda, A. Brain-type creatine kinase activates neuron-specific K⁺-Cl⁻ co-transporter KCC2. *J. Neurochem.* **2006**, *96*, 598-608.
- (445) Salin-Cantegrel, A.; Shekarabi, M.; Holbert, S.; Dion, P.; Rochefort, D.; Laganier, J.; Dacal, S.; Hince, P.; Karemera, L.; Gaspar, C.; Lapointe, J.; Rouleau, G. A. HMSN/ACC truncation mutations disrupt brain-type creatine kinase-dependant activation of K⁺/Cl⁻ co-transporter 3. *Hum. Mol. Genet.* **2008**, *17*, 2703-2711.
- (446) Florini, J. R. Assay of creatine kinase in microtiter plates using thio-NAD to allow monitoring at 405 nm. *Anal. Biochem.* **1989**, *182*, 399-404.
- (447) Tachikawa, M.; Fukaya, M.; Terasaki, T.; Ohtsuki, S.; Watanabe, M. Distinct cellular expressions of creatine synthetic enzyme GAMT and creatine kinases uCK-Mi and CK-B suggest a novel neuron-glia relationship for brain energy homeostasis. *Eur. J. Neurosci.* **2004**, *20*, 144-160.

- (448) Wyss, M.; Kaddurah-Daouk, R. Creatine and creatinine metabolism. *Physiol. Rev.* **2000**, *80*, 1107-1213.
- (449) Sauter, A.; Rudin, M. Determination of creatine kinase kinetic parameters in rat brain by NMR magnetization transfer. Correlation with brain function. *J. Biol. Chem.* **1993**, *268*, 13166-13171.
- (450) Chapman, A. G.; Meldrum, B. S.; Siesjö, B. K. Cerebral metabolic changes during prolonged epileptic seizures in rats. *J. Neurochem.* **1977**, *28*, 1025-1035.
- (451) Holtzman, D.; Meyers, R.; Khait, I.; Jensen, F. Brain creatine kinase reaction rates and reactant concentrations during seizures in developing rats. *Epilepsy Res.* **1997**, *27*, 7-11.
- (452) Erakovic, V.; Zupan, G.; Varljen, J.; Laginja, J.; Simonic, A. Altered activities of rat brain metabolic enzymes caused by pentylenetetrazol kindling and pentylenetetrazol -- induced seizures. *Epilepsy Res.* **2001**, *43*, 165-173.
- (453) Inoue, K.; Ueno, S.; Fukuda, A. Interaction of neuron-specific K⁺-Cl⁻ cotransporter, KCC2, with brain-type creatine kinase. *FEBS Lett.* **2004**, *564*, 131-135.
- (454) Cohen, I.; Navarro, V.; Clemenceau, S.; Baulac, M.; Miles, R. On the origin of interictal activity in human temporal lobe epilepsy in vitro. *Science* **2002**, *298*, 1418-1421.
- (455) Shin, J.; Streijger, F.; Beynon, A.; Peters, T.; Gadzalla, L.; McMillen, D.; Bystrom, C.; Zee, C. E. V. D.; Wallimann, T.; Gillespie, P. G. Hair bundles are specialized for ATP delivery via creatine kinase. *Neuron* **2007**, *53*, 371-386.
- (456) Jost, C. R.; Zee, C. E. E. M. V. D.; In 't Zandt, H. J. A.; Oerlemans, F.; Verheij, M.; Streijger, F.; Fransen, J.; Heerschap, A.; Cools, A. R.; Wieringa, B. Creatine kinase B-driven energy transfer in the brain is important for habituation and spatial learning behaviour, mossy fibre field size and determination of seizure susceptibility. *Eur. J. Neurosci.* **2002**, *15*, 1692-1706.
- (457) Bong, S. M.; Moon, J. H.; Jang, E. H.; Lee, K. S.; Chi, Y. M. Overexpression, purification, and preliminary X-ray crystallographic analysis of human brain-type creatine kinase. *J. Microbiol. Biotechnol.* **2008**, *18*, 295-298.
- (458) Bong, S. M.; Moon, J. H.; Nam, K. H.; Lee, K. S.; Chi, Y. M.; Hwang, K. Y. Structural studies of human brain-type creatine kinase complexed with the ADP-Mg²⁺-NO₃--creatine transition-state analogue complex. *FEBS Lett.* **2008**, *582*, 3959-3965.
- (459) Min, K.; Steghens, J.; Henry, R.; Doutheau, A.; Collombel, C. Dichloroaromatic phosphoguanidines are potent inhibitors but very poor

- substrates for cytosolic creatine kinase. *Biochim. Biophys. Acta* **1997**, 1357, 49-56.
- (460) Towler, E. M.; Wilson, L. K.; Zhou, Y. C.; Ma, T. S.; Fisher, R. J. A complete system for identifying inhibitors of creatine kinase B. *Anal. Biochem.* **2000**, 279, 96-99.
- (461) Lin, L.; Perryman, M. B.; Friedman, D.; Roberts, R.; Ma, T. S. Determination of the catalytic site of creatine kinase by site-directed mutagenesis. *Biochim. Biophys. Acta* **1994**, 1206, 97-104.
- (462) Ramagopal, S.; Subramanian, A. R. Alteration in the acetylation level of ribosomal protein L12 during growth cycle of *Escherichia coli*. *Proc. Natl. Acad. Sci. U.S.A* **1974**, 71, 2136-2140.
- (463) Charbaut, E.; Redeker, V.; Rossier, J.; Sobel, A. N-terminal acetylation of ectopic recombinant proteins in *Escherichia coli*. *FEBS Lett.* **2002**, 529, 341-345.
- (464) Louie, A. Y.; Meade, T. J. Metal complexes as enzyme inhibitors. *Chem. Rev.* **1999**, 99, 2711-2734.
- (465) Karlström, A. R.; Levine, R. L. Copper inhibits the protease from human immunodeficiency virus 1 by both cysteine-dependent and cysteine-independent mechanisms. *Proc. Natl. Acad. Sci. U.S.A.* **1991**, 88, 5552-5556.
- (466) Salomé, C.; Salomé-Grosjean, E.; Park, K. D.; Morieux, P.; Swendiman, R.; DeMarco, E.; Stables, J. P.; Kohn, H. Synthesis and anticonvulsant activities of (R)-N-(4'-substituted)benzyl 2-acetamido-3-methoxypropionamides. *J. Med. Chem.* **2010**, 53, 1288-1305.
- (467) Buechter, D. D.; Medzihradszky, K. F.; Burlingame, A. L.; Kenyon, G. L. The active site of creatine kinase. Affinity labeling of cysteine 282 with N-(2,3-epoxypropyl)-N-amidinoglycine. *J. Biol. Chem.* **1992**, 267, 2173-2178.
- (468) Goedert, M.; Pinnock, R. D.; Downes, C. P.; Mantyh, P. W.; Emson, P. C. Neurotensin stimulates inositol phospholipid hydrolysis in rat brain slices. *Brain Res.* **1984**, 323, 193-197.
- (469) Zimmermann, H. Signalling via ATP in the nervous system. *Trends Neurosci.* **1994**, 17, 420-426.
- (470) Bliss, T. V.; Collingridge, G. L. A synaptic model of memory: long-term potentiation in the hippocampus. *Nature* **1993**, 361, 31-39.
- (471) Kronfol, Z.; Remick, D. G. Cytokines and the brain: implications for clinical psychiatry. *Am. J. Psychiatry* **2000**, 157, 683-694.

- (472) Walker, S.; Sofia, M. J.; Kakarla, R.; Kogan, N. A.; Wierichs, L.; Longley, C. B.; Bruker, K.; Axelrod, H. R.; Midha, S.; Babu, S.; Kahne, D. Cationic facial amphiphiles: a promising class of transfection agents. *Proc. Natl. Acad. Sci. U.S.A.* **1996**, *93*, 1585-1590.
- (473) Zhao, Y. Facial amphiphiles in molecular recognition: From unusual aggregates to solvophobic driven foldamers. *Curr. Opin. Colloid. In.* **2007**, *12*, 92-97.
- (474) Lambeng, N.; Grossmann, M.; Chatelain, P.; Fuks, B. Solubilization and immunopurification of rat brain synaptic vesicle protein 2A with maintained binding properties. *Neurosci. Lett.* **2006**, *398*, 107-112.
- (475) Rardon, D.; Cefali, D.; Mitchell, R.; Seiler, S.; Jones, L. High molecular weight proteins purified from cardiac junctional sarcoplasmic reticulum vesicles are ryanodine-sensitive calcium channels. *Circ. Res.* **1989**, *64*, 779-789.
- (476) Zhang, Q.; Horst, R.; Geralt, M.; Ma, X.; Hong, W.; Finn, M. G.; Stevens, R. C.; Wüthrich, K. Micro-scale NMR screening of new detergents for membrane protein structural biology. *J. Am. Chem. Soc.* **2008**, *130*, 7357-7363.
- (477) Zhang, Q.; Ma, X.; Ward, A.; Hong, W.; Jaakola, V.; Stevens, R. C.; Finn, M. G.; Chang, G. Designing facial amphiphiles for the stabilization of integral membrane proteins. *Angew. Chem. Int. Ed.* **2007**, *46*, 7023-7025.
- (478) Demasi, M.; Davies, K. J. A. Proteasome inhibitors induce intracellular protein aggregation and cell death by an oxygen-dependent mechanism. *FEBS Lett.* **2003**, *542*, 89-94.
- (479) Paul, S.; Said, S. I. Characterization of receptors for vasoactive intestinal peptide solubilized from the lung. *J. Biol. Chem.* **1987**, *262*, 158-162.
- (480) Burghout, P.; van Boxtel, R.; Van Gelder, P.; Ringler, P.; Müller, S. A.; Tommassen, J.; Koster, M. Structure and electrophysiological properties of the YscC secretin from the type III secretion system of *Yersinia enterocolitica*. *J. Bacteriol.* **2004**, *186*, 4645-4654.
- (481) Dreher, C.; Prodöhl, A.; Weber, M.; Schneider, D. Heme binding properties of heterologously expressed spinach cytochrome b(6): implications for transmembrane b-type cytochrome formation. *FEBS Lett.* **2007**, *581*, 2647-2651.
- (482) Martens, J. R.; Sakamoto, N.; Sullivan, S. A.; Grobaski, T. D.; Tamkun, M. M. Isoform-specific localization of voltage-gated K⁺ channels to distinct lipid raft populations. Targeting of Kv1.5 to caveolae. *J. Biol. Chem.* **2001**, *276*, 8409-8414.

- (483) Keller, J. N.; Mark, R. J.; Bruce, A. J.; E. Blanc; Rothstein, J. D.; Uchida, K.; Waeg, G.; Mattson, M. P. 4-Hydroxynonenal, an aldehydic product of membrane lipid peroxidation, impairs glutamate transport and mitochondrial function in synaptosomes. *Neuroscience* **1997**, *80*, 685-696.
- (484) Kiedrowski, L. Elevated extracellular K(+) concentrations inhibit N-methyl-D-aspartate-induced Ca(2+) influx and excitotoxicity. *Mol. Pharmacol.* **1999**, *56*, 737-743.
- (485) Begley, J. G.; Butterfield, D. A.; Keller, J. N.; Koppal, T.; Drake, J.; Mattson, M. P. Cryopreservation of rat cortical synaptosomes and analysis of glucose and glutamate transporter activities, and mitochondrial function. *Brain Res. Protoc.* **1998**, *3*, 76-82.
- (486) Gray, E. G.; Whittaker, V. P. The isolation of nerve endings from brain: an electron-microscopic study of cell fragments derived by homogenization and centrifugation. *J. Anat.* **1962**, *96*, 79-88.
- (487) Whittaker, V. P.; Michaelson, I. A.; Kirkland, R. J. A. The separation of synaptic vesicles from nerve-ending particles ('synaptosomes'). *Biochem J.* **1964**, *90*, 293-303.
- (488) Lee, S. Y.; Voronov, S.; Letinic, K.; Nairn, A. C.; Di Paolo, G.; De Camilli, P. Regulation of the interaction between PIPKI gamma and talin by proline-directed protein kinases. *J. Cell Biol.* **2005**, *168*, 789-799.
- (489) Lauderback, C. M.; Hackett, J. M.; Keller, J. N.; Varadarajan, S.; Szweda, L.; Kindy, M.; Markesbery, W. R.; Butterfield, D. A. Vulnerability of synaptosomes from apoE knock-out mice to structural and oxidative modifications induced by A beta(1-40): implications for Alzheimer's disease. *Biochemistry* **2001**, *40*, 2548-2554.
- (490) Asermely, K. E.; Sterling, G. H.; McCafferty, M. R.; O'Neill, J. J. Synaptophysin is phosphorylated in rat cortical synaptosomes treated with botulinum toxin A. *Life Sci.* **1999**, *64*, 297-303.
- (491) Erecińska, M.; Pastuszko, A.; Wilson, D. F.; Nelson, D. Ammonia-induced release of neurotransmitters from rat brain synaptosomes: differences between the effects on amines and amino acids. *J. Neurochem.* **1987**, *49*, 1258-1265.
- (492) Hendrich, J.; Van Minh, A. T.; Heblich, F.; Nieto-Rostro, M.; Watschinger, K.; Striessnig, J.; Wratten, J.; Davies, A.; Dolphin, A. C. Pharmacological disruption of calcium channel trafficking by the alpha2delta ligand gabapentin. *Proc. Natl. Acad. Sci. U.S.A.* **2008**, *105*, 3628-3633.
- (493) Dunkley, P. R.; Jarvie, P. E.; Robinson, P. J. A rapid Percoll gradient procedure for preparation of synaptosomes. *Nat. Protoc.* **2008**, *3*, 1718-1728.

- (494) Löscher, W.; Böhme, G.; Müller, F.; Pagliusi, S. Improved method for isolating synaptosomes from 11 regions of one rat brain: electron microscopic and biochemical characterization and use in the study of drug effects on nerve terminal gamma-aminobutyric acid in vivo. *J. Neurochem.* **1985**, *45*, 879-889.
- (495) Fonnum, F. The 'compartmentation' of choline acetyltransferase within the synaptosome. *Biochem J.* **1967**, *103*, 262-270.
- (496) Enriquez, J. A.; Sánchez-Prieto, J.; Blanco, M. T. M.; Hernandez-Yago, J.; López-Pérez, M. J. Rat brain synaptosomes prepared by phase partition. *J. Neurochem.* **1990**, *55*, 1841-1849.
- (497) López-Pérez, M.; París, G.; Larsson, C. Highly purified mitochondria from rat brain prepared by phase partition. *BBA-Bioenergetics* **1981**, *635*, 359-368.
- (498) Krueger-Koplin, R. D.; Sorgen, P. L.; Krueger-Koplin, S. T.; Rivera-Torres, I. O.; Cahill, S. M.; Hicks, D. B.; Grinius, L.; Krulwich, T. A.; Girvin, M. E. An evaluation of detergents for NMR structural studies of membrane proteins. *J. Biomol. NMR* **2004**, *28*, 43-57.
- (499) Finbow, M. E.; Shuttleworth, J.; Hamilton, A. E.; Pitts, J. D. Analysis of vertebrate gap junction protein. *EMBO J.* **1983**, *2*, 1479-1486.
- (500) Brady, R. M.; Zinkowski, R. P.; Binder, L. I. Presence of tau in isolated nuclei from human brain. *Neurobiol. Aging* **1995**, *16*, 479-486.
- (501) Hoogland, G.; Blomenröhr, M.; Dijkstra, H.; de Wit, M.; Spierenburg, H. A.; van Veelen, C. W. M.; van Rijen, P. C.; van Huffelen, A. C.; Gispen, W. H.; de Graan, P. N. E. Characterization of neocortical and hippocampal synaptosomes from temporal lobe epilepsy patients. *Brain Res.* **1999**, *837*, 55-66.
- (502) Hens, J. J. H. In *Neurotransmitter methods*; Rayne, R. C., Ed.; Methods in Molecular Biology; Humana Press: Totowa, N.J., 1997; Vol. 72, pp. 61-69.
- (503) Votano, J. R.; Parham, M.; Hall, L. M.; Hall, L. H.; Kier, L. B.; Oloff, S.; Tropsha, A. QSAR modeling of human serum protein binding with several modeling techniques utilizing structure-information representation. *J. Med. Chem.* **2006**, *49*, 7169-7181.
- (504) Tawara, S.; Matsumoto, S.; Matsumoto, Y.; Kamimura, T.; Goto, S. Structure-binding relationship and binding sites of cephalosporins in human serum albumin. *J. Antibiot.* **1992**, *45*, 1346-1357.
- (505) Patel, I. H.; Levy, R. H. Valproic acid binding to human serum albumin and determination of free fraction in the presence of anticonvulsants and free fatty acids. *Epilepsia* **1979**, *20*, 85-90.

- (506) Kober, A.; Olsson, Y.; Sjöholm, I. Binding of drugs to human serum albumin. XIV. The theoretical basis for the interaction between phenytoin and valproate. *Mol. Pharmacol.* **1980**, *18*, 237-242.
- (507) Johansson, G. In *Affinity Chromatography: Methods and Protocols*; Bailon, P.; Ehrlich, G. K.; Fung, W. J.; Berthold, W., Eds.; Methods in Molecular Biology; Humana Press: Totowa, N.J., 2000; Vol. 147, pp. 105-117.
- (508) Burdman, J. A. Incorporation in vivo of radioactive leucine into neuronal and glial nuclear proteins of rat brain. *J. Neurochem.* **1970**, *17*, 1555-1562.
- (509) Burdman, J. Further observations on protein synthesis by isolated nuclei from rat brain cells. *Brain Res.* **1972**, *41*, 413-421.
- (510) Lovtrup-Rein, H.; McEwen, B. S. Isolation and fractionation of rat brain nuclei. *J. Cell Biol.* **1966**, *30*, 405-415.
- (511) Taniura, H.; Sng, J. C.; Yoneda, Y. Histone modifications in the brain. *Neurochem. Int.* **2007**, *51*, 85-91.
- (512) Balasubramanyam, K.; Varier, R. A.; Altaf, M.; Swaminathan, V.; Siddappa, N. B.; Ranga, U.; Kundu, T. K. Curcumin, a novel p300/CREB-binding protein-specific inhibitor of acetyltransferase, represses the acetylation of histone/nonhistone proteins and histone acetyltransferase-dependent chromatin transcription. *J. Biol. Chem.* **2004**, *279*, 51163-51171.
- (513) Bharal, N.; Sahaya, K.; Jain, S.; Mediratta, P. K.; Sharma, K. K. Curcumin has anticonvulsant activity on increasing current electroshock seizures in mice. *Phytother. Res.* **2008**, *22*, 1660-1664.
- (514) Gupta, Y. K.; Briyal, S.; Sharma, M. Protective effect of curcumin against kainic acid induced seizures and oxidative stress in rats. *Indian J. Physiol. Pharmacol.* **2009**, *53*, 39-46.
- (515) Monti, B.; Polazzi, E.; Contestabile, A. Biochemical, molecular and epigenetic mechanisms of valproic acid neuroprotection. *Curr. Mol. Pharmacol.* **2009**, *2*, 95-109.
- (516) Böttcher, T.; Sieber, S. A. Beta-lactones as privileged structures for the active-site labeling of versatile bacterial enzyme classes. *Angew. Chem. Int. Ed.* **2008**, *47*, 4600-4603.
- (517) Jessani, N.; Liu, Y.; Humphrey, M.; Cravatt, B. F. Enzyme activity profiles of the secreted and membrane proteome that depict cancer cell invasiveness. *Proc. Natl. Acad. Sci. U.S.A.* **2002**, *99*, 10335-10340.
- (518) Speers, A. E.; Cravatt, B. F. Chemical strategies for activity-based proteomics. *Chembiochem* **2004**, *5*, 41-47.

- (519) Konecny, G.; Untch, M.; Arboleda, J.; Wilson, C.; Kahlert, S.; Boettcher, B.; Felber, M.; Beryt, M.; Lude, S.; Hepp, H.; Slamon, D.; Pegram, M. Her-2/neu and urokinase-type plasminogen activator and its inhibitor in breast cancer. *Clin. Cancer Res.* **2001**, *7*, 2448-2457.
- (520) Williams, J. A.; Phillips, D. H. Mammary expression of xenobiotic metabolizing enzymes and their potential role in breast cancer. *Cancer Res.* **2000**, *60*, 4667-4677.
- (521) Staub, I.; Sieber, S. A. Beta-lactams as selective chemical probes for the in vivo labeling of bacterial enzymes involved in cell wall biosynthesis, antibiotic resistance, and virulence. *J. Am. Chem. Soc.* **2008**, *130*, 13400-13409.
- (522) Ritchie, J.; Rogart, R. The binding of saxitoxin and tetrodotoxin to excitable tissue. *Rev. Physiol. Biochem. Pharmacol.* **1977**, *79*, 1-50.